Trinity College Dublin
Coláiste na Tríonóide, Baile Átha Cliath
The University of Dublin

Investigation of the role of the complement system in the radioresistance of rectal cancer

Rebecca O'Brien
Student number: 14315794

Ph.D. Thesis
Submitted to Trinity College Dublin for the degree of Doctor of Philosophy

Thesis Supervisors: Dr Niamh Lynam-Lennon (Primary Supervisor)
Dr Joanne Lysaght (Co-Supervisor)

Department of Surgery, School of Medicine, Trinity Translational Medicine Institute, Trinity College Dublin and Trinity St. James's Cancer Institute
March 2023

Declaration

I declare that this thesis has not been submitted as an exercise for a degree at this or any other university and it is entirely my own work.

I agree to deposit this thesis in the University's open access institutional repository or allow the Library to do so on my behalf, subject to Irish Copyright Legislation and Trinity College Library conditions of use and acknowledgement.

I consent to the examiner retaining a copy of the thesis beyond the examining period, should they so wish (EU GDPR May 2018).

Signed

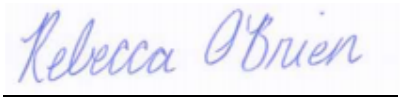

Rebecca O'Brien

24.03.2023

Rebecca O'Brien Date

Summary

Colorectal cancer (CRC) is the third most common cancer globally, accounting for approximately 10% of all cancer diagnoses. A third of CRCs occur in the rectum. The majority of CRCs are diagnosed at advanced stages and treatment for locally-advanced rectal cancer (LARC) is neo-adjuvant chemoradiation therapy (neo-CRT) followed by surgical removal of the tumour. Unfortunately, response rates to neo-CRT are modest, with less than 30% of patients achieving a complete pathological response (pCR). Therefore, there is a global unmet need to urgently elucidate the molecular factors influencing response to neo-CRT in rectal cancer to identify new therapeutic targets to boost response to therapy in this setting. Furthermore, the identification of novel predictive biomarkers of response to neo-CRT in rectal cancer would enable improved patient stratification prior to the initiation of treatment. The complement system is an essential arm of innate immunity which is becoming increasingly recognised in the context of cancer. Complement system components have been demonstrated to promote tumourigenesis and alter response to therapy in a number of human cancers. In this thesis, the role of the complement system in the radioresistance of rectal cancer was investigated, to assess the potential for complement as a therapeutic target and a predictive biomarker of response to neo-CRT in rectal cancer.

The inherent radiosensitivity of a panel of colon and rectal cancer cell lines was characterised, identifying HCT116 cells as an inherently radiosensitive cell line, while SW837, HRA-19 and SW1463 cells were inherently radioresistant. Expression of the complement system was characterised in these cells, demonstrating that colon and rectal cancer cells express the central complement components C3 and C5, which are present intracellularly and secreted. Complement was activated in CRC cells, with C3a and C5a anaphylatoxins secreted and retained intracellularly. The total intracellular concentration of C3 and C5 and their respective anaphylatoxins was increased in cells with increased radioresistance, suggesting a role for complement in the response to radiation in CRC. Furthermore, expression of C3 and C5 positively correlated with the surviving fraction of cells at a clinically-relevant dose of radiation. Expression of complement factor B (CFB), an alternative complement activation pathway component, suggested that complement activation may occur via this pathway. CRC cells were demonstrated to express the C3aR and C5aR complement receptors, and membrane-bound complement regulatory proteins, suggesting that they can respond to complement signalling and modulate complement activation, respectively.

In radiosensitive HCT116 cells and radioresistant HRA-19 cells, C3 was demonstrated to functionally modulate the response to radiation at a clinically-relevant dose of radiation. In HCT116 cells, C3 overexpression was not associated with alterations in viability, apoptosis, cell cycle distribution or DNA damage induction and repair, suggesting that C3 may modulate the response to radiation in these cells by another mechanism. In HRA-19 cells, C3 silencing and enhanced radiosensitivity was associated with increased levels of basal DNA damage and altered cell cycle distribution to a more radiosensitive phenotype. Immunoprecipitation of C3 from HRA-19 and HCT116 cells and analysis by mass spectrometry demonstrated that the C3 interactome is significantly altered

between these two cell lines, supporting the hypothesis that C3 may engage in different intracellular roles.

Investigation of the effect of tumour cell-derived C3 and recombinant C3a on T cell phenotype demonstrated that complement can maintain T cells in a naïve state. While this would suggest that complement does not boost effector function, assessment of T cell cytokine expression demonstrated that complement potentially shifts T cell responses away from T helper (Th)2-like towards an IFN-γ producing, Th1-like phenotype. No effect on T cell proliferation was demonstrated by either tumour cell-derived or recombinant complement.

Investigation of complement expression in pre-treatment rectal tumour biopsies demonstrated that central complement cascade and complement activation pathway components are expressed in rectal tissue at higher levels relative to non-cancer tissue. Expression of C5 mRNA was elevated in the tumour tissue of obese patients suggesting a relationship between obesity status and complement expression in rectal cancer. Complement activation was detected within the circulation in pre-treatment rectal cancer patient sera. Sera levels of C3a were associated with clinical tumour stage. For the first time, pre-treatment sera levels of C3a and C5b-9 were demonstrated to correlate with subsequently poor patient responses to neo-CRT, suggesting that complement may have potential as a circulating predictive biomarker of response to neo-CRT. C5b-9 was also elevated in the sera of patients with worse recurrence-free and overall survival.

Together this thesis demonstrates a functional role for C3 in the response to radiation *in vitro*, and highlights a potential role for circulating C3a and C5b-9 as predictive and prognostic biomarkers in rectal cancer.

Acknowledgements

It is an absolute pleasure to extend my gratitude to everyone who has helped me along the way in completing this PhD. It's true what they say – it really takes a village!

First, a massive thank you to Dr Niamh Lynam-Lennon who has been nothing short of an exceptional supervisor. Niamh, you have been a pleasure to work with from the moment I approached you in pursuit of research opportunities, all the way to correcting draft after draft of this thesis. Thank you for being a wonderful mentor and a constant support throughout the last 4 years. I will forever be grateful for the time you have invested in me, the skills you have shared and all of your advice.

I also have to extend a huge thank you to Dr Joanne Lysaght, for being a fantastic co-supervisor and a never-ending source of knowledge and encouragement. Working alongside the other members of your Tumour Immunology group has been invaluable, and I am greatly appreciative of your support every step of the way. Thank you for always being so helpful and approachable.

This PhD would not have been possible without funding from the Irish Cancer Society. I cannot thank the ICS team enough for supporting this project and having confidence in me as a researcher. Everyone at the ICS who has crossed my path has been just brilliant to work with, it has been a true privilege. A massive thank you for providing unmeasurable encouragement and support from the early days of applying for this PhD scholarship. I must also extend a huge thanks to all of the people who dedicate time to fundraising for the ICS and in doing so support the funding of research studies such as this.

Thank you to all members of the Department of Surgery who have played a role in the completion of this project. Thank you to everyone past and present who has worked on the Lower GI Biobank – Niamh Clarke, Dr Aisling Heeran, Dr Croí Buckley, Lorraine Smith and Dr Aisling Ui Mhaonaigh. Thank you to all of the clinical teams involved in recruiting patients to this study. Thanks to Dr Tim Nugent and Dr Noel Donlon for your tireless help in assisting with everything from ethics to the coordination of sample collection. Thank you to Dr Cara Dunne, Mr John Larkin, Mr Brian Mehigan, Mr Paul McCormack and Mr Michael Kelly in St. James's Hospital, and to Mr Adnan Hafeez, Mr Diarmuid O'Ríordáin, Mr Robert Hannon, Mr Paul Neary and Mr Reza Kalbassi in the Beacon Hospital for recruiting patients to this study.

I must express my profound gratitude to every patient who selflessly donated samples to this research. This research wouldn't have been possible without you.

I am very grateful for the wonderful collaborators who have contributed to this project. Thank you to Prof. Kathrine Røe Redalen and Dr. Sebastian Meltzer for generously sharing with us the pre-treatment patient sera from the OxyTarget patient cohort that was used in this study. Thank you to Sebastian for performing data analysis on this cohort.

Thank you to Dr Monica Olcina and all of the Immune Radiation Biology group at the MRC Oxford Institute for Radiation Oncology for so warmly welcoming me into your lab during my Mobility Element. Monica, I am extremely grateful for our valuable discussions and how generous you were with your time and knowledge. Huge thanks to Dominika, David and Kelly for all of your help in the lab, making my time in Oxford so enjoyable and teaching me how to punt! A special thanks to David for all of your hard work in performing IF for this project.

Thank you to Dr Iolanda Vendrell and Dr Roman Fischer at the Discovery Proteomics Facility at the Target Discovery Institute, University of Oxford for performing the mass spectrometry in this study. Your skills, expertise and guidance with data analysis are so greatly appreciated.

Thank you to all of the stellar PIs, post docs, PhD students and biobank managers in the Department of Surgery who have supported me over the course of this PhD. Thank you to Jacintha, Stephen, Melissa and Graham for fostering my research skills, providing constructive feedback and engaging in useful discussion of my experimental findings at Departmental meetings. This project was no doubt enhanced by all of your much appreciated input. I have been fortunate to work with and learn from many fantastic post docs. In particular, thank you to Aoife Cannon, my fellow complementologist, for all of your help and wisdom. Thank you also to Simone, Aisling H, Aoife K and Aisling U for all of your encouragement and guidance.

Thank you to everyone I have been lucky to share an office with; Croí, Andrew, Jason, Aisling, Maria, Noel, Christina, Brendan, Anshul, Cliona, Jim, Fiona, Klaudia, Eimear, Laura, Marina, Christine, Matt, Rebecca, Lorraine, Caroline, Niamh and David. You have made the Department a wonderful, memorable place to work and I am grateful for everyone's help and friendship. A very special thanks to Andrew and Jason for making me laugh every day and always being up for a coffee, I could not have done it without you! Thanks also to Croí, my PhD big sister, for your wonderful friendship and cheering me on until the end. It wouldn't have been the same without you!

Thank you to Martin, Kathy, Tony, Ken and Pierce from the Thoracic Oncology, Haematology and Pharmacology labs for helping me out in a pinch and being so generous with reagents and lab equipment whenever needed.

An important thank you to all of my friends outside of the lab who have been so patient with me over the last 4+ years. A huge thanks to Keith and Cody for always being so understanding and supporting me along the way. Thank you also to Joana for being the kindest, most wonderful friend. I am so lucky to have you! Maria, thank you for always being my cheerleader, even all the way from China! You are the kind of friend that everyone deserves and I am forever grateful for your encouragement and friendship.

I am tremendously lucky to have an incredible family that have always supported me in academic endeavours and beyond. Thank you to my Nana Sheila and Grandad Tom for keeping me company on my drive home from the lab, always providing me with much needed snacks and cups of tea and supporting me every day. I am eternally thankful to have you in my life and beyond grateful for your constant wise words and encouragement.

Thank you to my amazing sister Tara who is a best friend and sister in one. Thank you for everything you have done to make my life easier, all of the coffee walks, bakery runs, dog excursions with Poppy and Rosie and motivating me when I needed it. You are one in a million. I couldn't have done it without you!

The thank you necessary to acknowledge everything my amazing Mom and Dad have helped me with along the way exceeds anything I could put into words. I may be biased, but you are the most wonderful parents I could wish for. Thank you for always encouraging me to pursue whatever took my interest and supporting me in more ways than I could count. All of my successes in life are due to you and my gratitude for you is unmeasurable.

Finally, thank you to Aaron for sticking by my side through everything, listening to all of my worries and reminding me every day that I can do it. Thank you for being a constant encouragement and my best friend. I am beyond lucky to have you in my corner.

PhD Outputs

Publications

First author

O'Brien RM, Lynam-Lennon N, Olcina MM. Thinking inside the box: intracellular roles for complement system proteins come into focus. *British Journal of Cancer*. 2023 Jan 17:1-3**.**

O'Brien RM, Cannon A, Reynolds JV, Lysaght J, Lynam-Lennon N. Complement in tumourigenesis and the response to cancer therapy. *Cancers*. 2021 Mar 10;13(6):1209.

Co-author

Kane LE, Mellotte GS, Mylod E, **O'Brien RM**, O'Connell F, Buckley CE, Arlow J, Nguyen K, Mockler D, Meade AD, Ryan BM. Diagnostic accuracy of blood-based biomarkers for pancreatic cancer: A systematic review and meta-analysis. *Cancer Research Communications*. 2022 Oct 20;2(10):1229-43.

Davern M, **O'Brien RM**, McGrath J, Donlon NE, Melo AM, Buckley CE, Sheppard AD, Reynolds JV, Lynam-Lennon N, Maher SG, Lysaght J. PD-1 blockade enhances chemotherapy toxicity in oesophageal adenocarcinoma. *Scientific reports*. 2022 Feb 28;12(1):1-9.

Oral presentations (presenting author)

International

Annual Meeting of the Association of Radiation Research, Online, 12th-14th July 2021. Title: Investigating the role of the complement system in the radioresistance of rectal cancer.

Complement UK Training Course and Symposium, 25th & 28th January, 8th & 11th February 2021. Title: Investigation of the role of the complement cascade in the radioresistance of rectal cancer.

National

Irish Cancer Society's Research Awards 2023, Dublin, 27th February 2023. Title: Using immune proteins to improve treatment for people with bowel cancer.

Irish Radiation Research Society Scientific Annual Meeting 2021, Online, 16th-17th September 2021. Title: Investigating the role of the complement system in the radioresistance of rectal cancer.

Irish Cancer Society's Research Awards 2021, Online, 24th February 2021. Title: Using immune proteins to improve treatment for bowel cancer patients.

Irish Cancer Society's Research Awards 2020, The Richmond Education and Event Centre, 20th February 2020. Title: Can we use immune proteins to improve treatment for patients with bowel cancer?

Irish Cancer Society's in-house seminar series for Bowel Cancer Awareness month, 15th August 2019. Title: Can we use immune proteins to improve treatment for patients with rectal cancer?

Trinity Translational Medicine Institute Precision Medicine Cancer Symposium, TTMI, 15th February 2019. Title: Can we use immune proteins to tell which rectal cancer patients can be helped by radiation therapy?

Poster presentations (presenting author)

International

European Association for Cancer Research 2022 Congress – Innovative Cancer Science: Translating Biology to Medicine, Seville, 20th-23rd June, 2022. Title: Investigating the role of the complement system in the radioresistance of rectal cancer.

British Association for Cancer Research Response and Resistance in Cancer Therapy, Online, 6th -8th September 2021. Title: Investigating the role of the complement system in the radioresistance of rectal cancer.

6th European Congress of Immunology, Online, 1st-4th September 2021. Title: Investigating the role of the complement system in the radioresistance of rectal cancer.

European Association for Cancer Research 2021 Virtual Congress: Innovative Cancer Science, Online, 9th-12th June 2021. Title: Investigating the role of the complement system in the radioresistance of rectal cancer.

Complement UK Training Course and Symposium. Online, 25th & 28th January, 8th & 11th February 2021. Title: Investigation of the role of the complement cascade in the radioresistance of rectal cancer.

National

The Trinity St James's Cancer Institute 12th International Cancer Conference, Dublin, 13th-14th October 2022. Title: Complement proteins are associated with radioresistance, alter the T cell phenotype and can predict patient response to treatment in rectal cancer.

Irish Society for Immunology Annual Meeting, Maynooth, 1st-3rd September 2022. Title: Complement proteins are associated with radioresistance and can predict response to treatment in rectal cancer.

Irish Association for Cancer Research 58th Annual Meeting 2022, Cork, 30th March – 1st April 2022. Title: Investigating the role of the complement system in the radioresistance of rectal cancer.

Irish Association for Cancer Research Virtual Conference 2021, Online, 24th-26th March 2021. Title: Investigating the role of the complement cascade in the radioresistance of rectal cancer.

Irish Association for Cancer Research 56th Annual Meeting, Galway, 26-28th February 2020. Title: Investigation of the role of the complement system in the radioresistance of rectal cancer.

The 11th Trinity College Dublin International Cancer Conference, Dublin, 24th & 25th October 2019. Title: Investigating the complement cascade in the radioresistance of rectal cancer.

Irish Society for Immunology Annual Meeting, Dublin, 19th & 20th September 2019. Title: Investigating the complement cascade in the radioresistance of rectal cancer.

Breakthrough Cancer Research Breaking Through: Research to Transform Cancer Treatment, Cork, 5th & 6th September 2019. Title: Investigation of the role of the complement system in the radioresistance of rectal cancer.

Irish Association for Cancer Research 55th Annual Meeting, Belfast, 20th – 22nd February 2019. Title: Investigation of the role of the complement system in the radioresistance of rectal cancer.

Awards

Irish Cancer Society PhD Researcher of the Year 2023 – Awarded at the Irish Cancer Society Research Awards, Dublin, 27th February 2023.

Best Poster Award - Awarded at the Irish Association for Cancer Research 58th Annual Meeting 2022, Cork, 30th March –1st April 2022.

Oral Presentation Award – Awarded at the 28th International Complement Virtual Workshop, Online, 6th-10th December 2021.

Conference Bursary – On behalf of the Irish Society for Immunology /European Federation of Immunological Societies, to attend the 6th European Congress of Immunology, Online, 1st-4th September 2021.

Best Poster Award- Awarded at Irish Association for Cancer Research 56th Annual Meeting, Galway, 26-28th February 2020.

Travel Award – Awarded by Assay Genie for writing the top blog post, October 2019.

Table of contents

List of figures

List of tables

Abbreviations

ANOVA	Analysis of variance
AP	Alternative pathway
APC	Antigen presenting cell
ATM	Ataxia telangiectasia mutated
ATR	Ataxia telangiectasia mutated-rad3-related
AUC	Area under the curve
AV	Annexin V
BCA	Bicinchoninic acid
BER	Base excision repair
BMI	Body mass index
C1	Complement component 1
C1-INH	C1 inhibitor
C1QBP	C1q subcomponent binding PROTEIN
C3aR	C3a receptor
C4BP	C4-binding protein
C5aR	C5a receptor
CAF	Cancer associated fibroblast
cCR	Complete clinical response
CD	Cluster of differentiation
CDC	Complement dependent cytotoxicity
CDK	Cyclin-dependent kinase
cDNA	Complementary DNA
CEA	Carcinoembryonic antigen
CFB	Complement factor B
CFH	Complement factor H
CFI	Complement factor I
CFSE	Carboxyfluorescein succinimidyl ester
CHK	Checkpoint-transducer kinases
CIMP	CpG island methylator phenotype
CIN	Chromosomal instability
CM	Conditioned media
CMS	Consensus molecular subtypes

cN	Clinical nodal stage
CP	Classical pathway
CR	Complement receptor
CRC	Colorectal cancer
Ct	Threshold cycle
cT	Clinical tumour stage
CT	Computed tomography
CTSD	Cathepsin D
CTSL	Cathepsin L
DAF	Decay accelerating factor
DC	Dendritic cell
DDR	DNA damage response
DFS	Disease-free survival
5'DFUR	5'-deoxy-5-fluorouridine
DNA PKcs	DNA-dependent protein kinase catalytic subunit
dNTPs	Deoxynucleotides
DRE	Digital rectal examination
DSB	Double strand break
dTMP	Deoxythymidine monophosphate
dUMP	Deoxyuridine monophosphate
dUTP	Deoxyuridine triphosphate
EDTA	Ethylenediaminetetraacetic acid
ELISA	Enzyme-linked immunosorbent assay
EMT	Epithelial to mesenchymal transition
FACS	Fluorescence activated cell sorting
FBS	Foetal bovine serum
FdUMP	Fluorodeoxyuridine monophosphate
FdUTP	Fluorodeoxyuridine triphosphate
FFPE	Formalin-fixed paraffin-embedded
5-FU	5-fluorouracil
FUTP	Fluorouridine triphosphate
G	Gap
GI	Gastrointestinal

GO	Gene Ontology
HDI	Human development index
HIF	Hypoxia-inducible transcription factor
HR	Homologous recombination
HRE	Hypoxia-responsive element
IF	Immunofluorescence
Ig	Immunoglobulin
IHC	Immunohistochemistry
IL	Interleukin
IR	Ionising radiation
KEGG	Kyoto Encyclopedia of Genes and Genomes
L-15	Leibovitz's 15
LARC	Locally-advanced rectal cancer
LCRT	Long course radiation therapy
LIG	Ligase
LP	Lectin pathway
M	Mitosis
MAC	Membrane attack complex
MASP	MBL-associated serine proteases
MBL	Mannose-binding lectin
MCP	Membrane cofactor protein
mCRP	Membrane-bound complement regulatory protein
MFI	Mean fluorescence intensity
MMR	Mismatch repair
MSI	Microsatellite instability
mTOR	Mammalian target of rapamycin
n.d	Not detected
Neo-CRT	Neo-adjuvant chemoradiation therapy
Neo-RT	Neo-adjuvant radiation therapy
NHEJ	Non-homologous end-joining
NK cell	Natural killer cells
NSB	Nijmegen breakage syndrome
NSCLC	Non-small cell lung cancer

OAC	Oesophageal adenocarcinoma
OAC	Oesophageal adenocarcinoma
OS	Overall survival
p	Probability
p-adj	Adjusted *p* value
PAMP	Pathogen-associated molecular patterns
PBMC	Peripheral blood mononuclear cells
PBS	Phosphate buffered saline
pCR	Complete pathological response
PCR	Polymerase chain reaction
PE	Plating efficiency
PET	Positron emission tomography
PFS	Progression-free survival
PHD	Prolyl hydroxylase
PI	Propidium iodide
PI3K	Phosphatidylinositol-3 kinase
PIKK	Phosphatidylinositol-3-kinase-related kinase
PRDM15	PR-domain-containing protein 15
PTEN	Phosphate and tensin homolog
PTX	Paclitaxel
qPCR	Quantitative real-time PCR
RFS	Recurrence-free survival
RIPA	Radioimmunoprecipitation assay
ROS	Reactive oxygen species
RPM	Revolutions per minute
RPMI	Roswell park memorial institute
RT	Radiotherapy
S	Synthesis
SCC	Squamous cell carcinoma
SCRT	Short course radiation therapy
SEM	Standard error of the mean
SF	Surviving fraction
siRNA	Silent interfering RNA

SSB	Single strand break
SSBR	Single strand break repair
TCGA	The cancer genome atlas
TCM	Tumour conditioned media
TCR	T cell receptor
Th	T helper
TIL	Tumour infiltrating lymphocyte
TLR	Toll-like receptor
TME	Tumour microenvironment
TNF	Tumour necrosis factor
Tregs	Regulatory T cells
TRS	Tumour regression score
TS	Thymidylate synthase
TTC	Terminal complement complex
VC	Vector control
XRCC	X-ray repair cross-complementing protein

Units

°C	Degrees Celsius
d	Day
Gy	Gray
x g	Acceleration due to gravity
h	Hour
L	Litre
mA	Milliamp
min	Minute
mL	Millilitre
mM	Millimolar
ηg	Nanograms
ηM	Nanomolar
RT°	Room temperature
s	Second

μg	Microgram
μL	Microlitre
μM	Micromolar
V	volts
v/v	Volume per volume
w/v	Weight per volume

Chapter 1: General Introduction

This chapter has been published in part in;
O'Brien, R. M., Cannon, A., Reynolds, J. V., Lysaght, J., & Lynam-Lennon, N. (2021). Complement in Tumourigenesis and the Response to Cancer Therapy. *Cancers*, *13*(6), 1209.

1.1. Colorectal cancer

1.1.1. Epidemiology

Colorectal cancer (CRC) is a major contributor to the global cancer burden, representing the third most commonly diagnosed cancer worldwide[1]. In 2020, CRC accounted for more than 1.9 million new cancer diagnoses, approximately 10% of all cancer cases[1]. Of these, over 700,000 cases occurred in the rectum specifically. In Ireland, CRC is the second and third most commonly diagnosed cancer in males and females, respectively, responsible for almost 3000 new cancer diagnoses annually[2]. Of all CRCs diagnosed in Ireland, approximately one third occur in the rectum[2]. Between 2010 and 2014 in Ireland, 54.9% of colon cancers were diagnosed at advanced stages (stage II and III), while 60.3% of rectal cancers were diagnosed at advanced stages[3].

CRC greatly impacts mortality. The most recent report revealed that in 2020, CRC was the second leading cause of cancer death worldwide, responsible for 1 in 10, or approximately 935,000 cancer deaths[1]. Of these, more than 300,000 can be attributed to rectal cancer. CRC demonstrates a similar trend in Ireland, representing the second most common cause of cancer-related mortality and resulting in over 1000 deaths annually[2]. Based on sex, CRC on average is the second most common cause of cancer death in males, and the third most common in women, behind lung and breast cancer[2]. In Ireland, the 5-year survival rate for CRC increased from 50% between 1994-1999 to 66% between 2014-2018 (**Fig. 1-1**). Both the incidence of and mortality associated with CRC is greater in males than females[2,4,5]. The 5-year survival rate for rectal cancer specifically, is 61.6% [3].

The distribution of CRC varies globally. Highest rates of CRC occur in Europe, Australia/New Zealand and North American, with low incidence in most of Africa and also South Central Asia[1]. Increases in the human development index (HDI), a measure which encompasses life expectancy, the attainment of education and income, is accompanied by rising rates of CRC[6]. As such CRC is considered a socioeconomic developmental marker[1].

Worryingly, the incidence of CRC is rising, with new diagnoses projected to surpass 3 million in 2040[5]. The rising incidence of CRC is attributable to population growth and ageing, but increases in low HDI countries and young adults in higher-income settings are also linked to the adoption of a westernised diet and growing rates of obesity[5]. In 2020, more than 60% of all CRCs diagnosed globally occurred in patients between the ages of 50 and 74[5]. In Ireland, the majority of cases are diagnosed in those over 50, with less than 10% of CRCs occurring in patients under the age of 50[2]. CRC is increasing in younger people (<50) in particular, with more of these patients presenting with tumours in the rectum as

opposed to the colon[7,8]. Reportedly, diagnoses of rectal cancer in younger cohorts are delayed, often due to being symptomatic for a period of time prior to seeking medical attention and as a result of slow referral to necessary specialists after presenting at the clinic[9]. While earlier studies of CRC highlighted that younger patients were often diagnosed at later stages and had worse outcomes[10,11], more recent studies of rectal cancer specifically have suggested that tumour stage and 5 year survival is similar in younger and older patients[9,12].

It is estimated that global increases in CRC will be accompanied by a greater than 70% increase in deaths. The majority of these deaths are predicted to occur in high or very high HDI regions[5]. In Ireland particularly, rectal cancer deaths are projected to increase by 24.2% by the year 2035[13].

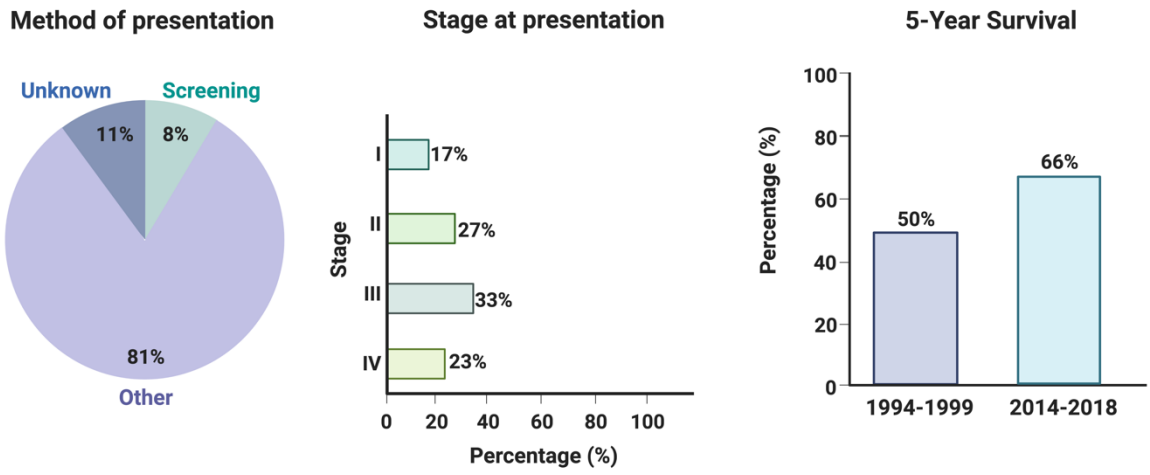

Figure 1-1: Presentation method, stage at diagnosis and 5-year survival of CRC in Ireland. Data from the National Cancer Registry Ireland[14]. Figure created with BioRender.com.

1.1.2. Molecular and clinical differences in colon and rectal cancers

A major percentage of CRCs (approximately 30%), occur in the rectum[1]. Given their close anatomical relationship, colon, rectal and anal cancers are generally classified together as CRC[1,15]. Despite this, evidence demonstrates that rectal cancers differ in aetiology, pathology and mutational burden, when compared to colon cancers.

It is hypothesised that colon and rectal cancers may arise at least partially via different mechanisms of oncogenesis[16]. Supporting this theory, study of tumour tissue from the rectum and colon has demonstrated that these cancers display differences in the expression

and mutation of both tumour suppressor and oncogenes. Moving from the right colon to the left colon to the rectum, the mutation frequencies of the p53 and adenomatous polyposis coli genes are demonstrated to increase, while decreasing mutational frequencies for genes including ataxia telangiectasia mutated (ATM) and phosphate and tensin homolog (PTEN) are reported[17]. Additionally, positive expression of p53 is more common in rectal cancers and significantly correlates with shorter disease-free survival (DFS) in rectal but not colon cancers[16]. Mutations in v-raf murine sarcoma viral oncogene homolog B1 *(BRAF)* can occur in both colon and rectal cancer, however they are less common in rectal tumours (25% of right-sided and 7% of left-sided colon vs. 3.2% of rectal)[17]. Furthermore, the majority of *BRAF* mutations in right and left-sided colon tumours are V600E mutations, compared with just 50% of rectal tumours[17]. Significantly greater amplification of human epidermal growth factor receptor 2 (HER2)/neu and lower activation of phosphatidylinositol-3 kinase (PI3K)/Akt/ mammalian target of rapamycin (mTOR) has also been noted in rectal cancers relative to colon cancers[17]. Rectal cancers display elevated nuclear expression of β-catenin, suggesting that greater activation of the β-catenin/ adenomatous polyposis coli pathway may occur in these tumours, relative to colon cancer[16]. These studies demonstrate that there are differences in the molecular landscape between colon and rectal cancers.

Most notably, the clinical behaviour of colon and rectal cancers differs. While the main challenge in treating rectal cancer is risk of local recurrence, a major concern for colon cancer is the development of distant metastases[16]. The rectum is located within the pelvis, a far less accessible region than the peritoneal cavity where the colon is located[18]. Although both rectal and colon surgeries are high-risk[19], the anatomical location of the rectum makes surgery more demanding, and poses increased risks of complications such as incontinence[20]. These features have led to the differences in management of colon and rectal cancers. While rectal cancer is treated with neo-adjuvant chemoradiation therapy (neo-CRT) to downstage tumours prior to resection[21], colon cancer patients instead generally receive adjuvant chemotherapy post-surgery[22].

Colon and rectal cancers also demonstrate different patterns of metastasis[23]. Aside from anatomical location, the blood supply and drainage differs within the colon and rectum[19]. While the right (proximal) colon is supplied by the superior mesenteric artery, the inferior mesenteric artery supplies the left (distal) colon and the rectum[18]. Drainage from the proximal colon is via the liver, while the distal colon and rectum venous drainage

bypasses the liver instead entering the lungs, leading to increased risk of pulmonary and bone metastases[19]. As the colon is located within the peritoneal cavity, metastasis to this region is more common[19]. In women, colon cancer presents an elevated risk of ovarian metastases, when compared to rectal cancer[23].

With regards to prognosis, there is no difference between early stage (I and II) colon and rectal cancers, however late stages (III and IV) rectal cancers demonstrate worse prognosis[24]. A seminal paper by Guinney *et al.* outlined four consensus molecular subtype (CMS) by which CRCs can be classified; CMS1 (immune), CMS2 (canonical), CMS3 (metabolic) and CMS4 (mesenchymal)[25]. When compared to right and left sided colon cancers, rectal cancers demonstrate a greater percentage of tumours classified as CMS4, the most aggressive and metastatic subtype, which tend to be advanced upon diagnosis[25].

1.1.3. Aetiology and risk factors for colon and rectal cancers

The differences in the incidence of colon and rectal cancers suggest that distinct risk factors separate tumours in these regions[8]. CRCs have a strong hereditary component. Two major familial forms of CRC exist; Lynch Syndrome or hereditary nonpolyposis colorectal cancer (HNPCC) and the rarer familial adenomatous polyposis (FAP), which give rise to tumours predominating in the right and left colon, respectively[18]. However, family history contributes less to rectal cancer than colon cancer[26].

Genomic instability is major contributor to tumourigenesis in the colorectum[27,28]. As outlined, different mutations of oncogene and tumour suppressor genes have been reported to predominate in colon and rectal cancers[16,17] There are three main pathways that dominate CRC tumours; microsatellite instability (MSI) which is characterised by deficient mismatch repair (MMR)[29], chromosomal instability (CIN)[30], which is associated with aneuploidy, defects in chromosomal segregation and oncogene mutations[31] and the epigenetically unstable CpG island methylator phenotype (CIMP)[32]. In rectal cancer, the majority of tumours develop as a result of the CIN pathway [21,30].

In terms of diet, total dietary fibre intake has an inverse relationship with the risk of developing both colon and rectal cancer[33]. However, different sources of fibre have been demonstrated to influence the risk of colon and rectal cancers to varying extents, with fibre from fruit and vegetables combined associated with a significantly lower risk of colon but not rectal cancer[33]. While the consumption of beef, lamb, pork and processed meat have been found to be associated with colon cancer, they are not associated with rectal cancer[26]

Reduced physical activity and increases in body weight are possible contributors to the increased incidence of rectal cancer in younger populations[34,35]. However, although exercise is demonstrated to reduce the risk of CRC, this association appears to have a greater preventative effect on the development of colon cancer, relative to rectal cancer[8,26] Given the large influence of lifestyle and dietary factors on the risk of developing CRC, disease prevention remains the major approach in tackling the global burden of CRC[1].

Another risk factor associated with rectal cancer is smoking. Smokers have a significantly greater risk of developing rectal cancer, when compared to never smokers. In never smokers, the incidence of rectal cancer is higher in men, however in smokers, there is a greater association between women and incidence of rectal cancer[36].

1.1.4. Screening, diagnosis and staging of colon and rectal cancers

CRC is among the few cancer types that are routinely screened by national programmes. Cancer screening programmes aim to detect pre-malignant conditions or early stage cancers and have been demonstrated to reduce cancer incidence and mortality[37]. In the United States, screening for CRC is recommended for ages 45-75, with further selective screening encouraged up to age 85[38]. At present in Ireland, those between the ages of 60 and 69 are for eligible for BowelScreen, the national CRC screening programme that occurs biennially[14]. Uptake of BowelScreen to date has been approximately 40%, with a greater uptake in females than males. The working goal is to extend the programme to everyone in the age range of 55-74[39]. Between 2018 and 2019, over 8000 adenomas/polyps and more than 900 sessile serrated lesions were removed as a result of screening in Ireland. A total of 304 cancers were detected, a rate of 1.4 per 1000 individuals screened[39]. Importantly, early-stage rectal cancers have been diagnosed more frequently since the introduction of BowelScreen, with 58% of tumours detected being stage I-II[40] . Initial screening for CRC involves detection of blood in stool samples, using a faecal immunochemical test (FIT) or a faecal occult blood test (FOBT) which are antibody and guaiac-based tests, respectively. It is estimated that 95% of people will require no further assessment, however the remaining 5% may require a colonoscopy[39].

In addition to screening, rectal cancer patients may also be identified following presentation in hospital with symptoms including changes in bowel habit, rectal bleeding and abdominal pain[41]. Diagnosis of rectal cancer in these patients and those with a positive faecal test, requires a digital rectal examination (DRE) and a colonoscopy to identify malignancy[21]. Rectal cancer is confirmed by histopathological examination of tumour

biopsy sample, taken at the time of colonoscopy[21]. Rectal cancer tumours are located ≤15 cm from the anal margin, while more proximal tumours are classified as colon cancer. Rectal cancers can further be defined as low, middle or high based on their location from this margin (up to 5cm, from 5-10 cm, from 10-15 cm, respectively)[21]. The classification of rectal cancers based on anatomical location is outlined in **Fig. 1-2**.

After determining tumour location and verifying malignancy from tissue biopsies, further clinical testing is required. A full blood count, functional tests of the liver and kidneys and assessment of serum carcinoembryonic antigen (CEA) should be performed[21]. Locoregional clinical staging of rectal tumours is performed using magnetic resonance imaging (MRI), which is the most accurate method to define clinical tumour stage (cT). For early stage tumours, the use of endoscopic rectal ultrasound (ERUS) together with MRI may be beneficial in deciding whether transanal endoscopic microsurgery (TEM) is a viable treatment option[42]. When disease is locally advanced, ERUS is of less value in defining treatment[42]. The presence of disease in regional lymph nodes, classified as clinical nodal stage (cN) is also assessed by MRI. To identify metastasis to the lungs, a thorax computed tomography (CT) scan is performed[43]. The abdomen and liver is also investigated using CT or magnetic resonance MRI[21]. In some instances, positron emission tomography (PET) may be useful to assess extensive disease spread that has occurred beyond the pelvis[44]. The Union for International Cancer Control (UICC) TNM staging classification (8th edition), defines the criteria for cT, cN and metastasis (M) stage. Details of this staging system are outlined in **Fig. 1-3.**

.

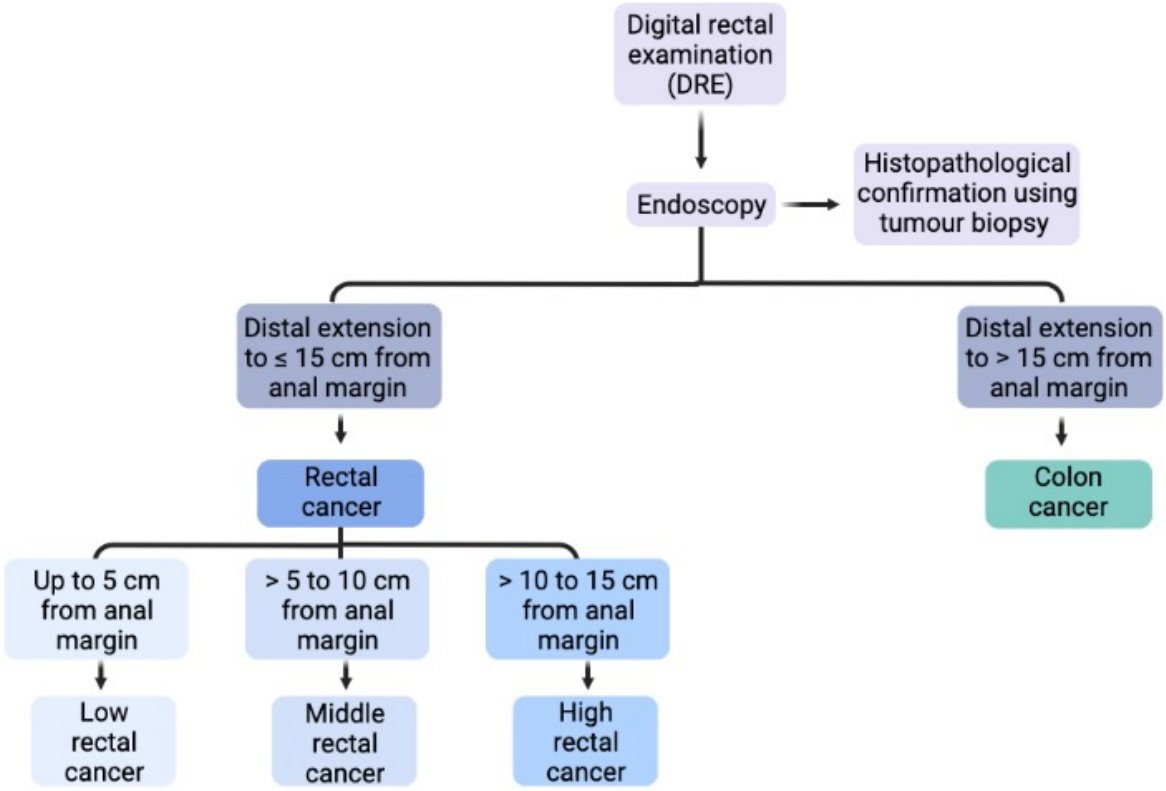

Figure 1-2: Anatomical classification of CRC into colon and rectal tumours. Colon and rectal tumours can be distinguished based on their proximity from the anal margin. Rectal tumours are defined as those less than or equal to 15 cm from the anal margin, and can further be sub-divided into low, middle or high cancers. Figure created with BioRender.com.

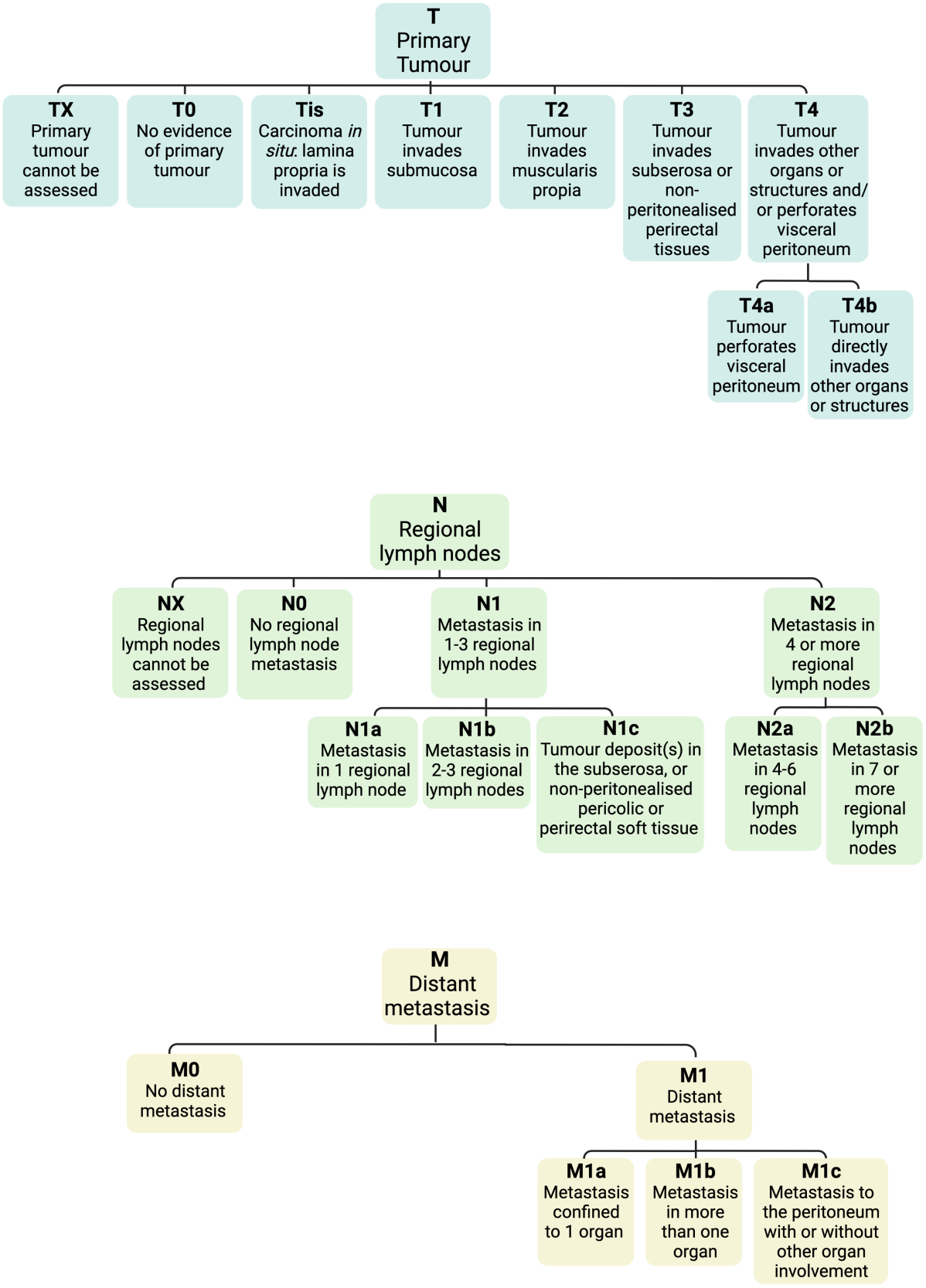

Figure 1-3: Overview of UICC TNM staging classification for rectal tumours. Rectal tumours are classified into stages based on the invasion of the primary tumour (T), the spread of cancer into lymph nodes (N) and the further dissemination of the cancer to give distant metastasis (M). Figure adapted from[21]. Figure created with BioRender.com.

1.2. Rectal cancer treatment

Treatment of rectal cancer patients is dependent on tumour stage. Very early stage tumours (T1), without nodal involvement, are most often suitable for TEM or another local excision procedure[45,46]. Early stage tumours (cT1-cT2 and node negative cT3a-cT3b middle and high rectal tumours) are advanced further than is suitable for TEM, and are at increased risk of recurrence and spread to mesorectal lymph nodes[46]. Therefore, radical total mesorectal excision is performed, a surgical approach that involves completely removing the rectum and excising all mesorectal fat, with the inclusion of the pararectal lymph nodes[47].

Intermediate tumours that are more locally advanced (cN1-N2, cT3a-cT3b low tumours) also are treated using total mesorectal excision[21]. The addition of preoperative radiation therapy (RT) either alone or in combination with chemotherapy to lower risk of local recurrence has been assessed in this setting, however use remains controversial[21]. Provided that a good plane of surgery is achieved when total mesorectal excision is performed, and lymph nodes are removed together, studies have demonstrated that risk of recurrence is low[48,49]

Locally advanced rectal cancers (LARC) are tumours beyond stage cT3b that are positive for extramural vascular invasion. To reduce the risk of local recurrence, LARC generally receive neo-CRT prior to total mesorectal excision[21]. There are two neo-adjuvant regimens for delivering RT. Short course RT (SCRT) consists of a total dose of 25 Gray (Gy), delivered in 5 fractions of 5 Gy, over a period of one week. Conventionally, surgery is performed within one week of completing SCRT, however, an alternative approach is to delay surgery for 4-8 weeks[50]. This is associated with fewer postoperative complications, and similar outcomes to immediate surgery[50]. Patients with LARC can also receive long course RT (LCRT), which is a total of 45-50 Gy delivered in 25-28 fractions. If the circumferential resection margin is at risk, a further boost of 5.4 Gy delivered in 3 fractions of 1.8.Gy may be administered[21]. For patients receiving neo-CRT, oral capecitabine and 5-fluorouracil (5-FU), delivered via continuous intravenous infusion rather than a bolus dose, are the recommended chemotherapy agents[21,51]

1.2.1. Response to neo-CRT

Response to neo-CRT is determined by histopathological assessment of resected surgical samples. In Ireland, the tumour regression score (TRS) is determined using the modified

Ryan tumour regression grading system[40]. This score is a 4-point grading system based on the recommendations outlined by the American Joint Committee of Cancer (**Table 1-1**)[52].

Table 1-1: Modified Ryan tumour regression grading system.

TRS	Response	Description
0	Complete	No viable tumour cells
1	Near-complete	Single or rare small groups of cancer cells
2	Partial	Residual cancer greater than single or small groups of cancer cells, with evident tumour regression
3	Poor or no	Residual cancer is extensive, no evident tumour regression

Abbreviations; TRS, tumour regression score.

A pathological complete response (pCR) to neo-CRT is associated with improved five-year survival, greater local control, increased metastasis-free survival and better overall survival (OS)[53]. However, unfortunately response rates to neo-CRT are modest with less than 30% of rectal cancer patients demonstrating a pCR[54–56]. This means that a majority of patients are subject to treatment-associated toxicities with no apparent therapeutic benefit and worse disease outcomes due to delay to surgery and disease progression[57].

A growing area of interest is whether surgery can be avoided in those patients who had a pCR following neo-CRT[58]. Until recently, response to therapy was only determined pathologically, post-surgery. More recently, evidence suggests that stringent clinical examination following neo-CRT may reliably identify patients with a complete clinical response (cCR)[58]. In this instance, there is an inability to detect residual tumour when patients are endoscopically or radiologically assessed[53]. For these patients, a wait-and-see approach as an alternative to immediate total mesorectal excision after neo-CRT has been proposed. Total mesorectal excision is associated with impairments in bowel, urinary and sexual function[59,60]. In addition to minimising these side-effects, motivation for a wait-and-see policy includes the avoidance of patient overtreatment[58]. While a wait-and-see policy has been debated in the literature, several large studies have demonstrated that in patients identified using strict selection criteria, it may be a safe management option, providing adequate follow-up takes place[53,61]. Similar recurrence rates and outcomes have been reported in wait-and-see and surgically resected patient cohorts[61–63]. In Ireland, a wait-and-

see approach has not been adopted for those demonstrating a cCR, however, National Clinical Guidelines recommend that it is discussed as an option with the patient, and may be a potential option following shared decision making[40].

1.2.2. Predictive markers of response to neo-CRT

Several studies have attempted to identify predictive biomarkers of response to neo-CRT in rectal tumours[54]. Clinical factors including tumour size, node positivity at diagnosis and the distance of the tumour from the anal verge have all been demonstrated to predict response to neo-CRT in rectal cancer[64]. Additionally, the length of the interval between neo-CRT and surgery has demonstrated predictive ability[64,65]. Some pathological features have also been noted as markers of response to neo-CRT, however, in general these clinicopathological features lack the necessary sensitivity and specificity required to be utilised as a clinical tool[66].

Molecular biomarkers in blood have been explored in several studies for their ability to identify responders to neo-CRT prior to the initiation of treatment[66]. CEA has been extensively studied in rectal cancer, and CEA levels at diagnosis have been demonstrated to predict response to neo-CRT[64,65] (and reviewed in[66]). Similarly, the expression of numerous tissue biomarkers has been demonstrated to discriminate between responders and non-responders to neo-CRT in rectal tumours[66]. Among these are p53, epidermal growth factor receptor (EGFR), vascular endothelial growth factor (VEGF), p21, B-cell lymphoma 2 (Bcl2), and BCL2-associated X protein (Bax)[66]. Gene expression profiling has demonstrated potential for determining the response to neo-RT in rectal cancer[66]. Using a novel 33 gene signature, Watanabe and colleagues discriminated responders from non-responders with an accuracy of 82.4%[67]. Within the signature there was an enrichment of genes associated with categories such as cell growth and signal transduction[67]. Subsequent studies have since demonstrated that differential gene expression may have potential to discriminate between responders and non-responders to neo-CRT in rectal cancer[68–70]. Despite this, no biomarkers are routinely used in the clinic to predict response to neo-CRT and aid in treatment decision making.

1.2.3. 5-FU

5-FU is a widely used chemotherapeutic agent, which has been used for over 40 y in the treatment of CRC, where it demonstrates the greatest anti-cancer effects[71]. An analogue of uracil, 5-FU has the advantage of transporting intracellularly using the same

system[72]. Once within the cell, 5-FU is converted to three active metabolites; fluorodeoxyuridine monophosphate (FdUMP), fluorodeoxyuridine triphosphate (FdUTP) and fluorouridine triphosphate (FUTP)[71]. FdUMP forms a ternary complex with 5,10-methylenetetrahydrafolate and thymidylate synthase (TS), a nucleotide synthetic enzyme. This blocks the nucleotide binding site of TS, preventing catalysis of deoxyuridine monophosphate (dUMP) to deoxythymidine monophosphate (dTMP)[73,74]. Inhibition of TS leads to imbalances in the pool of deoxynucleotides (dNTPs) and increased levels of deoxyuridine triphosphate (dUTP). Imbalances in the pool of dNTPs induce lethal DNA damage, which is understood to occur due to disruptions in DNA synthesis and repair[75,76]. Both dUTP and the 5-FU metabolite FdUTP can induce DNA damage by becoming mis-incorporated in DNA, inducing damage. RNA is also damaged by 5-FU. Incorporation of the 5-FU metabolite FUTP into RNA interferes with RNA processing and function, which can have toxic effects[71].

Capecitabine is an oral 5-FU pro-drug that is absorbed through the gastrointestinal (GI) tract. In the liver, capecitabine is sequentially converted to 5'-deoxy-5-fluorouridine (5'DFUR) by carboxylesterase and cytidine deaminase. Thymidine phosphorylase and/or uridine phosphorylase then convert 5'DFUR to 5-FU[77,78]. Importantly, capecitabine has demonstrated more favourable toxicity profiles in clinical trials, when compared to 5-FU[71].

1.2.4. RT

RT is a major cancer treatment modality, received by over 50% of cancer patients[79]. Approximately 40% of patients who are cured of their cancer will have received RT[80]. The number of patients requiring RT is estimated to rise by 16% by the year 2023, given the current projections for new cancer cases[81]. RT involves delivering ionising radiation (IR) in the form of X-rays or γ-rays[79]. Radiation is measured in units of Gy where 1 Gy is equivalent to 1 joule of absorbed energy per kg of tissue[82]. RT aims to induce tumour cell death by directly and indirectly damaging DNA. To maximise tumour kill while avoiding excessive damage to the surrounding normal tissue and adjacent organs, the total dose of radiation is administered in smaller doses, which are defined as fractions. A linear, quadratic formula is used in determining fractionation regimens, to ensure the time-dose factors for specific tumour types and normal tissues are taken into account[79,83]. The administration of RT in fractions aims to exploit the often inferior ability of cancer cells to repair sublethal DNA damage relative to normal cells, which proliferate slower, allowing

them more time to repair damaged DNA[83]. In the treatment of rectal cancer using LCRT, RT is delivered using 3-4 fields to the pelvis to ensure the tumour and a 2-5 cm margin, the presacral nodes and the internal iliac nodes are included[84]. SCRT may also include regions including the anal canal and lower lumbar lymph nodes[84]. RT is associated with both acute and long term side effects. Rectal cancer patients receiving either LCRT or SCRT often experience mild acute side effects including erythema, nausea and vomiting, which usually resolve in the weeks following treatment[85,86]. Furthermore, both regimens are associated with later side effects such as fecal or urine incontinence and poorer quality of life[86–88].

In 1975, Withers described the main factors that influence the cytotoxic outcome of fractionated RT and coined the 4 R's of radiobiology; repair of DNA damage, repopulation of tumour cells, reoxygenation of hypoxic areas and redistribution in the cell cycle[89]. Repair describes how fractionation exploits the differences in DNA repair ability in normal and cancer cells. While normal tissue can repair sublethal DNA damage induced by RT between fractions, cancer cells are often deficient in mechanisms of DNA repair, leading to the accumulation of sublethal damage and subsequent cell death[90]. Repopulation describes how tumours proliferate between fractions. This often proceeds at an increased rate during prolonged courses of RT[91]. Reoxygenation refers to the essential role of oxygen in the response to RT. Under conditions of low oxygen; hypoxia, tumour cells are three times less sensitive to RT, therefore leading to poor patient outcomes[92–94]. Redistribution considers that fact that cells display differing sensitivities to radiation when in different stages of the cell cycle; cells in gap (G) 2 and mitosis (M) phases are most sensitive, cells in G0 are more resistant, while cells in synthesis (S) phase are most resistant[95–97]. Therefore, fractionated doses of RT allow for redistribution of cells throughout the cell cycle. The impact of cancer stem cells on these 4 principles likely aids tumour escape of RT[89]. While these 4 R's are key influencers of response to RT, additional factors contribute to whether tumour control is achieved. In consideration of this, it has since been suggested that inherent radiosensitivity should be considered the 5th R of radiobiology[98]. Inherent radiosensitivity accounts for the different sensitivity between individual and cancer type specific tumours.

Although induction of direct and indirect DNA damage is the primary cause of cancer cell death, radiation can modulate anti-tumour responses and tumour cell recognition[99]. Studies have demonstrated that IR modifies the tumour microenvironment (TME) and can alter priming and recruitment of effector T cells[99–101]. Tumour regression that occurs outside of the field of irradiation, is known as the abscopal effect, and has also been linked to the indirect stimulation of anti-tumour immune responses by RT. Efforts to improve

tumour kill have demonstrated the addition of immunotherapy to RT regimens may enhance the abscopal effect[102,103]. Taking into account these essential roles for the immune system in response to RT, more recently a 6th R; reactivation of the immune response has been proposed[104] (**Fig. 1-4**).

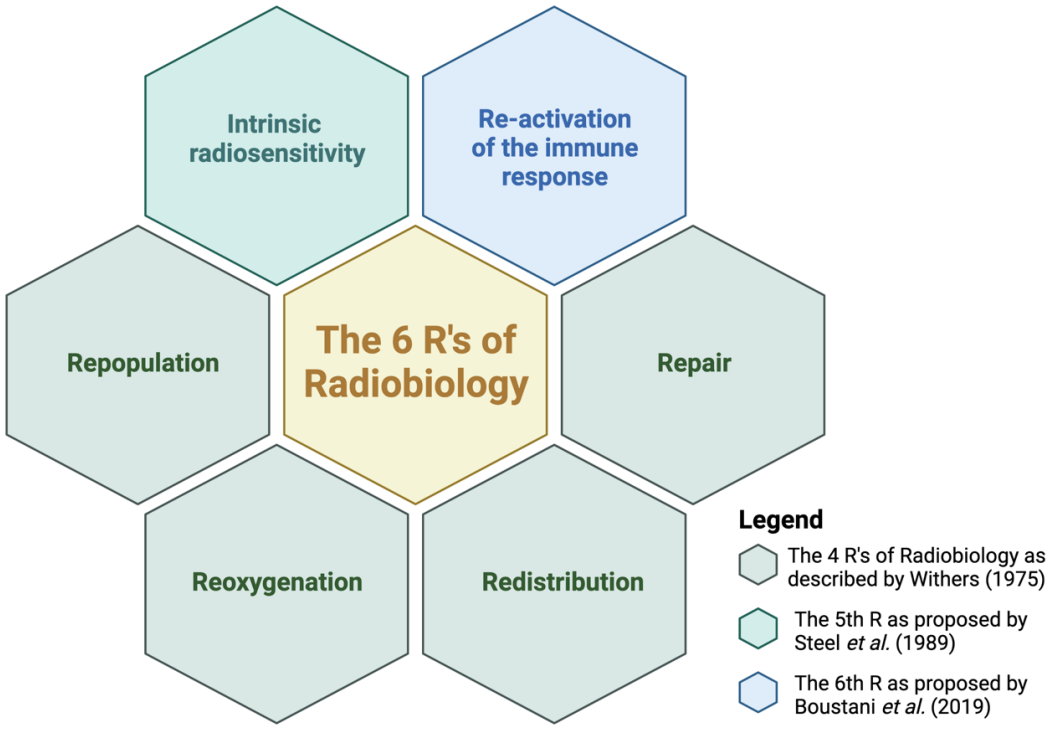

Figure 1-4: The 6 R's of Radiobiology. Repopulation, repair, reoxygenation and redistribution were described as the 4 R's of Radiobiology. Since then, intrinsic radiosensitivity and reactivation of the immune response have been proposed as the 5th and 6th R's of Radiobiology, respectively. Figure adapted from[104]. Figure created with BioRender.com.

1.2.4.1. Radiation-induced DNA damage

Cellular DNA is the critical target of RT[105]. IR induces significant DNA damage, mostly in the form of single-stranded breaks (SSBs) and double-stranded breaks (DSBs), the latter of which is considered the most lethal event[106]. Several other kinds of DNA lesions also result, including altered or mismatched bases, the formation of adducts and DNA cross-links[107]. A 1 Gy dose of IR induces approximately 1000 SSBs, 40 DSBs and 150 DNA-protein cross links, results in damage to 700 thymine bases and causes hydroxylation of 700 adenine bases[108].

IR-induced DNA damage occurs by direct and indirect mechanisms[79]. Direct DNA damage occurs due to direct energy deposition within the DNA molecule[108]. Indirect

damage to DNA occurs as a result of reactive oxygen species (ROS) formed when IR reacts with water in the cell. These ROS include superoxide, hydrogen peroxide and hydroxyl peroxyl and alkyl radicals[109] and contain one unpaired electron, making them highly unstable and therefore reactive with DNA[110]. Indirect damage to DNA accounts for approximately 70% of all radiation-induced DNA damage[111]. IR also affects the plasma membrane, altering membrane structure and organisation and stimulating signalling events which induce apoptosis or modulate cellular morphology[112]. In particular, IR-induced hydrolysis of sphingomyelin produces ceramide, which can trigger apoptosis[113].

Irreparable DNA damage induced by radiation causes tumour cell death via apoptosis and mitotic catastrophe, or leads to cell cycle arrest and senescence[114]. Regardless of whether repair or cell death is the outcome of radiation-induced DNA damage, the generation of DNA damage within the cell initiates a range of response mechanisms.

1.2.4.2. The DNA damage response

The DNA damage response (DDR) represents the intracellular mechanisms, which have evolved to detect, signal the presence of and repair DNA damage induced daily by endogenous and environmental agents[115]. There are an estimated 450 essential proteins involved in the DDR[116]. These are organised into sensors, which recognise damaged DNA, transducers, which amplify the signal and effector molecules, which are responsible for ultimately inducing a cellular response[117]. This response ranges from repair of damaged DNA or chromatin remodelling, to the induction of apoptosis or cell cycle arrest[115].

Activation of the DDR initiates a cascade of protein kinases. The most upstream of these are transducers from the phosphatidylinositol-3-kinase-related kinase (PIKK) family; DNA-dependent protein kinase catalytic subunit (DNA PKcs), ATM and ataxia telangiectasia mutated-rad3-related (ATR)[118]. ATM is generally considered the master regulator in response to DSBs[119], however, DNA PKcs function is also important in repairing DSBs, by non-homologous end-joining (NHEJ)[119]. ATR is activated by a wider range of lesions in proliferating cells and plays essential roles in DNA replication stress responses[120]. Together, these kinases are responsible for a range of essential phosphorylation events that drive the DDR signalling response[120].

Neoplastic transformation is associated with an accumulation of genomic instability, often rendering cancer cells defective in one or more DDR pathway[115,121]. This results in DDR dependencies that can be exploited by cytotoxic therapies that induce lethal DNA damage, such as DSBs, which are difficult to resolve[106,115]. However, cancer cells often

display alterations in DDR activity/genes, providing them with an enhanced ability to repair DNA damage and promoting radioresistance[122–124].

1.2.5. Mechanisms of resistance to treatment in rectal cancer

1.2.5.3. DNA repair

Several molecular parameters have been implicated in tumour resistance to RT, including alterations in DNA repair[122–124]. DNA repair occurs by five major pathways[125]. The mechanism by which DNA is repaired is dependent on both the type of DNA lesion and the phase of the cell cycle the cell is in[126].

DSBs are the most lethal DNA lesion induced by IR. Two mechanisms of DNA repair predominate for the resolution of DSBs; NHEJ and homologous recombination (HR). HR is largely restricted to the later S and G2 cell cycle phases[127]. Alterations in HR activity and mediators have been linked with response to radiation. The Mre11-Rad50-Nbs1 (MRN) complex is essential in the initiation of HR[128]. Elevated expression of RAD50, in pre-treatment rectal tumour biopsies has been demonstrated to associate with subsequently poor patient responses to neo-CRT[129]. Overexpression of the MRN complex is associated with worse DFS and OS following neo-CRT in rectal cancer[130]. The majority of DSBs are resolved by NHEJ which predominates in the G1 and early S phases of the cell cycle[127]. In rectal cancer, enhanced NHEJ[131] and cytoplasmic versus nuclear expression of essential NHEJ machinery[132] has also been linked with radioresistance. These data indicate that enhanced expression of DSB repair machinery is associated with poor responses to neo-CRT, suggesting alterations in DNA repair are a major mechanism of resistance to RT in rectal cancer.

1.2.5.4. The cell cycle and radioresistance

Alterations in cell cycle distribution and progression are also recognised as contributors to radioresistance. Four phases; G1, S, G2 and M compose the cell cycle, together with the G0 phase, which is outside the cell cycle[107]. Sensitivity to radiation is altered depending on phase of the cell cycle (**Fig. 1-5**), with cells in the G2 and M phases being most sensitive to radiation, cells in G0 being more resistant, while cells in S phase are most resistant[95–97]. Progression through the cell cycle is governed by various cell cycle checkpoints, which are activated during the DDR to halt progression to the next phase[107]. Activation of cell cycle checkpoints allows for repair of damaged DNA[126]. IR induces arrest in the G1, S and G2 phases of the cell cycle[133].

Radioresistance in rectal cancer related to cell cycle alterations often involves p53 and p21[134]. Rectal tumours positive for p53 both prior to[135] and following[136] IR are radioresistant, while p53 negative tumours demonstrate radiosensitivity[136–138]. In addition, tumour expression of p21 has been highlighted as a marker of radiosensitivity in rectal cancer[139]. Cell cycle checkpoint targeting drugs have been proposed as a viable method to enhance response to therapy including RT[140].

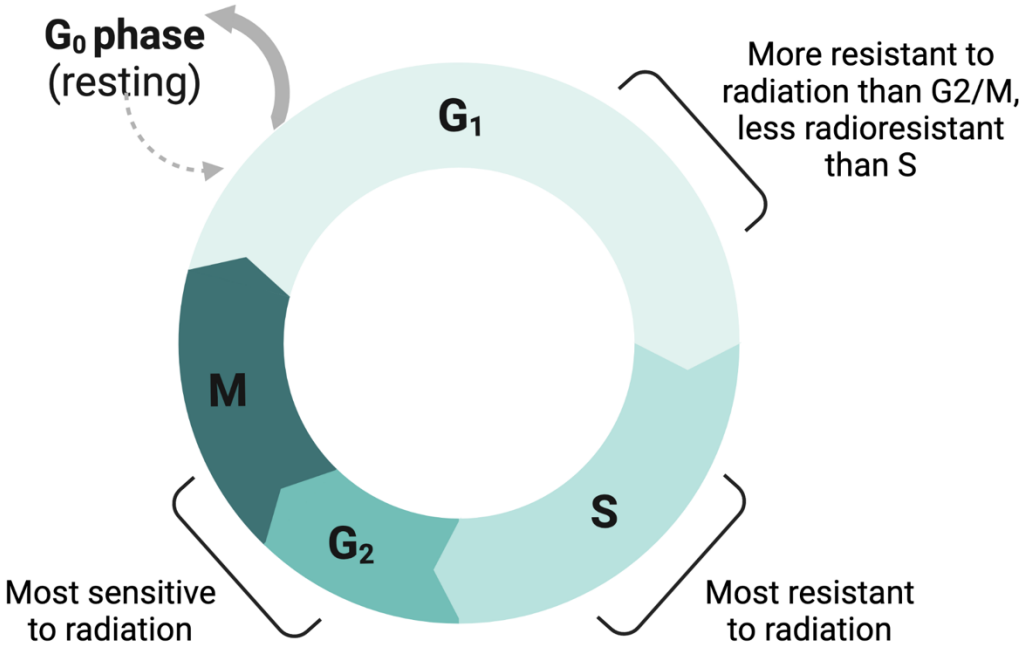

Figure 1-5: Cell cycle phases and sensitivity to radiation. The four cell cycle phases gap (G) 1, synthesis (S), G2 and mitosis (M), and also the G0 phase which is outside the cell cycle are shown. The G2/M phases are the most sensitive to radiation, G1 is more sensitive, while S is the most sensitive to radiation. Figure created with BioRender.com.

1.2.5.5. Apoptosis and radioresistance

If DNA damage cannot be repaired, cell death will occur[115]. This can occur as a result of mitotic catastrophe[114], when micronucleated interphase cells result from a combination of IR-induced DNA damage and defective cell cycle checkpoints[141,142]. Apoptosis may also be induced, which is a p53-dependent process[114].

The contribution of apoptosis to radiation-induced cell death is controversial and thought to play a modest role at least in the elimination of solid tumours[114]. However, in several cancer types including lung, breast and neuroblastoma, reduced apoptosis has been associated with radioresistance[143–145]. A study by Rödel *et al.* demonstrated that pre-treatment apoptosis was elevated in rectal tumours with good responses to neo-CRT, and therefore the pre-treatment apoptotic index, which relates the percentage of apoptotic cells within a tumour to the total number of tumour cells, was predictive of subsequent pCR[146]. Investigations by Scott *et al.* and Adell *et al.*[147,148] have similarly observed how increased pre-treatment tumour cell apoptosis is associated with reduced local recurrence[147,148].

1.2.6. The TME and radioresistance

Beyond cancer cells themselves, the TME is also implicated in radioresistance[149]. The TME refers to the biological interactions that take place between the tumour and its surrounding stroma, and includes the local vasculature and infiltrating immune cells[150]. The tumour not only shapes but dominates the TME, influencing a variety of molecular and cellular processes, altering immune cell infiltration and promoting hypoxia[150].

Hypoxia refers to oxygen deprived (< 2% O_2)[151] tumour regions, which arise due to the disorganised tumour vasculature and rapid proliferation of neoplastic cells[152]. Hypoxia-inducible transcription factor (HIF) signalling contributes to both the initiation and progression of tumour growth[151]. Tumour hypoxia is a major challenge to RT[109,153,154]. Hypoxic cancer cells are three times less sensitive to killing by radiation, when compared to oxygenated cancer cells, and as a result hypoxia is associated with poor patient prognosis and treatment outcomes[92–94]. Areas of hypoxia are present in rectal tumours[155,156]. Makers of hypoxia such as HIF-1α associate with DFS and OS in LARC[157,158] and in pre-treatment rectal tumour biopsies, HIF-1 expression is significantly elevated in patients with subsequently poor responses to neo-CRT[159]. This suggests that tumour hypoxia may at least in part contribute to radioresistance in rectal cancer.

Stromal cells recruited to the TME including immune cells, cancer-associated fibroblasts (CAFs) and angiogenic vascular cells contribute to the majority of the hallmarks of cancer and can promote resistance to therapy[160]. RT is an immunogenic process, initiating both innate and adaptive immune responses [99,114]. In rectal cancer, a subset of patients with immune 'hot' (immune infiltrated) tumours have previously been demonstrated to have good responses to neo-CRT and greater DFS, when compared to

those with poorly infiltrated, immune 'cold' tumours[161]. More recently, components of the complement system have been implicated in tumourigenesis and the response to cancer therapy[162]. This demonstrates that the immune TME is extensively involved in the response to treatment, and that immune cells themselves are not alone in promoting resistance to cancer treatment[162].

1.3. The complement system

1.3.1. Introduction to the complement system

The complement system is an essential arm of the innate immune system, which also functions to enhance adaptive immunity[163]. Early discovery of the complement system involved several key immunologists including Buchner, Bordet and Ehrlich[164]. In 1901, complement was described by Jules Bordet as a heat-labile factor present in serum, that augmented antibody-mediated bacterial lysis[165]. Although initially regarded as a single entity, a large body of research within the 20th century redefined complement as a family of many proteins[166]. Ferrata and Brand were the first to demonstrate that complement is separated into various components; describing 'midpiece' and 'endpiece' complement fractions, which are now known as complement (C)1 and C2, respectively[166–168].

1.3.2. Components of the complement system

Complement components are primarily produced by the liver before systemic dissemination via the bloodstream[169]. However, not all complement is hepatic in origin, with the majority of cell types capable of producing complement components locally[170]. T cells[171,172], macrophages[173], endothelial cells[174], CAFs[175] and tumour cells[176] have all been demonstrated to produce complement. This locally produced complement engages in context-dependent, often non-canonical roles[177].

The complement system is composed of approximately 50 soluble and membrane-bound complement effectors, regulators and receptors, with the main complement proteins numbered C1-C9[163]. Several complement components exist as zymogens, which require cleavage in order to gain functionality[178]. Cleavage of these components takes place following complement system activation, and is the responsibility of complement convertases, which are sequentially activated as part of an enzymatic cascade. Two enzymes, the C3 and C5 convertases are central to the complement cascade, cleaving C3 and C5 respectively to generate anaphylatoxins (C3a, C5a) and opsonins (C3b, C5b)[163,179]. Anaphylatoxins are small, potent, inflammatory mediators with many effector

functions[178,180]. Their activity is regulated by carboxypeptidases, which cleave the C3a and C5a C-terminal arginines to generate C3a desArg and C5a desArg, respectively[181,182]. C3a desArg has little functional ability[183], however, C5a desArg has been demonstrated to retain some activity[184,185]. C3a signals through the C3a receptor (C3aR)/CD88. while C5a can interact with both the C5a receptor (C5aR)1 and C5aR2, all of which are 7 trans-membrane receptors[186]. C3aR and C5aR1 are G-protein coupled receptors, however, in contrast, C5aR2 recruits β-arrestin[187–189]. The function of C5aR2 is less defined, when compared to C5aR1, however, it is generally considered to act as a negative modulator of C5aR1 signalling[190,191].

1.3.3. Systemic activation of complement

Systemic activation of complement can occur by three pathways; the classical, the lectin and the alternative pathways[186] (**Fig. 1-6**). The pathway of activation that takes place is dependent on the pathogen or foreign body initiating the cascade.

C1q, a component of the C1 complex is the pattern recognition molecule of the classical pathway (CP). The C1 complex is composed of C1q together with two copies of the C1r and C1s proteases[192]. The major initiating factors of CP are antigen-antibody (immunoglobulin (Ig) G or IgM containing) immune complexes. Activation of the CP can also be initiated via interaction of C1q with antibody-independent ligands such as c-reactive protein or viral proteins[193–199]. Conformational changes induced following interaction of C1q with its target antigen leads to activation of C1r, which subsequently activates C1s[192]. C1s can then cleave C4 and C2 to yield the C4a anaphylatoxin, the C2b opsonin and C2a and C4b, which assemble to form C4bC2a, the C3 convertase[186].

Viral and bacterial carbohydrate-based pathogen-associated molecular patterns (PAMPs) activate the lectin pathway (LP) by binding to mannose-binding lectin (MBL), ficolins or collectins[186,200–202]. MBL and ficolins circulate in association with MBL-associated serine proteases (MASPs). Similarly to C1s, target binding of MBL allows for MASP-mediated cleavage of C2 and C4, allowing for assembly of the C3 convertase[192].

Unlike the classical and lectin pathways, the alternative pathway does not contain a specific recognition molecule to identify foreign antigens. Instead, in a process known as ‘tick-over’, C3 is spontaneously hydrolysed to $C3H_2O$[203,204]. This functions as a constant surveillance mechanism for pathogens in healthy individuals[186], and can act as an activation loop for the CP and LP[179,205]. The AP may be amplified by bacterial and yeast

polysaccharides and damaged tissue[206,207]. An initial C3 convertase complex is formed when tick-over occurs in the presence of Factor B (FB) and Factor D (FD)[179]. $C3H_2O$ is bound by FB, which is then cleaved by FD to produce $C3H_2OBb$. C3 cleavage by $C3H_2OBb$ and FB by FD leads to assembly of C3bBb, the final AP C3 convertase[179].

All three activation pathways converge at a central point of the C3 convertase, from which is often referred to as the terminal pathway (TP). Cleavage of C3 yields the C3a anaphylatoxin and C3b, which joins the C3 convertase to form the C5 convertase (C4bC2aC3b in the CP and AP, and C3bBbC3b in the LP). The TP culminates with C5 cleavage and the assembly of C5b-9 to form a membrane attack complex (MAC), otherwise known as the terminal complement complex (TCC)[208,209]. MAC insertion into target cell membranes can trigger lysis known as complement-dependent cytotoxicity (CDC)[210], or at sub-lytic doses may activate signalling pathways to promote cell survival[211,212].

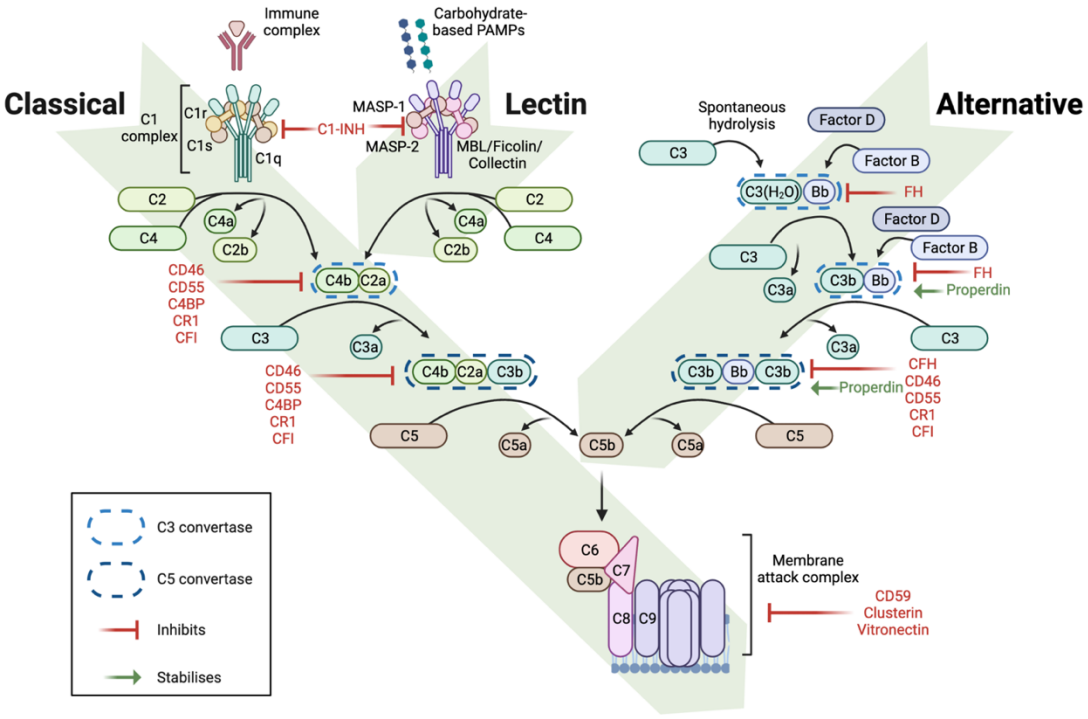

Figure 1-6: Complement activation pathways. There are three routes by which the complement system can become activated: the classical, the lectin and the alternative pathways. Classical pathway activation is initiated primarily by antigen-antibody immune complexes. C1q of the C1 complex (C1q, C1r and C1s) interacts with the fragment crystallisation (Fc) portion of antigen-bound immunoglobulins, activating C1r, which subsequently cleaves and activates C1s. Activated C1s cleaves C4 into C4a and C4b, and C2 into C2a and C2b leading to assembly of C4bC2a, the C3 convertase. Carbohydrate-based pathogen-associated molecular patterns (PAMPs) trigger activation of the lectin pathway. Mannose-binding lectin (MBL), ficolins or collectins recognise PAMPs, activating MBL-associated serine proteases (MASPs). Similar to the classical pathway, C4 and C2 are cleaved to generate C4bC2a. The classical and lectin complement activation pathways converge at this point to cleave C3 into the potent anaphylatoxin C3a, and C3b, which joins the C3 convertase to form C4bC2aC3b, the C5 convertase. Cleavage of C5 yields the C5a anaphylatoxin and C5b, which polymerises with C6, C7, C8 and C9 to form the membrane-attack complex (MAC). This inserts into target cell membranes to induce lysis. Spontaneous hydrolysis of C3 into $C3H_2O$ occurs in the alternative pathway. Cleavage of factor B (FB) by factor D yields Bb, which associates with $C3H_2O$ to form a C3 convertase. Cleavage of C3 and FB produces C3b and Bb, respectively. The binding of properdin to microbial surfaces recruits C3b, facilitating the assembly of the C3 convertase (C3bBb), and initiating pathway activation. Subsequent cleavage of C3 produces C3b, which combines with the C3 convertase to form a C5 convertase (C3bBbC3b). From this point, the terminal pathway is initiated to assemble the MAC, similarly to the classical and lectin pathways. Complement activation is regulated at various stages of the pathways by several membrane-bound complement regulatory proteins (Complement receptor 1 (CR1), CD46, CD55 and CD59) and circulating factors (C1- inhibitor (C1-INH), complement factor H (CFH), complement factor I (CFI), C4-binding protein (C4BP), clusterin and vitronectin), which are depicted in red, and properdin, in green, which stabilises the alternative pathway C3 convertase. Figure adapted from *O'Brien et al. 2020*[162]. Figure created with BioRender.com.

1.3.4. Regulation of complement activation

Activation of the complement system and subsequent amplification of this response induces a powerful inflammatory response. Within the complement system, there are numerous soluble and membrane-bound effector molecules, which modulate the pathway at various critical stages in order to minimise damage to host cells. These include the widely expressed membrane-bound complement regulatory proteins (mCRPs), (**Table 1-2**) and the fluid phase proteins, C1 inhibitor (C1-inh), C4b-binding protein (C4BP), complement factor H (CFH) and complement factor I (CFI) (**Table 1-3**), which negatively regulate complement activation [186,213,214]. Properdin positively regulates the AP via stabilisation of the C3 convertase[215,216]

Table 1-2: Membrane-bound complement regulatory proteins.

mCRP	Alternative Name (s)	Distribution	Function
CD35	Complement receptor 1 (CR1)	Lymphocytes, erythrocytes, phagocytes & dendritic cells primarily	Cofactor for C3b & C4b degradation by Factor H[217–221] Accelerates decay of C3 and C5 convertases
CD46	Membrane cofactor protein (MCP)	All nucleated cells	Cofactor for C3b and C4b degradation by Factor H[222–224]
CD55	Decay accelerating factor (DAF)	Ubiquitously expressed	Accelerates decay of C3 and C5 convertases[225–227]
CD59	Membrane-inhibitor of reactive lysis (MIRL), MAC inhibitory protein (MAC-IP), Protectin,	Ubiquitously expressed	Binds C5b-9 to prevent polymerization of C9[228,229]

Abbreviations; mCRP, membrane-bound complement regulatory protein
Table adapted from *O'Brien et al. 2020*[162].

Table 1-3: Fluid phase complement regulatory proteins.

Regulator	Pathway regulated	Function
C1 inhibitor (C1-inh)	CP & LP	Inactivation of C1r and C1s/ MASP-1 and MASP-2[230]
Complement Factor I (CFI)	CP, LP & AP	Degradation of C3b and C4b in the presence of a cofactor [231]
Complement Factor H (CFH)	AP	Accelerates decay of C3bBb. Acts as a cofactor for FI[232]
Factor H- like 1 (FHL-1)	AP	Accelerates decay of C3bBb. Acts as a cofactor for FI[233,234]
C4-binding protein (C4BP)	CP/LP	Accelerates decay of C4b-containing convertases. Cofactor for FI[235–237]
Clusterin	TP	Binds to C5b-9 preventing assembly[238]
Vitronectin	TP	Prevents assembly of C5b-9 via binding to C7-C9[239]

Abbreviations; CP, classical pathway; AP, alternative pathway; LP, lectin pathway.
Table adapted from[163].

1.3.5. Complement functions in innate immunity

The complement system plays several key innate immune functions[240]. Constant low-level complement activation that occurs in the tick-over loop of the AP pathway acts as constant surveillance mechanism for microbial challenge to healthy cells[241]. The central event resulting from activation of the complement system is MAC-induced lysis of target cells, however, complement anaphylatoxins and opsonins play essential roles in host defence via recruitment of phagocytic cells and promotion of phagocytosis, respectively[178]. C3a and C5a have been demonstrated to induce chemotaxis of mast cells[242,243] and eosinophils[244], with C5a additionally acting as a chemoattractant for macrophages[245], monocytes[246] neutrophils[246,247], basophils[248], and T and B lymphocytes[249,250]. Complement

opsonins including C3b and its degradation products iC3b and C3d aid phagocytosis by coating target cells and subsequently facilitating the engagement of phagocytes via complement receptor (CR) 1, CR3, CR4 and CR1g[163,251]. Furthermore, the phagocytic response to immune complexes may be enhanced by C5a-mediated upregulation of activating fragment crystallisation (Fc) γ receptors (FcγR) on the surface of phagocytes[180,252]. Complement is also intrinsically linked with toll-like receptors (TLRs), and has been demonstrated to cooperate with several TLRs including TLR2, TLR4 and TLR9 to promote inflammation[253].

1.3.6. Complement functions in adaptive immunity

1.3.6.6. Systemic complement

Complement cascade components also play key roles in orchestrating adaptive immunity. The complement receptors CR1 (CD35) and CR2 (CD21) are essential in the generation of B cell and follicular dendritic cell (DC) responses[254]. B cell responses are enhanced via CR2, which binds iC3b, C3dg and C3d[255]. In addition to an antigen receptor, B cells express a co-receptor complex composed of CR2, CD19 and CD81[256]. Binding of C3d-opsonised antigen results in co-engagement of the B cell receptor and this coreceptor by antigen and opsonin, respectively. This leads to enhanced signalling through the B cell receptor and subsequent lowering of the threshold for activation[257,258]. Additionally, CR1 and CR2 play important roles in the humoral response within lymphoid tissues, where they localise antigens to follicular DCs[254].

1.3.6.7. Locally produced complement

Complement components also play essential roles in T cell responses, however, this complement is produced locally. Firstly, complement is important during the stimulation of naïve T cells. Following cognate interactions between antigen-presenting cells (APCs) and T cells, complement components are produced and activated locally[171,259,260]. Both APCs and T cells express the AP components FB, FD and also C3, C5, C3aR and C5aR1[171]. Additionally, local activation of C3 and C5 generates C3a and C5a, respectively. Early studies observed that T cells stimulated with APCs deficient in DAF/CD55, which dissociates C3 and C5 convertases, demonstrated reduced proliferation and differentiation into effector cells[259,260] Subsequent investigations revealed that signalling via C3aR and C5aR1 enhances the expression of costimulatory molecules by both APCs and T cells[171].

Following these discoveries, complement was recognised as an important regulator of T cell homeostasis. Signalling via C3a/C3aR and C5a/C5aR1 axes enhances T cell proliferation through activation of PI3K-γ and subsequent phosphorylation of AKT[171]. Complement promotes the viability of T cells by limiting the induction of apoptosis[172]. Locally produced C5a engages C5aR1 expressed on the surface of T cells to upregulate Bcl-2, limiting Fas expression and preventing apoptosis[172]. In addition, several key studies identified that complement promotes the induction of a T helper (Th) 1 phenotype. Alongside upregulation of costimulatory molecules, C3a and C5a signals have been demonstrated to promote expression of innate cytokines including IL-12, which foster differentiation into an IFN-γ producing phenotype[171,260]. Importantly, complement also aids in the contraction of T cell responses. Engagement of $CD4^+$ T cell expressed CD46 by C3b, promotes Th1 induction, however, as a result of IL-2 accumulation, a switch occurs whereby IL-10 is expressed, switching cells instead to a regulatory phenotype and initiating a contraction phase[261].

1.3.6.8. Intracellular complement – the 'complosome'

Shortly after the importance of locally-produced complement in the immune response was recognised, complement was discovered intracellularly, providing greater functional insights into complement-mediated regulation of T cell responses[262]. This intracellular complement pool was coined the 'complosome'[169].

Liszewski *et al.* were the first to demonstrate that resting $CD4^+$ T cells contained intracellular stores of C3. They demonstrated that intracellular C3 is cleaved by cathepsin L (CTSL), resulting in intracellular stores of C3a and C3b[263]. This intracellular C3a engages lysosomal expressed C3aR, inducing homeostatic mTOR signals, which sustain T cell survival. Furthermore, following stimulation of the T cell receptor (TCR), this intracellular system translocates to the surface and CTSL cleaves C3, generating C3a and C3b, which engage extracellular C3aR and CD46, respectively[263]. Autocrine signalling through CD46 has been demonstrated to drive Th1 induction via regulation of glucose and amino acid transporters, thereby regulating nutrient intake and metabolic programming[264].

Intracellular C5a also orchestrates the induction of a Th1 phenotype[265]. Upon TCR and CD46 stimulation, intracellular C5 within $CD4^+$ T cells is cleaved by a currently unknown protease to generate C5a, which signals via intracellular C5aR1 to produce ROS and subsequently trigger NOD- LRR- and pyrin domain-containing protein 3 (NLRP3)

assembly[265]. This culminates with the production of IL-1β, which is necessary for Th1 induction. Surface bound C5aR2 acts as a negative regulator of this process[265].

Together, these studies demonstrate that intracellular activation of complement and subsequent anaphylatoxin signalling can alter key cellular phenotypes in immune cells, shaping the adaptive immune response. Additionally, recent work has also highlighted that an intracellular mitochondrial C5a/C5aR1 signalling axis modulates sterile inflammation in myeloid cells[266]. This novel role for intracellular complement in the induction of immune responses suggest that complement may also activate intracellular signalling pathways to drive disease pathogenesis. In general, the discovery of intracellular complement highlights that complement signalling is more complex than the well-defined canonical complement activation pathways, which function in an extracellular fashion.

1.3.7. Complement in homeostasis and beyond

In addition to orchestrating both innate and adaptive immune responses, the complement system 'complements' the resolution of immune responses and promotes homeostasis[163]. Complement can play a protective role by promoting tissue repair following damage to host cells[267,268]. Evidence also supports a role for complement in the developing nervous system. C1q and C3 facilitate complement-mediated elimination of unwanted synapses early in the postnatal period[269].

1.4. The complement system in cancer

As newer roles for the complement system in immunity have been elucidated, our understanding of complement in the context of cancer has also evolved. Chronic inflammation is now considered an enabling hallmark of developing tumours[270] and can promote angiogenesis, facilitate genomic instability and remodel the local immune cell populations within the TME[271]. This paradox, where a system designed to defend the host can act as a tumour promoter[272], has now too been recognised for the complement system. While the complement system is a key player in host defence, a growing body of evidence illustrates that dysregulated complement can contribute to tumour development.

1.4.1. Activation of the complement system in cancer

As a key mediator in host defence, traditionally complement has been considered to engage in anti-tumour immune functions. Indeed, several studies have demonstrated that

the complement system is activated systemically and within the TME. Increased MBL/MASP activity and MBL levels have been observed in the serum of patients with CRC, when compared to non-cancer controls[273]. In lung cancer cell lines, incubation with normal human serum activates complement and is associated with C5 deposition, when compared to cell lines derived from the normal bronchial epithelium, demonstrating complement recognition of tumour cells[274]. Furthermore, increased C5a levels have been reported in the plasma of non-small cell lung cancer (NSCLC) patients, when compared to healthy controls, suggesting that local activation of complement may be followed by systemic diffusion[274]. Complement components are deposited in many tumour tissues, for instance C4d, a C4-derived fragment, has been reported in oropharyngeal squamous cell carcinomas[275] and follicular and mucosal-associated lymphoid tissue lymphomas[276]. Similarly, others have demonstrated that C3c is abundantly deposited in tumour tissue from glioblastoma multiforme patients, when compared to non-malignant controls[277]. In addition, this study reported deposition of C5b-9 on tumour cells. The presence of C5b-9 in tumour tissue has also been reported in breast[278], gastric[279] and thyroid[280] cancers, and within ovarian cancer-associated ascitic fluid[281], demonstrating local complement activation up to advanced stages of disease. The complex relationship between cancer cells and the C5b-9 MAC has recently been reviewed in detail, including the pro-lytic signals responsible for mediating the necrotic cell death induced by MACs[282].

Collectively, these observations provide evidence for tumour-induced activation of the complement system. Given the role of complement in immune defence, it may be expected that complement activation within the TME would be associated with favourable outcomes. Paradoxically, complement system activity is observed to correlate with poor prognosis in several cancers including cervical[283], colorectal[284] and ovarian cancer[285]. This suggests that dysregulation of the complement system occurs in a number of human cancers. It is widely accepted that a chronic inflammatory state facilitates neoplastic transformation[271] and current evidence suggests that complement activity, even if primarily initiated as a mechanism of host defence, may become tumour promoting as a result of sustained inflammation within the TME.

1.4.2. Tumour expression of complement regulators

During tumour development, cancer cells employ a range of mechanisms to avoid immune destruction[270]. As outlined, host cells express mCRPs to limit complement activation and avoid damage to healthy tissue[214]. This strategy is exploited by cancer cells,

which often express complement regulators at levels higher than those observed in non-malignant tissue[286–289]. For example, head and neck squamous cell carcinoma (HNSCC) cells express significantly elevated levels of CD46, CD55 and CD59, when compared to benign keratinocyte cells. Furthermore, tumour infiltrating lymphocytes (TILs) from HNSCC patients have significantly increased expression of mCRPs, when compared to those from healthy controls[290]. Although there is evidence for complement activation in cancer, the expression of mCRPs within the TME provides evidence for tumour evasion of the complement system. In particular, analysis of 30 cancer types by Roumenina *et al.* identified CD59 as one of the most highly expressed complement genes, suggesting malignant cells efficiently evade complement-mediated attack[177]. This is further supported by evidence that mCRP expression correlates with poor clinical outcomes in cancer more often than not[291]. An extensive overview of the contribution of mCRPs to tumour growth and their current status as biomarkers is presented in a recent review by Geller and Yan[292].

Soluble complement regulators are also employed by tumours in a bid to regulate complement activation. Lung cancer cells produce and secrete CFH, and CFI is secreted by NSCLC cells providing them with protection from complement-mediated lysis[293–295]. Together with evidence for expression of mCRPs in the TME, this demonstrates a consistent and active attempt by tumours to evade detection by complement.

1.4.3. Roles for complement in tumour growth

Aside from evidence for a detection-evasion interplay between complement and the immune system, direct roles for complement in tumour growth have been identified. Several excellent reviews have recently discussed the role of complement in tumour growth and dissemination in detail[177,296,297], however, broadly speaking, mechanistic insights have mostly been obtained through the study of mouse models.

1.4.3.9. Tumour-promoting modulation of the immune milieu

A seminal paper in 2008 from Markiewski and colleagues provided the first clear evidence for a functional role for complement in tumourigenesis. Using a syngeneic TC-1 mouse model, they demonstrated that tumour growth was significantly impeded in $C3^{-/-}$, $C4^{-/-}$ and $C5aR^{-/-}$ mice[298]. It is well established that local cells within the TME, and the mediators they produce, play key roles in tumour growth[150]. In this model, they demonstrated that in the absence of C5a signalling, migration of myeloid-derived suppressor cells (MDSC) to tumours was reduced, allowing increased infiltration of $CD8^+$

T cells[298]. Since then, several others have demonstrated pro-tumour roles for complement, in particular providing evidence for complement-mediated modulation of the anti-tumour immune response (**Table 1-4**). Signalling through the C3a/C3aR and C5a/C5aR axes has been observed to remodel the TME, altering immune infiltrates and inducing immunosuppressive phenotypes. Complement-mediated regulation of T cell function is the most well described relationship between the complement system and an immune cell. This is likely due to the roles played by autocrine complement in T cell homeostasis, differentiation and metabolism[171,261,263,264].

1.4.3.10. Immune-independent promotion of tumour growth

Other immune-independent roles for complement in tumour growth have been identified. Expression of C1q in the TME of melanoma promotes proliferation and migration of tumour cells[299]. In a mouse model of ovarian cancer, autocrine activation of the C3a/C3aR and C5a/C5aR signalling axes resulted in elevated proliferation of cancer cells due to PI3K/AKT signalling[300]. C3, CFI and complement factor B (CFB) have been demonstrated to enhance proliferation and migration of cutaneous squamous cell carcinoma (cSCC) cells via autocrine signalling through extracellular signal regulated kinase (ERK) 1 and ERK2[301,302] Furthermore, complement has also been reported to induce angiogenesis[173,299,303] and foster acquisition of an epithelial-mesenchymal transition (EMT) phenotype by promoting expression of stemness genes[304], enhancing invasion[305–307] and increasing motility[308–311] of cells in several cancer types. Evidence for complement in metastasis has been presented in several cancers (reviewed in[296] and[312]). It is notable that whilst the majority of murine studies have demonstrated pro-oncogenic roles for complement, a small number of studies have reported anti-tumour functions for complement. In murine breast cancer models, protective roles for C3, C5a, C1q and Factor P have been demonstrated[313–316].

Expression of complement components has been demonstrated in human tumour tissue. At the gene level, mutations, in particular driver mutations, as well as alterations and deletions in complement system genes are prevalent across at least 32 cancer types including lung, pancreatic and haematological malignancies[287]. Complement appears to modulate disease progression, given that these alterations are associated with outcomes[287]. In gastric cancer, tumours exhibit enhanced deposition of C3 and C3a relative to adjacent healthy tissue[317]. This demonstrates activation of complement within tumours locally, which is occurring at increased rates relative to healthy tissue. With regards to functional

evidence, increased C5aR expression and phosphorylated PI3K/AKT has been observed in gastric cancer tissue, when compared to matched normal tissue, with *in vitro* studies demonstrating C5a-mediated activation of PI3K/AKT[318]. This suggests that complement-mediated signals may drive proliferation in gastric tumours. Similarly, C5a has been demonstrated to promote proliferation of breast cancer cell lines, suggesting a role for complement signalling in breast cancer progression[319].

Table 1-4: Functional effects of complement on immune cells that promote tumour growth in mouse models.

Immune Cell	Model	Component	Observation	Mechanism	Ref
MDSC $CD8^+$ T cell	Ovarian cancer, syngeneic (TC-1 cells)	C5a, C5aR	Tumour growth is impaired in $C5aR^{-/-}$ mice Pharmacological blockade of C5aR reduces tumour growth	Recruitment of PMN MDSCs to tumours and production of ROS/RNS by MO MDSCs, suppresses $CD8^+$ T cell responses	298
$CD8^+$ T cell	Melanoma, syngeneic (B16 cells) Breast cancer syngeneic (E0771)	C3, C3aR C5aR	Tumour growth is impaired in $C3^{-/-}$ mice C3aR and C5aR antagonism reduces tumour growth	Complement signalling inhibits IL-10 expression by $CD8^+$ TILs, hindering the anti-tumour response	320
$CD8^+$ T cell	Breast cancer, syngeneic (4T1 and 4TI-GFP cells)	C5a, C5aR	Reduces lung and liver metastases in $C5aR^{-/-}$ mice C5aR antagonism reduces lung metastases	Recruitment of MDSCs, and induction of TGFB and IL-10 production, leads to suppression of $CD8^+$ T cell function by Treg cells	321
$CD8^+$ T cell	Lung cancer, syngeneic $Kras^{LSL\text{-}G12D/+}$ mice (393P cells)	C5aR	Decreased tumour volume in $C5aR^{-/-}$ mice Pharmacological blockade of C5a and PD-1 impairs tumour growth	Fewer MDSCs accompanied by an increase in $CD8^+$ T cells, which had lower levels of exhaustion markers	322
CD8+ T cell	Colon cancer, syngeneic (MC38)	C3	Complement (C3) depletion using CVF impairs tumour growth	C3 contributes to the generation of an immunosuppressive environment (Increased MDSCs, fewer $CD8^+$ T cells, lower expression of CCL5, CXCL10 and CXCL11)	323
MDSC CD8+ T cell	Colitis-associated colorectal cancer (Induced by azoxymethane	C5aR	Tumour growth is impaired in $C5aR^{-/-}$ mice C5aR antagonism reduces tumour growth	C5a recruits MDSCs to CRC tissue, inhibiting $CD8^+$ T cell responses	324

	and dextran sulfate sodium)				
$CD4^+$ T cell $CD8^+$ T cell	Lymphoma, syngeneic (RMA-3CF4 and RMA-1474 cells)	C5a	Tumour growth is impaired in mice with lymphoma cells producing low C5a levels	Increase in effector (IFN-y producing) CD4 and $CD8^+$ T cells	[325]
$CD4^+$ T cell	Lung cancer, syngeneic and orthotopic (LLC-luc, CMT-luc and EML4-ALK cells)	C3, C3aR, C5aR	Tumour growth is impaired and metastases are reduced in $C3^{-/-}$ mice C3aR or C5aR antagonism reduces tumour growth	Signalling of C3 prevents cytokine production by $CD4^+$ T cells	[326]
MDSC	Lung cancer, syngeneic (3LL cells)	C5a, C5aR	C5aR antagonism reduces tumour growth	C5a contributes to the generation of an immunosuppressive microenvironment	[274]
MDSC	Hepatocellular carcinoma, syngenic (H22 cells)	C3	Tumour growth is impaired in mice with $C3^{-/-}$ hepatic stellate cells	Hepatic stellate cells produce C3 leading to MDSC accumulation and immunosuppression	[327]
Neutrophil	Small intestine tumourigenesis ($APC^{Min/+}$ mice)	C3aR	Tumour growth is impaired in $C3aR^{-/-}$ mice	Engagement of C3aR on neutrophils drives NETosis and coagulation pathways to induce protumourigenic low density neutrophils	[328]
Neutrophil	Colitis-associated colorectal cancer (Induced by azoxymethane and dextran sulfate sodium)	C3, C5, C5aR	Tumour growth is impaired in $C3^{-/-}$, $C5^{-/-}$ and $C5aR^{-/-}$ mice	C5a induces neutrophil infiltration and IL-1B expression which drives IL-17A production	[329]
Neutrophil	Melanoma, syngeneic (B16F10)	C3aR	Tumour growth is impaired in $C3aR^{-/-}$ mice. C3aR antagonism arrests growth of established tumours	C3aR signalling reduces infiltrating neutrophils and $CD4^+$ T cell populations	[330]
Macrophage	Melanoma, syngeneic (B16F10)	C3a, C3aR	C3a neutralization impairs tumour growth	C3a recruits macrophages which suppress the $CD8^+$ T cell response	[331]
Macrophage	Sarcoma (Induced by 3-methylcholanthrane)	PTX3, C5a	PTX3 controls complement activation by recruiting Factor H. *Ptx3*$^{-/-}$ mice are more susceptible to carcinogenesis	In the absence of PTX3, C5a generation is uninterrupted. An increase in CCL2 skews macrophages to an M2 phenotype	[332]
Macrophage	Colon cancer (metastatic), syngeneic (SL4 cells)	C5a, C5aR	Growth of hepatic metastases is impaired in $C5aR^{-/-}$ mice or when C5 is downregulated or targeted via	C5a induces MCP-1 production by macrophages via the Akt pathway and promotes an	[333]

	Colon cancer xenograft (HCT116 and SW116 cells)		pharmacological blockade	immunosuppressive microenvironment	
Macrophage	Pancreatic neuroendocrine tumours, transgenic (BT2B6)	C5aR	C5aR antagonism reduces tumour growth.	Increased infiltration of macrophages	[334]
Macrophage	Colon cancer, syngeneic (SL4-luc)	C5aR	Growth of hepatic metastases is impaired in $C5aR^{-/-}$ mice	C5a polarises tumour associated macrophages to an M2 phenotype via NF-kB signalling	[335]
Macrophage and Mast cells	Squamous cell carcinoma, transgenic (K14-HPV16)	C5aR	Tumour growth is impaired in $C5aR^{-/-}$ mice.	C5aR signalling activates macrophages and mast cells, promoting a pro-tumour microenvironment and limiting $CD8^+$ T cell responses	[336]
Natural Killer cell	Colorectal cancer, syngeneic (CT26 cells) Breast cancer, Syngeneic (JC cells)	C3a/C3aR	Tumour growth inhibited in $C3aR^{-/-}$ mice	C3a/C3aR signalling inhibits NK cell migration to tumours	[337]
Natural Killer cell	Pancreatic cancer, syngeneic (Pan02 cells) Xenograft (PANC-1 and MIAPaCa-2)	C3a/C3aR	Tumour growth is delayed when C3a/C3aR signalling is inhibited	C3a/C3aR signalling inhibits NK cell migration to tumours	[338]
Natural Killer cell	Melanoma, syngeneic (B16gp33 cells)	C3	Complement (C3) depletion using CVF impairs tumour growth	Complement limits NK cell-mediation of the $CD8^+$ T cell anti-tumour immune response	[339]
Natural Killer cell	Melanoma, syngeneic (B16-luc cells)	CR3	Metastases were reduced in $CD11b^{-/-}$ (CR3 deficient) mice and mice with CR3 deficient NK cells	Interaction of iC3b with CR3 supresses NK cells by activating SHIP and JNK pathways	[340]

Abbreviations; APC, adenomatous polyposis coli; C3aR, C3a receptor; C5aR, C5a receptor; CCL, chemokine (c-c motif) ligand; CR. Complement receptor; CVF, cobra venom factor; CXCL, chemokine (c-x-c motif) ligand; IL, interleukin; MDSC, myeloid-derived suppressor cell; MO, mononuclear; NET, neutrophil extracellular trap; NK, natural killer; PMN, polymorphonuclear; PTX, pentraxin 3; RNS, reactive nitrogen species; ROS, reactive oxygen species; TIL, tumour-infiltrating leukocyte. Table adapted from *O'Brien et al. 2020*[162].

1.4.3.11. Intracellular complement and the complosome in tumour growth

Recently, evidence for the complosome in cancer cells was presented by Ding *et al*.[341]. In CRC cells, they demonstrated intracellular cleavage of C5 by cathepsin D (CTSD) to generate C5a. Interestingly, they provide mechanistic insights that β-catenin, a known promoter of oncogene transcription and contributor to CRC carcinogenesis, is stabilised by intracellular C5a/C5aR signalling[341]. These findings illustrate that neoplastic transformation may be driven by intracellular complement signalling. In support of this, in patient tumour tissue, elevated expression of C5aR1, C5a and CTSD was accompanied by high β-catenin expression and poor prognosis. This provides evidence that intracellular complement may have roles in disease progression and/or patient response to treatment in cancer.

CFH has been identified in lysosomes in clear cell renal cell carcinoma (ccRCC) and lung adenocarcinoma, and this intracellular form engages in a pro-tumour role distinct from its membranous counterpart[342]. Intracellular CFH has been reported to promote tumour cell proliferation, migration and survival and is associated with poor patient outcomes[342].

C4BP-A is another complement component that has been identified intracellularly[343]. Within cells, C4BP-A has been observed to associate with the NF-kB family member RelA, to promote survival. This provides further evidence that location can influence the function of complement components[344]. An overview of the roles for autocrine and intracellular complement in cancer is presented in **Fig. 1-7.**

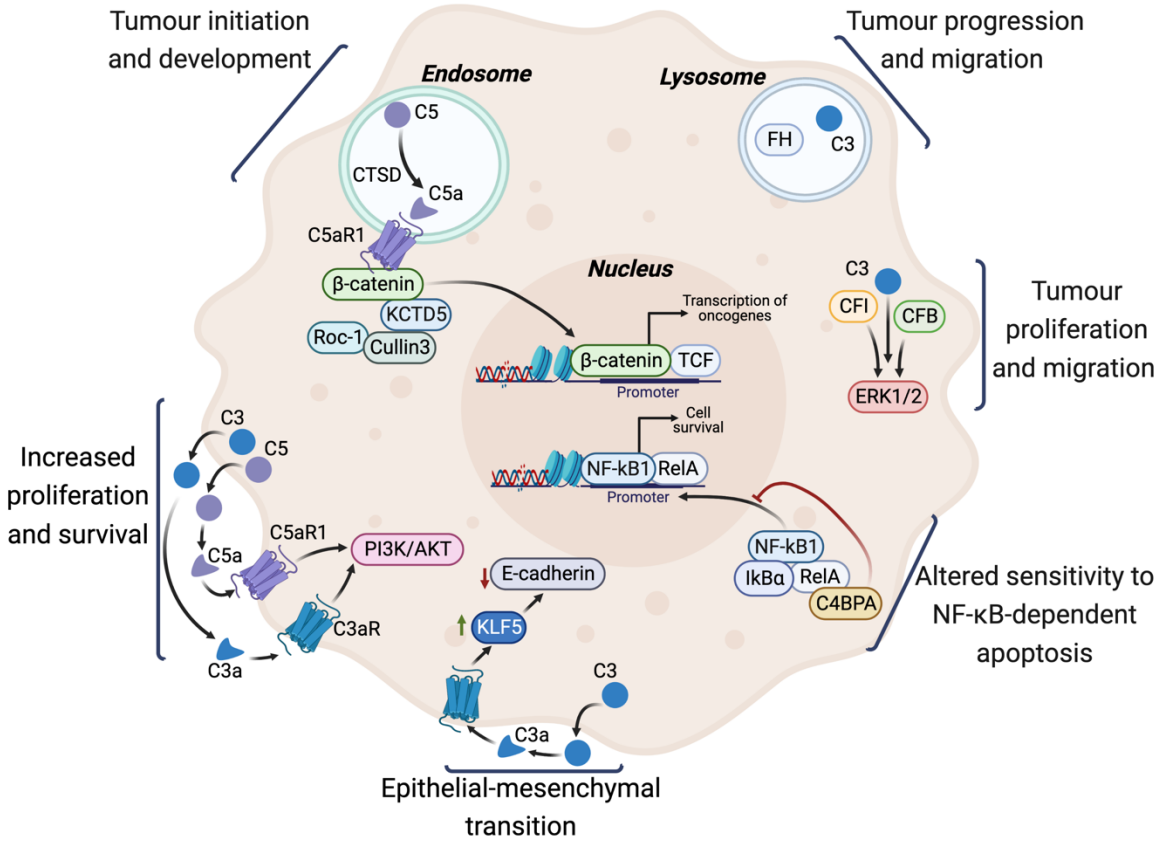

Figure 1-7: Autocrine and intracellular roles for complement in cancer cells. Summary of autocrine roles for complement in cancer including novel intracellular roles. Figure adapted from *O'Brien et al. 2023*[344]. Figure created with BioRender.com.

1.5. Complement and response to cancer therapy

1.5.1. Complement and the response to chemotherapy

Given that complement contributes to tumour growth and progression, it is unsurprising that complement has been implicated in the tumour response to anti-cancer therapy (**Fig. 1-8**). The interactions between complement and local immune cells may play a key role in this process. Medler *et al.* identified a role for macrophage-produced C5a in squamous cell carcinogenesis, whereby signalling through the C5aR activates mast cells and macrophages, promoting a pro-tumour, immunosuppressive microenvironment[336]. They demonstrated in a murine model that tumour response to paclitaxel (PTX) chemotherapy was improved following treatment with a C5aR antagonist, PMX-53. The combination of PTX and PMX-53 resulted in transcriptional reprogramming of tumour-associated macrophages and subsequent recruitment of $CXCR3^+$ effector and memory $CD8^+$ T cells to significantly reduce tumour burden, when compared to treatment with PTX alone[336]. This suggests that C5a signalling remodels the TME by restricting $CD8^+$ T cell

infiltration. Therefore, inhibiting complement within the TME of squamous cell carcinomas and other cancers therefore may have potential for improving response to chemotherapy.

More recently, a role for complement signalling in the response to chemotherapy in breast adenocarcinoma was identified. Transcriptomic analysis of intratumoural B cells highlighted an inducible T cell costimulatory ligand (ICOSL) positive B cell population, which was enriched following initiation of neo-adjuvant chemotherapy, when compared to pre-treatment[345]. In agreement, murine studies demonstrated a doxorubicin (DXR)-induced increase in $ICOSL^+$ $CR2^+$ B cells[345]. Importantly, $ICOSL^+$ B cells were clinically significant, correlating with improved DFS and OS, and were also associated with complement activation. Chemotherapy-associated immunogenic cell death was demonstrated to induce complement activation, generating activation fragments, which promote B cell switching to an $ICOSL^+$ phenotype by interacting with CR2. Expression levels of CD55, an mCRP that limits complement activation, negatively correlated with complement activation and infiltration of $ICOSL^+$ B cells, and elevated levels corresponded with chemoresistance and poorer patient outcomes[345]. Complement largely appears to protect against tumour growth in breast adenocarcinoma[313–316]. These data support that in this cancer type, complement activation has an anti-tumour function and is essential for chemotherapeutic efficacy[345]. Further study of the impact of $ICOSL^+$ B cells in the TME is required to determine their relevance in the response to therapy of other cancers [346].

In triple negative breast cancer (TNBC), targeting complement signalling has demonstrated potential in protecting against lung metastases. In murine models, adjuvant DXR treatment has been observed to promote immunosuppression in the lungs, where it fails to control tumour spread[175]. Within this metastatic niche, Monteran and colleagues demonstrated that T cells were dysfunctional and exhausted, C3aR and C5aR1 expressing MDSCs were present and CAFs demonstrated upregulated expression of complement components[175]. Therefore, they hypothesised that CAF-mediated complement signalling may promote immunosuppression. Interestingly, both C3aR or C5aR antagonism in combination with DXR attenuated metastatic burden and progression[175]. This study provides contrasting evidence to the aforementioned work, which demonstrates essential roles for complement in the response to chemotherapy in breast cancer. With regards to prognosis, breast cancer is among a group of cancers in which complement is of uncertain significance[177]. The impact of complement may also be uncertain in breast cancer in terms of subtype, and disease stage.

Complement has also been demonstrated to alter response to chemotherapy independent of immune cells. In glioblastoma, C5 has been demonstrated to promote repair of DNA damage induced by the chemotherapeutic agent temozolomide (TMZ), leading to chemoresistance[347]. Antagonism of the C5aR has a chemosensitising effect, providing evidence for complement signalling in resistance to chemotherapy[347]. Other complement components in addition to anaphylatoxins have been implicated in the response to cancer treatment. Endometrioid tumours overexpress CD55, relative to benign tissue[348]. This expression is associated with resistance to cisplatin chemotherapy, with CD55 positive cells exhibiting markedly increased self-renewing ability, when compared to CD55 negative cells[349]. In particular, CD55 is highly expressed by cancer-stem cells and cisplatin-resistant cancer cells. Functional studies have demonstrated that CD55 localises to lipid rafts to activate ROR2-JNK and lymphocyte-specific protein tyrosine kinase (LCK) pathways[349]. Signalling through these pathways drives self-renewal and resistance to cisplatin, respectively. LCK signals were associated with the induction of expression of DNA repair genes[349]. This tumour-promoting role for CD55 is in contrast with that elucidated by Lu *et al.* whereby expression of CD55 inhibits complement activation required for the B cell response to chemotherapy in breast cancer[345]. Together these studies provide further evidence of context-dependent roles for complement in the response to chemotherapy.

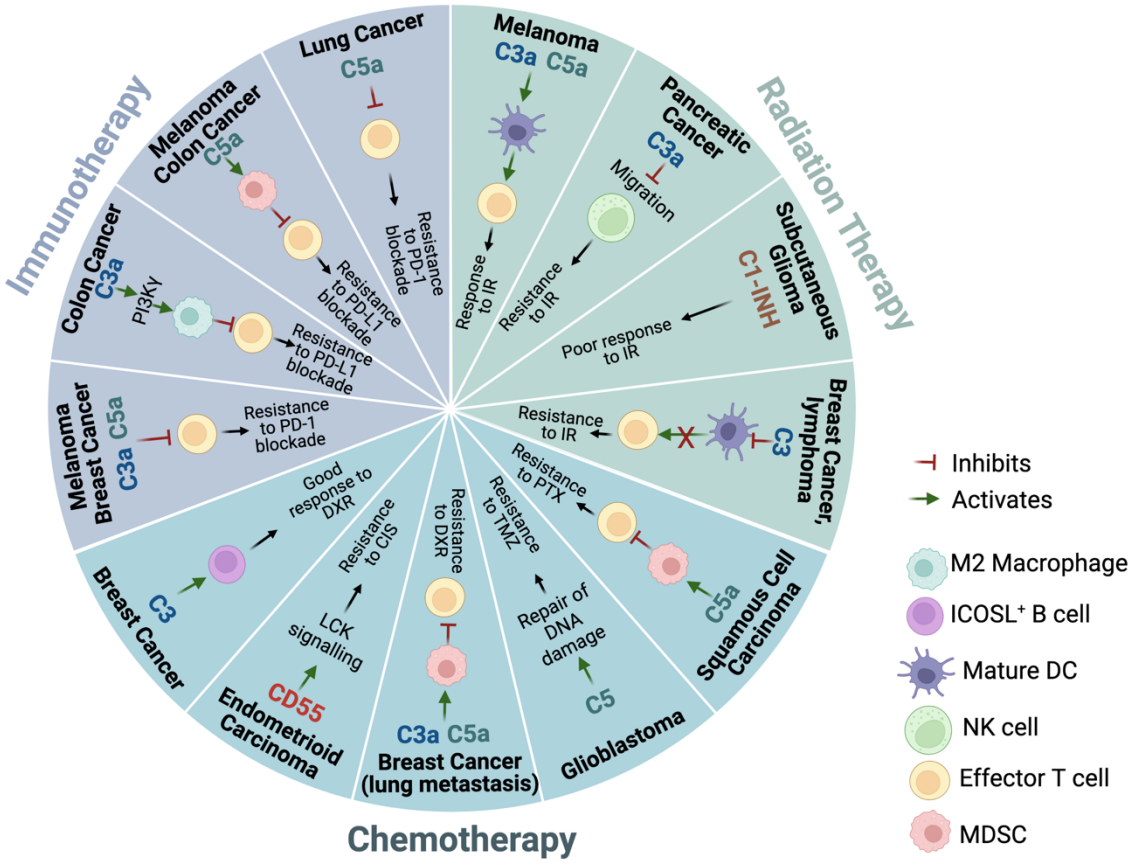

Figure 1-8: Roles for complement in the response to chemotherapy, immunotherapy and RT. The current understanding of the roles for complement in the response to radiotherapy, chemotherapy and monoclonal-antibody based immunotherapies are depicted. Green arrows illustrate events where complement component(s) have been demonstrated to activate an immune cell or signalling pathway, while inhibitory effects are shown in red. Black arrows indicate the observed influence of complement activities on the therapeutic efficacies of the designated chemotherapy, radiotherapy or immunotherapy treatment, in specified cancer types. Abbreviations; CIS, cisplatin; DXR, doxorubicin; IR, ionising radiation; PD-1, programmed cell death protein-1; PD-L1, PD-ligand 1; TMZ, Temozolomide.
Figure adapted from *O'Brien et al. 2020*[162]. Figure created with BioRender.com.

1.5.2. Complement and the response to RT

Recent evidence also suggests a role for complement in the tumour response to RT[338,350,351]. Irreparable DNA damage induced by IR causes tumour cell death via apoptosis and mitotic catastrophe, or cell cycle arrest leading to senescence[114]. Elvington *et al.* hypothesised that inhibiting complement would reduce complement-mediated clearance of apoptotic cells, resulting in increased inflammation and necrotic cells, and a more immunogenic environment[350]. In a murine model of lymphoma, they demonstrated that complement inhibition in combination with RT significantly reduced the tumour growth

rate, decreased tumour burden and improved survival, when compared to RT alone [350]. Although complement activation is an inflammatory process, in this model, inhibition of complement in combination with RT promoted inflammation, when compared to RT alone. This was characterised by increased levels of IFN-γ, IL-6 and IL-17[350]. Furthermore, early neutrophil infiltration followed by later infiltration of mature DCs and $CD8^+$ T cells was observed, resulting in an enhanced anti-tumour immune response[350]. Ultimately, targeting complement improved therapeutic efficacy, suggesting that complement can alter response to RT by restricting immune cell infiltration and the anti-tumour immune response [350].

Inhibition of complement has also been demonstrated to augment the tumour response to RT, in murine pancreatic cancer models[338]. In pancreatic cancer, exclusion of natural killer (NK) cells from the tumour is common and is associated with worse survival[338]. Complement signalling via the C3a/C3aR axis has previously been demonstrated to restrict tumour infiltration of NK cells in mouse models of CRC and breast cancer[337]. Similarly, using murine models of pancreatic cancer, Sodji *et al.* demonstrated that inhibition of the C3aR signalling axis is associated with elevated numbers of NK cells within the TME and delayed tumour growth[338]. To investigate the potential for targeting complement signalling in controlling tumour growth, C3aR antagonism was combined with RT. A combination of RT and C3aR antagonism demonstrated superior tumour control, when compared to RT alone[338]. These data further support a role for complement in negatively modulating the immune component of the TME, which impacts on the tumour response to RT. Other evidence supporting a role for complement inhibition in boosting RT responses has been demonstrated in models of subcutaneous glioblastoma, where combination use of C1-INH and RT significantly increased survival and resulted in decreased tumour size[352].

While these studies suggest that inhibiting complement may potentiate RT, evidence has also been provided for an essential role of complement in the response to RT. It is well established that RT induces immunogenic cell death and promotes anti-tumour immunity by enhancing T cell priming and effector phases[99–101,353]. However, the earliest step triggered by radiation that is responsible for initiating an immune response is unclear. A potential mechanism involving complement was uncovered by Surace *et al*. who demonstrated that radiation activated the complement system, producing anaphylatoxins, which were essential for the subsequent response to RT[351]. In both mouse and human tumours, the classical and alternative complement pathways were activated following

treatment with radiation. RT failed to control tumours in mice deficient in either C3, C3aR or C5aR, indicating a functional role for complement in treatment efficacy[351]. Analysis of tumour infiltrating immune cells, demonstrated that radiation induced complement expression in DCs and upregulated C3aR and C5aR expression[351]. In line with previous reports, complement signals were essential for DC activation[171]. In C3aR and C5aR deficient mice, $CD8^+$ T cells produced less IFN-γ post-radiation, when compared to controls[351]. These data demonstrate that in this model, complement is functionally important for activating DCs and promoting an efficient anti-tumour $CD8^+$ T cell response[351]. Combination RT and treatment with dexamethasone, a glucocorticoid that inhibits complement activation, abolished the therapeutic effect of RT, further highlighting the essential role for complement in the response to RT[351].

These studies present conflicting results with regards to whether complement enhances or hinders the tumour response to radiation. This is likely due to the context-dependent effects of complement in cancer, the models used and the radiation schedule. Importantly, these data highlight that complement regulates immune cells within the TME, which can influence response to RT.

1.5.3. Complement and the response to immunotherapy

Immune checkpoint inhibitors (ICI) target immune cell receptors or ligands which engage in inhibitory interactions that downregulate immune responses, such as cytotoxic T lymphocyte-associated protein 4 (CTLA-4) and programmed death-1 (PD-1) expressed by activated T and B cells[354,355]. Resistance to ICIs is a clinical challenge, with populations of patients displaying primary resistance and others acquiring resistance overtime to anti-PD-1 or anti-programmed death -ligand 1 (PD-L1) therapy[356,357]

A synergistic, combination approach to inhibit both the PD-1/PD-L1 axis and another immunomodulatory pathway has been suggested as potential way to overcome this resistance[358]. Within the TME, complement components including C1q and C5a have been linked with tumour expression of immune checkpoints including PD-L1, LAG3 and CTLA-4[173,274]. In metastatic melanoma, serum complement is associated with resistance to anti-PD-1 therapy[359]. Several studies have demonstrated that targeting complement in combination with ICIs may be an effective strategy to boost responses. Wang *et al.* demonstrated that complement signalling suppresses the $CD8^+$ T cell anti-tumour immune response[320]. In a model of melanoma, they demonstrated that C3aR and C5aR antagonism

in combination with PD-1 blockade was superior in controlling tumour growth, when compared to either alone[320]. This suggests that inhibition of complement signalling synergises with PD-1 blockade to overcome immunosuppression and restore anti-tumour immunity[320]. Similarly, in CRC, the C3a/C3aR signalling axis has been proposed as a potential mechanism by which to boost responses to anti-PD-1 immunotherapy[360]. Ajona *et al.* demonstrated in a model of lung cancer that combination C5aR and PD-1 inhibition more effectively controlled tumour growth, when compared to monotherapy[322]. In murine colon and melanoma models, evidence suggests that inhibition of C5aR signalling improves response to PD-L1 blockade, by relieving complement-mediated, MDSC suppressive activity[361]. C3 activity has also been implicated in resistance to PD-L1 therapy. In a colon cancer model, tumour cell-derived C3a has been demonstrated to engage C3aR expressed by TAMs to promote an M2 phenotype, suppressing effector $CD8^+$ T cells[362]. Study of C3-deficient colon tumours, indicated that PD-L1 therapy was more effective in these mice, when compared to controls[362].

Collectively, these studies establish complement as a modulator of immune cells within the TME, which subsequently may affect response to treatment.

1.6. Complement as a cancer biomarker

1.6.1. Prognostic biomarker

In patients, the expression of complement components is commonly associated with adverse features and poor outcomes[274,283,291,363]. Mutations in complement genes appear to functionally impact cancer progression, given the correlation between groups of complement mutations and survival; for example, the association of complement mutations with poor OS in low grade glioma[287]. In gastric cancer, high C3 deposition correlates with worse 5 year OS[317]. Similarly, in breast cancer, expression of C5aR is associated with larger tumours, metastases in the lymph nodes and advanced clinical stages[319]. Furthermore, patients with C5aR negative tumours had improved survival rates, when compared to those with C5aR positive tumours. In CRC, CMS4 tumours have the worst outcomes[25,161]. Interestingly, tumours within this subtype, demonstrate upregulated complement expression[25], suggesting that complement may associate with worse outcomes.

Conversely, complement has also been correlated with favourable clinical outcomes, suggesting a role for protection against tumour growth. High C3 levels are indicative of good prognosis in NSCLC, with greater numbers of infiltrating $CD4^+$ and $CD8^+$ T cells reported in tumours with increased C3 expression[364]. These studies

demonstrate that the relationship between complement and prognosis is inconsistent. This has been addressed by Roumenina *et al.* who identified that four groups could be defined based on the observed prognostic impact of complement on the cancer type; protective complement, protective C3, aggressive complement and complement of uncertain significance[177]. CRC is among the cancer types defined by 'aggressive complement'[177].

1.6.2. Predictive biomarker of treatment response

There is global interest in identifying biomarkers of response to chemotherapy, RT or combined chemoradiation therapy (CRT) with the aim of reducing treatment-associated toxicities and ensuring optimal treatment strategies for patients.

The expression of several complement cascade genes has recently been correlated with the chemosensitivity of soft tissue sarcomas (STS)[365]. Analysis of TCGA by Zhang *et al.* indicated that several genes were differentially expressed between STS subtypes with varying chemosensitivities, many of which encoded complement system components. Those STS that were relatively insensitive to chemotherapy treatment, expressed high levels of complement system genes, and this had clinical significance[365]. High expression of C3aR, C1QC and CFI, correlated with poor OS. Upregulation of C3aR was also associated with worse DFS, suggesting that these complement components play a role in the tumour response to chemotherapy in STS[365]. These genes thus represent novel biomarkers of tumour chemosensitivity and patient survival in STS.

Complement has also demonstrated predictive potential as a circulating biomarker of response to cancer therapy. In breast cancer, resistance to neo-adjuvant chemotherapy remains a clinical challenge. Proteomic analysis of human plasma from breast cancer patients has demonstrated that complement is modulated by epirubicin and docetaxel, with alterations in complement components reported as early as 24 h following the initiation of treatment[366]. Interestingly, the levels of C3 isoforms in plasma differed between responders and non-responders. As the immediate response in plasma correlated with the final tumour response to treatment, this suggests that C3 isoforms may have potential as early predictive biomarkers of response to epirubicin and docetaxel in breast cancer[366].

Within our Department, similar predictive potential of tumoural and circulating complement was identified in oesophageal adenocarcinoma (OAC). Proteomic profiling of pre-treatment serum samples from OAC patients was performed, demonstrating that increased C3a and C4a levels predict a subsequent poor response to neo-CRT[367]. This study was the first to implicate these anaphylatoxins in the response to neo-CRT. In support of

this, OAC patients with a subsequent poor pathological response to neo-CRT had increased pre-treatment tumoural expression of C3, when compared to good responders[368]. This suggests that complement may have potential as a tumoural and/or circulating biomarker of response to treatment. To determine the full potential of complement components as predictive markers of therapeutic response, further validation studies encompassing multiple cancer types and treatment regimens is required.

1.7. Mechanisms by which complement may modulate response to treatment

1.7.1. DNA repair

Alterations in DNA repair capabilities have been identified to associate with resistance to RT[122–124]. Previous studies in our Department demonstrated that C3 mRNA expression was significantly increased in pre-treatment tumour biopsies from OAC patients with a subsequent poor responses to neo-CRT[368]. Global micro-RNA (miR) profiling revealed that miR-187 was significantly decreased in these tissue samples. In miR-187-overexpressing OAC cell lines, C3 mRNA expression was downregulated, suggesting negative regulation of C3 by miR-187[368]. Interestingly, these *in vitro* studies demonstrated that overexpression of miR-187 sensitised OAC cells to both RT and cisplatin and this was accompanied by downregulation of several DDR genes[368]. MiR-187 mediated-regulation of C3 expression and DDR genes suggests that complement potentially interacts with the DDR to influence response to therapy[368]. Evidence suggests that C5 may also play a role in the DDR. In glioblastoma, C5 has been demonstrated to promote the repair of TMZ-mediated DNA damage[347]. C5aR1 antagonism in combination with TMZ induced significantly greater levels of DNA damage, when compared to TMZ alone, highlighting that complement signalling limited chemotherapy efficacy.

Further evidence that complement proteins play roles in DNA repair comes from the finding that C1q subcomponent binding protein (C1QBP) is implicated in HR repair of DSBs. Study of C1QBP demonstrated that it associates with MRE11, stabilising it and influencing the assembly and activation of the MRN complex[369]. Deficiency of C1QBP was associated with impaired activation of ATR and ATM and inefficient repair of IR-induced DNA damage, demonstrating that C1QBP plays an essential role in the repair of DNA damage[369]. These findings have relevance in the context of cancer, as immunohistochemical (IHC) analysis of breast cancer tissue revealed a strong positive correlation between C1QPB and MRE11[369]. Expression of C1QBP and MRE11 at high

levels was associated with worse OS in breast cancer. Furthermore, in ovarian cancer, poor prognosis following chemotherapy was also associated with high C1QBP expression[369].

Genetic polymorphisms in DNA repair genes can greatly contribute towards cancer development and result in therapeutic resistance. The DNA repair protein X-ray repair cross-complementing (XRCC) 3 is a key participant in HR of DNA DSBs[370]. Genotype variants at the rs1861539 polymorphic site of the XRCC3 gene result in defective DNA repair and are associated with increased risk for several cancers including lung and childhood acute lymphoblastic leukemia[371]. In a study of styrene-exposed individuals, low serum levels of complement C3 and C4 correlated with specific genotypes of the XRCC3 gene at this site, when compared to the wildtype genotype[372]. Although this study was not performed in the context of cancer, it highlights that polymorphisms in DNA repair genes correlate with altered complement expression levels, further suggesting a relationship between the DDR and complement.

1.7.2. Cell cycle

Cell cycle distribution can alter sensitivity to RT. Evidence suggests that complement may modulate cell cycle distribution. In a study of clear renal cell carcinoma cells, Daugan *et al*. demonstrated that silencing of CFH is associated with modifications in cell cycle distribution[342]. Interestingly, CFH-silenced cells were predominantly in the G0/G1 phase, with fewer radiosensitive G2/M phase cells, and a trend towards fewer radioresistant S phase cells[342]. Sublytic C5b-9 has been demonstrated to influence cell cycle distribution in oligodendrocytes, by activating the cell cycle and promoting entry into S phase[373]. Gastric cancer cell lines were observed to accumulate in the S phase, following the addition of C3 into cell culture medium[317]. This suggests that cell cycle alterations induced by C3 may alter cellular sensitivity, potentially altering responses to anti-cancer therapy. These studies demonstrate that components of the complement system may modify cell cycle, which may alter response to therapy.

1.7.3. Apoptosis

Apoptosis is another key parameter implicated in resistance to cancer therapy. While its impact on the therapeutic efficacy of RT remains controversial, radioresistance has been associated with lower rates of apoptosis in numerous cancer types[143–145].

The complement component C4BPA has recently been implicated in resistance to oxaliplatin, by modulating apoptosis[343]. In a study of HCT116 cells, Olcina *et al*.

demonstrated that C4BPA interacts with NF-κB family-member RelA[343]. Patient-specific mutations in C4BPA were demonstrated to alter the apoptotic response to oxaliplatin, with 'sensitive' mutations leading to retention of C4BPA in the cytoplasm, subsequently attenuating NF-κB signalling and leading to enhanced apoptosis[343]. This study demonstrates that intracellular complement can impact treatment response, with mutations in complement genes further impacting the relative therapeutic sensitivity.

Properdin has also been highlighted as a potential modulator of apoptosis in cancer. In breast cancer cell lines, elevated expression of properdin was associated with increased expression of DNA damage inducible transcript 3 (DDIT3), a pro-apoptotic transcription factor[313]. This highlights that properdin may act as a tumour suppressor in breast cancer[313], further demonstrating that tumour cell apoptosis can be regulated by complement components.

1.8. Aims and hypothesis

1.8.1. Overall hypothesis

The complement system is upregulated in treatment-resistant rectal cancer. Targeting the complement system may improve responses to RT and complement may act as a predictive tumoural or circulating biomarker of response to neo-CRT.

1.8.2. Overall aim

The overall aim of this thesis was to characterise the complement system in rectal and colon cancer cell lines and in pre-treatment tumour biopsies and sera from rectal cancer patients to investigate the functional role for complement in modulating the tumour response to RT and the potential role for complement as a predictive biomarker of response to treatment in rectal cancer. Additionally, this thesis aimed to investigate the potential effect of complement on T cell phenotype in CRC.

1.8.3. Specific aims

- Characterise expression of the complement system in a panel of colon and rectal cancer cell lines and correlate with inherent radiosensitivity.
- Assess whether modulating expression of C3 alters radiosensitivity in colon and rectal cell lines and characterise the effects of altered complement expression on apoptosis, DNA damage and repair and cell cycle distribution.

- Assess the effects of colon and rectal cancer cell-derived C3, and recombinant C3a on T cell viability, activation, proliferation and cytokine production.
- Investigate expression of complement genes in pre-treatment tumour biopsies from rectal cancer patients and correlate with clinicopathological factors including response to neo-CRT.
- Assess the circulating concentration of complement components in pre-treatment sera from rectal cancer patients and correlate with clinicopathological factors including response to neo-CRT and prognosis.

Chapter 2: Characterisation of the complement system in an *in vitro* model of radioresistant CRC

2.1. Introduction

CRC is a major cause of cancer-related death, with increasing global burden[15]. Colon and rectal cancers are often defined together as CRC, however approximately 30% of all CRCs occur in the rectum[374–376]. Globally, more than 700,000 cases of rectal cancer were diagnosed in 2020[1]. In Ireland, CRC is a major contributor to the national cancer burden and represents the second and third most common cancer in males and females, respectively[2]. In alignment with global figures, approximately a third of CRCs in Ireland are located in the rectum[2]. Worryingly, deaths from rectal cancer are projected to increase by 24.2% by the year 2035[13].

The current standard of care for LARC involves neo-CRT followed by total mesorectal excision, which aims to downstage rectal tumours, increasing local control and aiding resection[377]. Neo-CRT consists of RT delivered as SCRT (Total dose of 25 Gy, delivered in 5 x 5 Gy fractions) or LCRT (Total dose of 45-50 Gy, delivered in 1.8 or 2 Gy fractions), with 5-FU-based chemotherapy, prior to surgery[21,377]. A pCR is characterised by no viable tumour cells upon surgical resection post neo-CRT[52]. Achievement of a pCR is associated with reduced disease recurrence and improved survival[54,55]. Alarmingly, neo-CRT achieves complete loco-regional control in less than 30% of rectal cancer patients[21,55,56]. Consequently, the approximately 70% of rectal cancer patients who do not achieve a pCR are not only subject to toxicity and therapy-associated complications, but also a higher risk of mortality[54,55]. In addition, following potentially curative surgery, over 50% of patients with locally advanced disease develop distant metastases or recurrence of disease[378]. Improving the poor response rates to neo-CRT is essential to reduce the rising mortality rates in rectal cancer. Currently, there are no clinical markers available to predict, prior to treatment, those patients who will/will not respond to neo-CRT. There is therefore, an urgent global need to elucidate the molecular mechanisms governing the response to neo-CRT in rectal cancer, to (i) identify biomarkers prior to initiation of treatment that can predict therapy response for improved stratification of patients and (ii) identify novel therapeutic targets to boost the response to neo-CRT in those majority of patients who are resistant to the standard of care.

The complement system is a conserved branch of the innate immune system, which is essential for the elimination of foreign antigens and the induction of an inflammatory immune response[208,379]. This network of approximately 50 soluble and membrane-bound proteins compose three complement activation pathways[163,166]. Inflammation and other effector functions of the complement system are mediated by potent anaphylatoxins, C3a,

C4a and C5a, which are generated upon activation of the complement system[178,180]. Beyond a first line of defence, the complement system plays important roles in maintaining homeostasis and coordinating adaptive immune responses[163]. In the context of cancer, complement has traditionally been viewed as 'anti-tumour' in function, and indeed several studies have demonstrated that complement is capable of recognising and eliminating malignant cells[380]. However, a growing body of evidence supports a tumour promoting role for complement[380,381]. In recent years, a number of studies have demonstrated that complement components can aid tumourigenesis and promote metastasis[305,319,336,382,383]. At present, potential oncogenic roles for complement proteins contributing to every hallmark associated with carcinogenesis have been described[381]. In these studies, it is apparent that the effects of complement within the microenvironment are due to locally-derived complement components from tumour or immune cells. Additionally, as intracellular complement has come into focus, complement components have been identified intracellularly in cancer cells, where they engage in unique roles including modulating cell survival and promoting tumourigenesis[341,343]. This is unsurprising given that intracellular complement plays essential roles in orchestrating T cell homeostasis and metabolism during activation[261,263–265].

Novel roles for the complement system are also emerging in therapeutic response, with roles for complement components identified in the response to chemotherapy, immunotherapy and indeed RT[320,322,336,345,349,361,362]. As such, a potential role for complement as a biomarker of treatment response is emerging[162]. Our group were the first to implicate complement in the response to neo-CRT, demonstrating that increased levels of C3a and C4a in the sera of oesophageal cancer patients were predictive of a subsequent poor response to neo-CRT[367]. This was supported in oesophageal adenocarcinoma (OAC) tumours, where poor response to neo-CRT was associated with increased expression of C3[368]. Together, these studies suggest that the complement system may be important for the tumour response to neo-CRT in GI cancers.

Considering the novel roles for complement in tumourigenesis, metastasis and therapeutic resistance, it is evident that complement may be a powerful target for controlling tumour growth and enhancing response to treatment. As outlined, there is an imperative need to improve response rates to neo-CRT in rectal cancer. However, the role of complement in the response to neo-CRT in rectal cancer is largely unknown. Therefore, the objective of this chapter was to investigate the relationship between complement and the response to radiation in CRC *in vitro*. In this chapter, the inherent radiosensitivity of a

panel of CRC cell lines was determined and the expression, activation and regulation of the complement system was characterised.

2.2. Specific aims of Chapter 2

The aim of this chapter was to characterise the complement system in an *in vitro* model of inherent radiosensitivity and radioresistance in CRC.

The specific aims for Chapter 2 are;

1. Determine the inherent radiosensitivities of a panel of CRC cell lines consisting of the human colon carcinoma HCT116 cell line and the human rectal adenocarcinoma SW837, HRA-19 and SW1463 cell lines.
2. Investigate the expression of the central complement cascade components C3 and C5 basally and following 1.8 Gy of X-ray radiation in HCT116, SW837, HRA-19 and SW1463 cell lines.
3. Assess the production of complement anaphylatoxins C3a and C5a in HCT116, SW837, HRA-19 and SW1463 cell lines to determine if complement is activated in CRC.
4. Determine if complement activation correlates with inherent radiosensitivity in HCT116, SW837, HRA-19 and SW1463 cell lines.
5. Investigate which pathway complement activation may be occurring by in HCT116, SW837, HRA-19 and SW1463 cell lines.
6. Examine the expression of complement receptors and mCRPs in HCT116, SW837, HRA-19 and SW1463 cell lines.

2.3. Materials and methods

2.3.1. Cell culture

Aseptic technique was adopted for all cell culture procedures. Cell culture work was carried out in a grade II laminar flow hood, which was switched on for at least 20 min prior to use. Before use, the area was decontaminated using 70% (v/v) ethanol. All reagents and equipment were sterilised with 70% ethanol prior to placing in the laminar flow hood.

2.3.2. Cell lines

The HCT116 human colon carcinoma cell line and the SW837, HRA-19 and SW1463 rectal adenocarcinoma cell lines were obtained from the European Collection of Authenticated Cell Cultures (ECACC) (Salisbury, United Kingdom).

2.3.3. Cell maintenance

The HCT116 and HRA-19 cell lines were maintained in vented 75cm^2 flasks in Roswell Park Memorial Institute 1640 (RPMI 1640) (Gibco) supplemented with 10% (v/v) foetal bovine serum (FBS) (Gibco) and 1% (v/v) penicillin-streptomycin (Lonza, Basel, Switzerland) (complete media) at 37°C, 5% CO_2/ 95% humidified air.

The SW837 and SW1463 cell lines were maintained in Leibovitz's 15 (L-15) medium (Lonza, Basel, Switzerland) supplemented with 10% (v/v) FBS, 1% (v/v) penicillin-streptomycin and 1% (v/v) L-Glutamine (Lonza, Basel, Switzerland) (complete medium). Cell lines cultured in L-15 were maintained at 37°C in non-vented 75cm^2 flasks as these cells grow independently of CO_2.

2.3.4. Cell sub-culture

Cells were visually examined daily using a light microscope and sub-cultured upon reaching 70-80% confluency. Cell culture reagents were pre-warmed to 37°C in a water bath prior to use. Cell culture media from confluent flasks was disposed of using a Vacusafe Aspiration System (INTEGRA Biosciences, Thatcham, United Kingdom). A 3 mL volume of warm phosphate buffered saline (PBS, 13.8 mM NaCl, 2.7 mM KCl, pH 7.4) (Gibco) was added to wash cells and then removed to waste. Cells were detached from the surface of the flask using 1 mL (HCT116 cells) or 3 mL (SW837, HRA-19 and SW1463 cells) of 0.1% (w/v) trypsin with 0.04% (w/v) ethylenediaminetetraacetic acid (EDTA) (Sigma). Flasks were incubated for 2-5 min at 37°C, 5% CO_2/ 95% humidified air to allow cells to detach from the surface of the flask. Trypsin was neutralised using an equal volume of

complete medium. This solution was used to seed new flasks at the recommended subcultivation ratios (1:3-1:10).

2.3.5. Preparation of frozen cell stocks

Frozen cell stocks were prepared from cells in the exponential growth phase. Cells were detached from the flask by trypsinisation as previously described (Section 2.3.4). Trypsin was neutralised and the cell solution was transferred to a sterile 15 mL tube. Cells were pelleted by centrifugation at 1,300 RPM for 3 min. The pellet was resuspended in complete growth medium supplemented with 10% (v/v) dimethyl sulfoxide (DMSO), which was added drop-wise and with agitation. This cell solution was added in 1 mL volumes to sterile 2 mL cryotubes. Cryotubes were added to a Mr Frosty Freezing Container (Thermofisher Scientific, Massachusetts, United States), which gradually lowers the temperature of the cell solution by 1°C per min. Cell stocks were stored at -80°C or in a liquid nitrogen freezer until required.

2.3.6. Reconstitution of frozen cell stocks

Cell stocks were retrieved from the -80°C freezer or liquid nitrogen storage and thawed rapidly by holding the cryotube in a 37°C water bath. The cell solution was transferred to a 15 mL tube containing 5 mL of warm complete growth medium. Cells were pelleted by centrifugation at 1,300 RPM for 3 min. The supernatant was discarded to waste and the cell pellet was re-suspended in 1 mL of warm complete growth medium. This cell suspension was then added to a 25 cm^2 flask containing 5 mL of complete growth medium. Cells were cultured at 37°C, 5% CO_2/ 95% humidified air.

2.3.7. Mycoplasma testing

All cell lines in culture were routinely tested for mycoplasma. To perform mycoplasma testing, a 1 mL volume of cell supernatant was collected from confluent flasks. Cell debris was pelleted by centrifugation at 2,000 RPM for 1 min. In an appropriate polymerase chain reaction (PCR) hood, the PCR reaction was set up using cell culture supernatant, GoTaq Green Master Mix (Promega), sense and antisense primers (10 μM) (Integrated DNA Technologies, Iowa, United States) and AccuGENE Molecular Biology Water (Fisher Scientific) (**Table 2-1**). A negative control (sterile water) and a positive control (supernatant from a known mycoplasma contaminated cell line) were included. The

PCR reaction was set up as outlined in **Table 2-2** and the PCR products were run on a 2% agarose gel (2 g of agarose in 200 mL of 1X Tris-Borate-EDTA buffer diluted from 10X stock (165 g Tris, 27.5g boric acid, 9.3g EDTA in 1 L of H_2O, pH adjusted to 8.3 using acetic acid)) for 30 min.

Table 2-1: Master mix for PCR reaction to perform mycoplasma testing.

Reagent	Volume/sample (μL)
GoTaq Green Master Mix	25
Sense primer GPO-3 (5′- GGGAGCAAACAGGATTAGATACCCT-3′)	1
Antisense primer MGSO (5′-TGCACCATCTGTCACTCTGTTAACCTC-3′)	1
AccuGENE Molecular Biology Water	22
Cell culture supernatant	1

Table 2-2: **PCR protocol for mycoplasma testing.**

Step	Time	Temperature (°C)	No. of Cycles
Hold Stage	5 min	95	1
PCR Stage	30 s	94	40
PCR Stage	30 s	55	40
PCR Stage	1 min	72	40
Hold Stage	10 min	72	1

2.3.8. Cell counting

Cells were counted using a Neubauer haemocytometer (Marienfeld, Lauda-Königshofen, Germany). Cells in the exponential growth phase were trypsinised (Section 2.3.4) and collected in 15 mL tubes by centrifuging at 1,300 RPM for 3 min. The supernatant was discarded and the cell pellet was re-suspended in 1 mL of complete medium. A 20 μL volume of this cell suspension was added to 180 μL of Trypan Blue Stain (0.4%) (Gibco) and 10 μL of this was added to the haemocytometer. Viable cells were distinguished from dead cells based on their exclusion of trypan blue, due to an intact cell membrane. Viable cells in the four corner squares of the haemocytometer grid were counted. Cells touching the upper and left sides of the squares were excluded. The number of cells/mL were calculated using the formula;

$$Average\ no.of\ cells\ per\ corner\ \times\ 10\text{^}4\ \times\ 10\ (dilution\ factor)$$

2.3.9. X-ray irradiation

Cells were irradiated using an Xstrahl RS225 X-ray irradiator (Xstrahl, Walsall, United Kingdom) at a dose rate of 1.74 Gy/min. A broad radiation beam of 12.5 cm x 12.5 cm produced by 195kV and 15 mA ensured that X-ray radiation was delivered uniformly to cells. Control plates were mock irradiated by placing at RT°.

2.3.10. Clonogenic assay

The inherent radiosensitivity of HCT116, SW837, HRA-19 and SW1463 cell lines was assessed by clonogenic assay, which measures a cells replicative potential post treatment and is the gold standard for measuring radioresistance[384]. Cells in the exponential growth phase were trypsinised, counted (Section 2.3.8) and single cell suspensions were prepared. In 6-well plates, cells were seeded at optimised seeding densities (**Table 2-3**) in complete RPMI and allowed to adhere overnight at 37°C, 5% CO_2/95% humidified air. Cells were irradiated, whilst control plates were mock irradiated (Section 2.3.9) at 24 h post seeding and incubated for 8-21 days at 37°C, 5% CO_2/95% humidified air until colonies had formed but not merged.

2.3.11. Staining of colonies

Colonies were fixed for 10 min using 700 µL of 4% (w/v) paraformaldehyde (SantaCruz, Texas, United States) (HCT116) or 25% (v/v) methanol (Honeywell, South Carolina, United States) (SW837, SW1463 and HRA-19) and stained for 20 min using 700 µL of 0.05% (w/v) crystal violet. The crystal violet solution was discarded and wells were washed with 1 mL of water. Plates were left to air dry overnight.

Table 2-3: Optimised clonogenic seeding densities.

X-ray radiation dose	Number of cells seeded per well (6-well plates)			
	HCT116	**SW837**	**HRA-19**	**SW1463**
0 Gy	500	3,000	3,000	4,000
1.8 Gy	1,000	6,000	4,000	8,000
2 Gy	1,000	6,000	4,000	8,000
4 Gy	2,000	8,000	5,000	1,000
6 Gy	4,000	10,000	6,000	1,200

Abbreviations; Gy, Gray

2.3.12. Colony Counting

A GelCount™ (Oxford Optronix Ltd, Abingdon, United Kingdom) colony counter was used to count the total number of colonies consisting of at least 50 cells. The plating efficiency (PE) determines the ratio of colonies grown from untreated cells with respect to the number of cells seeded. PE was calculated using the formula:

$$PE = \frac{No.\ colonies}{No.\ cells\ seeded}$$

The surviving fraction (SF), representing the number of colonies formed from treated cells with respect to the PE, was calculated using the formula:

$$SF = \frac{No.\ colonies}{No.\ cells\ seeded\ x\ PE}$$

Survival curves were constructed by graphing SF versus radiation dose using Prism 9 Software (GraphPad, California, United States).

2.3.13. RNA isolation

Cells were plated at optimised seeding densities **(Table 2-4)** in 6-well plates in complete RPMI, incubated at 37°C, 5% CO_2/ 95% humidified air for 24 h before being irradiated or mock irradiated (Section 2.3.9). Supernatants were discarded after 24 h or 48 h and cells were harvested by trypsinisation and stored in 1.5 mL eppendorfs at -80°C. RNA was isolated using the TRI Reagent® method. Cell pellets were thawed to RT° for 30 min and re-suspended in 0.5 mL of TRIzol Reagent (Thermofisher Scientific, Massachusetts, United States). Repeated pipetting of each sample was performed to ensure complete lysis of cells before incubation at RT° for 5 min. A 50 µL volume of 1-bromo-3-chloropropane was added, samples were vortexed for 10 s and centrifuged at 13,400 x g for 15 min at 4°C to separate samples into 3 phases, an upper colourless aqueous phase, a white interphase and a lower red organic phase. The upper aqueous layer was transferred to a new 1.5 mL eppendorf and RNA was precipitated by adding 250 µL of isopropanol. Samples were vortexed for 10 s, incubated at RT° for 5 min and centrifuged at 13,400 x g for 8 min at 4°C. Supernatants were discarded and cell pellets were washed using 0.5 mL of ethanol (70% v/v). Samples were centrifuged at 7,500 x g for 5 min at 4°C. After centrifuging, the ethanol was removed and the RNA pellets were air dried at RT° for 5 min. Pellets were re-suspended in 30 µL of RNase-free molecular water (Qiagen, Hilden, Germany).

Table 2-4: Cell seeding densities for RNA isolation.

Cell Line	Number of cells seeded per well (6-well plates)
HCT116	300,000
SW837	500,000
HRA-19	400,000
SW1463	400,000

2.3.14. RNA quantification

RNA was quantified spectrophotometrically using a Micro-Volume Spectrophotometer (MaestroNano, Hsinchu City, Taiwan). The instrument was first blanked using 1 μL of RNase-free water. RNA concentration in ng/μL was measured by loading 1 μL of each sample onto the pedestal. The A260/280 and A260/230 ratios were recorded to assess the quality of RNA isolated. RNA samples were stored at -80°C.

2.3.15. cDNA synthesis

RNA samples were thawed on ice for 10 min. For each sample, 1 μg of RNA was prepared in a total volume of 11 μL molecular grade water (Fisher Bioreagents). A 1 μL volume of random hexamer primers (Meridian Bioscience, Ohio, United States) was added to each sample. Samples were briefly centrifuged to pool the contents in each tube. Samples were heated to 70°C for 10 min to enable primer annealing. A reverse transcriptase master mix was prepared using 5x Reaction Buffer, dNTPs (10mM, prepared using a 1:1:1:1 ratio of dGTP, dCTP, dTTP and dATP in molecular grade water and RiboSafe RNase Inhibitor, Bioscript™ Reverse Transcriptase Enzyme and molecular grade water (All Meridian Bioscience, Ohio, United States) (**Table 2-5**). An 8 μL volume of this master mix was added to each sample before vortexing. Samples were incubated at 37°C for 1 h, heated to 70°C for 10 min to inactivate the reverse transcriptase enzyme before being held at 4°C. cDNA samples were stored at -20°C.

Table 2-5: Reverse transcription Master Mix for cDNA synthesis.

Reagent	Volume/sample (μL)
5 X Reaction Buffer	4
dNTP mix	1
RiboSafe RNase Inhibitor	0.5
Bioscript ™ Reverse Transcriptase Enzyme	0.5
Molecular Grade Water	2

Abbreviations; dNTP, deoxyribonucleotide triphosphate.

2.3.16. Quantitative real time qPCR

cDNA was used as the template for quantitative real-time PCR (qPCR). Each sample was plated in triplicate for each target assessed. Master mixes were prepared to contain 10 µL Taqman™ Gene Expression Master Mix, 8 µl molecular grade water (Fisher BioReagents) and 1µL Taqman™ gene-specific primer (Applied Biosystems) per sample. To a MicroAmp™ Optical 96-Well Reaction Plate (Applied Biosystems), 19 µL of master mix and 1 µL of cDNA was added. Molecular grade water (1 µL) was utilised for a non-template control. The plate was sealed using an optical adhesive cover (4titude®) and briefly centrifuged to pool the contents. qPCR was performed using a Quant Studio 5 Real-Time PCR System (Applied Biosystems) and the protocol outlined in **Table 2-6**. Data collection was performed at the extension stage.

Table 2-6: qPCR protocol.

Step	Time	Temperature (°C)	No. of Cycles
Hold Stage	2 min	50	1
Hold Stage	10 min	95	1
PCR Stage	15 s	95	40
PCR Stage	1 min	60	40

Abbreviations; PCR, polymerase chain reaction; s, seconds; min, minute.

2.3.17. Quantitative real-time qPCR data analysis

Data analysis was performed using the qPCR Relative Quantification App on the ThermoFisher Connect™ platform. The threshold cycle (Ct) values of triplicate wells were inspected to remove outliers. Samples amplifying after 37 cycles (Ct values greater than 37) were excluded from the analysis. Expression of target genes was normalised to the expression of the endogenous control gene, 18S. Relative changes in gene expression were assessed using the $2^{-\Delta\Delta CT}$ (Livak) method using one sample set as the calibrator for analysis[385].

2.3.18. Supernatant collection from CRC cell lines

Cells were plated at optimised seeding densities (**Table 2-4**) in 6-well plates in complete RPMI and incubated at 37°C, 5% CO_2/ 95% humidified air for 24 h before being irradiated or mock irradiated (Section 2.3.9). Supernatants were removed after 24 h and centrifuged at 1,300 RPM for 10 min to pellet cell debris and stored at -80°C. Cells were harvested by trypsinisation and centrifuged for 3 min at 1300 RPM. Cell pellets were washed twice with 500 µl of cold PBS and stored at -80°C for protein isolation

2.3.19. Protein isolation

Protein was isolated from cell pellets prepared as in Section 2.3.18 using 1X radioimmunoprecipitation assay (RIPA) buffer supplemented with one PhosSTOP phosphatase inhibitor tablet (Roche, Basel, Switzerland) and one cOmplete, Mini Protease Inhibitor Cocktail tablet (Roche, Basel, Switzerland) per 10 mL of buffer, prepared on the day of use. Cell pellets were thawed on ice and resuspended in 30 µL of 1X supplemented RIPA buffer. Repeated pipetting was performed to ensure complete cell lysis. Cell lysates were incubated on ice for 20 min and centrifuged at 13,400 RPM for 20 min at 4°C. Supernatants were removed to new eppendorf tubes and stored at -80°C.

2.3.20. Bicinchoninic acid assay

Protein concentration was determined using the Pierce bicinchoninic acid (BCA) protein assay kit (Thermofisher Scientific, Massachusetts, United States). A series of albumin standards (0-2000 µg/mL) were prepared by serial dilution and samples were diluted 1:5 using PBS. All standards and samples were assessed in duplicate. A 200 µL volume of working reagent (50 parts Reagent B per 1 part Reagent A) was added to each well. The plate was mixed for 30 s using a plate shaker before incubation at 37°C for 30 min. The plate was allowed to cool to RT and absorbance was determined at 562nm using a VersaMax Microplate Reader (Molecular Devices, California, United States). A standard curve was constructed using Prism 9 and interpolated to determine the protein concentration of each sample.

2.3.21. C3 and C5 ELISAs

The concentration of C3 and C5 from cell supernatants (collected as in Section 2.3.18) and protein lysates (prepared as in Section 2.3.19) from HCT116, SW837, HRA-19 and SW1463 cells was determined by enzyme-linked immunosorbent assay (ELISA) (Abcam, Cambridge, United Kingdom). Standards were prepared via serial dilution as per the manufacturer's instructions. A 50 µL volume of sample or standard was added to the microplate in duplicate. Following 2 h incubation at RT°, excess sample or standard was removed by washing five times with 1X wash buffer. A 50 µL volume of biotinylated complement antibody specific for C3 or C5 was added to each well and the plate was incubated for a further 1 h, at RT°. The plate was washed five times before 50 µL of 1X streptavidin-peroxidase conjugate was added to each well and the plate was incubated for

30 min. Following five more wash cycles, 50 µL of chromogen substrate was added per well and the plate was incubated for 10-20 min. When an optimal blue colour had developed, 50 µL of stop solution was added to each well to quench the reaction. The absorbance was read on a VersaMax Microplate Reader at 450 nm and 570 nm. Absorbances read at 570 nm were subtracted from those read at 450 nm to correct for optimal imperfections. The mean absorbances of the standards were graphed relative to concentration, and a line of best fit was determined by regression analysis using a 4-parameter logistic fit. The concentration of unknown samples was determined using the standard curve. C3 and C5 protein concentration was normalised to total protein concentration determined by BCA assay (Section 2.3.20).

2.3.22. C3a and C5a ELISAs

The concentration of C3a and C5a from cell supernatants (collected as in Section 2.3.18) and protein lysates (prepared as in Section 2.3.19) from HCT116, SW837, HRA-19 and SW1463 cells was determined by ELISA (RayBiotech, Georgia, United States). Standards were prepared via serial dilution as per the manufacturer's instructions. A 100 µL volume of sample or standard was added to the microplate in duplicate. Following 2.5 h incubation at RT° with gentle shaking, excess sample or standard was removed by washing four times with 1X wash buffer. A 100 µL volume of biotinylated complement antibody specific for C3a or C5a was added to each well and the plate was incubated for a further 1 h at RT° with gentle shaking. The plate was washed four times before 100 µL of 1X horseradish peroxidase-streptavidin solution was added to each well and the plate was incubated for 45 min. Following four more wash cycles, 100 µL of chromogen one-step substrate solution was added per well and the plate was incubated for 30 min at RT° in the dark with gentle shaking. When an optimal blue colour had developed, 50 µL of stop solution was added to each well to quench the reaction. The absorbance was read immediately using a VersaMax Microplate Reader at 450 nm. The mean absorbances of the standards were graphed relative to concentration, and a line of best fit was determined by regression analysis using a 4-parameter logistic fit. The concentration of unknown samples was determined using the standard curve. C3a and C5a protein concentration was normalised to total protein concentration determined by BCA assay (Section 2.3.20).

2.3.23. Seeding CRC cell lines for flow cytometry

For flow cytometry experiments, cells were seeded in 12-well plates. HCT116 cells were plated at a density of 1 x 10^5 cells/well and SW837, SW1463 and HRA-19 cells were plated at a density of 2 x 10^5 cells/well. Cells were left to adhere overnight and incubated for 24 h at 37°C, 5% CO_2/ 95% humidified air before being irradiated or mock irradiated (Section 2.3.9).

2.3.24. Extracellular flow cytometry staining

The expression of the membrane-bound complement regulatory proteins (mCRPs) (CD46, CD55 and CD59) and extracellular complement receptors (C3aR and C5aR1) was assessed by flow cytometry. Cells were plated as described (Section 2.3.23). After 24 h, supernatants were discarded, cells were washed with PBS and detached by trypsinisation. Trypsin was neutralised using complete RPMI and cell suspensions were transferred to fluorescence-activated cell sorting (FACS) tubes. Cells were centrifuged for 3 min at 1,300 RPM and washed twice with PBS. To eliminate dead cells during analysis, cells were stained with Zombie NIR (1:100 dilution in PBS) (Biolegend, California, United States). Cells were stained in the dark at RT° for 10 min. Without washing off the Zombie NIR, samples were stained at RT° in the dark for 15 min using optimised volumes of antibodies for mCRPs (Biolegend, California, United States) or the C3aR and C5aR1 (Miltenyi, Bergisch Gladbach, Germany) (**Table 2-7**). The volume per sample was made up to 100 µl using FACS Buffer (PBS with 2% FBS, 0.01% Sodium Azide). Cells were washed twice with FACS buffer and resuspended in 250 µl of FACS buffer.

Table 2-7: Antibodies and staining volumes used to assess expression of membrane-bound regulatory proteins and complement receptors.

Antibody	Optimised Staining volume (µL)
CD46-APC	5
CD55-PE	5
CD59-FITC	5
C3aR-APC	5
C5aR1-PE	5

2.3.25. Intracellular flow cytometry staining

Intracellular expression of the complement receptors C3aR and C5aR1 was assessed by flow cytometry using the eBioscience Intracellular Fixation and Permeabilization Buffer Set (Thermofisher Scientific, Massachusetts, United States). Cells were plated at optimised seeding densities (Section 2.3.23) and collected in FACS tubes before staining with Zombie NIR as previously described (Section 2.3.24). Cells were washed with FACS buffer (0.5 mL) and pelleted by centrifugation at 1300 RPMI for 3 min. Supernatants were discarded and cells were fixed using 100 µl of intracellular fixation buffer. FACS tubes were vortexed well and incubated in the dark at RT° for 20 min. Cells were washed with 1 mL of 1X permeabilization buffer (10X permeabilization buffer diluted 1:10 with distilled water) and centrifuged at 1300 RPM for 3 min. Antibody staining was performed using optimised volumes of C3aR and C5aR1 antibodies (**Table 2-7**) in a final volume of 100 µl of 1X permeabilization buffer per sample. Samples were incubated in the dark at RT° for 20 min before being washed twice with 1mL of 1X permeabilization buffer. Cells were pelleted by centrifugation as before and resuspended in 250 µl of FACS buffer.

2.3.26. Compensation beads

Compensation beads were prepared using the BD CompBead anti-mouse Ig, k/ negative control particle set (BD Biosciences). Compensation beads were vortexed well and one drop of each was added to a FACS tube containing 100 µl of PBS. The optimised antibody volume per sample was added. FACS tubes were incubated in the dark at RT° for 20 min. Beads were washed twice with FACS buffer and resuspended in 300 µl of FACS buffer.

2.3.27. Flow cytometry acquisition and analysis

Samples were acquired using a BD FACSCANTO™ II instrument and FACSDIVA™ Software ((BD Biosciences, New Jersey, United States). Flow cytometric analysis was performed using version 10.7.1 of FlowJo software (BD Biosciences). Doublets were excluded by plotting FSC-H x FSC-A and analysis was performed by gating on cells negative for Zombie NIR to ensure results were representative of live cells **(Fig. 2-1)**.

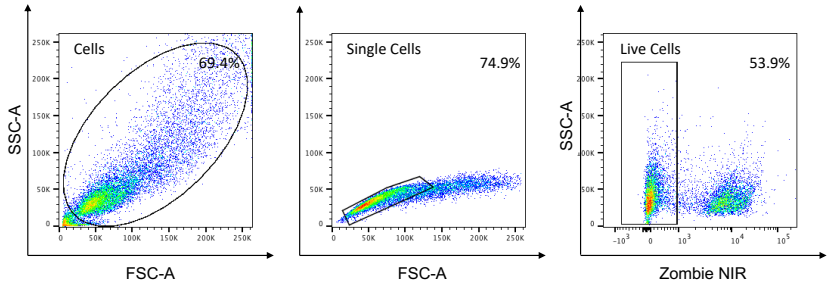

Figure 2-1: Gating strategy for identifying live cells during flow cytometric analysis of mCRPs or complement receptors.

2.3.28. Immunofluorescence to assess C3aR expression

Expression of the C3aR was assessed by immunofluorescence (IF) by David MacLean (University of Oxford). HCT116 cells in the exponential growth phase were trypsinised, resuspended in 10 mL of Dulbecco's Modified Eagles Medium (DMEM), supplemented with 10% FBS and 1% penicillin-streptomycin and counted using a Countess automated cell counter (Thermo Fisher Scientific). In a 6-well plate, coverslips were added to each well and 1.5 x 10^5 cells were carefully dispensed directly onto each coverslip. A 2 mL volume of complete media was carefully added to each well. To disperse cells over the coverslip, the plate was gently rocked three times in each direction. Plates were incubated for 24 h at 37°C, 5% CO_2/95% humidified air. After 24 h, cells were irradiated using a GSR D1 caesium-137 gamma irradiator (Gamma-Service Medical GmbG, Leipzig, Germany) at a dose rate of 1.7 Gy/min.

At 24 h post irradiation, media was carefully removed from each well and cells were gently washed using 1 mL of PBS, taking care to avoid dispensing the PBS directly onto the coverslip. A 500 µL volume of Fixation Buffer (4% (v/v) PFA in PBS) was carefully added in a drop-wise monition to each coverslip, and cells were fixed by incubating for 15 min at RT°. Fixation buffer was removed and cells were washed using 1 mL of PBS. Coverslips containing fixed cells were stored in 1-2 mL of PBS, in a 6-well plate, at 4°C until staining. Before staining, PBS was removed and cells were permeabilised by careful addition of 500 µL of Lysis Buffer (1% PBS-T; 1 mL Triton-X in 100 mL PBS) to each coverslip, and incubation for 10 min at RT°. Lysis Buffer was removed and replaced with 500 µL of Blocking Solution (2% bovine serum albumin (BSA) in 0.1% PBS-Triton-X; 0.2 g BSA, 10 µL Triton-X, 10 mL PBS) and cells were incubated for 1 h at RT°. Blocking Solution was removed and cells were carefully washed using 1 mL of ice-cold Wash Buffer (0.25% PBS-T; 250 µL Triton-X in 100 mL PBS). Wash Buffer was removed and cells

were stained with 75 µL of C3aR antibody (D-12) (Santa Cruz Biotechnology Inc, California, United States) (1:50 dilution in blocking buffer). The 6-well plate was incubated in a humidified chamber within a 37°C oven for 1 h. Primary antibody was removed and cells were washed three times using 1 mL of ice-cold Wash Buffer and once with 1 mL of PBS. A 75 µL volume of donkey anti-Mouse secondary antibody Donkey anti-Mouse IgG (H+L) Highly Cross-Adsorbed Secondary Antibody, Alexa Fluor™ Plus 594 (Thermo Fisher Scientific) (diluted 1:250 in blocking buffer) was added to each slide. Slides were incubated in a humidified chamber within a 37°C oven for 1 h. Cells were washed twice with 1 mL of Wash Buffer and once with 1 mL of PBS. A 75 µL volume of Phalloidin-iFluor 488 reagent (Abcam) (1:1000 dilution with Blocking Buffer) was added to each coverslip and the plate was incubated in a humidified chamber within a 37°C oven for 20 min. Cells were washed twice with 1 mL of Wash Buffer and once with 1 mL of PBS as before. Coverslips were mounted onto slides using 7 µL of ProLong Gold antifade mounting reagent with DAPI (Thermo Fisher Scientific). Slides were stored horizontally, protected from light overnight at RT°, then subsequently stored at 4°C until imaged.

Slides were imaged using a Zeiss LSM 710 confocal microscope (Carl Zeiss AG, Jena, Germany) and images were acquired and processed using ZEN (blue edition) software (Carl Zeiss AG), with 10 photos taken per condition. Signal quantification was performed using Cell Profiler cell image analysis software[386] (Cimini Lab, Broad Institute of MIT and Harvard, United States).

2.3.29. Statistical analysis

Graphing of results and statistical analysis was performed using Prism 9 Software (GraphPad, California, United States). All data are presented as mean ± standard error of the mean (SEM), unless otherwise indicated. Significance was determined by analysis of variance (ANOVA) with post-hoc Tukey's multiple comparisons testing or Student's *t*-test, as detailed in figure legends. Where comparison groups were paired (i.e. untreated vs. treated), a paired *t*-test was performed, otherwise unpaired *t*-tests were used. Results were considered significant where probability (p) ≤ 0.05. Correlations were performed using Pearson's correlation coefficient.

2.4. Results

2.4.1. CRC cell lines differ in inherent radiosensitivity

To investigate the potential role of complement in the radioresponse, the inherent radiosensitivity of a panel of human CRC cell lines was investigated to identify an *in vitro* model of inherent radioresistance/radiosensitivity. The radiosensitivity of the human colon carcinoma (HCT116) and human rectal adenocarcinoma (SW837, HRA-19 and SW1463) cell lines was assessed using the gold standard clonogenic assay, which measures a cells reproductive integrity post treatment. The surviving fraction (SF) of each cell line was assessed at 1.8, 2, 4 and 6 Gy bolus doses of X-ray radiation and survival curves were constructed **(Fig. 2-2 A)**. The area under the curve (AUC) was calculated for each cell line, demonstrating that HCT116 cells are overall significantly more radiosensitive, when compared to the human rectal adenocarcinoma SW837, HRA-19 and SW1463 cell lines ($p < 0.0001$ for all) (AUC ± SEM; HCT116 1.703 ± 0.027, SW837 3.376 ± 0.040, HRA-19 3.782 ± 0.079, SW1463 3.581 ± 0.120) **(Fig. 2-2 B)**.

The human colon carcinoma HCT116 cell line was demonstrated to be significantly more radiosensitive, when compared to the human rectal adenocarcinoma SW837, HRA-19 and SW1463 cell lines at clinically-relevant doses of 1.8 Gy and 2 Gy ($p < 0.0001$ for all) (SF at 1.8 Gy ± SEM; HCT116 0.324 ± 0.014, SW837 0.681 ± 0.025, HRA-19 0.709 ± 0.030, SW1463 0.836 ± 0.015) (SF at 2 Gy ± SEM; HCT116 0.313 ± 0.014, SW837 0.686 ± 0.016, HRA-19 0.738 ± 0.026, SW1463 0.836 ± 0.005) **(Fig. 2-2 C-D)**. HCT116 cells were also significantly more radiosensitive, when compared to SW837 ($p = 0.0001$), HRA-19 ($p < 0.0001$) and SW1463 ($p < 0.0001$) cells at 4 Gy (SF at 4 Gy ± SEM; HCT116 0.038 ± 0.001, SW837 0.394 ± 0.002, HRA-19 0.484 ± 0.019, SW1463 0.412 ± 0.055) **(Fig. 2-2 E)**. In addition, at 6 Gy HCT116 cells were significantly more radiosensitive, when compared to SW837 ($p = 0.0010$) and HRA-19 cells ($p < 0.0001$) (SF at 6 Gy ± SEM; HCT116 0.002 ± 0.0000732, SW837 0.215 ± 0.015, HRA-19 0.338 ± 0.045) **(Fig. 2-2 F)**.

Human rectal adenocarcinoma SW1463 cells were demonstrated to be significantly more radioresistant following irradiation with a clinically-relevant dose of 1.8 Gy, when compared to human rectal adenocarcinoma SW837 ($p = 0.0034$) and HRA-19 ($p = 0.0186$) cells (SF ± SEM; SW1463 0.836 ± 0.015, SW837 0.681 ± 0.025, HRA-19 0.709 ± 0.030) **(Fig. 2-2 C)**. SW1463 cells were also demonstrated to be significantly more radioresistant following 2 Gy of X-ray radiation, when compared to SW837 ($p = 0.0012$) and HRA-19 ($p = 0.0157$) rectal cancer cells (SF ± SEM; SW1463 0.836 ± 0.005, SW837 0.686 ± 0.016, HRA-19 0.738 ± 0.026) **(Fig. 2-2 D)**.

The HRA-19 cell line was demonstrated to be significantly more radioresistant, when compared to SW837 ($p = 0.0265$) and SW1463 ($p = 0.0003$) rectal cancer cells at 6 Gy. SW837 cells were also significantly more radioresistant at 6 Gy of X-ray radiation, when compared to SW1463 cells ($p = 0.0196$) (SF ± SEM; HRA-19 0.338 ± 0.045, SW837 0.215 ± 0.015, SW1463 0.085 ± 0.002) **(Fig. 2-2 F)**.

This data demonstrates that the human colon carcinoma HCT116 cell line is significantly more radiosensitive, when compared to the human rectal adenocarcinoma SW837, HRA-19 and SW1463 cell lines and thus this cell line panel represents an *in vitro* model of inherent radiosensitivity/radioresistance in CRC.

2.4.2. CRC cell lines express C3 and C5 mRNA

Having characterised the radiosensitivity of HCT116, SW837, HRA-19 and SW1463 cells, the expression of the central complement cascade components, C3 and C5 was assessed at the mRNA level by qPCR.

C3 mRNA was expressed in HCT116, HRA-19 and SW837 cells. The radioresistant HRA-19 rectal cancer cell line expressed significantly higher levels of C3 mRNA, when compared to the radiosensitive HCT116 cell line ($p = 0.0006$) and the SW837 cell line ($p = 0.004$). SW837 cells expressed significantly higher levels of C3 mRNA, when compared to HCT116 cells ($p = 0.0143$) (C3 relative mRNA expression ± SEM; HRA-19 40.27 ± 3.683, HCT116 2.631 ± 0.957, SW837 13.763 ± 2.511) **(Fig. 2-3 A)**. C3 mRNA expression was not detected in the SW1463 cell line.

Interestingly, all cell lines demonstrated C5 mRNA expression. The radioresistant SW1463 cell line expressed significantly higher levels of C5 mRNA, when compared to HCT116 ($p = 0.0011$), SW837 ($p = 0.0261$) and HRA-19 ($p = 0.0013$) cell lines (C5 relative mRNA expression ± SEM; SW1463 66.662 ± 7.827, HCT116 0.901 ± 0.189, HRA-19 3.223 ± 0.521, SW837 31.081 ± 6.726) **(Fig. 2-3 B)**. The SW837 cell line demonstrated significantly increased expression of C5 mRNA, when compared to the radiosensitive HCT116 cell line ($p = 0.0109$) and the HRA-19 cell line ($p = 0.0145$) (C5 relative mRNA expression ± SEM; SW837 31.081 ± 6.726, HCT116 0.901 ± 0.189, HRA-19 3.223 ± 0.521) **(Fig. 2-3 B)**. The radioresistant HRA-19 cell line expressed significantly higher levels of C5 mRNA, when compared to the radiosensitive HCT116 cell line ($p = 0.0138$) (C5 relative mRNA expression ± SEM; HRA-19 3.223 ± 0.521, HCT116 0.901 ± 0.189). This data demonstrates that central complement components are expressed by CRC cells, with relative expression levels differing between cell lines.

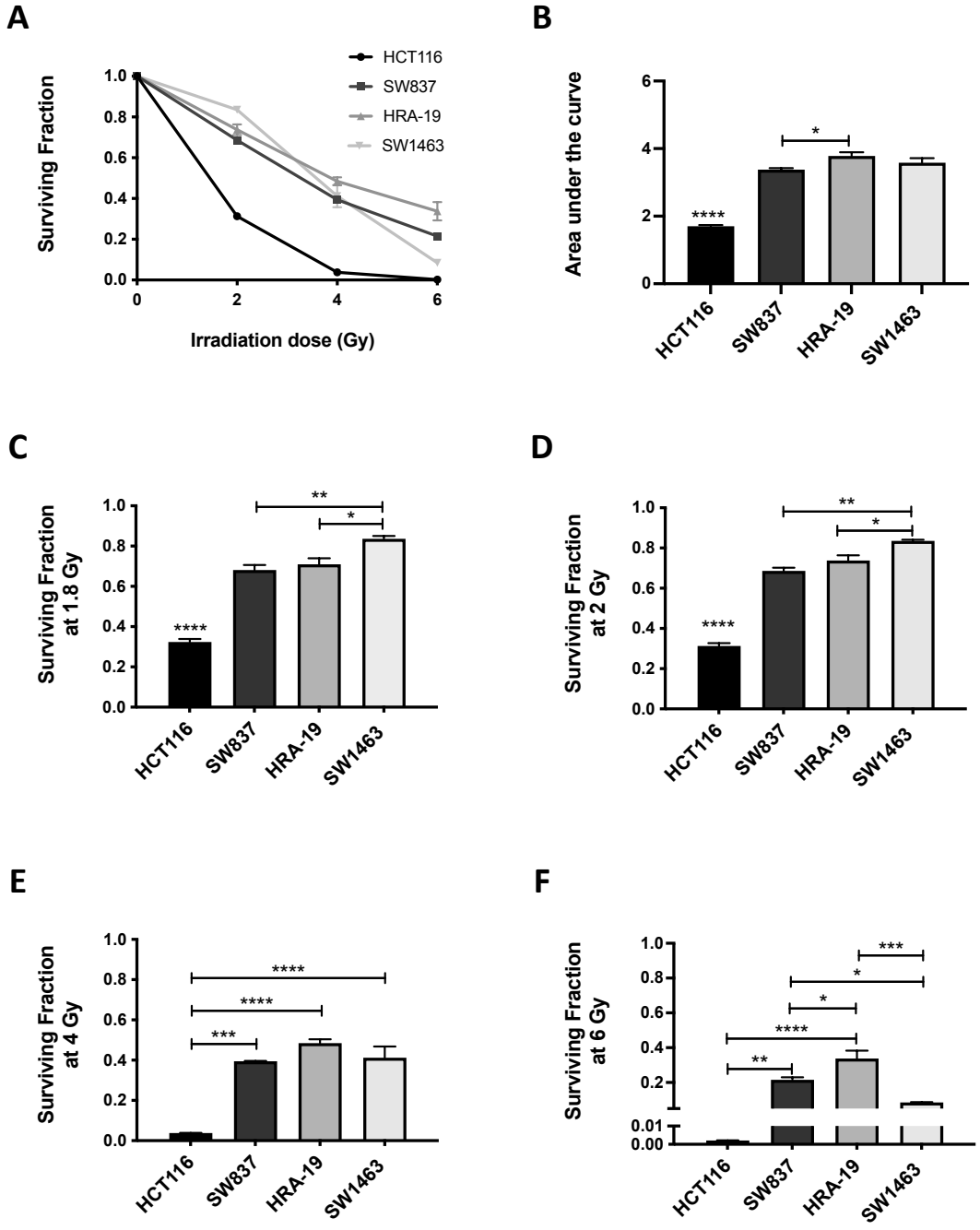

Figure 2-2: Radiosensitivity profiles of human colon carcinoma HCT116 and human rectal adenocarcinoma SW837, HRA-19 and SW1463 cell lines. The radiosensitivity of HCT116, SW837, HRA-19 and SW1463 cells was assessed by clonogenic assay. **(A)** Survival curves **(B)** Area under the curve and **(C-F)** surviving fraction following treatment with 0 Gy, 1.8 Gy, 2 Gy, 4 Gy and 6 Gy of X-ray radiation. Controls were mock-irradiated. Data are presented as mean SF ± SEM for 3 independent experiments. Statistical analysis was performed by one-way ANOVA and post-hoc Tukey's multiple comparisons testing. * $p < 0.05$, ** $p < 0.01$, *** $p < 0.001$, **** $p < 0.0001$.

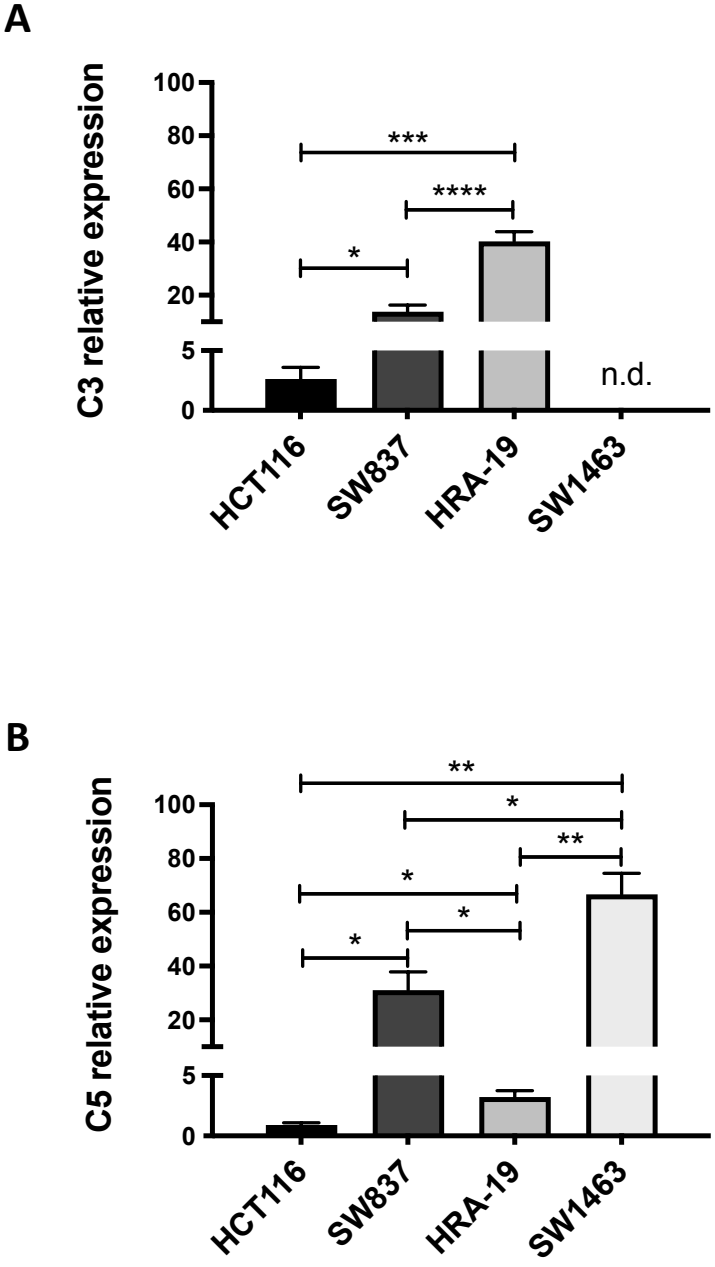

Figure 2-3: C3 and C5 mRNA is expressed by radiosensitive HCT116 and radioresistant SW837, HRA-19 and SW1463 cell lines. mRNA expression of **(A)** C3 and **(B)** C5 was assessed basally in HCT116, SW837, HRA-19 and SW1463 cells by qPCR. Data are presented as mean ± SEM for 3 independent experiments. Statistical analysis was performed by unpaired two-tailed Student's *t*-test. * $p < 0.05$, ** $p < 0.01$, *** $p < 0.001$, **** $p < 0.0001$. Abbreviations; n.d., not detected.

2.4.3. Total basal C3 and C5 mRNA expression is increased in radioresistant CRC cells

C3 and C5 are both central complement cascade components. To assess the overall C3 and C5 expression profile in CRC cell lines, the total expression of C3 and C5 mRNA was examined for each cell line. The radiosensitive HCT116 cell line expressed significantly lower relative levels of cumulative central complement cascade components (C3 and C5), when compared to SW837 ($p = 0.006$), HRA-19 ($p = 0.008$) and SW1463 ($p = 0.0004$) cell lines (Total relative C3 + C5 mRNA expression ± SEM; HCT116 3.532 ± 0.830, SW837 44.844 ± 9.001, HRA-19 43.494 ± 3.261, SW1463 66.729 ± 7.812) **(Fig. 2-4)**. This data suggests that complement expression is increased in radioresistant cell lines in CRC.

2.4.4. Radiation increases C5 mRNA expression in HCT116 cells

To investigate the potential effect of X-ray radiation on complement expression, C3 and C5 mRNA expression in CRC cell lines was assessed at 24 h and 48 h following a clinically-relevant dose of 1.8 Gy of X-ray radiation. There was no significant alteration in C3 mRNA expression at either 24 h or 48 h following 1.8 Gy, when compared to baseline levels in HCT116 **(Fig. 2-5 A)**, SW837 **(Fig. 2-5 B)** or HRA-19 cells **(Fig. 2-5 C)**.

Similar to C3, there were no significant alterations in C5 mRNA expression in SW837 **(Fig. 2-5 E)**, HRA-19 **(Fig. 2-5 F)** or SW1463 **(Fig. 2-5 G)** cell lines following X-ray radiation relative to basal expression. Interestingly, in the radiosensitive HCT116 cell line, C5 mRNA was significantly increased at 48 h following 1.8 Gy of X-ray radiation, when compared to basal levels ($p = 0.0326$) and levels at 24 h following radiation ($p = 0.0288$) (C5 relative mRNA expression ± SEM; HCT116 48 h post 1.8 Gy X-ray radiation 1.865 ± 0.210, HCT116 + 0 Gy X-ray radiation 0.901 ± 0.189, HCT116 24 h post 1.8 Gy X-ray radiation 0.751 ± 0.142) **(Fig. 2-5 D)**. These data demonstrate that radiation can induce alterations in complement expression in CRC, suggesting that radiation increases complement expression in radiosensitive cells.

2.4.5. CRC cell lines secrete C3 and C5 protein, with higher levels secreted by radioresistant cells

Having demonstrated that C3 and C5 were expressed by CRC cell lines at the mRNA level, the protein expression of these central complement cascade components was investigated by ELISA. To determine whether complement proteins were secreted from

CRC cells the concentration of C3 and C5 was assessed in supernatants generated from the panel of CRC cell line. Supporting the mRNA data, significantly lower levels of C3 protein were detected in the supernatant of HCT116 cells, when compared to SW837 ($p = 0.0005$) and HRA-19 cells ($p = 0.0274$) (C3 concentration (ng/mL) ± SEM; HCT116 0.191 ± 0.047, SW837 4.151 ± 0.376, HRA-19 11.142 ± 3.224) **(Fig. 2-6 A)**. C3 protein was not detected in supernatants collected from SW1463 cells **(Fig. 2-6 A)**.

C5 protein was present in supernatants from all CRC cell lines investigated. Significantly higher levels of C5 were secreted from SW1463 cells, when compared the HCT116 ($p = 0.0038$), SW837 ($p = 0.0049$), and HRA-19 ($p = 0.0275$) cell lines (C5 concentration (ng/mL) ± SEM; SW1463 2.878 ± 0.436, HCT116 0.246 ± 0.021, SW837 0.271 ± 0.156 HRA-19 1.036 ± 0.324) **(Fig. 2-6 B)**. This data demonstrates that complement is secreted from CRC cells at low levels, with higher levels secreted from radioresistant cells.

2.4.6. CRC cell lines contain C3 and C5 protein intracellularly, with higher levels present in radioresistant cells

To determine if complement was present intracellularly in CRC cells, the concentration of C3 and C5 in protein lysates prepared from each CRC cell line was assessed. C3 protein was present in lysates from all CRC cell lines in the panel, including SW1463 cells. Protein lysates from SW1463 cells contained significantly higher levels of C3 protein, when compared to HCT116 ($p < 0.0001$) and SW837 ($p = 0.0001$) cells (C3 concentration (ng/mL) ± SEM; SW1463 43.659 ± 1.731, HCT116 7.628 ± 1.239, SW837 10.887 ± 1.553) **(Fig. 2-6 C)**. Similarly, increased levels of C3 protein were present in protein lysates from HRA-19 cells when compared to HCT116 ($p = 0.0145$) and SW837 ($p = 0.0196$) cells (C3 concentration (ng/mL) ± SEM; HRA-19 46.838 ± 9.409, HCT116 7.628 ± 1.239, SW837 10.887 ± 1.553) **(Fig. 2-6 C)**. The concentration of C5 protein in lysates from the radiosensitive HCT116 cell line was significantly lower, when compared to the radioresistant HRA-19 ($p = 0.0145$) and SW1463 ($p < 0.0001$) cell lines (C5 concentration (ng/mL); HCT116 1.526 ± 0.248, HRA-19 9.368 ± 1.882, SW1463 8.732 ± 0.346). Similarly, lower levels of C5 protein were present in lysates from SW837 cells, when compared to HRA-19 cells ($p = 0.0157$) and SW1463 cells ($p < 0.0001$) (C5 concentration (ng/mL); SW837 1.723 ± 0.230, HRA-19 9.368 ± 1.882, SW1463 8.732 ± 0.346) **(Fig. 2-6 D)**. These data demonstrate that C3 and C5 protein are present intracellularly in CRC cells with increased complement production occurring in radioresistant cells

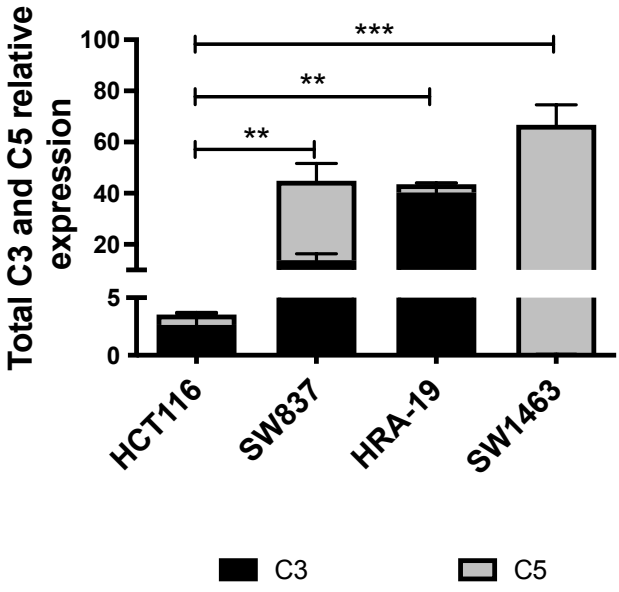

Figure 2-4: Total C3 and C5 mRNA expression in radiosensitive HCT116 and radioresistant SW837, HRA-19 and SW1463 cell lines. Overall cumulative expression of C3 and C5 mRNA in HCT116, SW837, HRA-19 and SW1463 cells was assessed at basal level by qPCR. Data are presented as mean ± SEM for 3 independent experiments. Statistical analysis was performed by one-way ANOVA and post-hoc Tukey's multiple comparisons testing. $^{**}p < 0.01$, $^{***}p < 0.001$.

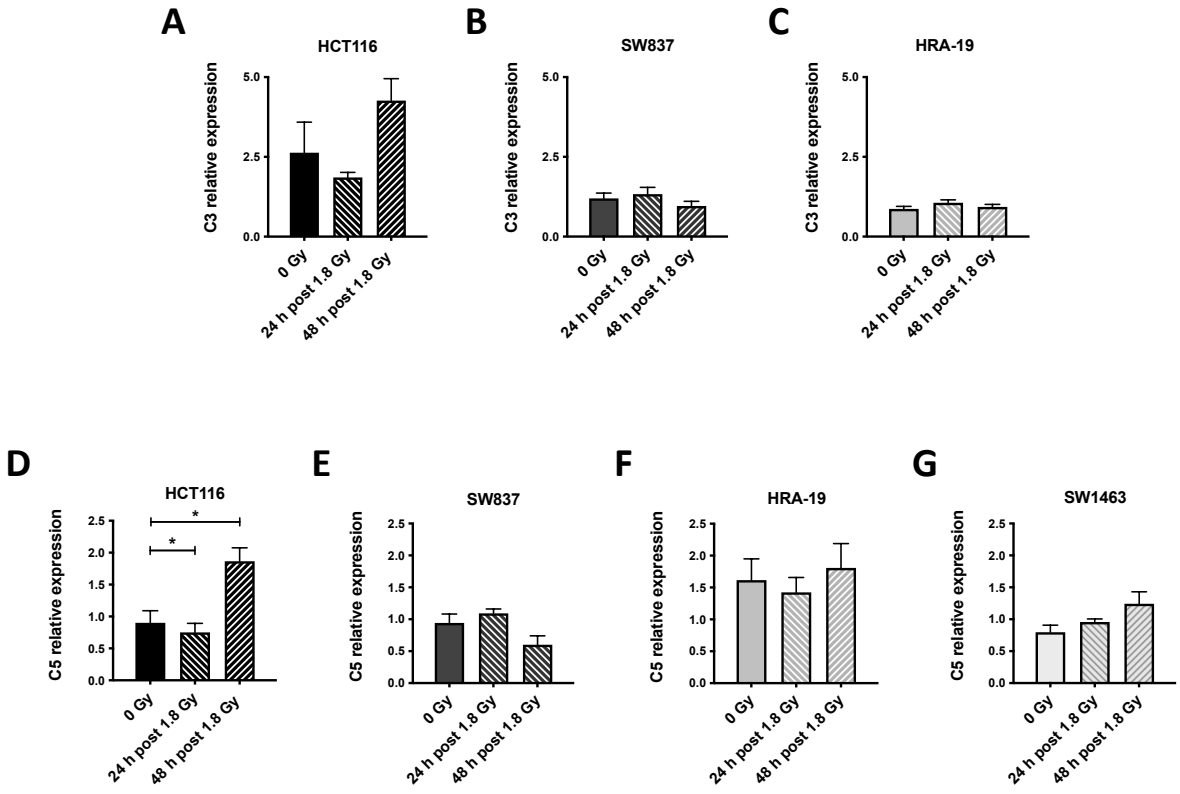

Figure 2-5: Radiation upregulates C5 mRNA expression in radiosensitive HCT116 cells. C3 mRNA expression basally relative to expression at 24 h and 48 h post 1.8 Gy of X-ray radiation in **(A)** HCT116, **(B)** SW837 and **(C)** HRA-19 cells. C5 mRNA expression basally relative to expression at 24 h and 48 h post 1.8 Gy of X-ray radiation in **(D)** HCT116, **(E)** SW837 **(F)** HRA-19 and **(G)** SW1463 cells. Data are presented as mean ± SEM for 3 independent experiments. Statistical analysis was performed by paired two-tailed Student's *t*-test. *$p < 0.05$.

.

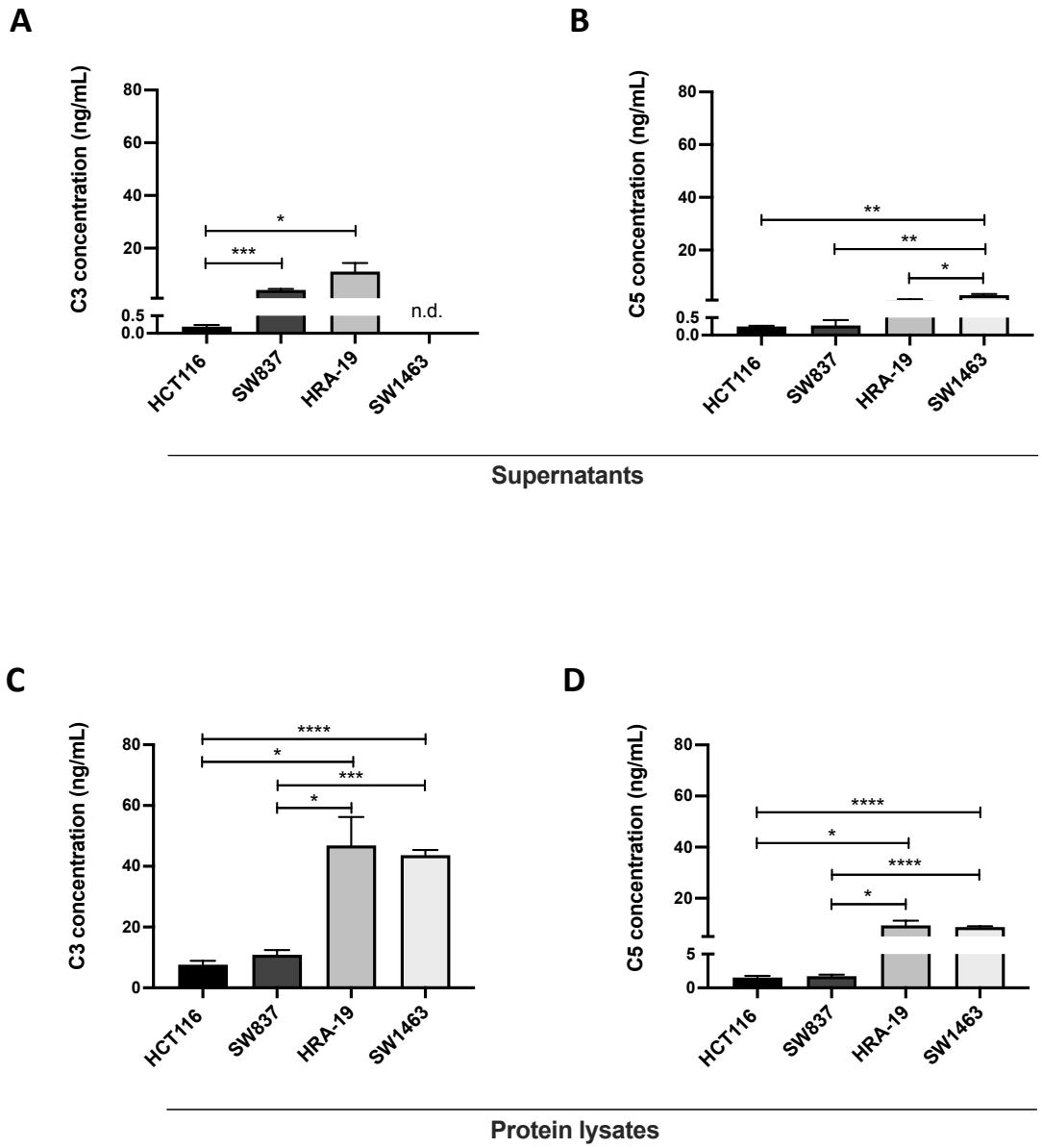

Figure 2-6: C3 and C5 protein is secreted from and present intracellularly in CRC cells. Protein concentration of C3 and C5 in **(A-B)** cell supernatants and **(C-D)** protein lysates from HCT116, SW837, HRA-19 and SW1463 cells. Data are presented as mean ± SEM for 3 independent experiments. Statistical analysis was performed by unpaired two-tailed Student's *t*-test. * $p < 0.05$, ** $p < 0.01$, *** $p < 0.001$, **** $p < 0.0001$. Abbreviations; n.d., not detected.

2.4.7. Radiation increases C3 and C5 protein production in HCT116 cells

Having demonstrated that C3 and C5 protein are produced by the CRC cell line panel, the effects of radiation on complement protein production was assessed. CRC cells were irradiated with a clinically-relevant dose of 1.8 Gy and C3 and C5 levels were investigated by ELISA. At the mRNA level, radiation induced alterations in C5 expression only in the radiosensitive HCT116 cell line (Section 2.4.4). Therefore, these experiments were performed using only HCT116 cells and one radioresistant cell line, the SW1463 cell line. Protein was isolated at 48 h post irradiation.

Radiation did not alter the concentration of C3 protein present in supernatants from HCT116 cells **(Fig. 2-7 A)**. In SW1463 cell supernatants, C3 protein was not detected basally or following radiation treatment. The concentration of C5 protein in supernatants from HCT116 cells was unaltered following radiation **(Fig. 2-7 B)**. In SW1463 cell supernatants however, significantly higher levels of C5 protein were detected 48 h post 1.8 Gy of X-ray radiation, when compared to basal levels (p = 0.0042) (C5 concentration (ng/mL) ± SEM; SW1463 0 Gy 2.878 ± 0.436, SW1463 48 h post 1.8 Gy 5.244 ± 0.304) **(Fig. 2-7 B)**.

In HCT116 cell lysates, C3 protein levels were significantly elevated 48 h following 1.8 Gy of radiation, when compared to basal levels (p = 0.0458) (C3 concentration (ng/mL) ± SEM; HCT116 0 Gy 7.628 ± 1.239, HCT116 24 h post 1.8 Gy 10.430 ± 1.532) (**Fig. 2-8 C**). There were no alterations in C3 protein levels in SW1463 cell lysates following 1.8 Gy of X-ray radiation, when compared to basal expression **(Fig. 2-7 C)**. Increased levels of C5 protein were also present in HCT116 cell lysates 48 h following 1.8 Gy of X-ray radiation, when compared to basal levels (p = 0.0458) (C5 concentration (ng/mL) ± SEM; HCT116 0 Gy 1.526 ± 0.248, HCT116 48 h post 1.8 Gy 2.086 ± 0.306) **(Fig. 2-7 D)**. There were no alterations in the levels of C5 protein present in SW1463 cell lysates at 48 h post 1.8 Gy of X-ray radiation, when compared to basal levels (**Fig. 2-7 D)**. These data demonstrate that radiation can upregulate the production of complement protein both in radiosensitive and radioresistant CRC cell lines.

2.4.8. The complement system is activated in CRC cells, with higher levels of activation in radioresistant cells

Having demonstrated that complement system components are expressed at both the mRNA and protein level, activation of the complement system within CRC cells was investigated. Activation of the complement system results in the production of C3a and

C5a, two potent anaphylatoxins derived from C3 and C5 proteins, respectively. The production of both secreted and intracellular C3a and C5a was assessed by ELISA.

C3a and C5a were detected in cell supernatants from HCT116, SW837, HRA-19 and SW1463 cells using commercially available ELISAs, however the levels were outside of the standard curve and could not be quantified. This suggests that these cells secrete anaphylatoxins at low levels.

Both C3a and C5a were present intracellularly in all cell lines investigated. Significantly lower levels of C3a were present in lysates from the radiosensitive HCT116 cell line, when compared to the SW837 ($p = 0.0167$), HRA-19 ($p = 0.0434$) and SW1463 ($p = 0.0247$) cell lines (Concentration C3a (ng/mL); HCT116 12.770 ± 1.431, SW837 21.120 ± 1.548, HRA-19 33.765 ± 7.056, SW1463 48.909 ± 10.197) **(Fig. 2-8 A)**. Similarly, the concentration of C5a was significantly lower in lysates from HCT116 ($p = 0.0185$) and SW837 cells ($p = 0.0166$), when compared to SW1463 cells (Concentration C5a (ng/mL); HCT116 0.324 ± 0.31, SW837 0.239 ± 0.128, SW1463 2.913 ± 0.661) **(Fig. 2-8 B)**. These results demonstrate that the complement system is activated intracellularly in CRC cells, with higher levels of anaphylatoxins produced by radioresistant cells.

2.4.9. Radiation does not alter complement anaphylatoxin production in CRC cells

Having determined that complement was activated intracellularly in CRC cell lines, the effect of X-ray radiation on anaphylatoxin production was assessed. Levels of C3a and C5a were investigated in cell supernatants from the radioresistant HCT116 cell line and the radioresistant SW1463 cell line at 48 h post 1.8 Gy of X-ray radiation. C3a and C5a were not detected in cell supernatants following radiation, suggesting that radiation does not induce the secretion of anaphylatoxins from CRC cells.

The effect of X-ray radiation on intracellular levels of C3a and C5a was also assessed at 48 h post 1.8 Gy of radiation. There were no alterations in the levels of C3a in protein lysates from HCT116 or SW1463 cells at 48 h post 1.8 Gy of X-ray radiation, when compared to controls (**Fig. 2-9 A-B**). Similarly, 1.8 Gy of X-ray radiation did not induce alterations in intracellular C5a production in HCT116 and SW1463 cells, when compared to basal levels (**Fig. 2-9 C-D**). These data suggest that complement anaphylatoxin production is not induced by X-ray radiation in CRC cells.

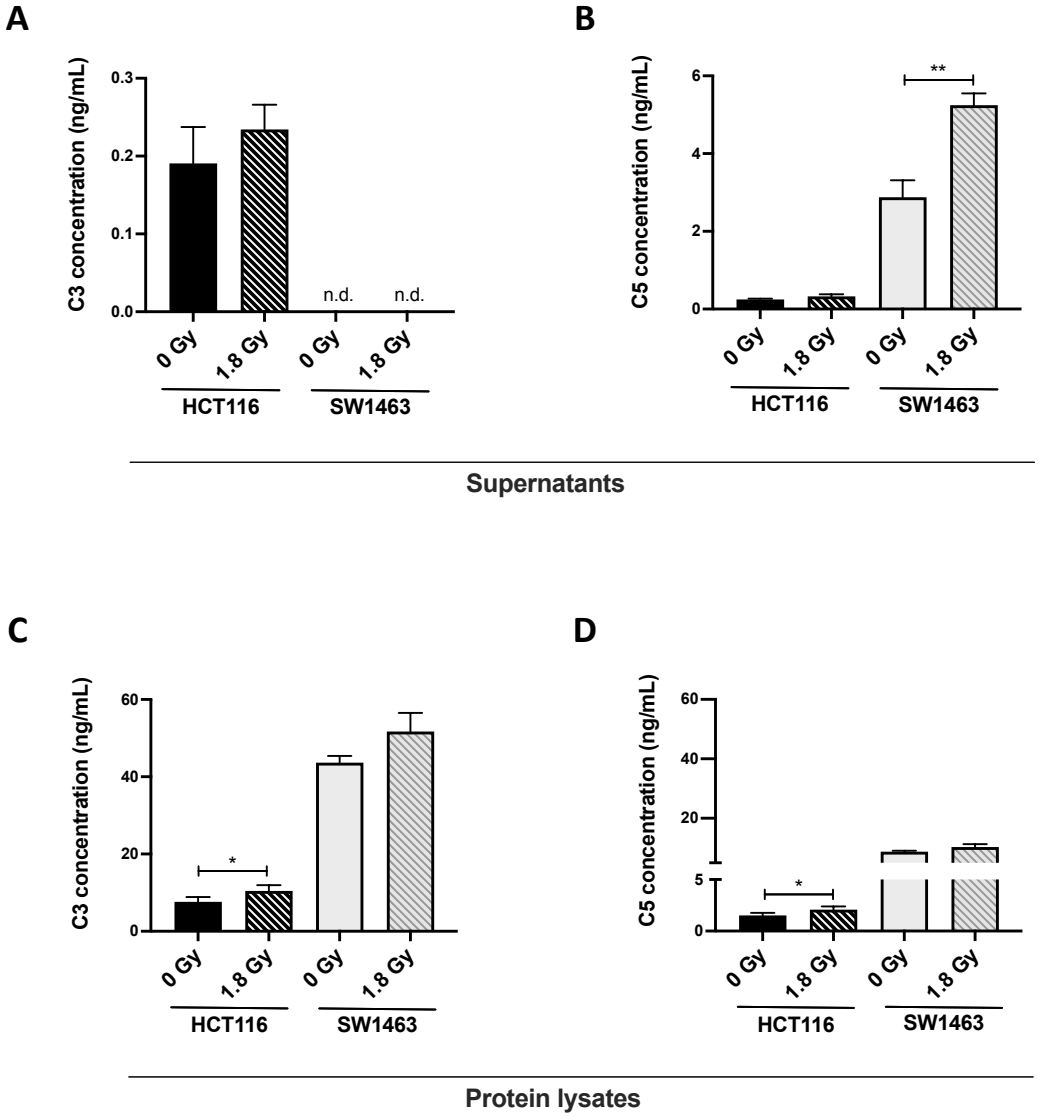

Figure 2-7: C3 and C5 protein expression is increased in radiosensitive HCT116 cells at 48 h post irradiation with 1.8 Gy. C3 and C5 protein was assessed basally and at 48 h post 1.8 Gy of X-ray radiation in HCT116 and SW1463 cells. **(A)** C3 and **(B)** C5 protein concentration was assessed in cell supernatants. **(C)** C3 and **(D)** C5 protein concentration was assessed in cell lysates. Data are presented as mean ± SEM for 3 independent experiments. Statistical analysis was performed by paired two-tailed Student's *t*-test. *$p < 0.05$, **$p < 0.01$. Abbreviations; n.d., not detected.

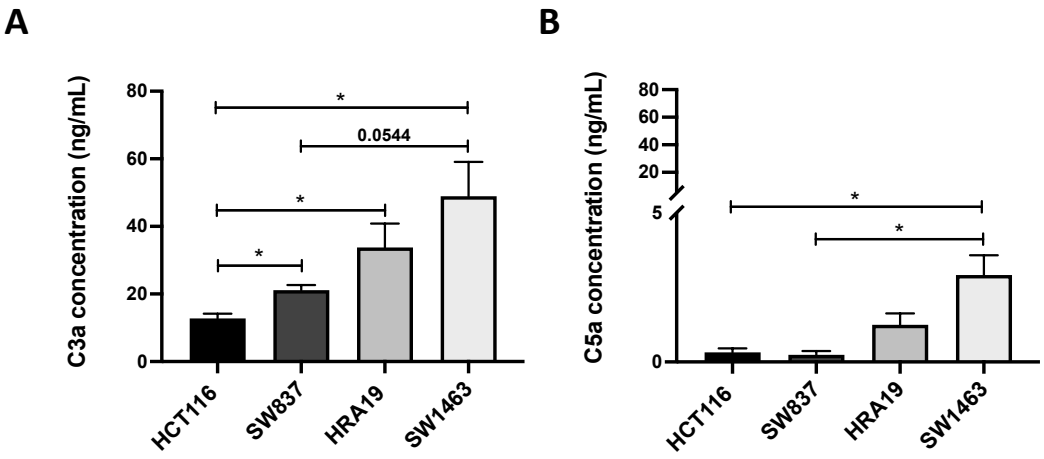

Figure 2-8: Complement anaphylatoxins are present intracellularly in radiosensitive HCT116 and radioresistant SW837, HRA-19 and SW1463 cell lines. The concentration of **(A)** C3a and **(B)** C5a was assessed in protein lysates from HCT116, SW837, HRA-19 and SW1463 cells. Data are presented as mean ± SEM for 3 independent experiments. Statistical analysis was performed by unpaired two-tailed Student's *t*-test. * $p < 0.05$.

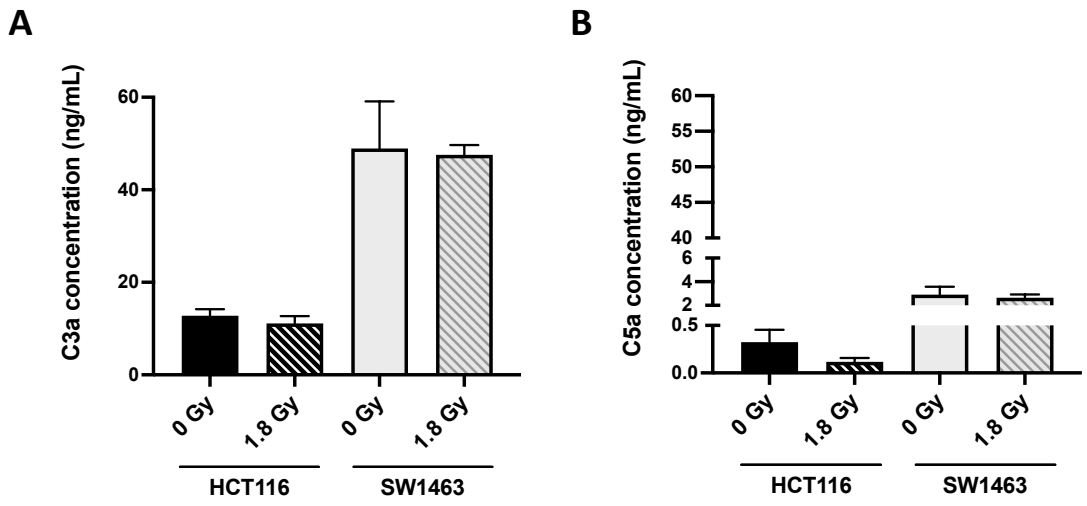

Figure 2-9: Radiation does not alter C3a or C5a anaphylatoxin production intracellularly in radiosensitive HCT116 and radioresistant SW1463 cell lines. The concentration of C3a and C5a anaphylatoxins was assessed basally and 48 h post 1.8 Gy of X-ray radiation in HCT116 and SW1463 cells. **(A)** C3a and **(B)** C5a protein concentration was assessed in cell lysates. Data are presented as mean ± SEM for 3 independent experiments. Statistical analysis was performed by paired two-tailed Student's *t*-test.

2.4.10. Radioresistant CRC cell lines produce higher intracellular levels of complement components

The relative expression of central complement genes (Section 2.4.3) and proteins (Section 2.4.6) by the CRC cell line panel suggests that higher levels of complement are expressed by radioresistant CRC cells. To determine whether there is a relationship between complement expression and inherent radiosensitivity in CRC, the total intracellular concentration of complement components (C3, C5, C3a and C5a) in cell lysates from HCT116, SW837, HRA-19 and SW1463 cells was calculated. The total intracellular concentration of complement proteins in the radiosensitive HCT116 cell line was significantly lower, when compared to the SW837 ($p = 0.0296$), HRA-19 ($p = 0.0191$) and SW1463 ($p = 0.0033$) cell lines. Similarly, the concentration of total complement protein expressed by SW837 cells was significantly lower, when compared to HRA-19 cells ($p = 0.0345$) and SW1463 cells ($p = 0.0060$) (Concentration total C3, C5, C3a and C5a (ng/mL); HCT116 22.248 ± 2.351, SW837 33.968 ± 2.643, HRA-19 91.21.7 ± 17.987, SW1463 104.212 ± 12.908) **(Fig. 2-10 A)**. This suggests that complement expression is increased in radioresistant CRC cells.

To further investigate the relationship between inherent radiosensitivity and complement expression in CRC, the total concentration of intracellular complement protein was correlated with the SF of each cell line at a clinically-relevant dose of 1.8 Gy. There was a significant positive correlation between SF at 1.8 Gy and intracellular concentration of complement ($p = 0.0081$, $R^2 = 0.059$) **(Fig. 2-10 B)**. This demonstrates that increased expression of intracellular complement protein is associated with increased radioresistance at 1.8 Gy of X-ray radiation.

2.4.11. CRC cells express CFB of the alternative complement activation pathway

Having determined that complement is activated in CRC, the potential pathway by which the complement system is activated in these cells was investigated. There are three pathways of complement activation, the classical, lectin and alternative pathways. The mRNA expression of Clq, mannose-binding lectin 2 (MBL2) and complement factor B (CFB), key initiating factors in the classical, lectin and alternative complement pathways, respectively, was assessed by qPCR. C1q and MBL2 mRNA was not detected in human colon carcinoma HCT116 and human rectal adenocarcinoma SW837, HRA-19 and SW1463 cells **(Appendix 1)**, suggesting that the classical and lectin pathways are not active in CRC cells.

However, CFB was expressed by all cell lines investigated, suggesting that complement may be activated via the alternative pathway in these cells. Interestingly, the radiosensitive HCT116 cell line expressed significantly lower levels of CFB, when compared to the SW837 ($p = 0.0078$), HRA-19 ($p < 0.0001$), and SW1463 ($p = 0.0004$) cell lines. SW837 cells expressed lower levels of CFB relative to HRA-19 ($p = 0.0002$) and SW1463 ($p = 0.0012$) cell lines (CFB relative mRNA expression ± SEM; HCT116 5.099 ± 3.370, SW837 88.181 ± 16.656, HRA-19 427.717 ± 19.931, SW1463 456.217 ± 41.624) **(Fig. 2-11 A)**.

CFB mRNA expression positively correlated with the total relative C3/C5 mRNA expression in HCT116, SW837, HRA-19 and SW1463 cells ($p = 0.0097$, R squared =0.5037) **(Fig. 2-11 B)**, suggesting that complement expression is occurring via the alternative pathway and may account for the increased activation of complement demonstrated in radioresistant cell lines.

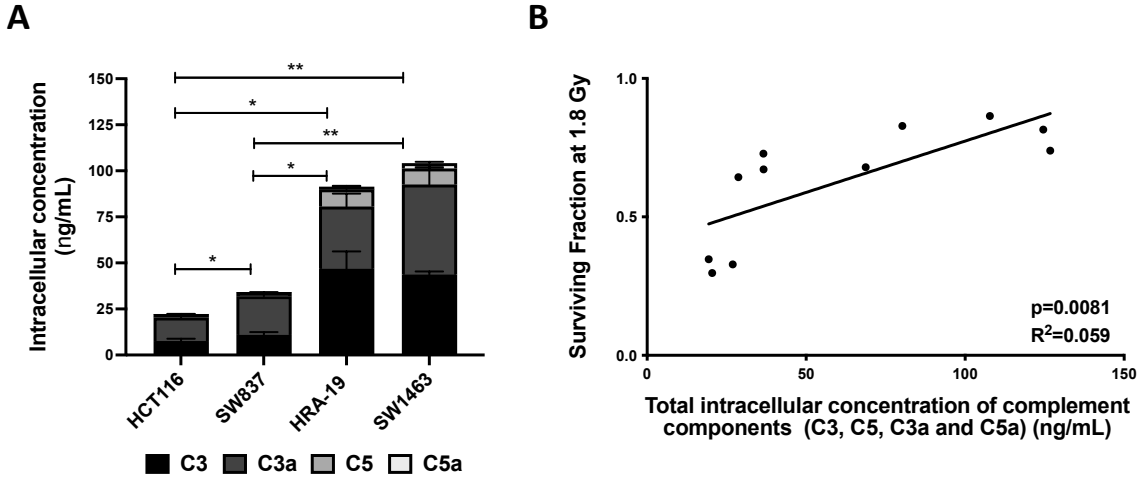

Figure 2-10: Total intracellular concentration of complement protein in CRC cell lines correlates with surviving fraction of cells at 1.8 Gy of radiation. The concentration of C3, C5, C3a and C5a was assessed basally by ELISA**. (A)** The cumulative concentration of complement was calculated for each cell line. Data are presented as mean ± SEM for 3 independent experiments. Statistical analysis was performed by unpaired two-tailed Student's *t*-test. * $p < 0.05$, ** $p < 0.01$. **(B)** Total intracellular concentration of complement components in HCT116, SW837, HRA-19 and SW1463 cells was correlated with surviving fraction at 1.8 Gy of X-ray radiation (n=12). Statistical analysis was performed by calculating the Pearson correlation coefficient.

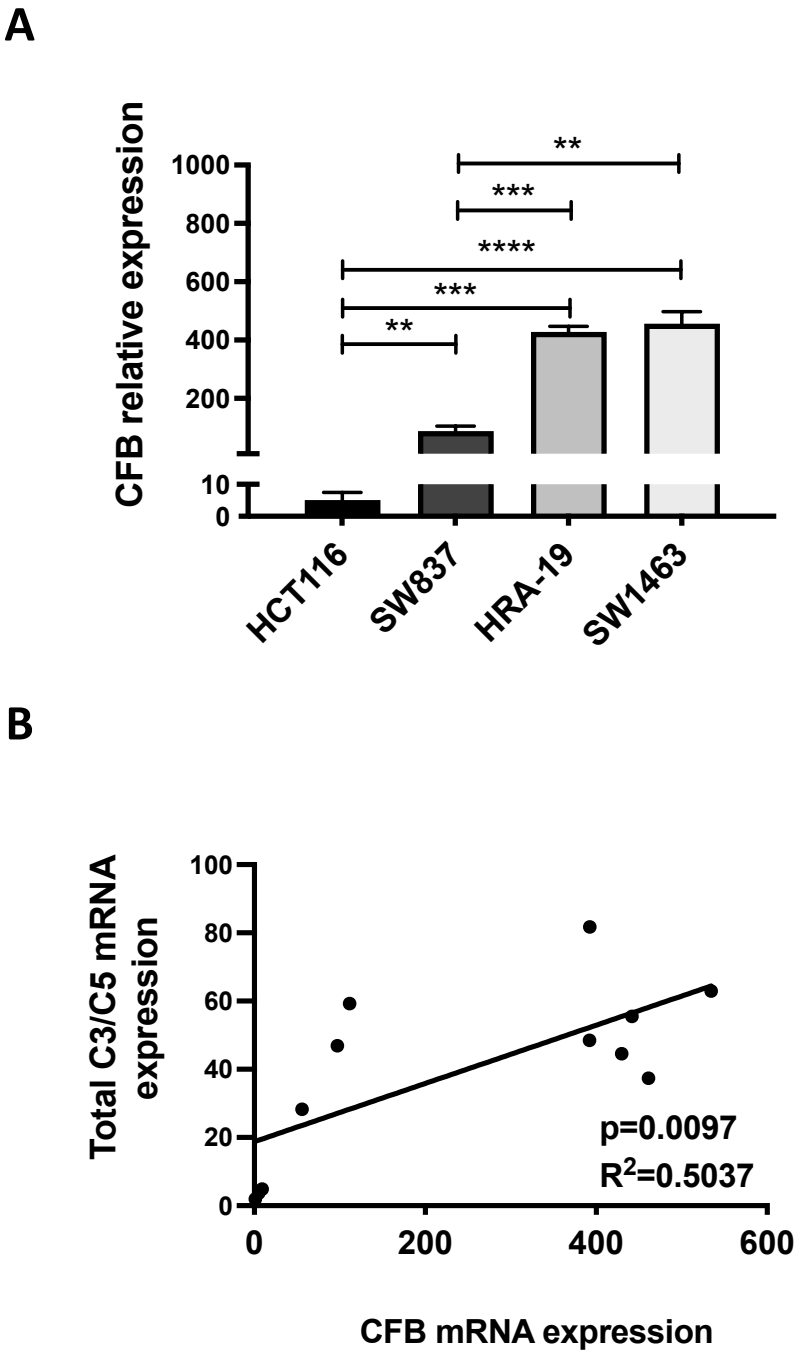

Figure 2-11: CFB mRNA expression correlates with total C3 and C5 mRNA expression in radiosensitive HCT116 and radioresistant SW837, HRA-19 and SW1463 cell lines. (A) mRNA expression of CFB was assessed basally in HCT116, SW837, HRA-19 and SW1463 cells by qPCR. Data are presented as mean ± SEM for 3 independent experiments. Statistical analysis was performed by unpaired two-tailed Student's *t*-test. $^{**}p < 0.01$, $^{***}p < 0.001$, $^{****}p < 0.0001$. **(B)** Total relative C3/C5 mRNA expression was correlated with CFB mRNA expression in HCT116, SW837, HRA-19 and SW1463 cells. Statistical analysis was performed by calculating the Pearson correlation coefficient.

2.4.12. Radiation does not alter CFB mRNA expression in CRC cell lines

Having demonstrated that CFB mRNA is expressed by CRC cell lines, the effect of X-ray radiation on CFB mRNA expression was assessed. There were no significant alterations in CFB mRNA expression at 24 h or 48 h post 1.8 Gy of X-ray radiation, when compared to basal levels in HCT116 (**Fig. 2-12 A**), SW837 (**Fig. 2-12 B**), HRA-19 (**Fig. 2-12 C**) and SW1463 (**Fig. 2-12 D**) cell lines.

2.4.13. CRC cell lines express extracellular C5aR1 but not C3aR

Having demonstrated that CRC cell lines produce complement anaphylatoxins, the potential of CRC cells to respond to complement signalling was investigated. The effects of the potent anaphylatoxins C3a and C5a are mediated via binding to their respective receptors, the C3aR and the C5aR1. Expression of both receptors was assessed in all cell lines by flow cytometry.

Basal expression of extracellular C3aR by HCT116, SW837, HRA-19 and SW1463 cells was not detected by flow cytometric analysis (**Appendix 2**). However, basal extracellular expression of the C5aR1 was detected in HCT116, SW837, HRA-19 and SW1463 cells. There were no significant alterations in C5aR1 expression across the cell lines (Mean % of $C5aR1^+$ cells ± SEM; HCT116 3.477 ± 0.828, SW837 5.655 ± 1.635, HRA-19 4.847 ± 1.381, SW1463 12.407 ± 3.460) **(Fig. 2-13)**.

2.4.14. Radiation increases extracellular C5aR1 expression in CRC cells

Expression of the C5aR1 in HCT116, SW837, HRA-19 and SW1463 cells following clinically-relevant doses of 1.8 Gy and 5 Gy of X-ray irradiation was assessed. Radiation had no effect on the percentage of HCT116, SW837, HRA-19 and SW1463 cells expressing the C5aR1 extracellularly **(Fig. 2-14 A)**. However, there was a significant increase in the fold change in mean fluorescence intensity (MFI) of C5aR1 expressed at 24 h post 5 Gy of X-ray irradiation, when compared to basal levels, by HCT116 ($p = 0.0059$), SW837 ($p = 0.0352$) and SW1463 ($p = 0.0270$) cells (Mean fold change in C5aR1 MFI at 24 h post 5 Gy relative to 0 Gy ± SEM; HCT116 2.572 ± 0.015, SW837 1.546 ± 0.105, HRA-19 1.311 ± 0.052) **(Fig. 2-14 B)**. There were no alterations in the MFI of C5aR1 expressed by HRA-19 cells at 24 h following 1.8 Gy or 5 Gy of X-ray radiation **(Fig. 2-14 B)**.

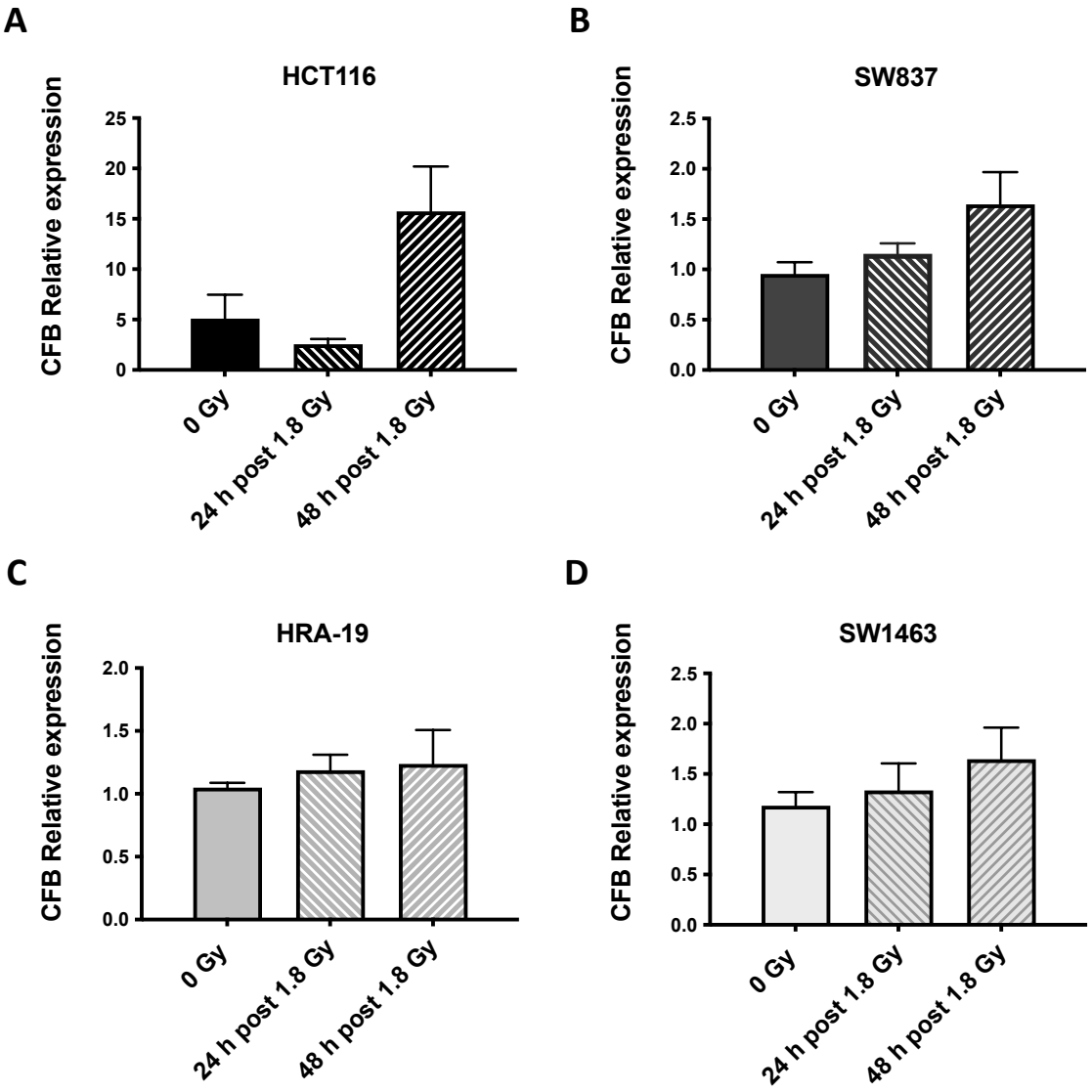

Figure 2-12: Radiation does not alter CFB mRNA expression in radiosensitive HCT116 and radioresistant SW837, HRA-19 and SW1463 cell lines. CFB mRNA expression basally and at 24 h and 48 h post 1.8 Gy of X-ray radiation in **(A)** HCT116, **(B)** SW837 **(C)** HRA-19 and **(D)** SW1463 cells. Data are presented as mean ± SEM for 3 independent experiments. Statistical analysis was performed by one-way ANOVA and post-hoc Tukey's multiple comparisons testing.

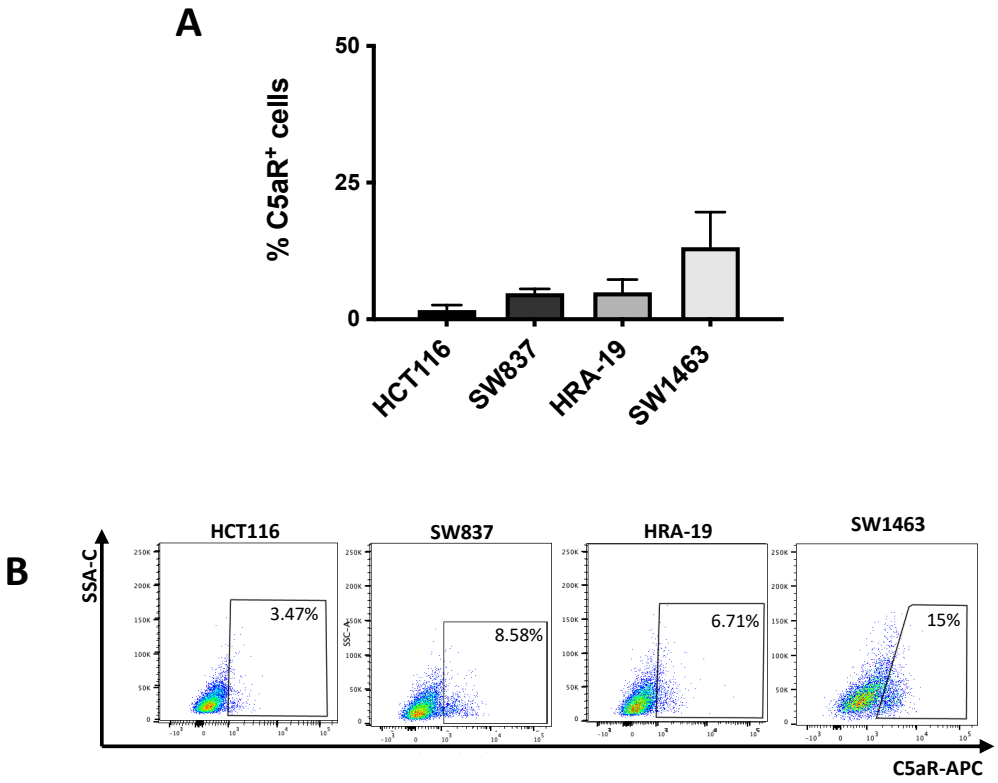

Figure 2-13: The C5aR1 is expressed extracellularly by radiosensitive HCT116 and radioresistant SW837, HRA-19 and SW1463 cell lines. Basal extracellular C5aR1 expression was assessed by flow cytometry. **(A)** Percentage of HCT116, SW837, HRA-19 and SW1463 cells expressing the C5aR1 extracellularly. Data are presented as mean ± SEM for 3 independent experiments. **(B)** Dot plots representative of data from 3 independent experiments. Statistical analysis was performed by one-way ANOVA and post-hoc Tukey's multiple comparisons testing.

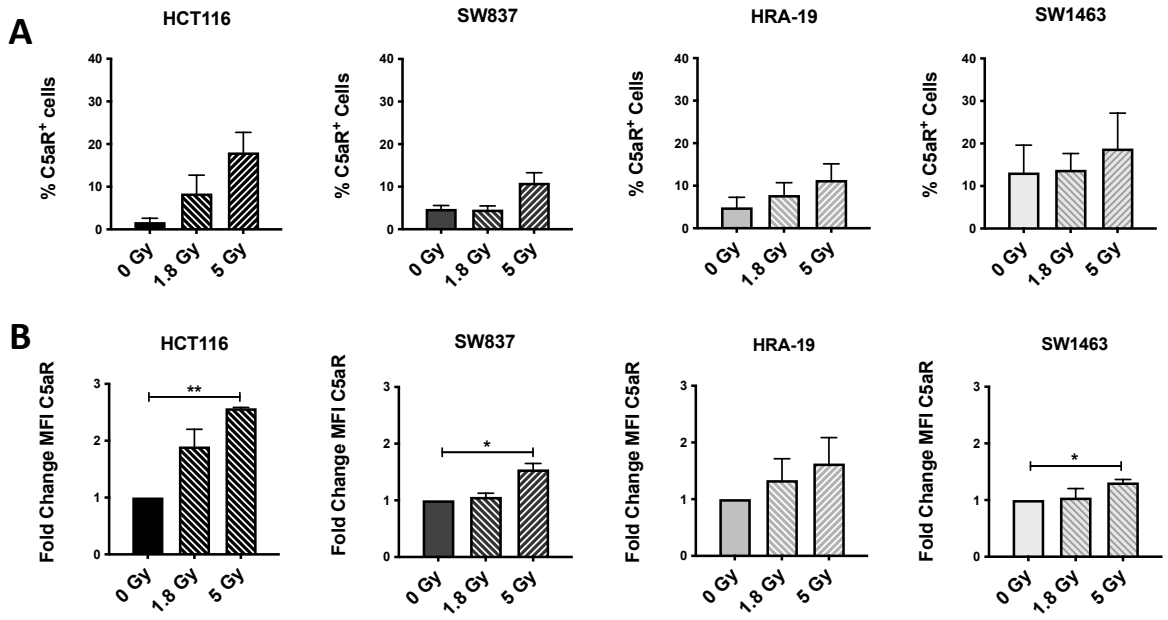

Figure 2-14: Radiation increases the MFI of extracellular C5aR1 expressed in radiosensitive HCT116 and radioresistant SW837 and SW1463 cell lines. C5aR1 expression was assessed by flow cytometry in HCT116, SW837, HRA-19 and SW1463 cells basally and at 24 h post irradiation with 1.8 Gy and 5 Gy of X-ray radiation. **(A)** Percentage of cells positive for extracellular C5aR1. Data are presented as mean percentage of cells ± SEM for 3 independent experiments. **(B)** Fold change in the MFI of C5aR1 expressed by each cell line at 24 h post irradiation with 1.8 Gy and 5 Gy of X-ray radiation relative to 0 Gy controls for 3 independent experiments. Statistical analysis was performed by paired two-tailed Student's *t*-test. $*p < 0.05$, $**p < 0.01$.

2.4.15. CRC cell lines express both the C3aR and C5aR1 intracellularly

Having demonstrated extracellular expression of the C5aR1, the intracellular expression of C3aR and C5aR1 was investigated in HCT116, SW837, HRA-19 and SW1463 cells by flow cytometry.

Interestingly, HCT116, SW837, HRA-19 and SW1463 cells expressed the C3aR intracellularly (Mean % of C3aR+ cells ± SEM; HCT116 97.133 ± 1.384, SW837 99.1 ± 0.529, HRA-19 79.833 ± 8.601, SW1463 87.250 ± 6.55) **(Fig. 2-15 A-B)**. HCT116, SW837, HRA-19 and SW1463 cells also all expressed the C5aR1 intracellularly (Mean % of C5aR1+ cells ± SEM; HCT116 99.733 ± 0.176, SW837 99.3 ± 0.557, HRA-19 94.6 ± 4.86, SW1463 97.3 ± 2) **(Fig. 2-15 C-D)**. There were no statistically significant alterations in the percentage expression of intracellular C3aR or C5aR1 between the CRC cell lines **(Fig. 2-15)**.

2.4.16. Radiation increases intracellular C5aR1 expressed by HCT116 cells

The expression of intracellular C3aR and C5aR1 in HCT116, SW837, HRA-19 and SW1463 cells following clinically-relevant doses of 1.8 Gy and 5 Gy of X-ray radiation was also assessed.

Radiation had no effect on the percentage of HCT116, SW837, HRA-19 and SW1463 cells expressing the C3aR intracellularly **(Fig. 2-16 A)**. Similarly, radiation had no effect on the fold change in MFI of C3aR expressed at 24 h post 1.8 Gy or 5 Gy of X-ray irradiation, when compared to basal levels **(Fig. 2-16 B)**. Similarly, the percentage of HCT116, SW837, HRA-19 and SW1463 cells expressing the C5aR1 intracellularly was unchanged following radiation **(Fig. 2-16 C)**. However, there was a significant increase in the fold change in MFI of C5aR1 expressed at 24 h post 5 Gy of X-ray radiation, when compared to basal levels by HCT116 cells ($p = 0.0188$) (Mean fold change in C5aR1 MFI at 24 h post 5 Gy relative to 0 Gy ± SEM; HCT116 1.393 ± 0.055) **(Fig. 2-16 D)**. There were no alterations in the fold change in MFI of intracellular C5aR1 expressed by SW837, HRA-19 and SW1463 cells 24 h following 1.8 Gy or 5 Gy of X-ray radiation, when compared to baseline **(Fig. 2-16 D)**. This suggests that radiation increases the amount of C5aR1 expressed by radiosensitive HCT116 cells, and not radioresistant CRC cell lines.

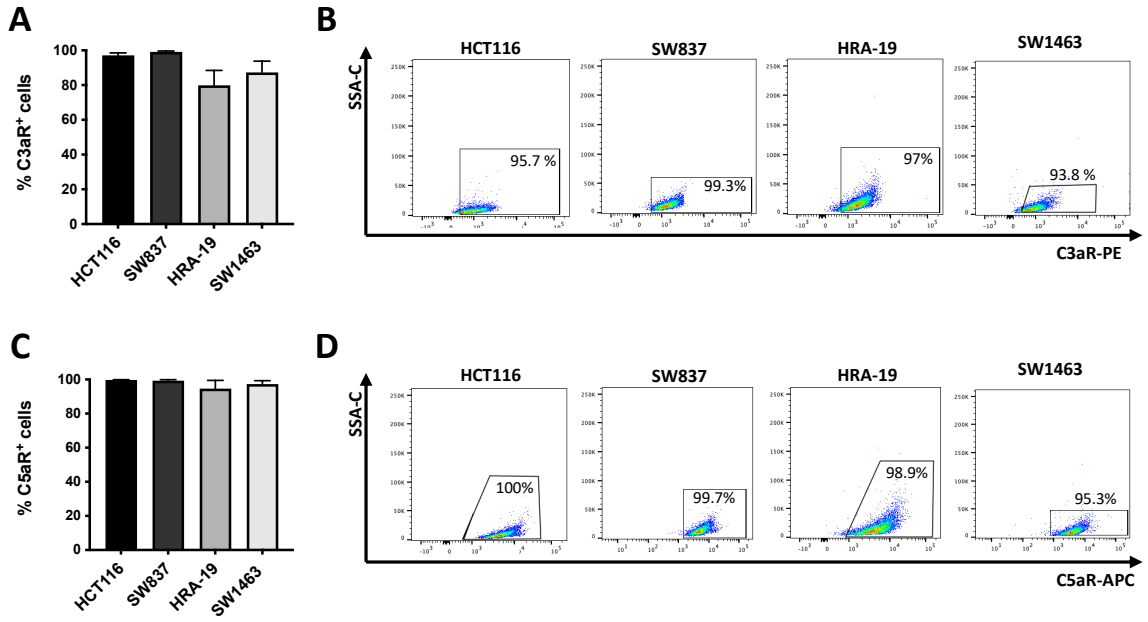

Figure 2-15: The C3aR and the C5aR1 are expressed intracellularly by radiosensitive HCT116 and radioresistant SW837, HRA-19 and SW1463 cell lines. CRC cell lines were fixed and permeabilized and intracellular C3aR and C5aR1 expression was assessed by flow cytometry. **(A)** Percentage and **(B)** representative dot plot of cells expressing intracellular C3aR. **(C)** Percentage and **(D)** representative dot plot of cells expressing intracellular C5aR1. Data are presented as mean ± SEM for 3 independent experiments. Dot plots are representative of data from 3 independent experiments. Statistical analysis was performed by one-way ANOVA and post-hoc Tukey's multiple comparisons testing.

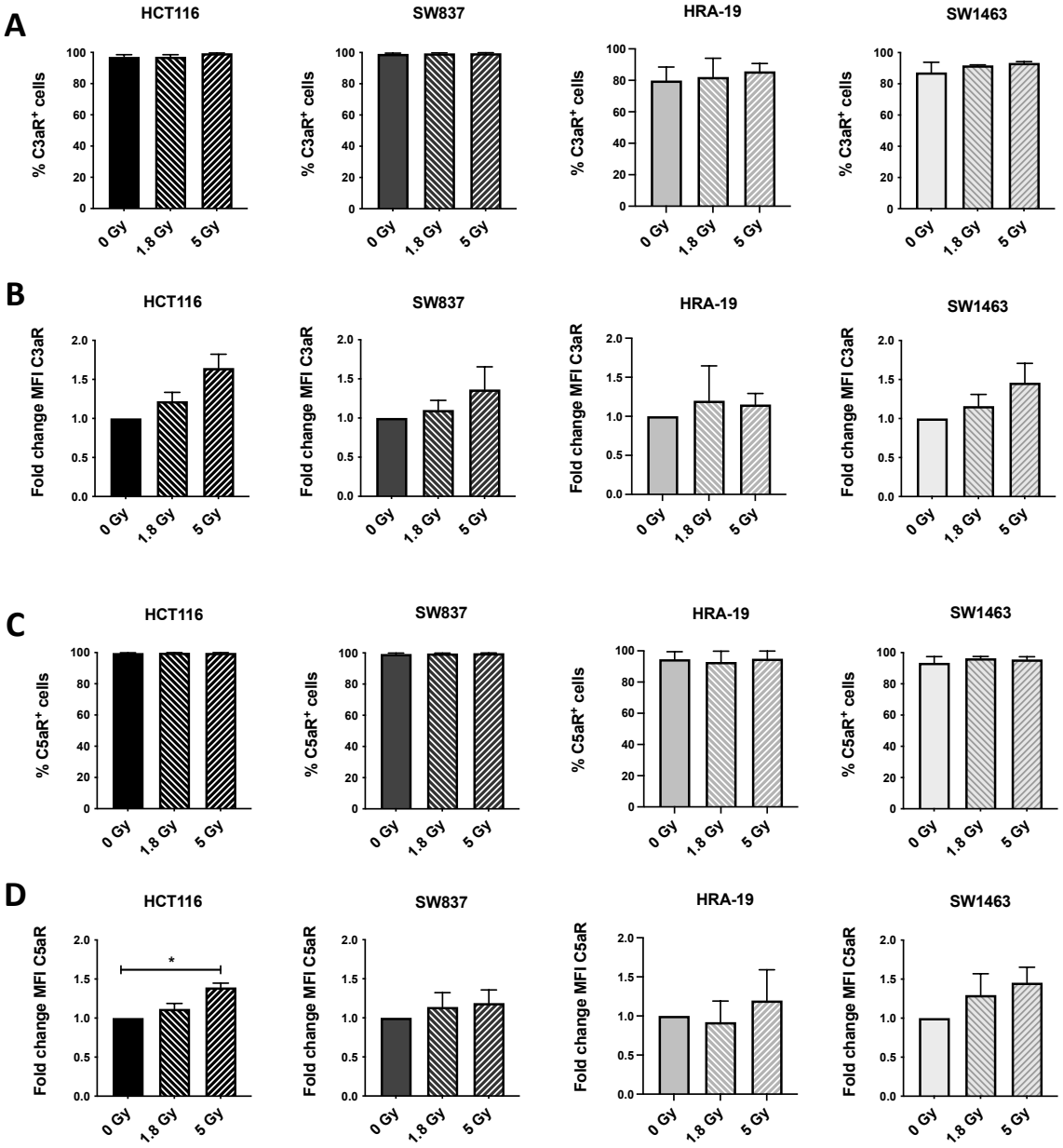

Figure 2-16: Radiation increases the MFI of intracellular C5aR1 expressed by radiosensitive HCT116 cells. CRC cell lines were fixed and permeabilized and intracellular C3aR and C5aR1 expression was assessed by flow cytometry basally and at 24 h post irradiation with 1.8 Gy and 5 Gy of X-ray radiation. **(A)** Percentage of cells positive for intracellular C3aR. **(B)** Fold change in the MFI of C3aR expressed by each cell line at 24 h post irradiation with 1.8 Gy and 5 Gy of X-ray radiation relative to basal levels. **(C)** Percentage of cells positive for intracellular C5aR1. **(D)** Fold change in the MFI of C5aR1 expressed by each cell line at 24 h post irradiation with 1.8 Gy and 5 Gy of X-ray radiation relative to basal levels. Data are presented as mean percentage of cells ± SEM or fold change in the MFI of C5aR1 or C3aR expression relative to 0 Gy controls. Data are representative of 3 independent experiments. Statistical analysis was performed by paired two-tailed Student's *t*-test. $*p < 0.05$.

2.4.17. The C3aR is expressed within the cytoplasm and nucleus in HCT116 cells

To investigate the intracellular location of the C3aR, HCT116 cells were assessed using IF staining and confocal microscopy. Interestingly C3aR was detected intracellularly in HCT116 cells in both the cytoplasm and the nucleus **(Fig. 2-17 A)**. THP-1 cells were used as a positive control and demonstrated an observably lower expression relative to HCT116 cells **(Fig. 2-17 B)**.

Having demonstrated that IR increased the MFI of intracellular C5aR1 expressed by HCT116 cells, with a trend towards an increase in MFI of C3aR expression, C3aR expression was assessed following clinically-relevant doses of radiation to determine whether expression was altered within different cellular locations following radiation. Interestingly, 1.8 Gy and 5 Gy doses of radiation significantly increased ($p < 0.0001$ for both) the integrated intensity of C3aR expressed across the whole cell (Mean integrated intensity of C3aR ± SEM; 0 Gy 24.04 ± 0.32, 1.8 Gy 43.32 ± 0.81, 5 Gy 52.85 ± 1.12) **(Fig. 2-17 C)**. Furthermore, within the cytoplasm, 1.8 Gy and 5 Gy doses of radiation significantly increased ($p < 0.0001$ for both) the integrated intensity of C3aR (Mean integrated intensity of C3aR ± SEM; 0 Gy 12.1 ± 0.2, 1.8 Gy 24.43 ± 0.52, 5 Gy 30.69 ± 0.75) **(Fig. 2-17 D)**. Similarly, following 1.8 Gy and 5 Gy doses of radiation, expression of the C3aR was significantly increased within the nucleus ($p < 0.0001$ for both) (Mean integrated intensity of C3aR ± SEM; 0 Gy 12.14 ± 0.14, 1.8 Gy 19.21 ± 0.31, 5 Gy 22.94 ± 0.43) **(Fig. 2-17 E)**. This demonstrates that C3aR localises within both the cytoplasm and the nucleus in HCT116 cells, with increased expression observed following radiation.

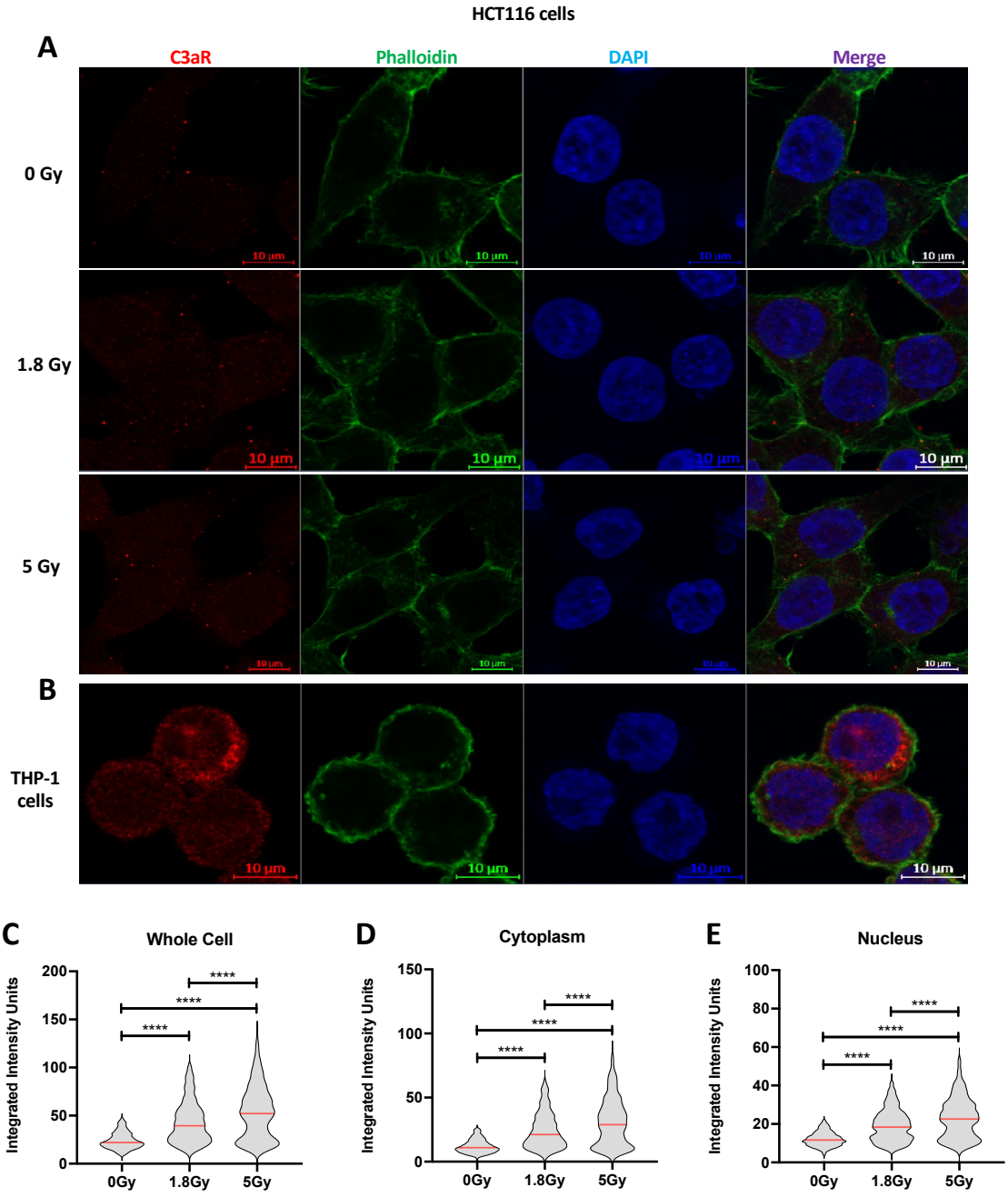

Figure 2-17: The C3aR is expressed within the nucleus and cytoplasm of HCT116 cells. HCT116 cells were assessed for intracellular C3aR expression by confocal microscopy. Representative images of C3aR staining in **(A)** HCT116 cells basally and following irradiation with 1.8 or 5 Gy of X-ray radiation. **(B)** C3aR expression was assessed in THP-1 cells basally as a positive control. Image magnification is 63X. The integrated intensity of C3aR expression was quantified **(C)** across the whole cell **(D)** in the cytoplasm and **(E)** in the nucleus, basally and 24 h post irradiation with 1.8 Gy or 5 Gy. Data are presented as violin plots of the integrated intensity of C3aR signal showing the median, for 3 independent experiments. A minimum of 100 cells were analysed per experimental replicate. Outliers were removed using whisker plots and the Tukey method. Statistical analysis was performed by one-way ANOVA and post-hoc Tukey's multiple comparisons testing. ****$p < 0.0001$. (IF staining performed by the University of Oxford).

2.4.18. CRC cell lines express mCRPs

The complement system is regulated by an extensive network of membrane-bound and soluble regulators, which act to modulate complement activation at various stages of the pathway. To investigate the ability of CRC cells to control complement activation, the expression of the surface-expressed mCRPs CD46, CD55 and CD59 was assessed by flow cytometry.

CD46, or membrane cofactor protein, acts as a cofactor for the degradation of C3b and C4b by complement factor H[222–224]. HCT116, SW837, HRA-19 and SW1463 cells all expressed CD46, with similar percentage expression demonstrated in each cell line (Mean percentage of CD46+ cells ± SEM; HCT116 96 ± 2.957, SW837 98.333 ± 0.867, HRA-19 95.533 ± 1.559, SW1463 96.450 ± 2.850) **(Fig. 2-18 A-B)**.

CD55, otherwise known as decay accelerating factor (DAF) accelerates the decay of C3 and C5 convertases to limit complement cascade activation[225–227]. CD55 was expressed by all four CRC cell lines. A significantly lower percentage of both HRA-19 and SW1463 cells expressed CD55, when compared to HCT116 and SW837 cells ($p < 0.0001$ for all). An increased percentage of HRA-19 cells expressed CD55, when compared to SW1463 cells ($p = 0.0081$) (Mean percentage of CD55 + cells ± SEM; HCT116 96.167 ± 3.06, SW837 94.4 ± 2.982, HRA-19 29.233 ± 2.373, SW1463 9.345 ± 0.285) **(Fig. 2-18 C-D)**.

CD59 interferes with the polymerisation of the membrane attack complex, which is essential for inducing target cell lysis[228,229]. CD59 was expressed by HCT116, SW837, HRA-19 and SW1463 cells, with no alterations in percentage expression across the panel (Mean percentage of CD59 + cells ± SEM; HCT116 95.5 ± 3.089, SW837 98.567 ± 0.273, HRA-19 93.933 ± 1.408, SW1463 95.250 ± 2.450) **(Fig. 2-18 E-F)**.

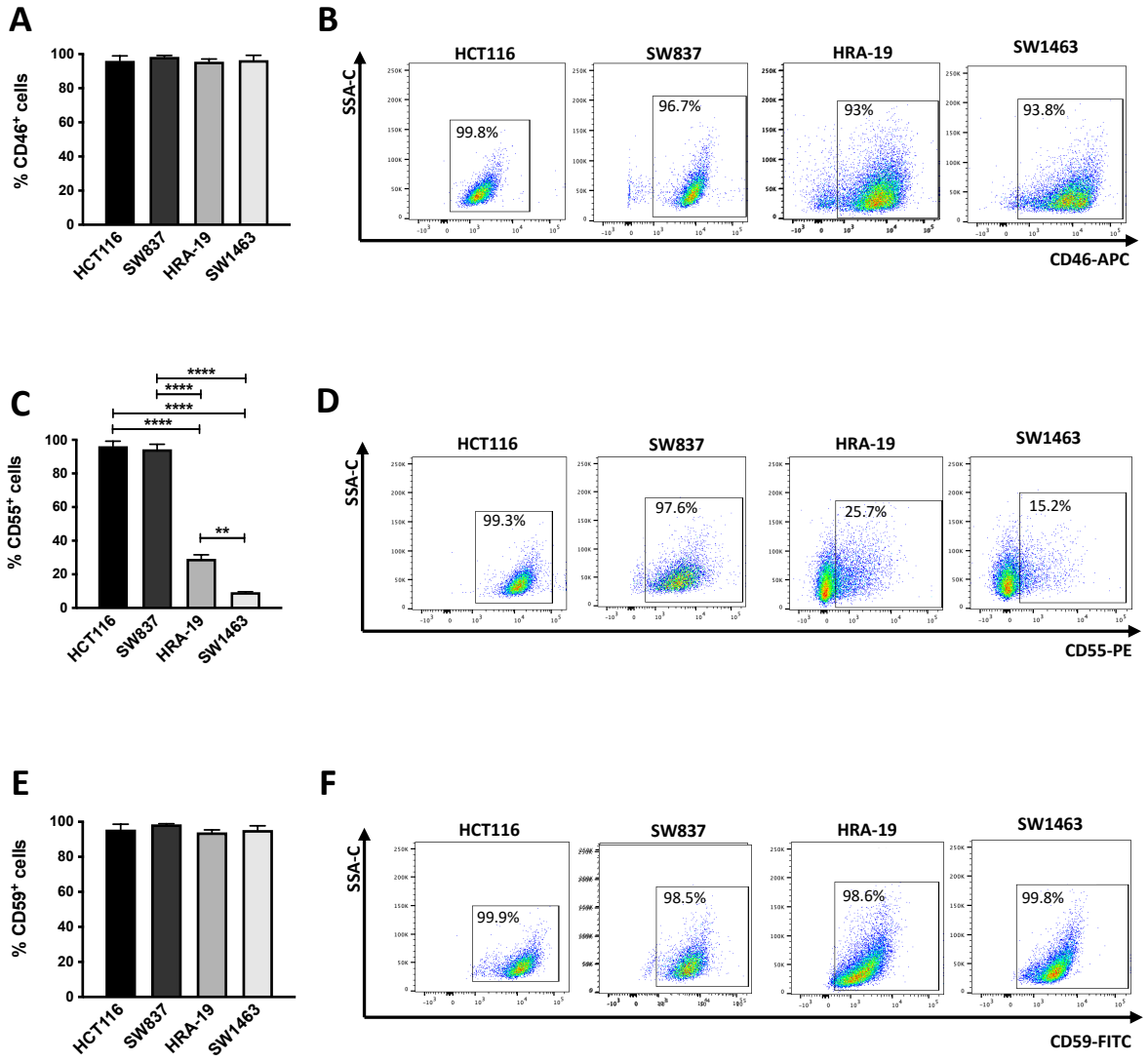

Figure 2-18: The mCRPs CD46, CD55 and CD59 are expressed by the radiosensitive HCT116 and radioresistant SW837, HRA-19 and SW1463 cell lines. Basal expression of surface-bound mCRPs was assessed by flow cytometry. **(A)** Percentage and **(B)** representative dot plot of cells expressing CD46. **(C)** Percentage and **(D)** representative dot plot of cells expressing CD55. **(E)** Percentage and **(F)** representative dot plot of cells expressing CD59. Data are presented as mean percentage of cells positive ± SEM for 3 independent experiments. Dot plots are representative of data from 3 independent experiments. Statistical analysis was performed by one-way ANOVA and post-hoc Tukey's multiple comparisons testing. ****$p < 0.0001$.

2.4.19. Radiation does not alter mCRP expression in CRC cells

To investigate the potential effect of X-ray radiation on mCRP expression, the expression of CD46, CD55 and CD59 was assessed at 24 h post treatment with a clinically-relevant dose of 1.8 Gy.

There were no alterations in the percentage of HCT116, SW837, HRA-19 or SW1463 cells expressing CD46, CD55 or CD59 **(Fig. 2-19 A-C)** following radiation. To investigate whether radiation altered the level of mCRP expression by the CRC cell line panel, the fold change in MFI of mCRPs was assessed. There were no alterations in fold change of the MFI of CD46 CD55 or CD59 **(Fig. 2-20 A-C)** expressed by the CRC cell line panel following irradiation. These data suggest that radiation does not alter expression of mCRPs in CRC cells.

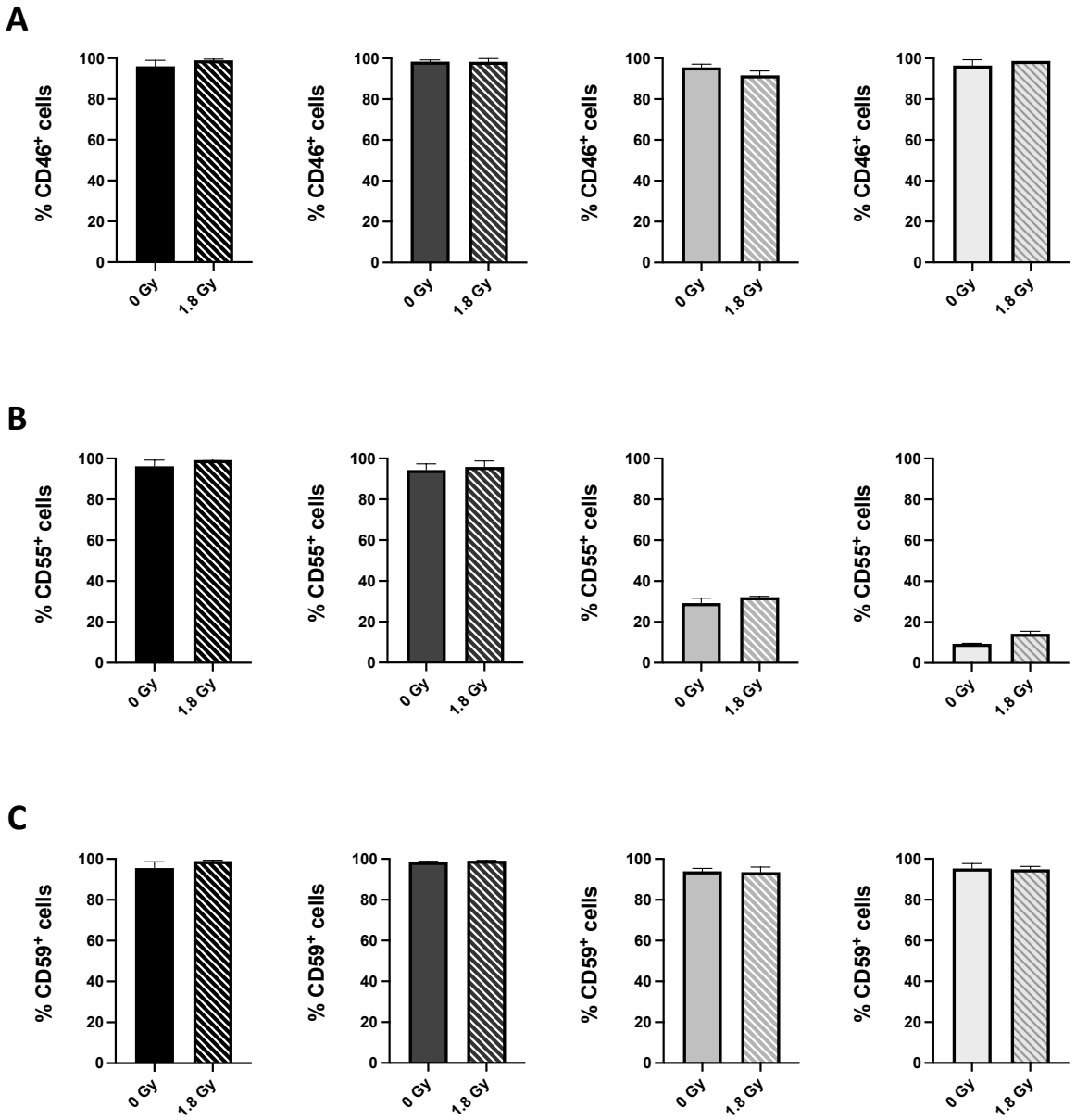

Figure 2-19: Radiation does not increase the percentage of HCT116, SW837, HRA-19 or SW1463 cells expressing CD46, CD55 or CD59. Surface expression of CD46, CD55 and CD59 was assessed basally and at 24 h post 1.8 Gy of X-ray radiation by flow cytometry. The percentage expression of **(A)** CD46, **(B)** CD55 and **(C)** CD59 in HCT116, SW837, HRA-19 and SW1463 cells. Data are presented as mean percentage of cells positive ± SEM for 3 independent experiments. Statistical analysis was performed by paired two-tailed Student's *t*-test.

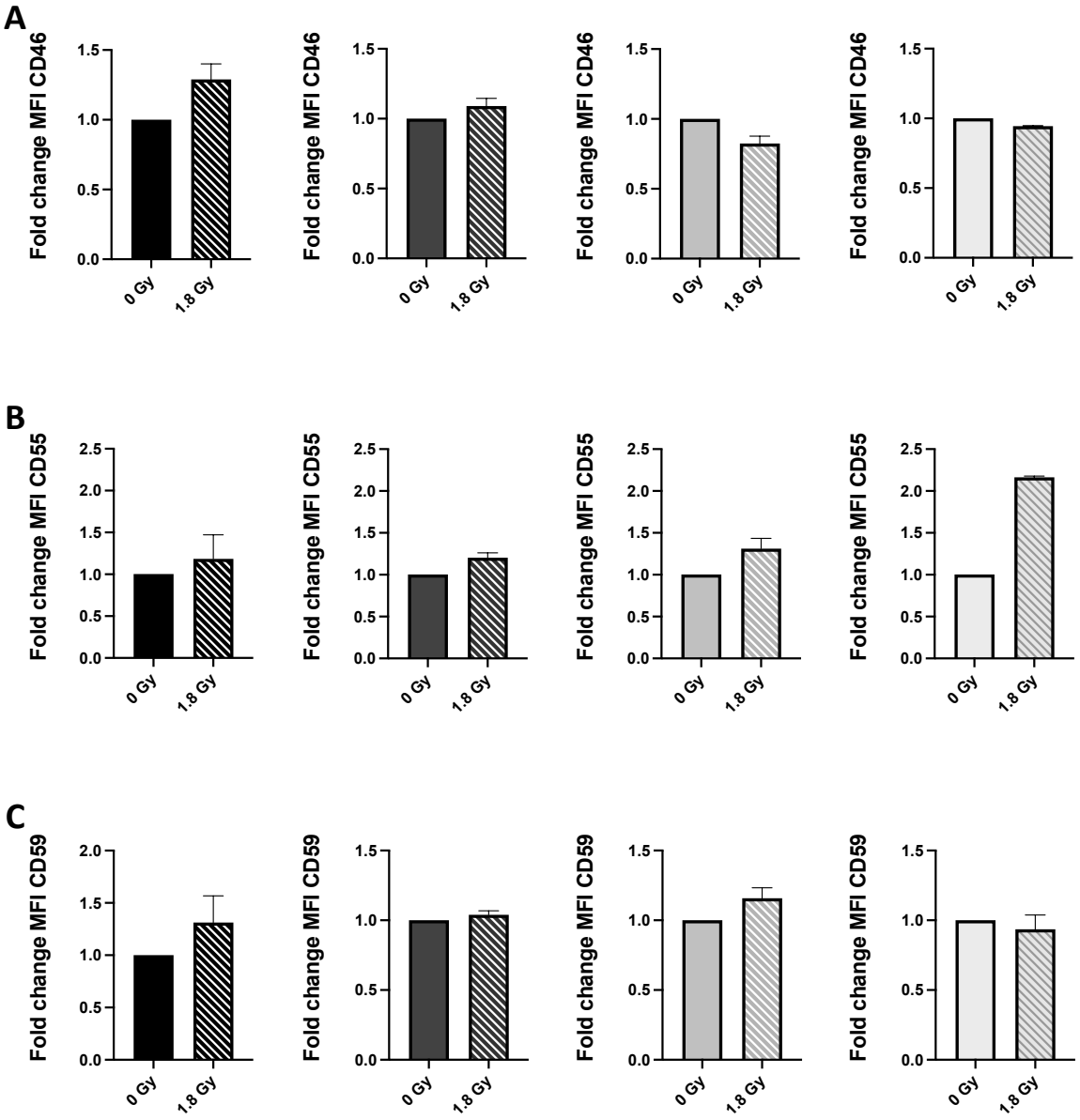

Figure 2-20: Radiation does not increase the expression level of CD46, CD55 and CD59 in HCT116, SW837, HRA-19 or SW1463 cells. Surface expression of CD46, CD55 and CD59 was assessed basally and at 24 h post 1.8 Gy of X-ray radiation by flow cytometry. Fold change in MFI of **(A)** CD46, **(B)** CD55 and **(C)** CD59 expressed by HCT116, SW837, HRA-19 and SW1463 cells. Data are presented as mean fold change in MFI ± SEM for 3 independent experiments. Statistical analysis was performed by paired two-tailed Student's *t*-test.

2.5. Discussion

The overall objective of this chapter was to investigate the relationship between the complement system and the response to radiation in CRC *in vitro*, through the identification of an *in vitro* model of radiosensitive/radioresistant CRC and the characterisation of complement production, activation and regulation in this model.

To establish an *in vitro* model for studying radiosensitivity/radioresistance in CRC, the human colon carcinoma HCT116 and human rectal adenocarcinoma SW837, HRA-19 and SW1463 cell lines were selected. Although RT is not included in standard treatment regimens for colon cancer, the HCT116 colon cancer cell line was utilised as there are a limited number of cell lines established from rectal tumours. Consequently, other studies investigating the radiobiology of CRC have also utilised colon cancer cells[387]. Additionally, the radioresponse of HCT116 cells is well-characterised in the literature[388–391]. The radioresponses of rectal cancer cell lines are poorly characterised in the literature, with few published studies reporting the radioresistance of the SW1463 and SW837 cell lines[387,390–393]. The inherent radiosensitivity of the HRA-19 cell line has not previously been reported. To our knowledge, this is the first time that the inherent radiosensitivity of this cell line has been profiled.

The human colon carcinoma HCT116 cells were identified as the most radiosensitive cell line of the panel. This finding is supported by several studies in the literature which have previously demonstrated the sensitivity of these cells to radiation[388–391]. Previously uncharacterised in the literature, the HRA-19 cell line was demonstrated to be inherently radioresistant, like the majority of established rectal cancer cell lines[387,390–393]. The inherent radiosensitivity profile of the SW1463 cell line did not follow the same trend as the other rectal cancer cell lines assessed (SW837 and HRA-19), however, the survival curve of these cells is similar to that demonstrated by others[392]. In this study, SW1463 cells were the most radioresistant cell line at low doses of radiation such as 1.8 Gy and 2 Gy. The SF of SW1463 cells at these doses are slightly higher than those reported in other studies, however they consistently are demonstrated to be inherently radioresistant cells[387,393]. Differences in results may be due to variations in seeding densities. In addition, SW1463 cells grow in a clumped morphology, which can compound accurate cell counting, and may impact on the resulting surviving fraction. While SW1463 and SW837 cell lines are both inherently radioresistant, SW1463 cells have been reported as more radiosensitive than SW837 cells at increasing doses of X-ray radiation[390]. This is supported by the data in this chapter, which demonstrates that SW1463 cells are significantly more radiosensitive

at 6 Gy of X-ray radiation than SW837, and also HRA-19 cells. From this characterisation, radiosensitive (HCT116) and radioresistant (SW837, HRA-19 and SW1463) cell lines were identified, providing an *in vitro* model of radioresistance and radiosensitivity in CRC to investigate complement.

Complement components are primarily produced in the liver, but production also occurs locally in most cell types[169]. The last decade of research has demonstrated that this extends to the TME, with both tumour and immune cells capable of complement production[177,297]. Analysis of TCGA data has demonstrated that complement is widely expressed in human cancers[177]. C3 is a central complement cascade component and is expressed by many cancer cell lines, including those originating from renal, squamous cell, gastric and ovarian tumours[300,301,304,394]. For the first time, the HCT116, SW837 and HRA-19 cell lines were demonstrated to express C3 mRNA and protein. In SW1463 cells, expression of C3 mRNA was not detected, however C3 protein was detected in protein lysates. A possible explanation for this is a rapid translation of C3 mRNA to protein, preventing detection of C3 mRNA by qPCR. C5 is also a central component of the complement cascade, linking complement activation pathways with the terminal complement pathway[395]. All four cell lines in the CRC cell line panel expressed C5, with both C3 and C5 identified as being secreted and present intracellularly.

Previous work by Surace *et al*. has demonstrated upregulation of several complement gene transcripts in immune cells, mouse tumours and patient biopsies following radiation[351]. In this CRC cell line panel, there were no alterations in complement components expressed by the radioresistant SW837, HRA-19 and SW1463 cells following radiation. However in the radiosensitive HCT116 cell line, X-ray radiation led to significantly increased C5 mRNA expression, suggesting that radiation may upregulate complement genes in radiosensitive CRC cells.

Activation of the complement system plays an important role in the innate immune response. A hallmark of complement system activation is the generation of the C3a and C5a anaphylatoxins from C3 and C5 proteins, respectively. Several studies have provided evidence for systemic and local activation of the complement system in cancer[273–278]. C3a and C5a was detected in cell supernatants from this cell line panel at low levels that could not be quantified using the standard curve. C3a has been detected in the supernatant of HCT116 cells in a recent study, at a concentration of approximately 40 pg/μL[337]. The assay used here was limited by a sensitivity of 63 pg/μL. Interestingly, C3a and C5a were present

in protein lysates from HCT116, SW837, HRA-19 and SW1463 cell lines, demonstrating that the complement system is activated intracellularly in CRC. This supports recent findings that C5a is produced intracellularly in colon cancer cells[341]. Although complement activation has been observed in cancer, this may not always be beneficial. In cervical, colorectal, renal and ovarian cancers, activation of complement has been observed to associate with poor prognosis[283–285,394]. Here, in radiosensitive HCT116 cells, lower levels of complement anaphylatoxins were detected, when compared to radioresistant CRC cell lines. This demonstrates that complement activation is elevated in radioresistant rectal cancer cell lines, suggesting that complement activation is associated with a radioresistant phenotype in CRC. Previously, radiation has been demonstrated to induce complement activation, generating anaphylatoxins which impact the radioresponse[350,351]. In this study, radiation did not alter anaphylatoxin production in CRC cell lines, suggesting that radiation does not activate the complement system in this model, and highlighting the context-dependent nature of complement across human cancer types.

Complement activation can occur via 3 pathways, the classical, the lectin and the alternative pathway[186,208]. Altered expression of complement pathway components have been reported in several human cancers including ovarian, cervical and colorectal[273,283–285,396,397]. Having demonstrated that complement was activated in the CRC cell line panel, the potential pathway by which complement activation is occurring was assessed. Previously in CRC patients, increased expression of mannose-binding lectin and ficolins, components of lectin pathway components, has been demonstrated[396,397]. The expression of complement cascade components in rectal cancer specifically has not been characterised, however rectal surgery has been reported to activate complement via the alternative pathway, demonstrating that this is an active pathway in this cancer type[398]. This supports the results in this chapter, which demonstrate that although HCT116, SW837, HRA-19 and SW1463 cells do not express C1q and MBL2 of the classical and lectin pathways, respectively, they all express the alternative pathway component CFB. CFB mRNA expression positively correlated with total C3 and C5 mRNA expression, suggesting that the alternative complement pathway may be active in CRC cells. Expression levels of CFB varied across the cell line panel, with the radiosensitive HCT116 cells expressing the lowest relative levels, when compared to radioresistant rectal cancer cell lines. A study by Huang *et al*. compared gene expression profiles between CRC cell lines with varying radiosensitivities[389]. They similarly used the radiosensitive HCT116 cells, but in combination with the radioresistant SW480 and SW403 colon cancer cell lines.

Interestingly, they discovered that CFB was among the genes discriminating response to RT, with higher expression demonstrated in radioresistant cells[389]. This supports the results outlined in this chapter, which demonstrate higher levels of CFB mRNA expression in radioresistant CRC lines. These data highlight an association between the alternative complement pathway and the radioresponse in CRC. Importantly, Ding *et al.* have recently provided evidence for intracellular generation of C5a, independent of canonical activation of the complement system. In their study, they identify CTSD as the enzyme responsible for cleavage of intracellular C5 to generate C5a[341]. This highlights that cleavage of C3 and C5 in rectal cancer cell lines may occur via an enzyme outside of the traditional complement activation pathways.

Radiation has been reported to induce activation of the classical and alternative complement pathways in a murine model of melanoma[351]. In the CRC cell panel there were no significant alterations in CFB expression following radiation. This may suggest that radiation does not activate the complement system in CRC, again highlighting the context-dependent nature of complement in cancer.

The data in this chapter demonstrates complement production and activation in CRC cells. Across the CRC cell line panel, the greatest levels of complement genes, proteins and anaphylatoxins were detected in the most radioresistant cell lines. This suggests that complement may be associated with the response to radiation in CRC. Expression of complement components has been correlated with various clinical parameters across many cancer types. In breast cancer, expression of the C5aR1 has been linked to larger tumours, lymph node metastases, advanced clinical stages and poorer outcomes[319]. High expression of C1s is associated with poor prognosis in ccRCC[394]. Furthermore, mounting evidence supports a role for complement in patient response to treatment[162]. In soft tissue sarcomas, high expression of complement components has been correlated with resistance to chemotherapy and subsequent poor patient OS[365]. Our group have previously correlated elevated levels of pre-treatment circulating and tumoural complement with subsequent poor responses to neo-CRT in OAC[367,368]. Here, interestingly, the radiosensitive HCT116 cell line express significantly lower levels of C3 and C5, when compared to radioresistant SW837, HRA-19 and SW1463 rectal cancer cells. Intracellular levels of C3, C5, C3a and C5a exceeded secreted levels, and the total intracellular concentration of these components positively correlated with SF of cells at 1.8 Gy, a clinically-relevant dose of X-ray radiation. This demonstrates that there is a relationship between complement expression and the radioresponse in this CRC cell line panel. These

data suggest for the first time a role for complement in the response to radiation in rectal cancer.

Several studies have provided direct functional evidence for complement components both in the response to chemotherapy and immunotherapy[320,322,336,345,349,361,362]. At present, few studies have interrogated the relationship between complement system components and the radioresponse. Those that have, have demonstrated functional roles for complement anaphylatoxins in the response to radiation[350,351]. Importantly, these functional effects were due to complement-mediated regulation of immune cells within the TME. While the relationship between T cells and CRC cell-derived complement will be explored later in this thesis, the results from this chapter are derived purely from *in vitro* studies, which do not recapitulate the TME. This suggests that the effects of tumour cell-derived complement on the radioresponse *in vitro* in CRC are a result of autocrine signals, which promote radioresistance. In the literature, evidence for autocrine C3a/C3aR and C5a/C5aR1 signalling that enhances cancer cell proliferation, migration and invasiveness has been described[300,383]. To investigate the potential for complement signalling in CRC cells, the expression of complement receptors was assessed. The C3aR was not detected on the surface of CRC cells, however, low numbers of CRC cells were detected to express the C5aR1 extracellularly. Expression of the C5aR1 has been correlated with poor patient prognosis in a number of human cancers including ovarian, breast and non-small cell lung cancer[300,319,363]. This suggests that C5aR1 expression could contribute to the pathogenesis and therapeutic response of CRC cells.

In recent years, the functional significance of intracellular C3aR and C5aR1 expressed by T cells, among other cell types, is becoming increasingly apparent. Signalling through intracellular complement receptors is, for example, essential during the induction of Th1 responses[261,263–265]. Additionally, a growing body of research has demonstrated that intracellular complement is of functional importance both in normal cellular processes and in the context of cancer[261,263–265,342]. Recently, in ccRCC, pro-tumour roles for CFH, a complement regulatory protein, intracellularly, have been described. Interestingly, the pro-tumour functions of intracellular CFH are mediated through a non-canonical mechanism, and are distinct from those of the membrane-associated CFH[342]. Having demonstrated that complement is present intracellularly in CRC cells, the intracellular expression of complement receptors was investigated. Despite lacking expression of extracellular C3aR, it was demonstrated that almost 100% of HCT116, SW837, HRA-19 and SW1463 cells expressed both the C3aR and C5aR1 intracellularly. Intracellular C3aR in HCT116 cells

localised within the cytoplasm and the nucleus. This supports the hypothesis that signalling through intracellular C3aR and/or C5aR1 is of functional importance in CRC and may promote a radioresistant phenotype. In colon cancer cell lines, an intracellular C5a/C5aR1 signalling axis has recently been identified[341]. Signalling of C5a via C5aR1 expressed on endosomes stabilises β-catenin to drive gene transcription and promote tumourigenesis[341]. This highlights that intracellular complement signalling axes may play important roles in tumour progression and response to therapy. Interestingly, radiation was demonstrated to upregulate intracellular C5aR1 expression in the HCT116, SW837 and SW1463 cell lines, with a trend towards upregulation observed in HRA-19 cells. Upregulation of intracellular C3aR expression was also determined in HCT116 cells. This suggests that radiation may promote complement signalling in CRC cells.

The powerful inflammatory response resulting from complement activation requires regulation to avoid uncontrolled inflammation and damage to healthy tissue. This is the responsibility of several soluble and membrane-bound effectors, including the widely expressed mCRPs CD46, CD55 and CD59[214]. Expression of mCRPs can halt complement activation at various stages of the pathway, a strategy exploited by cancer cells, which often demonstrate elevated expression of complement regulators, when compared to non-malignant tissue, allowing them to evade the complement system[286–289]. Unfortunately, this evasion strategy appears successful, as expression of mCRPs generally correlates with poor clinical outcomes in cancer[291]. CD46, CD55 and CD59 were demonstrated to be expressed in HCT116, SW837, HRA-19 and SW1463 cells, with no alterations in expression occurring following radiation. While there was widespread expression of CD46 and CD59, there were variations in the percentage of cells expressing CD55. CD55 was expressed at lower levels in the radioresistant HRA-19 and SW1463 cells. CD55 has been demonstrated to regulate cisplatin resistance and self-renewal independently of complement, in endometroid tumours[349]. It is also a poor prognostic marker in several human cancers including non-small cell lung cancer, breast cancer and CRC[287,363,399]. Despite correlation with a poor response in CRC, CD55 was expressed at lower levels in the most radioresistant CRC lines used in this chapter. This suggests that the relationship between CD55 and poor outcomes in CRC is due to other functional effects, which are independent of the response to radiation.

In summary, to our knowledge this is the first time the complement system has been characterised in this CRC cell line panel. CRC cell lines were demonstrated to express

central and pathway specific complement components and activation of the complement system was observed. CRC cells expressed complement receptors and regulators, suggesting that they can respond to complement signals and modulate complement activation, respectively. Interestingly, total intracellular complement correlated with radioresistance, suggesting a role for complement in the radioresponse in CRC. In particular, intracellular complement is significant as despite low extracellular expression of C5aR1, CRC cells expressed high levels of C3aR and C5aR1 intracellularly. This suggests there may be an important intracellular signalling axis in CRC. The results in this chapter demonstrate that complement is associated with the response to radiation in CRC *in vitro*.

Chapter 3: C3 functionally modulates radioresistance in CRC cells

3.1. Introduction

Radioresistance is a major clinical challenge in the treatment of LARC. Despite being the current standard of care, neo-CRT fails to achieve loco-regional control in up to 70% of patients[21,55,56]. The molecular factors governing response to therapy in this setting are poorly understood. Identifying novel therapeutic targets with the aim of increasing radiosensitivity is essential to improve response rates and outcomes in rectal cancer.

In the last decade, study of the complement system has demonstrated that targeting complement components may have potential in restoring anti-tumour immunity and boosting cancer treatment response[162]. Aberrant expression of complement components has been demonstrated in many human cancers including ovarian, breast and gastric cancer, and is frequently associated with adverse features and poor outcomes[285,317,319]. Across more than 32 cancer types, mutations in complement genes have been identified[287] and demonstrated to correlate with poor OS, suggesting that alterations in complement play a functional role in tumourigenesis[287]. The overexpression of complement in cancer suggests that targeting complement may have potential as a novel therapeutic approach. Study of murine models has demonstrated that within the TME, dysregulated expression of complement can suppress anti-tumour immunity, promoting tumour growth and progression[298] (summarised in [162]). In addition to modulation of immune cells, complement signalling has been demonstrated to drive tumourigenesis by activating the PI3K/AKT and JAK/STAT pathways[300,306,317,318,362].

Considering these novel roles in cancer, it is unsurprising that components of the complement system have been implicated in the tumour response to anti-cancer therapy. In addition to enhancing tumour growth, complement has been demonstrated to aid therapeutic resistance to RT, chemotherapy and immunotherapy by promoting immunosuppression[320,322,350,361,362]. Supporting this, previous work in our Department has demonstrated that high pre-treatment serum levels of C3a and C4a are predictive of subsequent poor responses to neo-CRT in OAC patients[367]. In addition, C3 expression was demonstrated to be elevated in pre-treatment OAC tumour tissue from patients with a subsequent poor response to neo-CRT[368]. These data highlight a potential role for complement in the response to treatment in GI cancers[367].

The relationship between complement and radiation response has been explored in two previous studies, both of which link C3a and C5a anaphylatoxins to the response to radiation[350,351]. In both of these studies, complement is demonstrated to alter the radioresponse via its extracellular functions, through modulation of immune cells.

However, increasing evidence demonstrates that complement is expressed intracellularly in immune cells and cancer cells, with intracellular complement demonstrating canonical and non-canonical roles[400]. In CRC, intracellular C5a/C5aR signalling stabilises β-catenin to promote transcription of oncogenes including cyclooxygenase-2 (COX-2) and cyclin D1[341]. Intracellular CFH has been demonstrated to enhance tumour cell proliferation, survival, migration and is associated with poor patient prognosis in lung adenocarcinoma and ccRCC[342]. This suggests that intracellular complement may also play a role in the tumour response to therapy. Supporting this, in endometrial cancer, CD55 overexpression was demonstrated to drive cisplatin resistance via intracellular activation of lymphocyte-specific protein tyrosine kinase (LCK) signalling[349]. Currently, the role of intracellular complement in the response to RT is yet to be elucidated. Data presented in Chapter 2 demonstrated that expression of key complement system components are elevated in radioresistant CRC cell lines and positively correlate with inherent radioresistance to a clinically-relevant dose of X-ray radiation. This suggests that intracellular functions of complement, independent of immune cell-modulation, may be involved in the tumour response to RT in CRC. However, the mechanism (s) by which intracellular complement may modulate treatment response is largely unknown.

Whilst the leading cause for radioresistance is yet to be elucidated, there are several known parameters that impact on the tumour response to radiation. Alterations in DNA repair capabilities are often implicated in radioresistance[122–124]. The DDR is activated following the induction and detection of DNA damage. This triggers a DNA repair pathway or other downstream signals including programmed cell death[106,117]. Neoplastic transformation is associated with an accumulation of genomic instability, often rendering cancer cells defective in one or more DNA repair pathway[115,121]. This is exploited by cytotoxic therapies which induce lethal DNA damage, such as double-strand breaks (DSBs) that are difficult to resolve[106,115]. However, an enhanced ability to repair DNA damage has been demonstrated in radioresistant cancer cells[122–124].

Alterations in cell cycle distribution and progression are also recognised as contributors to radioresistance. Four phases, gap (G) 1, synthesis, G2 and mitosis (M) compose the cell cycle, together with the G0 phase which is outside the cell cycle[107]. Sensitivity to radiation is altered depending on phase of the cell cycle, with cells in the G2 and M phases being most sensitive to radiation, cells in G0 being more resistant, while cells in S phase are most resistant[95–97]. Progression through the cell cycle is governed by various

cell cycle checkpoints, which are activated during the DDR to halt progression to the next phase[107]. At each phase of the cell cycle various DDR pathways are active, therefore activation of cell cycle checkpoints allows for repair of damaged DNA[126]. Cancer cells demonstrate defective checkpoint operation, and loss of the G1 checkpoint is common[401,402]. Thus, cell cycle checkpoint targeting drugs have been proposed as a viable method to enhance response to therapy including RT[140]. Understanding the mechanisms by which cancer cells alter dependency on cell cycle checkpoints is also essential to boosting therapeutic efficacy.

Apoptosis is another parameter linked with DNA repair pathways and the DDR[126]. If DNA damage cannot be repaired, cells may undergo apoptosis or senescence[115]. Apoptosis can occur by two pathways; the intrinsic or mitochondrial-mediated pathway, and the extrinsic or death receptor-mediated pathway, both of which have been implicated in radiation-induced apoptosis[114]. The contribution of apoptosis to radiation-induced cell death is controversial, and thought to play a modest role at least in the elimination of solid tumours[114]. However, in several cancer types including lung, breast and neuroblastoma, reduced apoptosis has been associated with radioresistance[143–145].

The mechanisms by which complement may be modulating the tumour response to RT and its relationship with pathways implicated in radioresistance is unknown. Therefore the aim of this chapter was to investigate how complement functionally modulates the response to radiation in CRC.

3.2. Specific aims of Chapter 3

The aim of this chapter was to investigate the functional role of C3 in the radioresponse of CRC cells.

The specific aims of Chapter 3 are;

1. Optimise overexpression of C3 in HCT116 cell lines, which express lower levels of C3, using a complementary DNA (cDNA) vector for C3.
2. Assess the effect of C3 overexpression on radiosensitivity in HCT116 cells.
3. Optimise silencing of C3 in the radioresistant SW837 and HRA-19 cell lines, which express higher levels of C3 relative to the radiosensitive HCT116 cell line, using small interfering RNA (siRNA) for C3.
4. Assess the effect of C3 siRNA silencing on the radiosensitivity of the SW837 and HRA-19 cell lines line by clonogenic assay.

5. Investigate the mechanism (s) by which C3 contributes to radioresistance by characterising viability, cell cycle distribution, DNA damage induction and DNA repair in CRC cells, basally and post modulation of C3 expression.
6. Investigate potential interactors of C3 in HCT116 and HRA-19 cells by mass spectrometry

3.3. Materials and methods

3.3.1. Transformation of competent E. coli for vector amplification

C3 was overexpressed in HCT116 cells using a Human untagged complement component 3 cDNA ORF Clone DNA plasmid (SinoBiological, Beijing, China). Negative controls were set up in parallel using pCMV3-untagged Negative Control Vector (SinoBiological, Beijing, China). These vectors were amplified using chemically competent E. coli (XL10-Gold Ultracompetent Cells) (Agilent, California, United States).

Chemically competent E. coli were thawed on ice. C3 or vector control (VC) plasmid DNA was added at a concentration of 0.5 μg and incubated on ice for 5 min. E. coli were transformed by heat shock by incubating in a water bath for 45 s at 42°C, before incubating on ice for 2 min. Fast-Media Amp Terrific Broth (200 mL) (InvivoGen, San Diego, California) was prepared according to the manufacturer's instructions, inoculated with the transformed E. coli solution and incubated at 37°C with agitation overnight in a Stuart SI50 Orbital Incubator (Cole Palmer, Illinois, United States).

3.3.2. Purification of DNA plasmids

Bacterial cultures were harvested by centrifugation at 4,000 RPM for 20 min at 4°C. DNA plasmids were purified using the Qiagen Plasmid Midi Kit (Qiagen, Hilden, Germany) according to the manufacturer’s instructions. DNA was precipitated using isopropanol and resuspended in molecular grade water.

3.3.3. Quantification of purified DNA plasmids

Purified DNA plasmids were quantified and assessed for purity spectrophotometrically using a DS-11 Series Spectrophotometer/Fluor (DeNovix, Delaware, United States). The pedestal was cleaned using molecular grade water and the machine was blanked using 1 μL of molecular grade water. The A260/280 and A260/230 ratios were recorded to assess the quality of DNA isolated. DNA concentration in ng/mL was measured by loading 1 μL of each sample onto the pedestal. DNA plasmids were stored at -20°C until required.

3.3.4. Reverse transfection of CRC cells for transient overexpression of C3 plasmid DNA

Expression of purified C3 and VC plasmids was achieved by transient reverse transfection, which involves combining transfection complexes with cells that are in suspension, rather than adhered to the plate or flask. This can improve transfection efficiency, as a greater cell surface area is exposed. C3 or VC DNA plasmids (0.1 µg or 0.25 µg) were diluted to a final volume of 100 µL per well to be transfected with RPMI. A 5 µL volume of the transfection reagent, Lipofectamine 2000 (Invitrogen), was diluted to 100 µL per well to be transfected with RPMI. The diluted plasmids and lipofectamine were incubated at RT for 5 min. The diluted Lipofectamine was added to the diluted plasmids, mixed gently and incubated for 20 min at RT° to allow the transfection complexes to form. Cells in the exponential growth phase were harvested by trypsinisation as previously described (Section 2.3.4), counted (Section 2.3.8) and adjusted to a final concentration of 2 x 10^5 cells per mL in RPMI supplemented with 10% FBS. In 6-well plates, 200 µL of C3 or VC plasmid/lipofectamine complex was added to each well. Cell only control wells were prepared by adding a 200 µL volume of RPMI only. A 1.5 mL volume of cell suspension (3 x 10^5 cells) was added to all wells. Plates were rocked back and forth gently for 10 s and incubated at 37°C, 5% CO_2/ 95% humidified air. After 4 h incubation, media was replaced with fresh RPMI supplemented with 10% FBS. RNA was isolated at 24 h and 48 h and 72 h post transfection as previously described (Section 2.3.13) to confirm transfection efficiency. Protein was isolated at 24 h post transfection as previously described (Section 2.3.19). C3 overexpression was confirmed at the gene and protein level by qPCR and ELISA (as described in Section 2.3.16 and Section 2.3.21, respectively).

3.3.5. siRNA transient transfection

C3 was transiently silenced in HRA-19 and SW837 cells using FlexiTube siRNA (Qiagen, Hilden, Germany) by transient reverse transfection. FlexiTube siRNAs for C3 and the AllStars Negative control siRNA (Qiagen, Hilden, Germany) (10 nM or 50 nM) were diluted to a final volume of 300 µL per well to be transfected, with RPMI. A 5 µL volume of the transfection reagent, Lipofectamine 2000 (Invitrogen), was diluted to 300 µL per well to be transfected using RPMI. The diluted siRNA and Lipofectamine were incubated at RT° for 5 min. Following this, the diluted Lipofectamine was added to the diluted siRNA, mixed gently and incubated for 20 min at RT° to allow the transfection complexes to form.

Cells in the exponential growth phase were harvested by trypsinisation as previously described (Section 2.3.4), counted (Section 2.3.8) and adjusted to a final concentration of 1 x 10^5 cells per mL in RPMI supplemented with 10% FBS. In 6-well plates, 600 µL of C3 (termed si-C3) or control siRNA (termed si-scr)/lipofectamine complex was added to each well. A 600 µL volume of RPMI only was added to cells only (no transfection complexes), control wells. A 2.4 mL volume of cell suspension (2.4 x 10^5 cells) was added to each well. Plates were rocked back and forth gently for 10 s and incubated at 37°C, 5% CO_2/ 95% humidified air. RNA was isolated at 24 h and 48 h post transfection as previously described (Section 2.3.13) to confirm transfection efficiency. Protein was isolated at 24 h post transfection as previously described (Section 2.3.19). C3 silencing was confirmed at the gene and protein level by qPCR and ELISA (as described in Section 2.3.16 and Section 2.3.21, respectively).

3.3.6. Clonogenic survival following transient transfection

The effect of complement silencing or overexpression on radiosensitivity in CRC cells was assessed by clonogenic assay. At 24 h post transfection with siRNA (as described in Section 3.3.5) or plasmid DNA (as described in Section 3.3.4), cells were irradiated with 1.8 Gy or mock irradiated (as described in Section 2.3.9). Cells were incubated for 1 h at 37°C, 5% CO_2/ 95% humidified air before being trypsinised, counted and seeded in 6-well plates (as described in Section 2.3.10), at optimised seeding densities (**Table 3-1**). Cells were incubated for 8-21 days at 37°C, 5% CO_2/95% humidified air until colonies had formed but not merged. Colonies were stained with crystal violet (as described in Section 2.3.11) before colonies were counted and the surviving fraction of cells calculated (as described in Section 2.3.12).

Table 3-1: Seeding densities to assess clonogenic survival following transient transfection.

Radiation dose	Number of cells seeded per well (6-well plate)		
	HCT116	**SW837**	**HRA-19**
0 Gy	500	3000	3000
1.8 Gy	1000	6000	4000

3.3.7. Annexin V (AV)/ propidium iodide (PI) assay to assess cell death

Cell death was assessed by flow cytometry using the AV/PI assay. AV binds phosphatidylserine, a component of the plasma membrane, which is exposed during apoptosis, so can detect apoptotic cells. PI is a fluorescent DNA-binding dye. Live cells, and those in early-stage apoptosis are not detected by PI, as they have an intact plasma membrane and exclude the dye. Late-stage apoptotic/dead cells and necrotic cells have compromised plasma membranes and so are detected by PI. Together, AV and PI can distinguish cells into four categories; live (AV^-PI^-), early-stage apoptotic (AV^+PI^-), late-stage apoptotic/dead (AV^+PI^+) and necrotic (AV^-PI^+) (**Fig. 3-1**).

HRA-19 cells were transfected with siRNA (Section 3.3.5) and HCT116 cells were transfected with DNA plasmids (Section 3.3.4). At 24 h post transfection, cells were irradiated or mock irradiated as previously described (Section 2.3.9). At 24 h post irradiation, supernatants were collected in 5 mL round-bottom polystyrene falcon tubes (Becton, Dickinson and Company, New Jersey, United States). The addition of these supernatants to the tubes ensures that unadhered and/or dead cells are kept for analysis. Adhered cells were washed with 500 µL of PBS and trypsinised as previously described (Section 2.3.4). Trypsin was neutralised using 500 µL of RPMI and cell suspensions were transferred to the tubes containing their corresponding supernatants. Cells were pelleted by centrifugation at 1,300 RPM for 3 min at RT° and the supernatants discarded. Cells were washed with 1 mL of PBS and pelleted as before.

The supernatant was discarded to waste and the cells were washed with 500 µL of 1X AV binding buffer (Diluted 1:10 with PBS from 10X stock, (0.1 M HEPES pH 7.4, 1.4 M NaCl, 25 Mm CaCl2 in dH_2O)). Cells were pelleted again by centrifugation at 1,300 RPM for 3 min at RT°. Cells were stained with 100 µL of AV-FITC antibody staining solution (Biolegend, San Diego, United States) stain (2 µL of AV-FITC antibody in 98 µL of 1X AV binding buffer) in the dark at RT° for 20 min. Following incubation, cells were washed with 500 µL of 1X AV binding buffer and pelleted. Cells were resuspended in 250 µL of 1X AV binding buffer. PI (Invitrogen, Massachusetts, United States) was diluted 1:4000 using 1X AV binding buffer. Immediately before sample acquisition, 250 µL of PI staining solution was added to each tube, resulting in a final dilution of 1:8000. Samples were acquired using a BD FACSCanto II (Becton, Dickinson and Company, New Jersey, United States) and FACSDiva Software (Becton, Dickinson and Company, New Jersey, United States). Analysis was performed using FlowJo v10 Software (Becton, Dickinson and Company, New Jersey, United States).

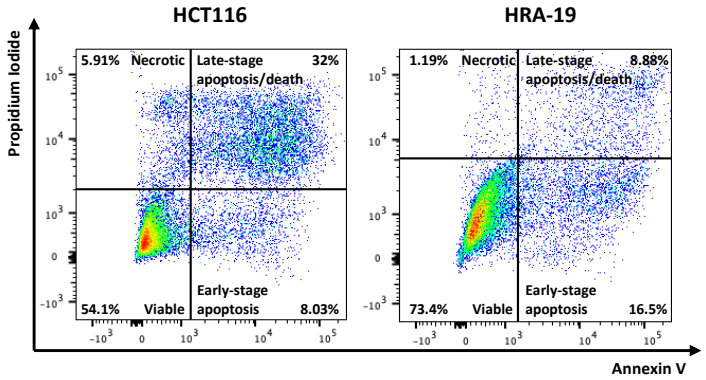

Figure 3-1: Representative dot plots of AV/PI staining on HCT116 and HRA-19 cells. Dot plots illustrate the live (AV^-PI^-), early apoptotic (AV^+PI^-), late apoptotic/dead (AV^+PI^+) and necrotic (AV^-PI^+) populations, which can be distinguished using this assay.

3.3.8. Assessment of cell cycle distribution and DNA damage

Cell cycle distribution and DNA damage was assessed by flow cytometry. PI staining was used to quantify the percentage of cells in each phase of the cell cycle. In the G0/G1 phases, cells have a DNA content of 2n. This increases as DNA is synthesised in the S phase, resulting in a DNA content of 4n when cells are in the G2/M phase. Cells in the S phase therefore have an intermediate DNA content, somewhere between 2n and 4n. As PI is a DNA-binding dye, the fluorescence intensity of PI staining will be proportional to the DNA content of a cell, distinguishing the proportion of cells in each phase of the cell cycle. The addition of ribonuclease (RNase) depletes RNA within the cell to ensure that only DNA is quantified.

The induction and repair of DNA damage in the form of DSBs, can be identified by measuring phosphorylated H2A histone family member X (γH_2AX). γH_2AX is a sensitive marker of DNA damage as phosphorylation occurs rapidly at the site of DSBs. Additionally, loss of H_2AX phosphorylation correlates with repair of DSBs, allowing for the kinetics of DNA repair to be assessed. This can be measured by flow cytometry using a γH_2AX antibody conjugated to a fluorescent fluorophore.

Cells in the exponential growth phase were harvested by trypsinisation as previously described (Section 2.3.4), counted (Section 2.3.8) and transfected with appropriate DNA vectors (3.3.4) or siRNA (3.3.5) in 6-well plates. Transfected cells were incubated for 24 h at 37°C, 5% CO_2/ 95% humidified air before being irradiated with 1.8 Gy or mock-irradiated (0 Gy), as previously described (Section 2.3.9). At 20 min, 6 h, 10 h and 24 h post irradiation or mock irradiation, cells were fixed and stained for analysis.

Cell supernatants were discarded to waste and each well was washed with 1 mL of warm PBS. Cells were trypsinised using 500 uL of Trypsin, neutralised with an equal volume of complete RPMI and cell suspensions were transferred to labelled 5 mL FACS tubes. Cells were pelleted by centrifugation at 1,300 RPM for 3 min at RT° and the supernatants discarded. Cells were washed with 1 mL of PBS and pelleted as described. Cells were re-suspended in 1 mL of PBS and fixed by dropwise addition of 2.5 mL 90% (v/v in deionised water) ethanol while vortexing, to prevent cell clumping. Cells were incubated for 30 min in the dark at RT°. Cells were pelleted by centrifugation at 1,300 RPM for 3 min at RT°, resuspended in 1 mL of PBS and stored at 4°C until staining. When cells for each time point had been collected and fixed, all cells were pelleted by centrifugation at 1,300 RPM for 3 min at RT° and supernatants were discarded. Cells were stained for γH2AX using 100 µL of γH2AX antibody staining solution (1:100 dilution of γH2AX-Alexa Fluor 488 antibody (Biolegend) in PBS/FBS (2%)/ Triton X-100 (0.1%)). As a positive control for γH2AX, cells irradiated with 10 Gy of X-ray radiation were stained using the γH2AX antibody staining solution. All cells were incubated in the dark for 2 h at RT°. Cells were washed with 1 mL of PBS/FBS (2%), pelleted by centrifugation as before, and supernatants were discarded. PI staining solution was prepared (PBS/PI (0.025 mg/mL)/RNAase A (0.1 mg/mL)/Triton X-100 (0.1%)) and cells were resuspended in 500 µL of PI staining solution. The PI staining solution was not added to the γH_2AX positive control. Cells were vortexed and incubated for 30 min at 37°C, in the dark. Samples were acquired using a BD FACSCanto II (Becton, Dickinson and Company, New Jersey, United States) and FACSDiva Software (Becton, Dickinson and Company, New Jersey, United States). Analysis was performed using FlowJo v10 Software (Becton, Dickinson and Company, New Jersey, United States).

3.3.9. Preparation of C3-FLAG plasmid

Transient overexpression of a FLAG-tagged C3 plasmid (C3 (NM_000064) ORF Clone) (GenScript Biotech Corp, New Jersey, United States) was performed using HCT116 and HRA-19 cells in preparation for immunoprecipitation (IP) and mass spectrometry. Vector amplification was performed by transforming chemically competent E. coli (Section 3.3.1). DNA plasmids were purified using the Qiagen Plasmid Midi Kit (Section 3.3.2), and quantified as previously outlined (Section 3.3.3).

3.3.10. Reverse transfection of CRC cells for transient overexpression of C3-FLAG plasmid DNA

Expression of purified C3-FLAG plasmid DNA was achieved by transient reverse transfection. C3-FLAG DNA plasmid (9 µg) was diluted to a final volume of 600 µL per 10 cm petri-dish to be transfected with RPMI. A 24 µL volume of the transfection reagent, Lipofectamine 2000 (Invitrogen), was diluted to 600 µL per petri-dish to be transfected with RPMI. The diluted plasmids and lipofectamine were incubated at RT for 5 min. The diluted Lipofectamine was added to the diluted plasmids, mixed gently and incubated for 20 min at RT° to allow the transfection complexes to form. Cells in the exponential growth phase were harvested by trypsinisation as previously described (Section 2.3.4), counted (Section 2.3.8) and adjusted to a final concentration of 1.8 x 10^6 cells per 5 mL in RPMI supplemented with 10% FBS. A 1.2 mL volume of C3-FLAG /lipofectamine complex was added to each 10 cm petri-dish. Cell only control wells were prepared by adding a 1.2 mL volume of RPMI only. A 5 mL volume of cell suspension (1.8 x 10^6 cells) was added to all wells, and the total petri-dish volume was adjusted to 9 mL using RPMI supplemented with 10% FBS. For each condition (HRA-19 or HCT116 cells, C3-FLAG transfected or cell only controls) three, 10 cm petri-dishes of cells were transfected. Dishes were rocked back forth gently for 10 s and incubated at 37°C, 5% CO_2/ 95% humidified air. After 4 h incubation, media was replaced with fresh RPMI supplemented with 10% FBS.

3.3.11. Preparation of protein lysates for IP

At 24 h post transfection, petri-dishes of transfected cells (prepared in Section 3.3.10) were placed on ice. Supernatants were removed and cells were gently washed using 1 mL of ice-cold PBS. To each plate 180 µL of protein lysis buffer (50 mM Tris-HCL pH 7.4, 0.5% NP-40, 150 mM NaCl, 20 mM $MgCl_2$) containing cOmplete, Mini Protease Inhibitor Cocktail (Roche, Basel, Switzerland) (one tablet per 10 mL of buffer) was added, and cells were detached using a cell scraper. The protein lysates were added to new 1.5 mL eppendorf tubes and incubated on ice for 30 min. Eppendorfs were centrifuged for 10 min at 4°C at 14,000 RPM, and supernatants were transferred to new eppendorf tubes. Protein concentration was determined by BCA assay (Section 2.3.20).

3.3.12. Preparation of ANTI-FLAG M2 magnetic beads

IP was performed using ANTI-FLAG M2 magnetic beads (Merck Millipore, Massachusetts. Prior to the addition of protein lysates (prepared in Section 3.3.11), beads were equilibrated. The ANTI-FLAG M2 magnetic bead resin was resuspended by gentle inversion and 40 µL of suspension (20 µL of packed gel volume) per sample was removed to an eppendorf. The eppendorf was placed in a magnetic separator to remove the storage buffer and collect the beads. Beads were washed twice with 10 packed gel volumes of 1X TBS (10X TBS (24 g Tris-HCl, 5.6 g Tris base, 88g NaCl adjusted to 1 L with H_2O) diluted 1:10 with H_2O), and then resuspended in 1X TBS and divided into eppendorf tubes according to the number of samples being prepared.

3.3.13. Immunoprecipitation

Protein lysates (1 mg) were diluted 5-fold using ice cold NET buffer (50 mM Tris pH 7.5, 5mM EDTA, 150 mM NaCl, 0.5% NP-40). To analyse the input fraction, 10% was removed and stored at -80°C. Lysates were pre-cleared by the addition of 50 µL of Protein G Plus/Protein A Agarose (Merck Millipore) (previously washed three times in NET buffer), and incubation on a rotator for 1 h at 4°C. Samples were centrifuged for 5 min at 5,000 RPM at 4°C and supernatants were transferred to a new eppendorf. Eppendorfs containing ANTI-FLAG M2 magnetic beads (prepared in Section 3.3.12) were placed in a magnetic separator and the 1X TBS removed. Protein lysate samples were added to the magnetic beads and incubated overnight on a rotator at 4°C overnight. The next day, supernatants were removed and stored for quality control (QC) experiments. The magnetic beads were washed twice using 500 µL of PBS, 5% were removed for silver stain QC checks and the remainder were stored at -80°C

3.3.14. SDS-PAGE and western blotting

C3-FLAG expression in CRC cells was detected by SDS-polyacrylamide gel electrophoresis (PAGE) and western blotting. Samples were resolved on a 4-15% mini-PROTEAN TGX Stain-Free Precast Gel (Bio-Rad, California, United States), using a mini-PROTEAN Tetra cell (Bio-Rad). Gels were placed in the running module within the cell, the comb was carefully removed and 1X running buffer (10X running buffer (30.2 g of Tris base, 144g glycine, 10g SDS, H_2O up to 1 L) diluted 1:10 with H_2O) was added. Input samples were diluted 1:2 with sample buffer (3.3% SDS, 6 M urea, 17mM Tris-HC1, 0.07

M β-mercaptoethanol and 0.01% bromophenol blue) and boiled for 5 min at 100°C. Magnetic beads were boiled in 20 µL of sample buffer for 5 min at 100°C and the buffer was carefully removed from the beads. The input and sample buffer from the boiled magnetic beads were carefully loaded into the gel wells. A 5 µL volume of Precision Plus Protein™ Kaleidoscope™ Prestained Protein Standards (Bio-Rad) was loaded into the first well. Samples were separated by electrophoresis for 1 h at 120 V.

3.3.15. Protein detection

Resolved proteins were transferred to a polyvinylidene difluoride (PVDF) membrane using a Trans-Blot Turbo Transfer System (Bio-Rad). The PVDF membrane and filter papers were soaked in 1X transfer buffer (10X transfer buffer (30.2 g Tris base, 144g glycine, H_2O up to 1 L) diluted 1:10 with H_2O). A transfer 'sandwich' was assembled in the cassette by stacking two transfer buffer-soaked filter papers, next adding the membrane, before adding the gel and finally a second filter paper stack. The gel was transferred onto the PVDF membrane for 7 min and then blocked with agitation for 1 h at RT° in 10 mL of blocking buffer (50:50 1X TBST (1X TBS with 0.1% Tween-20) and Intercept (TBS) Blocking Buffer (Li-Cor, Nebraska, United States))

Primary antibodies were prepared at the optimised dilution factor (**Table 3-2**) in 5 mL of blocking buffer. Blots were incubated with agitation overnight at 4°C. Primary antibodies were removed and the blot was washed five times in TBST. Secondary antibodies were prepared in 10 mL of blocking buffer at the optimised dilution factor (**Table 3-2**) and blots were incubated for 1 h at RT° with agitation. Blots were washed twice in TBST and once in TBS before imaging using a Li-Cor Odessey Infrared Imager.

Table 3-2: Primary and secondary antibodies and dilution factors for IP QC.

Antibody	**Primary**	**Primary**	**Secondary**
	Complement C3 Polyclonal Antibody	Anti-FLAG M2 Antibody	IRDye 680CW Goat Anti-Rabbit
Manufacturer	Invitrogen	Sigma Aldrich	Li-Cor
Dilution factor	1:1000	1:2000	1:10,000

3.3.16. SDS-PAGE and Silver staining

Prior to mass spectrometry analysis, SDS-PAGE and silver staining was performed to ensure the IP samples contained sufficient protein content. SDS-PAGE was performed using a mini-PROTEAN Tetra cell (Bio-Rad). The glass casting apparatus was thoroughly cleaned with warm water and 70% (v/v) ethanol and assembled. A 7.5% resolving gel was prepared (**Table 3-3**) and gently pipetted between the two plates. To ensure an even gel and assist polymerisation a layer of isopropanol was pipetted on top. When the gel had polymerised (approx. 30 min), the isopropanol was carefully removed, the stacking gel (**Table 3-4**) was pipetted on top and a 10-well comb was inserted into the gel. When the gel had polymerised (approx. 30 min), the gel was clamped into a gasket which was then fitted into the running module in the cell. The cell was filled with the indicated amount of 1X running buffer (10X running buffer (30.3 g Tris base, 144g glycine, 100 mL 10% SDS, H_2O up to 1 L) diluted 1:10 with H_2O). The 1X running buffer was also added up to the top of the gasket. The well comb was carefully removed vertically and the wells were flushed with 1X running buffer using a 1 mL syringe to remove residual polymerised stacking gel. A 5 µL volume of PageRuler Plus Prestained Ladder (Thermo Fisher Scientific) was loaded to the first well. The supernatant and 5% magnetic bead IP fractions (prepared in Section 3.3.13) were prepared for loading. A 10 µL volume of sample buffer (125 mM Tris-HCL pH 6.8, 4% SDS, 30% (v/v) glycerol, 0.0004% bromophenol blue) was added to 10 µL of supernatant, and 20 µL of sample buffer was added to the magnetic beads and samples were boiled at 5 min at 100°C. The magnetic beads were separated from the sample buffer, and samples were allowed to cool before loading into the gel. Samples were separated by electrophoresis for 1 h at 120 V.

Silver staining of gels was performed using the Pierce Silver Stain Kit (Thermo Fisher Scientific, Massachusetts, United States) according to the manufacturer's instructions. Briefly, gels were carefully removed from the glass plates and washed twice for 5 min in ultrapure H_2O. Gels were fixed by incubating in 30% ethanol:10% acetic acid solution twice for 15 min. Gels were then washed twice in 10% ethanol for 5 min and twice in ultra-pure H_2O for 5 min. The Sensitiser Working Solution (50 µL Sensitiser in 25 mL H_2O) was prepared and gels were sensitised for exactly 1 min before washing twice in ultrapure H_2O for 1 min. The Stain Working Solution was prepared (0.5 mL Enhancer in 25 mL Stain) and the gels were stained for 30 min. The Developer Working Solution was prepared (0.5 mL Enhancer in 25 mL Developer). Gels were washed twice for 20 s with

ultrapure H_2O and then developed for 2-3 min until bands appeared. The development was stopped by incubating the gel in 5% acetic acid for 10 min. As the silver stain bands are visible by eye, gels were imaged in their staining trays.

Table 3-3: Resolving gel (7.5%) components and volumes.

Component	7.5%
H_2O	7.4 mL
1.5 M Tris pH 8.8	3.75 mL
Acrylamide	3.65 mL
10% SDS	150 µL
10% APS	75 µL
TEMED	18 µL

Table 3-4: Stacking gel components and volumes.

Component	Volume
H_2O	6.1 mL
0.5 M Tris pH 6.8	2.5 mL
Acrylamide	1.3 mL
10% SDS	100 µL
10% APS	100 µL
TEMED	20 µL

3.3.17. Mass spectrometry to identify interactors of C3

Mass spectrometry was performed in collaboration with Dr Monica Olcina, at the University of Oxford. On-bead digest of samples (prepared in Section 3.3.13) was performed using SMART Digest Trypsin (Thermo Fisher Scientific), according to the manufacturer's instructions, and analysed by liquid chromatography with tandem mass spectrometry (LCMSMS) by Dr Iolanda Vendrell and Assoc. Prof. Roman Fischer at the Discovery Proteomics Facility, Target Discovery Institute, University of Oxford. Mass spectrometry data was label-free acquired in data-independent acquisition (DIA) mode and label-free quantification (LFQ) was performed using DIA-NN software (Demichev, Ralser and Lilley labs)[403]. The data were further analysed in Perseus[404]. Protein intensity as determined by LFQ was log2 transformed, and a median centred normalisation was

performed. To increase the robustness of the dataset, a filtering step was introduced which retained all proteins with quantitative values on all three biological replicates at least in one of the groups.

3.3.1. Statistical analysis

Graphing of results and statistical analysis was performed using Prism 9 Software (GraphPad, California, United States). All data are presented as mean ± SEM, unless otherwise indicated. Significance was determined by ANOVA with post-hoc Tukey's multiple comparisons testing or Student's *t*-test, as detailed in figure legends. Where comparison groups were paired (i.e. untreated vs. treated), a paired *t*-test was performed, otherwise unpaired *t*-tests were used. Results were considered significant where $p \leq 0.05$.

For mass spectrometry data, significant proteins ($p < 0.05$) were identified using the two-sample Student's *t*-test combined with permutation false discovery rate (FDR) (5%) to calculate adjusted p-values (*p*-adj) ($q < 0.05$). Further clustering analysis was performed for proteins where *p*-adj was significant, to generate heatmaps and profile plots. The STRING online database of known and predicted protein-protein interactions was used to generate predicted protein networks and perform functional enrichment analysis.

3.4. Results

3.4.1. Optimisation of transient transfection of C3 overexpression vector

The optimum conditions for transient transfection of a C3 overexpression vector was determined in HCT116 cells. To determine the optimum DNA plasmid concentration, HCT116 cells were reverse transfected with either 0.1 µg or 0.25 µg of a C3 or a VC DNA plasmid and the relative C3 expression levels were assessed by qPCR.

C3 mRNA expression was upregulated following transfection with 0.1 µg of C3 plasmid DNA by > 214,000 fold at 24 h post transfection, when compared to VCs (Relative C3 mRNA expression; Cells only 1, VC 2.158, C3 462,573) (**Fig. 3-2 A**). Elevated expression was maintained, when compared to VCs at both 48 h (Relative C3 mRNA expression; Cells only 0.014, VC 0.053, C3 812.241) and 72 h post transfection (Relative C3 mRNA expression; Cells only 0.07, VC 0.011, C3 523.9) (**Fig. 3-2 A**). Similarly, transfection with 0.25 µg of C3 plasmid DNA resulted in a large upregulation of C3 mRNA (> 535,000 fold) by 24 h post transfection, when compared to VC. (Relative C3 mRNA expression; Cells only 1, VC 2.584, C3 1,383,000) (**Fig. 3-2 A**). Elevated expression was maintained, when compared to VCs at both 48 h (Relative C3 mRNA expression; Cells only 0.014, VC 0.02, C3 61,478.1) and 72 h post transfection (Relative C3 mRNA expression; Cells only 0.07, VC 0.007, C3 112.92) (**Fig. 3-2 B**). As both plasmid concentrations investigated resulted in increased expression of C3 at 24 h, 48 h and 72 h post transfection, a concentration of 0.1 µg was selected for all downstream experiments.

Expression of C3 was assessed by ELISA to confirm upregulation at the protein level. Using a concentration of 0.1 µg C3 plasmid, HCT116 cells expressed > 2-fold more C3 protein, when compared to VC, at 24 h post transfection (Relative C3 protein expression; Cells only 1, VC 3.916, C3 8.046) (**Fig. 3-2 C**).

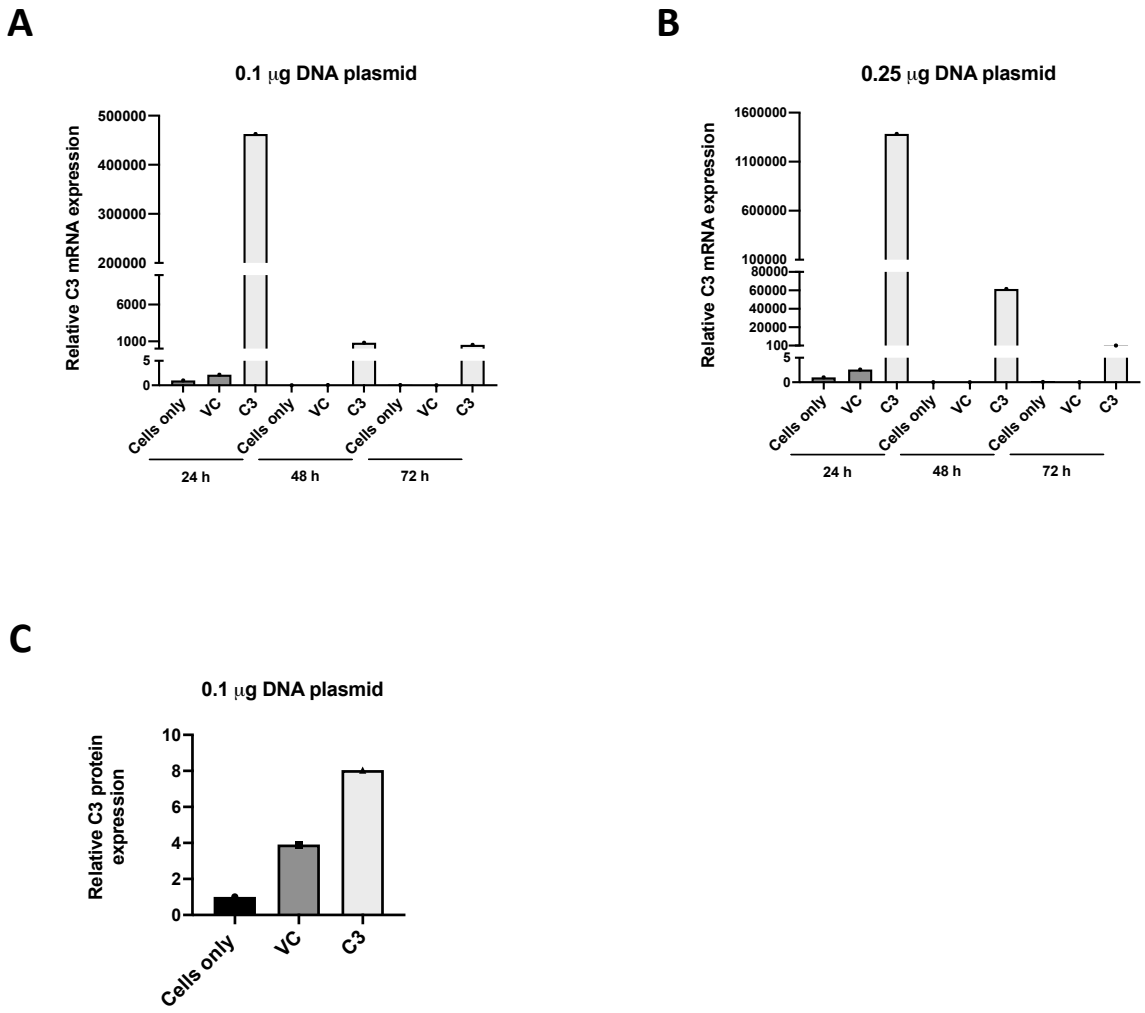

Figure 3-2: Optimisation of C3 overexpression plasmid DNA concentration in HCT116 cells. HCT116 cells were transfected with either **(A)** 0.1 μg or **(B)** 0.25 μg of C3 or vector control (VC) plasmid DNA. Relative C3 mRNA expression was assessed by qPCR at 24 h, 48 h and 72 h post transfection. Data are presented as the relative expression of C3 from a single experiment. **(C)** Relative C3 protein expression was assessed by ELISA at 24 h post transfection with 0.1 μg of plasmid DNA. Data are presented as the relative expression of C3 protein from a single experiment.

3.4.2. Overexpression of C3 enhances radioresistance in HCT116 cells

As demonstrated in Chapter 2, the HCT116 cell line is inherently radiosensitive and expresses significantly lower levels of C3, when compared to the more radioresistant cell lines characterised (**Fig. 2-3, Fig. 2-6)**. These data suggest that C3 may play a role in the radioresponse of CRC cells. To investigate whether C3 functionally modulates the response to radiation, the effect of C3 overexpression on the radiosensitivity of HCT116 cells at a clinically-relevant dose of 1.8 Gy was assessed using the gold standard clonogenic assay.

Overexpression of C3 was confirmed by qPCR (as described in Section 2.3.16) (**Fig. 3-3 A**). Cells transfected with VC DNA plasmid demonstrated an upregulation of C3, when compared to untransfected cells (Relative C3 expression ± SEM; 52.6 ± 41.4 vs 1.19 ± 0.19, respectively), however, cells transfected with C3 DNA plasmid demonstrated much greater upregulation of C3 (> 20 fold), when compared to VCs (Relative C3 expression ± SEM; 1008 ± 560 vs. 52.6 ± 41.4, respectively). At 1.8 Gy, cells transfected with C3 still demonstrated upregulated expression of C3, relative to cells transfected with a VC (Relative C3 expression ± SEM; 22786 ± 13717 vs. 7.724 ± 4.865, respectively).

Irradiation with 1.8 Gy greatly reduced survival in HCT116 cells transfected with C3 or VC (0.439 ± 0.038 or 0.243 ± 0.037, respectively), when compared to an unirradiated control set at 1.00 (**Fig. 3-3 B**). Interestingly, HCT116 cells transfected with C3 were significantly ($p = 0.0263$) more resistant to 1.8 Gy, when compared to VC transfected cells, suggesting that C3 plays a functional role in modulating radioresistance in HCT116 cells.

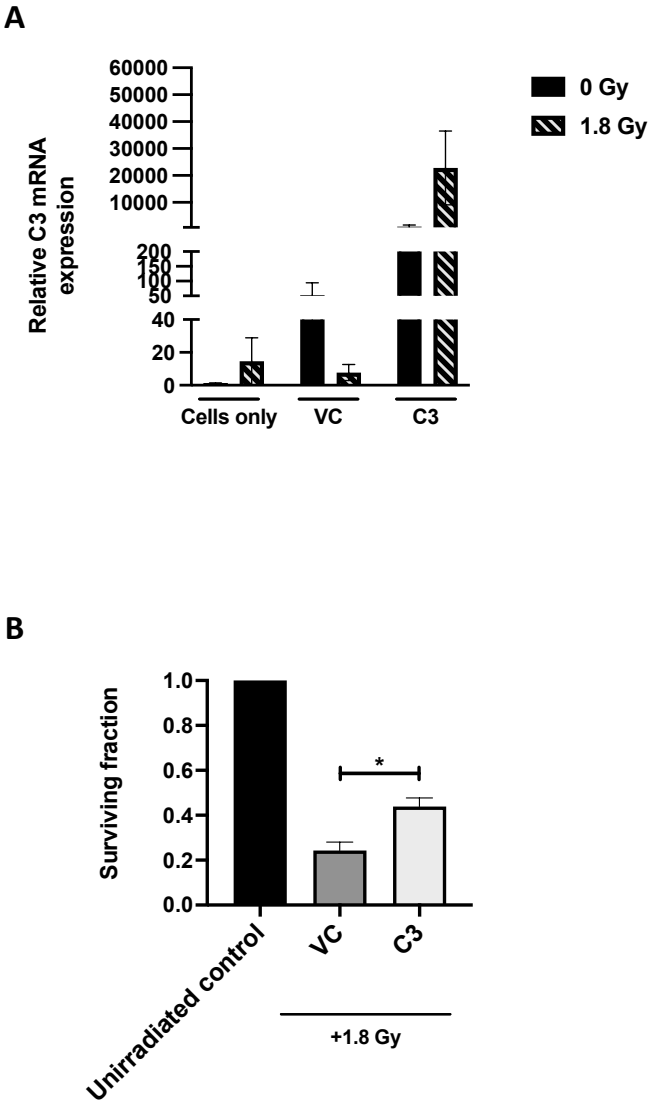

Figure 3-3: Overexpression of C3 significantly enhances the radioresistance of HCT116 cells at 1.8 Gy of X-ray radiation. HCT116 cells were transfected with 0.1 µg of C3 or a VC plasmid DNA. At 24 h post transfection, cells were irradiated with 1.8 Gy whilst control cells were mock irradiated. At 25 h post transfection cells were trypsinised, counted and seeded at optimised clonogenic seeding densities. RNA was also isolated. **(A)** C3 upregulation was confirmed by qPCR. Data are presented as mean ± SEM for 2 independent experiments. C3 was upregulated in cells that had been transfected with C3 plasmid DNA. **(B)** Surviving colonies at the end of the clonogenic incubation period were counted and the surviving fraction determined. Data are presented as mean ± SEM for 4 independent experiments. Statistical analysis was performed by paired two-tailed Student's *t*-test. *$p < 0.05$.

3.4.3. C3 overexpression does not alter basal apoptosis in HCT116 cells

Having demonstrated that overexpression of C3 in HCT116 cells results in enhanced radioresistance, the potential mechanism(s) by which C3-mediated radioresistance is occurring was investigated. Alterations in apoptosis have been implicated in the therapeutic response to RT[143–145] and consequently, the effects of C3 overexpression on apoptosis in HCT116 cells was investigated. HCT116 cells were transfected with a C3 or VC plasmid. At 24 h post transfection, cells were irradiated with 1.8 Gy or mock-irradiated (0 Gy) and cell viability was assessed at 24 h and 48 h following irradiation using the AV/PI assay.

The percentage of live VC and C3 transfected HCT116 cells was significantly reduced, when compared to RPMI controls at 24 h (p = 0.0458, p = 0.013, respectively) (Mean % of AV^-PI^- cells ± SEM; RPMI 91.87% ± 2.05, VC 46.93 ±7.966, C3 46.833 ±3.18) (**Fig. 3-4 A**) and 48 h (p = 0.0045, p = 0.0289, respectively) (Mean % of AV^-PI^- cells ± SEM; RPMI 88.03% ± 1.43, VC 57.9 ± 3.45, C3 56.4 ± 6.2) (**Fig. 3-5 A**). The percentage of late apoptotic/dead (AV^+PI^+) cells was significantly elevated in mock irradiated VC and C3 HCT116 cells, when compared to RPMI controls at 24 h (p =0.0385, p = 0.0265, respectively) (Mean % of AV^+PI^+ cells ± SEM; RPMI 1.61 % ± 0.696, VC 36.067 ± 6.398, C3 33.567 ± 1.69) (**Fig. 3-4 C**) and 48 h timepoints (p = 0.0048, p = 0.0389, respectively) (Mean % of AV^+PI^+ cells ± SEM; RPMI 4.517 % ± 1.461, VC 25.3 ± 2.095, C3 27.83 ± 5.62) (**Fig. 3-5 C**), suggesting that transfection altered viability of HCT116 cells. However, there were no significant alterations in viability demonstrated between C3 or VC transfected HCT116 cells at both 24 h (**Fig. 3-4 A)** or 48 h **(Fig. 3-5A)** timepoints. Additionally, the percentage of early apoptotic, late apoptotic/dead or necrotic cells was comparable at 24 h and 48 h (**Fig. 3-4 B-D, Fig. 3-5 B-D**) in cells transfected with C3 or VC. This suggests that C3 does not alter basal apoptosis in HCT116 cells

3.4.4. C3 overexpression does not alter radiation-induced apoptosis in HCT116 cells

To investigate whether radiation-induced apoptosis was altered in HCT116 cells overexpressing C3, apoptosis was assessed at 24 h and 48 h following 1.8 Gy of X-ray radiation. Radiation did not significantly induce early apoptosis, late apoptosis/death or necrosis, when compared to mock-irradiated controls in HCT116 cells transfected with either C3 or a VC at 24 h (**Fig. 3-4 B-D**) or 48 h (**Fig. 3-5 B-D**) post 1.8 Gy. There were no alterations in the percentage of live HCT116 cells transfected with either C3 or a VC at 24 h (**Fig. 3-4 A**) or at 48 h post irradiation (**Fig. 3-5 A**). This suggests that radiation-

induced apoptosis is not a major mechanism of cell death in C3 and VC transfected HCT116 cells.

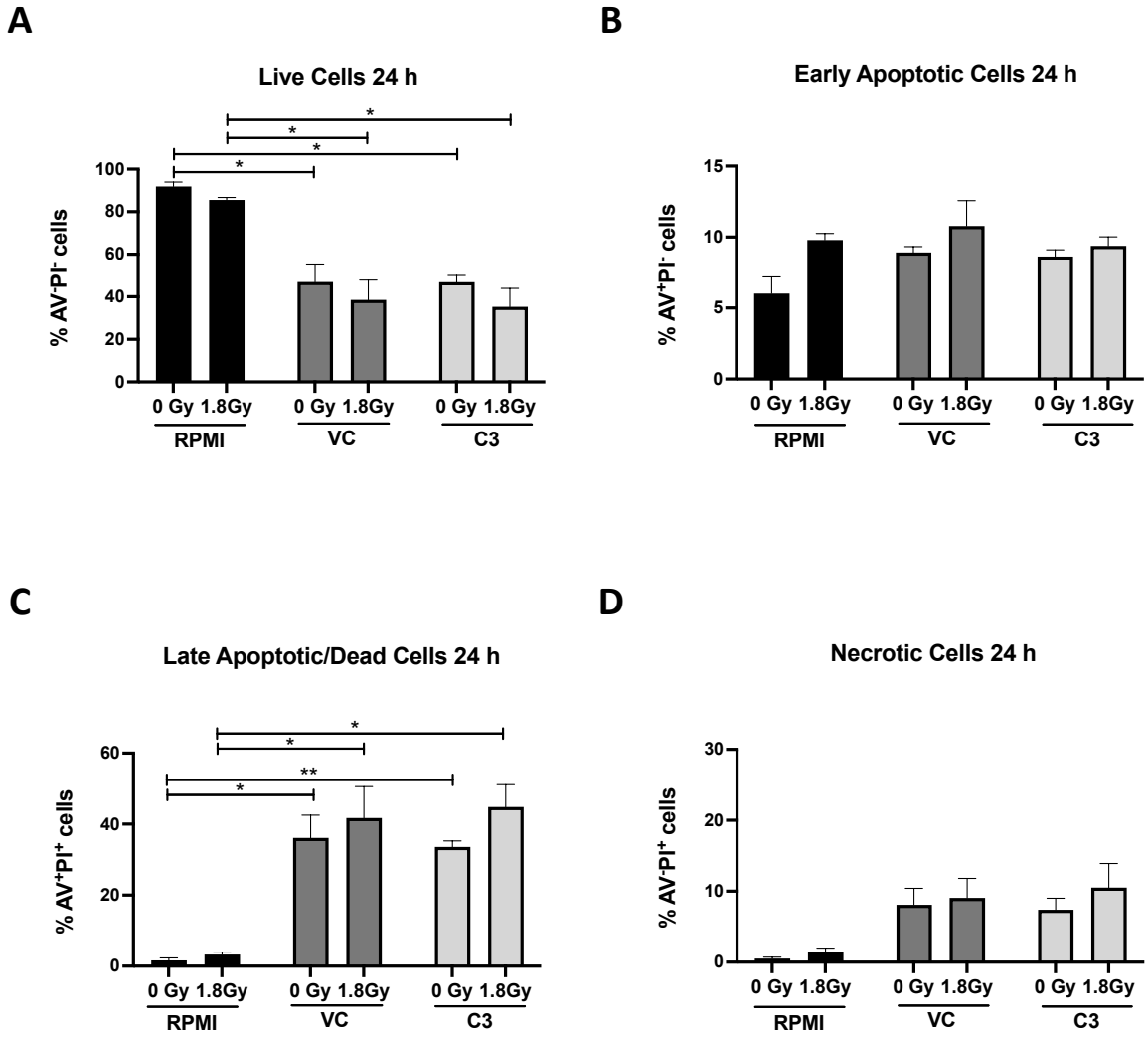

Figure 3-4: C3 overexpression does not alter the viability of HCT116 cells basally or at 24 h following irradiation. HCT116 cells were transfected with C3 or a VC plasmid. At 24 h post transfection, cells were irradiated with 1.8 Gy or mock irradiated and apoptosis was assessed at 24 h post irradiation by AV/PI assay. Percentage of **(A)** live (AV^-PI^-), **(B)** early apoptotic (AV^+PI^-), **(C)** late apoptotic/dead (AV^+PI^+) and **(D)** necrotic (AV^-PI^+) C3, VC, and RPMI control HCT116 cells were analysed. Data are presented as mean ± SEM for 3 independent experiments. Statistical analysis was performed by paired two-tailed Student's *t*-test. $*p < 0.05$, $**p < 0.01$.

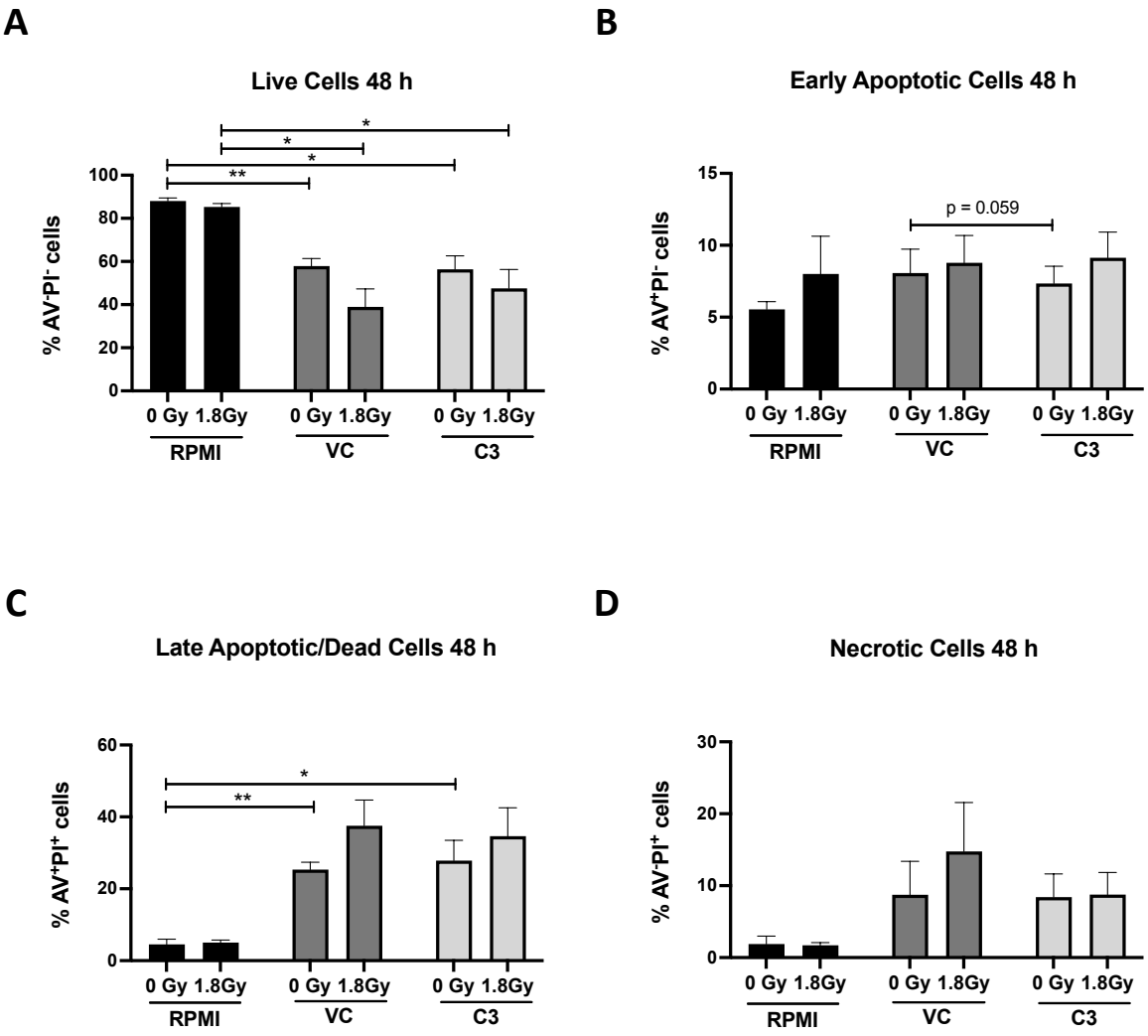

Figure 3-5 C3 overexpression does not alter the viability of HCT116 cells basally or at 48 h following irradiation. HCT116 cells were transfected with C3 or a VC plasmid. At 24 h post transfection, cells were irradiated with 1.8 Gy, or mock irradiated and apoptosis was assessed at 48 h post irradiation by AV/PI assay. Percentage of **(A)** live (AV^-PI^-), **(B)** early apoptotic (AV^+PI^-), **(C)** late apoptotic/dead (AV^+PI^+) and **(D)** necrotic (AV^-PI^+) C3, VC, and RPMI control HCT116 cells were analysed. Data are presented as mean ± SEM for 3 independent experiments. Statistical analysis was performed by paired two-tailed Student's *t*-test. *$p < 0.05$, **$p < 0.01$.

3.4.1. C3 overexpression does not alter basal DNA damage in HCT116 cells

DNA is the critical target of radiation and alterations in DNA damage contribute to radioresistance. To investigate the potential contribution of DNA damage to C3-mediated enhancement of radioresistance, HCT116 cells were transfected with C3 or a VC and at 24 h and 48 h post transfection basal DNA damage was assessed by measurement of γH_2AX using flow cytometry. H_2AX is a sensitive marker of DNA damage, becoming rapidly phosphorylated to γH_2AX at the sites of DSBs[405].

There were no alterations in the MFI of γH_2AX in HCT116 cells transfected with C3, when compared to HCT116 cells transfected with a VC at 24 h (**Fig. 3-6 A)** or 48 h (**Fig. 3-6 B)** post transfection. These data suggest that overexpression of C3 in HCT116 cells does not alter basal DNA damage levels.

3.4.2. C3 overexpression does not alter radiation-induced DNA damage in HCT116 cells

Having demonstrated that HCT116 cells overexpressing C3 are significantly more radioresistant following 1.8 Gy of X-ray radiation, when compared to cells transfected with a VC, DNA damage was assessed at 20 min post irradiation to investigate whether C3 overexpression is associated with altered radiation-induced DNA damage induction.

There were no alterations in γH_2AX fluorescence in C3, VC, or RPMI control HCT116 cells 20 min post 1.8 Gy **(Fig. 3-7 A)**, when compared to their unirradiated controls. This suggests that C3 does not alter radiation-induced DNA damage in HCT116 cells at this clinically-relevant dose.

3.4.3. C3 overexpression does not alter repair of radiation-induced DNA damage in HCT116 cells

γH_2AX is a sensitive marker of DNA damage, and loss of phosphorylation corresponds with repair of DNA damage[405]. Therefore, fluorescence can be measured over time to monitor the kinetics of DNA repair. The kinetics of DNA repair were assessed in HCT116 cells transfected with C3 or a VC at 6 h, 10 h or 24 h post irradiation with 1.8 Gy.

Similar levels of γH_2AX were demonstrated in cells transfected with C3 or VC at all time points investigated **(Fig. 3-7 B-D)**. This suggests that overexpression of C3 does not alter repair of radiation-induced DNA damage in HCT116 cells.

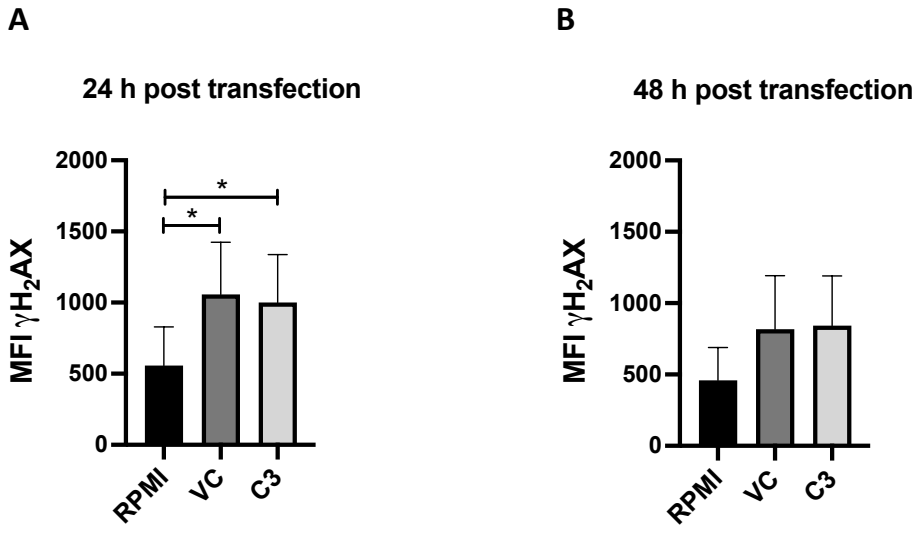

Figure 3-6: C3 overexpression does not alter basal DNA damage in HCT116 cells. HCT116 cells were transfected with C3 or a VC plasmid and DNA damage was assessed by measurement of γH_2AX by flow cytometry. MFI of γH_2AX at **(A)** 24 h and **(B)** 48 h post transfection. Data are presented as mean ± SEM for 4 independent experiments for 24 h and 3 independent experiments for 48 h. Statistical analysis was performed by paired two-tailed Student's *t*-test. $*p < 0.05$.

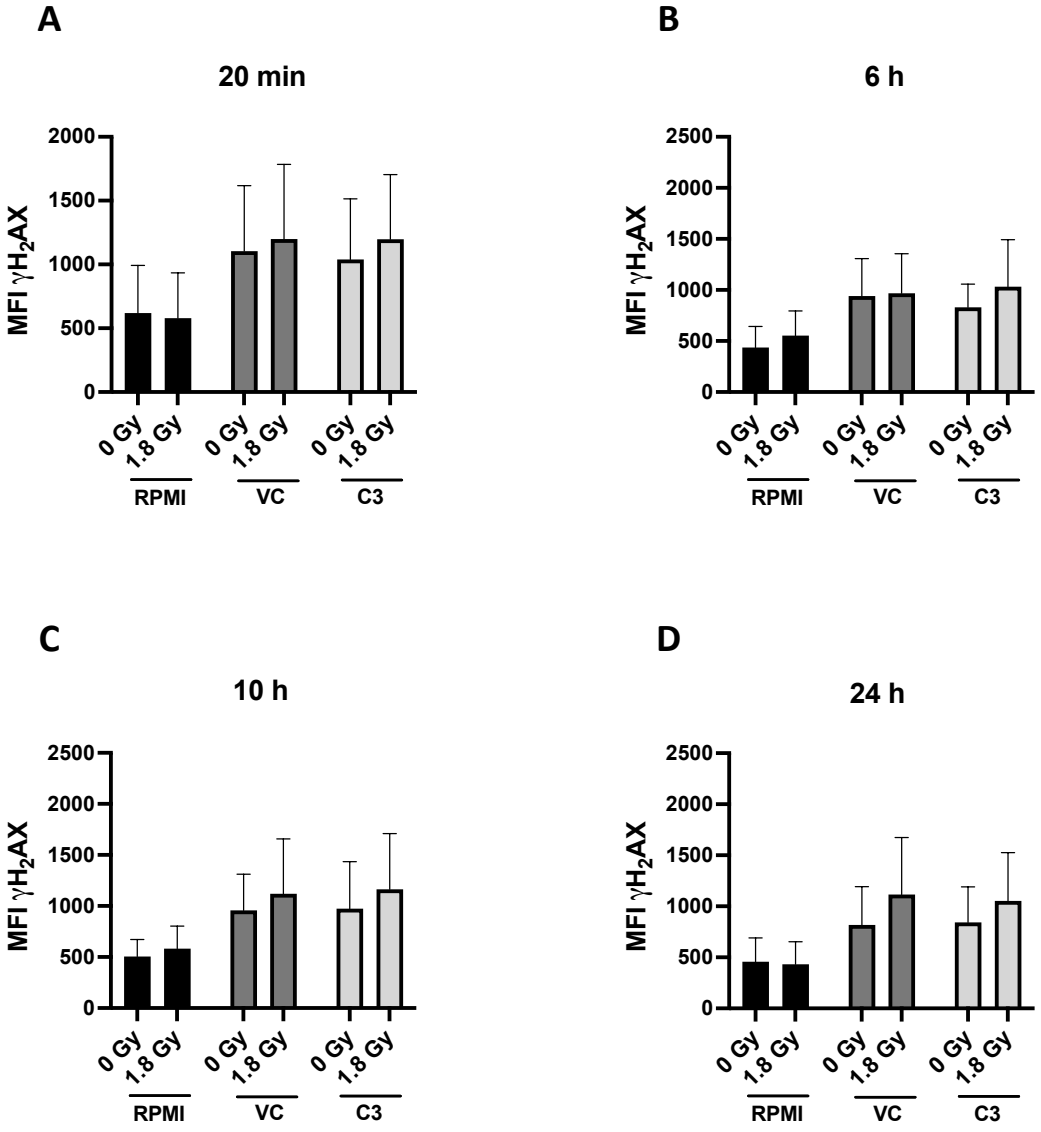

Figure 3-7: Overexpression of C3 does not alter the induction or repair of radiation-induced DNA damage in HCT116 cells. HCT116 cells were transfected with C3 or a VC plasmid and irradiated with 1.8 Gy at 24 h post transfection. Control cells were mock irradiated. Cells were fixed and MFI of γH_2AX was assessed by flow cytometry at **(A)** 20 min post irradiation to assess induction of radiation-induced DNA damage and at **(B)** 6 h, **(C)** 10 h and **(D)** 24 h post irradiation to examine the kinetics of DNA damage repair. Data are presented as mean ± SEM for 3 independent experiments. Statistical analysis was performed by paired two-tailed Student's *t*-test.

3.4.4. C3 overexpression does not alter basal cell cycle distribution in HCT116 cells

Alterations in cell cycle distribution are demonstrated to play a role in cellular radioresistance. To investigate if cell cycle alterations are a mechanism involved in C3-mediated enhancement of radioresistance, HCT116 cells were transfected with C3 or a VC and basal cell cycle was assessed at 24 h post transfection by PI staining and flow cytometry.

There were no differences in the percentage of cells in G0/G1, S and G2/M phases in HCT116 cells transfected with C3, when compared to cells transfected with a VC at 24 h (**Fig. 3-8 A**) or 48 h post transfection (**Fig. 3-8 B)**. These data suggest that overexpression of C3 does not alter basal cell cycle distributions in HCT116 cells.

3.4.5. C3 overexpression does not alter cell cycle distribution following irradiation in HCT116 cells

Sensitivity to radiation is altered depending on the phase of the cell cycle, with cells in the G2 and M phases being most sensitive to radiation, cells in G0 being more resistant, while cells in S phase are most resistant[95–97]. Having demonstrated no alterations in basal cell cycle distribution between C3 and VC transfected HCT116 cells, the effect of 1.8 Gy of radiation on cell cycle distribution was investigated using PI staining and flow cytometry.

At 20 min post irradiation, there were no alterations in the percentage of HCT116 cells transfected with C3 in the G0/G1, S or G2/M phases, when compared to cells transfected with a VC (**Fig. 3-9 A**). Similarly, at 6 h, 10 h and 24 h post irradiation, cell cycle distribution was unaltered in HCT116 cells transfected with C3, when compared to cells transfected with a VC (**Fig. 3-9 B-D**). These data demonstrate that C3 overexpression does not affect cell cycle distribution in HCT116 cells, suggesting that alterations in cell cycle distribution do not account for the enhanced radioresistance of these cells.

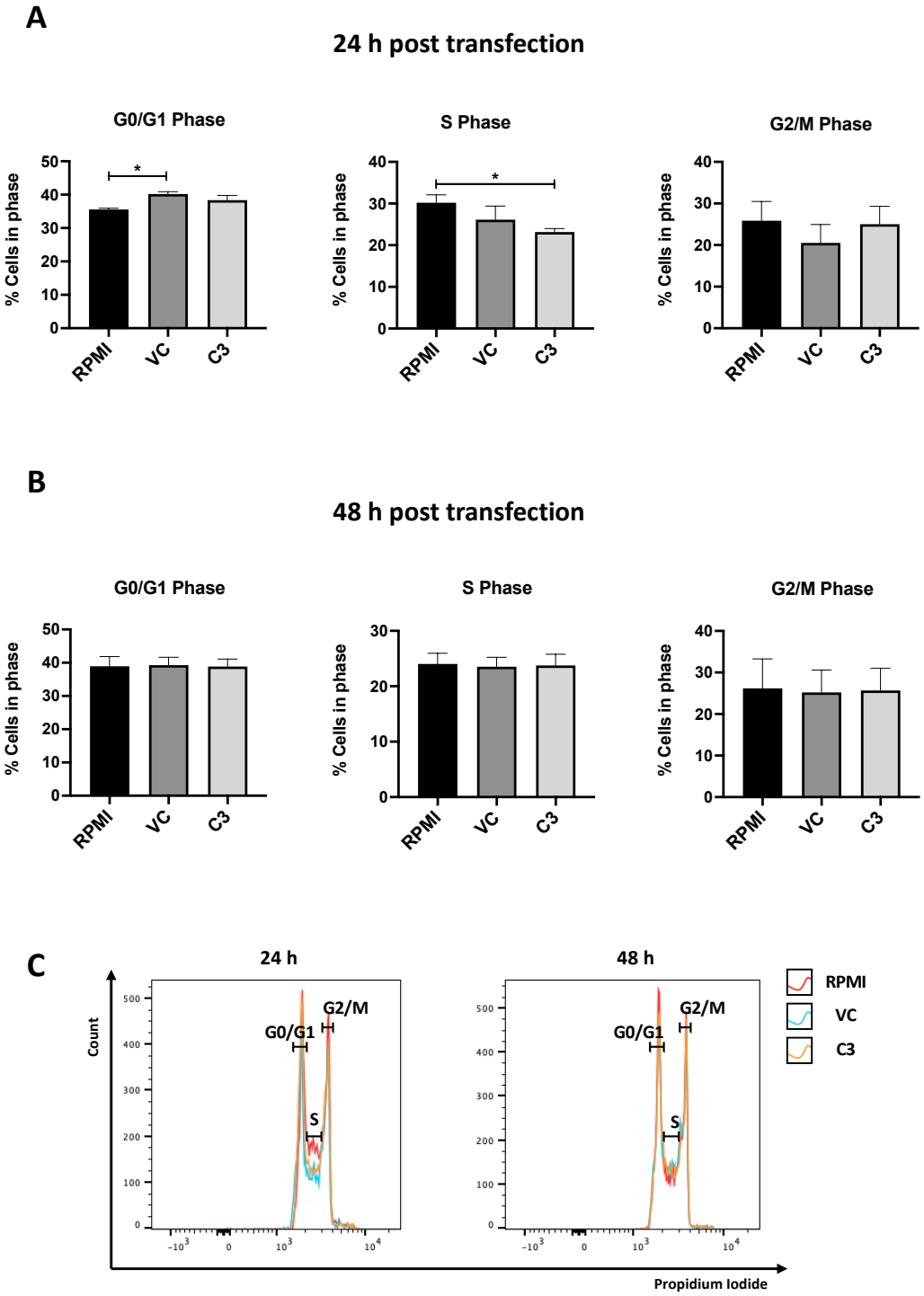

Figure 3-8: Overexpression of C3 does not alter basal cell cycle distribution in HCT116 cells. HCT116 cells were transfected with C3 or a VC plasmid. At **(A)** 24 h and **(B)** 48 h following transfection, cells were fixed, stained with PI and cell cycle distribution was assessed by flow cytometry. **(C)** Representative histograms demonstrating gating by which the percentage of cells in the G0/G1, S and G2/M phases was assessed**.** Data are presented as mean ± SEM for 3 independent experiments. Statistical analysis was performed by paired two-tailed Student's *t*-test. **p* < 0.05.

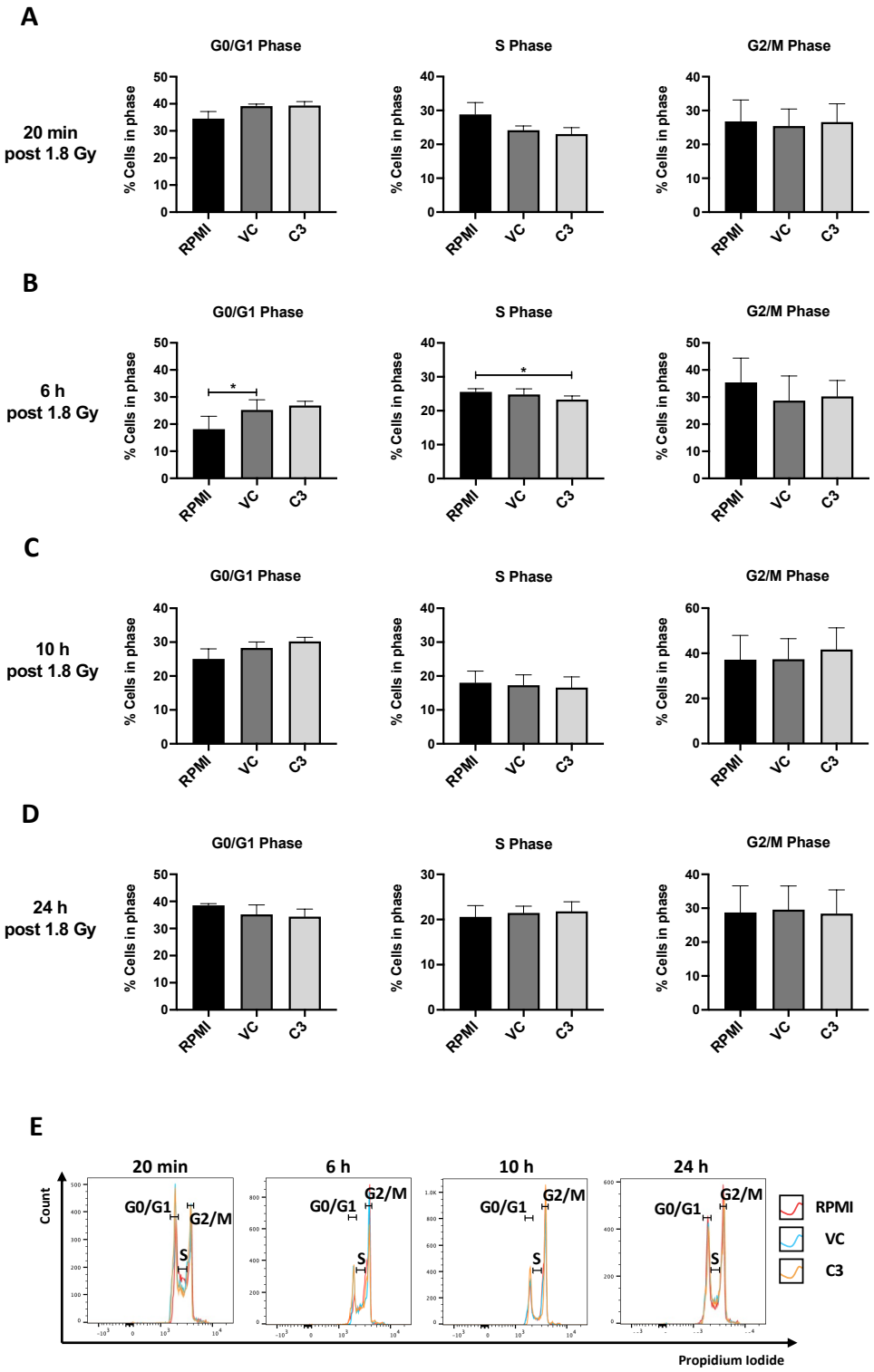

Figure 3-9: Overexpression of C3 does not alter cell cycle distribution following radiation in HCT116 cells. HCT116 cells were transfected with C3 or a VC plasmid. At 24 h post transfection, cells were irradiated with 1.8 Gy. Control cells were mock irradiated. At **(A)** 20 min, **(B)** 6 h, **(C)** 10 h and **(D)** 24 h following irradiation, cells were fixed, stained with PI and cell cycle distribution was assessed by flow cytometry. **(E)** Representative histograms demonstrating gating by which the percentage of cells in the G0/G1, S and G2/M phases was assessed**.** Data are presented as mean ± SEM for 3 independent experiments. Statistical analysis was performed by paired two-tailed Student's *t*-test.

3.4.6. Optimisation of transient C3 siRNA transfection

Having demonstrated that upregulation of C3 in the radiosensitive HCT116 cell line results in enhanced radioresistance, the effect of silencing C3 on the radiosensitivity of the radioresistant HRA-19 cell line was assessed. The optimum conditions for transient transfection of a C3 targeting siRNA (si-C3) was determined in HRA-19 cells. To determine the optimum siRNA concentration, HRA-19 cells were reverse transfected with either 10 nM or 50 nM of si-C3 or scrambled control siRNA (si-scr) and the relative C3 expression levels were assessed by qPCR.

C3 mRNA expression was downregulated following transfection of HRA-19 cells with 10 nM of si-C3 by 83.45% at 24 h post transfection, when compared to HRA-19 cells transfected with si-scr (Relative C3 mRNA expression; Cells only 1, si-scr 0.707, si-C3 0.117) (**Fig. 3-10 A)**. Downregulated expression was maintained, when compared to si-scr transfected cells, at 48 h post transfection (Relative C3 mRNA expression; Cells only 1.559, si-scr 1.671, si-C3 0.159) (**Fig. 3-10 A**). Similarly, transfection with 50 nM of si-C3 downregulated C3 mRNA expression by 87.58% at 24 h post transfection (Relative C3 mRNA expression; Cells only 1, si-scr 0.636, si-C3 0.079) (**Fig. 3-10 B)**. Downregulated expression of C3 was also maintained, when compared to si-scr transfected cells, at 48 h post transfection (Relative C3 mRNA expression; Cells only 0.681, si-scr 2.323, si-C3 0.099) (**Fig. 3-10 B**).

As both concentrations of si-C3 investigated reduced mRNA expression of C3 by over 70%, a concentration of 10 nM was selected for all downstream experiments. The expression of C3 at the protein level following transfection with 10 nM of siRNA was assessed by ELISA to confirm downregulation of C3 protein. At 24 h post transfection, 10 nM of si-C3 reduced C3 protein expression by 71.2% when compared to si-scr controls (Relative C3 protein expression ± SEM; Cells only 1 , si-scr 1.18, si-C3 0.34) **(Fig. 3-10 C)**.

The effect of 10 nM of si-C3 on C3 expression in SW837 cells was also assessed. C3 mRNA expression was downregulated following transfection of SW837 cells with 10 nM of si-C3 by 75.64% at 24 h post transfection, when compared to SW837 cells transfected with si-scr (Relative C3 mRNA expression; Cells only 1, si-scr 0.546, si-C3 0.133) (**Fig. 3-10 D)**. Downregulated expression was maintained, when compared to si-scr transfected cells, at 48 h post transfection (Relative C3 mRNA expression; Cells only 0.602, si-scr 0.896, si-C3 0.136) (**Fig. 3-10 D**). These data demonstrated that 10 nM of si-C3 sufficiently reduces expression of C3 in SW837 cells.

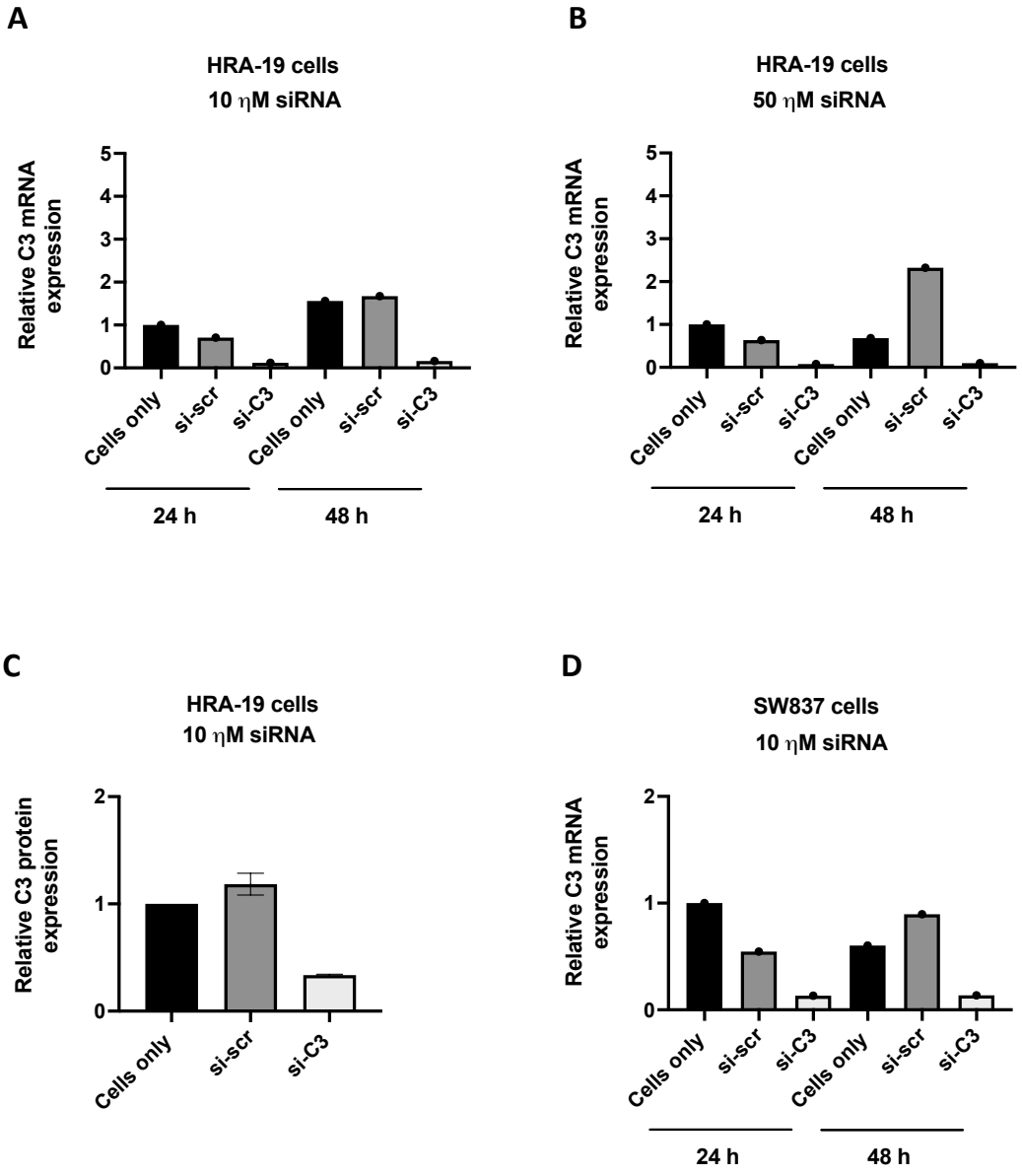

Figure 3-10: Optimisation of si-C3 concentration in HRA-19 and SW837 cells. HRA-19 cells were transfected with either **(A)** 10 nM or **(B)** 50 nM of C3 siRNA (si-C3) or a scrambled control siRNA (si-scr) siRNA. Relative C3 mRNA expression was assessed by qPCR at 24 h and 48 h post transfection. Data are presented as the relative expression of C3 from a single experiment. **(C)** Relative C3 protein expression was assessed at 24 h post transfection with 10 nM si-C3 or si-scr by ELISA. Data are presented as mean ± SEM for 2 independent experiments. **(D)** SW837 cells were transfected with 10 nM of si-C3 or si-scr. Relative C3 mRNA expression was assessed by qPCR at 24 h and 48 h post transfection. Data are presented as the relative expression of C3 from a single experiment

3.4.7. Transient silencing of C3 significantly enhances radiosensitivity in HRA-19 cells

The HRA-19 cell line expresses significantly elevated levels of C3 **(Fig. 2-3 A)** and is significantly more radioresistant following 1.8 Gy of X-ray irradiation (**Fig. 2-2 C**), when compared to HCT116 cells. Having demonstrated that C3 overexpression enhances the radiosensitivity of HCT116 cells, the effect of transient C3 silencing on the radiosensitivity of HRA-19 cells at a clinically-relevant dose of 1.8 Gy was assessed using the gold standard clonogenic assay.

Silencing of C3 was confirmed by qPCR (as described in Section 2.3.16) (**Fig. 3-11 A**). Only cells transfected with si-C3 demonstrated downregulation of C3, when compared to si-scr controls (Relative C3 expression 0.3205 vs 0.9975, respectively). Irradiation with 1.8 Gy greatly reduced survival in HRA-19 cells transfected with si-C3 or si-scr (0.394 ± 0.022 and 0.538 ± 0.014, respectively), when compared to an unirradiated control set at 1.00 (**Fig. 3-11 B**). Interestingly, HRA-19 cells transfected with si-C3 were significantly (p = 0.0180) more sensitive to 1.8 Gy, when compared to si-scr transfected cells, suggesting that C3 plays a functional role in modulating radioresistance in HRA-19 cells.

3.4.8. Transient silencing of C3 does not enhance radiosensitivity in SW837 cells

Having demonstrated that C3 silencing enhances radiosensitivity in HRA-19 cells, the effect of C3 silencing on radiosensitivity was investigated in the SW837 rectal cancer cell line. Similar to HRA-19 cells, the SW837 cell line is significantly more radioresistant following 1.8 Gy of X-ray radiation **(Fig. 2-2 C)** and expresses significantly higher levels of C3 (**Fig. 2-6 and Fig. 2-3)**, when compared to the HCT116 cell line.

Silencing of C3 was confirmed by qPCR (as described in Section 2.3.16) (**Fig. 3-12 A**). Only cells transfected with si-C3 demonstrated downregulation of C3, when compared to si-scr controls (Relative C3 expression 0.7915 vs 0.3125, respectively). Irradiation with 1.8 Gy greatly reduced survival in SW837 cells transfected with si-C3 or si-scr (0.595 ± 0.039 and 0.661 ± 0.099, respectively), when compared to an unirradiated control set at 1.00 (**Fig. 3-12 B**). SW837 cells transfected with si-C3 were not significantly more sensitive to 1.8 Gy, when compared to si-scr transfected cells, suggesting that C3 does not play a functional role in modulating radioresistance in SW837 cells.

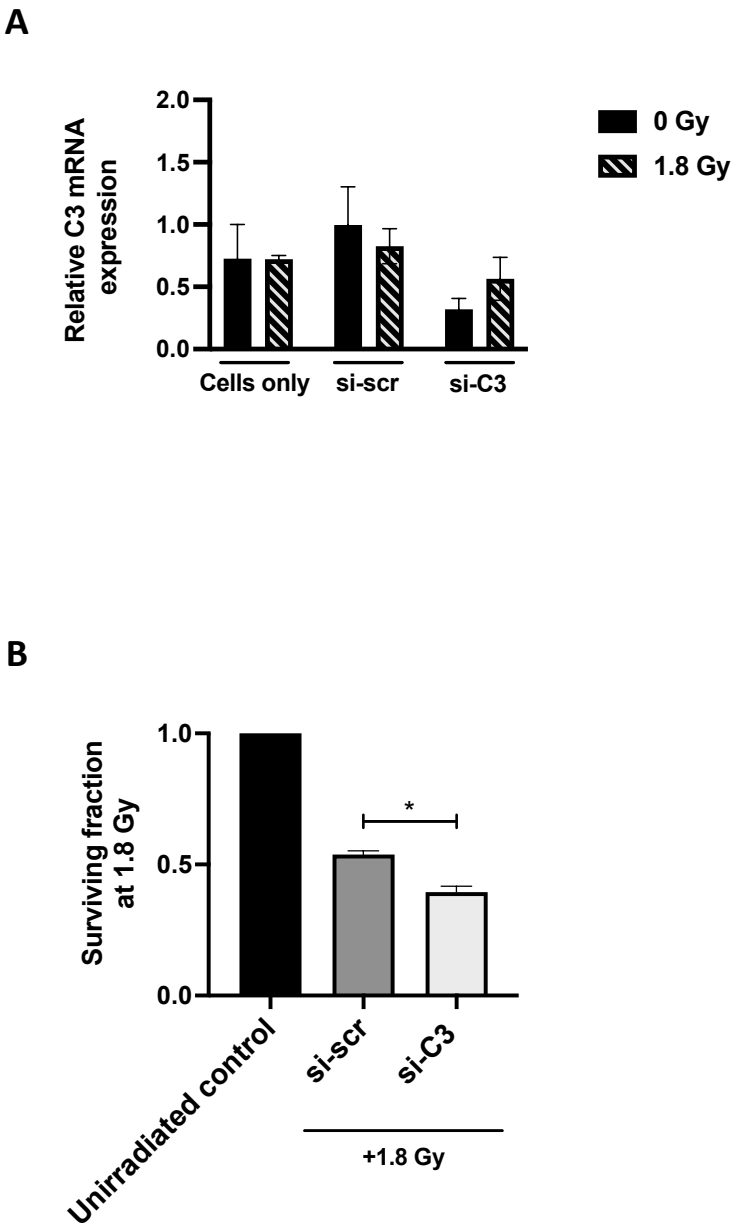

Figure 3-11: Silencing of C3 significantly enhances the radiosensitivity of HRA-19 cells at 1.8 Gy of X-ray radiation. HRA-19 cells were transfected with 10 nM of C3 (si-C3) or a scrambled control (si-scr) siRNA. Cells were irradiated with 1.8 Gy at 24 h post transfection and control cells were mock irradiated. At 25 h post transfection cells were seeded for clonogenic assay and RNA was also isolated. **(A)** C3 silencing was confirmed by qPCR. Data are presented as mean ± SEM for 2 independent experiments. **(B)** Surviving colonies at the end of the clonogenic incubation period were counted and the surviving fraction determined. Data are presented as mean ± SEM for 3 independent experiments. Statistical analysis was performed by paired two-tailed Student's *t*-test. *$p < 0.05$.

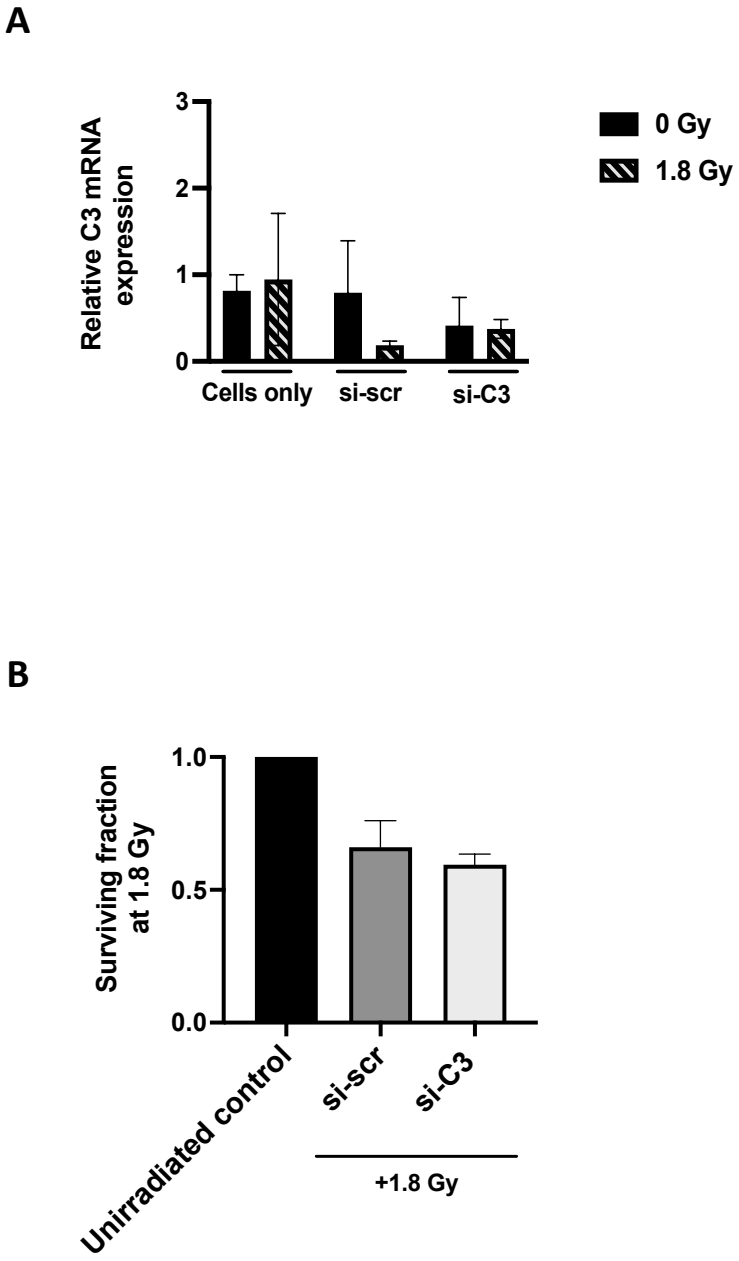

Figure 3-12: Silencing of C3 does not alter the radiosensitivity of SW837 cells at 1.8 Gy of X-ray radiation. SW837 cells were transfected with 10 nM of C3 (si-C3) or a scrambled control (si-scr) siRNA. Cells were irradiated with 1.8 Gy at 24 h post transfection and control cells were mock irradiated. At 25 h post transfection cells were seeded for clonogenic assay and RNA was also isolated. **(A)** C3 silencing was confirmed by qPCR. Data are presented as mean ± SEM for 2 independent experiments. **(B)** Surviving colonies at the end of the clonogenic incubation period were counted and the surviving fraction determined. Data are presented as mean ± SEM for 3 independent experiments. Statistical analysis was performed by paired two-tailed Student's t-test.

3.4.9. Transient silencing of C3 does not alter basal or radiation-induced apoptosis in HRA-19 cells

Having demonstrated that transient silencing of C3 significantly enhanced radiosensitivity to 1.8 Gy in HRA-19 cells, the potential mechanism by which C3 may be modulating the radioresponse in HRA-19 cells was investigated. The effect of transient C3 silencing on apoptosis in HRA-19 cells was investigated to determine if the enhanced radiosensitivity of C3 silenced HRA-19 cells is associated with altered apoptosis. HRA-19 cells were transfected with si-C3 or si-scr. At 24 h post transfection, cells were irradiated with 1.8 Gy or mock-irradiated and cell death was assessed at 24 h and 48 h post irradiation using the AV/PI assay.

Alterations in cell death were assessed in mock irradiated si-scr and si-C3 transfected HRA-19 cells, when compared to RPMI controls, to investigate the effect of transfection on basal viability. At 24 h, increased early apoptosis was demonstrated in si-C3 cells relative to RPMI controls (p = 0.0265), with a trend towards increased early apoptosis demonstrated in si-scr cells, when compared to RPMI controls (p =0.0506) (Mean % of AV^+PI^- cells ± SEM; RPMI 8.680 ± 3.073, si-scr 15.6 ± 4.524, si-C3 13.76 ± 3.774) (**Fig. 3-13 B**). Similarly, at 48 h, early apoptosis and late apoptosis/death were significantly increased in si-scr cells (p = 0.0044, p = 0.0154, respectively) and si-C3 cells (p = 0.0024, p = 0.028, respectively), when compared to RPMI controls (**Fig. 3-14 B-C)**. No changes in necrosis were demonstrated at 24 h (**Fig. 3-13 D**) or 48 h (**Fig. 3-14 D**). These data demonstrate that transfection with siRNA induces slight but significant alterations in the basal viability of HRA-19 cells.

Mock irradiated cells were analysed to assess differences in basal viability between si-scr and si-C3 transfected HRA-19 cells. The percentage of live and necrotic si-scr or si-C3 transfected HRA-19 cells at both 24 h (**Fig. 3-13 A** & **D)** and 48 h **(Fig. 3-14 A** & **D)** timepoints was similar. At 48 h, there was a significant increase in the percentage of HRA-19 cells transfected with si-C3 undergoing early apoptosis, when compared to si-scr controls (p = 0.0363) (Mean % of AV^+PI^- cells ± SEM; si-scr 15.533 ± 3.667, si-C3 17.567 ± 3.619) (**Fig. 3-14 B**). However, this was accompanied by a corresponding significant decrease in late apoptosis/death, when compared to si-scr cells controls (p = 0.0332) (Mean % of AV^+PI^- cells ± SEM; si-scr 13.3 ± 1.848, si-C3 12.393 ± 1.858) (**Fig. 3-14 C**). These data demonstrate that transient silencing of C3 does not alter basal apoptosis in HRA-19 cells, suggesting that the increased radiosensitivity of HRA cells transfected with si-C3 is not a result of altered basal apoptosis.

To investigate whether radiation-induced cell death was altered in cells transfected with si-C3, viability was assessed 24 h and 48 h following 1.8 Gy of X-ray radiation. There were no significant alterations in the percentage of live, early apoptotic, late apoptotic/dead or necrotic si-scr or si-C3 cells, when compared to their respective mock irradiated controls at 24 h (**Fig. 3-13**) or 48 h (**Fig. 3-14**) post 1.8 Gy. This suggests that downregulation of C3 does not alter radiation-induced apoptosis in these cells. However, at 24 h post 1.8 Gy of X-ray radiation the viability of HRA-19 cells transfected with si-C3 was significantly greater, when compared to si-scr cells (Mean % of AV^-PI^- cells ± SEM; si-C3 1.8 Gy 66.167 ± 39.342, si-scr 1.8 Gy 63.633 ± 9.19) (**Fig. 3-13 A**). This suggests that C3 may reduce the viability of HRA-19 cells following irradiation with 1.8 Gy.

3.4.10. Transient silencing of C3 significantly increases basal levels of DNA damage in HRA-19 cells

To determine if alterations in basal DNA damage are involved in the enhanced radiosensitivity of HRA-19 cells following transient C3 silencing, HRA-19 cells were transfected with si-C3 or si-scr and basal DNA damage was assessed by measurement of γH_2AX using flow cytometry at 24 h and 48 h post transfection.

There were no significant alterations in basal DNA damage demonstrated in HRA-19 cells transfected with si-C3, when compared to cells transfected with si-scr at 24 h post transfection (**Fig. 3-15 A**). However, DNA damage was significantly ($p = 0.0299$) elevated in HRA-19 cells transfected with si-C3, when compared to cells transfected with si-scr at 48 h post transfection (Mean MFI γH_2AX ± SEM; si-scr 1318 ± 269.587, si-C3 1538.333 ± 246.646) (**Fig. 3-15 B**). These data demonstrate that downregulation of C3 induces significant basal DNA damage in HRA-19 cells.

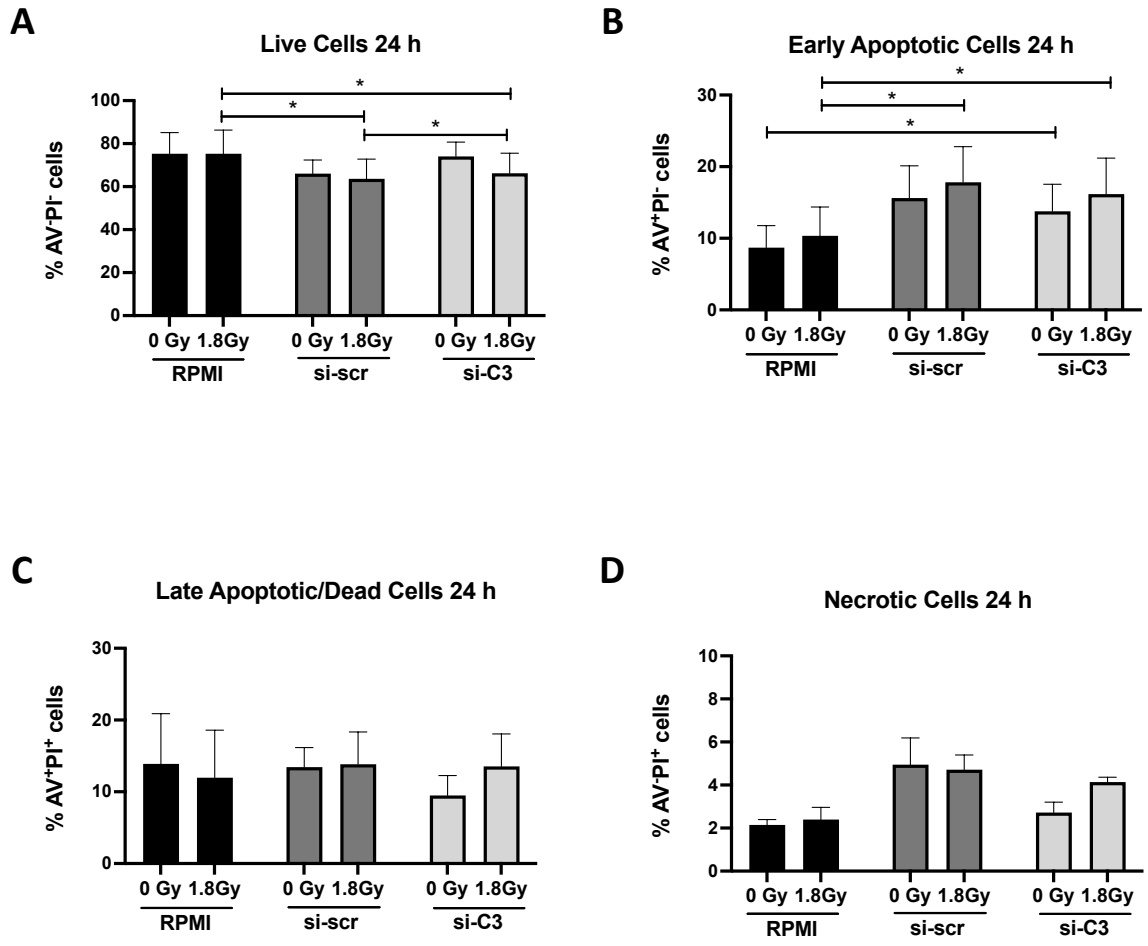

Figure 3-13: Transient C3 silencing does not alter the viability of HRA-19 cells basally or at 24 h following irradiation. HRA-19 cells were transfected with C3 (si-C3) or a scrambled control (si-scr) siRNA. At 24 h post transfection, cells were irradiated with 1.8 Gy or mock irradiated and apoptosis was assessed at 24 h post irradiation by AV/PI assay. Percentage of **(A)** live (AV^-PI^-), **(B)** early apoptotic (AV^+PI^-), **(C)** late apoptotic/dead (AV^+PI^+) and **(D)** necrotic (AV^-PI^+) si-C3, si-scr, and RPMI control HRA-19 cells were analysed. Data are presented as mean ± SEM for 3 independent experiments. Statistical analysis was performed by paired two-tailed Student's *t*-test. $*p < 0.05$.

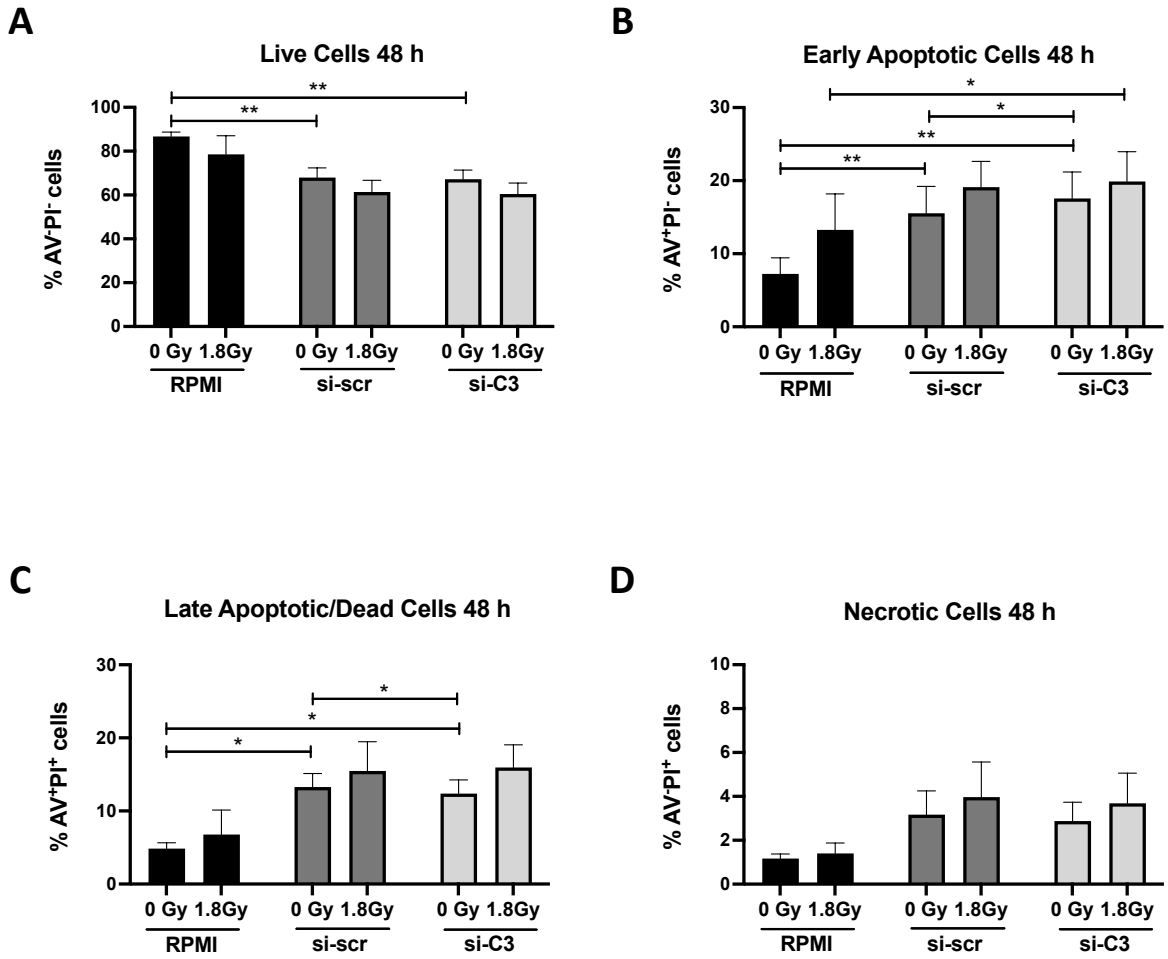

Figure 3-14: Transient C3 silencing does not alter the viability of HRA-19 cells basally or at 48 h following irradiation. HRA-19 cells were transfected with C3 (si-C3) or a scrambled control (si-scr) siRNA. At 24 h post transfection, cells were irradiated with 1.8 Gy or mock irradiated and apoptosis was assessed 48 h post irradiation by AV/PI assay. Percentage of **(A)** live (AV^-PI^-), **(B)** early apoptotic (AV^+PI^-), **(C)** late apoptotic/dead (AV^+PI^+) and **(D)** necrotic (AV^-PI^+) si-C3, si-scr, and RPMI control HRA-19 cells were analysed. Data are presented as mean ± SEM for 3 independent experiments. Statistical analysis was performed by paired two-tailed Student's *t*-test. $*p < 0.05$, $**p < 0.01$.

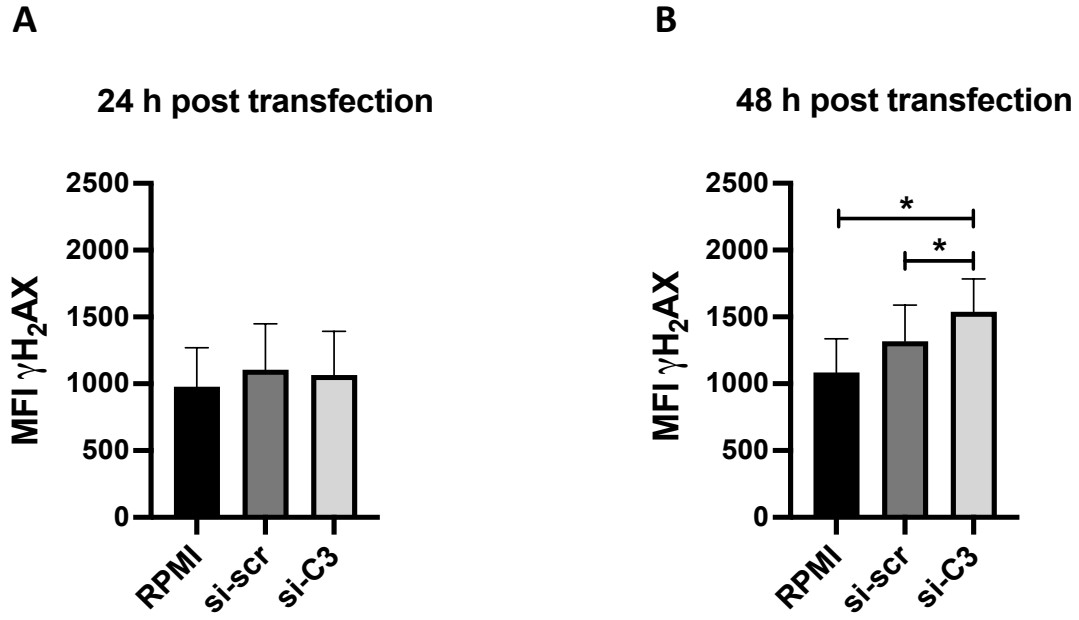

Figure 3-15: Transient C3 silencing induces basal DNA damage in HRA-19 cells. HRA-19 cells were transfected with C3 siRNA (si-C3) or a scrambled control (si-scr) siRNA and DNA damage was assessed by measurement of γH_2AX by flow cytometry. MFI of γH_2AX at **(A)** 24 h and **(B)** 48 h post transfection. Data are presented as mean ± SEM for 4 independent experiments for 24 h and 3 independent experiments for 48 h. Statistical analysis was performed by paired two-tailed Student's *t*-test. *$p < 0.05$.

3.4.11. Transient silencing of C3 significantly increases radiation-induced DNA damage in HRA-19 cells

Having demonstrated that silencing of C3 induces DNA damage basally in HRA-19 cells, the effect of transient C3 silencing on radiation-induced DNA damage was investigated. HRA-19 cells were transfected with a si-C3 or si-scr siRNA. At 24 h post transfection, cells were irradiated with 1.8 Gy or mock-irradiated and DNA damage was assessed by measurement of γH_2AX using flow cytometry at 20 min post irradiation.

In cells transfected with si-C3 siRNA, 1.8 Gy of X-ray radiation induced significant DNA damage relative to unirradiated controls at 20 min post irradiation ($p = 0.0487$) (Mean MFI $\gamma H_2AX \pm$ SEM; si-C3 0 Gy 1065.5 ± 327.962, si-C3 1.8 Gy 1753.75 ± 447.698) (**Fig. 3-16 A)**. Although there was a trend towards elevated DNA damage in si-scr controls irradiated with 1.8 Gy, this was not significant ($p = 0.0869$) (**Fig. 3-16 A)**. Similarly, irradiation of RPMI controls with 1.8 Gy did not induce significant DNA damage, suggesting that C3 may modulate radiation-induced DNA damage in HRA-19 cells.

3.4.12. Transient C3 silencing alters the kinetics of DNA repair in HRA-19 cells

To investigate the effect of C3 silencing on the kinetics of DNA repair, γH_2AX was assessed at 6 h, 10 h and 24 h post irradiation with 1.8 Gy. At 6 h post irradiation, cells transfected with si-C3 demonstrated a trend toward increased DNA damage, when compared to unirradiated controls ($p = 0.0572$) (**Fig. 3-16 B)**. Similarly, at 10 h post irradiation, significantly elevated levels of DNA damage were demonstrated in cells transfected with si-C3, when compared to unirradiated controls ($p = 0.0211$) (Mean MFI $\gamma H_2AX \pm$ SEM; si-C3 1.8 Gy 1668.34 ± 144.044, , si-C3 0 Gy 1143.67 ± 146.56) (**Fig. 3-16 C)**. By 24 h, levels of DNA damage were no longer significantly elevated in irradiated si-C3 cells, when compared to unirradiated controls, suggesting that radiation-induced DNA damage had been repaired at this timepoint (**Fig. 3-16 D)**. Interestingly, there were no significant alterations in DNA damage demonstrated in cells transfected with si-scr control at 6 h, 10 h or 24 h post irradiation, when compared to unirradiated controls. These data demonstrate that downregulation of C3 in HRA-19 cells results in significantly elevated levels of radiation-induced DNA damage, which still persists at 10 h post irradiation, suggesting that C3 may modulate repair of IR-induced DNA damage in CRC, which may contribute to the cellular radioresponse.

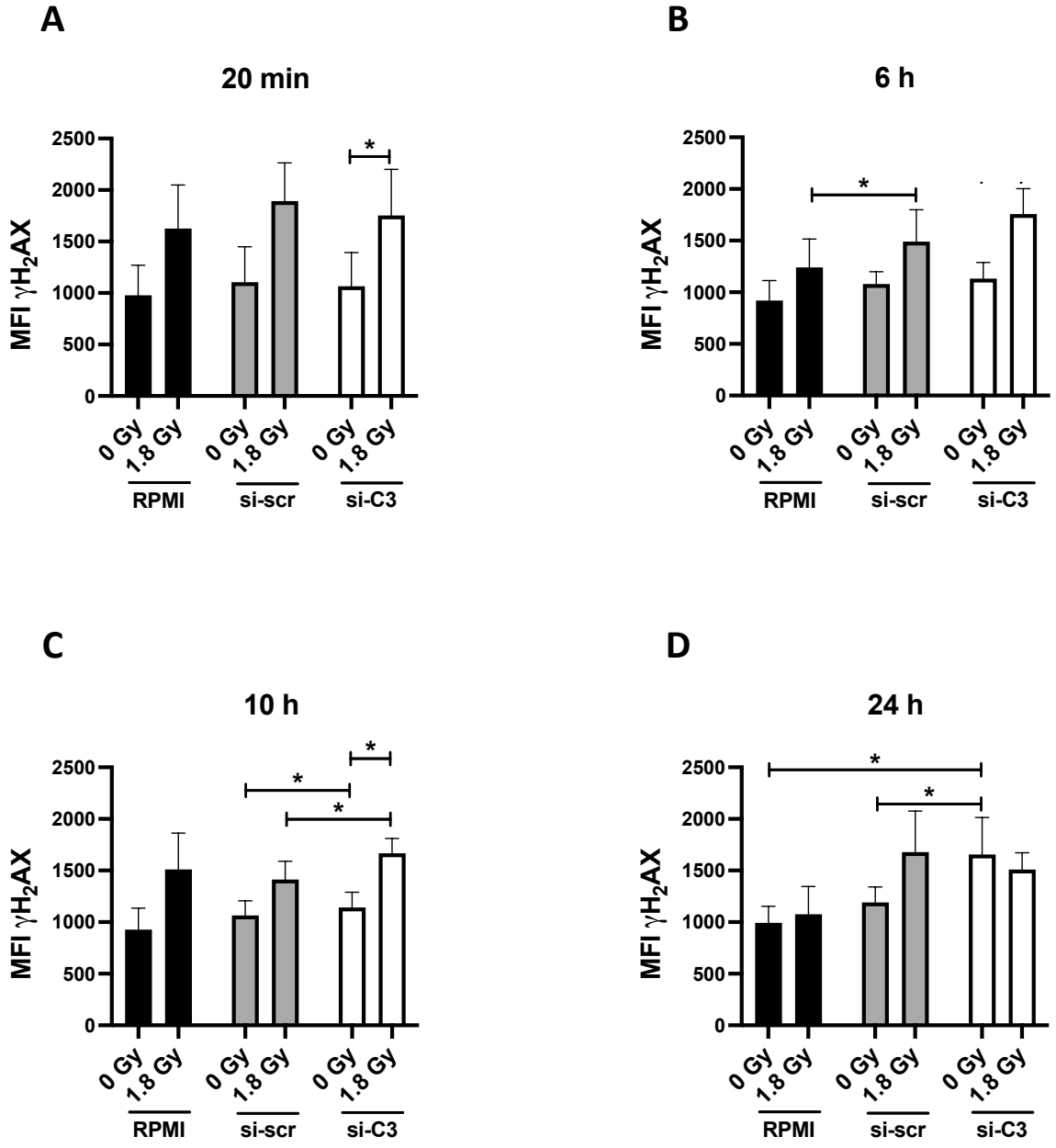

Figure 3-16: Transient C3 silencing induces significant radiation-induced DNA damage in HRA-19 cells. HRA-19 cells were transfected with C3 (si-C3) or a scrambled control (si-scr) siRNA and were irradiated with 1.8 Gy at 24 h post transfection. Control cells were mock irradiated. Cells were fixed and MFI of γH_2AX was assessed by flow cytometry at **(A)** 20 min to assess induction of DNA damage and at **(B)** 6 h, **(C)** 10 h and **(D)** 24 h post irradiation to examine the kinetics of DNA damage repair. Data are presented as mean ± SEM for 3 independent experiments. Statistical analysis was performed by paired two-tailed Student's *t*-test. $*p < 0.05$.

3.4.13. Transient silencing of C3 alters basal cell cycle distribution in HRA-19 cells

Having demonstrated that C3 silencing was associated with alterations in basal and radiation-induced levels of DNA damage in HRA-19 cells, the effect of C3 silencing on basal cell cycle distribution was assessed.

Interestingly, at 24 h post transfection C3 silencing was associated with a significant decrease in the percentage of radioresistant, S phase si-C3 cells, when compared to si-scr cells ($p = 0.0187$) and RPMI controls ($p = 0.0117$) (Mean % cells in phase ± SEM; RPMI 25.033 ± 1.501, si-scr 22.167 ± 1.660, si-C3 20.767 ± 1.392). This was accompanied by a corresponding increase in the percentage of si-C3 cells in the radiosensitive G2/M phase, when compared to si-scr cells ($p = 0.0438$) and RPMI controls ($p = 0.0140$) (Mean % cells in phase ± SEM; RPMI: 30.733 ± 1.084, si-scr 31.3 ± 1.595, si-C3 32.933 ± 1.388) (**Fig. 3-17 A**). This suggests that C3 silencing results in a partial G2/M arrest at 24 h post transfection. At 48 h post transfection, significantly more si-C3 cells were in the G0/G1 phase, when compared to si-scr cells ($p = 0.0149$) and RPMI controls ($p = 0.0060$) (Mean % cells in phase ± SEM; RPMI 23.867 ± 5.774, si-scr 26.2 ± 6.022, si-C3 29.767 ± 6.129) (**Fig. 3-17 B**). This further demonstrates that C3 alters basal cell cycle distribution in HRA-19 cells.

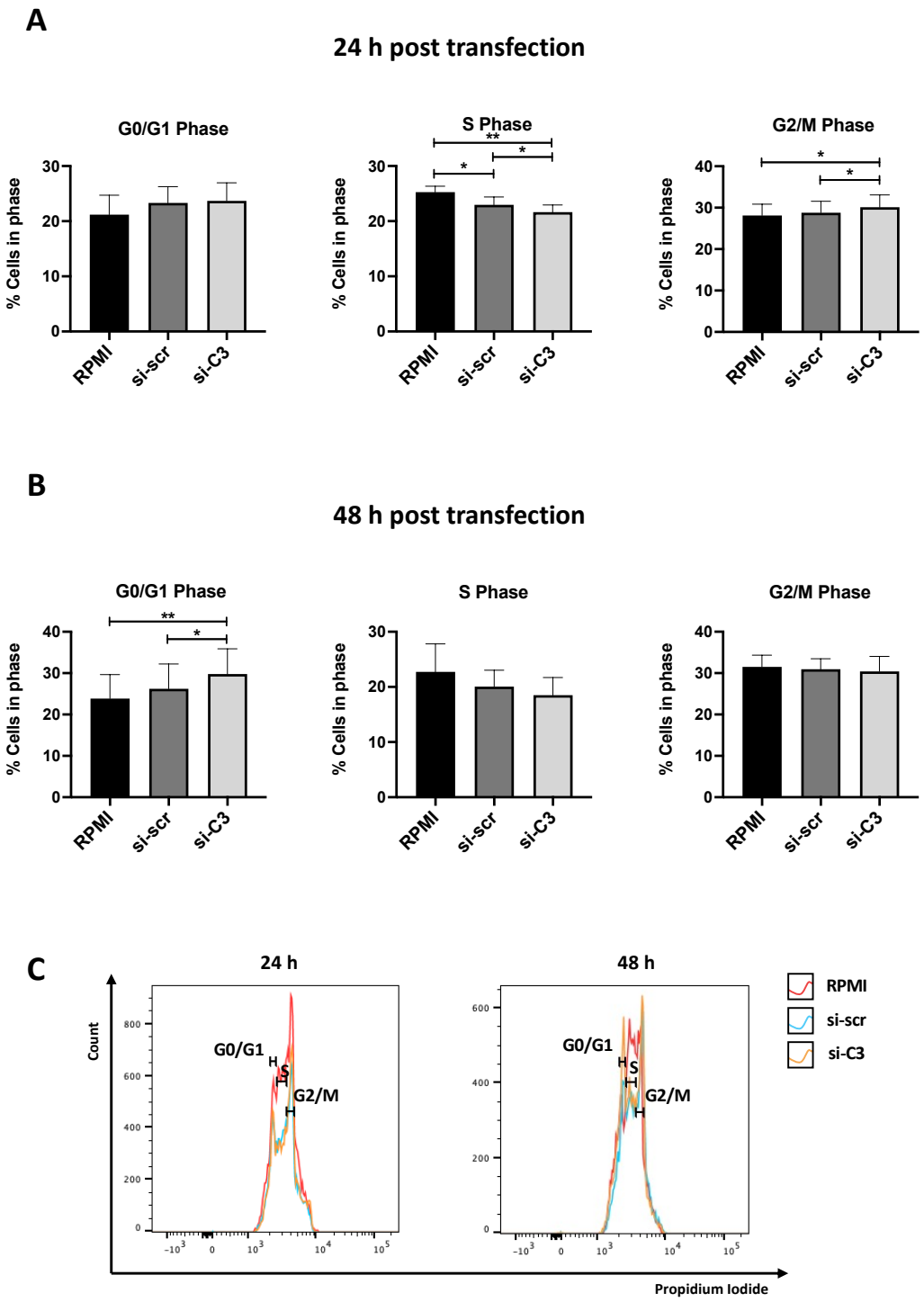

Figure 3-17: Transient C3 silencing alters basal cell cycle distribution in HRA-19 cells. HRA-19 cells were transfected with C3 siRNA (si-C3) or a scrambled siRNA control (si-scr). At **(A)** 24 h and **(B)** 48 h following transfection, cells were fixed, stained with PI and cell cycle distribution was assessed by flow cytometry. **(C)** Representative histograms demonstrating gating by which the percentage of cells in the G0/G1, S and G2/M phases was assessed**.** Data are presented as mean ± SEM for 3 independent experiments. Statistical analysis was performed by paired two-tailed Student's *t*-test. **p* < 0.05, ***p* < 0.01.

3.4.14. Transient C3 silencing is associated with radiation-induced alterations in cell cycle distribution in HRA-19 cells

Having demonstrated that transient C3 silencing alters basal cell cycle distribution in HRA-19 cells, the effect of silencing C3 on cell cycle distribution following irradiation with 1.8 Gy was investigated.

At 20 min post irradiation, cells transfected with si-C3 demonstrated a significantly lower percentage of cells in the radioresistant S phase, when compared to si-scr cells (p = 0.011) (Mean % cells in phase ± SEM; si-C3 21.567 ± 1.991, si-scr 22.4 ± 2.060) (**Fig. 3-18 A**). There were no alterations demonstrated in cell cycle phase in cells transfected with si-C3 at 6 h and 10 h post 1.8 Gy (**Fig. 3-18 B-C**). By 24 h post irradiation, there were significantly more si-C3 transfected cells in the G0/G1 phase, and concomitantly fewer S phase cells, when compared to si-scr cells (p = 0.0048) (Mean % cells in phase ± SEM; si-C3 30.167 ± 5.790, si-scr: 28.433 ± 5.907) (**Fig. 3-18 D**). (Mean % cells in phase ± SEM; si-C3 17.2 ± 3.151, si-scr 19.867 ± 3.353, RPMI 21.2 ± 2.651) (**Fig. 3-18 D**). These data demonstrate that downregulation of C3 in HRA-19 cells alters cell cycle distribution following irradiation.

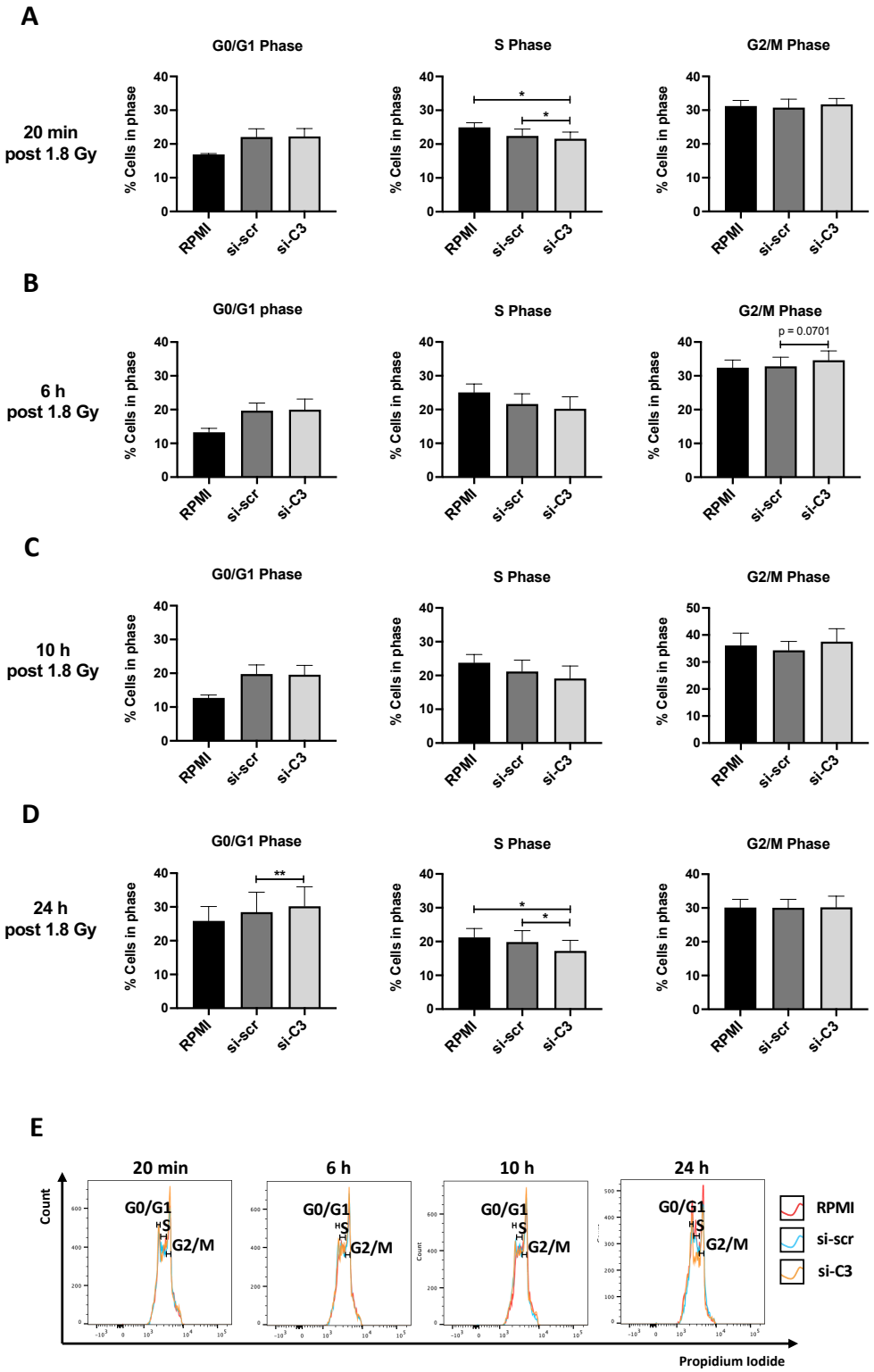

Figure 3-18: Transient C3 silencing alters cell cycle distribution post irradiation in HRA-19 cells. HRA-19 cells were transfected with C3 siRNA (si-C3) or a scrambled siRNA control (si-scr). At 24 h post transfection, cells were irradiated with 1.8 Gy. Control cells were mock irradiated. At **(A)** 20 min, **(B)** 6 h, **(C)** 10 h and **(D)** 24 h following irradiation, cell cycle was assessed by flow cytometry. **(E)** Representative histograms demonstrating gating by which the percentage of cells in the G0/G1, S and G2/M phases was assessed**.** Data are presented as mean ± SEM for 3 independent experiments. Statistical analysis was performed by paired two-tailed Student's *t*-test. **p* < 0.05, ***p* < 0.01.

3.4.15. The interactome of C3 differs between radiosensitive HCT116 and radioresistant HRA-19 cell lines

Modulation of C3 in both radiosensitive HCT116 and radioresistant HRA-19 cells altered radiosensitivity. Having demonstrated that modulation of C3 expression induces alterations in DNA damage induction and cell cycle distribution in HRA-19 cells but not HCT116 cells, mass spectrometry was performed to investigate if the interactome of C3 in these cell lines differed. C3-FLAG was overexpressed in HCT116 and HRA-19 cells and anti-FLAG IP was performed. QC experiments demonstrated that C3 and FLAG-M2 could be detected in input and IP fractions from both HCT116 and HRA-19 cells overexpressing C3 (**Appendix 3 A-D**). Prior to performing mass spectrometry, supernatant and IP fractions were separated by SDS-PAGE to confirm pull-down of C3 from C3-FLAG overexpressing samples and to confirm protein quantity was sufficient (**Appendix 3 E-F**).

The PCA plot demonstrates clustering of samples based on sample type, with HCT116 and HRA-19 cells overexpressing C3-FLAG seemingly separating based on component 2 (**Fig. 3-19 A**). The initial data set contained 2362 proteins, with a final number of 2109 proteins retained following a filtering step to remove any protein not detected in all three replicates of at least one condition. In the initial dataset, 13-29% of protein values were missing, while 8-23% were missing post-filtering (**Fig. 3-19 B**). C3 was present in the dataset (**Fig. 3-19 C**).

Differential expression analysis demonstrated that a total of 456 proteins were differentially expressed ($p < 0.05$) in C3 IP fractions from HRA-19 and HCT116 cells (**Fig. 3-20 A**). Of these, 285 proteins were downregulated and 171 were upregulated in the C3 interactome of HRA-19 cells, relative to HCT116 cells. The top 20 most upregulated and downregulated proteins from HRA-19 cells, are demonstrated in **Fig. 3-20 B-C.** Melanoma-associated antigen B2 (MAGEB2) was the most downregulated protein in the C3 interactome of HRA-19 cells, when compared to HCT116 cells (**Fig. 3-20 B**). The most upregulated protein identified in the C3 interactome of HRA-19 cells relative to HCT116 cells was galectin 4 (LEG4) (**Fig. 3-20 C**), which is a demonstrated tumour suppressor in CRC[406]. These data suggests that the C3 interactome differs between radiosensitive HCT116 and radioresistant HRA-19 cells. Notably, C3 was among the top 20 most downregulated proteins identified associated with HRA-19 cells relative to HCT116 cells suggesting a greater transfection efficiency in HCT116 cells.

To assess whether the top 20 most significantly upregulated or downregulated proteins may directly interact with C3, predicted protein networks were generated using

STRING. None of the 20 most downregulated proteins detected within the C3 IP of HRA-19 cells were predicted to directly interact with C3 (**Fig. 3-20 D**), however interestingly, of the most upregulated proteins, CXCL10 and CCL5 were predicted to directly interact with C3 (**Fig. 3-20 E**).

The top 30 proteins most significantly altered between the C3 interactome in HRA-19 and HCT116 cells are displayed in **Table 3-5**. HSPA1A/ B was the most significantly downregulated protein, as determined by *p*-adj (*p*-adj = 0.03289) in the HRA-19 C3 interactome, when compared to the HCT116 interactome. ZC3H4 was identified as the most significantly upregulated protein in the HRA-19 C3 interactome, when compared to the HCT116 interactome, as determined by *p*-adj (*p*-adj = 03394).

3.4.16. Three protein clusters are differentially expressed between the C3 IP fractions from HRA-19 and HCT116 cells

Having demonstrated that over 456 proteins were significantly altered ($p < 0.05$) between HCT116 and HRA-19 cells, a further clustering analysis was performed using *p*-adj, which resulted in 3 cluster groups (**Fig. 3-21 A**). The proteins identified in these clusters are outlined in **Appendix 4**. Clusters 1 and 2 contain 6 and 32 proteins, respectively and are both increased in HRA-19 cells relative to HCT116 cells (**Fig. 3-21 B**). Cluster 3 contains 45 proteins and is increased in HCT116 cells, relative to HRA-19 cells. Using STRING, these protein clusters were investigated to determine whether any of the proteins within the cluster are predicted to be direct interactors of C3. None of the proteins in Cluster 1 were predicted to be direct interactors with C3 (**Fig. 3-21 C**). Within Cluster 2, CXCL10 and CCL5 were predicted to directly interact with C3 (**Fig. 3-21 D**), while C1QBP was predicted to be a direct interactor with C3 in Cluster 3 (**Fig. 3-21 E**).

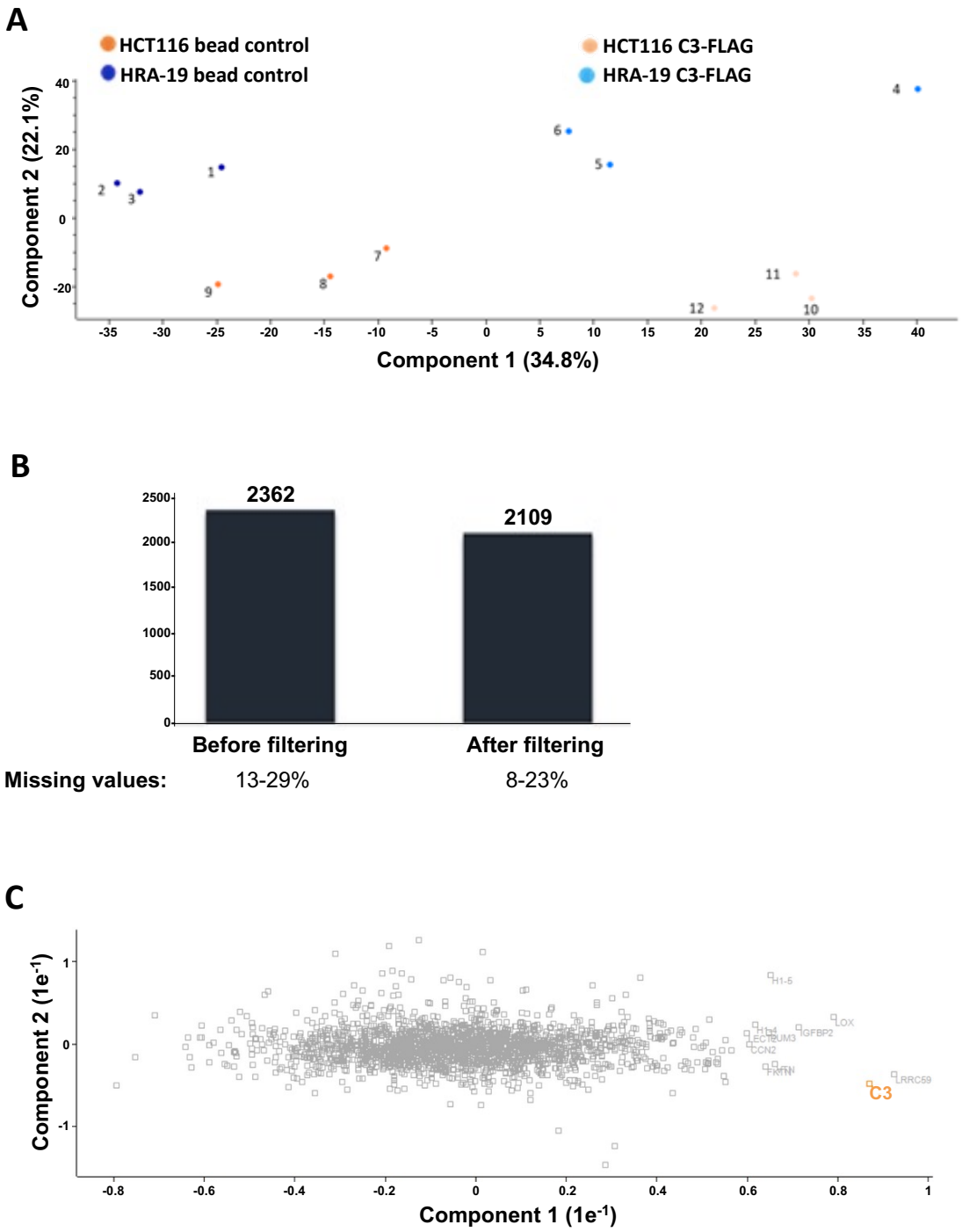

Figure 3-19: C3 IP from HCT116 and HRA-19 cells identified more than 2000 proteins associated with C3. C3-FLAG was overexpressed in HRA-19 and HCT116 cells and IP was performed using FLAG-M2 magnetic beads. Bead controls are representative of IP fractions that were prepared by incubating wild-type HCT116 and HRA-19 cells with FLAG-M2 magnetic beads. The experiment was performed in triplicate. **(A)** Principal component analysis (PCA) plot demonstrates clustering based on sample type. Component 1 (x-axis) accounts for 34.8% of variation between groups while 22.1% of variation is accounted for by component 2 (y-axis). (**B**) Total number of proteins identified in the initial dataset and proteins retained following a filtering step to remove any proteins not detected in at least all three replicates of one condition. (**C**) C3 is present within the protein dataset. Mass Spectrometry was performed by the Discovery Proteomics Facility at the Target Discovery Institute, University of Oxford.

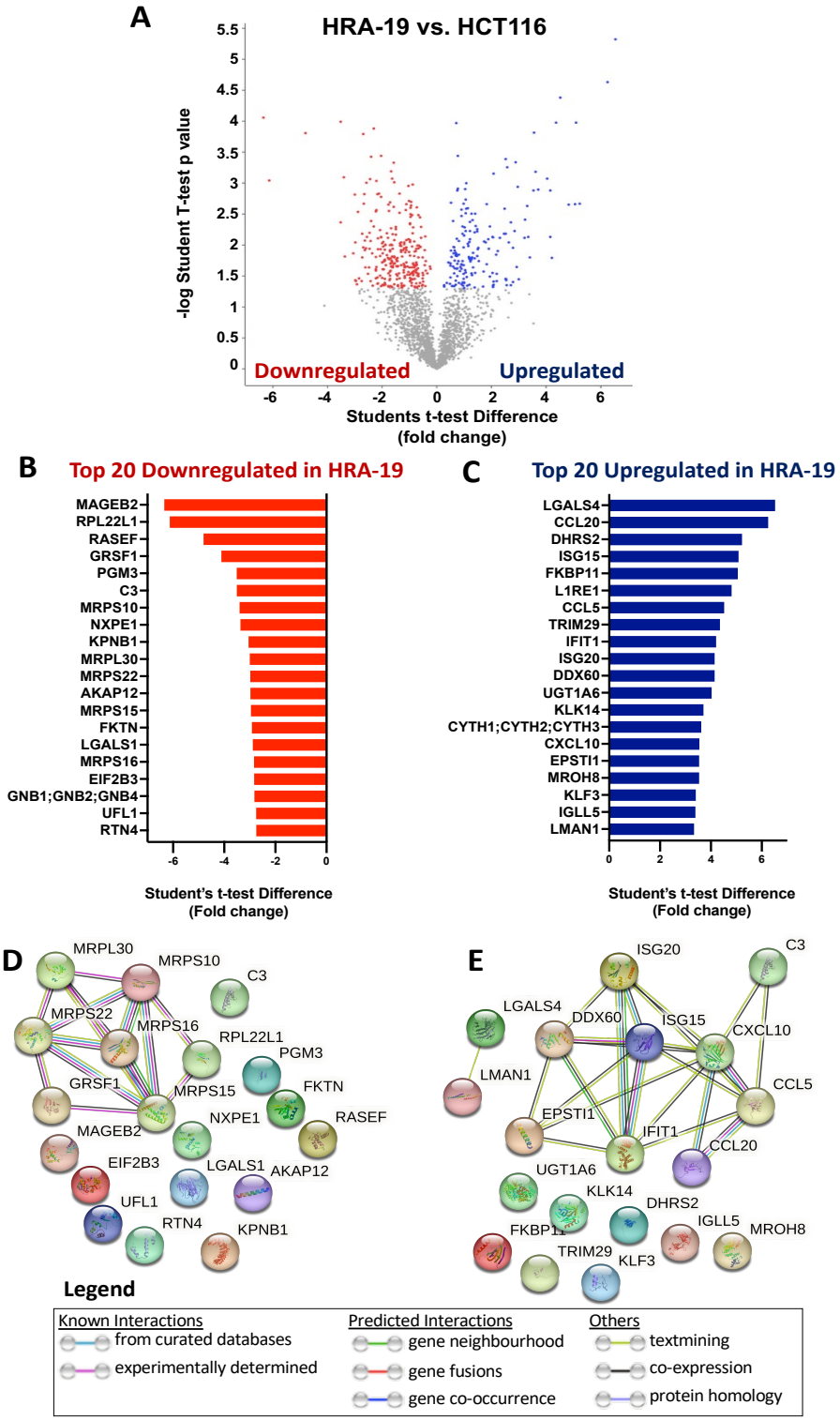

Figure 3-20: The C3 interactome differs between radiosensitive HCT116 and radioresistant HRA-19 cells. (A) Volcano plot illustrating 456 significant differentially expressed proteins ($p < 0.05$) in the C3 interactome of HRA-19 cells, when compared to HCT116 cells where blue dots and red dots represent upregulated and downregulated proteins, respectively. Statistical analysis was performed by Student's t-test. The top 20 most **(B)** downregulated and **(C)** upregulated proteins between HRA-19 and HCT116 cells were identified based on fold change in expression and **(D-E)** assessed for direct interaction with C3 by generating predicted protein networks using STRING. Mass Spectrometry was performed by the Discovery Proteomics Facility at the Target Discovery Institute, University of Oxford.

Table 3-5: Top 30 significantly altered proteins between the C3 interactome of HRA-19 and HCT116 cells. Up or downregulation of proteins is outlined in HRA-19 cells relative to HCT116 cells. Mass Spectrometry was performed by the Discovery Proteomics Facility at the Target Discovery Institute, University of Oxford.

Protein name	Up/Down regulated in HRA-19	*p*-adjusted	Fold change
HSPA1A;HSPA1B	Down	0.03288889	-2.2937593
ERCC3	Down	0.03366667	-2.6858315
ZC3H4	Up	0.03393548	1.07134088
EXOSC4	Down	0.03506667	-2.5634485
HSP90AB1	Down	0.03627586	-1.5621128
RASEF	Down	0.03672727	-4.8098523
VAT1	Down	0.03675	-0.8809849
NRGN	Down	0.03692308	-2.4391561
MANF	Up	0.037	0.71346601
HSPA5	Down	0.03757143	-2.2069969
SP6	Up	0.038	2.08468978
ESF1	Down	0.03809524	-1.3614817
ZC2HC1A	Down	0.0384	-1.6282228
RPL22L1	Down	0.03896296	-6.1307888
CD44	Down	0.03902439	-2.1142961
EI24	Down	0.03918182	-2.1720618
CYTH1;CYTH2;CYTH3	Up	0.03980952	3.62142769
UGT1A6	Up	0.04	4.02792088
DDX60	Up	0.04	4.14411664
PHLDA2	Down	0.04009302	-2.6437287
CXCL10	Up	0.0404	3.54825513
SNRPD3	Up	0.04102564	0.74357732
MRPL30	Down	0.04106667	-3.0014724
MRPS10	Down	0.04173913	-3.4024151
DNAJA2	Down	0.0418	-1.6636276
ELOA	Up	0.04188889	1.04111004
EPSTI1	Up	0.04210526	3.53634063
ISG15	Up	0.04228571	5.08771388
CCDC124	Down	0.04242424	-1.0294825
DHX35	Up	0.04308571	0.76225122

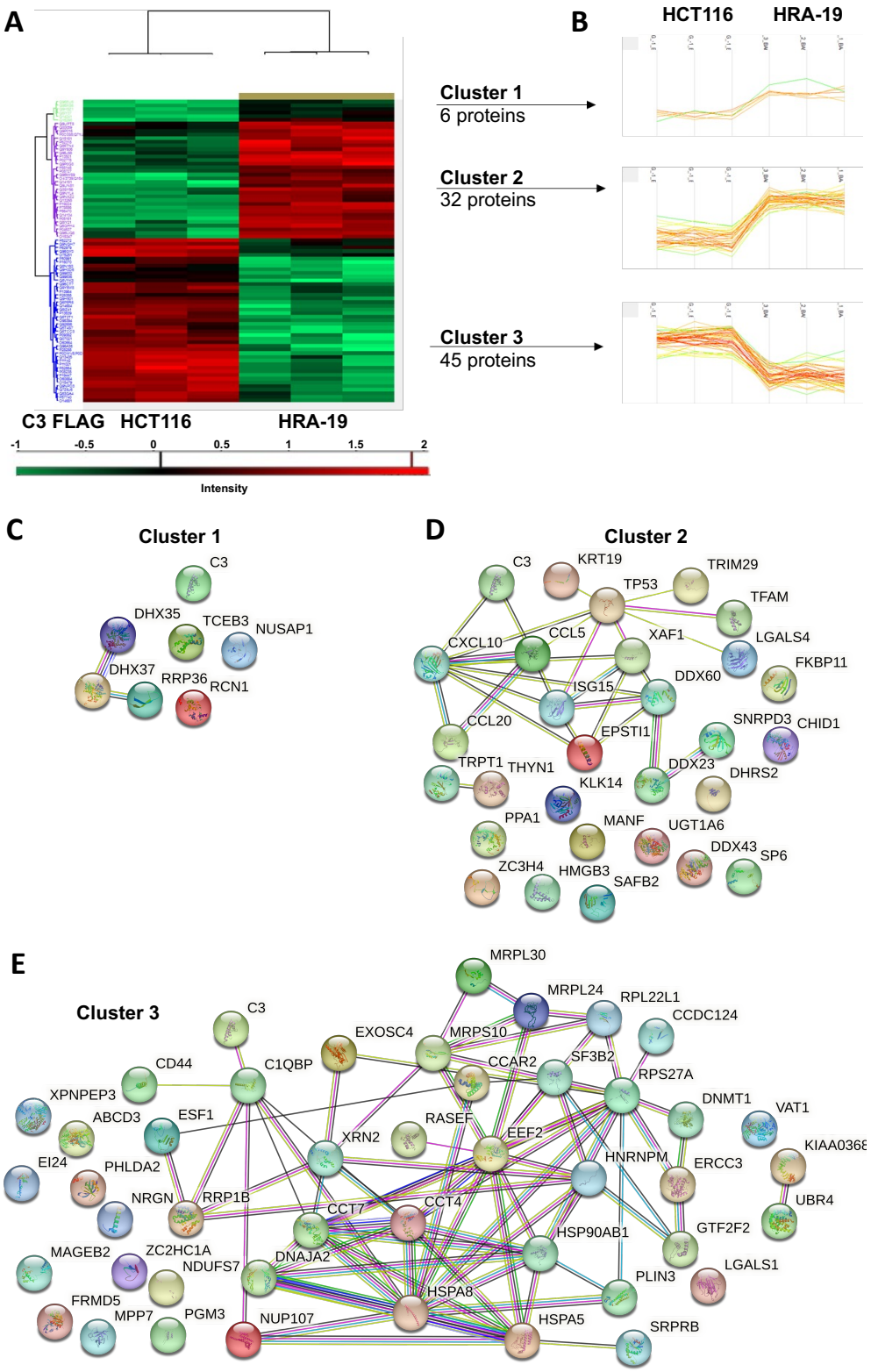

Figure 3-21: Three protein clusters are differentially expressed between the HRA-19 cell-derived and HCT116 cell-derived C3 interactome. Clustering analysis was performed using proteins significantly altered between HRA-19 and HCT116 cells (p-adj < 0.05). (**A**) Protein heatmap identifying **(B)** three protein clusters differentially expressed by HRA-19 and HCT116 cells. (**C-E**) Proteins in each cluster were assessed for potential interaction with C3 using STRING. Mass Spectrometry was performed by the Discovery Proteomics Facility at the Target Discovery Institute, University of Oxford.

3.4.17. The C3 interactome in HRA-19 cells demonstrates enrichments in lymphocyte chemotaxis and chemokine activity

Having demonstrated differential protein expression between the C3 IP fractions of HRA-19 and HCT116 cells, functional enrichment analysis was performed using STRING to identify whether Biological Processes, Molecular Function or Kyoto Encyclopedia of Genes and Genomes (KEGG) pathways were predicted to be altered between the two cell lines. Analysis was performed using the fold change values for all of the 2109 proteins identified in the initial data set.

For Biological Processes, there were 11 Gene Ontology (GO)-terms predicted to be enriched in HRA-19 cells, relative to HCT116 cells, which are detailed in **Table 3-6**. Lymphocyte chemotaxis was predicted to be the most enriched, with an enrichment score of 6.23. For Molecular Function, there were 4 GO-terms predicted to be enriched in HRA-19 cells, which are detailed in **Table 3-7**. Chemokine activity was the molecular process predicted to most significantly enriched, with an enrichment score of 7.39. The top 5 KEGG pathways predicted to be enriched in the C3 interactome of HRA-19 cells, when compared to HCT116 cells are outlined in **Table 3-8**. Cytokine-cytokine receptor interaction was the KEGG pathway predicted to be most significantly enriched, with an enrichment score of 7.39.

3.4.18. Common protein interactors with C3 exist between HRA-19 and HCT116 cells

While the C3 interactome was significantly altered between HRA-19 and HCT116 cells, the total protein dataset identified (2109) was assessed using STRING for potential common interactors of C3 derived from HRA-19 and HCT116 cells. A total of 23 proteins were identified that were predicted to directly interact with C3, none of which were expressed at significantly altered levels between HRA-19 and HCT116 cells. (**Fig. 3-22**) The fold change and -log(*p*-value) for these common interactors of C3 are outlined in **Appendix 5.** This demonstrates that while the C3 interactome is significantly altered between HCT116 and HRA-19 cells, common C3 binding partners potentially exist within these cell lines.

Table 3-6: Biological processes predicted to be enriched in the C3 interactome of HRA-19 cells, relative to HCT116 cells.

GO term ID	Term Description	Enrichment Score	FDR	Proteins from input
0048247	Lymphocyte chemotaxis	6.23651	0.00071	CCL20, CCL5, CXCL10, SLC12A2
0070098	Chemokine-mediated signalling pathway	5.77438	0.0018	CCL20, CCL5, CXCL10, RBM15
2000406	Positive regulation of T cell migration	5.672	0.0020	CCL20, CCL5, CXCL10, RHOA
2000404	Regulation of T cell migration	4.7012	0.0034	CCL20, CCL5, CXCL10, CRKL, RHOA
1990869	Cellular response to chemokine	3.9363	0.0020	CCL20, CCL5, CXCL10, SLC12A2, LOX, RBM15, RHOA
0060337	Type I interferon signalling pathway	3.50624	4.9E-05	OAS3, OASL, SAMHD1, ISG20, OAS2, JAK1, STAT1, XAF1, ADAR, IFIT1, IFIT3, HLA-C, ISG15, HLA-A, MX1, HLA-B
0034340	Response to type I interferon	3.23397	4.9E-05	OAS3, OASL, SAMHD1, ISG20, SHMT2, OAS2, JAK1, STAT1, XAF1, ADAR, IFIT1, IFIT3, HLA-C, ISG15, HLA-A, MX1, HLA-B
0045071	Negative regulation of viral genome replication	2.66903	4.9E-05	OAS3, LTF, EIF2AK2, ZC3HAV1, TRIM28, OASL, ISG20, KIAA1551, OAS2, VAPA, IFIT5, IFIT1, SRPK1, ISG15, MX1, ILF3, VAPB, HMGA2, CCL5
0070268	Cornification	1.64672	0.0050	PKP2, KRT14, KRT23, CAPNS1, KRT9, KRT5, KRT1, KRT6B, KRT15, KRT71, KRT10, ST14, KRT16, KRT17, KRT2, KRT7, PKP3, KRT19, DSP, KRT6A, KRT18, KLK14, JUP, CAPN1, KRT8
0006457	Protein folding	0.922026	5.86E-05	FKBP4, CD74, ST13, AHSA1, CSNK2A1, SGTA, CDC37, WFS1, MLEC, MOGS, HSPE1, TRAP1, CANX, HSPB1, LMAN1, DNAJB1, CCT7, PPIG, PSMC1, ERP29, DNAJB6, DNAJA3, CSNK2A2, DNAJC10, CCT6A, CCT5, RANBP2, PDIA4, PPIL3, CCT8, CCT3, HSPA9, CCT2, HSP90B1, PPIB, PDIA3, PPID, DNAJA2, GAK, TCP1, HSPH1, CHORDC1, NUDC, CALR, PDIA5, HSPA5, CCT6B, P4HB, HSP90AA1, GANAB, RAD23B, VCP, PFDN2, GNAI3, BAG2, HSP90AB1, PPIL1, HSPA1A,

				CSNK2B, PRDX4, DNAJA1, DNAJC21, DNAJC19, HSPD1, CCT4, PFDN6, PDIA6, DNAJC7, UNC45A, DNAJB11, PPIA, HSPA8, B2M, PRKCSH, RUVBL2, GNB1
0006119	Oxidative phosphorylation	0.741185	0.0018	NDUFB4, NDUFS7, ATP5E, NDUFA10, COX5B, NDUFB5, ATP5B, NDUFS3, NDUFA9, UQCRC2, NDUFB10, NDUFB9, ATP5O, ATP5J2, NDUFS4, ATP5L, NDUFA7, ATP5H, ATP5I, CYCS, GBAS, NDUFS8, CYC1, COX5A, NDUFV1, NDUFV2, NDUFA12, NDUFB1, UQCR10, NDUFA4, STOML2, ATP5C1, MTCO2, NDUFS2 ,ATP5F1, OX7A2, NDUFS5, NDUFA8, UQCRQ, ATP5A1, NDUFS1, NDUFA13, COX6C, UQCRB, COX4I1

Abbreviations; GO, gene ontology; FDR, False discovery rate.

Table 3-7: Molecular functions predicted to be enriched in the C3 interactome of HRA-19 cells, relative to HCT116 cells.

GO term ID	Term Description	Enrichment Score	FDR	Proteins from input
0008009	Chemokine activity	7.39111	0.00054	CXCL10, CCL20, CCL5
0042379	Chemokine receptor binding	3.93996	0.0039	NARS, CXCL10, CCL20, STAT1, YARS, CCL5
0003735	Structural constituent of ribosome	1.05585	0.0031	MRPS35, MRPS34, RPL18A, MRPL32, RPL19, MRPL27, RPS12, MRPS7, RPS16, MRPL34, MRPL4, MRPS25, MRPS36, MRPS9, RPL35, MRPS18B, RPL8, RPS11, RPS27A, MRPS5, RPS3, MRPL49, RPMS17, MRPL17, MRPL10, MRPL33, RPS23, MRPL16, NDUFA7, RPS9, RPL13, MRPL11, RPL15, RPL38, MRPL57, RPL4, MRPL46, MRPS31, MRPS11, MRPS24, RPS15A, MRPS23, RPLP2, RPS27L, MRPL54, MRPL12, MRPL30, RPS7, RPL7,MRPL43, RPS2, RPS21, RPL3, RPL36AL, RPL27A, RPL21, RPLP1, RPS17, RPS3A, RPSA, RPL22L1, RPL22, RPS26, MRPL24, RPL12, RPL39, MRPL18, DAP3, RPS27, MRPL9, RPL5, MRPL41, MRPS2, RPL7A, MRPL14, MRPS18A, MRPS16, MRPS15, RPS4X, RPL10A, RPL11, RPS6, RPL13A, MRPS33, RPL24, RPL34, RPS29, RPL14, RPS8, RPL23L, MRPS6, MRPS12, RPS14, RPL31, UBA52, RPL23A, RPS18, RPL17, RPL9, RPL6, MRPL55, RPL36A, RPL10, RPS24, RPL32, MRPL47, MRPS22, RPL37A, RPL7L1, RPL29, RPL35A, RPL23, MRPS14, RPL30, RPL26L1, RPS20, MRPL22, RPS25, FAU, RPS13, RPL18, RPLP0, RPL28, MRPS21, RPL26, RPL36, RPL27, RPS15, RPS19, RPS28, RPS5, RPS10
0051082	Unfolded protein binding	0.929661	0.00051	ST13, CDC37, HSPE1, TRAP1, CANX, LMAN1, DNAJB1, CCT7, DNAJB6, DNAJA3, AFG3L2, CCT6A, CCT5, CCT8, CCT3, NPM1, HSPA9, HEATR3, CCT2, HSP90B1, PPIB, DNAJA2, CHAF1B, TCP1, NUDC, CALR, HSPA5, CCT6B, HSP90AA1, TUBB4B, TOMM20, PFDN2, HSP90AB1, HSPA1A, DNAJA1, NAP1L4, HSPD1, CCT4, PFDN6, DNAJB11, PPIA, SRSF10, HSPA8, SERPINH1, NACA, RUVBL2

Abbreviations; GO, gene ontology; FDR, False discovery rate.

Table 3-8: Top 5 KEGG pathways predicted to be enriched in the C3 interactome of HRA-19 cells, relative to HCT116 cells.

Term Description	Enrichment Score	FDR	Proteins from input
Cytokine-cytokine receptor interaction	7.39111	8.18x 10^{-5}	CXCL10, CCL20, CCL5
Viral protein interaction with cytokine and cytokine receptor	7.39111	8.18 x 10^{-5}	CXCL10, CCL20, CCL5
Cytosolic DNA-sensing pathway	3.17812	0.0075	POLR1D,CXCL10,POLR2L,POLR2K,ADAR, CCL5
Ribosome	1.14612	0.00058	MRPS10, RPL18A, MRPL32, RPL19, MRPL27, RPS12, MRPS7, RPS16, MRPL34, MRPL4, MRPS9, RPL35, RPL8, RPS11, RPS27A, MRPS5, RPMS17, MRPL17, MRPL10, MRPL33, RPS23, MRPL16, RPS9, RPL13, MRPL11, RPL15, RPL38, RPL4, MRPS11, RPS15A, RPLP2, RPS27L, MRPL12, MRPL30, RPS7, RPL7, RPS2, RPS21, RPL3, RPL36AL, RPL27A, RPL21, RPLP1, RPS1, RPS3A, RPSA, RPL22L1, RPL22, RPS26, MRPL24, RPL12, RPL39, MRPL18, RPS27, MRPL9, RPL5, MRPS2, RPL7A, MRPL14, MRPS18A, MRPS16, MRPS15, RPS4X, RPL10A, RPL11, RPS6, RPL13A, RPL24, RPL34, RPS29, RPL14, RPS8, RPL23L, MRPS6, MRPS12, RPS14, RPL31, UBA52, RPL23A, RPS18, RPL17, RPL9, RPL6, RPL36A, RPL10, RPS24, RPL32, RPL37A, RPL29, RPL35A, RPL23, MRPS14, RPL30, RPL26L1, RPS20, MRPL22, RPS25, FAU, RPS13, RPL18, RPLP0, RPL28, MRPS21, RPL26, RPL36, RPL27, RPS15, RPS19, RPS28, RPS5, RPS10
Oxidative phosphorylation	0.666638	0.00038	NDUFB4, ATP6V1D, NDUFS7, ATP5E, NDUFA10, COX5B, NDUFB5, ATP5B, NDUFS3, NDUFA9, UQCRC2, NDUFB10, ATP6V1A, NDUFB9, ATP5O, ATP5J2, NDUFS4, ATP5L, NDUFA7, ATP5H, ATP5I, NDUFS8, CYC1, COX5A, NDUFV1, NDUFV2, NDUFA12, NDUFB1, UQCR10, NDUFA4, ATP5C1, MT-CO2, NDUFS2, ATP5F1, COX7A2, NDUFS5, PPA1, NDUFA8, ATP6V1G1, UQCRQ, ATP5A1, NDUFS1, NDUFA13, COX6C, UQCRB, COX4I1

Abbreviations; FDR, False discovery rate.

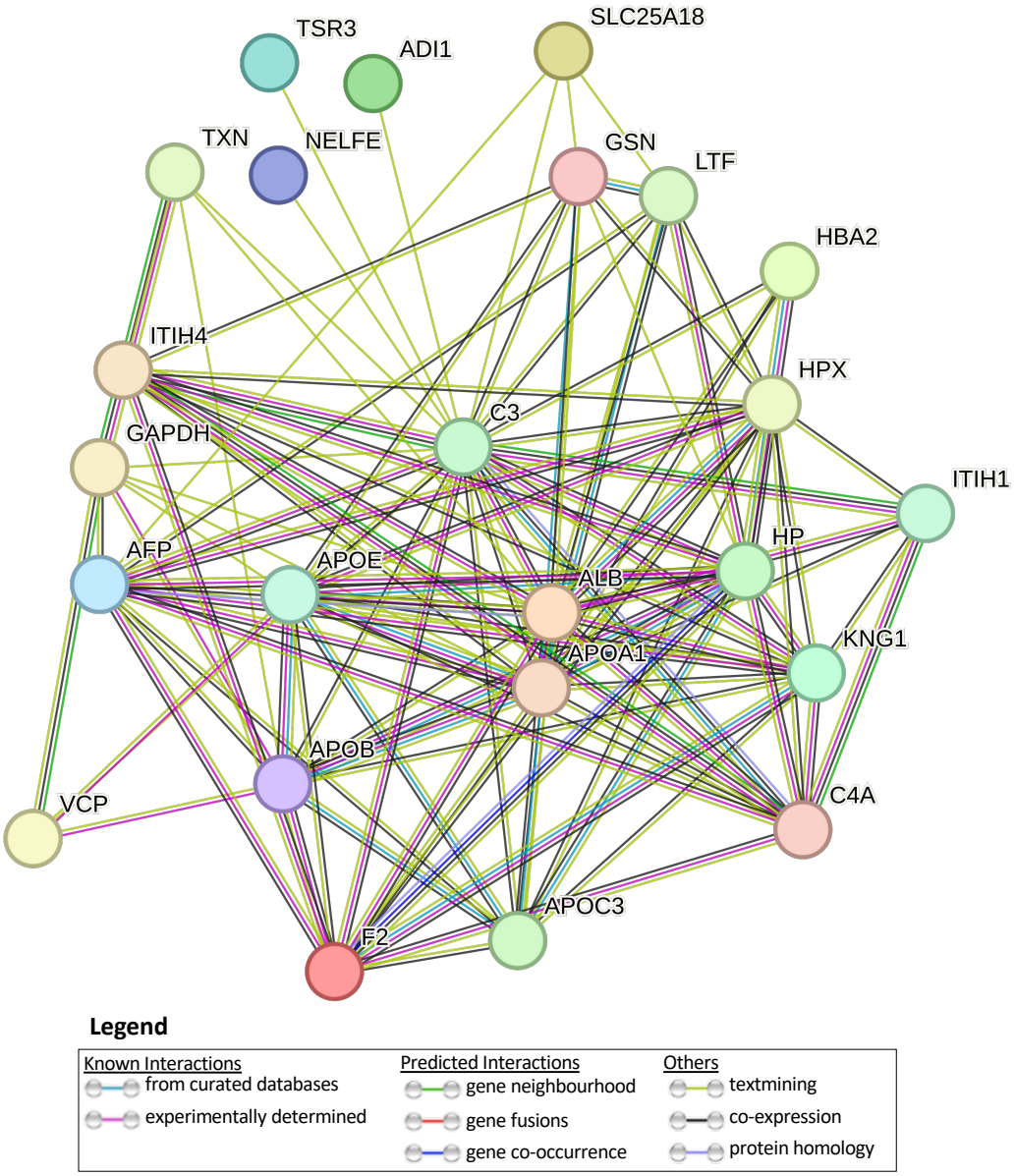

Figure 3-22: Proteins predicted to directly interact with C3 in HRA-19 and HCT116 cells. The initial (2109) protein dataset was analysed using STRING to identify proteins predicted to be direct interactors with C3. A total of 23 proteins were predicted to directly interact with C3 that were not expressed at significantly altered levels between HRA-19 and HCT116 cells.

3.5. Discussion

Increasing evidence suggests a role for complement in the tumour response to anti-cancer therapy, however, the role of complement in functionally modulating the response to radiation in CRC is currently unknown. Characterisation of a panel of CRC cell lines (Chapter 2), demonstrated that complement is activated in CRC cells and importantly, increased complement activation correlates with increased radioresistance to a clinically-relevant dose of radiation. This suggests a potential role for complement in modulating the radioresponse in CRC cells.

This chapter aimed to investigate the functional role of the central complement component C3 in modulating radiosensitivity in CRC cells through the use of a C3 overexpression plasmid and C3 siRNA. In the radiosensitive HCT116 cell line, which express low levels of C3, transient C3 overexpression resulted in a significant increase in radioresistance to a clinically-relevant dose, when compared to cells transfected with a VC. In the radioresistant HRA-19 cell line, which expresses increased levels of C3, downregulation of C3 enhanced radiosensitivity to a clinically-relevant dose. This demonstrates for the first time that intracellular C3 plays a functional role in modulating radioresistance in CRC *in vitro*. Surprisingly, transient silencing of C3 in another radioresistant line, the SW837 rectal adenocarcinoma cell line did not alter radiosensitivity. HRA-19 and SW837 cells were selected to study the functional role of C3 in the radioresponse as they were demonstrated to express significantly higher levels of complement, when compared to the radiosensitive HCT116 cell line (Chapter 2). However, whilst relative C3 mRNA expression in SW837 and HRA-19 cells was significantly greater than that in HCT116 cells, at the protein level, only HRA-19 cells expressed significantly higher levels of C3, when compared to HCT116 cells. Furthermore, while both SW837 and HRA-19 cells express greater levels of complement overall, when compared to HCT116 cells, (Chapter 2, **Fig. 2-10 A**), HRA-19 cells express significantly elevated levels of complement, when compared to SW837 cells. Therefore, alterations in the level of endogenous, intracellular C3 expression may account for the differing effects of C3 silencing on the radioresponse in SW837 and HCT116 cells. Additionally, while silencing of C3 was confirmed in SW837 cells relative to si-scr transfected controls, notably the degree of silencing was variable between experimental replicates. Furthermore, irradiation of SW837 cells transfected with si-scr RNA resulted in a downregulation of C3, when compared to unirradiated controls. As C3 expression was therefore downregulated in both

si-C3 and si-scr transfected SW837 cells, this may account for why there were no differences in the surviving fraction of these cells.

Having demonstrated that C3 modulates response to radiation in HCT116 and HRA-19 cells, the potential functional mechanism underlying this C3-mediated radioresistance was investigated. The functional role of complement in the radioresponse has previously been explored in two independent studies. Both of these highlighted complement anaphylatoxins as the functional mediators of the radioresponse. Work by Elvington and colleagues, demonstrated that combining complement inhibition with RT, therefore reducing anaphylatoxin generation, improved response to treatment by relieving immunosuppression and restoring the anti-tumour immune response[350]. In contrast, Surace *et al*. demonstrated that anaphylatoxins were essential for RT efficacy, demonstrating that tumour control was lost in C3, C3aR or C5aR deficient mice when complement was inhibited[351]. Despite these seemingly opposing results, Elvington and Surace utilised different murine models, fractionation schedules and methods of complement inhibition, which may have resulted in the dichotomy of responses observed. Regardless, the complement-mediated regulation of therapeutic response demonstrated in these studies was dependent on immune cells within the TME, a factor that cannot be recapitulated by *in vitro* experiments. Therefore, the demonstrated C3-mediated modulation of radiosensitivity/radioresistance in HRA-19 and HCT116 cells in this chapter, supports a novel, non-canonical function for endogenous tumour-derived complement.

In several cancer types including CRC, tumour-derived complement has been demonstrated to have autocrine effects on tumourigenesis[324,342]. Furthermore, increasing evidence demonstrates that complement components exist intracellularly, which may have canonical or non-canonical roles[344]. Study of complement in T cells identified this 'complosome'[407], which demonstrated that activation of C3 and C5 occurs intracellularly to generate C3a and C5a, which play essential roles in survival and effector differentiation[263,265]. The complosome is also present in myeloid cells, where intracellular C5a/C5aR signalling in mitochondria modulates sterile inflammation[266]. Aside from immune cells, intracellular complement has also been described in cancer. CFH resides in lysosomes in lung adenocarcinoma and clear cell renal cell carcinoma, where it co-localises with C3 and promotes tumour cell survival, proliferation and migration[342]. Additionally, intracellular C4BPA has been demonstrated to regulate NF-κB-dependent apoptosis in cancer cells[343]. In CRC, Ding *et al*. have recently described a role for endosomal C5a/C5aR

in promoting tumourigenesis via stabilisation of β-catenin[341]. Given these novel roles for intracellular complement in cancer, it was hypothesised that C3 may modulate the radioresponse of CRC cells via an intracellular function.

To investigate potential mechanism(s) by which C3 may be modulating radiosensitivity in CRC cells, the effect of modulating C3 expression on key parameters associated with radioresistance; apoptosis, DNA damage induction and repair and cell cycle were investigated. In HCT116 cells, transient overexpression of C3 did not impact any of these parameters basally, or following a clinically-relevant dose (1.8 Gy) of radiation. In contrast, silencing of C3 induced alterations in the phenotype of HRA-19 cells. This was unexpected, having demonstrated that modulation of C3 in both of these cell lines altered radiosensitivity. An important consideration is that these experiments were performed *in vitro* using cell lines. Cell lines are imperfect models as they arise from different driver mutations, and are characterised by different genetic backgrounds. Importantly, the HCT116 cell line is derived from a colon carcinoma, while the HRA-19 cell line was established from a rectal adenocarcinoma. This may suggest that the increased radioresistance demonstrated in HCT116 cells following C3 overexpression occurs by an independent mechanism not assessed in this chapter. While apoptosis, DNA damage and cell cycle are all implicated in resistance to RT[134], there are additional parameters including metabolism and oxidative stress, which are involved in treatment response[408]. Full characterisation of both HCT116 and HRA-19 cells basally and post modulation of complement may identify the important mechanisms affecting response to radiation in CRC.

Having demonstrated differences between HCT116 and HRA-19 cells, it raises the suggestion of whether an isogenic model would be useful to assess whether radioresistance is accompanied by altered complement expression. Previously within our Department, we have demonstrated using our in-house generated isogenic model of radioresistance in OAC, that radioresistant cells express significantly higher levels of C3, when compared to their parent counterparts (unpublished data). As isogenic models eliminate the genetic variation associated with the use of different cell lines, it would be useful to directly investigate which other genes and biological functions are altered. However, previous attempts by our research group to generate an isogenic model of radioresistance in rectal cancer using both the HRA-19 and SW837 cell lines has been unsuccessful, most likely due to the already high inherent radioresistance of these cells. Irrespective of this, isogenic models are still

accompanied by their own limitations, given that they reflect acquired radioresistance. To elucidate the function of C3 in rectal cancer that is inherently radioresistant or that displays a response followed by resistance to RT phenotype, other models would be required.

In addition, the experimental set up may also account for the differing effect of C3 modulation on the parameters of radioresistance investigated in HCT116 and HRA-19 cells. While in HRA-19 cells, endogenous C3 expression was silenced, an experimental over-expression of exogenous C3 via DNA plasmid was performed in HCT116 cells. Potentially, overexpression of exogenous C3 may produce a form distinct from endogenous C3, which is involved in different cellular processes. Kremlitzka *et al.* have demonstrated alternative translation of C3 resulting in distinct cytosolic and secreted forms[409]. Interestingly, cytosolic C3 engages in unique roles following invasion of staphylococcus aureus. This provides evidence that distinct forms of C3 can exist within cells, which reside in different cellular compartments, and have different functions[409]. In clear cell renal cell carcinoma and lung adenocarcinoma, CFH has been identified in two cellular compartments; membranous and intracellular[342]. Distinct from the membranous form, intracellular CFH resided in lysosomes, and engaged in non-canonical functions including the promotion of tumour cell proliferation, migration and motility. In patients, tumoural expression of intracellular CFH correlated with poor prognosis[342]. These data demonstrate that in cancer, distinct forms of complement that occupy separate regions within the cell can have differing effects on tumour growth and patient outcomes. Considering both of these new studies, it is feasible to suggest that overexpression of exogenous C3 in HCT116 cells potentially generates a form of C3 that is functionally distinct from endogenous C3. Theoretically speaking, this form of C3 may contribute to radiosensitivity in an alternative mechanism to that within HRA-19 cells.

Alterations in apoptosis have been linked with resistance to RT[143–145]. Previous work by Olcina *et al*. has provided evidence that complement can regulate apoptosis[343]. In an elegant study, they elucidated a role for C4BPA in regulating NF-κB-dependent apoptosis in cancer cells in response to oxaliplatin[343]. Although this doesn't provide us with insights into C3, it highlights how complement system components are continually being identified in previously unconsidered roles. Similarly to HCT116 cells, modulation of C3 expression in HRA-19 cells did not alter basal or radiation-induced apoptosis. These data suggest that apoptosis is not a major pathway of radiation-induced cell death in these cells. This contrasts with previous evidence in the literature that in rectal cancer, high levels of

apoptosis prior to neo-CRT correlate with good responses and reduced local recurrence[146–148]. Similarly, in CRC cell lines, radioresistance has been observed to associate with lower rates of spontaneous and radiation-induced apoptosis[410]. However, the role of apoptosis in the response to radiation is controversial and has long been debated. Evidence that apoptosis determines the response to RT is strong only for some haematological malignancies[411]. Importantly, the induction of apoptosis that occurs 24 – 48 h post irradiation is likely to be secondary to an aberrant mitotic event, which is instead the determining factor in response to radiation[412]. These data support the hypothesis that other mechanisms of cell death play a more central role in the response to radiation in CRC. Furthermore, these results suggest that in HCT116 and HRA-19 cells, complement-mediated apoptosis is not an important mediator of the tumour response to radiation. Importantly, experiments performed in this chapter utilised one dose of 1.8 Gy, and induction of apoptosis in HRA-19 and HCT116 cells may require multiple fractionated doses of radiation.

DNA is the critical target of RT. Consequently, DNA damage induction and repair play a critical role in the response to radiation. In HRA-19 cells, downregulation of C3 was associated with increased basal DNA damage at 48 h post transfection. DNA damage was also significantly induced following irradiation, which was detectable at 10 h post radiation, suggesting persistent damage. As DNA damage was not induced in si-scr cells, it is not possible to compare the kinetics of DNA repair in si-scr and si-C3 cells. However, these results suggest that downregulation of C3 in HRA-19 cells significantly induces DNA damage, both basally and following IR, which can sensitise cells to radiation. This finding is supported by previous work in our Department, which highlighted that C3 expression is increased in pre-treatment tumour tissue from OAC patients with subsequent poor responses to neo-CRT. Within these same tumour biopsies, miR-187 expression was significantly decreased[368]. This was explored *in vitro* using an isogenic OAC model of radioresistance, which demonstrated that transient overexpression of miR-187 in radioresistant cells had a significant radiosensitising effect. Interestingly, this was accompanied by a downregulation of several DDR genes and C3[368]. These data highlight that C3 may be involved in the DDR and subsequently tumoural responses to radiation. The suggestion that complement components are implicated in the DDR are supported by recent studies which have identified a role for C1QBP in stabilising the MRN complex to promote HR in response to DSBs[369], and a role for C5 in repairing chemotherapy-induced DNA damage[347]. Elucidating whether C3 modulates the DDR in HRA-19 cells would

require assessing expression of DDR genes following C3 silencing, to determine which, if any, pathways are implicated.

Silencing of C3 in HRA-19 cells was also associated with alterations in basal cell cycle distribution. Cell cycle phase can impact on radiosensitivity, with cells in the G2 and M phases being most sensitive, cells in G0 being more resistant, and cells in S phase being most resistant to radiation[95–97]. Interestingly, at 24 h post C3 silencing, HRA-19 cells demonstrated a significant increase in cells in the radiosensitive G2/M phase, when compared to scrambled controls. This was accompanied by a reduction in the percentage of radioresistant S phase cells. This demonstrates that basally, C3 silencing alters cell cycle distribution in HRA-19 cells to a more radiosensitive phenotype. Complement components have previously been implicated in cell cycle distribution[342]. In a study of clear renal cell carcinoma cells, Daugan *et al*. demonstrated that silencing of CFH is associated with modifications in cell cycle distribution, including an increased percentage of cells in the G0/G1 phase[342]. Sublytic C5b-9 is another element of the complement system that has been demonstrated to influence cell cycle distribution in oligodendrocytes, by inducing cell cycle activation and entry into S phase[373]. While results presented in this chapter relate to the role of C3 in CRC, these studies support the hypothesis that modulating complement expression can induce modifications in cell cycle distribution. Interestingly, addition of C3 to the culture medium of gastric cancer cell lines has been demonstrated to enhance accumulation in S phase[317]. Given that fewer C3 silenced HRA-19 cells resided in S phase, this supports a role for C3 in accumulating cells in S phase, which is the most radioresistant cell cycle phase. Thus, therapeutically, targeting C3 may reduce S phase accumulation, leading to increased radiosensitivity.

In addition to alterations in basal cell cycle distribution, silencing of C3 also modified cell cycle distribution following irradiation. Silencing of C3 resulted in a reduced distribution of cells in S phase, which was concomitant with an increased percentage of G0/G1 cells following irradiation. This shift suggests that complement influences cell cycle progression in response to radiation, and further highlights a relationship between C3 and S phase accumulation. No studies to date have explored the relationship between complement and cell cycle progression in the response to radiation. However, in radioresistant colon cancer cells, silencing of survivin, an anti-apoptotic protein, has previously been associated with G2/M arrest and elevated levels of DNA damage in the form of DSBs, post irradiation[413]. To our knowledge, the results presented here are the first

to demonstrate an association between C3 expression and altered cell cycle distribution in rectal cancer.

Results presented in this chapter suggest that C3 may potentially engage in a different interactome, within radiosensitive and radioresistant cells. In support of potential differing roles for C3 in HCT116 and HRA-19 cells, overexpression and IP of C3 demonstrated differential expression of proteins associated with C3 between these two cell lines, with 3 protein clusters also identified. Elongin A (ELOA1, TCEB3) was among the proteins identified in Cluster 1, which was upregulated in HRA-19 cells relative to HCT116 cells. As the transcriptionally active subunit of the Elongin complex, ELOA1 has been identified as a key contributor to efficient transcript elongation[414]. Study of ELOA1 in mammalian cells following ultra-violet radiation suggests that ELOA1 may contribute to the ubiquitylation and degradation of stalled RNA polymerase II (pol II) which has encountered damaged DNA, allowing gene transcription by another pol II molecule[414]. Nucleolar and spindle associated protein 1 (NUSAP1), another protein in Cluster 1, has been implicated in DNA damage and repair. NUSAP1 is reportedly overexpressed in colon cancer and associated with poor patient OS[415]. In chronic lymphocytic leukemia, interaction of NUSAP1 with RAD51 promotes resistance to chemotherapy by contributing to HR-mediated DNA repair[415]. Together, the findings in these studies highlight that ELOA1 and NUSAP1 contribute to the resolution of DNA damage. Given the upregulation of these proteins in HRA-19 cells, they may potentially contribute to enhanced DNA damage repair in HRA-19 cells, relative to HCT116 cells. However, neither ELOA1 or NUSAP 1 were predicted to directly interact with C3, so how exactly or if C3 expression is influencing this process requires further investigation.

Proteins identified in Cluster 2, which was upregulated in HRA-19 cells, when compared to HCT116 cells, also suggest that repair of DNA damage is a mechanism by which C3 mediates radioresistance in HRA-19 cells. Among the proteins in Cluster 2 are tripartite motif-containing protein 29 (TRIM29) and high-mobility group box 3 (HMGB3), which have been implicated in DNA repair and resistance to RT[416,417]. Within Cluster 2, the only predicted direct interactor with C3 was chemokine (c-x-c) motif ligand 10 (CXCL10). High expression of CXCL10 is associated with poor response to RT in SCC of the tongue[418], highlighting a potential role for CXCL10 in the radioresponse in CRC. C1QBP, identified in Cluster 3, which was enriched in HCT116 cells, has been identified as a promoter of HR in response to DSBs[369]. While results in this chapter did not identify

altered DNA damage and repair following modulation of C3 expression in HCT116 cells, it further highlights a relationship between C3 and the DDR.

Several biological and molecular pathways were functionally enriched in the C3 interactome of HRA-19 cells relative to HCT116 cells. In particular, lymphocyte chemotaxis and chemokine activity were identified. KEGG pathway analysis highlighted enrichment of oxidative phosphorylation, which has previously been implicated in the response of rectal cancer cells to radiation in our department (unpublished data). Together, these data have identified potential pathways involved in C3-mediated radioresistance in CRC that warrant further investigation.

Interestingly, several proteins were predicted to be direct interactors with C3 that were not significantly altered between HRA-19 and HCT116 cells. In particular, among these common, potential binding partners for C3 were several apolipoproteins (APO), APOE, APOA1, APOB and APOC3, suggesting a relationship between complement and cholesterol metabolism.

Intracellular complement is gaining increasing attention both within and outside of the cancer research landscape. The data presented here demonstrate that in CRC cells, intracellular C3 functionally modulates radioresistance. Transient silencing of C3 in the radioresistant HRA-19 rectal cancer cell line is associated with significantly enhanced radiosensitivity. In these cells, C3 silencing induced elevated levels of basal DNA damage and shifted cell cycle distribution to a more radiosensitive phenotype. Mass spectrometry analysis following C3 pull-down from HCT116 and HRA-19 cells suggests that C3 engages with different interactomes in these cells, which potentially contributes to different mechanisms of radioresistance. Complement components are well accepted to function in an often context-dependent manner in human cancers[177]. This likely extends to the role of intracellular complement in treatment response. Given the recent discovery that intracellular C5a/C5aR signalling can promote tumourigenesis in CRC[341], it is highly likely that C3/C3a also can modulate cellular phenotype and function. An important question is whether endogenous intracellular complement in this context is a different form to C3 that is secreted. Until recently, it was largely unknown whether intracellular complement is secreted before being re-internalized by the cell, or whether it gets diverted away from the secretory pathway[409,419]. Understanding this in the context of CRC is essential to fully elucidate the role for C3 in the radioresponse and assess its potential as a therapeutic target.

Chapter 4: Investigating the effect of CRC cell-derived C3 on T cell phenotype

4.1. Introduction

In addition to acting as a first line of defence, the complement system is integral in coordinating the adaptive immune response and can modulate immune cell phenotype and function[255]. Complement enhances the induction of humoral responses, with complement receptor 2 (CR2) forming a B cell co-receptor with CD19 and CD81[256]. When complement-opsonised antigens are co-ligated by the CR2 complex and the B cell receptor, the B cell threshold for activation is lowered[254,257,258]. In addition to augmenting the antibody response, complement plays key roles in the induction of T cell immunity. Cognate interactions between T cells and APCs result in local production of complement components, with upregulation of C3aR and C5aR and signalling of locally produced anaphylatoxins aiding co-stimulation[171,259,260]. In naïve T cells, C3a and C5a signals play roles in survival[171], and following activation, C5a can control the expansion of effector T cells by suppressing activation-induced apoptosis[172].

Importantly, local complement signals during activation can influence T cell phenotype. Together with antigen presentation and co-stimulation, polarising cytokines are a third critical signal during T cell activation, which induce differentiation into specific T cell subsets. Differentiation of Th1 cells is induced by interleukin (IL)-12[420], IL-4 and IL-13 induce differentiation into Th2 cells[421,422], and IL-10 promotes differentiation of regulatory T cells (Tregs)[423]. The functions of these T cell subsets are shaped by the cytokines they produce, for example; production of IFN-γ, TNF-α and IL-2 by Th1 cells drives their pro-inflammatory, anti-tumour role[424]. Engagement of C5aR expressed by APCs, by locally produced C5a, upregulates IL-12 production, fostering a Th1 IFN-γ-producing phenotype[171,260]. Local complement signals have also been demonstrated to drive differentiation of Th17 cells[425]. The importance of C3aR and C5aR signalling in providing co-stimulatory and survival signals is demonstrated by the enhanced induction of Tregs, which occurs due to elevated IL-10 levels produced in the absence of these complement signals[261,426]. Furthermore, recent evidence demonstrates that complement is activated intracellularly in T cells[263,265]. Activation of both intracellular C3[263] and C5[265] has important roles in normal T cell activation and the secretion of IFN-γ[407]. This intracellular T cell 'complosome' has also been demonstrated to regulate nutrient uptake and metabolic processes during T cell activation[264,427].

Unsurprisingly, given the demonstrated role of complement in T cell activation, complement has been demonstrated to modulate T cells in the context of cancer. To date,

many of the pro-tumour roles complement engages in can be attributed to the regulation of immune cells[162]. Evidence for complement-mediated immunosuppression has been demonstrated in models of ovarian[298], breast[321], lung[274,326], and colon cancers[323], and also in models of melanoma[330,331] and sarcoma[332]. Activation of local complement yields anaphylatoxins, which can promote tumour growth by modulating the immune cell populations within the TME, often impacting anti-tumour T cell responses. In a syngeneic model of ovarian cancer, the C5a/C5aR signalling axis has been demonstrated to recruit MDSCs, which limit the responses and tumour infiltration of $CD8^+$ T cells[298]. Similar observations have been reported in models of colitis-associated CRC[324]. Reduced T cell production of pro-inflammatory Th1 cytokines such as IFN-γ has been demonstrated in cancer, following C3a and C5a signalling[325,326]. Complement-mediated immunosuppression can additionally contribute to tumour progression by facilitating the growth of metastases. In a murine model of breast cancer, C5aR signalling not only recruited MDSCs, but stimulated their production of IL-10 and TGFβ[321]. This was associated with the generation of Tregs, which reduced T cell infiltration and responses in pre-metastatic lung niches[321]. Similarly, C3a/C3aR signalling has been demonstrated to restrict $CD4^+$ T cell infiltration and promote metastasis, in a murine model of lung cancer[326]. These studies highlight a role for complement in the promotion of tumour growth via remodelling of the TME and immune cell phenotypes.

Beyond tumour growth, complement-mediated regulation of T cells has been implicated in the response to cancer treatment. C5a/C5aR signalling in squamous cell carcinoma limits the infiltration of $CD8^+$ T cells, which is associated with a poor response to chemotherapy[336]. Suppression of $CD8^+$ T cell responses by complement has also been linked with poor responses to anti-PD-1 and anti-PDL-1 therapy[320,322,361,362]. In this context, C3a has been demonstrated to reduce IL-10 production[320] and C5a has been demonstrated to recruit MDSCs[322] or increase the suppressive capacity of MDSCs[361], all of which limit the effector function of $CD8^+$ T cells and contribute to poor responses to anti-PD-1 monoclonal antibodies. C3a/C3aR has additionally been demonstrated to activate PI3Kγ signalling to promote the immunosuppressive functions of tumour associated macrophages, subsequently limiting responses to anti-PD-L1 therapy[362]. Evidence highlights that the therapeutic efficacy of RT can be influenced by complement-mediated modulation of local immune cells[350,351]. RT has been demonstrated to generate complement anaphylatoxins, which play essential roles in DC and subsequently anti-tumour T cell activation, and are

indispensable for therapeutic efficacy[351]. In contrast, others have demonstrated that RT-induced activation of complement restricts immune cell infiltration and suppresses anti-tumour responses[350]. While these studies report contrasting results, they demonstrate that the impact of complement signalling on the immune milieu within the TME, extends to altering treatment response. Complement has also been identified to modulate NK cells, with C3a signals restricting tumour infiltration in murine models of breast and colon cancer[337]. Antagonism of the C3a/C3aR signalling axis resulted in slower tumour growth and increased infiltration of NK cells[338]. In these models, complement-mediated modulation of NK cells was demonstrated to hinder the therapeutic efficacy of RT, as combined RT and complement inhibition demonstrated superior tumour control, when compared to RT alone[338]. These studies highlight that complement can negatively modulate immune cells within the TME, leading to poor therapeutic response.

In rectal tumours, T cell infiltration has been demonstrated to correspond with response to neo-CRT[428,429]. Understanding whether tumour-derived complement impacts the T cell phenotype in rectal cancer may provide essential insights into controlling tumour growth, and importantly, targeting resistance to cancer treatment. Given their roles in tumour promotion and progression, C3aR and C5aR have been proposed as a novel class of immune checkpoint receptors[320,430]. In the literature, little is known about the effects of tumour-derived complement, in particular C3/C3a, on T cells in CRC. Having characterised a panel of CRC cell lines, and demonstrated that complement is expressed by and activated within these cells, this chapter investigated the effect of CRC cell-derived C3 and recombinant C3a on T cell phenotype.

4.2. Specific aims of Chapter 4

This chapter aimed to assess the effects of CRC cell-derived C3 and recombinant C3a on T cell phenotype *in vitro*.

The specific aims of Chapter 4 are;

1. To investigate the effect of CRC cell-derived complement on T cell viability, activation and cytokine production, in the context of activation followed by movement to a complement-rich TME, by pre-stimulating peripheral blood mononuclear cells (PBMCs) and then co-culturing with conditioned media (CM) from HRA-19 or HCT116 cells basally and following transient silencing or overexpression of C3, respectively.

2. To investigate the effect of recombinant C3a on T cell viability, activation and cytokine production, in the context of activation followed by movement to a complement-rich TME, by pre-stimulating PBMCs and then treating with recombinant C3a.
3. To investigate the effect of CRC cell-derived complement on T cell viability, proliferation, activation and cytokine production, in the context of T cell activation within a complement-rich lymph node, by activating PBMCs while co-culturing with HRA-19 or HCT116 CM.
4. To investigate the effect of recombinant C3a on T cell viability, proliferation, activation and cytokine production, in the context of T cell activation within a complement-rich lymph node, by activating PBMCs in the presence of recombinant C3a.

4.3. Materials and methods

4.3.1. Ethical approval

This study utilised blood samples from healthy donors and was approved by the Faculty of Health Sciences Research Ethics Committee at Trinity College Dublin.

4.3.2. Consent of healthy donors

Volunteers for blood donation provided written, informed consent prior to sample collection. Venous blood (maximum of 36 mL) was drawn from consenting healthy donors by a qualified phlebotomist. In line with GDPR regulations, blood samples were anonymised to protect donor privacy.

4.3.3. PBMC isolation

PBMC isolation was performed in a laminar flow hood (Bioquell, Andover, United Kingdom). Aseptic technique was adopted for all procedures involving PBMCs and work was carried out in a laminar flow hood, which was switched on for at least 20 min prior to use. Before entering the hood, the area was decontaminated using 70% (v/v) ethanol. All reagents and equipment were sterilised with 70% (v/v) ethanol before they were placed in the laminar flow hood. PBMCs were isolated from whole blood by density gradient centrifugation using Lymphoprep™ (STEMCELL Technologies, Vancouver, Canada). Whole blood was diluted 1:1 using complete RPMI and layered carefully over Lymphoprep at a ratio of 2:1 diluted blood to Lymphoprep, in a 50 mL falcon tube. Tubes were centrifuged at 2,000 RPM for 25 min (Acceleration 3, Deceleration 0). The white cloudy PBMC buffy layer was transferred to a new 50 mL falcon tube and the volume was made up to 50 mL with PBS. PBMCs were washed by centrifugation at 1,800 RPM for 10 min. Supernatants were discarded to waste and washed again as before. The pellet was re-suspended in 1 mL of RPMI and 5 µL of this was added to 195 µL Trypan Blue (1:40 dilution). Cells were counted using a haemocytomer as previously described (Section 2.3.8). PBMCs/mL were calculated using the formula:

$$\text{Number of cells/mL} = \frac{Total\ number\ of\ cells}{4}\ x\ 10^4 x\ 40\ (dilution\ factor)$$

PBMCs were re-suspended in RPMI at a concentration of 1 x 10^6 cells/mL and incubated at 37°C, 5% CO_2/ 95% humidified air until required.

4.3.4. T cell activation using anti-CD3 and anti-CD28

The PBMC buffy coat layer isolated from whole blood contains monocytes and T cells. To stimulate activation of T cells, PBMCs were stimulated using plate-bound anti-CD3 and anti-CD28 antibodies.

A 2 μg/mL goat anti-mouse immunoglobulin G (IgG) (Sigma Aldrich, Merck) in sterile PBS was prepared and 300 μL was added to each well of a 12 -well plate. Plates were carefully sealed with parafilm and incubated for 2 h at 37°C, 5% CO_2/ 95% humidified air. Unbound IgG antibody was removed by carefully washing wells twice with PBS. An ultra Leaf™ anti-CD3 (2 μg/mL) (Biolegend, California, United States) and anti-CD28 (5 μg/mL) (Ancell, Minnesota, United States) solution was prepared in sterile PBS and 300 μL was added to IgG coated wells. The plate was incubated at 37°C for at least 2 h to allow anti-CD3/CD28 antibodies to bind to IgG. Prior to seeding PBMCs (Section 4.3.8), unbound anti-CD3/CD28 was removed by carefully washing wells twice with sterile PBS.

4.3.5. Assessing C3aR expression on PBMCs

C3aR expression was assessed extracellularly on unactivated and activated PBMCs. PBMCs were activated by culturing in 2 mL of complete RPMI in 12-well plates coated with anti-CD3/CD28 (Section 4.3.4) at 37°C, 5% CO_2/ 95% humidified air for 72 h. Unactivated PBMCs were cultured in 2 mL of complete RPMI in 12-well plates at 37°C, 5% CO_2/ 95% humidified air for 72 h.

To stain, PBMCs were collected in FACS tubes and pelleted by centrifugation at 1,300 RPM for 3 min at RT°. Supernatants were discarded and PBMCs were washed with 1 mL of FACS buffer (PBS with 2% FBS, 0.1% Sodium Azide) and pelleted as before. Supernatants were discarded and to eliminate dead cells during analysis, cells were stained with Zombie NIR (1:1000 dilution in PBS) (Biolegend, California, United States). Cells were stained in the dark at RT° for 15 min. Without washing off the Zombie NIR, PBMCs were stained using the extracellular antibodies detailed in **Table 4-1** made up to a total volume of 100 μL with FACS buffer. Staining was performed in the dark at RT° for 20 min. PBMCs were washed twice with FACS buffer and resuspended in 250 μL FACS buffer.

Table 4-1: Optimised volumes of extracellular antibodies used to distinguish T cell populations and assess expression of the C3aR.

Antibody	Company	Clone	Vol (µL) / tube
CD3-Pe/Cy7	Biolegend	OKT3	1
CD4-APC	Biolegend	OKT4	1
CD8-BV421	Biolegend	SK1	1
C3aR-PE	Miltenyi	hC3aRZ8	5

4.3.6. Generation of CM

CM was generated from HCT116 and HRA-19 cells basally and following C3 overexpression or silencing, respectively (**Fig**. **4-1**).

C3 was knocked down in HRA-19 cells using siRNA (Qiagen, Hilden, Germany). Reverse transfection was performed using 10 nM si-C3 or si-scr in 6-well plates. Briefly, HRA-19 cells in the exponential growth phase were harvested by trypsinisation as previously described (Section 2.3.4), counted (Section 2.3.8) and adjusted to a final concentration of 1 x 10^5 cells per mL in RPMI supplemented with 10% FBS. Reverse transfection was carried out as described in Section 3.3.5. A 2.4 mL volume of cell suspension (2.4 x 10^5 cells) was added to each well. Plates were rocked back and forth gently for 10 s and incubated at 37°C, 5% CO_2/ 95% humidified air for 24 h. After 24 h incubation, CM was removed and stored at -20°C until required.

C3 was overexpressed in HCT116 cells using C3 and VC plasmids (SinoBiological, Beijing, China). Briefly, HCT116 cells in the exponential growth phase were harvested by trypsinisation as previously described (Section 2.3.4), counted (Section 2.3.8) and adjusted to a final concentration of 2 x 10^5 cells per mL in RPMI supplemented with 10% FBS. Reverse transfection was carried out as described in Section 3.3.4. A 1.5 mL volume of cell suspension (3 x 10^5 cells) was added to each well. Plates were rocked back and forth gently for 10 s and incubated at 37°C, 5% CO_2/ 95% humidified air for 4 h. After 4 h, media was carefully removed and replaced with 3 mL of fresh RPMI supplemented with 10% FBS. After 24 h incubation, CM was removed and stored at -20°C until required.

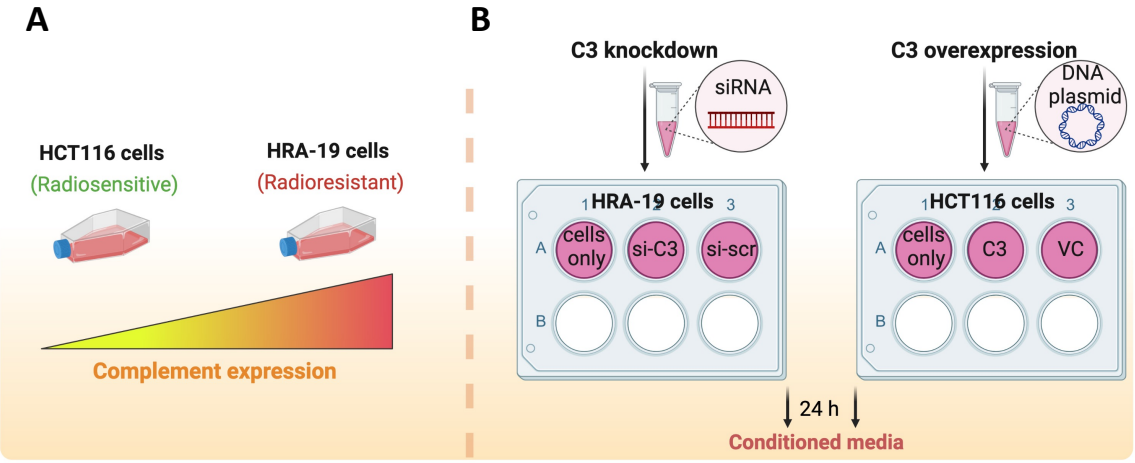

Figure 4-1: CM generation from HCT116 and HRA-19 cell lines. (A) The radiosensitive HCT116 cell line expresses significantly lower levels of complement, when compared to the radioresistant HRA-19 cell line. **(B)** CM was generated from HRA-19 cells lines basally (cells only) or following transient transfection with siRNA for C3 (si-C3) or a scrambled siRNA control (si-scr) and from HCT116 cells lines basally (cells only) or following transient transfection with a cDNA plasmid for C3 (C3) or a vector control (VC) plasmid. At 24 h post transfection, CM was removed and stored at -20°C until required.

4.3.7. Preparation of recombinant C3a

Recombinant human C3a (Bio-Techne, Minnesota, United States) was reconstituted in sterile PBS at a concentration of 250 µg/mL. Serial dilution of recombinant C3a (250 µg/mL) in complete RPMI was performed immediately prior to use as outlined in **Table 4-2**.

Table 4-2: Preparation of C3a working stock.

Volume recombinant C3a	Volume RPMI	Dilution factor	Final Concentration
6 µL of 250 µg/mL stock	744 µL	1:125	2000 ng/mL
300 µL of 2000 ng/mL working stock	300 µL	1:2	1000 ng/mL
250 µL of 1000 ng/mL working stock	250 µL	1:2	500 ng/mL

4.3.8. Co-culture of PBMCs with CM or recombinant C3a

PBMCs were co-cultured with CM or recombinant C3a using two experimental set ups. Experimental set up 1 aimed to recapitulate pre-activated T cells coming in contact with complement after trafficking back to the TME (**Fig. 4-2 A**). PBMCs were resuspended in RPMI at a concentration of 2 x 10^6 cells/mL. A 500 µL volume of cell suspension (1 x 10^6 cells) was added to 12-well plates pre-coated with anti-CD3/CD38 (Section 4.3.4). For CM co-cultures, 500 µL CM from HCT116 or HRA-19 cells (as generated in Section 4.3.6) was added to appropriate wells (1:2 dilution of CM). For recombinant C3a treatments, 100 µL of recombinant C3a working stock (500 ng/mL, 1000 ng/mL or 2000 ng/mL) (**Table 4-2**) was added to appropriate wells, followed by 400 µL RPMI to achieve a final well volume of 1 mL (1:10 dilution of recombinant C3a resulting in final concentrations of 50 ng/mL, 100 ng/mL and 200 ng/mL). PBS (0.8% in RPMI) was used as a vehicle control. PBMCs were incubated at 37°C, 5% CO_2/ 95% humidified air for 48 h (**Fig. 4-2 C**).

Experimental set up 2 aimed to recapitulate T cell activation within the tumour-draining lymph node in the presence of tumour-derived complement (**Fig. 4-2 B**). PBMCs were resuspended in RPMI at a concentration of 1 x 10^6 cells/mL. A 1 mL volume of cell suspension (1 x 10^6 cells) was added to 12-well plates pre-coated with anti-CD3/CD38 (Section 4.3.4), and PBMCs were incubated at 37°C, 5% CO_2/ 95% humidified air for 24 h. After 24 h activation, plates were centrifuged at 1,300 RPM for 3 min at RT° to pellet PBMCs and 500 µL of media was carefully removed. For CM co-cultures, 500 µL CM from HCT116 or HRA-19 cells (as generated in Section 4.3.6) was added to appropriate wells (1:2 dilution of CM). For recombinant C3a treatments, 100 µL recombinant C3a working stock (500 ng/mL, 1000 ng/mL or 2000 ng/mL) (**Table 4-2**) was added to appropriate wells, followed by 400 µL RPMI, to achieve a final well volume of 1 mL (1:10 dilution of recombinant C3a resulting in final concentrations of 50 ng/mL, 100 ng/mL and 200 ng/mL). PBS (0.8% in RPMI) was used as a vehicle control. PBMCs were incubated at 37°C, 5% CO_2/ 95% humidified air for a further 24 h (**Fig. 4-2 D**).

4.3.9. Carboxyfluorescein succinimidyl ester (CFSE) labelling to monitor proliferation

Proliferation of PBMCs was assessed using CFSE, which is a cell permeable dye. Following passive diffusion into cells, intracellular esters cleave CFSE ester groups, converting them into fluorescent esters, which bind intracellular proteins. CFSE is stable,

retained within the cell, and is passed on to daughter cells following divisions. At the time of sample acquisition, CFSE positive populations of varying fluorescence intensity can be identified, each corresponding to cell division.

Lyophilised CFSE was reconstituted to a concentration of 5 mM in DMSO. A 5 µM working solution of CFSE was prepared in sterile PBS. PBMCs were pelleted by centrifugation at 1,300 RPM for 3 min at RT° and resuspended in the 5 µM CFSE working solution at a concentration of 10 x 10^6 cells/mL. PBMCs were incubated in CFSE staining solution for 20 min at 37°C, 5% CO_2/ 95% humidified air in the dark. The stain was quenched by the addition of 5 times the original staining volume of complete medium. CFSE-labelled PBMCs were pelleted by centrifugation as before and resuspended in complete medium at a concentration of 1 x 10^6 cells/mL. CFSE-labelled PBMCs (1 x 10^6 cells) were seeded into 12-well plates pre-coated with anti-CD3/CD28 antibodies in a total volume of 2 mL complete medium. As controls, unstained PBMCs were also stimulated in anti-CD3/CD28 coated plates (unstained, activated), and CFSE-labelled PBMCs were seeded in an uncoated 12-well plate (stained, unactivated). PBMCs were incubated at 37°C, 5% CO_2/ 95% humidified air for 5 d. After 5 d, PBMCs were collected in FACS tubes and pelleted by centrifugation at 1,300 RPM for 3 min at RT°. The supernatants were discarded and PBMCs were washed with 1 mL FACS buffer (PBS with 2% FBS, 0.1% sodium azide). PBMCs were stained using 2 µL CD3-PeCy7 antibody (Biolegend, California, United States) in 98 µL FACS buffer in the dark at RT° for 20 min. PBMCs were washed twice with FACS buffer and resuspended in 250 µL FACS buffer.

4.3.10. AV/PI assay to assess viability

The viability of PBMCs co-cultured with CM or treated with recombinant C3a (Section 4.3.8) was assessed using the AV/PI assay.

Cells were collected in 5 mL round bottom polystyrene falcon tubes (Becton, Dickinson and Company, New Jersey, United States). Cells were pelleted by centrifugation at 1,300 RPM for 3 min at RT° and the supernatants were discarded. Cells were washed with 500 µL 1X AV binding buffer (Diluted 1:10 with PBS from 10X stock, (0.1 M HEPES pH 7.4, 1.4 M NaCl, 25 Mm CaCl2 in dH2O)). Cells were pelleted again by centrifugation at 1,300 RPM for 3 min at RT° and stained with 100 µL AV-FITC antibody staining solution (Biolegend, San Diego, United States) (2 µL AV-FITC antibody in 98 µL 1X AV binding buffer) in the dark at RT° for 20 min. After incubation, cells were washed with 500

µL 1X AV binding buffer and pelleted as before. Cells were resuspended in 250 µL 1X AV binding buffer. PI (Invitrogen, Massachusetts, United States) was diluted 1:4000 using 1X AV binding buffer immediately before sample acquisition and 250 µL diluted PI solution was added to each tube, resulting in a final dilution of 1:8000.

4.3.11. Flow cytometry staining to assess T cell activation

The expression of activation markers on the surface of PBMCs co-cultured with CM or treated with recombinant C3a (Section 4.3.8) was assessed by flow cytometry.

PBMCs were collected in FACS tubes and pelleted by centrifugation at 1,300 RPM for 3 min at RT°. Supernatants were discarded and PBMCs were washed with 1 mL FACS buffer and pelleted as before. Supernatants were discarded and to eliminate dead cells during analysis, cells were stained with Zombie NIR (1:1000 dilution in PBS). Cells were stained in the dark at RT° for 15 min. Without washing off the Zombie NIR, PBMCs were stained for cell surface activation markers using the extracellular antibodies detailed in **Table 4-3** made up to a total volume of 100 µL with FACs buffer. Staining was performed in the dark at RT° for 20 min. PBMCs were washed twice with FACS buffer and resuspended in 250 µL FACS buffer.

Table 4-3: Optimised volumes of extracellular antibodies used to distinguish T cell populations and assess expression of activation markers.

Antibody	Company	Clone	Vol (µL) / tube
CD3-Pe/Cy7	Biolegend	OKT3	1
CD4-APC	Biolegend	OKT4	1
CD8-BV421	Biolegend	SK1	1
CD69-PE	BD Biosciences	FN50	2
CD62L-Pe/Cy5	BD Biosciences	DREG-56	2
CD45RA-V500	BD Biosciences	HI100	1
CD45RO-FITC	Biolegend	UCHL1	1

4.3.12. Intracellular flow cytometry staining to assess cytokine production

Cytokine production by PBMCs co-cultured with CM or treated with recombinant C3a (Section 4.3.8) was assessed by flow cytometry.

Prior to staining, PBMCs were treated with PMA (10 ng/mL) and Ionomycin (1 μg/mL) (both Sigma Aldrich, Missouri, United States) during the last 4 h of incubation. For the final 3 h of incubation, PBMCs were additionally treated with Brefeldin A (10 μg/mL) (eBiosciences, Thermofisher Scientific, Massachusetts, United States).

PBMCs were collected in FACS tubes, washed and stained with Zombie NIR as previously described (Section 4.3.11). Without washing off the Zombie NIR, PBMCs were stained using extracellular antibodies for CD3, CD4 and CD8 using the optimised volumes outlined in **Table 4-4** made up to a total volume of 100 μL with FACS buffer. Staining was performed in the dark at RT° for 20 min. PBMCs were washed using 1mL FACS buffer, pelleted by centrifugation as before and supernatants were discarded.

To assess intracellular cytokine expression the eBioscience Intracellular Fixation and Permeabilization Buffer Set (Thermofisher Scientific, Massachusetts, United States) was used. PBMCs were fixed using 100 μL intracellular fixation buffer. FACS tubes were vortexed well and incubated in the dark at RT° for 20 min. PBMCs were washed with 1 mL 1X permeabilization buffer (10X permeabilization buffer diluted 1:10 with distilled water) and centrifuged at 1300 RPMI for 3 min. PBMCs were stained for intracellular cytokines using the optimised volumes of intracellular antibodies presented in **Table 4-5**, in a final volume of 100 μL 1X permeabilization buffer per sample. Samples were incubated in the dark at RT° for 20 min before being washed twice with 1mL of 1X permeabilization buffer and resuspended in 250 μl FACS buffer.

Table 4-4: Optimised volumes of extracellular antibodies used to distinguish T cell populations.

Antibody	Company	Clone	Vol / tube
CD3-PerCP	Biolegend	HIT3a	1 μL
CD4-FITC	Biolegend	OKT4	1 μL
CD8-BV421	Biolegend	SK1	1 μL

Table 4-5: Optimised volumes of intracellular antibodies used to assess cytokine expression.

Antibody	Company	Clone	Vol / tube
IL-10-PE	Biolegend	JESS-19F1	1 µL
IL-4-Pe/Cy7	Biolegend	MP4-25D2	1 µL
IL-17A-APC	Biolegend	BL168	1 µL
IFN- γ-BV510	Biolegend	4S.B3	1 µL

4.3.13. Flow cytometry acquisition and analysis

All samples were acquired using a BD FACSCanto II (Becton, Dickinson and Company, New Jersey, United States) and FACSDiva Software (Becton, Dickinson and Company, New Jersey, United States). Analysis was performed using FlowJo v10 Software (Becton, Dickinson and Company, New Jersey, United States). Gating strategies to assess expression of the C3aR, surface activation markers and intracellular cytokines are presented in **Appendices 6**,**7**, and **8** respectively.

4.3.14. Statistical analysis

Graphing of results and statistical analysis was performed using Prism 9 Software (GraphPad, California, United States). All data are presented as mean ± SEM, unless otherwise indicated. Significance was determined by ANOVA with post-hoc Tukey's multiple comparisons testing or Student's *t*-test, as detailed in figure legends. Where comparison groups were paired (i.e. untreated vs. treated), a paired *t*-test was performed, otherwise unpaired *t*-tests were used. Results were considered significant where $p \leq 0.05$.

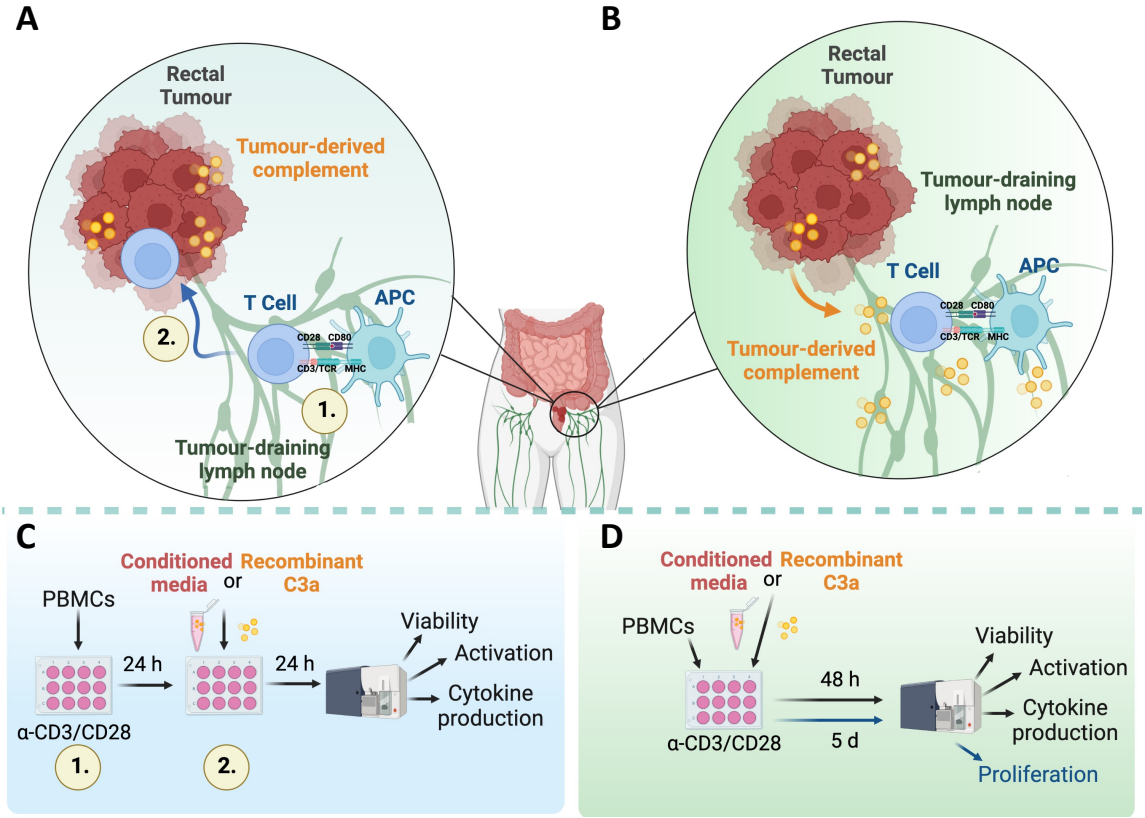

Figure 4-2: Experimental set ups for PBMC co-cultures with CM or recombinant C3a. Experiments were performed using two experimental set ups. **(A)** Experimental set up 1 aimed to recapitulate T cell activation followed by movement to a complement-rich TME. To assess the effect of this on T cell phenotype *in vitro* **(C)** PBMCs were pre-stimulated using plate-bound anti-CD3/CD28 for 24 h (1), before being co-cultured with CM from HCT116 or HRA-19 cells or treated with recombinant C3a (2). **(B)** Experimental set up 2 aimed to recapitulate T cell activation within the tumour-draining lymph node in the presence of tumoural complement. To assess the effects of this on T cell phenotype *in vitro*, **(D)** PBMCs were activated using plate-bound anti-CD3/CD28 while being co-cultured with CM from HCT116 or HRA-19 cells or treated with recombinant C3a.

4.4. Results

4.4.1. T cell expression of the C3aR increases following activation

C3a signals through the C3aR expressed on the surface of tumour cells and immune cells. Extracellular expression of the C3aR on T cells was assessed by flow cytometry using both unactivated T cells and T cells stimulated using anti-CD3/CD28 for 3 d.

The C3aR was expressed by both activated and unactivated T cells (**Fig. 4-3**). Expression of the C3aR was significantly elevated ($p = 0.0032$) on the surface of activated $CD3^+$ T cells, when compared to unactivated $CD3^+$ T cells (Mean % of $CD3^+$ cells expressing C3aR ± SEM; activated 53.6 ± 3.089, unactivated 11.06 ± 1.323). C3aR expression was also significantly increased ($p = 0.0017$) on activated, when compared to unactivated $CD3^+CD4^+$ T cells (Mean % of $CD3^+CD4^+$ cells expressing C3aR ± SEM; activated 53.90 ± 2.307, unactivated 13.83 ± 2.398). Similarly, $CD3^+CD8^+$ T cells demonstrated significantly increased expression of C3aR following activation ($p = 0.0283$) (Mean % of $CD3^+CD8^+$ cells expressing C3aR ± SEM; activated 55 ± 6.710, unactivated 11.15 ± 1.651). This demonstrates low basal expression of C3aR on T cells which increases following activation.

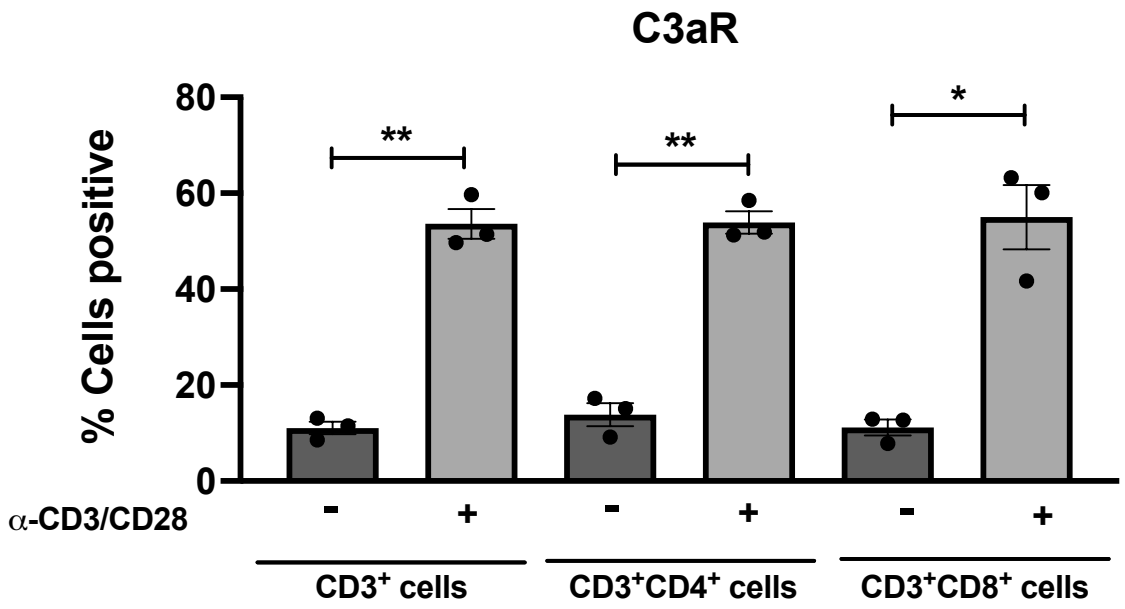

Figure 4-3: T cell expression of C3aR significantly increases following activation. Expression of C3aR was assessed on $CD3^+$, $CD3^+$ $CD4^+$ and $CD3^+$ $CD8^+$ T cells by flow cytometry. Data are presented as mean ± SEM for 3 biological replicates. Statistical analysis was performed by paired two-tailed Student's *t*-test. *$p < 0.05$, **$p < 0.01$.

4.4.2. CM from si-C3 transfected HRA-19 cells induces elevated early-stage apoptosis in PBMCs

HRA-19 cells express C3 protein that can be detected in CM generated from these cells. To investigate potential effects of HRA-19-derived complement on PBMCs, CM was generated basally and following transient C3 silencing using siRNA (As illustrated in **Fig. 4-1**). Transient C3 silencing was demonstrated to reduce the concentration of C3 protein in CM from HRA-19 cells by approximately 50% (**Fig. 4-4 A**).

PBMCs were pre-activated using plate-bound anti-CD3/CD28 and then cultured for a further 24 h in the presence of HRA-19 CM (as illustrated in **Fig. 4-5 A)**, with the aim of recapitulating uninterrupted T cell activation followed by movement to a complement-rich TME (**Fig. 4-2 A**). Viability was assessed using the AV/PI assay and flow cytometry. The percentage of viable (AV^-PI^-) cells was similar when PBMCs were cultured in RPMI or with CM from HRA-19 cells, si-C3 transfected HRA-19 cells or si-scr transfected HRA-19 cells (**Fig. 4-5 C**). PBMCs co-cultured with CM from si-C3 HRA-19 cells demonstrated significantly elevated levels of early-stage apoptosis (AV^+PI), when compared to those co-cultured with si-scr CM (**Fig. 4-5 D)**. There were no alterations in the percentage of PBMCs undergoing late stage apoptosis/death (AV^+PI^+) (**Fig. 4-5 E**) or necrosis (AV^-PI^+) when co-cultured with CM from si-C3 HRA-19 cells, when compared to controls (**Fig. 4-5 F**).

These data demonstrate that in the absence of C3-derived from HRA-19 cells, early-stage apoptosis of PBMCs is elevated, suggesting that tumour cell-derived C3 may promote PBMC viability in CRC.

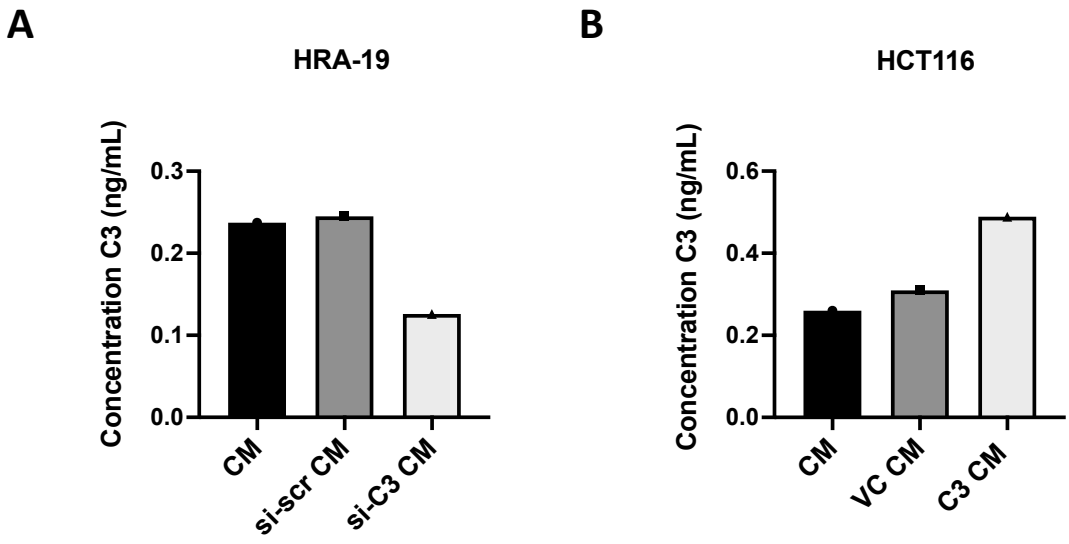

Figure 4-4: Concentration of C3 in CM generated from HCT116 and HRA-19 cells. C3 expression was transiently silenced in HRA-19 cells using siRNA (si-C3), or transiently overexpressed in HCT116 cells using a C3 DNA plasmid (C3). Controls were transfected with scrambled siRNA (si-scr), or vector control (VC) DNA plasmids, respectively. Cells were cultured for 24 h before CM was removed. Concentration of C3 in CM generated from **(A)** HRA-19 cells and **(B)** HCT116 cells was assessed by ELISA. Data are representative of results from a single experiment.

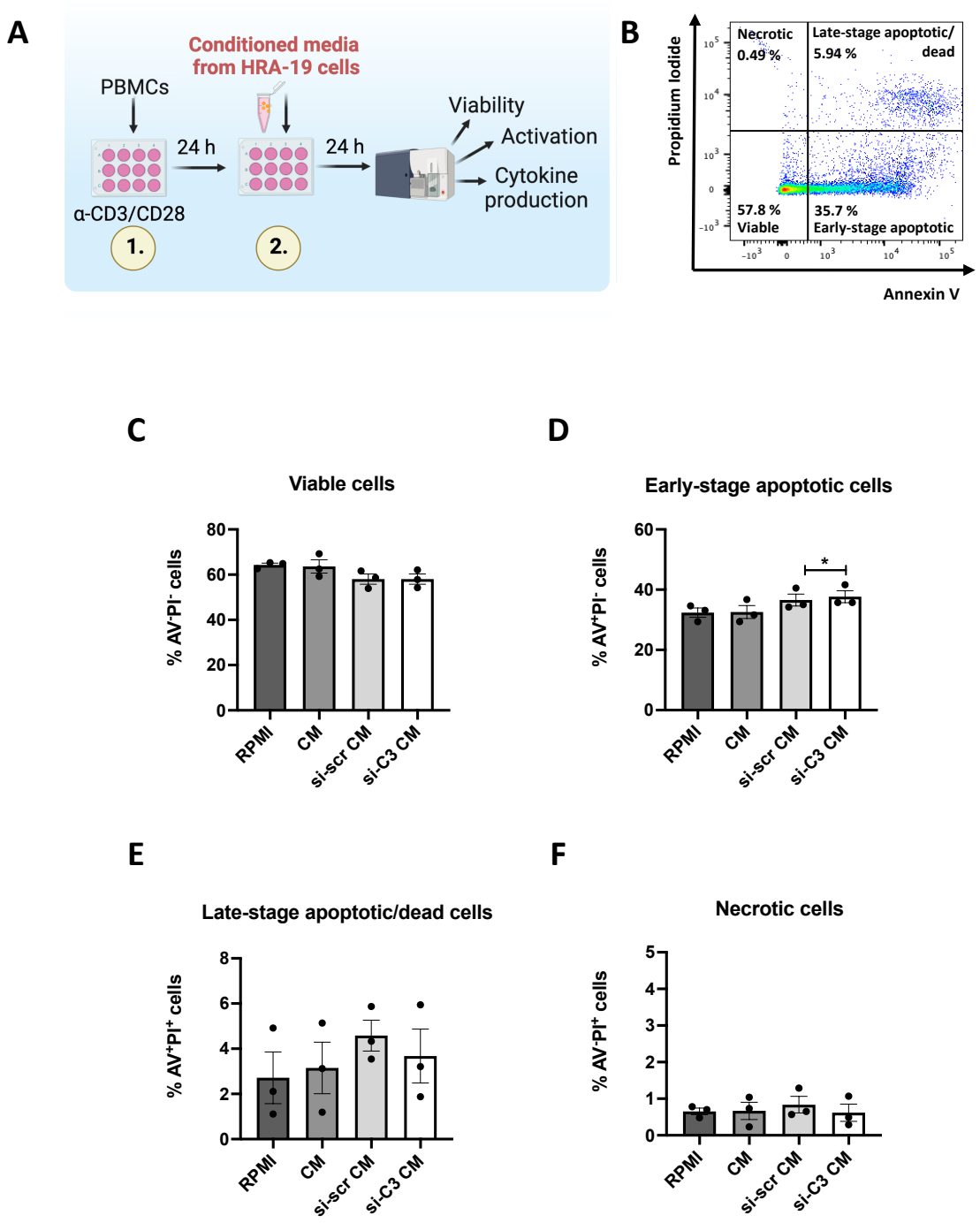

Figure 4-5: CM from si-C3 transfected HRA-19 cells induces significant early apoptosis in pre-activated PBMCs. (A) PBMCs were pre-activated for 24 h with plate-bound anti-CD3/CD28 and then co-cultured for a further 24 h with CM from HRA-19 cells basally or following transient transfection with C3 siRNA (si-C3), or a scrambled control siRNA (si-scr). Viability was assessed by flow cytometry using the AV/PI assay. **(B)** Representative dot plot. The percentage of **(C)** live (AV^-PI^-), **(D)** early apoptotic (AV^+PI^-), **(E)** late apoptotic/dead (AV^+PI^+) and **(F)** necrotic (AV^-PI^+) PBMCs was analysed. Data are presented as mean ± SEM for 3 biological replicates. Statistical analysis was performed by paired two-tailed Student's *t*-test. *$p < 0.05$.

4.4.3. CM from si-C3 transfected HRA-19 cells increases CD4RO expression in pre-activated $CD8^+$ T cells

The effect of CM from HRA-19 cells on T cell activation was assessed. Using the same experimental set up (as illustrated in **Fig. 4-5 A**), PBMCs activated for 24 h and co-cultured with CM from HRA-19 cells were assessed for surface activation marker expression by flow cytometry (**Fig. 4-6)**.

There were no differences in the percentages of $CD3^+$, $CD3^+CD4^+$ or $CD3^+CD8^+$ T cells expressing CD69, CD62L and CD45RA following co-culture with CM from si-C3 HRA-19 cells, when compared to CM from si-scr cells (**Fig. 4-6 A-C)**. There was a significant increase in the percentage of $CD3^+CD8^+$ T cells expressing CD45RO following co-culture with CM from si-C3 cells, when compared to CM from si-scr cells ($p = 0.0132$) (Mean % of $CD3^+CD8^+$ cells expressing CD45RO ± SEM; si-C3 co-cultured 13.113 ± 2.547, si-scr co-cultured 12.27 ± 2.606) (**Fig. 4-6 D)**. This demonstrates that $CD8^+$ T cells are significantly more activated when exposed to lower concentrations of C3 derived from HRA-19 cells, suggesting that HRA-19 cell-derived C3 may contribute to the maintenance of a naïve state.

MFI of activation markers expressed by $CD3^+$, $CD3^+$ $CD4^+$ or $CD3^+$ $CD8^+$ T cells co-cultured with CM from HRA-19 cells was also assessed. No alterations in the MFI of CD69, CD62L, CD45RA or CD45RO were demonstrated when the concentration of HRA-19 cell-derived C3 was reduced (**Fig. 4-6 E-H)**, suggesting that in this setting, C3 derived from HRA-19 cells does not alter the degree of activation markers expressed by T cells.

4.4.4. CM from si-C3 transfected HRA-19 cells does not alter cytokine expression in pre-activated T cells

Having demonstrated that HRA-19 CM induces alterations in surface expression of activation markers by pre-activated T cells, the effects of HRA-19 CM on T cell cytokine expression was assessed. Similarly, PBMCs activated for 24 h were co-cultured with CM from HRA-19 cells (as illustrated in **Fig. 4-5 A**), and intracellular cytokine expression was assessed by flow cytometry (**Fig. 4-7)**. As PMA downregulates human CD4, for this experiment $CD4^+$ T cells were classified as $CD3^+CD8^-$.

The percentage of $CD3^+$, $CD3^+CD8^+$ or $CD3^+CD8^-$ T cells expressing IFN-γ, IL-10, IL-4 or IL-17A was unchanged following co-culture with CM from si-C3 HRA-19 cells, when compared to CM from si-scr controls (**Fig. 4-7 A-D)**. Additionally, the MFI of

cytokines expressed by $CD3^+$, $CD3^+CD8^+$ or $CD3^+CD8^-$ T cells was unchanged following co-culture with CM from si-C3 HRA-19 cells, when compared to CM from si-scr controls (**Fig. 4-7 E-H)**. These data demonstrate that cytokine expression is similar in pre-activated T cells co-cultured with CM from si-C3 and si-scr HRA-19 cells. This suggests that C3 derived from HRA-19 cells does not alter cytokine production in pre-activated T cells.

4.4.5. CM from HCT116 cells overexpressing C3 does not alter the viability of pre-activated PBMCs

Having investigated the effect of HRA-19 cell-derived C3 on T cell phenotype in the context of pre-activated T cell movement to a complement-rich TME (**Fig. 4-2 A)**, the effect of C3 derived from another CRC cell line, HCT116 cells, was investigated.

HCT116 cells produce C3 protein at low levels that is present at low levels (<1 ng/mL) in CM generated from these cells. To investigate the effect of HCT116-derived complement on PBMCs, CM was generated from HCT116 cells basally and following transfection with a C3 overexpression vector or VC (As illustrated in **Fig. 4-1**). PBMCs were pre-activated using plate-bound anti-CD3/CD28 and then cultured for a further 24 h in the presence of HCT116 CM (as illustrated in **Fig. 4-8 A**).

The percentage of viable (AV^-PI^-) PBMCs was unchanged following co-culture with CM from HCT116 cells overexpressing C3 (**Fig. 4-8 C**). Similarly, CM from HCT116 cells overexpressing C3 did not alter the percentage of PBMCs that were undergoing early stage apoptosis (AV^+PI^-) (**Fig. 4-8 D**), late stage apoptosis/death (AV^+PI^+) (**Fig. 4-8 E**) or necrosis (AV^-PI^+) (**Fig. 4-8 F**), when compared to CM from HCT116 cells transfected with a VC or RPMI controls. Overall these data demonstrate that viability is similar in pre-activated T cells co-cultured with CM from HCT116 cells overexpressing C3, suggesting that C3 derived from HCT116 cells does not alter the viability of PBMCs.

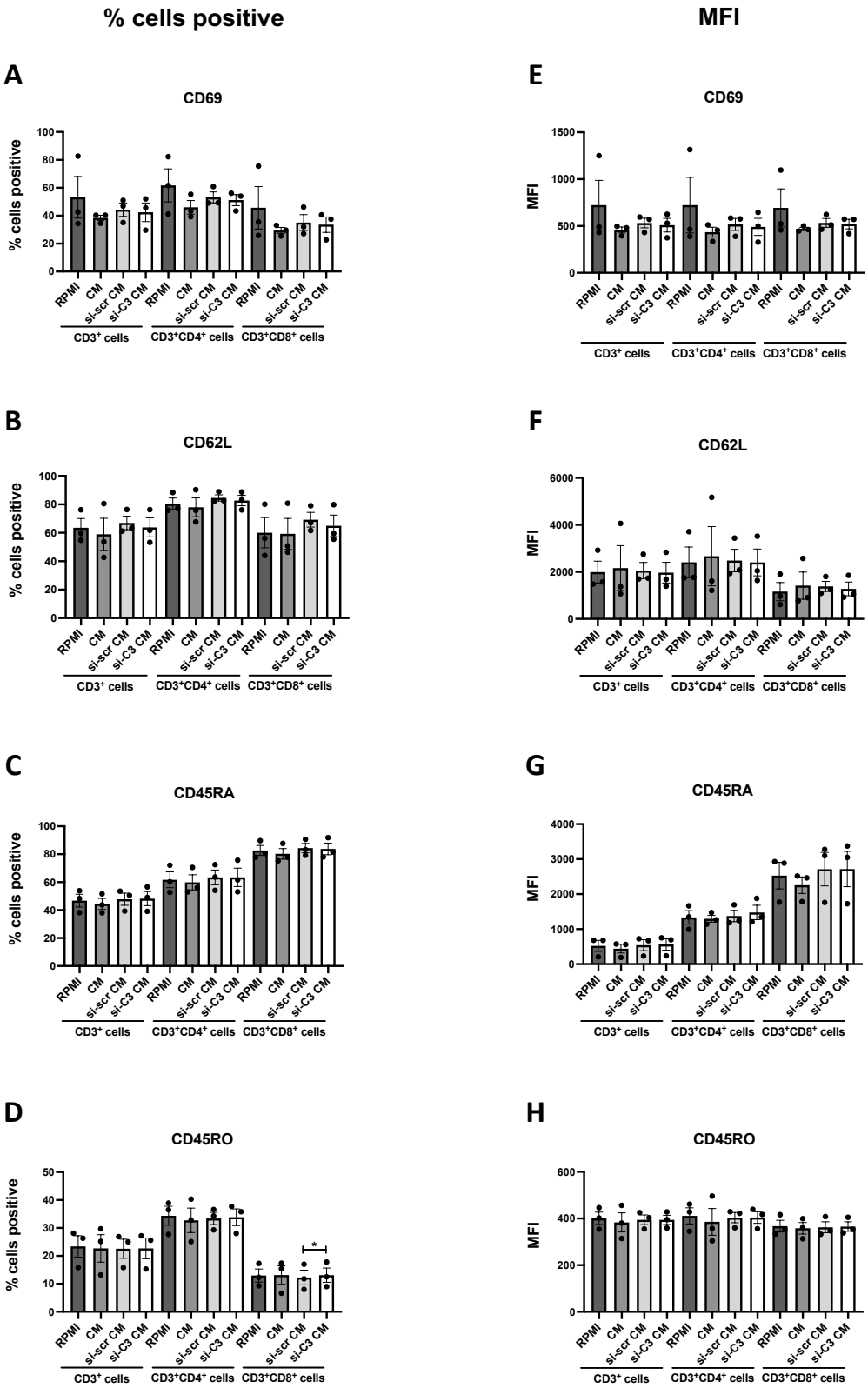

Figure 4-6: CM from si-C3 transfected HRA-19 cells increases CD45RO expression in pre-activated CD8$^+$ T cells. PBMCs were pre-activated for 24 h with plate-bound anti-CD3/CD28 and then co-cultured for a further 24 h with CM from HRA-19 cells basally or following transient transfection with C3 siRNA (si-C3), or a scrambled control siRNA (si-scr). The percentage of CD3$^+$, CD3$^+$CD4$^+$ and CD3$^+$CD8$^+$ T cells expressing **(A)** CD69, **(B)** CD62L, **(C)** CD45RA and **(D)** CD45RO was assessed by flow cytometry. **(E-H)** MFI of markers expressed. Data are presented as mean ± SEM for 3 biological replicates. Statistical analysis was performed by paired two-tailed Student's *t*-test. *$p < 0.05$.

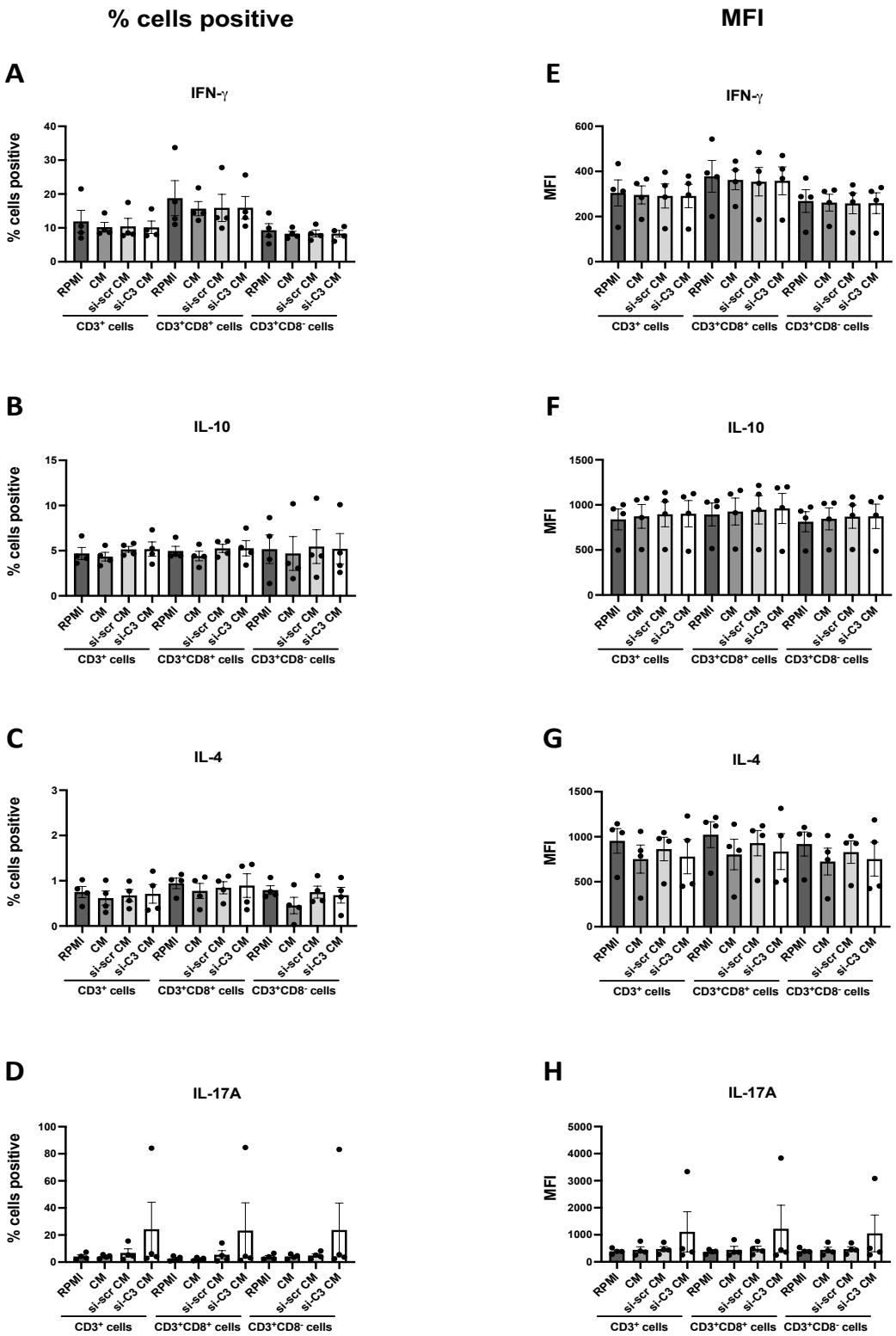

Figure 4-7: **CM from si-C3 transfected HRA-19 cells does not alter cytokine expression in pre-activated T cells.** PBMCs were pre-activated for 24 h with plate-bound anti-CD3/CD28 and then co-cultured for a further 24 h with CM from HRA-19 cells basally or following transient transfection with C3 siRNA (si-C3), or a scrambled control siRNA (si-scr). The percentage of $CD3^+$, $CD3^+CD8^+$ and $CD3^+CD8^-$ T cells expressing **(A)** IFN-γ, **(B)** IL-10, **(C)** IL-4 and **(D)** IL-17A was assessed by flow cytometry. **(E-H)** MFI of cytokines expressed. Data are presented as mean ± SEM for 4 biological replicates. Statistical analysis was performed by paired two-tailed Student's *t*-test.

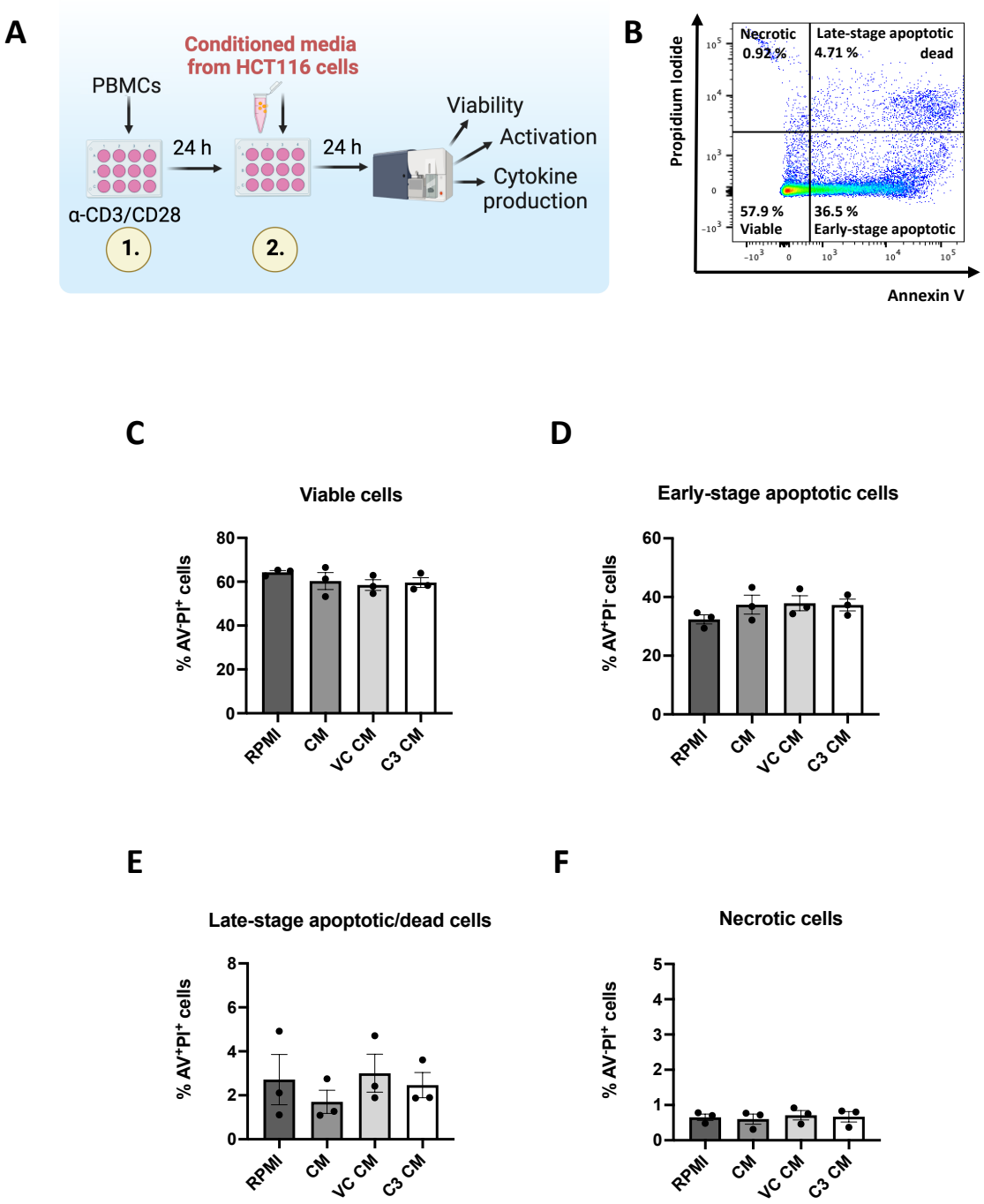

Figure 4-8: CM media from HCT116 cells overexpressing C3 does not alter the viability of PBMCs. (A) PBMCs were pre-activated for 24 h with plate-bound anti-CD3/CD28 and then co-cultured for a further 24 h with CM from HCT116 cells basally or following transient transfection with a C3 DNA plasmid or a VC plasmid. Viability was assessed by flow cytometry using the AV/PI assay. **(B)** Representative dot plot. The percentage of **(C)** live (AV^-PI^-), **(D)** early apoptotic (AV^+PI^-), **(E)** late apoptotic/dead (AV^+PI^+) and **(F)** necrotic (AV^-PI^+) PBMCs were analysed. Data are presented as mean ± SEM for 3 biological replicates. Statistical analysis was performed by paired two-tailed Student's *t*-test.

4.4.6. CM from HCT116 cells overexpressing C3 does not alter activation marker expression in pre-activated T cells

The effect of CM from HCT116 cells on T cell activation was assessed. PBMCs pre-activated for 24 h and co-cultured with CM from HCT116 cells (as illustrated in **Fig. 4-8 A**) were assessed for activation marker expression by flow cytometry (**Fig. 4-9)**.

There were no differences in the percentage of $CD3^+$, $CD3^+CD4^+$ or $CD3^+CD8^+$ T cells expressing CD69, CD62L, CD45RA or CD45RO following co-culture with CM from HCT116 cells overexpressing C3, when compared to CM from HCT116 cells transfected with a VC (**Fig. 4-9 A-D)**. MFI of activation markers expressed by $CD3^+$, $CD3^+CD4^+$ or $CD3^+CD8^+$ T cells co-cultured with C3 CM, when compared to those co-cultured with VC CM was also assessed. No alterations in the MFI of CD69, CD62L, CD45RA or CD45RO expression were demonstrated (**Fig. 4-9 E-H)**. These data demonstrate that activation marker expression in pre-activated T cells is unchanged following co-culture with CM from HCT116 cells overexpressing C3, suggesting that HCT116 cell-derived C3 does not alter T cell activation.

4.4.7. CM from HCT116 cells overexpressing C3 does not alter cytokine expression in pre-activated T cells

Having demonstrated that HCT116 CM does not induce alterations in surface expression of activation markers by pre-activated T cells, the effects of HCT116 CM on T cell cytokine expression was assessed. PBMCs activated for 24 h were co-cultured with CM from HCT116 cells (as illustrated in **Fig. 4-8 A**), and intracellular cytokine expression was assessed by flow cytometry (**Fig. 4-10)**. As PMA downregulates human CD4, for this experiment $CD4^+$ T cells were classified as $CD3^+CD8^-$.

The percentage of $CD3^+$, $CD3^+CD8^+$ or $CD3^+CD8^-$ T cells expressing IFN-γ, IL-10, IL-4 or IL-17A was unchanged following co-culture with CM from HCT116 cells overexpressing C3, when compared to CM from HCT116 cells transfected with a VC (**Fig. 4-10 A-D)**. Additionally, the MFI of cytokines expressed by $CD3^+$, $CD3^+CD8^+$ or $CD3^+CD8^-$ T cells was unchanged (**Fig. 4-10 E-H)**. These data demonstrate that cytokine expression in pre-activated T cells is unchanged following co-culture with CM from HCT116 cells overexpressing C3, suggesting that HCT116 cell-derived C3 does not alter cytokine expression.

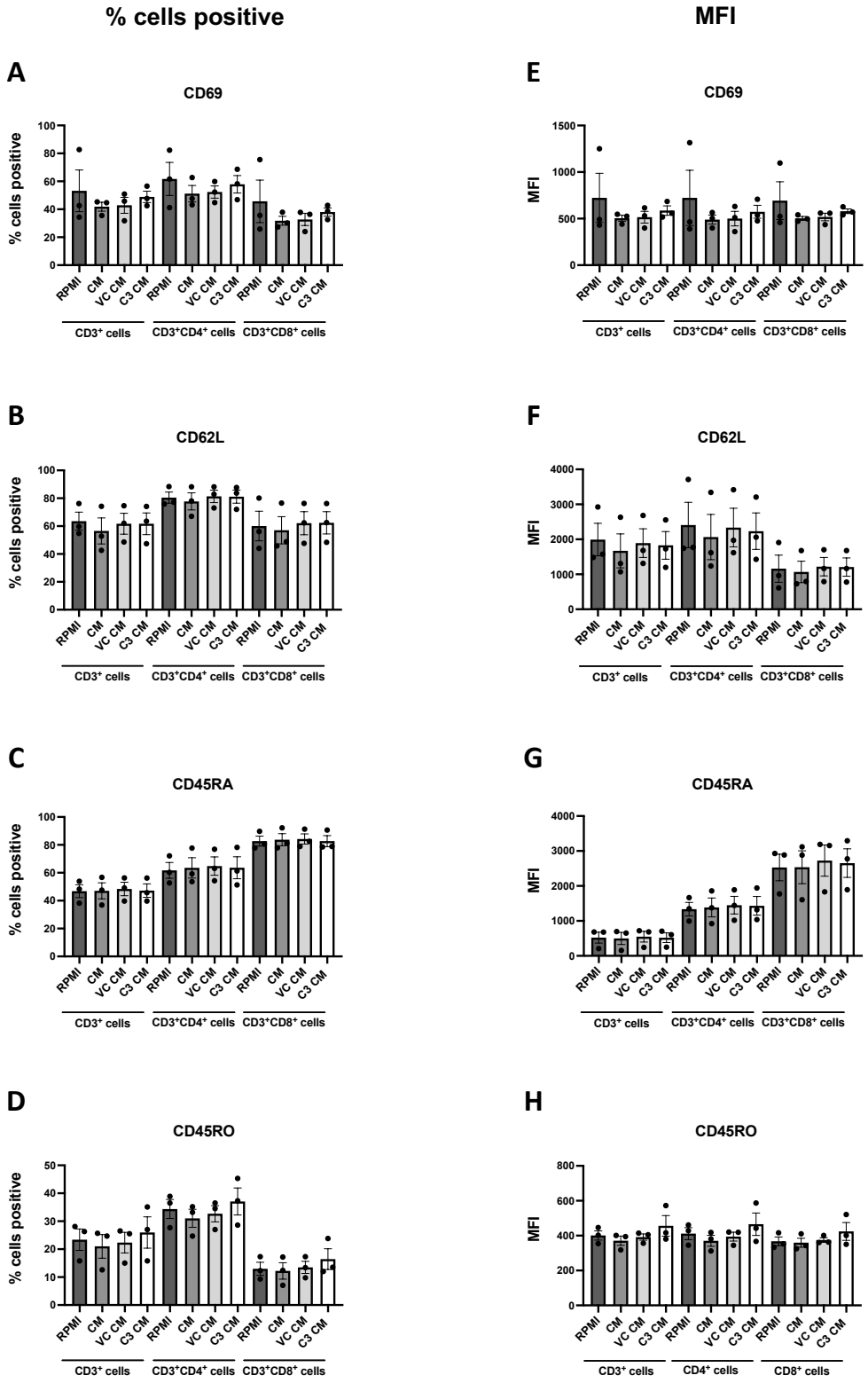

Figure 4-9: CM from HCT116 cells overexpressing C3 does not alter activation marker expression in pre-activated T cells. PBMCs were pre-activated for 24 h with plate-bound anti-CD3/CD28 and then co-cultured for a further 24 h with CM from HCT116 cells basally or following transient transfection with a C3 DNA plasmid, or a VC DNA plasmid. The percentage of $CD3^+$, $CD3^+CD4^+$ and $CD3^+CD8^+$ T cells expressing **(A)** CD69, **(B)** CD62L, **(C)** CD45RA and **(D)** CD45RO was assessed by flow cytometry. **(E-H)** MFI of markers expressed. Data are presented as mean ± SEM for 3 biological replicates. Statistical analysis was performed by paired two-tailed Student's *t*-test.

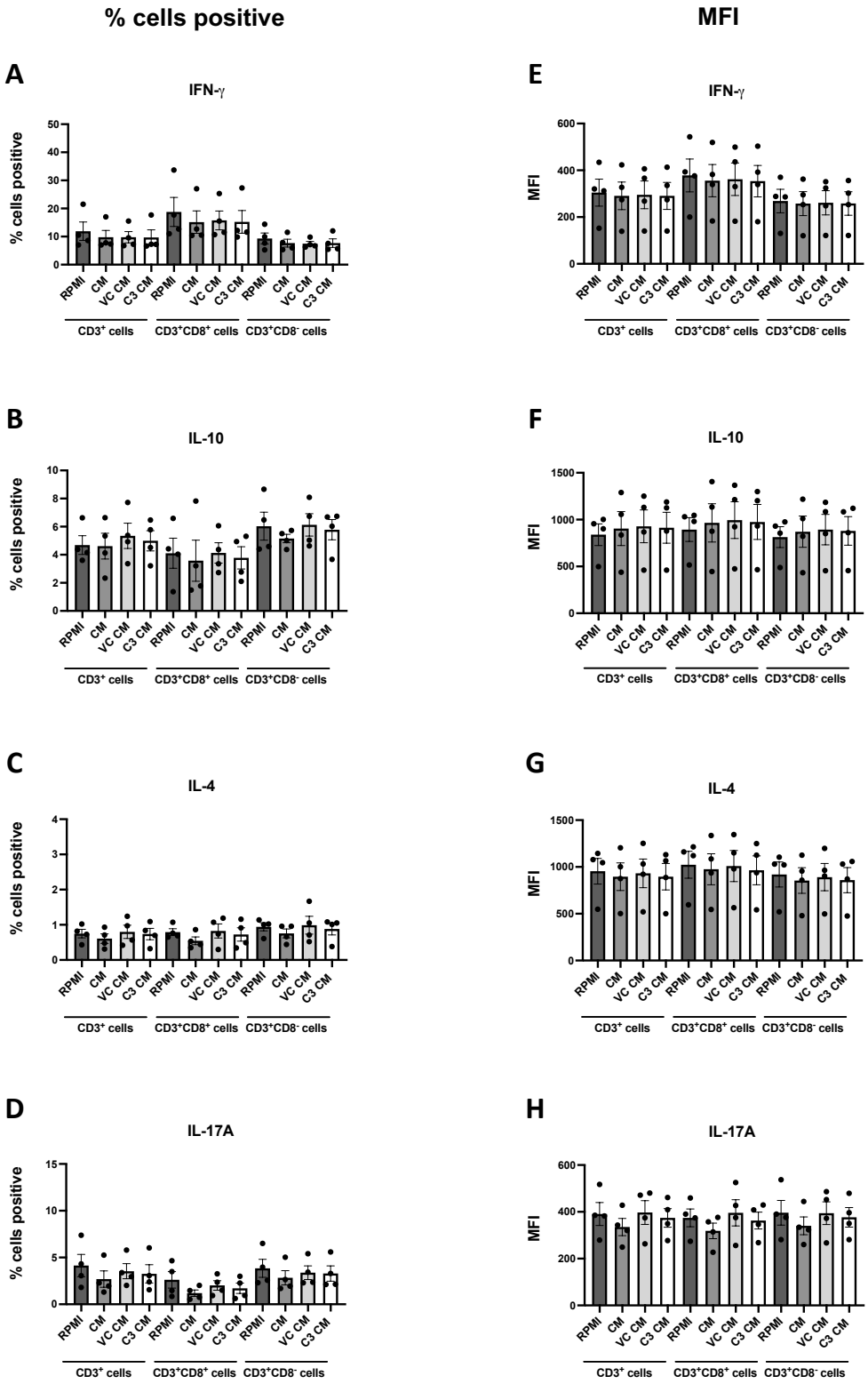

Figure 4-10: CM from HCT116 cells overexpressing C3 does not alter cytokine expression in pre-activated T cells. PBMCs were pre-activated for 24 h with plate-bound anti-CD3/CD28 and then co-cultured for a further 24 h with CM from HCT116 cells basally or following transient transfection with a C3 DNA plasmid or a VC plasmid. The percentage of $CD3^+$, $CD3^+CD8^+$ and $CD3^+CD8^-$ T cells expressing **(A)** IFN-γ, **(B)** IL-10, **(C)** IL-4 and **(D)** IL-17A was assessed by flow cytometry. **(E-H)** MFI of cytokines expressed. Data are presented as mean ± SEM for 4 biological replicates. Statistical analysis was performed by paired two-tailed Student's *t*-test.

4.4.8. Recombinant C3a does not alter the viability of pre-activated PBMCs

Having investigated the effects of CRC cell-derived complement on pre-activated PBMCs, the effect of recombinant C3a on T cell phenotype was assessed. In a similar manner to HRA-19 or HCT116 CM experiments, PBMCs were pre-activated using plate-bound anti-CD3/CD28 and then cultured for a further 24 h with recombinant C3a (**Fig. 4-11 A)**.

At all concentrations used, recombinant C3a did not alter the percentage of viable PBMCs when compared to vehicle or RPMI controls (**Fig. 4-11 C)**. Recombinant C3a at a concentration of 50 ng /mL resulted in a significant increase in the percentage of PBMCs undergoing early-stage apoptosis, when compared to vehicle controls ($p = 0.0238$) (Mean % of AV^+PI^- PBMCs ± SEM; 50 ng/mL C3a 38.9 ± 1.609, Veh 33.733 ± 1.257) (**Fig. 4-11 D)**. This was accompanied by a corresponding decrease in the percentage of cells undergoing late-stage apoptosis/death ($p = 0.0126$) (Mean % of AV^+PI^+ PBMCs ± SEM; 50 ng/mL C3a 1.527 ± 0.252, Veh 3.057 ± 0.386) (**Fig. 4-11 E)**. There were no alterations in the percentage of necrotic PBMCs after treatment with recombinant C3a (**Fig. 4-11 F)**.

4.4.9. Recombinant C3a increases expression of CD62L by pre-activated $CD4^+$ T cells

PBMCs activated for 24 h and then treated with recombinant C3a (**Fig. 4-11 A)** were assessed for activation marker expression by flow cytometry to further investigate the effects of recombinant C3a on T cell activation (**Fig. 4-12)**.

There were no differences in the percentage of $CD3^+$, $CD3^+CD4^+$ or $CD3^+CD8^+$ T cells expressing CD69, CD45RA or CD45RO following treatment with recombinant C3a, when compared to RPMI or vehicle controls (**Fig. 4-12 A, C-D)**. The percentage of $CD3^+CD4^+$ T cells expressing CD62L was significantly elevated following treatment with recombinant C3a (100 ng/mL), when compared to vehicle control ($p = 0.0094$) (Mean % of $CD3^+CD4^+$ cells expressing CD62L ± SEM; C3a 100 ng/mL 83.167 ± 5.357, Vehicle 80.933 ± 5.407) (**Fig. 4-12 B**). CD62L is a lymph node homing and naïve T cell marker[431]. These data suggest that C3a may promote retention of $CD4^+$ T cells in the lymph nodes. MFI of activation markers expressed by $CD3^+$, $CD3^+CD4^+$ or $CD3^+CD8^+$ T cells was also assessed. No alterations in the MFI of CD69, CD62L, CD45RA or CD45RO expressed by T cells following treatment with recombinant C3a were demonstrated (**Fig. 4-12 E-H)**.

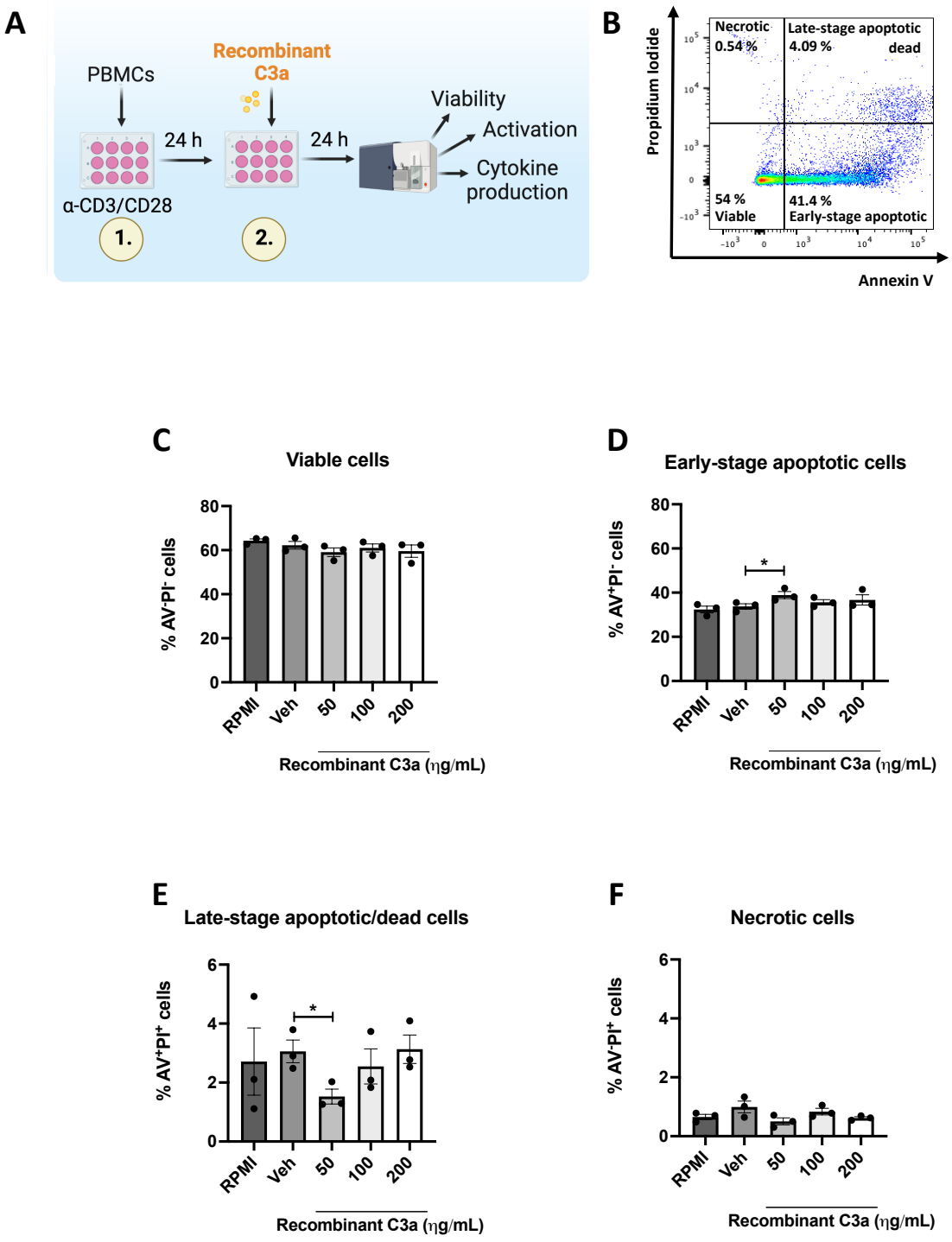

Figure 4-11: Recombinant C3a alters the viability of pre-activated PBMCs. (A) PBMCs were pre-activated for 24 h with plate-bound anti-CD3/CD28 and then treated for a further 24 h with recombinant C3a or the vehicle control (PBS). Viability was assessed by flow cytometry using the AV/PI assay. Percentage of **(C)** live (AV^-PI^-), **(D)** early apoptotic (AV^+PI^-), **(E)** late apoptotic/dead (AV^+PI^+) and **(F)** necrotic (AV^-PI^+) PBMCs analysed. **(B)** Representative dot plot. Data are presented as mean ± SEM for 3 biological replicates. Statistical analysis was performed by paired two-tailed Student's *t*-test.

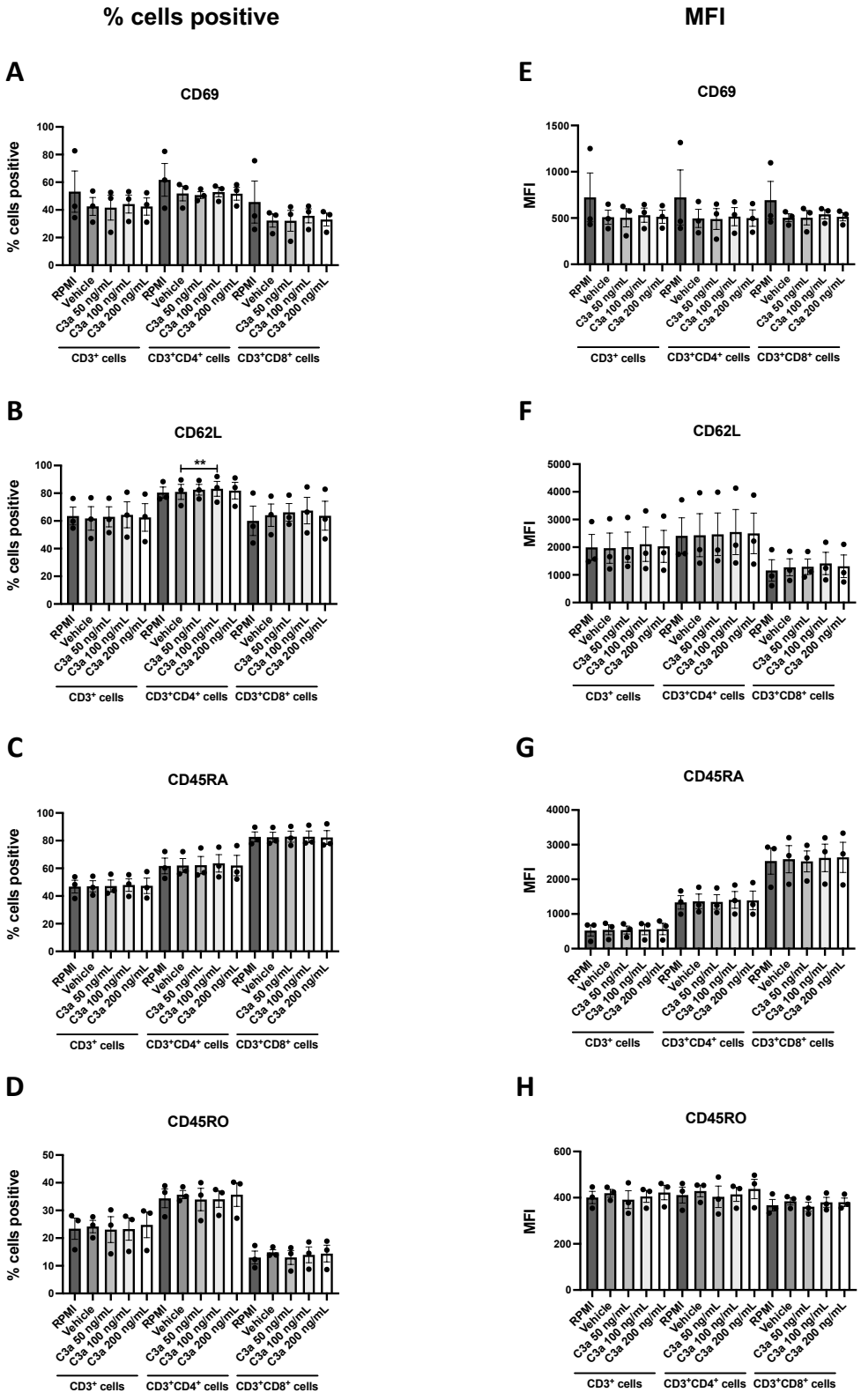

Figure 4-12: CD62L expression is elevated in pre-activated CD4$^+$ T cells following treatment with recombinant C3a. PBMCs were pre-activated for 24 h with plate-bound anti-CD3/CD28 and then treated for a further 24 h with recombinant C3a or vehicle control (PBS). The percentage of CD3$^+$, CD3$^+$CD4$^+$ and CD3$^+$CD8$^+$ T cells expressing **(A)** CD69, **(B)** CD62L, **(C)** CD45RA and **(D)** CD45RO was assessed by flow cytometry. **(E-H)** MFI of markers expressed. Data are presented as mean ± SEM for 3 biological replicates. Statistical analysis was performed by paired two-tailed Student's *t*-test.

4.4.10. Recombinant C3a reduces IL-4 expression in pre-activated T cells

The effects of recombinant C3a on cytokine expression were also assessed using PBMCs activated for 24 h (**Fig. 4-11 A**). T cell expression of IFN-γ, IL-10 and IL-17A was unchanged following treatment with recombinant C3a (**Fig. 4-13 A-B, D**). The percentage of IL-4 producing $CD3^+$ cells was significantly reduced following treatment with recombinant C3a (50 ng/mL), when compared to vehicle controls (**Fig. 4-13 C**) ($p = 0.01$) (Mean % of $CD3^+$ cells expressing IL-4 ± SEM; C3a 50 ng/mL 0.53 ± 0.13, Vehicle 0.693 ± 0.121). Similar was demonstrated in $CD3^+CD8^-$ cells (**Fig. 4-13 C**) ($p = 0.0393$) (Mean % of $CD3^+$ $CD8^-$ cells expressing IL-4 ± SEM; C3a 50 ng/mL 0.468 ± 0.103, Vehicle 0.64 ± 0.089). No alterations in the MFI of IFN-γ, IL-10, IL-4 and IL-17A expressed by T cells following treatment with recombinant C3a were demonstrated (**Fig. 4-13 E-H)**. These data demonstrate that recombinant C3a reduces T cell expression of IL-4.

4.4.11. CM from si-C3 transfected HRA-19 cells reduces late-stage apoptosis in PBMCs during activation

Having investigated the effects of complement in the context of the TME, these experiments aimed to recapitulate T cell activation within the tumour-draining lymph node, in the presence of tumour-derived complement (**Fig. 4-2 B**). Local lymph nodes play a central role in the anti-tumour immune response, and drainage of soluble mediators produced by tumour cells to this region via the lymphatic system can influence B and T cell activation[432,433].

PBMCs were activated using plate-bound anti-CD3/CD28 while being co-cultured with CM from HRA-19 cells (as illustrated in **Fig. 4-14 A**).The percentages of viable and early-stage apoptotic PBMCs was unchanged when co-cultured with CM from si-C3 transfected HRA-19 cells, when compared to si-scr CM (**Fig. 4-14 C-D**). Co-culture with CM from HRA-19 cells transfected with si-C3 significantly reduced the percentage of PBMCs undergoing late apoptosis/death (AV^+PI^+), when compared to CM from HRA-19 cells transfected with si-scr (**Fig. 4-14 E**) ($p = 0.0354$) (Mean % of AV^+PI^+ PBMCs ± SEM; si-C3 CM 3.413 ± 0.56, si-scr CM 3.983 ± 0.592). PBMCs co-cultured with CM from si-C3 transfected HRA-19 cells demonstrated a trend towards decreased necrosis relative to si-scr CM, however this was not significant ($p = 0.0549$) (**Fig. 4-14 F**). These data demonstrate that less HRA-19 cell-derived C3 reduces late-stage apoptosis in PBMCs, suggesting that HRA-19-derived C3 may promote cell death during PBMC activation.

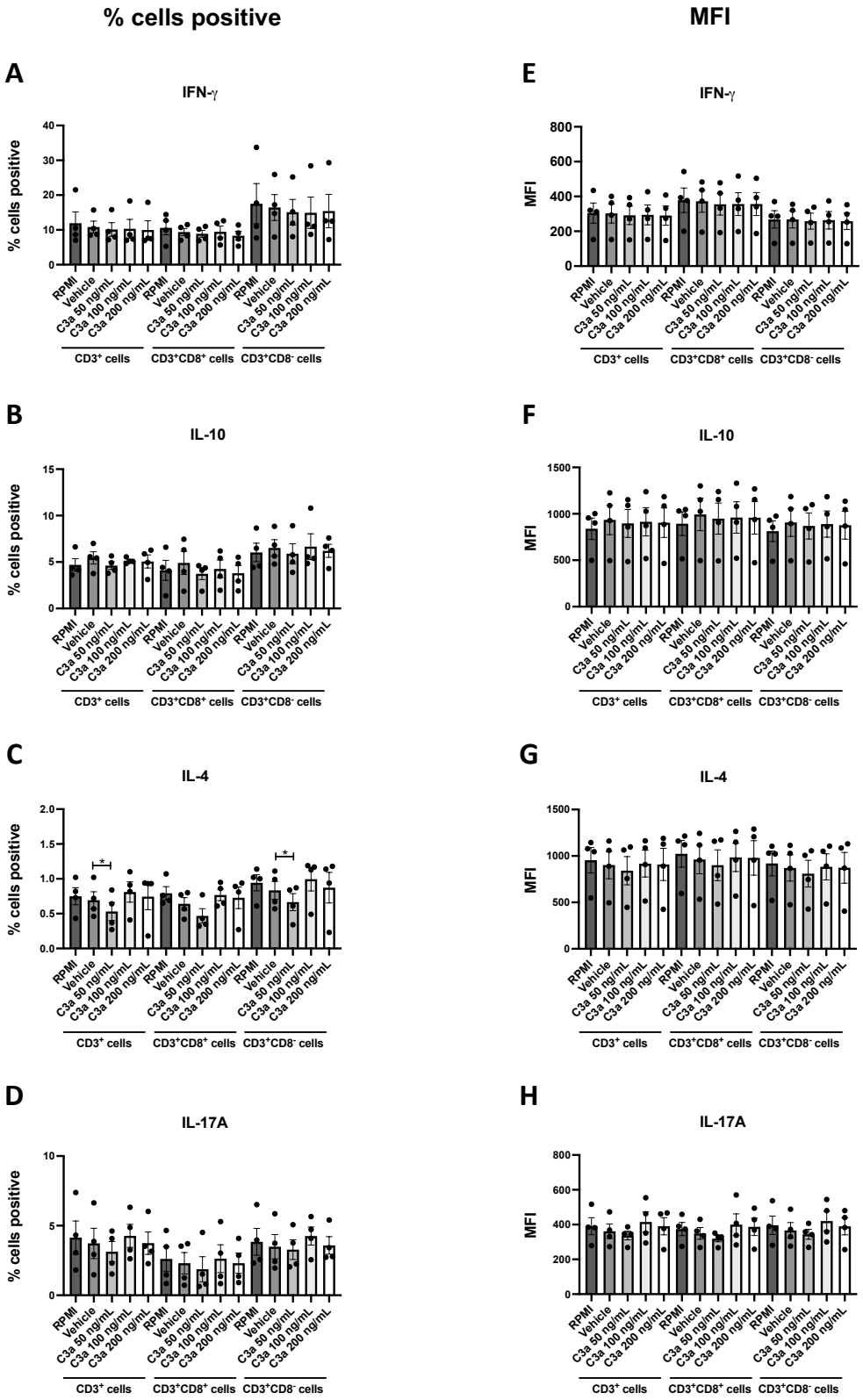

Figure 4-13: Recombinant C3a decreases IL-4 expression in pre-activated T cells. PBMCs were pre-activated for 24 h with plate-bound anti-CD3/CD28 and then treated for a further 24 h with recombinant C3a or vehicle control (PBS). The percentage of $CD3^+$, $CD3^+CD8^+$ and $CD3^+CD8^-$ T cells expressing **(A)** IFN-γ, **(B)** IL-10, **(C)** IL-4 and **(D)** IL-17A was assessed by flow cytometry. **(E-H)** MFI of cytokines expressed. Data are presented as mean ± SEM for 4 biological replicates. Statistical analysis was performed by paired two-tailed Student's *t*-test. $*p < 0.05$.

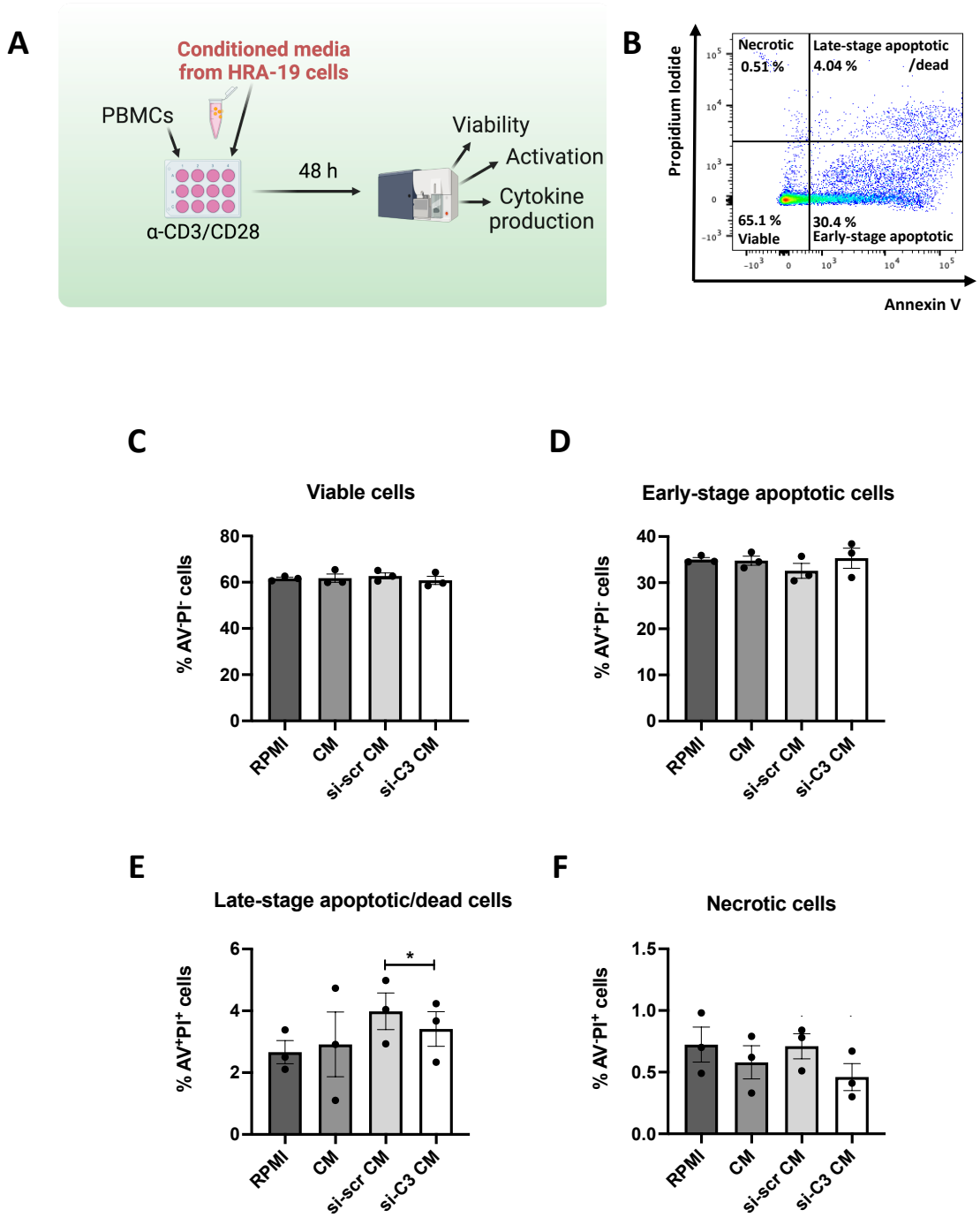

Figure 4-14: CM from si-C3 transfected HRA-19 cells reduces late-stage apoptosis of PBMCs during activation. (A) PBMCs were activated using plate-bound anti-CD3/CD28 and co-cultured with CM from HRA-19 cells basally or following transient transfection with C3 siRNA (si-C3 CM), or a scrambled control siRNA (si-scr), for 48 h. Viability was assessed by flow cytometry using the AV/PI assay. **(B)** Representative dot plot. Percentage of **(C)** live (AV^-PI^-), **(D)** early apoptotic (AV^+PI^-), **(E)** late apoptotic/dead (AV^+PI^+) and **(F)** necrotic (AV^-PI^+) PBMCs were assessed. Data are presented as mean ± SEM for 3 biological replicates. Statistical analysis was performed by paired two-tailed Student's *t*-test. $*p < 0.05$.

4.4.12. CM from si-C3 transfected HRA-19 cells does not alter proliferation of $CD3^+$ T cells

The effect of HRA-19 cell-derived C3 on T cell proliferation was assessed. PBMCs were stained with CFSE and activated using plate-bound anti-CD3/CD28 while being co-cultured with CM from HRA-19 cells, for 5 d (**Fig. 4-15**).

Co-culture with CM from HRA-19 cells transfected with si-C3 did not result in alterations to the total percentage of $CD3^+$ that had proliferated, when compared to CM from HRA-19 cells transfected with si-scr or RPMI controls (**Fig. 4-15 B**). The percentage of $CD3^+$ cells in each division was quantified, however the distribution across the 7 cell divisions was similar for all conditions (**Fig. 4-15 C**). These data suggest that C3 derived from HRA-19 cells does not alter T cell proliferation during activation.

4.4.13. CM from si-C3 transfected HRA-19 cells reduces T cell expression of CD62L

The effects of HRA-19 cell derived complement on T cell activation marker expression was assessed by flow cytometry (as illustrated in **Fig. 4-14 A**).

Co-culture of PBMCs with CM from si-C3 transfected HRA-19 cells during anti-CD3/CD28 activation did not result in alterations in the percentage expression of CD69, CD62L, CD45RA or CD45RO by $CD3^+$, $CD3^+CD4^+$ or $CD3^+CD8^+$ T cells (**Fig. 4-16 A-D)**. There were similarly no alterations in MFI of CD69, CD45RA and CD45RO in T cells (**Fig. 4-16 E, G-H)**. Interestingly, the MFI of CD62L expressed by $CD3^+$ and $CD3^+$CD4 T cells was significantly reduced following co-culture with si-C3 CM, when compared to si-scr CM ($p = 0.0138$ and $p = 0.0241$, respectively) (Mean MFI CD62L ± SEM; $CD3^+$; si-C3 CM 3215 ± 1063, si-scr CM 3884 ± 1105. $CD3^+$ $CD4^+$; si-C3 CM 3953 ± 1422 si-scr CM 4724 ± 1435) (**Fig. 4-16 F)**. These data suggest that C3 derived from HRA-19 cells may promote a lymph node homing, naïve phenotype in T cells.

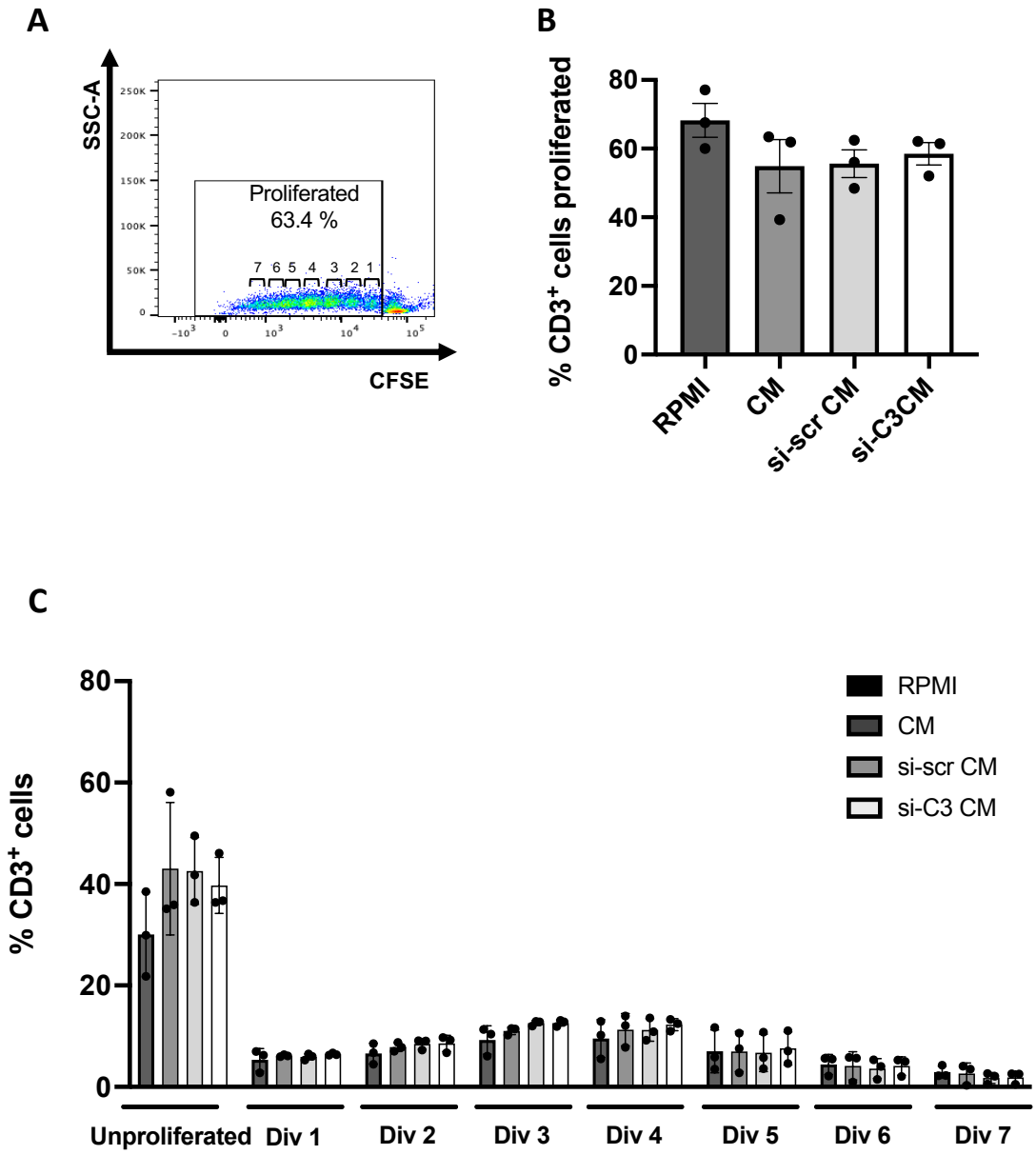

Figure 4-15: CM from si-C3 transfected HRA-19 cells does not alter proliferation of CD3$^+$ T cells during activation. PBMCs were stained with CFSE and co-cultured with CM from HRA-19 cells basally or following transfection with C3 siRNA (si-C3), or a scrambled control siRNA (si-scr) for 5 d, while being activated by plate-bound anti-CD3/CD28 **(A)** Representative dot plot demonstrating gating strategies to determine the total percentage of CD3$^+$ proliferated cells and the number of cell divisions that has taken place. **(B)** Total percentage of proliferated CD3$^+$ T cells. Statistical analysis was performed by paired two-tailed Student's *t*-test. **(C)** Percentage of unproliferated CD3$^+$ T cells, and the percentages of proliferated cells per division (Div). Data are presented as mean ± SEM for 3 biological replicates. Statistical analysis was performed by two-way ANOVA. *$p < 0.05$, ***$p < 0.001$.

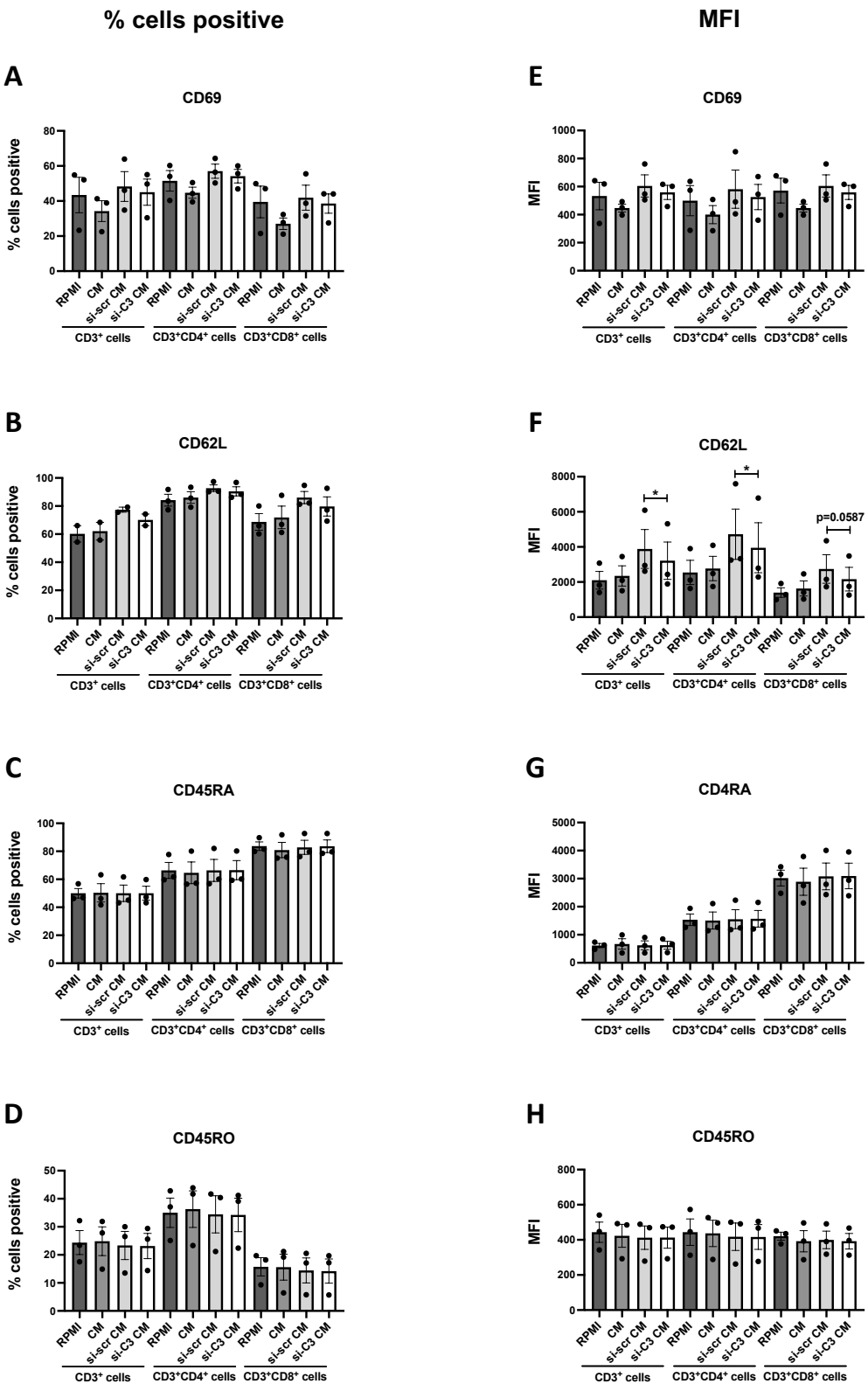

Figure 4-16: CM from si-C3 transfected HRA-19 cells reduces T cell expression of CD62L. PBMCs were activated using plate-bound anti-CD3/CD28 and co-cultured with CM from HRA-19 cells basally or following transient transfection with C3 siRNA (si-C3), or a scrambled control siRNA (si-scr), for 48 h. The percentage of $CD3^+$, $CD3^+CD4^+$ and $CD3^+CD8^+$ T cells expressing **(A)** CD69, **(B)** CD62L, **(C)** CD45RA and **(D)** CD45RO was assessed by flow cytometry. **(E-H)** MFI of markers expressed. Data are presented as mean ± SEM for 3 biological replicates. Statistical analysis was performed by paired two-tailed Student's *t*-test. *$p < 0.05$.

4.4.14. CM from si-C3 HRA-19 cells does not alter T cell cytokine production during activation

The effect of HRA-19 cell-derived C3 on T cell cytokine expression during T cell activation was assessed. PBMCs were co-cultured with CM from HRA-19 cells transfected with si-C3 or si-scr (as illustrated in **Fig. 4-14 A**) and intracellular cytokine expression was assessed by flow cytometry (**Fig. 4-17)**. As PMA downregulates human CD4, for this experiment $CD4^+$ T cells were classified as $CD3^+CD8^-$.

The percentage of $CD3^+$, $CD3^+$ $CD8^+$ or $CD3^+$ $CD8^-$ T cells expressing IFN-γ, IL-10, IL-4 or IL-17A was unchanged following co-culture with CM from si-C3 transfected HRA-19 cells, when compared to CM from si-scr transfected HRA-19 cells (**Fig. 4-17 A-D)**. Additionally, the MFI of cytokines expressed by $CD3^+$, $CD3^+$ $CD8^+$ or $CD3^+$ $CD8^-$ T cells was unchanged following co-culture with CM from si-C3 HRA-19 cells (**Fig. 4-17 E-H)**. These data demonstrate that C3 derived from HRA-19 cells does not alter cytokine expression in T cells during activation.

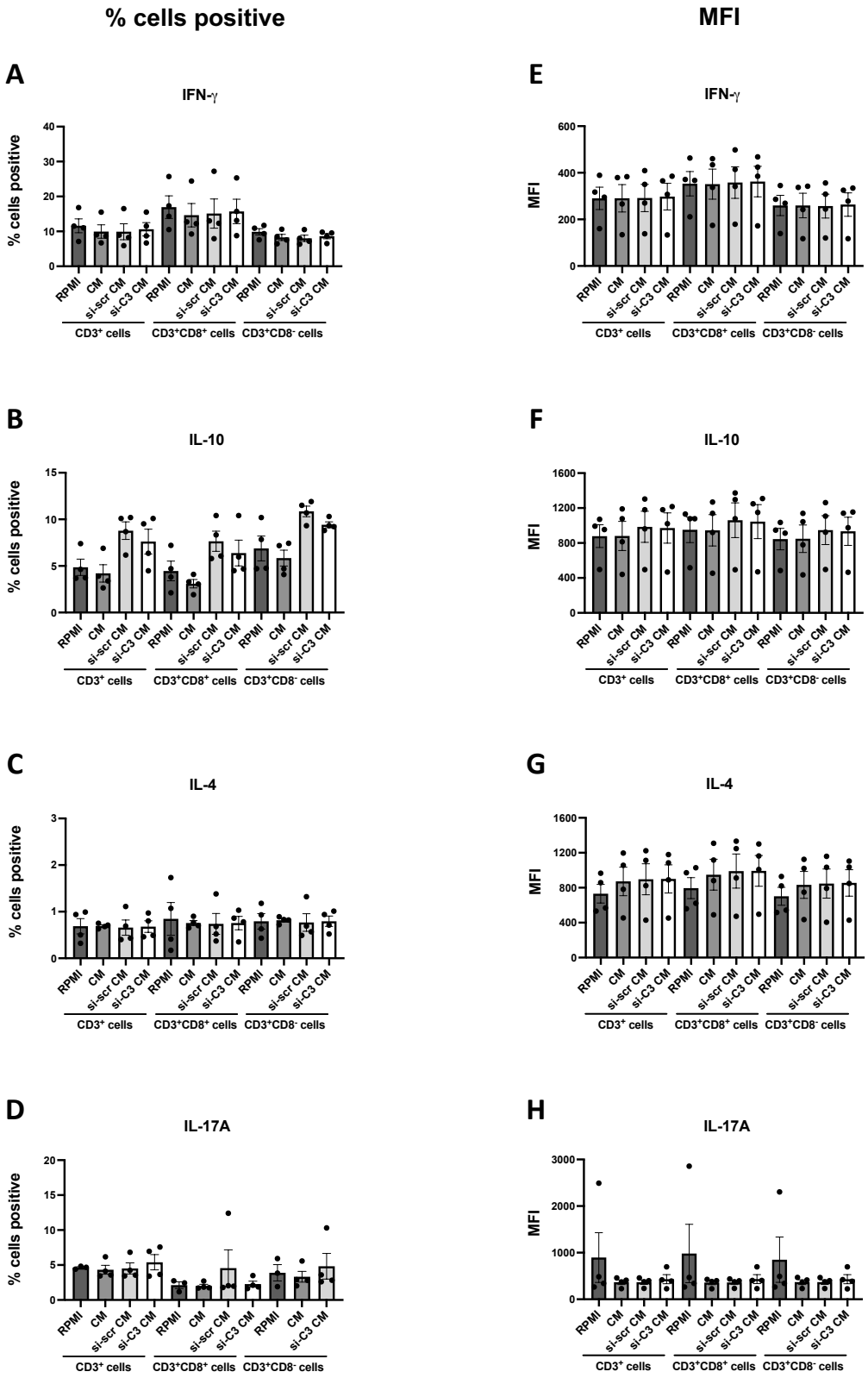

Figure 4-17: CM from si-C3 transfected HRA-19 cells does not alter T cell cytokine production during activation. PBMCs were activated using plate-bound anti-CD3/CD28 and co-cultured with CM from HRA-19 cells basally or following transient transfection with C3 siRNA (si-C3), or a scrambled control siRNA (si-scr), for 48 h. The percentage of $CD3^+$, $CD3^+CD8^+$ and $CD3^+CD8^-$ T cells expressing **(A)** IFN-γ, **(B)** IL-10, **(C)** IL-4 and **(D)** IL-17A was assessed by flow cytometry. **(E-H)** MFI of cytokines expressed. Data are presented as mean ± SEM for 4 biological replicates.

4.4.15. CM media from HCT116 cells overexpressing C3 does not alter the viability of PBMCs during activation

To further investigate the effects of complement in the context of the tumour-draining lymph node, the effect of C3 derived from HCT116 cells on T cell phenotype during activation was assessed (**Fig. 4-18 A**).

Using the AV/PI assay and flow cytometry, co-culture of PBMCs with CM from HCT116 cells overexpressing C3 was not demonstrated to alter the percentage of viable, early-stage apoptotic/dead, late-stage apoptotic or necrotic cells, when compared to RPMI or VC controls (**Fig. 4-18 C-F**). These data suggest that HCT116 cell-derived C3 does not alter PBMC viability.

4.4.16. CM from HCT116 cells overexpressing C3 does not alter proliferation of $CD3^+$ T cells

The effect of HCT116 cell-derived C3 on T cell proliferation was assessed. PBMCs were stained with CFSE and activated using plate-bound anti-CD3/CD28 while being co-cultured with CM from HCT116 cells, for 5 d (**Fig. 4-19**).

Co-culture with CM from HCT116 cells overexpressing C3 did not alter the total percentage of $CD3^+$ that had proliferated, when compared to CM from HCT116 cells expressing a VC or RPMI (**Fig. 4-19 B**). The percentage of $CD3^+$ cells in each division was quantified, however the distribution across the 7 cell divisions was similar for all conditions (**Fig. 4-19 C**). These data suggest that HCT116 cell-derived C3 does not alter T cell proliferation.

4.4.17. CM from HCT116 cells overexpressing C3 does not alter T cell expression of activation markers

The effects of HCT116 cell-derived complement on T cell activation marker expression, during activation was assessed by flow cytometry (**Fig. 4-20)**.

Co-culture of PBMCs with CM from HCT116 cells overexpressing C3 did not alter the expression of CD69, CD62L, CD45RA or CD45RO by $CD3^+$, $CD3^+CD4^+$ or $CD3^+CD8^+$ T cells (**Fig. 4-20 A-D)**. Similarly, there were no alterations in the MFI of any of the activation markers accessed (**Fig. 4-20 E-H).** These data suggest that C3 derived from HCT116 cells does not alter expression of activation markers by T cells.

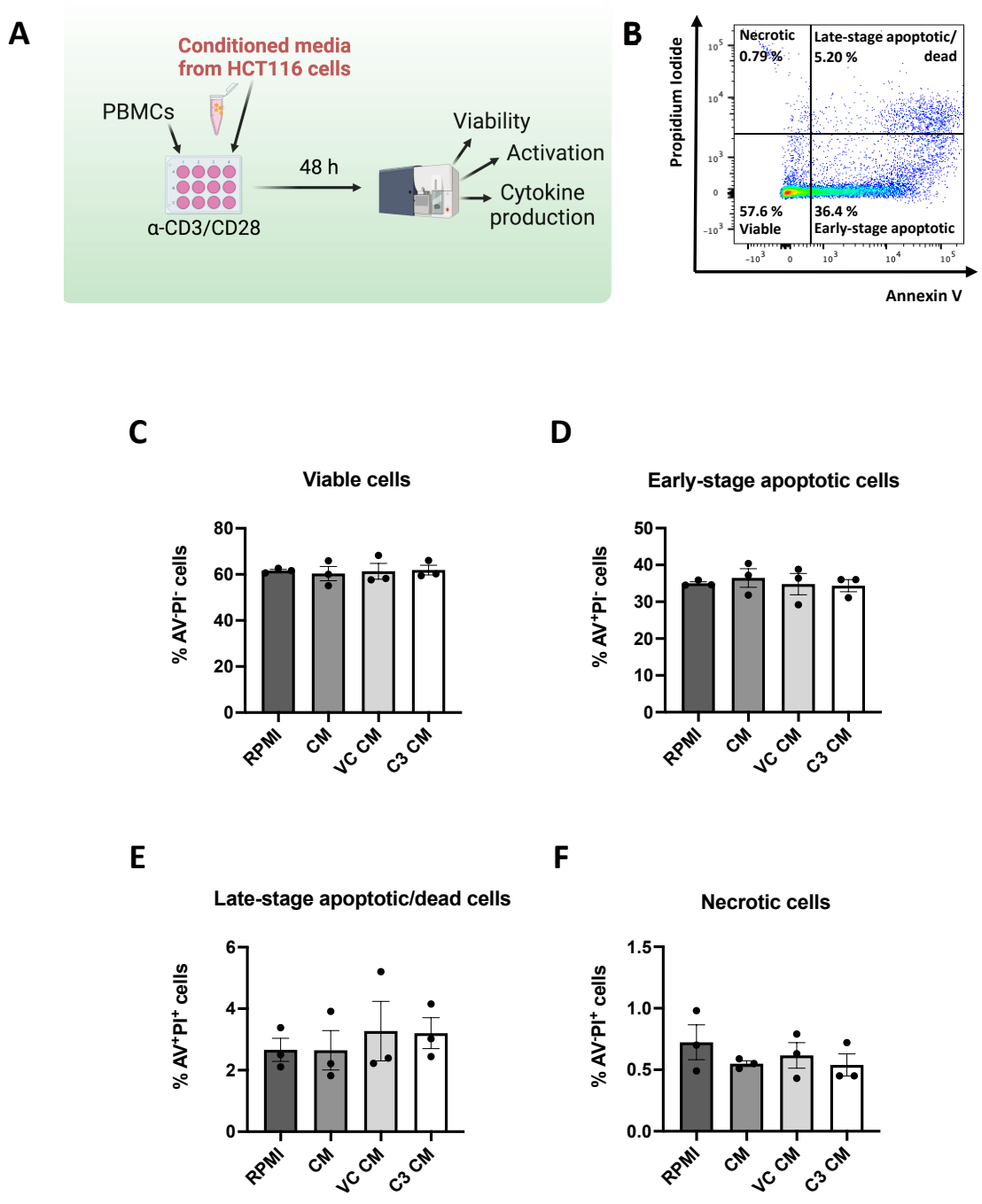

Figure 4-18: CM from HCT116 cells overexpressing C3 during activation does not alter PBMC viability. (A) PBMCs were activated using plate-bound anti-CD3/CD28 and co-cultured with CM from HCT116 cells basally or following transient transfection with a C3 DNA plasmid or a VC plasmid, for 48 h. Viability was assessed by flow cytometry using the AV/PI assay. **(B)** Representative dot plot. Percentage of **(C)** live (AV^-PI^-), **(D)** early apoptotic (AV^+PI^-), **(E)** late apoptotic/dead (AV^+PI^+) and **(F)** necrotic (AV^-PI^+) PBMCs were assessed. Data are presented as mean ± SEM for 3 biological replicates. Statistical analysis was performed by paired *t*-test. **p* < 0.05.

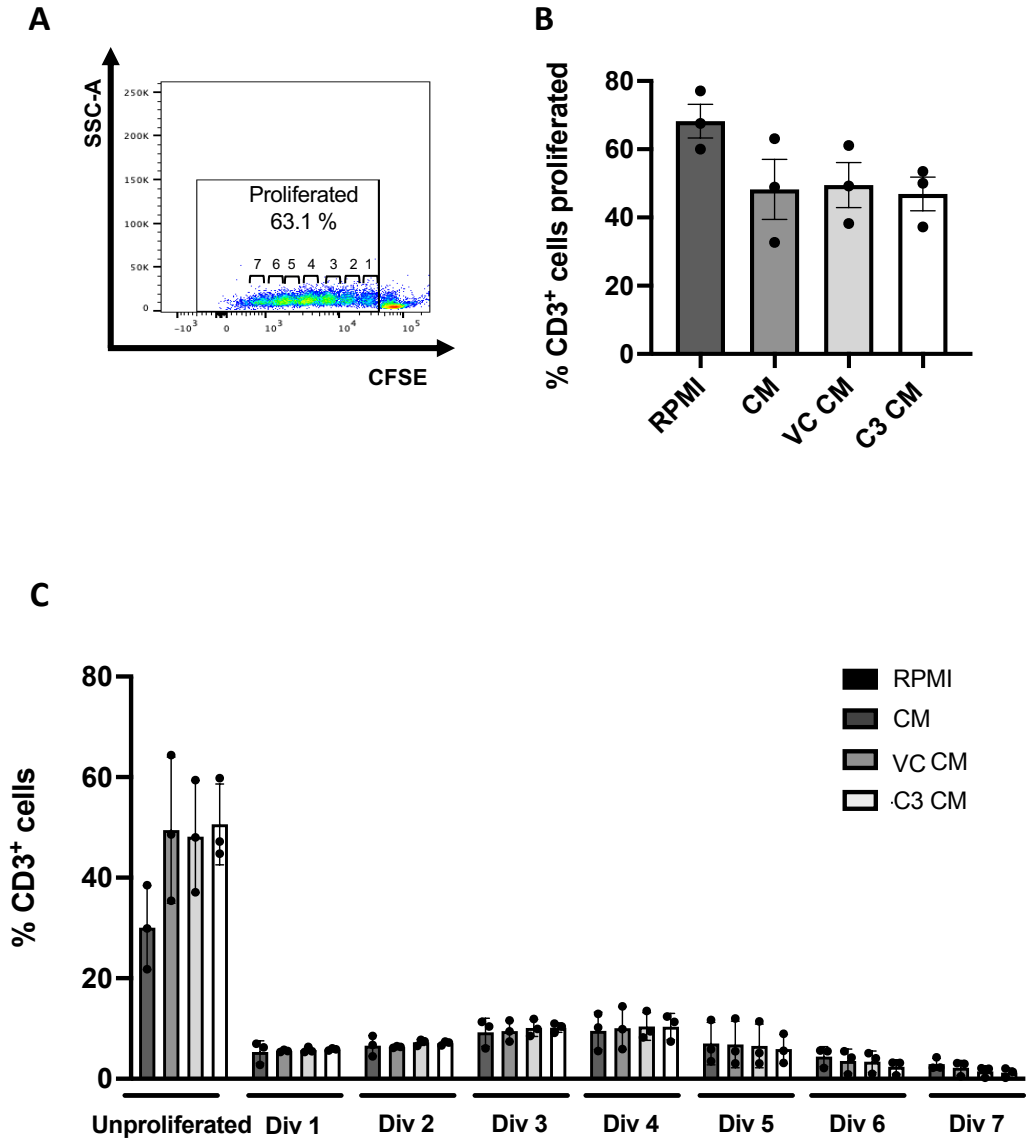

Figure 4-19: **CM from HCT116 cells overexpressing C3 does not alter proliferation of CD3$^+$ T cells during activation.** PBMCs were stained with CFSE and co-cultured with CM from HCT116 cells basally or following transient transfection with a C3 DNA plasmid or a VC plasmid for 5 d, while being activated by plate-bound anti-CD3/CD28. **(A)** Representative dot plot demonstrating gating strategies to determine the total percentage of CD3$^+$ proliferated cells and the number of cell divisions that has taken place. **(B)** Total percentage of proliferated CD3$^+$ T cells. Statistical analysis was performed by paired two-tailed Student's *t*-test. **(C)** Percentage of unproliferated CD3$^+$ T cells, and the percentages of proliferated cells per division (Div). Data are presented as mean ± SEM for 3 biological replicates. Statistical analysis was performed by two-way ANOVA.

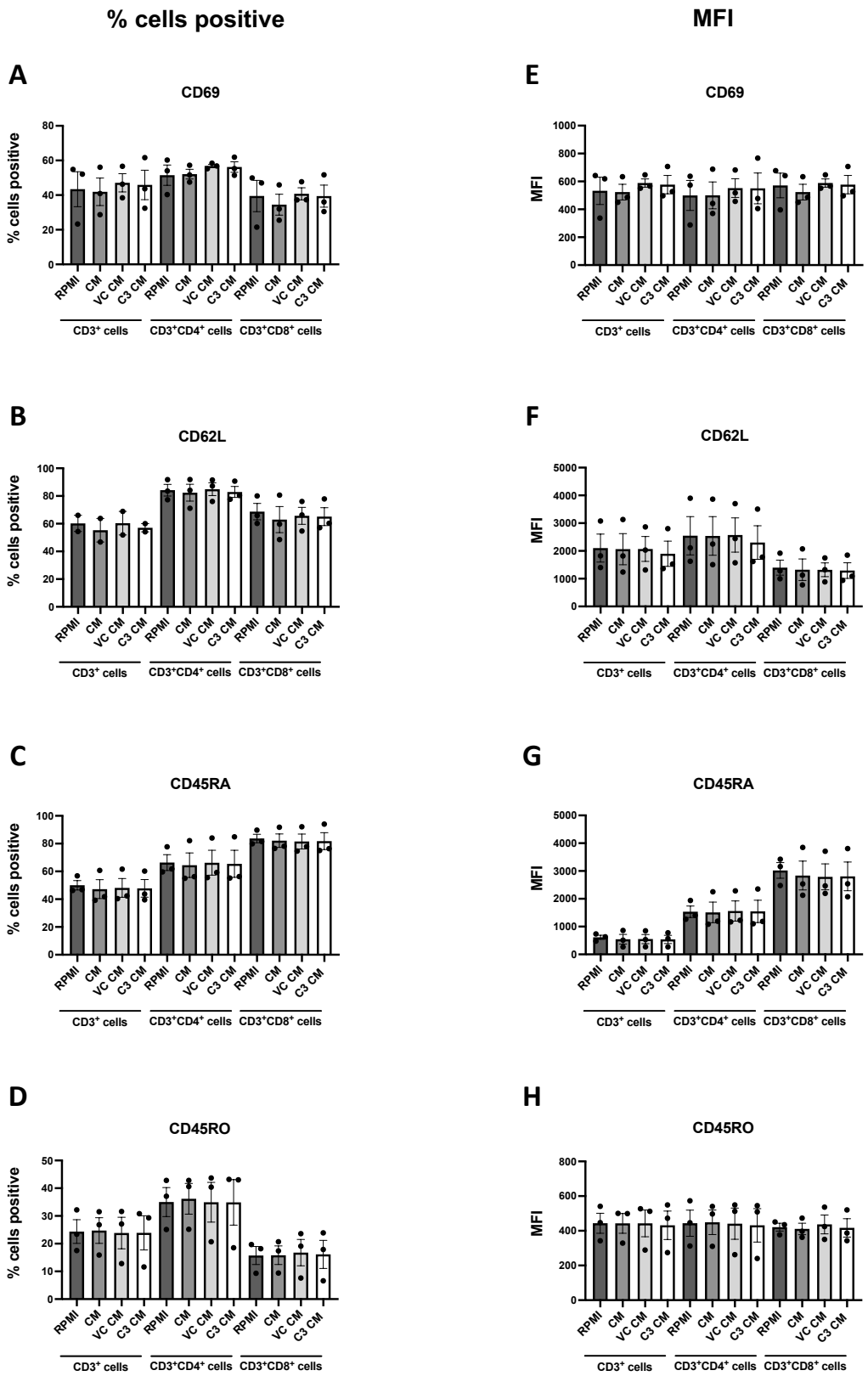

Figure 4-20: CM from HCT116 cells overexpressing C3 does not alter T cell expression of activation markers. PBMCs were activated using plate-bound anti-CD3/CD28 and co-cultured with CM from HCT116 cells basally or following transient transfection with a C3 or VC DNA plasmid for 48 h. The percentage of $CD3^+$, $CD3^+CD4^+$ and $CD3^+CD8^+$ T cells expressing **(A)** CD69, **(B)** CD62L, **(C)** CD45RA and **(D)** CD45RO was assessed by flow cytometry. **(E-H)** MFI of markers expressed. Data are presented as mean ± SEM for 3 biological replicates. Statistical analysis was performed by paired two-tailed Student's *t*-test.

4.4.18. CM from HCT116 cells overexpressing C3 alters T cell expression of intracellular cytokines

The effect of CM from HCT116 cells on intracellular cytokine expression, during activation, was also assessed by flow cytometry (**Fig. 4-21).** As PMA downregulates human CD4, for this experiment $CD4^+$ T cells were classified as $CD3^+CD8^-$.

Co-culture with CM from HCT116 cells overexpressing C3 during activation significantly increased ($p = 0.0149$) the percentage of $CD3^+$ $CD8^+$ cells expressing IFN-γ, when compared to CM from HCT116 cells expressing a VC (Mean % of IFN-γ^+ cells ± SEM; C3 CM 16.14 ± 4.588, VC CM 15.31 ± 4.529) (**Fig. 4-21 A).** These data suggest that C3 derived from HCT116 cells promotes more $CD8^+$ T cells to express IFN-γ. There were no alterations in MFI of IFN-γ expression (**Fig. 4-21 E)**.

Percentage expression and MFI of IL-10 was unchanged following co-culture with CM from HCT116 cells overexpressing C3 (**Fig. 4-21 B, F)**.

While there were no alterations in the percentage of IL-4 producing cells (**Fig. 4-21 C)**, the MFI of IL-4 expressed by $CD3^+$ and $CD3^+$ $CD8^-$ cells was significantly reduced after co-culture with CM from HCT116 cells overexpressing C3, when compared to CM from HCT116 cells expressing a VC ($p = 0.0272$ and $p = 0.0042$, respectively) (Mean MFI IL-4 ± SEM; $CD3^+$; C3 CM 850.75 ± 127, VC CM 861.5 ± 128. $CD3^+CD8^-$; C3 CM 808 ± 121.56, VC CM 823.25 ± 122.772) (**Fig. 4-21 G)**.

The percentage of $CD3^+$, $CD3^+CD8^+$ or $CD3^+CD8^-$ T cells positive for IL-17A was unchanged following co-culture with CM from HCT116 cells overexpressing C3, when compared to CM from HCT116 cells expressing a VC (**Fig. 4-21 D)**. However, $CD3^+CD8^+$ cells expressed significantly more IL-17A following co-culture with CM from C3 HCT116 cells, when compared to CM from HCT116 cells expressing a VC ($p = 0.027$) (Mean MFI IL-17A ± SEM; C3 CM 382.25 ± 50.553 , VC CM 327.750 ± 45.735) (**Fig. 4-21 H).** These data suggest that HCT116 cell-derived C3 alters T cell cytokine production during activation.

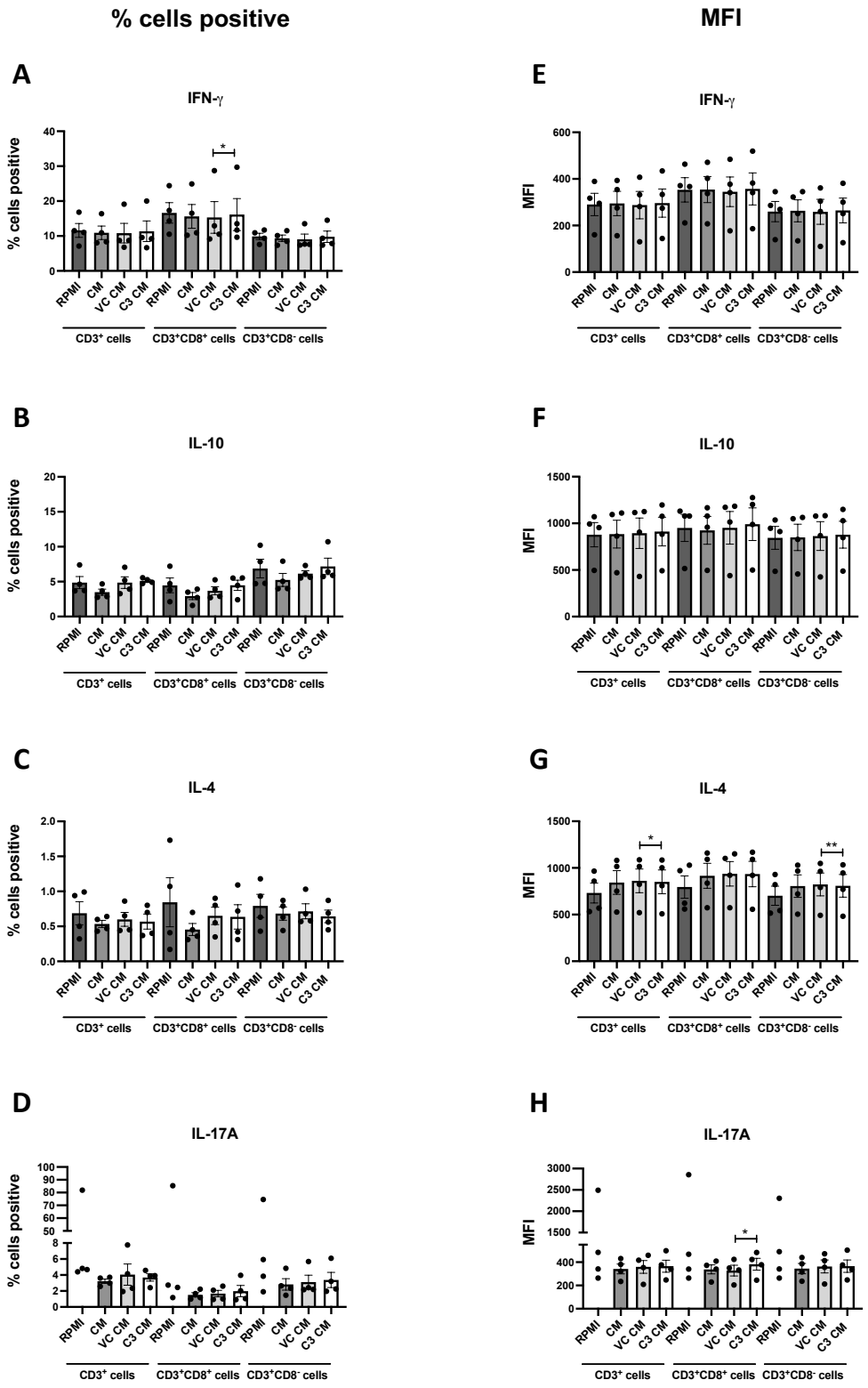

Figure 4-21: CM from HCT116 cells overexpressing C3 alters T cell cytokine production during activation. PBMCs were activated using plate-bound anti-CD3/CD28 and co-cultured with CM from HCT116 cells basally or following transient transfection with a C3 or VC DNA plasmid, for 48 h. The percentage of $CD3^+$, $CD3^+CD8^+$ and $CD3^+CD8^-$ T cells expressing **(A)** IFN-γ, **(B)** IL-10, **(C)** IL-4 and **(D)** IL-17A was assessed by flow cytometry. **(E-H)** MFI of cytokines expressed. Data are presented as mean ± SEM for 4 biological replicates. Statistical analysis was performed by paired two-tailed Student's *t*-test. *$p < 0.05$.

4.4.19. Recombinant C3a decreases late-stage apoptosis of PBMCs during activation

Having investigated the effects of CRC cell-derived complement on PBMCs during activation, the effect of recombinant C3a on T cell phenotype was assessed. In a similar manner to HRA-19 or HCT116 CM experiments, PBMCs were activated using plate-bound anti-CD3/CD28, in the presence of recombinant C3a, for 48 h **(Fig. 4-22 A)**

Treatment with recombinant C3a did not alter the percentage of viable, early-stage apoptotic or necrotic PBMCs, when compared to vehicle or RPMI controls **(Fig. 4-22 C-D, F)**. Interestingly, there was a significant decrease in the percentage of PBMCs undergoing late-stage apoptosis/cell death treated with recombinant C3a (50 ng/mL), when compared to the vehicle control ($p = 0.0104$) (Mean % of AV^+PI^+ PBMCs; C3a 50 ng/mL 2.303 ± 0.377, Veh 3.37 ± 0.454, **(Fig. 4-22 E)**. This suggests that recombinant C3a enhances PBMC viability during activation.

4.4.20. Recombinant C3a does not alter the proliferation of $CD3^+$ cells

The effect of recombinant C3a on T cell proliferation was also assessed. PBMCs were stained with CFSE and activated while in the presence of recombinant C3a for 5 d (**Fig. 4-23**).

Recombinant C3a did not alter the total percentage of $CD3^+$ cells that had proliferated in this setting, when compared to vehicle controls (**Fig. 4-23 B**). The percentage of $CD3^+$ cells in each cellular division was quantified, but the distribution across the 7 cell divisions was similar for all conditions (**Fig. 4-23 C**). These data suggest that recombinant C3a does not alter proliferation of $CD3^+$ cells.

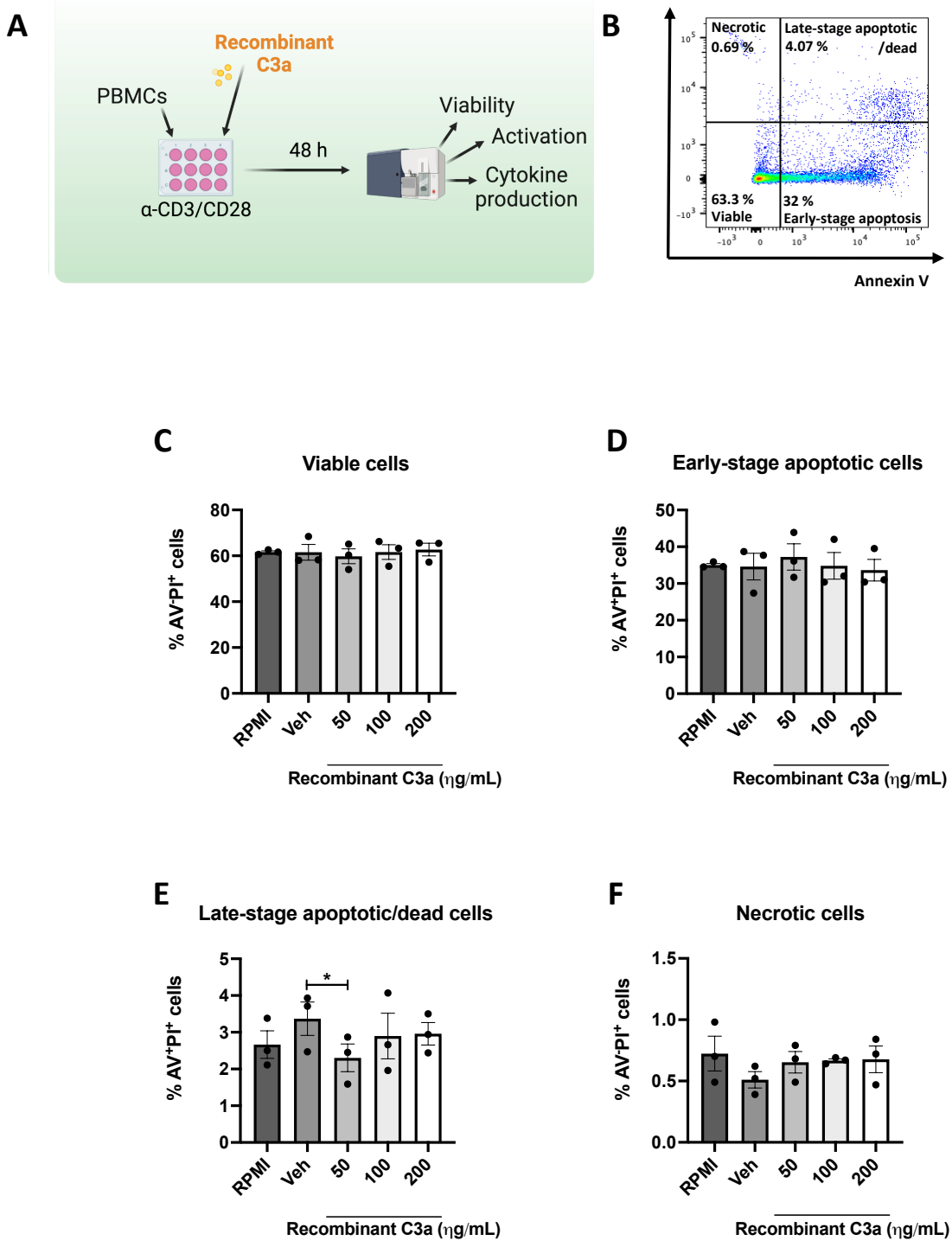

Figure 4-22: Recombinant C3a reduces late-stage apoptosis in PBMCs during activation. (A) PBMCs were activated with plate-bound anti-CD3/CD28 in the presence of recombinant C3a or the vehicle control (PBS) for 48 h. Viability was assessed by flow cytometry using the AV/PI assay. **(B)** Representative dot plot. Percentage of **(C)** live (AV^-PI^-), **(D)** early apoptotic (AV^+PI^-), **(E)** late apoptotic/dead (AV^+PI^+) and **(F)** necrotic (AV^-PI^+) PBMCs analysed. Data are presented as mean ± SEM for 3 biological replicates. Statistical analysis was performed by paired two-tailed Student's *t*-test. *$p < 0.05$.

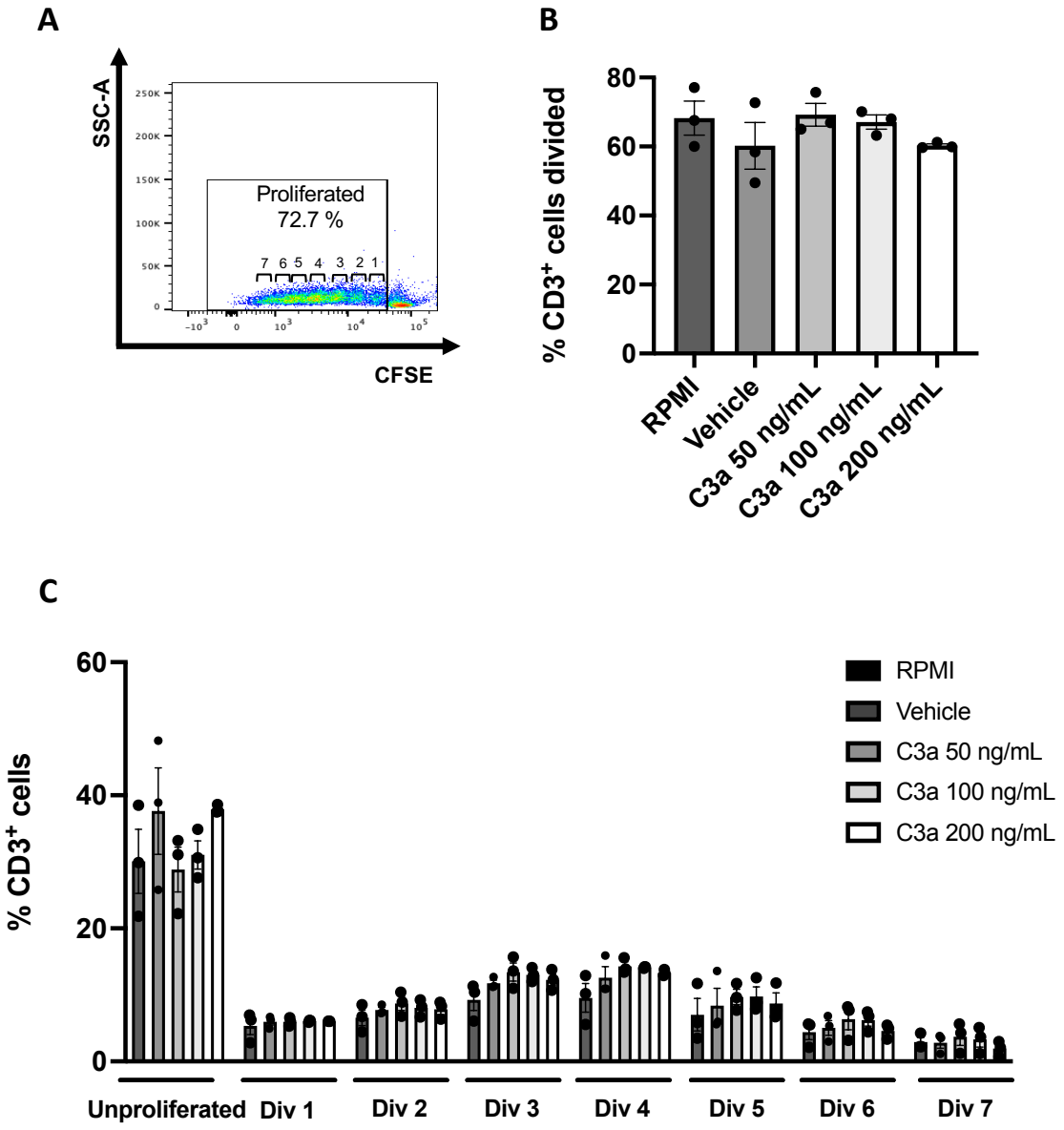

Figure 4-23: Recombinant C3a does not alter proliferation of CD3$^+$ T cells during activation. PBMCs were stained with CFSE and activated with plate-bound anti-CD3/CD28 in the presence of recombinant C3a or the vehicle control (PBS) for 5 d, while being activated by plate-bound anti-CD3/CD28. **(A)** Representative dot plot demonstrating gating strategies to determine the total percentage of CD3$^+$ proliferated cells and the number of cell divisions that has taken place. **(B)** Total percentage of proliferated CD3$^+$ T cells. **(C)** Percentage of unproliferated CD3$^+$ T cells, and the percentages of proliferated cells per division (Div). Data are presented as mean ± SEM for 3 biological replicates. Statistical analysis was performed by two-way ANOVA.

4.4.21. Recombinant C3a increases T cell expression of naïve markers during activation

PBMCs treated with recombinant C3a for 48 h during activation were assessed for the effects of C3a on the expression of T cell activation markers (**Fig. 4-24**).

Recombinant C3a did not alter the percentage of cells expressing CD69, or the MFI of CD69 expressed by T cells at all concentrations assessed (**Fig. 4-24 A, E**). Similarly, the percentage expression and MFI of CD45RO on the surface of $CD3^+$, $CD3^+CD8^+$ and $CD3^+CD8^-$ cells was unaltered by recombinant C3a treatment (**Fig. 4-24 D, H**). Interestingly however, recombinant C3a (50 ng/mL) was increased the percentage of CD62L-expressing $CD3^+$ and $CD3^+CD4^+$ cells ($p = 0.0353$, $p = 0.0214$, respectively) (Mean % of cells expressing CD62L ± SEM; $CD3^+$; C3a 50 ng/mL 62.5 ± 5.3, Vehicle 60.7 ± 5.4. $CD3^+CD4^+$; C3a 50 ng/mL 86.767 ± 4.113, Vehicle 84.933 ± 3.931). This increase was also demonstrated in the MFI of CD62L expressed by $CD3^+$ and $CD3^+CD8^+$ cells ($p = 0.0075$, $p = 0.0273$, respectively) (Mean MFI CD62L; $CD3^+$; C3a 50 ng/mL 2404.667 ± 615.239, Vehicle 2269 ± 603.541; $CD3^+CD8^+$; C3a 50 ng/mL 2942.33 ± 792.835, Vehicle 2741.667 ± 784.64). Recombinant C3a was also demonstrated to significantly increase the percentage of $CD3^+CD4^+$ cells expressing CD45RA, when compared to vehicle control ($p = 0.0315$) (Mean % of $CD3^+CD4^+$ cells expressing CD45RA; C3a (50 ng/mL) 63.733 ± 6.729, Vehicle 63 ± 6.596) (**Fig. 4-24 C**). These data demonstrate that recombinant C3a (50 ng/mL) is associated with expression of naïve T cell markers, suggesting that in the context of T cell activation, C3a promotes a naïve phenotype.

4.4.22. Recombinant C3a does not alter T cell cytokine production

The effect of recombinant C3a on cytokine expression during T cell activation was assessed. PBMCs were treated with recombinant C3a during activation, and intracellular cytokine expression was assessed by flow cytometry (**Fig. 4-25)**. As PMA downregulates human CD4, for this experiment $CD4^+$ T cells were classified as $CD3^+CD8^-$.

The percentage of $CD3^+$, $CD3^+CD8^+$ or $CD3^+CD8^-$ T cells producing IFN-γ, IL-10, IL-4 or IL-17A was unchanged following co-culture with recombinant C3a (**Fig. 4-25 A-D)**. Similarly, the MFI of cytokines expressed by $CD3^+$, $CD3^+CD8^+$ or $CD3^+CD8^-$ T cells was unchanged following co-culture with recombinant C3a (**Fig. 4-25 E-H)**. These data suggest that recombinant C3a does not alter cytokine expression during T cell activation.

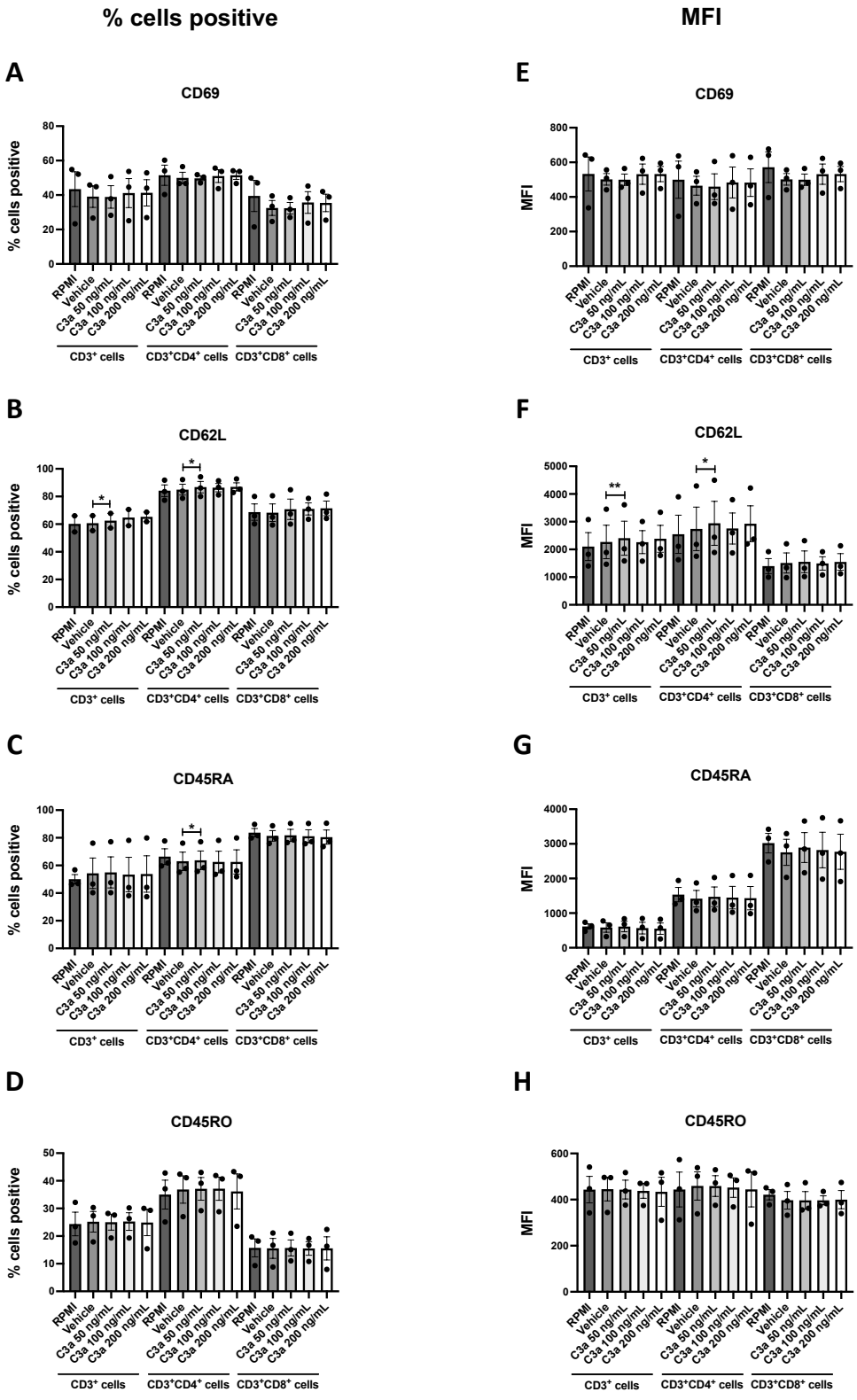

Figure 4-24: Recombinant C3a alters T cell expression of activation markers during anti-CD3/CD28 stimulation. PBMCs were activated using plate-bound anti-CD3/CD28 and treated with recombinant C3a or the vehicle control (PBS) for 48 h. The percentage of $CD3^+$, $CD3^+CD4^+$ and $CD3^+CD8^+$ T cells expressing **(A)** CD69, **(B)** CD62L, **(C)** CD45RA and **(D)** CD45RO was assessed by flow cytometry. **(E-H)** MFI of markers expressed. Data are presented as mean ± SEM for 3 biological replicates. Statistical analysis was performed by paired two-tailed Student's *t*-test. $*p < 0.05$, $**p < 0.01$.

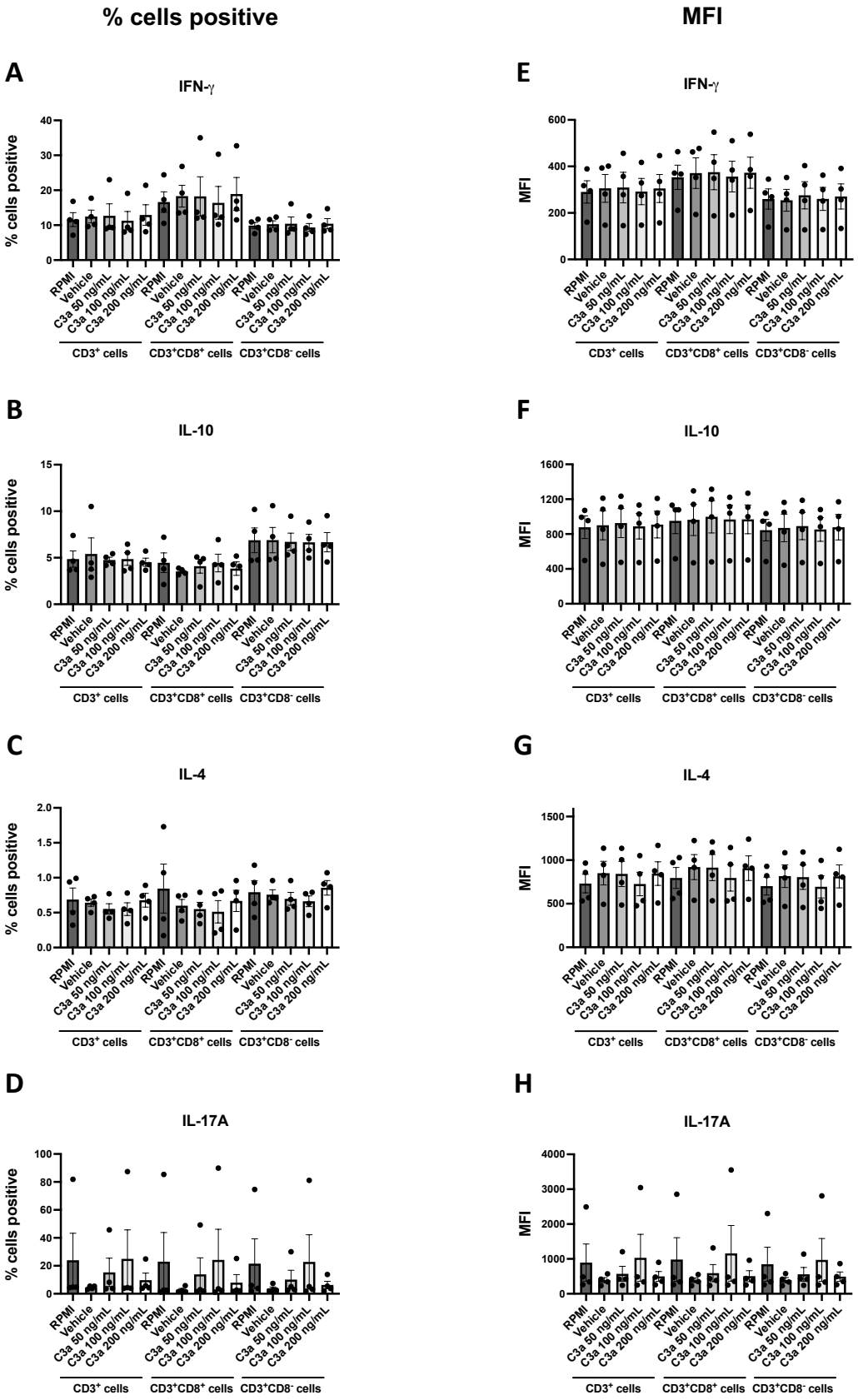

Figure 4-25: Recombinant C3a does not alter T cell cytokine production during activation. PBMCs were activated using plate-bound anti-CD3/CD28 and treated with recombinant C3a or the vehicle control (PBS) for 48 h. The percentage of $CD3^+$, $CD3^+CD8^+$ and $CD3^+CD8^-$ T cells expressing **(A)** IFN-γ, **(B)** IL-10, **(C)** IL-4 and **(D)** IL-17A was assessed by flow cytometry. **(E-H)** MFI of markers expressed. Data are presented as mean ± SEM for 4 biological replicates

4.5. Discussion

The immune system is well recognised as an important mediator in the response to cancer therapy, and immune infiltrates correspond with clinical outcomes in CRC[434,435]. In rectal tumours, T cell infiltration has been demonstrated to correspond with response to neo-CRT[428,429]. Several 'immune subtypes' have been defined for CRC, with tumours displaying heterogenous immune profiles within the TME[436]. The therapeutic efficacy of RT is at least in part dependent on immune infiltrates, which provide innate immune recognition of IR-induced DNA damage and subsequent priming of anti-tumour $CD8^+$ T cells[437,438]. Therefore, tackling poor response rates to neo-CRT in rectal cancer requires understanding the molecular factors and microenvironmental influences behind the immune profiles of these tumours. In 2015, a comprehensive study by Guinney *et al.* defined the CMS classification system for CRCs[25]. One of these subtypes, CMS4, is characterised by worse OS and relapse-free survival, and demonstrates an upregulation of genes involved in EMT. Notably, these CMS4 classified tumours were associated with an upregulation of the complement system[25]. This highlights that in CRC, the complement system may have functional roles that affect patient outcomes. Complement has been demonstrated to modify immune cell populations within the TME; recruiting MDSCs[298,321–324,327], skewing macrophages toward an M2 phenotype[332,335], limiting NK cell responses[339,340] and reducing T cell function and infiltration. While both C3 and C5 have been implicated in the modulation of T cell activity[298,320], little is known about the role of tumour cell-derived C3 on T cell phenotype in the context of CRC. This chapter aimed to characterise the effects of CRC cell-derived C3 on T cell viability, proliferation, activation and cytokine production.

Complement signals play important roles in maintaining the viability of naïve $CD4^+$ T cells[171,263]. To assess the effects of CRC cell-derived complement on T cell phenotype, this chapter used CM generated from HRA-119 and HCT116 cells basally and after modulation of C3 expression. Data presented in this chapter demonstrate that CM generated from HRA-19 cells following transient C3 silencing, significantly increases early apoptosis in pre-activated PBMCs. This suggests that PBMCs that are already undergoing activation are protected from apoptosis by C3 derived from HRA-19 cells. While to date there are no studies in the literature that report the effects of tumour-derived C3 on T cell viability in cancer, these results agree with evidence that complement maintains T cell viability under normal physiological conditions[171,263]. From a clinical perspective, this may suggest that tumour production of C3 and release into the TME may enhance the viability of pre-

activated T cells that have migrated to the tumour, potentially augmenting anti-tumour immune responses. This was further investigated using C3 derived from HCT116 cells. Conversely, CM generated from HCT116 cells following C3 overexpression did not alter the viability of pre-activated PBMCs. As discussed in Chapter 3, overexpression of exogenous C3 in HCT116 cells may produce a form of C3 that is distinct from the endogenous form. Recent data from Kremlitzka *et al*. demonstrates that C3 can be alternatively translated, resulting in a form distinct in functionality and cellular location[409]. This may be why culture with CM from HCT116 cells overexpressing C3 does not enhance viability of PBMCs. Additionally, as HRA-19 and HCT116 cell lines are derived from rectal and colon tumours, respectively, they may express varying forms of C3, with the ability to differentially alter PBMC viability.

Effects of CRC cell-derived C3 on PBMC viability were also assessed when PBMCs were cultured with CM during activation. Co-culture of PBMCs during activation with CM from HRA-19 cells in which C3 was silenced, resulted in decreased percentages of late apoptotic/dead and necrotic cells. This may suggest that HRA-19 cell-derived C3 reduces PBMC viability during activation. Under normal homeostasis, complement signals are important for maintaining $CD4^+$ T cells in a naïve state[171,263]. This experimental set up aimed to recapitulate activation of T cells in the tumour-draining lymph node, where tumour-derived complement is present. Therefore, these data suggest that in cancer, complement may have the opposite effect on viability[171,263]. Given the two experimental set ups used; whereby complement is present during T cell activation or post activation only, it suggests that the effect of complement on viability is context-dependent and may depend on the sequence in which T cells are activated and encounter tumour-derived complement.

Expression levels of complement in tumours varies, with overexpression or mutations often correlating with poor prognosis in several human cancers[287,317,318,394,439] including CRC[284,335]. In rectal cancer patients with high tumoural expression of complement, if complement remains localised within the TME, it may have a positive effect on anti-tumour immunity by promoting T cell viability. However, if tumoural complement drains to local lymph nodes, it may favour T cell death and the anti-tumour immune response may be hindered. An important question to be considered in future studies is whether anaphylatoxin generation solely occurs in the TME in rectal cancer, or whether cleavage of central complement components can be activated following drainage to local lymph nodes. One function of mCRPs is the regulation of C3 and C5 cleavage to

produce their respective anaphylatoxins[186]. In head and neck cancers, mCRPs are expressed in metastatic lymph node tissue, suggesting that complement can be regulated at this location[290]. Expression of mCRPs in the draining lymph nodes in rectal cancer may prevent cleavage of C3 to C3a. This may mean that less C3a is present and encountered by T cells during their activation, and clinically may translate to a more viable T cell population. Whether tumour-derived complement is retained within the TME or the majority drains to the tumour-draining lymph node is therefore an important question to answer when considering complement as a therapeutic target. Removing tumour-derived complement would either, reduce T cell viability or enhance it, if complement predominates in the TME or lymph nodes, respectively.

The concentration of C3 protein secreted by both HCT116 and HRA-19 cell lines and therefore within CM generated, is within the low ng/mL range. To assess the effects of higher concentrations of complement on the T cell parameters explored in this chapter, experiments were performed using recombinant complement. Recombinant C3a was used at concentrations of 50, 100 and 200 ng/mL. These concentrations were selected not only as they are much greater than the level of endogenous complement present in CM from HRA-19 and HCT116 cell lines, but also as they align with previously utilised concentrations reported in the literature[171,440]. Data presented in Chapter 2 of this study demonstrate that both HRA-19 and HCT116 cells possess an intrinsic ability to cleave C3 to produce the C3a anaphylatoxin. The concentration of C3a was assessed in CM from HCT116 and HRA-19 cells in Chapter 2, however although detectable, the levels were lower than the standard curve. Therefore, the inclusion of recombinant C3a had the additional benefit of assessing the effects of known concentrations of C3a, on T cell phenotype. Surprisingly, recombinant C3a had the same effect of increasing the percentage of pre-activated PBMCs undergoing early stage apoptosis, as CM from HRA-19 cells transfected with si-C3 did. Furthermore, when PBMCs were activated during treatment with recombinant C3a, late apoptosis/cell death was increased, again having the same effect as CM from si-C3 transfected HRA-19 cells. This suggests that endogenous complement is distinct from recombinant complement. A recent study, which investigated the effect of tumour-derived C1s on T cell phenotype demonstrated differing effects of tumour cell- and plasma-derived C1s on T cell activation[394], suggesting that recombinant C3a and tumour-derived C3a have different effects. A limitation of these viability experiments is that analysis was performed on whole $CD3^+$ populations rather than specific T cell subsets.

Therefore, future investigations would benefit from examining $CD4^+$ and $CD8^+$ T cells to assess whether alterations in viability vary between these populations.

Neither CM from HRA-19 or HCT116 cells, or recombinant C3a induced alterations in $CD3^+$ T cell proliferation. This is supported by a study by Zha *et al.,* who investigated the effect of CT26 (a colon carcinoma cell line) cell-derived C3 on T cell proliferation. In their study, they report that within C3 knockout colon tumours, the proliferative ability of T cells was enhanced[362]. However, similar to the results presented here, *in vitro* addition of C3a to T cells had no effect on proliferation. They suggest, that the effects of tumour-derived C3 on T cell proliferation occurs via an indirect mechanism[362]. This may suggest that C3 derived from the CRC cell lines studied here may have effects on T cell proliferation that cannot be recapitulated *in vitro*. Therefore, to gain further insight into the role of HCT116 and HRA-19 cell-derived C3 on T cell proliferation, a murine model that contains other elements of the TME may be essential.

Activated effector T cells are essential for the recognition and elimination of tumours but also for effective responses to cancer therapy[441]. CM generated from both HCT116 and HRA-19 cells following modulation of complement expression, did not induce alterations in activation marker expression by T cells that were pre-activated before exposure to the CM. This suggests that movement of activated T cells to a TME where CRC-derived C3 is present, does not affect their activation status. Therefore, if patients have tumours that express and release complement that remains within the TME, this may not impact on T cell activation, and therefore effector function. However, when pre-activated T cells were treated with recombinant C3a (100 ng/mL), the percentage of $CD4^+$ T cells expressing CD62L, was significantly increased. CD62L, also known as L-selectin, is a lymph node homing marker required for the retention of naïve T cells, which is shed by activated T cells allowing them to egress from the lymph node[442]. These data suggest that C3a may limit the movement of pre-activated T cells. Assessing the effect of recombinant or CRC cell-derived C3 on T cell activation marker expression, during activation, also highlighted that C3 alters CD62L expression. CM from C3 silenced HRA-19 cells, significantly decreased the MFI of CD62L expressed by $CD3^+$ and $CD4^+$ T cells, with a similar trend demonstrated in $CD8^+$ T cells. In contrast, recombinant C3a (50 ng/mL) increased both the percentage and MFI of CD62L expressed by $CD3^+$ and $CD4^+$ T cells. Recombinant C3a also increased the percentage of $CD4^+$ T cells expressing CD45RA, a naïve T cell marker. These data suggest that if complement is present in the tumour-draining lymph node during activation, a naïve, lymph node homing T cell phenotype may

be favoured. Therefore, if complement drains to local lymph nodes it may prevent T cell movement to the tumour and patients may have a reduced anti-tumour immune response, with potentially larger tumours and poor responses to cancer therapy. C3 has been demonstrated to both negatively and positively correlate with tumour infiltration of T cells. In non-small cell lung cancer, C3 expression positively correlates with $CD4^+$ and $CD8^+$ T cell infiltration[364]. In contrast, in murine colon cancer tumours, C3 has previously been linked with lower numbers of infiltrating T cells[323]. Complement inhibition enhanced T cell infiltration, reduced the numbers of MDSCs and upregulated chemo-attractive cytokines such as CCL5. This suggests that the restricted movement of T cells within the TME was indirectly mediated by complement[323]. More recently, expression of the C3aR in tumours from colon and rectal cancer patients has been demonstrated to associate with the number of innate and adaptive infiltrating immune cells[360]. In both patient and murine models, reduced C3aR expression correlated with elevated immune infiltrates[360]. These data suggest a role for C3a/C3aR-mediated modulated of immune cell migration in CRC. The effect of C3 on CD62L expression demonstrated in this chapter further suggests that complement may play direct roles in modulating T cell movement. To fully explore the role of CRC cell-derived C3 in modulating T cell movement, migration-specific assays would be required.

T cell expression of CD69, an early activation marker[443] was unaltered by CRC cell-derived C3 or recombinant C3a, in both experimental set ups. This is supported by a study by Daugan *et al*., where they similarly demonstrated that CD69 expression was unaltered in pre-activated T cells treated with recombinant C3a[394]. These data suggest that complement does not alter CD69 expression *in vitro.* Similarly, no effects on CD45RO were demonstrated here, however at present there are no reports in the literature assessing expression of this activation marker following exposure to tumour-derived or recombinant complement. While only CD62L expression was altered, these data suggest that complement, including tumour cell-derived complement may limit $CD4^+$ T cell activation. In support of this, Kwak *et al.,* have previously demonstrated that in a model of lung cancer, $CD4^+$ and $CD8^+$ T cells were more activated in C3 deficient mice[326]. Study of CRC cell-derived C3 using an *in vivo* model in the future may provide greater insights.

The effector functions of T cell subsets are shaped by the cytokines they produce[424]. Cytokine expression in pre-activated T cells was unchanged by CM from HRA-19 and HCT116 cells following modulation of C3 expression, however, recombinant C3a reduced the MFI of IL-4 expressed by $CD3^+$ and $CD8^-$ T cells. IL-4 is a cytokine with an important

role in humoral immunity, produced by Th2 cells alongside IL-10 and IL-5[444]. Th2 cells can inhibit the pro-inflammatory functions of Th1 cells, shifting the immune response towards pro-tumour[445,446] These data suggest that when pre-activated T cells are exposed to complement it promotes a pro-inflammatory, anti-tumour immune response. Similar effects were demonstrated when T cells were exposed to CRC cell-derived C3 during activation. A significant decrease in the percentage of $CD8^-$ T cells expressing IL-4 during activation, resulted from co-culture with CM from HCT116 cells overexpressing C3. Th2 cytokines have been implicated in complement-mediated tumour progression. The lung is a common site of metastasis for breast cancer, with pulmonary mesenchymal stromal cells (MSCs) playing an essential role in facilitating the development of pre-metastatic niches[447]. Recently, Th2 cytokines have been demonstrated to induce C3 expression in MSCs, which recruits neutrophils leading to neutrophil extracellular trap formation and subsequent metastasis in the lung[447]. Therefore, the results presented here demonstrating that both recombinant and CRC cell-derived complement lowers IL-4 expression, suggests that tumour-derived complement may favour the induction of a pro-inflammatory immune response. These alterations in the expression of Th2-like cytokines may also have wider anti-tumour effects within the TME, such as limiting complement expression in stromal cells that potentially promotes tumour progression.

Changes in IFN-γ expression further support the observation that complement may promote a pro-inflammatory, Th-1 like immune response. IFN-γ is a multifunctional cytokine, promoting both $CD4^+$ and $CD8^+$ T cell responses, which positively impact cancer patient survival outcomes[448]. Increased numbers of $CD8^+$ T cells expressed IFN-γ following co-culture with CM from C3 overexpressing HCT116 cells, during activation, suggesting that HCT116-derived C3 promotes expression of IFN-γ. This is in contrast with murine lung[326] and colon[362] cancer models, whereby C3 deficiency was associated with increased numbers of IFN-γ^+ T cells. However, these studies differ in terms of model and set up, when compared to this *in vitro* study, which lacks additional immune or TME influences and may account for the differences observed. In further support of a pro-inflammatory role for complement in T cell cytokine production, CM from C3 overexpressing HCT116 cells also increased IL-17A production in $CD8^+$ T cells. IL-17A has contradictory roles in tumourigenesis, with both pro- and anti-tumour functions associated with $CD8^+$ T cells[449]. As IL-17A has been reported to have anti-tumour functions

when secreted in combination with IFN-γ, overall the trend in these results suggests CRC cell-derived C3 potentially promotes an anti-tumour response.

No alterations in IL-10 expression were induced by recombinant or CRC cell-derived complement, suggesting that complement does not affect IL-10 production. However, previous studies have demonstrated that autocrine production of C3 by $CD8^+$ T cells inhibits IL-10 production[320,362]. Again, these contrasting results may be a feature of the models used. As these experiments were performed using CM generated from CRC cell lines, future *in vitro* studies may yield further insights if T cells were co-cultured directly with CRC cells themselves following C3 silencing or overexpression. This may more closely recapitulate T cells coming into contact with tumour-derived complement within the TME. Using different ratios of T cells to CRC cells would be useful to model tumours with varying degrees of immune infiltration. As the *in vitro* culture used here is devoid of other immune influences, elucidating the full extent of the effects of CRC cell-derived complement on T cell phenotype would require an *in vivo* model. Given that interactions between T cells and APCs produce complement components that are indispensable for normal function, it seems plausible to suggest that investigating the effects of tumour-derived complement on T cell phenotype require T cells to be in a setting where this normal complement activity can also take place. Furthermore, an important consideration for future studies is the expression of complement within the lymph node itself, and how this affects T cell phenotype. In lymph node metastases arising from luminal breast cancer, expression of C3 is reduced relative to the primary tumour, providing evidence for alterations in complement gene expression during cancer progression[450]. The contribution of complement derived from secondary tumour sites, and whether this may be enhanced by complement which drains from the primary tumour, has largely been unexplored in *in vivo* studies.

To conclude, data presented in this chapter aligns with existing literature demonstrating that complement can function in maintaining T cells in a naïve state, with both recombinant and CRC cell-derived C3 observed to decrease expression of CD62L on $CD4^+$ cells. While this would suggest that complement does not boost effector function, assessment of T cell cytokine expression demonstrated that complement potentially shifts T cell responses away from Th2-like towards an IFN-γ producing, Th1-like phenotype. No effect on T cell proliferation was demonstrated by either tumour cell-derived or recombinant complement, however this may be a feature of the model used. Collectively,

these results demonstrate that CRC cell-derived C3 has the ability to modulate T cell phenotype (**Fig. 4-26**), which may have implications for the pathogenesis and treatment response of CRC.

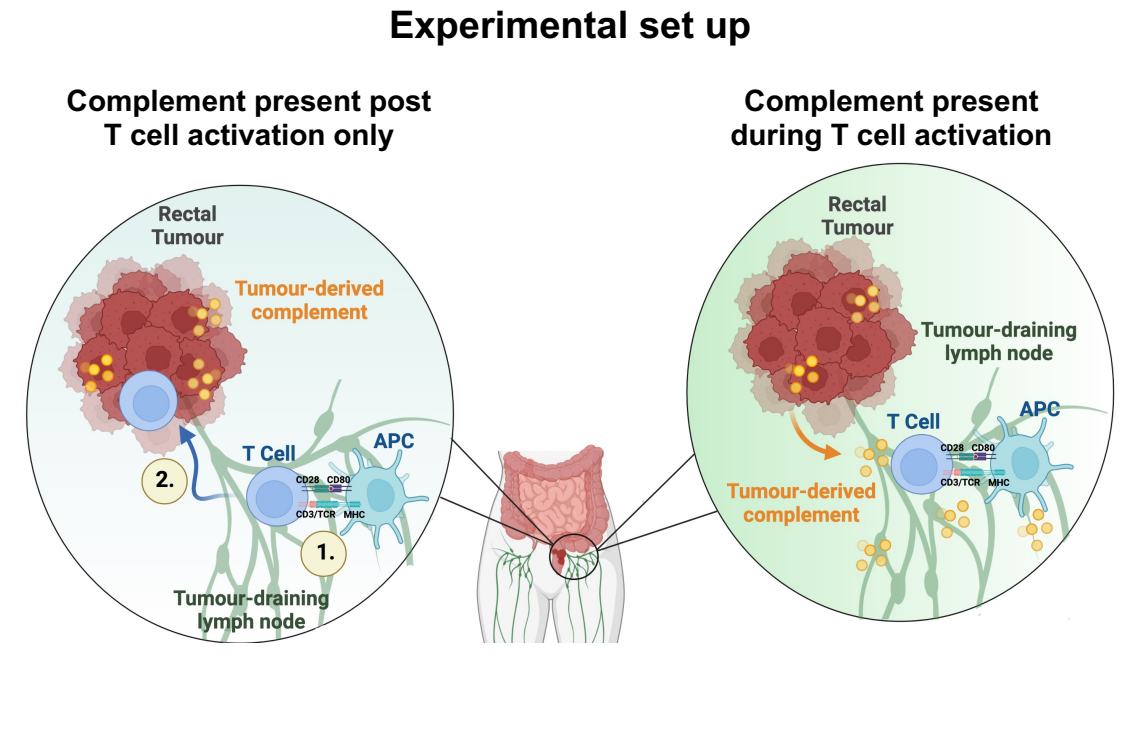

Summary of Results

	HRA-19 siC3 conditioned media	HCT116 C3 conditioned media	Recombinant C3a		HRA-19 siC3 conditioned media	HCT116 C3 conditioned media	Recombinant C3a
Viability	↑ Early stage apoptosis	No effect	↑ Early stage apoptosis ↓ Late stage apoptosis / death	**Viability**	↓ Late stage apoptosis / death ↓ Necrosis	No effect	↓ Late stage apoptosis / death
Activation	No effect	No effect	↑ % $CD4^+$ $CD62L^+$ cells	**Activation**	↓ MFI CD62L $CD3^+$ and $CD4^+$ cells	No effect	↑ % $CD3^+$ & $CD4^+$ $CD62L^+$ cells ↑ MFI CD62L $CD3^+$ & $CD4^+$ cells ↑ % $CD45RA^+$ $CD4^+$ cells
Cytokine Expression	No effect	No effect	↓ MFI IL-4 $CD3^+$ and $CD8^-$ cells	**Cytokine Expression**	No effect	↑ % $CD8^+$ $IFN\gamma^+$ cells ↑ MFI IL-17A $CD8^+$ cells ↓ MFI IL-4 $CD3^+$ and $CD8^-$ cells	No effect

Figure 4-26: CM from HCT116 cells overexpressing C3, CM from C3 silenced HRA-19 cells and recombinant C3a alters T cell phenotype. Summary of results based on two experimental set ups; C3/C3a present post T cell activation only, or if C3/C3a is present during T cell activation.

Chapter 5: Characterisation of complement in pre-treatment tumour biopsies and sera from rectal cancer patients

5.1. Introduction

Rectal cancer significantly contributes to the global cancer burden. Of the approximately 1.9 million new global cancer cases in 2020, more than 700,000 occurred in the rectum[1]. In Ireland, rectal cancers account for approximately one third of all CRCs diagnosed[2]. Furthermore, CRC accounts for 10% of all cancer-related deaths, with rectal cancer responsible for over 300,000 global deaths in 2020 alone[2]. Worryingly, the incidence of CRC is rising, with new diagnoses projected to surpass 3 million in 2040[5]. CRC is increasing in particular in younger people (<50 y), with more of these patients presenting with tumours in the rectum as opposed to the colon[7,8].

For patients with locally advanced rectal cancer, the current standard of care is neo-CRT followed by total mesorectal excision, which involves surgical excision of the rectum including mesorectal fat and the pararectal lymph nodes[21]. Neo-CRT consists of short course RT (SCRT) (25 Gy in 5 Gy fractions, delivered over one week) or long course RT (LCRT) (45-50 Gy delivered in 25-28 fractions over several weeks), and chemotherapy[21]. Oral capecitabine and/or 5-fluorouracil (5-FU), delivered via continuous intravenous infusion rather than a bolus dose, are the recommended chemotherapy agents[21,51].

The addition of neo-CRT prior to surgery aims to reduce local recurrence rates post-surgery. Neo-CRT can aid resection by downstaging tumours prior to surgery, however LCRT has been demonstrated to achieve increased rates of downstaging relative to SCRT[451]. The tumour response to neo-CRT is assessed pathologically following surgical resection. In Ireland, tumour regression score (TRS) is determined using the modified Ryan tumour regression grading system. This score is a 4-point grading system based on the recommendations outlined by the American Joint Committee of Cancer[52]. TRS 0 (a complete response) is defined as no viable tumour cells, TRS 1 (a near-complete response) refers to single or small groups of cancer cells, TRS 2 (a partial response) describes evident tumour regression with evidence of residual tumour beyond single or groups of cancer cells and TRS 3 (a poor or no response) defines residual cancer that is extensive, with no evidence of tumour regression[452]. Rectal cancer patients who achieve a pCR (TRS 0) following neo-CRT have significantly improved disease-free and overall survival[53]. Unfortunately, a pCR is limited to less than 30% of rectal cancer patients who receive neo-CRT[21,55,56]. This means that the majority of patients are subject to therapeutic-toxicities without apparent therapeutic benefit. Additionally, the delay to surgery while neo-CRT is administered may allow time for disease progression, leading to more advanced tumours that are more difficult to resect. The ability to predict prior to initiation of treatment those

patients who are likely to respond to treatment and conversely those patients who are likely to be resistant to treatment, for improved patient stratification, would be of significant clinical benefit. A variety of biomarkers spanning clinical and histopathological features, the TME and molecular markers have demonstrated some degree of predictive ability in the response to neo-CRT in rectal cancer[453]. Despite this, no single or combination biomarker has been clinically approved by the United States Food and Drug Administration (FDA) to indicate prior to the initiation of neo-CRT, whether a patient is likely to respond.

For the majority of patients who are resistant to the current standard of care, there are no alternative treatment options. Therefore, there is an unmet global need to identify novel therapeutic targets to enhance the radiosensitivity of rectal tumours to neo-CRT, and boost treatment outcomes for rectal cancer patients. Total mesorectal excision is a major procedure and is associated with increased risk of perioperative mortality and morbidity and has long term impacts on the quality of life for cancer survivors[454]. Therefore, there is an increasing interest in the identification of treatment strategies that can facilitate organ preservation[455]. Previously, accurate detection of response to neo-CRT was only possible post-surgery, by pathological examination of the resected specimen. More recently, evidence suggests that stringent clinical examination following neo-CRT may reliably identify patients with a complete clinical response (cCR)[58]. In this instance, endoscopic or radiologic assessment of patients does not detect residual tumour[53]. This presents a potential opportunity to employ a wait-and-see-strategy as an alternative to immediate total mesorectal excision after neo-CRT. Motivation for a wait-and-see policy includes the avoidance of patient overtreatment[58] and reduction of total mesorectal excision-associated impairments in bowel, urinary and sexual function[59,60]. Several large studies have demonstrated that in patients identified using strict selection criteria it may be a safe management option, providing adequate follow-up takes place[53,61]. Similar recurrence rates and outcomes have been reported in wait-and-see and surgically resected patient cohorts[61–63]. With this in mind, the ability to identify novel therapeutic targets to improve tumour responses to neo-CRT in rectal cancer may have the ability to increase the number of patients who can be managed using a wait-and-see strategy, subsequently reducing patient overtreatment and improving survival and quality of life for patients.

Expression of components of the complement system in cancer have been demonstrated to correlate with a variety of clinical and pathological parameters. In primary human tumours, high expression of C5aR has been demonstrated to correlate with vascular invasion[310]. C4d, a complement activation product, associates with nodal invasion, tumour

differentiation grade and disease stage in oropharyngeal squamous cell carcinoma[275]. In breast cancer, expression of C5aR correlates with larger tumours, lymph node metastasis and advanced clinical stages[319]. While these studies suggest a potential role for complement components as biomarkers of aggressive disease, a number of studies have also highlighted that expression of complement components are associated with survival outcomes. A study of gastric cancer patients demonstrated that patients with high tumour expression of C5aR had a significantly reduced 5-year OS[383]. Similarly in breast cancer, patients with C5aR positive tumours had poorer survival than patients with C5aR negative tumours[319]. Expression of C3aR has similarly been demonstrated to correlate with decreased OS, in lung and ovarian tumours[300]. The prognostic significance of complement expression appears to be largely context-dependent[456].

Aberrant expression of complement components has also been demonstrated to have biomarker potential in response to anti-cancer therapy. Assessment of differentially expressed genes in soft tissue sarcomas with varying sensitivities to chemotherapy, demonstrated that complement cascade genes including C3aR, C1QC and CFI were significantly upregulated in chemoresistant tissues, when compared to chemosensitive tissue[365]. Neo-CRT prior to surgery is also a mainstay of treatment for OAC patients with resectable, locally-advanced disease[457]. In a previous study performed in our Department, high expression of C3 in pre-treatment OAC tumour biopsies was associated with subsequent poor responses to neo-CRT[368].

In addition to tumoural expression, circulating levels of complement components have demonstrated potential as prognostic or predictive biomarkers. While tumoural biomarkers have clinical potential to inform and support the design of patient treatment plans, circulating biomarkers represent a more convenient, less invasive and potentially more cost-effective option[458]. A study investigating chemoresistance in ovarian cancer has demonstrated that plasma levels of C3 were decreased, while C4-A was increased, in patients who were resistant to platinum-based chemotherapy, when compared to patients with chemosensitive tumours[459]. Furthermore, isoforms of C3 and C4 in the plasma of breast cancer patients have been demonstrated to correlate with response to neoadjuvant chemotherapy[366]. Evidence has also been presented for complement as a circulating biomarker in the response to immune checkpoint inhibitors (ICI). In renal cell carcinoma, poor responses to nivolumab (anti-PD-1) or nivolumab in combination with ipilimumab (anti-CTLA-4), were associated with increased plasma levels of complement factor D and CFH and decreased levels of C5b-9 and CFI. Reduced C5b-9 levels in combination with

elevated C5a additionally predicted worse responses to ICI[460]. Previous work in our Department also demonstrated that pre-treatment sera levels of C3a and C4a were elevated in OAC patients with subsequent poor pathological responses to neo-CRT, when compared to those who had good responses[367]. This suggests that complement anaphylatoxins may have potential as circulating biomarkers of response to neo-CRT.

Data presented in Chapters 2 and 3 demonstrates that complement components are increased in radioresistant rectal cancer cells and that C3 plays a functional role in the tumoural response to radiation. However, the circulating and tumoural expression of complement components in rectal cancer patients is largely unknown. Therefore, the aim of this chapter was to profile key complement components in pre-treatment tumour tissue and sera from rectal cancer patients, and rectal tissue samples from non-cancer controls to determine if alterations in complement levels are associated with key clinicopathological factors including response to neo-CRT and prognosis.

5.2. Specific aims of Chapter 5

This chapter aimed to characterise complement in pre-treatment tumour biopsies and sera from rectal cancer patients and determine if there is a relationship between complement and key clinicopathological factors including response to neo-CRT and prognosis.

The specific aims of Chapter 5 are:

1. Assess the expression of central complement cascade components (C3, C5) and complement activation pathway components (CFB, C1q, MBL2) in pre-treatment rectal tumour biopsies and normal non-cancer rectal tissue to determine if complement expression is altered in rectal cancer.
2. Investigate the relationship between tumoural complement expression and key clinicopathological factors including pathological tumour stage, Body Mass Index (BMI) and TRS.
3. Investigate the relationship between tumour and circulating levels of C3 in a pilot cohort of rectal cancer patients.
4. Assess the relationship between C3 and IL-6 in sera and tumour conditioned media (TCM) from rectal cancer patients.
5. Investigate the relationship between circulating complement components (C3, C3a, C5, C5a and C5b-9) in pre-treatment sera from rectal cancer patients and key clinicopathological factors including pathological tumour stage, BMI, TRS and prognosis.

5.3. Materials and methods

5.3.1. Patient recruitment and ethical approval

Two patient cohorts were utilised in this chapter. The analyses performed on each of these cohorts is outlined in **Figure 5-1**.

5.3.1.1. St James's Hospital/Beacon Hospital, Dublin patient cohort

Following Ethical approval (Joint St. James's Hospital / AMNCH ethical review board and the Beacon Hospital Research Ethics Committee) and written informed consent, sera and rectal tumour tissue were taken from rectal cancer patients and normal non-cancer rectal tissue was taken from healthy controls undergoing colonoscopy for symptoms including unexplained rectal bleeding and changes in bowel habit, between January 2018 and August 2021, at St James's Hospital and Beacon Hospital, Dublin. Samples from cancer patients were obtained prior to neo-CRT. All patient data was pseudo-anonymised and given a unique biobank identifier.

5.3.1.2. OxyTarget patient cohort

Following Ethical approval (Regional Committee for Medical and Health Research Ethics of South-East Norway (reference number REK 2013/152) and the Institutional Review Board (reference number 12-106)) and written informed consent, sera samples were taken from rectal adenocarcinoma patients between October 2013 and November 2017, at Akershus University Hospital (Lørenskog, Norway) (ClinicalTrials.gov NCT01816607) prior to neo-CRT.

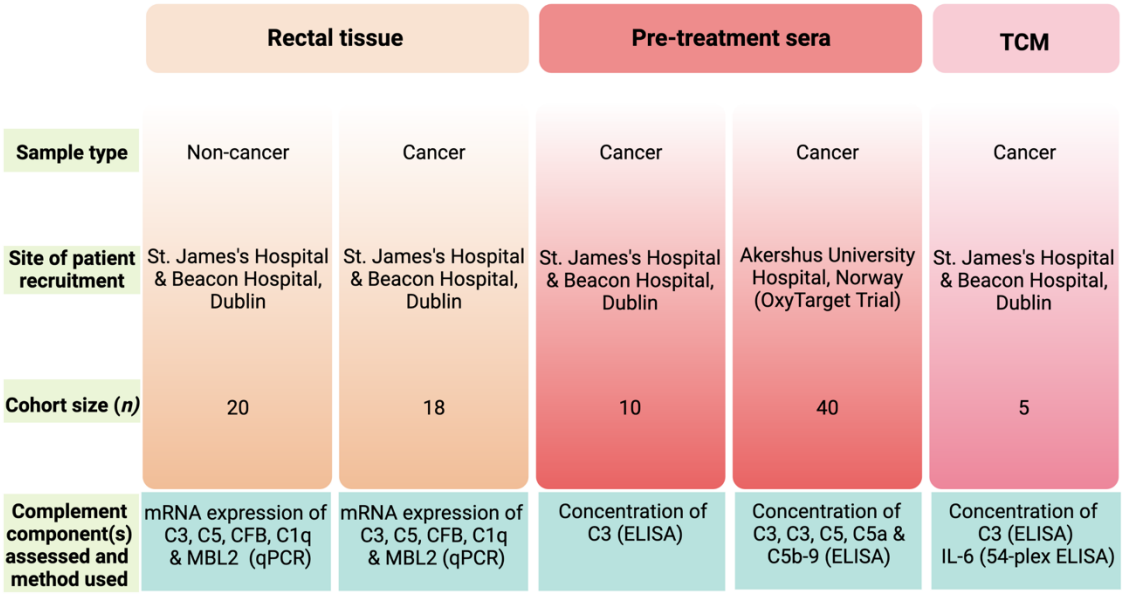

Figure 5-1: Overview of patient cohorts. Non-cancer and pre-treatment rectal cancer tissue, pre-treatment sera from rectal cancer patients and TCM generated from rectal tumour biopsies were utilised for experiments in this chapter. The site of patient recruitment, the cohort size, the complement components assessed and methods used are outlined.

5.3.2. Patient treatment

5.3.2.3. St James's Hospital/Beacon Hospital patient cohort

Patients were treated according to the prevailing national guidelines with neo-CRT and radical pelvic surgery. Chemotherapy consisted of FOLFOX (leucovorin, 5-FU, oxaliplatin) or FOLFIRI (leucovorin, fluorouracil, irinotecan hydrochloride). RT was delivered in 28 fractions of 1.8 Gy.

5.3.2.4. OxyTarget patient cohort

Patients were treated according to the prevailing national guidelines with neo-CRT and radical pelvic surgery. The absence of metastatic disease at the time of diagnosis was established on CT scans of the thoracic and abdominal cavities. Chemotherapy consisted of capecitabine, FLOX (fluorouracil, leucovorin, oxaliplatin) or FLV (5-FU, leucovorin). RT was delivered in either 25 fractions of 2 Gy, or 5 fractions of 5 Gy. All patients were followed systematically with clinical examination and CT scans at 3, 6, 12, 18 and 24 months and then every year for a total of 5 years after surgery.

5.3.3. Pathological response to neo-CRT

Tumour response to neo-CRT was assessed pathologically using resected rectal specimens. TRS was determined in the St James's Hospital and Beacon Hospital patient cohort using the modified Ryan tumour regression system. In the OxyTarget patient cohort, TRS was assessed using the American Joint Committee of Cancer and College of American Pathologists (AJCC/CAP) system. Both of these grading schemes use the ratio of fibrosis to residual tumour and are identical 4 tier grading systems, where 0 (a complete response) is defined as no viable tumour cells, 1 (a near-complete response) refers to single or small groups of cancer cells, 2 (a partial response) describes tumour regression that is evident to a greater extent than single or groups of cancer cells and 3 (a poor or no response) defines residual cancer that is extensive, with no evidence of tumour regression[452].

5.3.4. Rectal tissue collection and processing

Pre-treatment tumour biopsies were obtained from consenting rectal cancer patients, prior to neo-CRT, and were taken by a qualified endoscopist during diagnostic colonoscopy. Normal (non-cancer) rectal biopsies were obtained from consenting patients undergoing colonoscopy, that did not have cancer. Tissue biopsies were placed in RNAlater (Thermo Fisher Scientific, Massachusetts, United States) and refrigerated at 4°C. After 24 h, RNAlater was removed and biopsies were snap frozen in liquid nitrogen, before being stored at -80°C. Tumour and non-tumour tissue was confirmed using haematoxylin and eosin staining by an experienced GI pathologist.

5.3.5. RNA isolation from tissue biopsies

RNA was isolated using the miRNeasy Mini Kit (Qiagen, Hilden, Germany). Tissue samples were lysed by the addition of 700 µL of QIAzol Lysis Reagent. Samples were pipetted repeatedly to ensure complete lysis, briefly vortexed and incubated for 5 min at RT°. A 140 µL volume of 1-bromo-3-chloropropane was added and the homogenate was shaken for 15 s, before resting for 1 min at RT°. Homogenates were centrifuged for 15 min at 4°C at 12,000 x g to allow for phase separation. The RNA-containing, upper, aqueous phase was carefully removed to a new 1.5 mL eppendorf. A 525 µL volume of ethanol was added to each eppendorf, and samples were mixed by repeated pipetting. RNeasy spin columns were placed in 2 mL collection tubes and 700 µL of each sample was transferred. Tubes were centrifuged for 15 s at RT° at 10,000 x g. The flow-through was discarded and

the remaining samples were added to the spin columns and centrifuged as before. To wash, 700 µL of RWT buffer was added to each spin column before centrifugation for 15 s at RT° at 10,000 x g. A 500 µL volume of RPE buffer was then added to each spin column before centrifugation again for 15 s at RT° at 10,000 x g. This was repeated, instead with centrifugation for 2 min at RT° at 10,000 x g, to dry the spin column membrane. To elute the RNA, spin columns were transferred to new collection tubes and 30 µL of RNase-free H_2O was added to each column, before centrifugation for 1 min at full speed, at RT°. RNA was quantified as previously described (Section 2.3.14).

5.3.6. Assessing rectal tissue expression of complement components

Gene expression of C3, C5, CFB, C1q and MBL2 was assessed by qPCR. RNA isolated from tissue biopsies (Section 5.3.5) was reverse transcribed to cDNA (Section 2.3.15), which was used as the template for qPCR. qPCR was performed as outlined in Section 2.3.16, using Taqman™ gene-specific primers (Applied Biosystems). Results were analysed using the qPCR Relative Quantification App on the ThermoFisher Connect™ platform (Section 2.3.17).

5.3.7. Processing of whole blood to isolate serum

Pre-treatment blood samples were obtained from consenting rectal cancer patients attending St James's Hospital, Dublin and Beacon Hospital, Dublin. To isolate serum, blood tubes were centrifuged at 3,000 RPM for 10 min at RT°. Serum was carefully removed from the top of the blood tubes using a pipette, and added to 2 mL eppendorf tubes in 1 mL aliquots. Serum samples were stored at -80° until required. Serum samples obtained from the OxyTarget patient cohort had already been isolated from whole blood so did not require further processing.

5.3.8. Assessing circulating levels of complement components

The circulating levels of complement components in pre-treatment sera was assessed using several ELISAs. Details of the ELISAs used and the dilution factor of sera that was performed for each assay is outlined in **Table 5-1**.

All ELISAs were performed according to the manufacturer's instructions. Following the specified incubation times, ELISA plates were read using a GloMax® Explorer Multimode Plate Reader (Promega, Wisconsin, United States). Graphical and

statistical analysis was performed using GraphPad Prism and standard curves were constructed using the absorbance readings of the standards. This standard curve was used to interpolate the absorbance readings of sera samples to determine the concentration of complement components present in these samples.

Table 5-1: Details of ELISAs used to assess circulating levels of complement components.

Complement Component	Manufacturer	Dilution Factor
C3	Abcam (Cambridge, United Kingdom)	1:800 in 1 X Diluent M (from kit)
C3a	Invitrogen (Massachusetts, United States)	1:5000 in 1 X Assay Buffer (from kit)
C5	Abcam (Cambridge, United Kingdom)	1:80,000 in 1 X Diluent N (from kit)
C5a	Abcam (Cambridge, United Kingdom)	1:40 in 1 X Assay Diluent A (from kit)
C5b-9	Novus Biologicals (Minnesota, United States)	1:10 in Sample Diluent (from kit)

5.3.9. TCM generation

TCM was generated from fresh pre-treatment rectal tumour biopsies. Within 30 min of sampling, biopsies were washed gently four times in PBS supplemented with 1% penicillin-streptomycin, 1% Fungizone® (amphotericin B) and 0.1% gentamicin. In a 12-well plate, each biopsy was then incubated in 1 mL of M199 medium supplemented with 10% FBS, 1% penicillin-streptomycin, 1% Fungizone®, 0.1% gentamicin and 1 µg/mL insulin for 24 h at 37°C, 5% CO_2/ 95% humidified air. After 24 h, TCM was collected and biopsies were removed and snap-frozen in liquid nitrogen. Both the TCM and snap frozen biopsies were stored at -80°C until required.

5.3.10. Determining IL-6 levels in sera and TCM

The level of IL-6 was assessed in the OxyTarget sera cohort using a custom Luminex (Luminex Corporation, Texas, United States) multi-plex assay. This was performed by Dr Sebastian Meltzer in Akershus University Hospital (Lørenskog, Norway).

The level of IL-6 in TCM generated from pre-treatment rectal cancer biopsies was assessed using the V-Plex Proinflammatory Panel 1 Human Kit, from the Meso Scale Diagnostics (MSD) (Maryland, United States) Human Biomarker 54-plex kit. The assay was performed as instructed by the manufacturer's guidelines, and incubations were performed overnight. TCM samples were assessed neat. Data was normalised to protein

concentration of the biopsies used to generate the TCM, as assessed by BCA assay (Section 2.3.20).

5.3.11. Determining the level of C3 in TCM

The level of C3 in TCM (generated as outlined in Section 5.3.9) was assessed by ELISA (Abcam). TCMs were assessed neat and the ELISA was performed according to the manufacturer's instructions. The plate was read using a GloMax® Explorer Multimode Plate Reader (Promega, Wisconsin, United States). Graphical and statistical analysis was performed using GraphPad Prism and standard curves were constructed using the absorbance readings of the standards. This standard curve was used to interpolate the absorbance readings of the TCM samples to determine the concentration of complement components present in these samples. TCM samples exceeded the standard curve so relative absorbance readings were obtained. Relative absorbances were normalised to protein concentration of the biopsies used to generate the TCM, as assessed by BCA assay (Section 2.3.20).

5.3.12. Statistical analysis

Graphing of results and statistical analysis was performed using Prism 9 Software (GraphPad, California, United States). All data are presented as mean ± SEM, unless otherwise indicated. Significance was determined by ANOVA with post-hoc Tukey's multiple comparisons testing or Student's *t*-test, as detailed in figure legends. Where comparison groups were paired (i.e. untreated vs. treated), a paired *t*-test was performed, otherwise unpaired *t*-tests were used. Results were considered significant where $p \leq 0.05$. Correlations were performed using Pearson's correlation coefficient.

Data analysis of the central complement components C3 and C5 and their respective anaphylatoxins, C3a and C5a, was performed by Andrew Sheppard (Dept. of Surgery, TCD) using R Studio.

The probability of recurrence-free survival (RFS) and OS data was determined in accordance with the REMARK checklist[461], as encouraged by the equator network, by performing Cox regression analysis and the Kaplan-Meier (log-rank) test using the median as a cut-off. This was performed by Dr Sebastian Meltzer (Akershus University Hospital, Lørenskog, Norway).

5.4. Results

5.4.1. Expression of C3 and C5 is elevated in rectal tumour biopsies, when compared to non-cancer rectal tissue

Elevated expression of complement components has been reported in several human cancers. To assess whether complement components are altered in rectal tumour tissue, levels of C3 and C5 were assessed in pre-treatment rectal tumour biopsies (*n*=18) and normal non-cancer (confirmed histologically) rectal tissue biopsies (*n*=20) taken from patients undergoing investigative colonoscopy. Rectal cancer patient characteristics are outlined in **Table 5-2**. Non-cancer rectal tissue was obtained from *n*=20 patients (Male *n*=8 Female *n*=12). The non-cancer cohort had an age range of 28-79, with a median age of 54.

Interestingly, relative expression of C3 mRNA was significantly (p = 0.0063) upregulated in rectal tumour tissue, when compared to non-cancer rectal tissue (Mean relative C3 mRNA expression ± SEM; cancer 4.324 ± 0.9351, non-cancer 1.298 ± 0.4938) (**Fig. 5-2 A)**. Similarly, relative expression of C5 mRNA was significantly (p = 0.0023) greater in rectal tumour tissue, when compared to non-cancer rectal tissue (Mean relative C5 mRNA expression ± SEM; cancer 1.747 ± 0.2527, non-cancer 0.7729 ± 0.1669) (**Fig. 5-2 B)**. These data demonstrate that expression of central complement components are increased in rectal tumours in this rectal cancer patient cohort.

5.4.2. Expression of CFB and C1q are differentially altered in rectal tumour biopsies, when compared to non-cancer rectal tissue

Having demonstrated elevated levels of C3 and C5 in rectal tumour tissue, the mRNA expression of Clq, MBL2 and CFB, key factors in the initiating stages of the classical, lectin and alternative complement pathways, respectively, were assessed by qPCR in pre-treatment rectal cancer tissue and normal non-cancer rectal tissue.

MBL2 was not detected in cancer or non-cancer rectal tissue (**Appendix 9**). Relative expression of CFB mRNA was significantly ($p < 0.0001$) greater in rectal tumour tissue, when compared to non-cancer rectal tissue (Mean relative CFB mRNA expression ± SEM; cancer 1.274 ± 0.1904, non-cancer 0.2021 ± 0.0376) (**Fig. 5-2 C)**. In contrast, relative expression of C1q mRNA was significantly (p = 0.0023) reduced in rectal tumour tissue, when compared to non-cancer rectal tissue (Mean relative C1q mRNA expression ± SEM; cancer 4.882 ± 1.916, non-cancer 32.48 ± 8.579) (**Fig. 5-2 D)**. These data suggest that the classical and alternative pathways may be more active in non-cancer and cancerous rectal tissue, respectively.

Table 5-2: Patient characteristics of patient cohort in which tumour biopsies were assessed for complement gene expression.

		Cancer (*n*=18)
Gender	**Male (*n*)**	11
	Female (*n*)	7
Age at diagnosis	**Median (y)**	65.5
	Range (y)	48-89
Histology	**Adenocarcinoma (*n*)**	18
Differentiation	**Poor-moderate (*n*)**	2
	Moderate (*n*)	14
	Well (*n*)	1
	Unknown (*n*)	1
BMI at diagnosis	**Normal (18.5-24.9) (*n*)**	3
	Overweight (25-29.9) (*n*)	5
	Obese (>30) (*n*)	6
	N/A (*n*)	4
Pathological T stage	**0 (*n*)**	5
	1 (*n*)	2
	2 (*n*)	4
	3 (*n*)	6
	N/A (*n*)	1
Treatment received	**Neo-CRT**	16
	Neo-RT	2
TRS (Modified Ryan Scale)	**0 (*n*)**	5
	1 (*n*)	7
	2 (*n*)	4
	3 (*n*)	1
	N/A (*n*)	1

Abbreviations; BMI, body mass index; CRT, chemoradiation therapy; N/A, not available; neo, neo-adjuvant; RT, radiation therapy; TRS, tumour regression score; T stage, tumour stage; y, years.

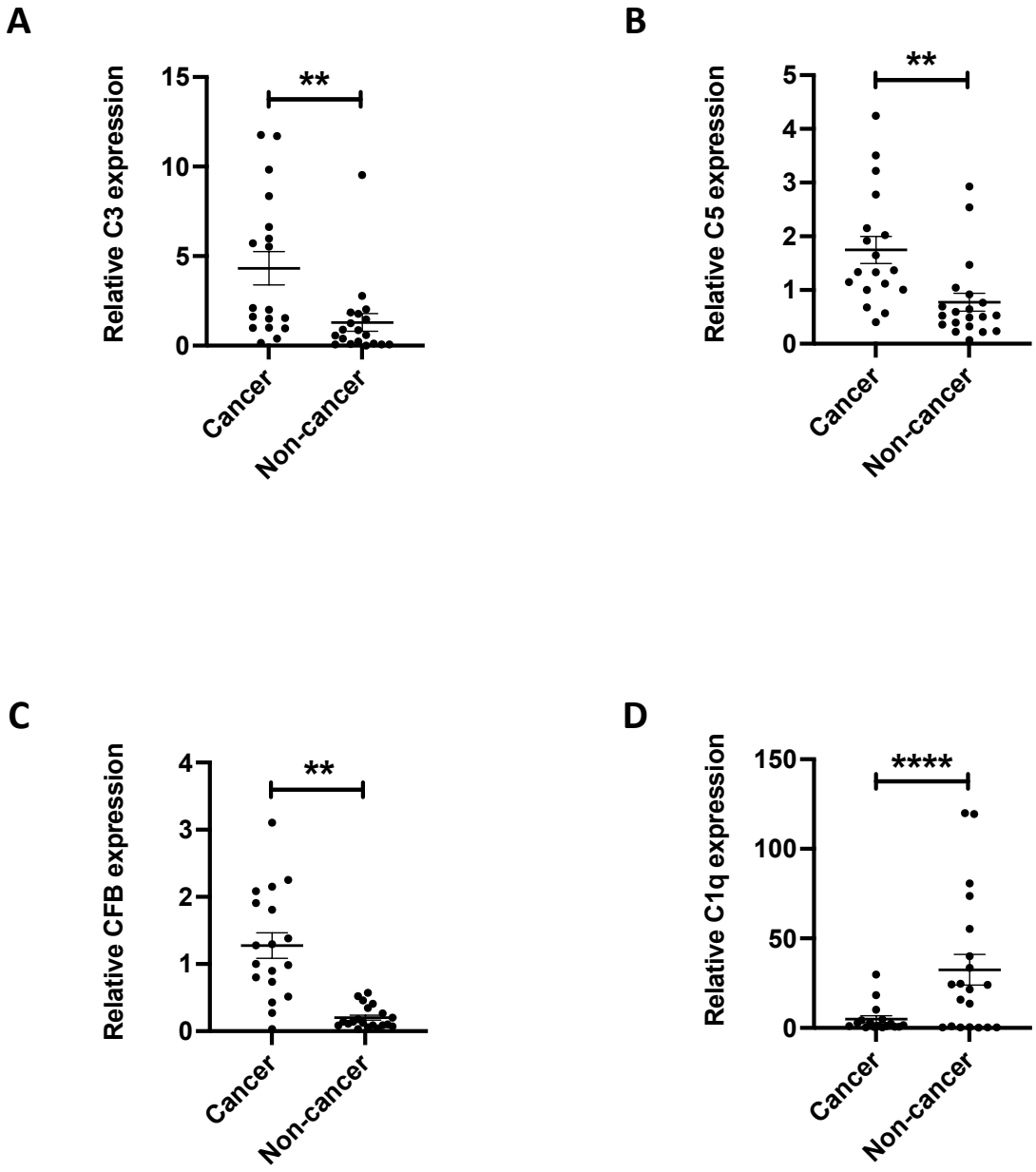

Figure 5-2: Expression of complement components differs in rectal tumour tissue and non-cancer rectal tissue. Expression of C3, C5, CFB and C1q in pre-treatment rectal cancer tissue (n=18) and non-cancer rectal tissue (n=20) was assessed by qPCR. Statistical analysis was performed by unpaired two-tailed Student's t-test. **$p < 0.01$, ****$p < 0.0001$.

5.4.3. Expression of C3 and C5 in pre-treatment rectal tumour biopsies does not correspond with subsequent pathological response to neo-CRT

Having demonstrated that the expression of complement components is altered in rectal tumour tissue, when compared to normal non-cancer rectal tissue, the relationship between complement expression in tumour tissue and subsequent TRS was explored. Expression of C3 and C5, two central complement cascade components was assessed at the gene level in pre-treatment rectal tumour biopsies (n=18) using qPCR and correlated with subsequent pathological response (TRS) to neo-CRT. Patient cohort characteristics are outlined in **Table 5-2**, and TRS was available for n=17 patients.

Expression of C3 (**Fig. 5-3 A**) or C5 (**Fig. 5-3 B)** mRNA was similar in tumours from patients achieving a subsequent TRS 0, 1, 2 or 3. As this patient cohort was relatively small, patients were also grouped based on a good (TRS 0 or 1) or poor (TRS 2 or 3) response to neo-CRT. No trends in C3 or C5 expression were demonstrated when TRS 0-1 (n=12) vs TRS 2 (n=4) (**Fig. 5-3 C-D**), TRS 0-1 (n=12) vs TRS 2-3 (n=5) (**Fig. 5-3 E-F**), TRS 1 (n=7) vs TRS 2 (n=4) (**Fig. 5-3 G-H**), or TRS 0 (n=5) vs TRS 2 (n=4) (**Fig. 5-3 I-J**) were compared.

These data demonstrate that at the mRNA level, C3 and C5 expression in pre-treatment rectal tumour biopsies is not associated with subsequent TRS in this cohort of rectal cancer patients.

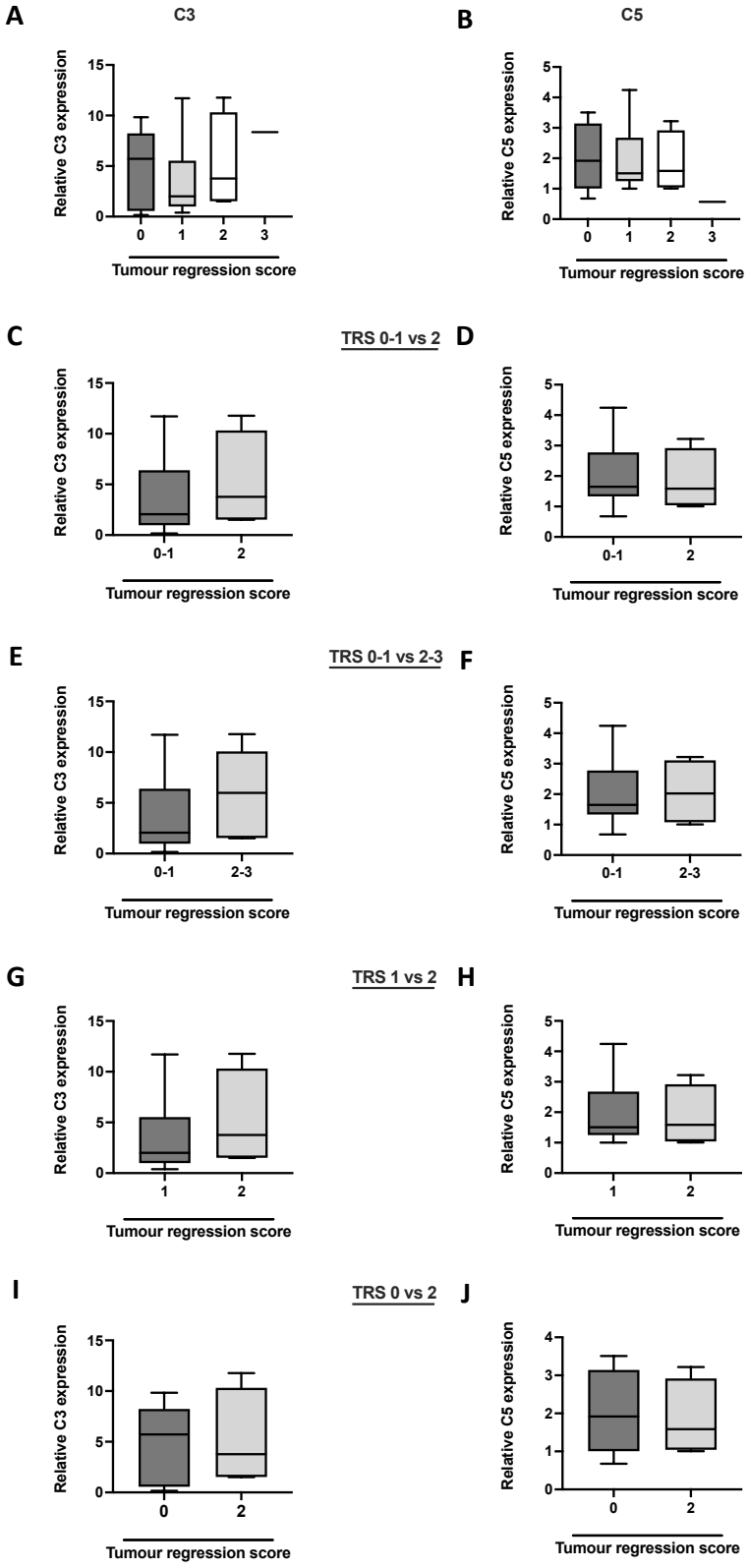

Figure 5-3: Tumour expression of central complement cascade components does not correlate with TRS in rectal cancer. Relative **(A)** C3 and **(B)** C5 mRNA expression levels were assessed in pre-treatment rectal cancer biopsies (*n*=18), TRS 0 *n*=5, TRS 1 *n*=7, TRS 2 *n*=4, TRS 3 *n*=1. **(C-D)** Relative C3 and C5 mRNA expression in patients with TRS 0-1 vs 2, (**E-F)** TRS 0-1 vs 2-3, (**G-H)** TRS 1 vs 2 and (**I-J)** TRS 0 vs 2 was compared. Statistical analysis was performed by unpaired two-tailed Student's *t*-test.

5.4.4. Expression of complement activation pathway components in pre-treatment rectal tumour tissue does not correspond with subsequent pathological response to neo-CRT

Having assessed the mRNA expression of Clq, MBL2 and CFB, key factors in the initiating stages of the classical, lectin and alternative complement pathways, respectively, in pre-treatment rectal cancer tissue by qPCR, the relationship with subsequent TRS was investigated. Patient cohort characteristics are outlined in **Table 5-2**, and TRS was available for *n*=17 patients.

MBL2 mRNA was not detected in rectal cancer tissue (**Appendix 9**). Expression of C1q (**Fig. 5-4 A**) and CFB (**Fig. 5-4 B)** mRNA was similar in tumours from patients with a subsequent TRS of 0, 1, 2 or 3. Patients were grouped based on a good (TRS 0 or 1) or poor (TRS 2 or 3) response to neo-CRT. No trends in C1q or CFB expression were demonstrated when TRS 0-1 (*n*=12) vs TRS 2 (*n*=4) (**Fig. 5-4 C-D**), TRS 0-1 (*n*=12) vs TRS 2-3 (*n*=5) (**Fig. 5-4 E-F**), TRS 1 (*n*=7) vs TRS 2 (*n*=4) (**Fig. 5-4 G-H**), or TRS 0 vs TRS 2 (*n*=4) (**Fig. 5-4 I-J**) were compared.

These data demonstrate that at the mRNA level, C1q and CFB expression does not associate with TRS, suggesting that C1q and CFB mRNA expression is not predictive of subsequent response to neo-CRT in this cohort of rectal cancer patients.

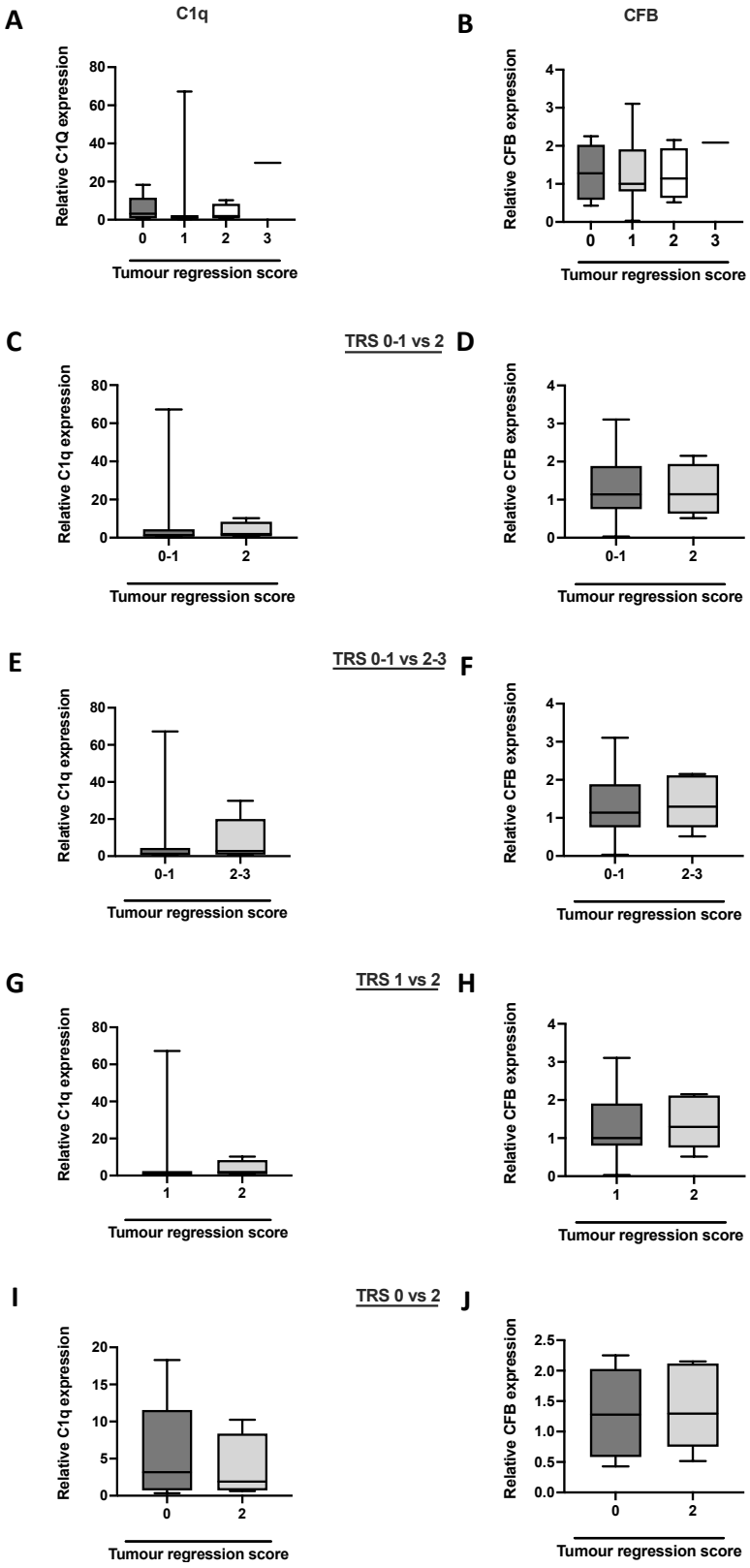

Figure 5-4: Tumour expression of classical and alternative pathway components is not associated with TRS in rectal cancer. Relative **(A)** C1Q and **(B)** CFB mRNA expression levels were assessed in pre-treatment rectal cancer biopsies (*n*=18), TRS 0 *n*=5, TRS 1 *n*=7, TRS 2 *n*=4, TRS 3 *n*=1. **(C-D)** Relative C1Q and CFB mRNA expression in patients with TRS 0-1 vs 2, (**E-F)** TRS 0-1 vs 2-3, (**G-H)** TRS 1 vs 2 and (**I-J)** TRS 0 vs 2 was compared. Statistical analysis was performed by unpaired two-tailed Student's *t*-test.

5.4.5. Expression of central complement components is not associated with expression of complement activation pathway components in rectal tumour tissue

To investigate whether there was a relationship between tumour expression of the central complement components C3 and C5 in rectal cancer tissue, a simple linear regression was performed. Relative C3 mRNA expression did not significantly correlate with relative C5 mRNA expression (p = 0.5479) (**Fig. 5-5 A**). This may suggest the relationship between C3 and C5 mRNA expression in rectal cancer tissue is not linear.

Having demonstrated that classical (C1q) and alternative (CFB) activation pathway components are expressed by rectal cancer tissue, their expression was correlated with C3 and C5 expression to assess whether complement expression is associated with a particular activation pathway. Relative expression of C3 positively correlated with relative CFB expression, but the trend didn't reach statistical significance (p = 0.0506) (**Fig. 5-5 B**). There was no correlation between relative C5 and CFB expression (**Fig. 5-5 C**). Relative C1q mRNA expression did not correlate with the relative expression level of C3 mRNA (**Fig. 5-5 D**) or C5 mRNA (**Fig. 5-5 E**) mRNA. These data suggest that in this rectal cancer patient cohort, tumoural expression of C3 may be associated with CFB at the mRNA level, suggesting the alternative pathway as a pathway of activation in rectal tumours.

5.4.6. Expression of C3, C5, C1q or CFB does not associate with pathological tumour stage in rectal cancer.

To assess whether expression of central complement components is elevated in patients with advanced tumour stages, relative C3 and C5 mRNA expression was assessed in patients based on pathological tumour stage. Expression of C3 (**Fig. 5-6 A**) and C5 (**Fig. 5-6 B**) was similar in patients with a pathological tumour stage of 0 (n=5), 1 (n=2), 2 (n=4) or 3 (n=6). This suggests that expression of C3 and C5 in pre-treatment tumour biopsies is not associated with pathological tumour stage in this cohort of rectal cancer patients.

To assess whether expression of complement components from the alternative and classical pathways is elevated in patients with advanced tumour stages, relative expression of CFB and C1q mRNA was assessed in patients based on pathological tumour stage.

Expression of CFB (**Fig. 5-6 C**) and C1q (**Fig. 5-6 D**) was similar in patients with a pathological tumour stage of 0, 1, 2 or 3. This suggests that expression of complement activation pathway components is not associated with pathological tumour stage in this cohort of rectal cancer patients.

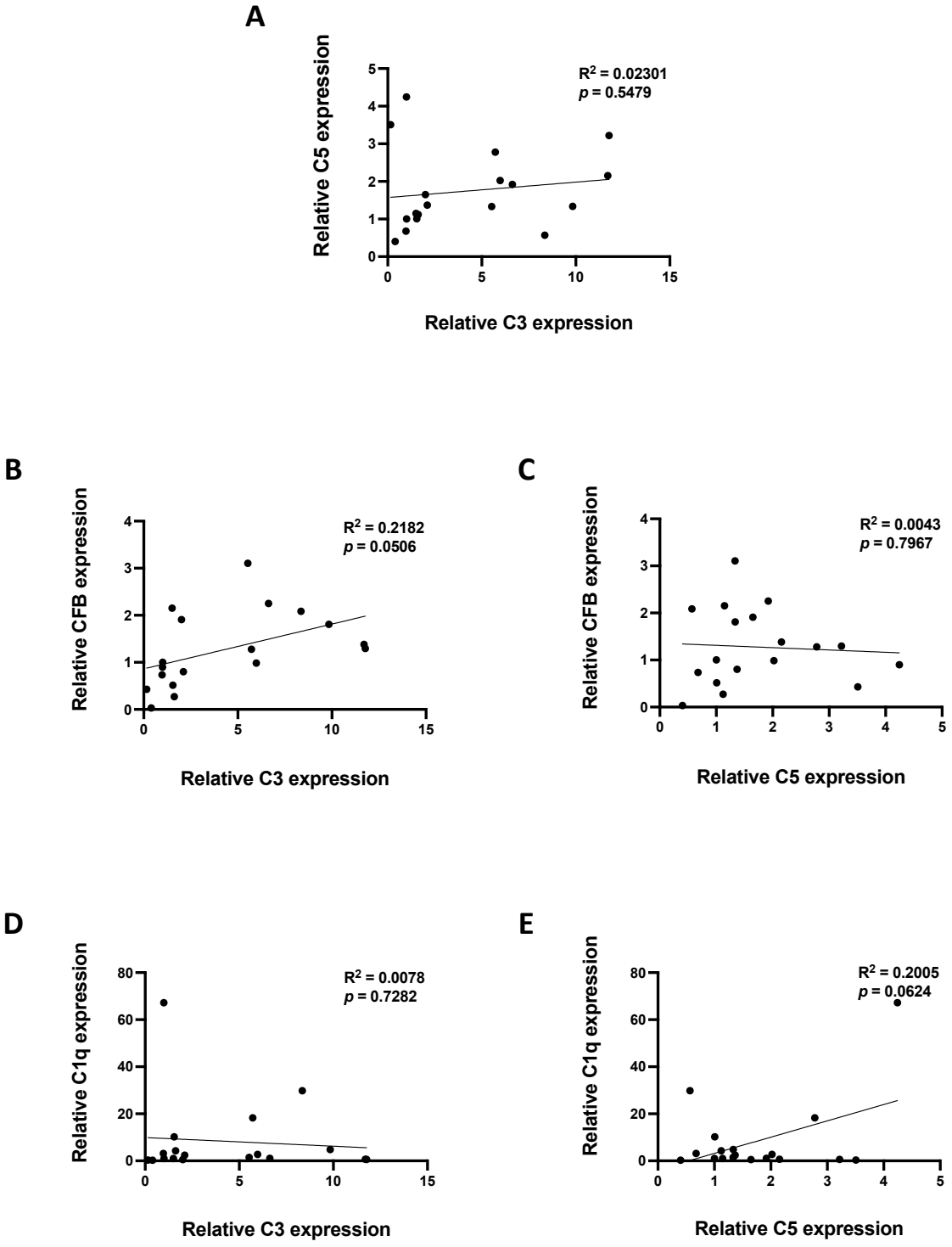

Figure 5-5: Relative mRNA expression of C3 and C5 do not correlate with each other, or expression of C1q or CFB in rectal cancer tissue. Expression of C3, C5, C1q and CFB in pre-treatment rectal cancer tissue (n=18) was assessed by qPCR. **(A)** Relative mRNA expression of C3 does not correlate with relative expression of C5. **(B)** Relative mRNA expression of C3 demonstrated a trend towards a positive correlation with relative CFB expression. **(C)** Relative mRNA expression of C5 does not correlate with relative expression of CFB. Relative mRNA expression of **(D)** C3 and **(E)** C5 does not correlate with relative expression of C1q. Statistical analysis was performed by simple linear regression.

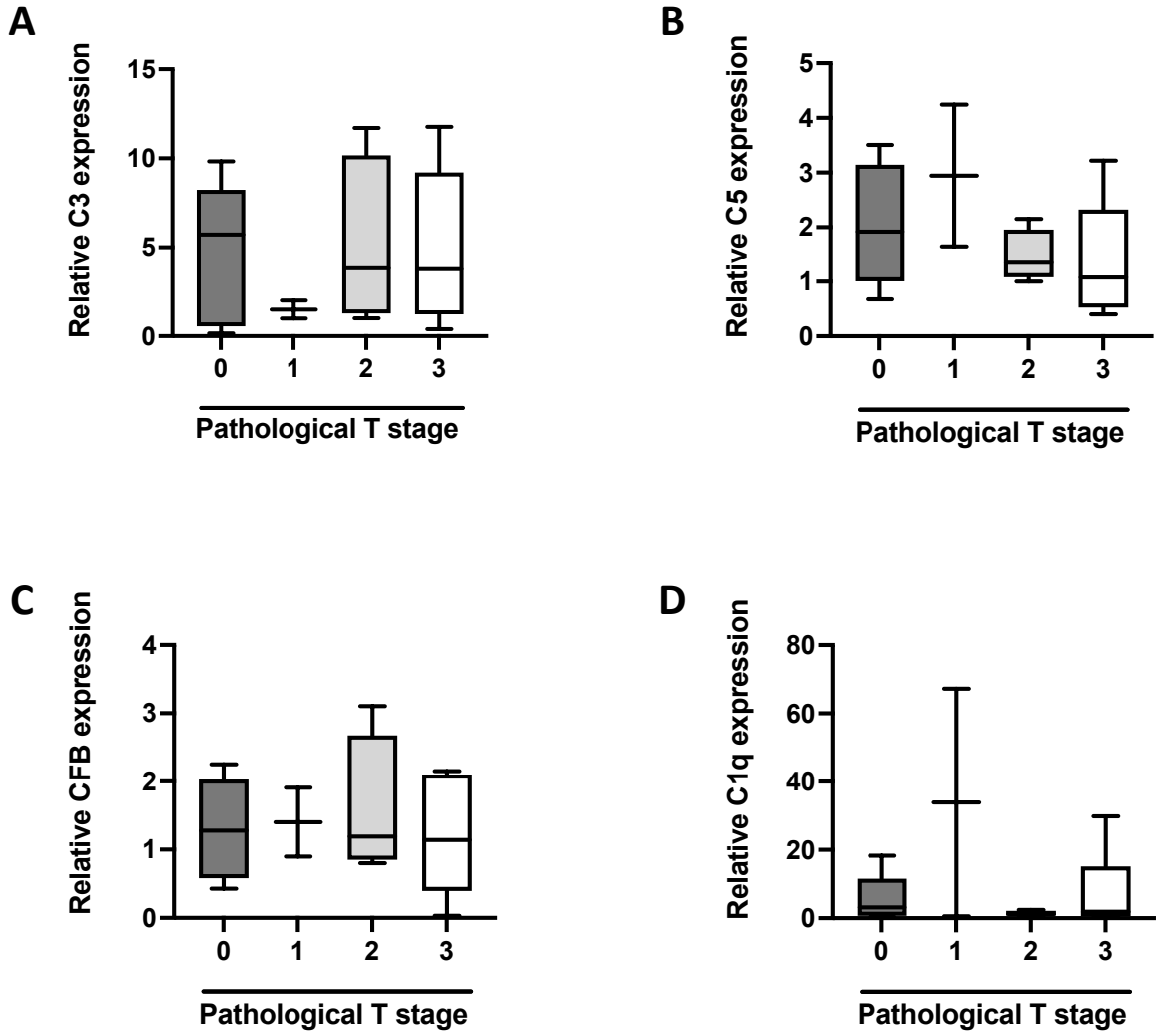

Figure 5-6: Tumour expression of C3, C5, CFB and C1q is not altered based on pathological tumour stage in rectal cancer patients. Expression of C3, C5, C1q and MBL2 in pre-treatment rectal cancer tissue (*n*=17) was assessed by qPCR. Relative mRNA expression of **(A)** C3, **(B)** C5, **(C)** CFB and **(D)** C1q was assessed in patients with a pathological tumour (T) stage of 0 (*n*=5), 1 (*n*=2), 2 (*n*=4) and 3 (*n*=6). Expression of complement components did not significantly vary based on pathological T stage. Statistical analysis was performed by one-way ANOVA and post-hoc Tukey's multiple comparisons testing.

5.4.7. C5 mRNA is elevated in rectal tumours from obese patients, when compared to overweight patients

Obesity is a recognised driver of cancer development[462], however in some instances, paradoxically may associate with better outcomes[463]. In rectal cancer, obesity has been demonstrated to associate with poorer responses to neo-CRT in some studies, while others report it is a positive prognostic factor[464]. To explore the relationship between obesity and complement expression in rectal cancer, relative expression levels of complement components was correlated with body mass index (BMI). Patients for whom BMI information was available were grouped into normal (BMI 18.5-24.9) (n=3) overweight (BMI 25-29.9) (n=5) and obese (BMI ≥ 30) (n=6) categories[465] to assess whether relative expression levels varied across these categories.

Relative expression of C3 mRNA did not correlate with BMI (**Fig. 5-7 A)** or differ based on BMI group (**Fig. 5-7 B**). However, relative C5 mRNA expression demonstrated a significant positive correlation with BMI (p = 0.0326) (**Fig. 5-7 C**). Interestingly relative expression levels of C5 were significantly higher (p = 0.0464) in tumour tissue from obese rectal cancer patients, when compared to overweight patients (Mean relative C5 mRNA expression ± SEM; obese 2.757 ± 0.4765, overweight 1.457 ± 0.2423) (**Fig. 5-7 D)**. This suggests that C5 expression may increase with obesity in this rectal cancer patient cohort.

5.4.8. C1q and CFB expression in rectal cancer tissue is not associated with BMI

Having demonstrated that tumoural C5 expression is associated with obesity in rectal cancer, the relationship between complement activation pathway components CFB and C1q and BMI was also assessed.

Neither CFB (**Fig. 5-7 E)** nor C1q (**Fig. 5-7 G)** relative mRNA expression levels correlated with BMI. Similarly, relative expression levels of CFB (**Fig. 5-7 F)** and C1q (**Fig. 5-7 H)** did not alter across BMI groups. This suggests that expression of complement activation pathway components is not associated with BMI in this rectal cancer patient cohort.

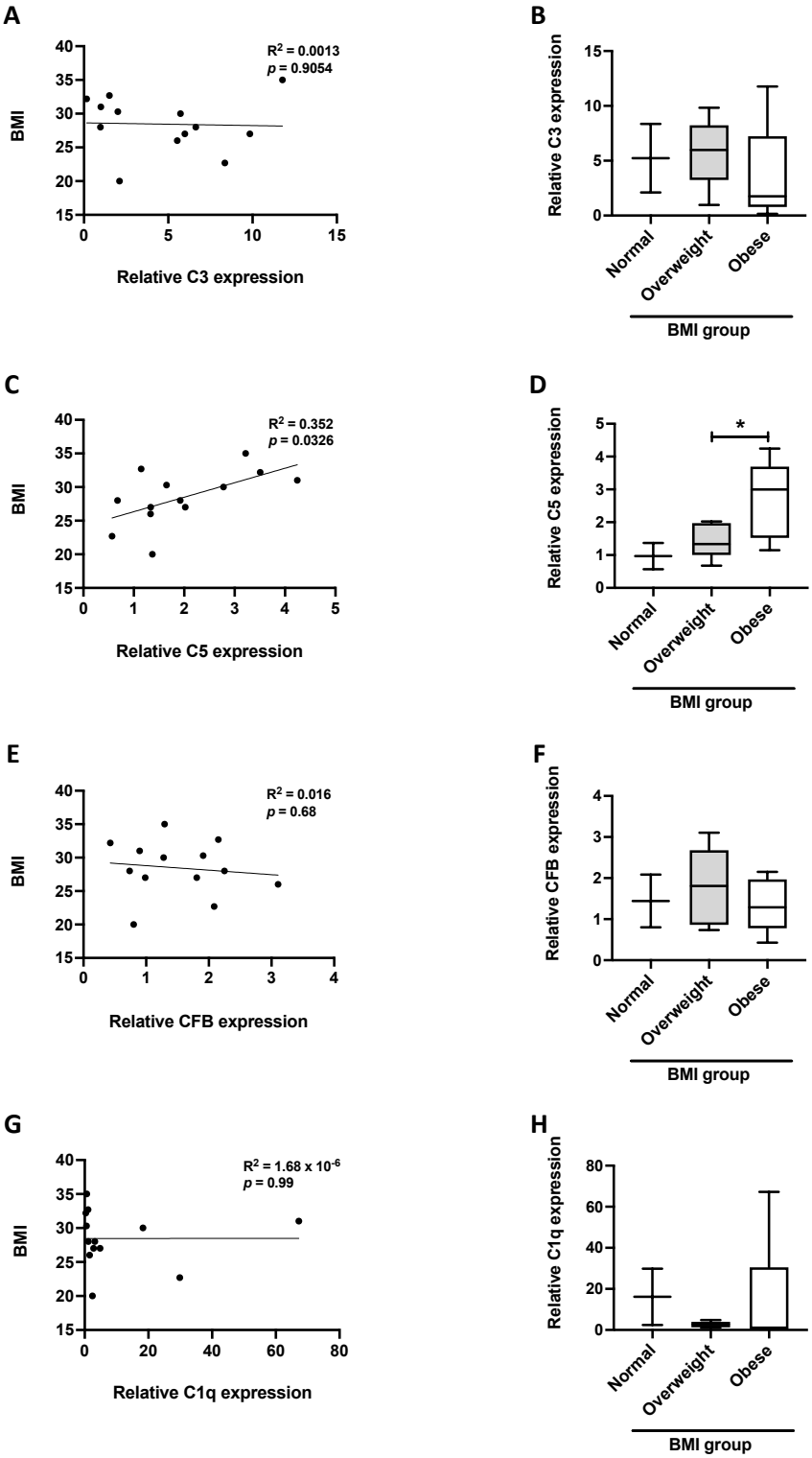

Figure 5-7: Tumour expression of C5 is elevated in obese rectal cancer patients. Expression of C3, C5, CFB and C1q in pre-treatment rectal cancer tissue (n=13) was assessed by qPCR. Relative mRNA expression of **(A)** C3 **(C)** C5 **(E)** CFB and **(G)** C1q was correlated with body mass index (BMI). Statistical analysis was performed by simple linear regression. Patients were grouped based on BMI into normal (n=3), overweight (n=5) and obese (n=6) and relative mRNA expression of **(B)** C3 **(D)** C5 **(F)** CFB and **(H)** C1q were assessed in these groups. Statistical analysis was performed by one-way ANOVA and post-hoc Tukey's multiple comparisons testing. *$p < 0.05$.

5.4.9. Tumour-derived C3 expression does not significantly correlate with sera levels of C3

Matched pre-treatment sera samples were available for *n*=10 patients from the cohort used to assess tumoural mRNA expression of complement components. To investigate whether tumoural expression of complement is associated with circulating levels of complement in this cohort, serum level of C3 was assessed by ELISA and correlated with C3 mRNA expression levels in these matched patients. Patient cohort characteristics are outlined in **Table 5-3**.

There was no significant correlation between pre-treatment sera C3 levels and C3 mRNA expression in pre-treatment rectal tumour biopsies in this cohort of matched patients. However, there was a trend towards increasing circulating levels of C3 with decreasing tumoural expression of C3 ($p = 0.0828$) (**Fig. 5-8**). This may suggest a potential inverse relationship between tumoural and circulating C3.

Table 5-3: Patient characteristics of patient cohort used for correlation of C3 expression in tumour biopsies with circulating levels of C3 in sera.

		Cancer (*n*=10)
Gender	**Male (*n*)**	7
	Female (*n*)	3
Age at diagnosis	**Median (y)**	71
	Range (y)	53-89
Histology	**Adenocarcinoma (*n*)**	10
Differentiation	**Poor-moderate (*n*)**	8
	Moderate (*n*)	2
BMI at diagnosis	**Normal (18.5-24.9) (*n*)**	2
	Overweight (25-29) (*n*)	2
	Obese (>30) (*n*)	5
	N/A (*n*)	1
Pathological T stage	**0 (*n*)**	3
	1 (*n*)	2
	2 (*n*)	0
	3 (*n*)	5
Treatment received	**Neo-CRT**	8
	Neo-RT	2
TRS (Modified Ryan Scale)	**0 (*n*)**	3
	1 (*n*)	3
	2 (*n*)	3
	3 (*n*)	1

Abbreviations; BMI, body mass index; CRT, chemoradiation therapy; N/A, not available; neo, neo-adjuvant; RT, radiation therapy; TRS, tumour regression score; T stage, tumour stage; y, years.

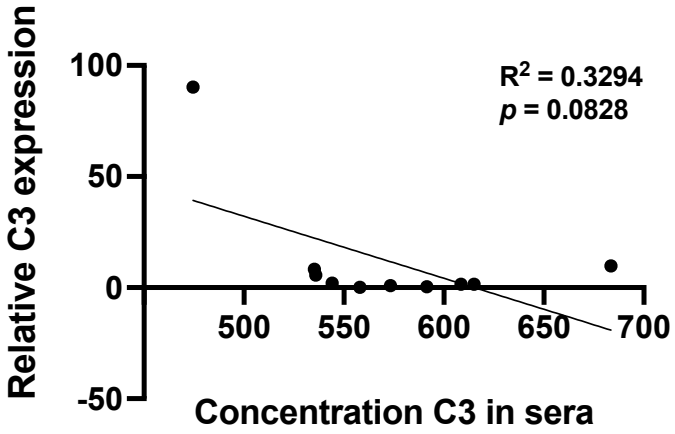

Figure 5-8: Circulating C3 levels do not correlate with tumoural expression of C3 mRNA in rectal cancer patients. The concentration of C3 was assessed in pre-treatment sera from rectal cancer patients and correlated with C3 mRNA expression in tumour biopsies from matched patients (*n*=10). Statistical analysis was performed by simple linear regression and calculating Pearson's correlation coefficient.

5.4.10. Complement components are circulating in pre-treatment sera from rectal cancer patients

Having demonstrated that complement was expressed in pre-treatment tumour biopsies, the levels of circulating complement components were assessed in pre-treatment sera from rectal cancer patients in the OxyTarget cohort. The levels of C3, C5 and the C3a and C5a anaphylatoxins were assessed by ELISA in pre-treatment sera samples from rectal cancer patients (n=40). Patient cohort characteristics are outlined in **Table 5-4**.

All components assessed were detected in all samples. C3 was the most abundant complement component in rectal cancer patient sera, present at significantly higher ($p < 0.0001$ for all) levels, when compared to C3a, C5 and C5a. The level of C3a was significantly higher than C5a ($p < 0.0001$) (Mean concentration (ng/mL) ± SEM; C3 381777 ± 15601, C3a 4578 ± 576.6, C5 72409 ± 2226, C5a 16.81 ± 1.762) (**Fig. 5-9)**. These data demonstrate that systemic activation of central complement cascade components C3 and C5 to generate anaphylatoxins (C3a and C5a) occurs in rectal cancer patients.

5.4.11. C3 positively correlates with C3a levels in pre-treatment sera from rectal cancer patients

To investigate the relationship between circulating complement components and anaphylatoxins in pre-treatment sera from rectal cancer, analysis was performed using R studio.

The circulating levels of C3 and C3a were positively correlated and significantly associated ($p = 0.0072$), suggesting that increased production of C3a is associated with higher circulating levels of C3 (**Fig. 5-10 A**). In contrast, there was no correlation between circulating C5 and C5a levels (**Fig. 5-10 B**). Circulating C3a levels were positively correlated and significantly associated with C5a levels ($p = 0.00079$). Interestingly, this relationship remained significant ($p = 0.00439$) when the association was adjusted for age, sex and circulating C3 and C5 levels (**Fig. 5-10 C**). This suggests that the levels of C3a and C5a are associated independently of the levels of C3 and C5 in pre-treatment sera from rectal cancer patients.

Table 5-4: Patient characteristics of OxyTarget pre-treatment rectal cancer sera cohort.

		Cancer (*n*=40)
Gender	**Male (*n*)**	24
	Female (*n*)	16
Age at study inclusion	**Median (y)**	65
	Range (y)	41-79
Histology	**Adenocarcinoma (*n*)**	40
Differentiation	**Low (*n*)**	3
	Mean/Moderate (*n*)	25
	High (*n*)	7
	N/A (*n*)	5
BMI at diagnosis	**Underweight (< 18.5) (*n*)**	2
	Normal (18.5-24.9) (*n*)	16
	Overweight (25-29.9) (*n*)	14
	Obese (> 30) (*n*)	8
Pathological T stage	**1 (*n*)**	4
	2 (*n*)	3
	3 (*n*)	31
	4 (*n*)	2
Clinical T stage	**2 (*n*)**	2
	3 (*n*)	17
	4 (*n*)	21
Treatment received	**Neo-CRT**	40
TRS (CAP/AJCC)	**1 (*n*)**	13
	2 (*n*)	16
	3 (*n*)	11

Abbreviations; AJCC, American Joint Committee on Cancer; BMI, body mass index; CAP, college of American pathologists; N/A, not available; neo-CRT, neo-adjuvant chemoradiation therapy; TRS, tumour regression score; T stage, tumour stage; y, years.

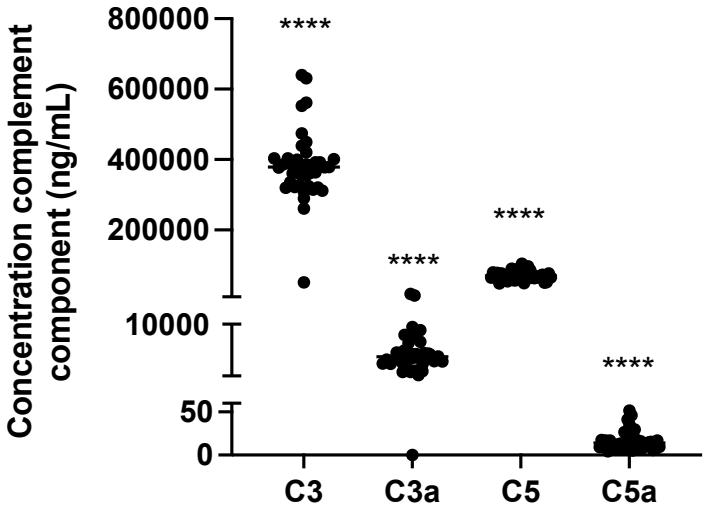

Figure 5-9: Circulating complement components are detected in pre-treatment sera from rectal cancer patients. Circulating levels of C3, C3a, C5 and C5a were assessed by ELISA in pre-treatment rectal cancer sera (n=40). Statistical analysis was performed by one-way ANOVA with Tukey's multiple comparisons testing. **** $p < 0.0001$, where significance is between the indicated components and every other component.

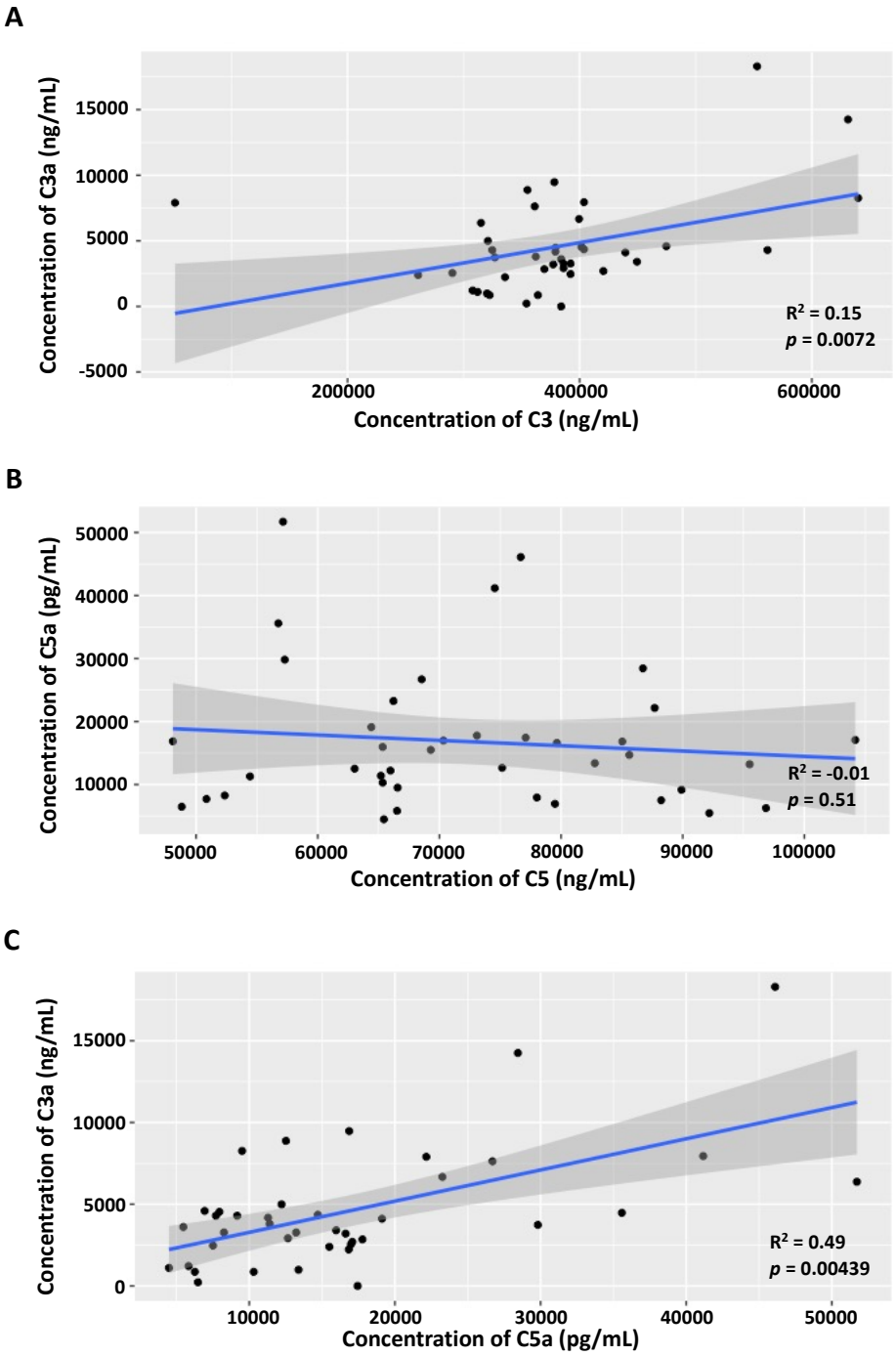

Figure 5-10: Circulating C3 and C3a levels are positively associated in pre-treatment sera from rectal cancer patients. Levels of circulating complement components were assessed in pre-treatment rectal cancer patient sera (*n*=40). **(A)** C3 and C3a are positively correlated and significantly associated. **(B)** C5 and C5a are not significantly associated**.** Linear regression was performed to assess the strength of the association and calculate the R^2 value. **(C)** C3a and C5a are positively correlated and significantly associated, independent of C3, C5, age and sex. Multiple linear regression was carried out to determine the R^2 value and assess the strength of the association independent of these parameters.

5.4.12. Sera levels of C3a are associated with clinical tumour stage

Having demonstrated that C3, C3a, C5 and C5a are present at detectable levels in pre-treatment rectal cancer patient sera, the relationship between these circulating complement components and tumour stage was investigated.

Circulating levels of C3 (**Fig. 5-11 A)**, C5 (**Fig. 5-11 C**) and C5a (**Fig. 5-11 D)** were not altered in patients with a clinical tumour stage of 2 (*n*=2), 3 (*n*=17) or 4 (*n*=21). Interestingly, circulating levels of C3a were significantly higher (p = 0.0247) in patients with a clinical tumour stage of 4, when compared to those with a clinical tumour stage of 3 (Mean concentration of C3a (ng/mL) ± SEM; clinical tumour stage of 3: 3104 ± 369.5, clinical tumour stage of 4: 6158 ± 987.6) (**Fig. 5-11 B**).

Having demonstrated that C3a levels were altered based on clinical tumour stage, the relationship between circulating complement levels and pathological tumour stage was assessed. There were no significant alterations in circulating levels of C3, C3a, C5 or C5a in patients having a pathological tumour stage of 1 (*n*=4), 2 (*n*=3), 3 (*n*=31), or 4 (*n*=2), (**Fig. 5-12)**.These data suggest that circulating levels of C3, C3a, C5 and C5a in sera are not associated with pathological tumour stage in this cohort of rectal cancer patients.

5.4.13. Sera levels of C3, C3a, C5 and C5a are not associated with BMI

Having demonstrated that expression of C5 mRNA is elevated in tumours from obese rectal cancer patients, when compared to overweight rectal cancer patients in the St James's Hospital/Beacon Hospital patient cohort, the relationship between circulating complement components and BMI was assessed in the OxyTarget patient cohort .

Circulating levels of C3 (**Fig. 5-13 A)**, C3a (**Fig. 5-13 C)**, C5 (**Fig. 5-13 E)**, and C5a (**Fig. 5-13 G)** did not correlate with BMI. Similarly, sera levels of these complement components were unaltered when patients were grouped by BMI into underweight (BMI <18.5) (*n*=2), normal (BMI 18.5-24.9) (*n*=16) overweight (BMI 25-29.9) (*n*=14) and obese (BMI ≥ 30) (*n*=8) categories (**Fig. 5-13**). This suggests that the circulating levels of complement components are not associated with BMI in this cohort of rectal cancer patients.

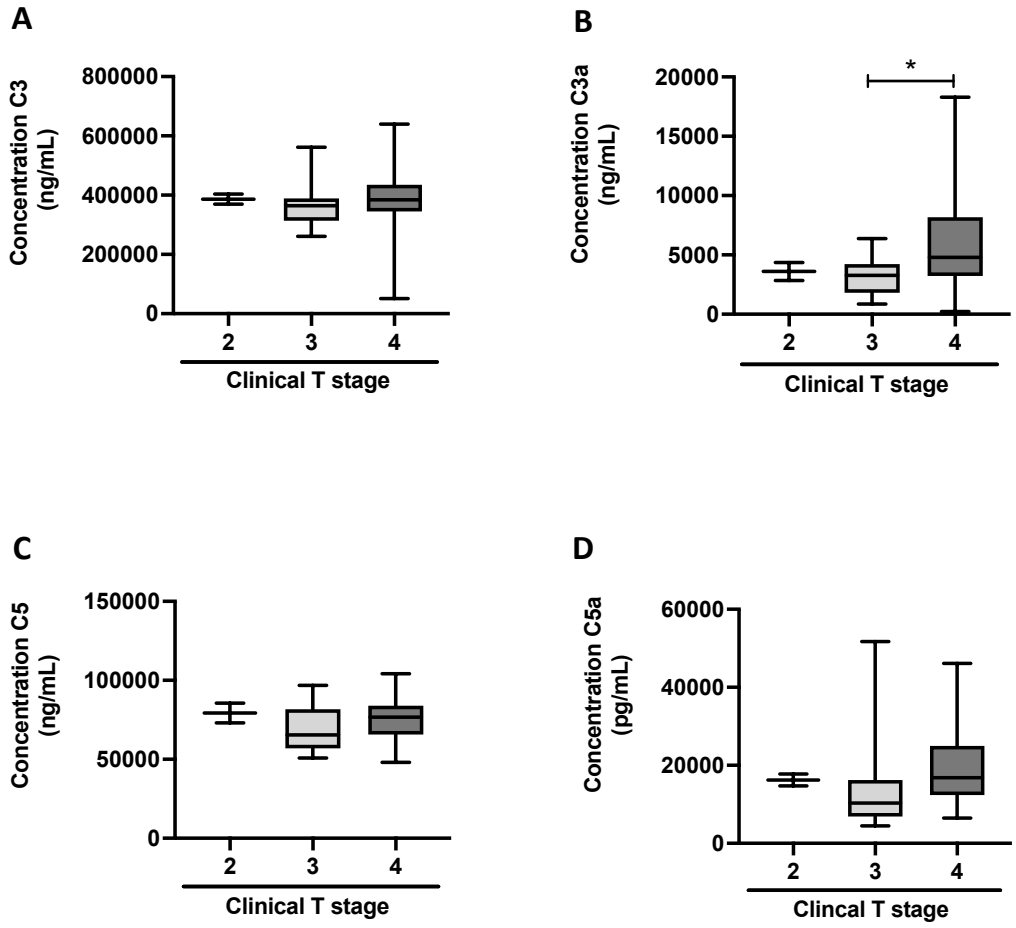

Figure 5-11: Circulating levels of C3a in pre-treatment sera from rectal cancer patients are altered across clinical T stage. Levels of circulating complement components were assessed in pre-treatment rectal cancer patient sera **(***n*=40). Patients were grouped based on clinical tumour (T) stage; 2, (*n*=2), 3 (*n*=17) and 4 (*n*=21) and circulating levels of **(A)** C3 **(B)** C3a **(C)** C5 and **(D)** C5a were assessed in these groups. Statistical analysis was performed by one-way ANOVA and post-hoc Tukey's multiple comparisons testing. *$p. < 0.05$.

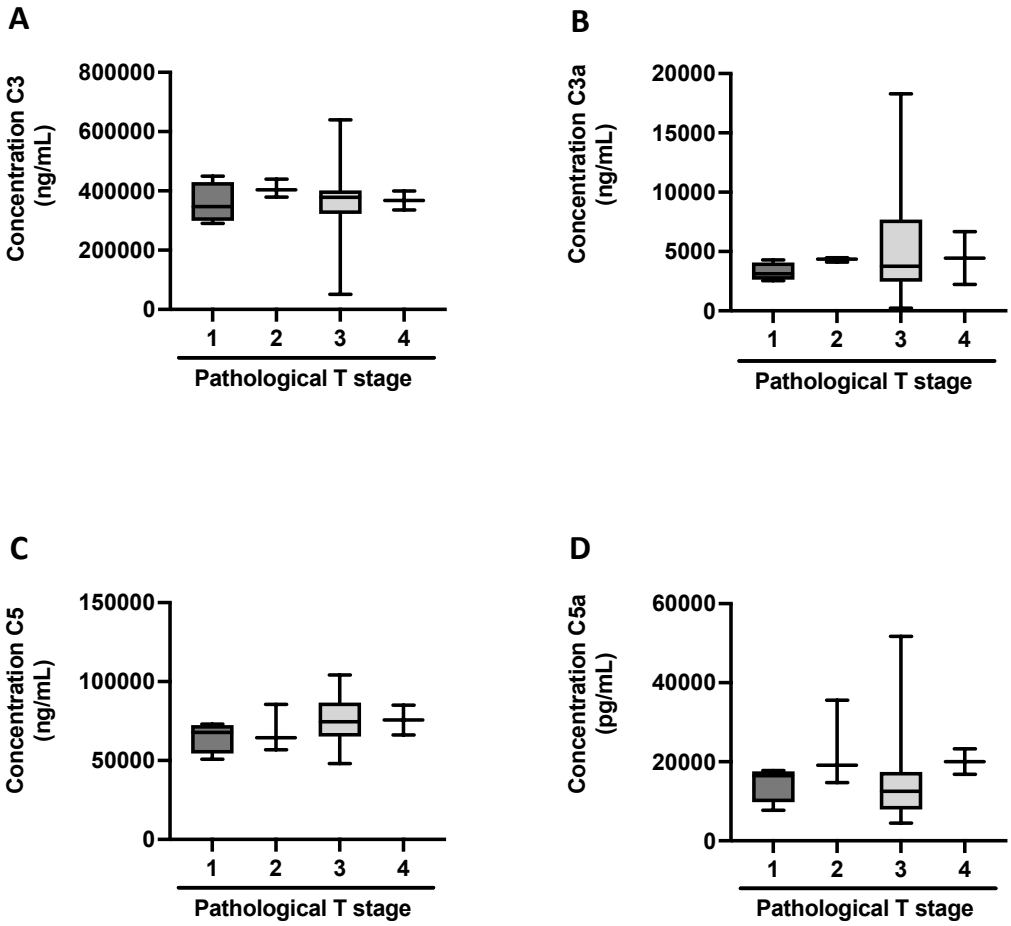

Figure 5-12: Circulating levels of complement components in pre-treatment sera from rectal cancer patients are not altered based on pathological tumour stage. Levels of circulating complement components were assessed in pre-treatment rectal cancer patient sera (*n*=40). Patients were grouped based on pathological tumour (T) stage; 1 (*n*=4), 2, (*n*=3), 3 (*n*=31) and 4 (*n*=2) and circulating levels of **(A)** C3 **(B)** C3a **(C)** C5 and **(D)** C5a were assessed in these groups. Statistical analysis was performed by one-way ANOVA and post-hoc Tukey's multiple comparisons testing.

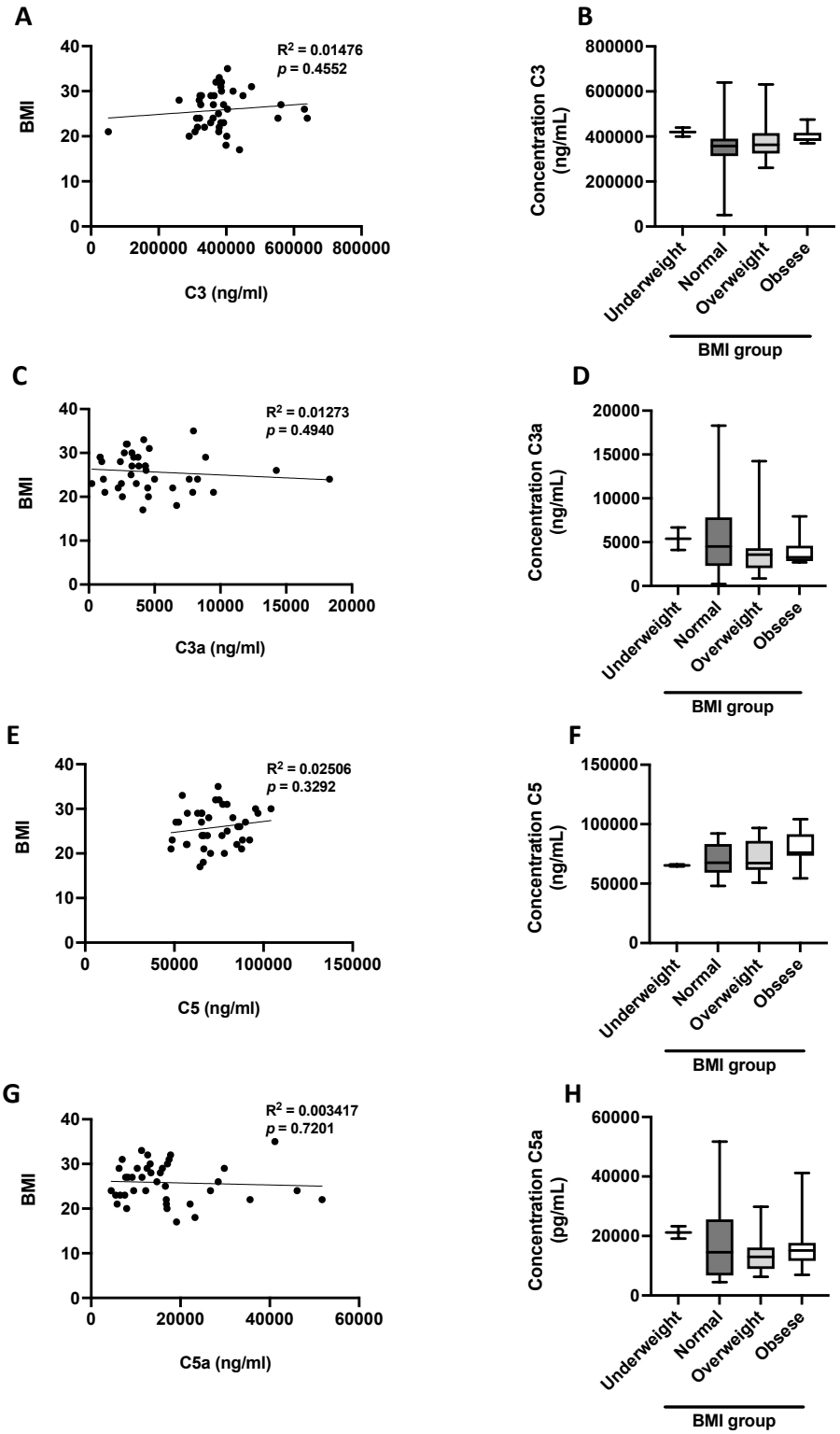

Figure 5-13: Circulating levels of complement components in pre-treatment sera from rectal cancer patients are not altered based on BMI group. Levels of circulating complement components were assessed in pre-treatment rectal cancer patient sera (*n*=40). Sera levels of **(A)** C3 **(C)** C3a **(E)** C5 and **(G)** C5a were correlated with body mass index (BMI). Statistical analysis was performed by simple linear regression. Patients were grouped based on BMI into underweight (*n*=2), normal (*n*=16), overweight (*n*=14) and obese (*n*=8) and circulating levels of **(B)** C3 **(D)** C3a **(F)** C5 and **(H)** C5a were assessed in these groups. Statistical analysis was performed by one-way ANOVA and post-hoc Tukey's multiple comparisons testing.

5.4.14. Circulating levels of C3 positively correlate with circulating levels of IL-6

IL-6 is a pleiotropic cytokine which is upregulated in several cancers and can have immunosuppressive effects[466]. In CRC, IL-6 has been demonstrated to promote tumourigenesis and elevated IL-6 levels of IL-6 are demonstrated to correlate with and reduced survival[467]. Previous profiling of the sera from the OxyTarget patient cohort by Multiplex ELISA (performed by collaborators at Akershus University Hospital, Lørenskog, Norway) had investigated circulating levels of IL-6 in this patient cohort. The relationship between IL-6 levels and levels of C3, C5, C3a and C5a pre-treatment sera samples from the OxyTarget patient cohort (n=40) was investigated. Interestingly, the levels of C3 and IL-6 demonstrated a significantly positive correlation (p = 0.021, rho = 0.363) (**Fig. 5-14**), suggesting a relationship between circulating levels of IL-6 and C3 in this cohort of rectal cancer patients.

5.4.15. Secreted levels of C3 from rectal tumour biopsies positively correlates with secreted levels of IL-6 in the TME

Having demonstrated that circulating C3 and IL-6 levels positively correlate in rectal cancer patient sera, the relationship between secreted C3 and IL-6 in TCM generated from pre-treatment rectal tumour biopsies was assessed (n=5). Patient cohort characteristics are outlined in **Table 5-5**.

The concentration of C3 in rectal cancer TCM exceeded the standard curve so relative absorbances relating to C3 concentration in each TCM sample was calculated. The relative absorbance of C3 in TCM significantly positively correlated with the level of IL-6 in TCM (p = 0.0272, R^2 = 0.08) (**Fig. 5-15**), suggesting a relationship between IL-6 and C3 within the TME in rectal cancer.

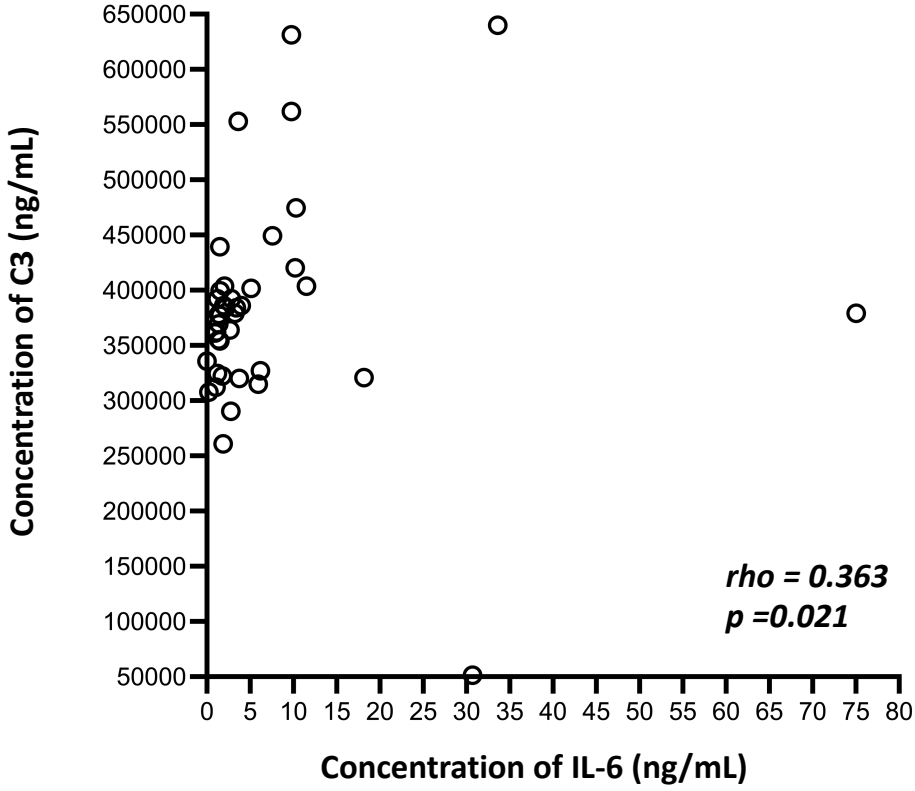

Figure 5-14: Circulating levels of C3 positively correlate with circulating levels of IL-6 in pre-treatment sera from rectal cancer patients. The concentration of C3 was assessed in pre-treatment sera from rectal cancer patients (OxyTarget Cohort) and correlated with the concentration of IL-6 determined in these samples (n=40). Statistical analysis was performed by assessing Spearman's rho.

Table 5-5: Patient characteristics of patient cohort in which TCM was assessed.

		Cancer (*n*=5)
Gender	**Male (*n*)**	3
	Female (*n*)	2
Age at diagnosis	**Median (y)**	
	Range (y)	47-78
Histology	**Adenocarcinoma (*n*)**	5
Differentiation	**Poor-moderate (*n*)**	1
	Moderate (*n*)	2
	Well (*n*)	1
	N/A (*n*)	1
BMI	**Normal (18.5-24.9) (*n*)**	1
	Overweight (25-29.9) (*n*)	2
	Obese (>30) (*n*)	2
Pathological T stage	**1 (*n*)**	2
	3 (*n*)	2
	N/A (*n*)	1
Treatment received	**Neo-CRT (*n*)**	2
	Surgery only (*n*)	2
	Unknown (*n*)	1
TRS (Modified Ryan Scale)	**2 (*n*)**	1
	3 (*n*)	1
	N/A (*n*)	3

Abbreviations; BMI, body mass index; N/A, not available; neo-CRT, neo-adjuvant chemoradiation therapy; TRS, tumour regression score; T stage, tumour stage; y, years.

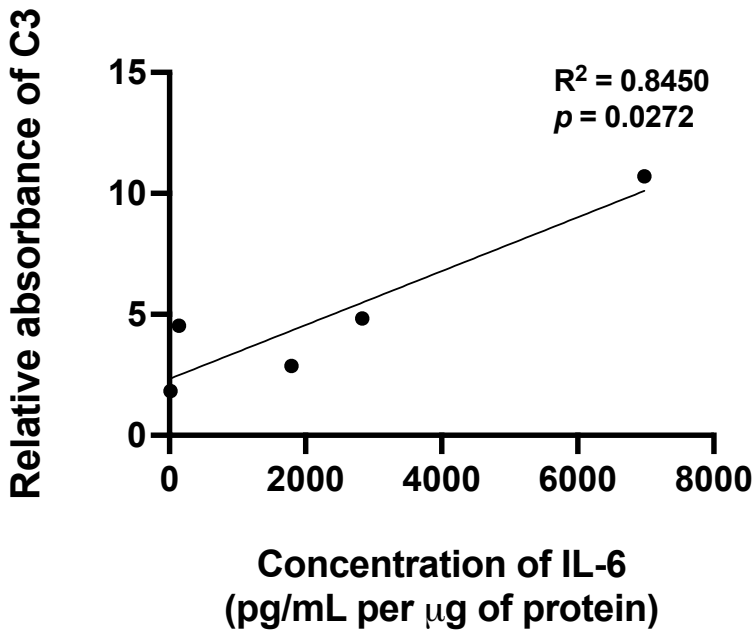

Figure 5-15: Relative absorbance of secreted C3 positively correlates with the level of secreted IL-6 in TCM from pre-treatment rectal cancer biopsies. The concentration of C3 and IL-6 was assessed in TCM generated from pre-treatment rectal cancer biopsies (*n*=5) by ELISA and Multi-Plex ELISA, respectively. Statistical analysis was performed using simple linear regression.

5.4.16. Pre-treatment sera levels of C3a are elevated in patients with subsequent poor responses to neo-CRT in rectal cancer

Having determined the circulating levels of C3, C5, C3 and C5a in pre-treatment sera from rectal cancer patients, the relationship between circulating complement and subsequent pathological response to neo-CRT was investigated. Patient cohort (n=40) characteristics are outlined in **Table 5-4**.

Circulating C3 (**Fig. 5-16 A**), C5 (**Fig. 5-16 C**) and C5a (**Fig. 5-16 D**) levels were similar in pre-treatment sera from rectal cancer patients with a TRS of 1, 2 or 3. However, interestingly, pre-treatment C3a levels were significantly (p = 0.0432) higher in patients with a subsequent TRS of 3, when compared to patients with a TRS of 1 (Mean concentration of C3a (ng/mL) ± SEM; TRS 1 3232 ± 352.5, TRS 3 6906 ± 1770) (**Fig. 5-16 B**). These data suggest that elevated pre-treatment levels of C3a may have potential as a predictive biomarker of poor response to neo-CRT.

5.4.17. Pre-treatment sera levels of C3, C3a, C5 and C5a are not associated with recurrence-free or overall survival

Pathological response to neo-CRT in rectal cancer is associated with outcome, with attainment of a pCR associated with reduced disease recurrence and improved survival[53]. Having demonstrated that elevated circulating levels of C3a correlate with a poor response to neo-CRT in this cohort of rectal cancer patients, the relationship between circulating complement components and recurrence-free survival (RFS) and OS was assessed using Cox regression analysis and log-rank testing. There were no statistically significant associations between circulating levels of C3 and C5 and RFS or OS when Cox regression analysis was performed (**Table 5-6**). Cox regression analysis of circulating C3a levels demonstrated a significant association with both RFS and OS (**Table 5-6**). However, using Kaplan Meier log-rank testing, there was no statistically significant association between levels of C3a and RFS (**Fig. 5-17 A**) or OS (**Fig. 5-17 B**). Similarly, Cox regression analysis demonstrated that circulating C5a levels were significantly associated with RFS (p = 0.002) (**Table 5-6**), however log-rank analysis demonstrated that circulating C5a was did not significantly associate with RFS or OS (**Fig. 5-17 C-D**).

These data suggest that in this rectal cancer patient cohort circulating levels of C3, C5 and their respective anaphylatoxins are not associated with survival.

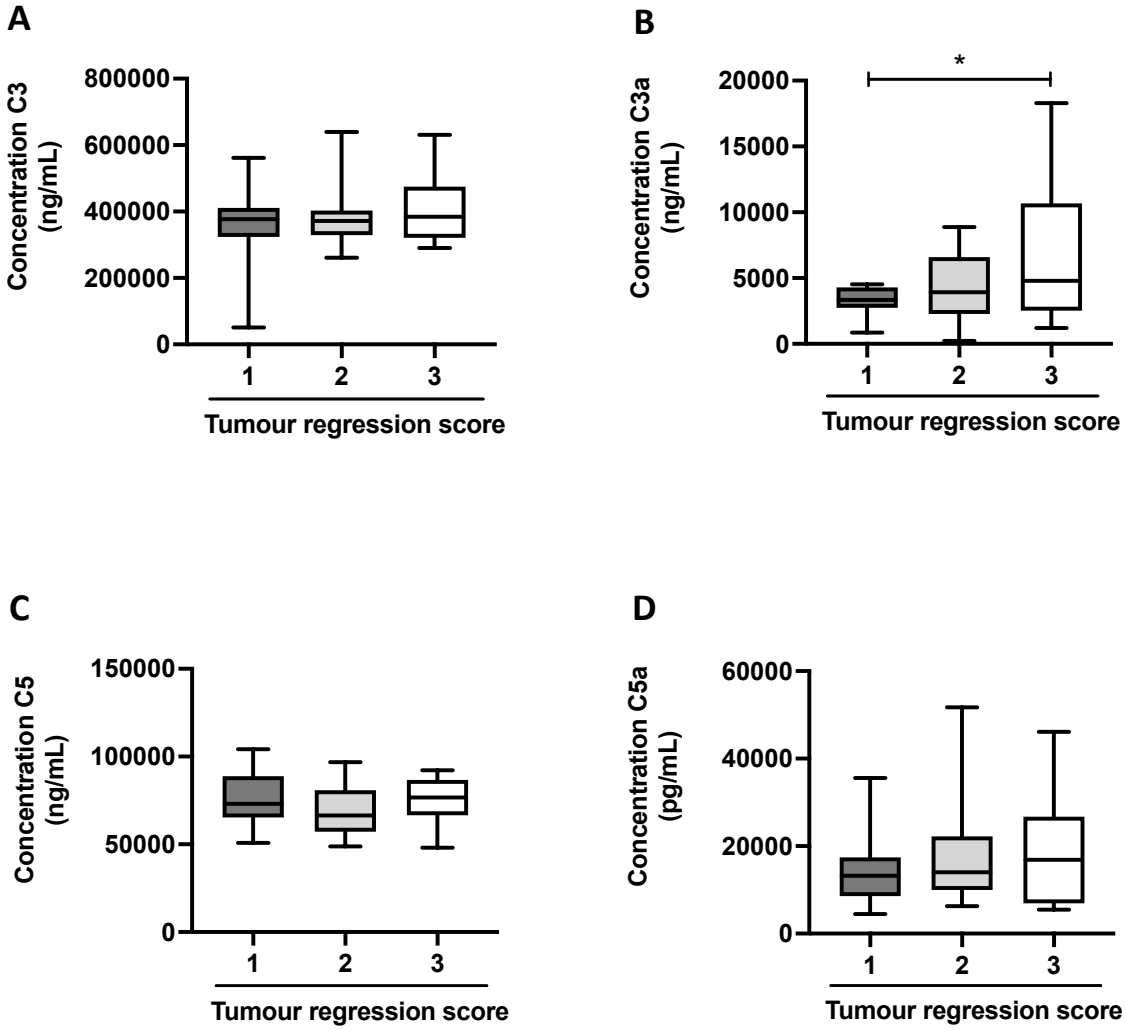

Figure 5-16: C3a is significantly elevated in pre-treatment sera from rectal patients with a subsequent poor pathological response to neo-CRT. Levels of circulating complement components were assessed in pre-treatment rectal cancer patient sera (*n*=40). Patients were grouped based on tumour regression score; 1 (*n*=13), 2 (*n*=16) or 3 (*n*=11) and circulating levels of **(A)** C3 **(B)** C3a **(C)** C5 and **(D)** C5a were assessed in these groups. Statistical analysis was performed by one-way ANOVA and post-hoc Tukey's multiple comparisons testing. *$p < 0.05$.

Table 5-6: Results of Cox regression analysis (HR) and log-rank test to investigate the effect of circulating complement levels on recurrence-free and overall survival in rectal cancer.

	RFS				OS			
	n	**HR (95% CI)**	***p***	**Log-rank *p* (median)**	***n***	**HR (95% CI)**	***p***	**Log-rank *p* (median)**
C3	32	1.000 (1.000-1.000)	0.800	0.4029	40	1.000 (1.000-1.000)	0.500	0.9768
C3a	32	1.000 (1.000-1.000)	0.040	0.7279	39	1.000 (1.000-1.000)	<0.001	0.1613
C5	32	1.000 (0.999-1.000)	0.600	0.7680	40	1.000 (1.000-1.000)	0.600	0.1644
C5a	32	1.000 (1.000-1.000)	0.002	0.0777	40	1.000 (1.000-1.000)	0.100	0.2316

Abbreviations; CI, confidence interval; HR, hazard ratio; OS, overall survival; RFS, recurrence-free survival.

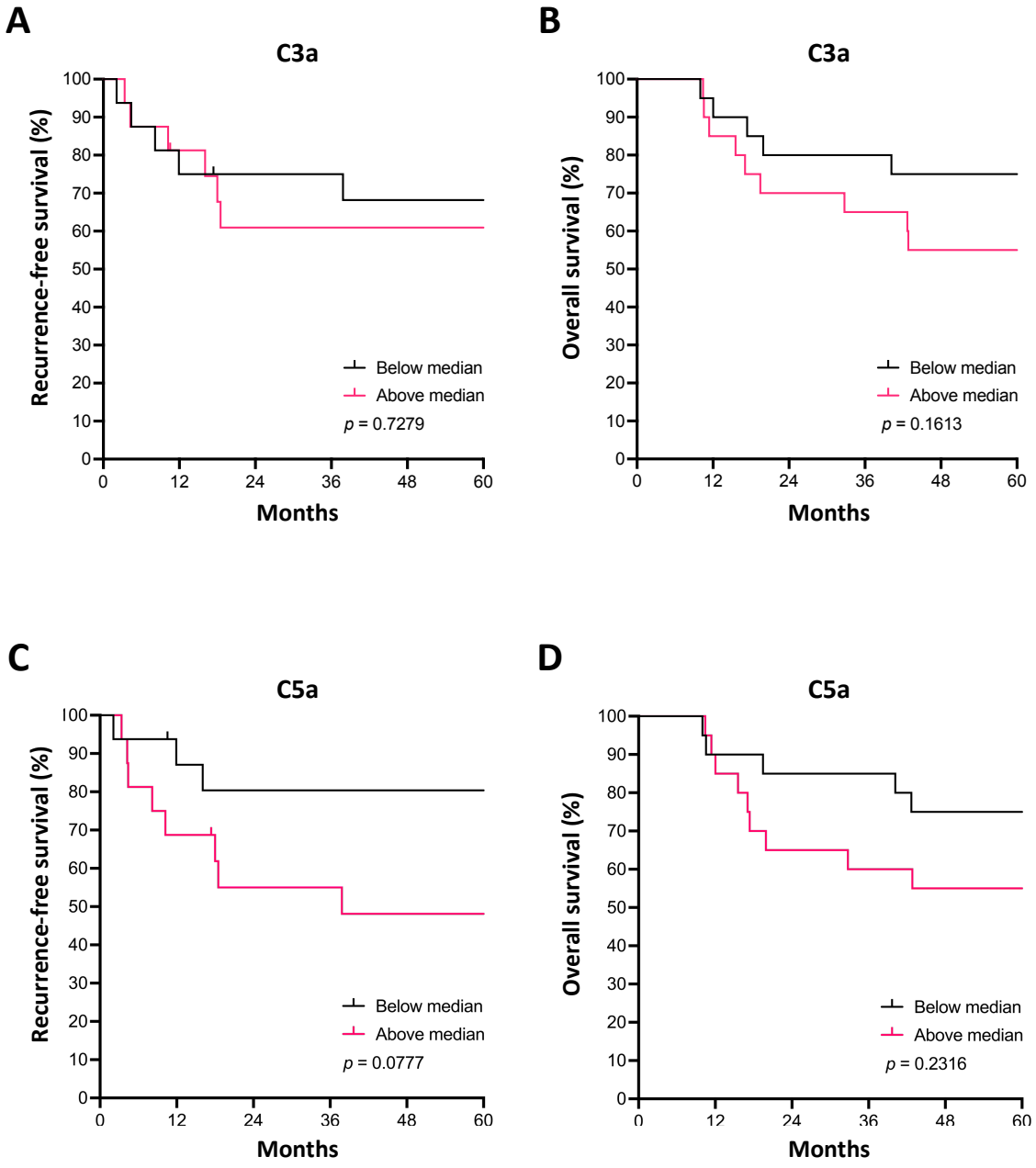

Figure 5-17: Circulating C3a and C5a levels in pre-treatment sera are not associated with recurrence-free survival or overall survival in rectal cancer patients. Kaplan Meier curves demonstrating the effect of pre-treatment circulating C3a levels on **(A)** recurrence-free survival and **(B)** overall survival in rectal cancer (n=32 and n=39, respectively). Levels of C3a were separated into two groups; above the median and below the median. Survival is measured in months. Analysis was performed using the log-rank test.

5.4.18. Pre-treatment sera levels of C5b-9 are not associated with tumour stage or BMI

Having demonstrated that the complement anaphylatoxins C3a and C5a are present in the serum of rectal cancer patients, the levels of C5b-9, the terminal complement component (TCC), was assessed in pre-treatment sera by ELISA, to assess whether activation of the terminal complement pathway occurs in rectal cancer. The relationship between circulating C5b-9 and tumour stage and BMI was assessed. Patient cohort (n=40) characteristics are outlined in **Table 5-4**.

C5b-9 was present in all pre-treatment sera samples tested. There were no significant alterations in circulating C5b-9 levels across clinical or pathological tumour stage (**Fig. 5-18 A-B**), suggesting that C5b-9 does not correlate with tumour stage in this cohort of rectal cancer patients. Similarly, levels of C5b-9 did not correlate with BMI or associate with BMI groups, suggesting that C5b-9 is not related with obesity status in this cohort of rectal cancer patients (**Fig. 5-18 C-D**).

5.4.19. Pre-treatment sera levels of C5b-9 are elevated in patients with subsequent poor responses to neo-CRT in rectal cancer

Having demonstrated that C5b-9 was present in pre-treatment sera from rectal cancer patients, the relationship between C5b-9 and subsequent pathological response to neo-CRT was assessed. Patient cohort (n=40) characteristics are outlined in **Table 5-4**.

Levels of C5b-9 in pre-treatment sera were significantly (p = 0.0134) elevated in rectal cancer patients with a subsequent TRS of 3, when compared to those with a TRS of 1 (Mean concentration of C5b-9 (ng/mL) ± SEM; TRS 1 457.7 ± 34.09, TRS 3 797.5 ± 129) (**Fig. 5-19 A**). This data suggests that increased circulating levels of C5b-9 is associated with a poorer response to neo-CRT, highlighting C5b-9 as a potential predictive biomarker of response to neo-CRT.

5.4.20. Elevated pre-treatment sera levels of C5b-9 are associated with worse recurrence-free and overall survival in rectal cancer patients

Having demonstrated that increased levels of C5b-9 in pre-treatment sera is associated with a poor response to neo-CRT, the relationship between circulating C5b-9 levels and RFS and OS was assessed using Cox regression analysis and log-rank testing (**Table 5-7**). Pre-treatment sera levels of C5b-9 were significantly increased in patients with poorer RFS (**Fig. 5-19 B**) and OS (**Fig. 5-19 C**), suggesting a potential role for complement in the

pathogenesis of rectal cancer and highlighting C5b-9 as a potential prognostic biomarker in rectal cancer.

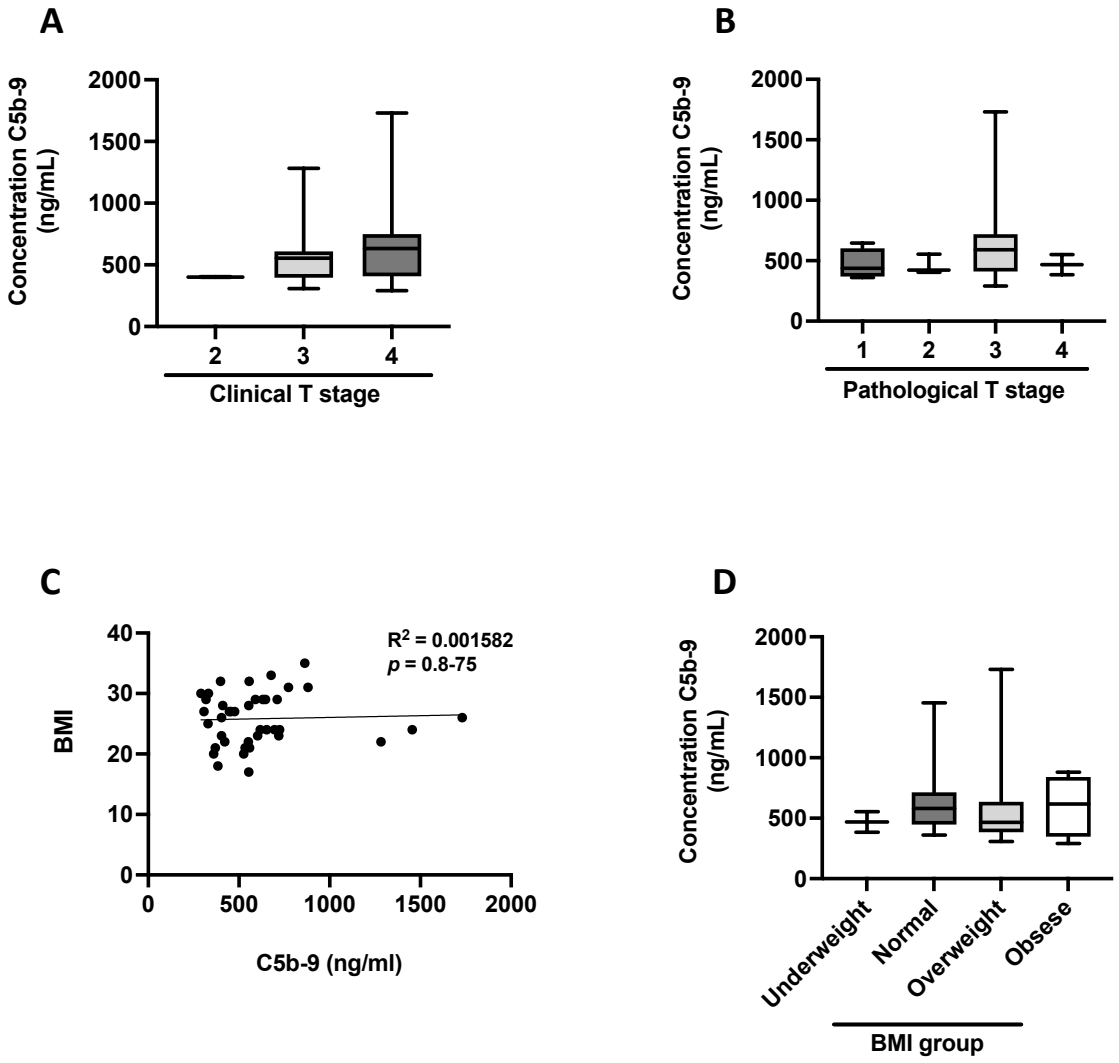

Figure 5-18: Circulating levels of C5b-9 in pre-treatment sera from rectal cancer patients are not associated with tumour stage or BMI. Levels of C5b-9 were assessed in pre-treatment sera from rectal cancer patients (*n*=40) by ELISA. Patients were grouped based on **(A)** clinical tumour (T) stage; 2 (*n*=2), 3, (*n*=17) and 3 (*n*=21) and **(B)** pathological T stage; 1 (*n*=4), 2, (*n*=3), 3 (*n*=31) and 4 (*n*=2). **(C)** Sera levels of C5b-9 were correlated with BMI and **(D)** patients were also grouped by BMI into underweight (*n*=2), normal (*n*=16), overweight (*n*=14) and obese (*n*=8). Statistical analysis was performed by simple linear regression and by one-way ANOVA and post-hoc Tukey's multiple comparisons testing.

Table 5-7: Results of Cox regression analysis (HR) and log-rank testing performed to investigate the effect of circulating C5b-9 levels on recurrence-free and overall survival in rectal cancer.

	RFS				OS			
	n	**HR (95% CI)**	***p***	**Log-rank *p* (median)**	***n***	**HR (95% CI)**	***p***	**Log-rank *p* (median)**
C5b-9	32	1.002 (1.001-1.004)	0.005	0.0040	40	1.002 (1.001-1.003)	0.006	0.0023

Abbreviations; CI, confidence interval; HR, hazard ratio; OS, overall survival; RFS, recurrence-free survival.

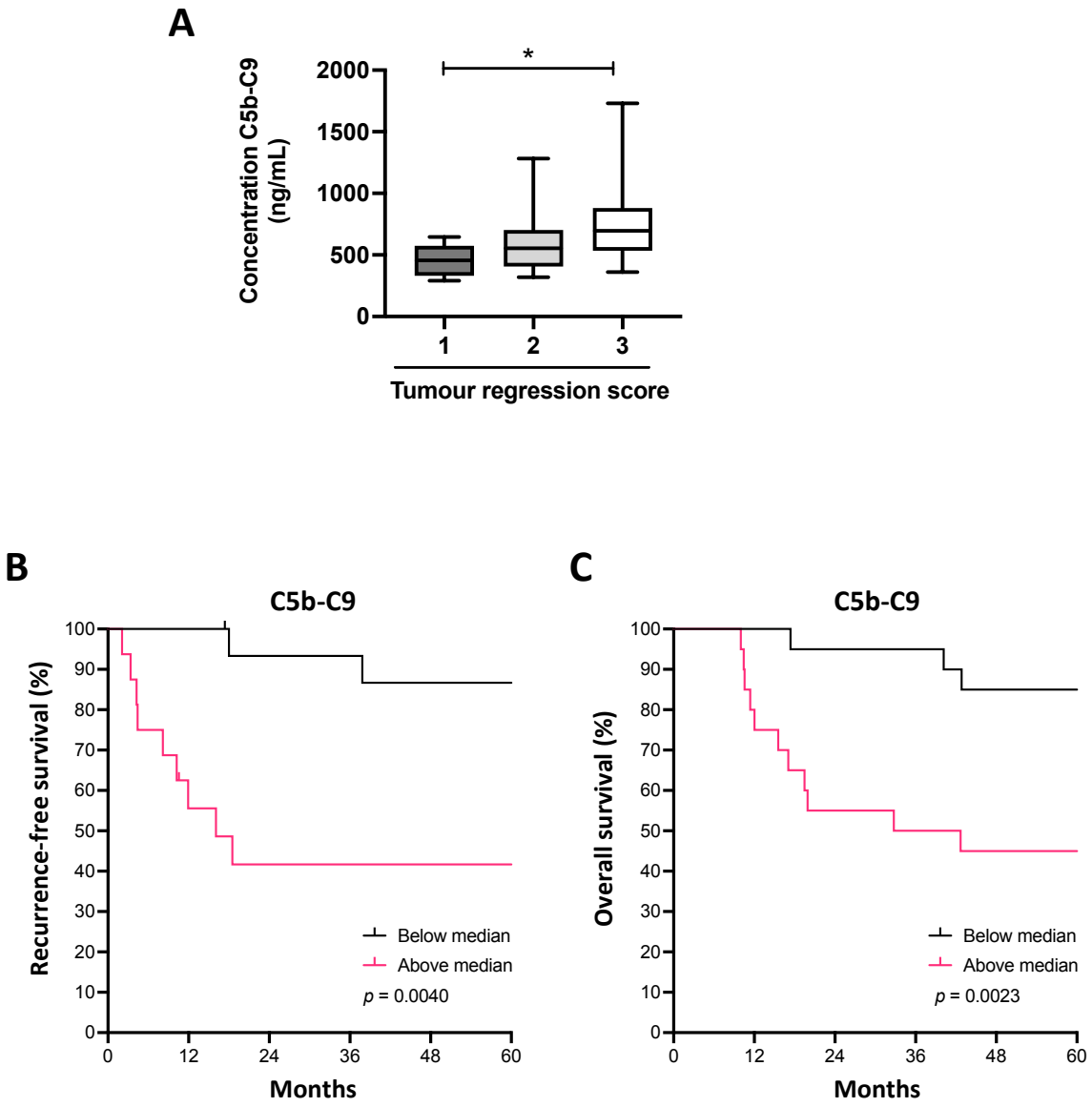

Figure 5-19: Circulating levels of C5b-9 are significantly elevated in pre-treatment sera from rectal cancer patients with subsequent poor responses to neo-CRT and poorer survival. Levels of C5b-9 were assessed in pre-treatment rectal cancer patient sera (*n*=40). **(A)** Patients were grouped based on TRS; 1 (*n*=13), 2 (*n*=16) or 3 (*n*=11) and C5b-9 levels were significantly elevated in patients with a subsequent TRS of 3, when compared to those with a TRS of 1. Statistical analysis was performed by one-way ANOVA with post-hoc Tukey's multiple comparisons testing. Kaplan Meier curves demonstrating the effect of pre-treatment circulating C5b-9 levels on **(A)** recurrence-free survival and **(B)** overall survival in rectal cancer (*n*=32 and *n*=40, respectively). Levels of C5b-9 were separated into two groups; above the median and below the median. Survival is measured in months. Analysis was performed using the log-rank test.

5.5. Discussion

There is an urgent need to identify predictive biomarkers of response to neo-CRT in rectal cancer and to elucidate molecular factors influencing response to treatment to develop novel therapeutic strategies to boost treatment response and survival for patients. This chapter aimed to profile the expression of key complement components in pre-treatment rectal tumour biopsies and pre-treatment sera from rectal cancer patients.

Complement components have frequently been reported as overexpressed in tumour tissue, when compared to healthy tissue[456], however, the expression level of complement components in normal non-cancer rectal tissue is currently unknown. Supporting previous studies in gastric, CRC and skin cancers, we demonstrate that expression of C3 is increased in rectal tumour tissue, when compared to rectal tissue from non-cancer controls[301,317,468]. We also demonstrate upregulation of C5 in rectal tumour tissue, when compared to non-cancer rectal tissue. This supports a potential role for dysregulated complement expression in the progression from normal to malignant rectal tissue. Elucidating whether tumour-expressed complement has potential as a therapeutic target or biomarker of response requires investigating complement expression in normal non-cancer tissue. Here we demonstrate that complement is expressed at low levels in non-cancer rectal tissue, which may be beneficial from a therapeutic perspective. Further investigation using matched tumour and adjacent non-cancer rectal tissue is required to establish whether this may aid the targeting of complement in rectal tumours.

Expression of complement activation pathway components has been reported in several cancer types. In squamous cell carcinoma, upregulation of CFB relative to normal tissue has been reported, demonstrating an upregulation of complement activation pathway components in cancer[301]. This is supported by data presented in this chapter, which demonstrate elevated expression of CFB in rectal tumour biopsies, when compared to non-cancer tissue. Interestingly, C1q of the classical pathway was expressed at significantly higher levels in non-cancer rectal tissue, when compared to rectal tumour tissue. In the literature at present, there are no studies to indicate that different complement activation pathways predominate in tumour tissue when compared to normal tissue. However, results presented here suggest that different complement activation pathways may be enriched in cancer, when compared to normal tissue. If complement activation is occurring via these canonical pathways, this may be beneficial from a therapeutic perspective as it may provide an opportunity to selectively target tumour tissue while sparing normal tissue.

Supporting *in vitro* data presented in Chapter 2, assessment of tumoural expression of complement components in pre-treatment rectal tumour biopsies demonstrated that C3 and C5 are expressed in rectal tumour biopsies. Importantly, gene expression of complement components was assessed using whole tumour biopsies, which contain stromal and epithelial cells. While expression of complement was demonstrated in CRC cell lines in Chapter 2, which are of epithelial origin, further investigation using formalin-fixed paraffin-embedded (FFPE) tumour tissue is necessary to pinpoint the location of complement expression in rectal tumours.

The presence of C4d deposits in oropharyngeal SSC and C5aR expression in breast cancer tissue has been previously demonstrated to correlate with tumour stage[275,319], suggesting a relationship between complement and tumour stage in cancer. In this study, the expression of C3 and C5 mRNA in biopsies from rectal cancer patients was not associated with pathological tumour stage. C4d and C5aR are reflective of complement activation and a potential to transduce complement signals, respectively, both of which have a functional ability to modify the TME. Considering these findings, it may be useful in future studies to directly investigate complement activation within the rectal TME by assessing for the presence of complement activation products (such as C3d). In addition to complement expression, complement activation could be correlated with tumour stage, to assess whether there is a relationship between the activation of complement and rectal cancer stage.

Within the circulation, complement components and anaphylatoxins were detected in pre-treatment sera from rectal cancer patients, highlighting systemic activation of complement in rectal cancer. Interestingly, C3a was elevated in the sera of patients with a clinical tumour stage of 4, when compared to those with a clinical tumour stage of 3. This supports previous studies suggesting a relationship between complement and tumour stage[275,319]. Importantly, the relationship between circulating and tumoural complement is far from understood and requires further study to elucidate how tumour stage and sera levels may be related.

A major area of interest in the investigation of complement in cancer is whether tumoural levels of complement are reflective of or related to circulating levels. Although circulating complement is hepatic in origin, whether or not tumour-derived complement can contribute to the circulating pool of complement components is largely unexplored. In an attempt to address this question in part, tumour biopsy expression of C3 at the mRNA level was correlated with the circulating level of C3 in pre-treatment sera from a small pilot

cohort of matched patients. While no significant associations were demonstrated, there was a strong trend towards an inverse relationship, suggesting that further investigation in a larger cohort is warranted. This is supported by a study of gastric cancer, in which pre-treatment tumoural deposition of C3 was inversely related to pre-treatment C3 levels in plasma[317]. Importantly, investigation of the expression of C3 at the protein level in rectal tumour biopsies is required, as mRNA levels may not be reflective of the protein level. A small number of studies have explored whether the pool of tumoural complement is distinct to circulating complement. In oral squamous cell carcinoma (OSCC), salivary and plasma levels of C4d were significantly associated[275]. More recently, in clear cell renal cell carcinoma, Daugan and colleagues proposed that CFH produced by the tumour has little to no contribution to the plasmatic pool[342]. These studies highlight once again the context-dependent nature of complement in cancer.

CRC risk increases with obesity[469]. Elevated expression of complement components has been observed in obese individuals[470] and C3 has been demonstrated to correlate with obesity and BMI[471]. In this study, C3 mRNA expression was not associated with BMI, however C5 mRNA expression in pre-treatment rectal tumour biopsies positively correlated with BMI, with higher levels expressed in tumours from obese patients, when compared to overweight patients. To our knowledge, this is the first indication of a potential relationship between obesity and tumoural expression of complement genes in rectal cancer. These data suggest that obesity may result in dysregulated complement expression in rectal cancer. In patients with metabolic disease, circulating complement is dysregulated[472]. However, circulating levels of complement were not associated with BMI or a particular BMI category, in contrast with results from tumour tissue. This further suggests that in rectal cancer, tumoural complement and circulating complement are distinct pools, with different biological effects. Notably, there are limitations with using BMI to define obesity, as it does not distinguish subcutaneous or visceral fat and cannot take muscle or bone mass into account[473]. As such, other markers including waist-to-hip ratio, visceral fat area as defined by CT or MRI, and waist circumference are more accurate indicators of visceral obesity. Therefore, to further investigate the relationship between tumoural complement expression and obesity, data should be analysed with respect to these clinical measurements.

IL-6 is a pro-inflammatory cytokine, which can promote tumourigenesis in CRC[474]. In this study, C3 levels correlated with IL-6 levels, in both pre-treatment sera and TCM generated from pre-treatment rectal tumour biopsies. This suggests that both within the

circulation and the TME, there is a relationship between IL-6 and C3. There are few studies in the literature, which have reported a relationship between IL-6 and C3 in cancer. In a small cohort of women with breast cancer in Iraq, it has been suggested that C3 and IL-6 together with TNF-α and IgA may predict disease recurrence. This was based on the observation that women who developed recurrences had altered serum levels of each of these markers, including elevated C3 and IL-6, relative to women who did not[475]. In rectal cancer, following neo-CRT, elevated plasma levels of IL-6 have previously been demonstrated in rectal cancer patients with poor responses[476]. Similar results were demonstrated in another study, where although not significant, patients achieving a pCR tended to have lower pre-treatment concentrations of IL-6 in sera[477]. These studies highlight that IL-6 may negatively affect patient response to neo-CRT in rectal cancer. Importantly, IL-6 has been demonstrated to induce the synthesis of C3 in the liver, skin fibroblasts and germinal centre cells[478–480]. Potentially, in rectal cancer there is a cross-talk between IL-6 and C3 to promote inflammation and negatively affect disease pathogenesis.

Determining the molecular, cellular and microenvironmental factors influencing response to neo-CRT in rectal cancer is essential to improving patient outcomes, and may identify predictive biomarkers of response. Additionally, improving tumour response to neo-CRT may allow organ preservation. Wilkins *et al.* have recently demonstrated that complement activation pathways are enriched in rectal tumours that respond poorly to neo-CRT[481]. While specific genes were not named, the study highlighted that complement components may associate and play a role in the tumour response to neo-CRT in rectal cancer. One of the main objectives of this Chapter was to assess whether tumour expression of complement components is altered based on tumour response to neo-CRT in rectal cancer. However, tumoural expression of C3, C5, CFB, or C1q was not altered based on TRS, indicating that pre-treatment expression of both central and activation pathway complement components do not influence subsequent patient response to neo-CRT. Although no associations between TRS and expression of central or pathway complement components were demonstrated here, this may be a feature of the patient cohort, which was limited in size and distribution across TRS groups (12 patients with TRS 0 or 1, 5 patients TRS 2 or 3). Further investigation of the relationship between tumour-derived complement expression and TRS in larger, independent cohorts is required. Additionally, while in this study tumour expression of C3, C5, CFB and C1q mRNA did not associate with TRS, potentially expression at the gene level is not reflective of protein expression in these biopsies. Further investigation of the protein expression of key complement components in

rectal tumours is required to elucidate the relationship between complement expression and TRS.

It is also possible that associations between complement and treatment response in rectal cancer are more complex than simply the levels at which components are expressed in good and poor responders. An elegant study by Olcina *et al.,* demonstrated that in CRC, mutations in complement components are associated with poor OS[287]. Analysis of differentially expressed genes in the tumours of patients with and without complement mutations revealed alterations in a hypoxia signature [287]. This highlights that dysregulation of complement converges on other important cellular processes, which may have major implications on patient outcomes. Potentially, investigation into the relationship between tumoural expression of complement and response to neo-CRT in rectal cancer may require analysis of specific mutations rather than simply the relative expression levels of individual components, to ascertain whether complement expression impacts on the tumour response to neo-CRT.

This study also investigated the potential of circulating complement components as biomarkers of response to neo-CRT. Interestingly, pre-treatment circulating levels of C3a were increased in patients with subsequent poor responses to neo-CRT, those with a TRS of 3. This highlights that activation of the complement system systemically may have an impact on patient prognosis, potentially by having an immunosuppressive effect on immune cells. Furthermore, it demonstrates that complement may have potential as a minimally-invasive biomarker of response to neo-CRT in rectal cancer. This supports previous studies within our department, which highlighted that increased sera levels of C3a and C4a anaphylatoxins are associated with subsequent poor responses to neo-CRT in OAC[367]. The results presented in this chapter further support a role for complement anaphylatoxins in the response to neo-CRT in GI cancers. The implication of circulating C3a in the poor response of rectal tumours to neo-CRT raises the question of whether circulating C3a plays a functional role in the response to treatment, or whether elevated levels in poor responders are secondary to another event.

C5b-9 was detected in pre-treatment sera from rectal cancer patients, providing further evidence for systemic activation of the complement system in rectal cancer. This finding is supported by a previous study, which demonstrated circulating C5b-9 in plasma from rectal cancer patients[398]. In this chapter, levels of C5b-9 were significantly higher in patients with a subsequent poor response to neo-CRT. This further supports a role for complement as a

predictive biomarker of response to neo-CRT in rectal cancer and highlights that circulating complement may influence the tumour response to treatment.

Prognostic biomarkers have much importance in providing treatment-independent information on outcomes such as RFS and OS[482]. Overexpression of C3 in colon but not rectal cancer negatively correlates with OS, highlighting the prognostic significance of complement in cancer[483]. Results presented in this chapter suggest that increased activation of the complement system has a negative effect on patient outcomes in rectal cancer, with elevated circulating levels of C5b-9 associated with worse RFS and OS. This suggests that C5b-9 may have prognostic potential in rectal cancer. Elucidating the functional importance of C5b-9 in this context and the initiating factors in assembling C5b-9 are necessary. Considering this, understanding the mechanism of complement activation and the complement activation pathway (s) that function in the context of this cancer is essential for effective targeting of the complement cascade. Supporting *in vitro* results in Chapter 3, analysis of complement gene expression in pre-treatment rectal tumour biopsies demonstrated that CFB is expressed in rectal tissue. While serum levels of components specific to the different complement activation pathways were not assessed as part of this study, previous study of circulating complement activation products has demonstrated that the alternative pathway is activated systemically in rectal cancer[398]. This provides further evidence that the alternative complement activation pathway may predominate in rectal tumours and systemically. However, in CRC, lectin pathway components have been detected in the circulation, with increased activity observed in patients relative to non-cancer controls and elevated levels of components such as MASP-2 demonstrated to correlate with disease recurrence and poor survival[273,284]. Expression of MBL of the lectin pathway was not detected in pre-treatment rectal tumour biopsies, therefore further investigation of expression of additional components of the lectin pathway is required to determine whether this pathway is involved in the pathogenesis of rectal cancer. Although often grouped together, colon and rectal cancers are distinct diseases[452]. Potentially there are differences between the complement pathways of activation that dominate each of these cancer types. Additionally, as discussed, whether circulating complement reflects tumoural complement levels in rectal cancer remains largely to be elucidated. Further study is necessary to determine whether complement activation varies within the TME, when compared to systemic activation.

While results presented in this chapter highlight two complement activation products, C3a and C5b-9, as potential biomarkers of poor response to neo-CRT and poor

OS, this requires extensive further validation. In the literature, assessing the potential of complement as clinically-relevant biomarkers is associated with challenges. Many of the biomarker investigative studies for complement components to date, are in part limited by a small sample size. A systematic approach on a larger scale is essential for validation of the clinical utility of complement as a biomarker[456].

In summary, the results presented in this chapter confirm that central and activation pathway components of the complement system are expressed in pre-treatment rectal tumour biopsies. Although tumour expression of complement does not correlate with tumour stage, C5 mRNA expression positively correlates with BMI suggesting a potential relationship between complement and obesity in CRC. Tumoural expression of C3 was not reflective of C3 levels in the sera suggesting that in rectal cancer these complement pools may be distinct. In the circulation, C3, C5 and their respective anaphylatoxins C3a and C5a were detected, demonstrating complement activation. The presence of C5b-9 further supports systemic activation of the complement system in rectal cancer. Circulating levels of C3a were elevated in patients with advanced clinical stages suggesting a relationship between tumour stage and complement in rectal cancer. Interestingly levels of both C3a and C5b-9 were elevated in patients with subsequent poor responses to neo-CRT and C5b-9 levels were elevated in those with worse RFS and OS. This highlights that complement activation in rectal cancer is associated with worse outcomes and suggests that complement has potential as a circulating predictive and prognostic biomarker of response to neo-CRT in rectal cancer.

Chapter 6: Concluding Discussion and Future Directions

CRC significantly contributes to the global cancer burden, representing the third most commonly diagnosed cancer type, and the second most common cause of cancer death[1]. Rectal cancer accounts for approximately one third of all CRCs and was responsible for over 300,000 deaths worldwide in 2020[1]. In Ireland, the majority of rectal cancers are at late stage upon diagnosis[14], and the average 5-year survival irrespective of stage is around 60%[3]. Worryingly, the incidence of CRC is rising, particularly in younger populations (<50), with tumours occurring more frequently in the rectum relative to the colon[7,8]. The high mortality rates and projected increase in incidence over the next decade represents a global health burden, highlighting the critical need for improved treatment strategies for rectal cancer patients.

A multimodal approach to treatment is now the standard of care for LARC, with patients receiving neo-CRT followed by surgical total mesorectal excision. Patients who attain a pCR following neo-CRT, have significantly improved outcomes; significantly reduced disease recurrence and significantly improved metastasis-free, 5 year and OS[53]. However, unfortunately response rates are modest, with only ~30% of patients demonstrating a pCR following neo-CRT[54–56]. The remaining patients are subject to therapy-associated toxicities without apparent therapeutic gain and their prognosis may be worsened by the delay to surgery[57]. Consequently, there is a global unmet need to elucidate the molecular mechanism(s) underpinning response to neo-CRT in rectal cancer. The identification of novel therapeutic targets is essential to improve the efficacy of current treatment and increase the proportion of patients demonstrating a pCR following neo-CRT. Furthermore, at present there are no clinically approved predictive biomarkers to indicate prior to the initiation of treatment, whether patients are likely to respond to neo-CRT. This would have the added benefit of potentially increasing the number of patients who may be eligible for a 'wait-and-see' approach, which avoids proceeding straight to surgery following neo-CRT and enables organ preservation. With strict selection criteria this management has been demonstrated as a safe option, once appropriate follow up takes place[53,61].

Combining chemotherapy with RT aims to achieve an enhanced therapeutic effect, which can occur by several mechanisms, independent of an additive effect[484]. One of these is spatial co-operation, which describes how the systemic effects of chemotherapy can augment the locoregional tumour control which is exerted by RT[484]. Therefore, this suggests that with regards to locoregional tumour control, resistance to RT is largely accountable for treatment failure. Resistance to RT has been linked to several parameters

including DNA damage and repair, tumour cell repopulation, redistribution within the cell cycle, tissue reoxygenation, intrinsic radiosensitivity and more recently, the immune response[104]. Although DNA is the critical target of RT, radiation can also modulate anti-tumour immune responses[99]. Dysregulation of the immune system promotes tumour growth and can alter responses to anti-cancer therapy including RT. The most recent immune component to be included in this paradox is the complement system, which has been demonstrated to play roles in both of these processes[162]. Previous findings within our Department demonstrated that components of the complement system were upregulated in an isogenic *in vitro* model of radioresistant OAC (unpublished data), and in pre-treatment sera and tumour biopsies from OAC patients who subsequently had poor pathological responses neo-CRT[367,368]. As the complement system has been largely unexplored in rectal cancer, this study aimed to characterise the inherent radiosensitivity of a panel of CRC cell lines and profile the expression of the complement system in these cells. Furthermore, the effect of modulating C3 expression on the radiosensitivity of colon and rectal cancer cell lines was assessed and characterised in terms of apoptosis, DNA damage and repair and cell cycle distribution. The effects of colon and rectal cancer cell-derived C3 and recombinant C3a on T cell phenotype (viability, activation, proliferation and cytokine production) was assessed, in the context of T cell activation in the presence of complement, or activation followed by migration to a complement-rich environment. Additionally, little is known about the circulating levels and tumoural expression of complement components in rectal cancer patient sera and tumour tissue, respectively. To investigate this, key complement components were profiled using samples from rectal cancer patients to assess whether alterations in complement levels are associated with key clinicopathological factors including response to neo-CRT and prognosis.

To identify an *in vitro* model for studying radiosensitivity/radioresistance in CRC, a panel of CRC cell lines was selected for study in Chapter 2. This consisted of the HCT116 human colon carcinoma cell line and SW837, HRA-19 and SW1463 cells, three human rectal adenocarcinoma lines. A challenge in studying radioresistance in rectal cancer is that few cell lines have been established from rectal tumours and as a result the majority of published studies have employed colon cancer cells[387]. As HCT116 cells are an extensively characterised colon cancer cell line in radiobiology studies, it was selected for inclusion in this panel. In support of previous studies, HCT116 cells were demonstrated to be inherently radiosensitive[388–391]. To date, the radioresponses of rectal cancer cell lines have been poorly characterised in the literature, with minimal studies reporting the radioresistance of the

SW1463 and SW837 cell lines[387,390–393]. In agreement, all three rectal cancer lines assessed in this study were inherently radioresistant, when compared to HCT116 cells, supporting this panel of cell lines as an *in vitro* model of inherent radiosensitivity/ radioresistance. The SW1463 cell line was the most radioresistant at 1.8 Gy and 2 Gy doses of IR, while the HRA-19 cell line emerged as the predominant radioresistant line at higher doses of IR. To our knowledge, this study is the first to report the inherent radioresistance of the HRA-19 cell line.

A growing body of research has provided evidence that complement components are expressed by cancer cells[177]. The central complement cascade proteins C3 and C5 were expressed by all four CRC cell lines in the panel. Previous investigations of the role of complement in the response to radiation have observed that complement gene transcripts are upregulated after radiation in a variety of cell types including immune cells and murine and human tumours[351]. This suggests that radiation may upregulate complement in cancer. Supporting these findings, in this study HCT116 cells upregulated expression of C3 and C5 following radiation, highlighting that radiation may increase complement expression in radiosensitive cancer cells.

The potent C3a and C5a anaphylatoxins are cleaved from the C3 and C5 proteins, and are traditionally considered a marker of complement activation. Evidence for systemic and local activation of the complement system in cancer has been demonstrated in several studies[273–278]. Supporting this, we demonstrate that activation of C3 and C5 to produce C3a and C5a occurs in CRC cell lines. Interestingly, C3a and C5a was present in protein lysates from these cells suggesting that C3a and C5a are present intracellularly. In this study, C3a and C5a were detected at low levels (below the standard curve) in supernatants from these cell lines, likely due to the sensitivity of the assay. Previous studies have demonstrated that CRC cells secrete C3a[337] and C5a[333], however, the assay sensitivity in these publications exceeded those which were used for this study, an important consideration for future investigations.

The complement system can be activated in cancer, with evidence demonstrating that across cancer types this activation encompasses the classical, lectin and alternative pathways[275,293,485]. Importantly, activation of the complement system has been reported to correlate with poor prognosis in several human cancers, including CRC[283–285,394]. In this study, expression of both C1q and MBL2, key initiating components of the classical and lectin pathways, respectively, were not detected in the CRC panel. Interestingly, expression of CFB, an alternative pathway component, correlated with total C3 and C5 mRNA

expression, and was elevated in radioresistant cells. This may suggest that in CRC, complement activation is occurring via the alternative pathway. However, recent evidence presented by Ding *et al.* demonstrates that within CRC cells, cleavage of C5 can occur independently of the complement cascade by CTSD[341], similar to C3 processing by CTSL which occurs in T cells[263]. In the CRC cell line panel assessed in this study, similar cleavage of C5 and C3 may occur. Further study is required to elucidate the specific mechanisms responsible for anaphylatoxin generation.

In addition, C1q of the classical pathway has been demonstrated to promote tumour growth in a murine model of melanoma, indicating that independent of complement activation, key initiating members of activation pathways may have pro-tumour roles[299]. Similarly, CFB has been observed to promote the growth of cSCC cells, with the authors of this study raising the possibility that this may occur independent of complement activation[301]. Therefore, while proteases independent of the alternative complement cascade may activate C3 and C5, CFB may also engage in a pro-tumour role in CRC cells.

The identification of mCRPs expressed by CRC cells suggests that these cells can modulate complement activation. Interestingly, CD46, CD55 and CD59 were all expressed on the surface of each cell line within the CRC panel. CD55 appears to be an unfavourable prognostic marker in CRC, with upregulation associated with disease progression, relapse and worse 7-year survival[486–488]. While this suggests that CD55 may be upregulated in radioresistant cell lines, our characterisation demonstrated that CD55 expression was decreased in the HRA-19 and SW1463 radioresistant cell lines. SW837 cells are also inherently radioresistant and demonstrated elevated CD55 expression, when compared to the other rectal cancer cell lines, suggesting that CD55 may not be involved in the radioresponse in CRC. Further study is required to elucidate the mechanisms by which CD55 expression is altered in CRC.

Complement signalling via C3a and C5a receptors is a key mechanism by which complement activation can remodel the cellular environment[489]. We demonstrate for the first time that colon and rectal cancer cells express the C3aR intracellularly and C3aR is localised within the cytoplasm and the nucleus in colon cancer cells. In addition, we support recent findings that C5aR1 is expressed in colon cancer cells[341], and demonstrate for the first time that the C5aR1 is expressed on the surface and intracellularly in rectal cancer cells. These data suggest that intracellular complement signalling axes may be important in CRC. Supporting this, Ding *et al*. have recently demonstrated intracellular signalling of C5a via C5aR1, to drive the assembly of a complex of potassium channel tetramerization

domain 5(KCTD5)/cullin3/Roc-1[341]. This complex stabilises β-catenin, allowing for transcription of oncogenes including COX-2 and cyclin D, providing direct evidence that intracellular complement signalling can drive tumourigenesis[341]. In Chapter 2, the intracellular concentration of C3, C5 and their respective anaphylatoxins was elevated in radioresistant CRC cells. Intracellular complement also positively correlated with the surviving fraction of cells at a clinically-relevant dose of IR. This suggests that complement may play functional roles in the response of CRC to radiation, potentially via an intracellular signalling axis.

Autocrine roles for tumour cell-derived complement have been demonstrated to influence tumour cell proliferation, migration and invasion, with intracellular roles for complement recently coming into focus[344]. Intracellular C4BP-A has the ability to alter sensitivity to oxaliplatin-induced apoptosis in an NF-κB-dependent manner, providing evidence for intracellular complement in the response to cancer therapy[343]. In Chapter 3, the role of C3 in functionally modulating the response to IR in CRC cell lines was investigated. Overexpression of C3 in the radiosensitive HCT116 cell line, which express low basal levels of C3 resulted in enhanced radioresistance, while transient silencing of C3 significantly sensitised the radioresistant HRA-19 cells to a clinically-relevant dose of IR. Silencing of C3 in the radioresistant SW837 cell line was not associated with enhanced radiosensitivity, however this may be due to lower basal expression levels of C3, when compared to HRA-19 cells, the apparent downregulation of C3 in si-scr controls following irradiation, and also a degree of variability between experimental replicates. Further optimisation of C3 silencing in SW837 cells, is required to interrogate the role of C3 in the response to IR in this cell line model.

In order to gain greater insight into how C3 functionally modulates the response to radiation in CRC cells, the relationship between C3 and key parameters associated with radioresistance; apoptosis, DNA damage induction and repair and cell cycle distribution were investigated. Alterations in apoptosis have been linked with radioresistance in several cancer types[143–145]. In C3 silenced HRA-19 cells and C3 overexpressing HCT116 cells, both basal and radiation-induced apoptosis was unaltered. While this suggests that altered apoptosis may not be implicated in complement-mediated modulation of the radioresponse, this needs to be further investigated using larger fractions of IR or multi-fraction doses of IR.

Alterations in DNA repair capabilities have been reported to confer radioresistance in cancer cells[122–124]. Complement components including C5 and C1QBP have been implicated in DNA repair and response to chemotherapy[347,369]. In a previous study, in OAC patient biopsies, elevated C3 expression correlated with poor response to neo-CRT and in OAC cell lines miR-187 negatively regulates the expression of both C3 and several DDR genes, suggesting a relationship between complement, DNA repair and response to RT[368]. These studies highlight that complement potentially interacts with DDR genes to influence response to therapy. In this study, while overexpression of exogenous C3 in HCT116 cells did not alter basal or radiation-induced DNA damage, transient silencing of endogenous C3 was associated with elevated basal levels of DNA damage in HRA-19 cells, and significant levels of DNA damage persisted up to 10 h post irradiation. This suggests that within radioresistant rectal cancer cells, C3-mediated alterations in DNA damage and repair may alter the response to radiation.

The position of a cell within the cell cycle can influence response to radiation, with G2/M phase cells demonstrating superior radiosensitivity, when compared to the more resistant G0 cells and the inherently radioresistant S phase cells[95–97]. Similar to the other parameters assessed, HCT116 cells did not demonstrate basal or radiation-induced alterations in cell cycle distribution following overexpression of C3. In contrast, in the basal state, C3 silenced HRA-19 cells demonstrated a partial arrest in the G2/M phase and a reduction in the percentage of radioresistant S phase cells following irradiation. This indicates that radioresistance in rectal cancer may arise in part due to complement-mediated dysregulation of cell cycle distribution, which favours a more radioresistant phenotype.

In a recent study, alternative translation of C3 resulting in distinct cytosolic and secreted forms has been reported[409]. Furthermore, intracellular CFH has been demonstrated to perform different roles relative to its membranous counterpart, with intracellular CFH associated with unfavourable patient prognosis[409]. Together these studies provide evidence that distinct forms of complement components exist, which can engage unique roles and may impact on cancer pathogenesis and subsequent outcomes. We postulate that the observed differences in the effects of C3 modulation in HCT116 and HRA-19 cells on the parameters assessed may have been due to our experimental set up; whereby overexpression of exogenous C3 in HCT116 cells generates an alternative form of C3, which interacts with intracellular signalling networks in a manner distinct from endogenous C3. Furthermore, given that the underlying biology of HCT116 and HRA-19 cells reflects their tumour of origin; colon and rectal tumours, respectively, and that differing molecular

drivers are evident in colon and rectal cancers, this may suggest that C3 has differing functions in these cell types. With collaborators at the University of Oxford, we overexpressed C3 in HRA-19 and HCT116 cells and performed IP and mass spectrometry to interrogate differences between the C3 interactome in these cells. We demonstrate that the C3 interactome is significantly altered between HRA-19 and HCT116 cells. In particular, 3 proteins clusters were identified, which were present in different abundances in HCT116 and HRA-19 cells, suggesting that the C3 interactome is altered in radiosensitive and radioresistant cells. This provides evidence that within these cell lines, C3 may differentially modulate the response to radiation. Interestingly, functional enrichment analysis of significantly altered proteins between the C3 interactomes of HRA-19 and HCT116 cells, identified that several KEGG pathways[490–492] were functionally enriched in the C3 interactome of HRA-19 cells. Interestingly, one of these pathways was oxidative phosphorylation, which our Department has previously demonstrated to play a role in the response to radiation of rectal cancer cells (unpublished data) and OAC[493], suggesting a potential relationship between complement and metabolic reprogramming, which warrants further investigation.

Tumour cell-derived complement has been demonstrated to modulate immune cell phenotype and function in cancer[326,337,494]. Increasing evidence demonstrates that complement signalling axes limit anti-tumour immune responses, therefore, complement anaphylatoxin receptors have been proposed as a novel immune checkpoint for relieving complement-mediated immunosuppression within the TME[430]. Immunosuppressive roles for C3 and the C3a/C3aR signalling axis on T cells have been identified in breast, lung and colon cancers[320,323,326]. In rectal tumours, tumour infiltration by T cells has been demonstrated to correspond with response to neo-CRT[428,429]. However, little is known with regards to the effect of rectal cancer-derived complement on immune cell phenotypes.

Zha *et al.* have demonstrated that in CRC, expression of C3 correlates with a TME characterised by immunosuppression and T cell dysfunction[362]. In Chapter 4, the effect of CM from HCT116 and HRA-19 cells and recombinant C3a on T cell phenotype was assessed. Existing literature has provided evidence that complement plays roles in maintaining T cell viability and T cells within a naïve state[171,263]. There is currently no evidence in the literature for the effects of tumour cell-derived C3 on T cell viability. Data presented in Chapter 4 suggests that C3-derived from rectal cancer cells may have differing effects on viability, depending on whether PBMCs are stimulated in the presence of, or pre-stimulated and then exposed to tumour-derived complement. Cell death was decreased in

PBMCs cultured with CM from si-C3 transfected HRA-19 cells during activation, while pre-stimulated cells demonstrated increased early-stage apoptosis. Considering this, C3 may promote viability as naïve cells become activated, but once activation has initiated, encountering C3 may decrease viability. This suggests that the effects of rectal cancer cell-derived C3 on T cell viability in cancer may be context-dependent. No alterations in the viability of PBMCs were induced by CM from HCT116 cells overexpressing C3, suggesting that colon cancer cell-derived C3 may have different effects relative to C3 derived from rectal cancer cells. In a recent study, alternative translation of C3 generated a distinct form, which localises in a different cellular region and engages in a unique role[409]. Therefore, the different effects observed may also be a feature of the silencing of endogenous C3 in HRA-19 cells, versus the overexpression of exogenous C3 in HCT116 cells.

Previous studies have demonstrated that *in vitro* addition of C3a to T cells does not promote proliferation, with the study authors suggesting that C3a affects T cell proliferation via an indirect mechanism[362]. Supporting this, altered T cell proliferation was not observed following treatment with CM from CRC cell lines, or recombinant C3a. This suggests that *in vitro* experiments are a limiting factor in assessing the effects of tumour cell-derived complement on T cell proliferation.

Tumoural expression of complement has been linked with dysregulated anti-tumour immune responses. In a murine model of colon cancer, restricted T cell infiltration is associated with C3 expression[323]. Analysis of T cell activation marker expression in Chapter 4 suggests that regardless of the set up used; whether complement is present during T cell activation or post activation only, CD62L expression is increased. This suggests that complement rich tumours may promote a lymph node homing phenotype, restricting migration to the tumour. However, cytokine expression in T cells following culture in the presence of HCT116 cell-derived C3 or following pre-stimulation and then culture with recombinant C3a, suggests that T cell responses may be shifted away from Th2-like towards an IFN-γ producing, Th1-like phenotype. Therefore, this may suggest that tumoural expression of C3 in rectal cancer patients may allow for an improved anti-tumour response with better responses to therapy. However, in several studies, immunosuppression of T cells by complement does not occur directly and is mediated by MDSCs. This relies on successful T cell migration to the tumour, which may be impeded by CD62L expression and retention in the lymph node. In order to confirm whether CRC cell-derived C3 has a

favourable effect on the immune response, a mouse model which contains other immune and microenvironmental factors is required.

A recent study reported that the C3-mediated immune response differs between colon and rectal cancers[483]. Liang *et al*. identified C3 as a core differentially expressed gene between colon and rectal cancers, which positively correlates with colon cancer immune scores and has prognostic significance in colon but not rectal cancer[483]. These results suggest that the C3 present within the TME of these cancer types differentially affects the immune cell milieu. Results in Chapter 4, suggest that C3 derived from HCT116 and HRA-19 cells may have different direct effects on T cell phenotype, including viability and activation. While study of the C3-mediated immune response by Liang and colleagues suggests that within the TME of colon and rectal tumours, C3 differentially affects the immune cell milieu[483], the data presented in this chapter suggest that C3 derived from colon and rectal cancer cells differentially alters T cell phenotype. Both the anti-tumour and pro-tumour immune cell populations have been demonstrated to be elevated in colon cancers, when compared to rectal cancers[483], supporting our observations that colon cancer cell-derived C3 may promote a Th1-like response, which would have anti-tumour effects.

Importantly, within our study, the effects of CRC cell-derived complement on the T cell phenotype were assessed basally. The potential shift towards a Th1 phenotype suggests that a complement rich TME may enhance the anti-tumour immune response in the context of RT. However, the findings in Chapter 4 suggest that inhibition of complement may instead reduce CD62L expression, allowing T cells to infiltrate the tumour, which may augment the response to RT. Given the vast body of evidence that demonstrates complement-mediated regulation of immune cells, elucidating the relationship between complement, T cell responses and response to RT, requires mouse models. Current evidence supporting a role for complement in modulating the T cell response following radiation is conflicting. Elvington *et al*. demonstrate that complement inhibition in combination with RT enhances the tumour response to radiation and is associated with increased DC maturation and infiltration of $CD8^+$ T cells[350]. In contrast, Surace *et al*. provide evidence in their model that complement is essential to the therapeutic response to RT, due to the maturation of DCs and subsequent induction of T cell effector responses[351]. Among the differences between these two studies, is the dose of IR used; Surace *et al*. utilised a large 20 Gy bolus dose of IR[351], which was necessary for the model used, while Elvington *et al*. used fractionated IR in doses of 1.5 and 5 Gy[350]. Importantly, when Surace *et al*. delivered 5 x 5 Gy doses of IR, the accumulation and anti-tumour

function of $CD8^+$ T cells was not supported[351]. This suggests that in this model it is the bolus delivery of IR, and not the total dose that may be responsible for the favourable impact of complement on response to radiation. Whether the benefit of complement in the context of RT translates to a clinical setting, where bolus doses of IR such as 20 Gy are not delivered, remains to be further investigated. In the context of rectal cancer, fractionated doses of IR (1.8/2 Gy and 5 Gy) are of clinical relevance, as they are delivered as part of LCRT and SCRT. Considering the findings by Elvington *et al*. and the data presented in Chapter 5, which demonstrates that complement is expressed in rectal tumour biopsies, this provides a rationale for investigating combination RT and complement inhibition in models of rectal cancer.

In chapter 5, expression of complement was assessed in cancer and non-cancer tissue. Expression of central complement components are often overexpressed in tumour tissue relative to healthy tissue[456]. An example of this is expression of C3 in gastric cancer, CRC and cSCC tissue[301,317,468]. Both C3 and C5 mRNA were expressed at significantly higher levels in rectal tumour tissue, when compared to normal tissue. When expression of key initiating components in complement activation pathways was assessed, CFB was also expressed at higher levels in rectal tumour tissue. This supports experiments performed in Chapter 2 which demonstrated that CFB is expressed in CRC cell lines. In contrast, in non-cancer rectal tissue, relative expression levels of C1q were elevated, when compared to tumour tissue, suggesting that the expression of complement activation pathway components differs in malignant tissue relative to healthy rectal tissue. To confirm that complement expression is of epithelial origin, study of FFPE tumour biopsy tissue is required.

In OAC, tumour expression of C3 has been demonstrated to correlate with response to neo-CRT[368]. In Chapter 2, expression of C3 and C5 was elevated in radioresistant CRC cell lines and correlated positively with SF at 1.8 Gy of IR. This suggests that complement may play a role in the radioresponse. When tumoural expression of C3, C5 and complement pathway components was assessed in Chapter 5, expression did not correlate with TRS in this rectal cancer cohort, suggesting that complement may not have predictive power in rectal cancer patients. However, further investigation in a larger independent patient cohort is required to determine whether this is just due to small sample size. In addition, mRNA expression of complement components may not be reflective of protein levels, therefore, further investigation of tumour-derived complement protein expression and the relationship with subsequent TRS is required.

Expression of C3, CFB and C1q mRNA in rectal tumour biopsies did not correlate with pathological T stage or BMI, suggesting that expression of these components is independent of such clinical factors. C5 mRNA expression was elevated in the tumour tissue from obese patients, relative to overweight patients suggesting there may be a relationship between expression of C5 and increasing BMI.

In chapter 5, activation of the complement system was demonstrated systemically, with C3a, C5a and C5b-9 detected in rectal cancer patient sera. Circulating members of the lectin pathway including MBL, collectin-liver 1 and M-ficolin have been reported within the circulation in CRC[273,284,396,397]. This highlights that the lectin pathway may be of importance in CRC. Analysis of whole rectal tumour biopsies demonstrated that MBL2 was not detected at the mRNA level. Interestingly, CFB of the alternative pathway was demonstrated to be overexpressed in tumour tissue, when compared to normal tissue, suggesting a potential role for this activation pathway in rectal tumourigenesis. While circulating complement components were assessed in pre-treatment sera from rectal cancer patients, pathway-specific components were not profiled, so the activation pathway responsible for generation of anaphylatoxins within the circulation in rectal cancer is unknown. Elucidating how complement is activated in rectal cancer requires further investigation of the expression of complement pathway-specific components both within tumour tissue and blood samples.

Furthermore, whether tumoural and circulating complement are related in rectal cancer remains to be determined. In a pilot cohort (n=10), we demonstrated a trend towards a negative correlation between the circulating and tumoural expression of C3 in rectal cancer patients. To determine whether circulating complement levels are reflective of tumoural complement expression, further study in a larger patient cohort is required.

While the relationship between circulating and tumoural complement remains to be determined, in both pre-treatment serum and TCM generated from pre-treatment tumour biopsies, C3 positively correlated with IL-6. Serum levels of IL-6 have previously been associated with response to neo-CRT in rectal cancer[476,477], and IL-6 has previously been implicated in the promotion of CRC tumourigenesis[474]. Considering our findings in rectal cancer, this suggests that an IL-6-C3 relationship may be significant in the pathogenesis of rectal cancer and warrants further investigation. Functional enrichment analysis of proteins that were significantly altered between the HRA-19 and HCT116 cell C3 interactomes identified several KEGG pathways[490–492] which were functionally enriched in HRA-19 cells. Interestingly, one of these was the cytosolic DNA sensing pathway within which IL-

6 production can occur via both the NF-κB and retinoic acid-inducible gene I (RIG-I)-like receptor signalling pathway. This further suggests a potential relationship between IL-6 and C3 in rectal cancer that may influence the response to RT.

Pre-treatment circulating levels of C3, C5, C3a, C5a and C5b-9 were not altered in rectal cancer patients based on BMI or pathological T stage. This suggests that similar to the expression of complement in pre-treatment biopsies, circulating complement is independent of these factors. Circulating levels of C3a were elevated in patients with clinical T stage of 4, when compared to a clinical T stage of 3. Importantly, we demonstrated for the first time that pre-treatment circulating C3a and C5b-9 levels are associated with subsequent poor responses to neo-CRT in rectal cancer. This suggests a role for circulating markers of complement activation as potential predictive biomarkers of response to neo-CRT in rectal cancer, supporting previous data from our Department in OAC[367]. Elucidating how circulating levels of complement may be influencing response to neo-CRT in rectal cancer remains unknown, but investigations in murine models to extensively characterise the effects of complement on the immune milieu in rectal cancer may provide useful insights.

The prognostic significance of complement component expression is often negative [274,283,291,363], however, in some cancer types such as NSCLC, complement associates with favourable prognosis[364]. Interestingly, pre-treatment circulating levels of C5b-9 emerged as a potential prognostic biomarker, with elevated C5b-9 levels associated with worse RFS and OS in a cohort of rectal cancer patients. Activation of the complement system culminates with the assembly and insertion of the TCC, C5b-9, into target cells to induce cell lysis[208,209]. C5b-9 is composed of C5b, C7, C8 and C9 and has been detected in ovarian cancer-associated ascitic fluid[281] and several tumour tissues including breast[278], gastric[279] and thyroid[280]. TCGA analysis of complement genes performed by Roumenina *et al*. demonstrated that expression of C8A, C8B and C9 is low across the majority of cancer types, therefore they suggest that activation of the terminal complement pathway (to form C5b-9) is unlikely to occur as a result of this in situ complement[177]. This may suggest that circulating C5b-9 is derived solely from the systemic pool of complement and not tumour-produced complement components, which may be useful in interrogating how C5b-9 levels are related to outcomes in rectal cancer.

Biomarkers demonstrating predictive potential for response to neo-CRT in rectal cancer span clinical features, molecular markers, histopathological features and the tumour

environment[453]. To our knowledge, this is the first study to implicate circulating complement in the response to neo-CRT in rectal cancer. Biomarker investigative studies for complement components to date, are in part limited by a low sample size. Validation of the clinical utility of complement as both a predictive and prognostic biomarker necessitates a large scale, systematic approach[456].

This thesis has demonstrated that complement may represent a therapeutic target in rectal cancer, and may modulate T cell phenotype within the TME. Understanding the role of complement in rectal cancer requires critical consideration of previous work by Olcina and colleagues, which demonstrated that the prognostic association between complement components and poor OS was a result of the mutational status of complement genes[287]. This suggests that in instances where complement is modulating response to treatment in cancer it may be necessary to characterise the expression of complement beyond relative expression levels. Additionally in rectal tumours, four immune subtypes have been identified which are linked to prognosis and in some cases, response to immunotherapy[495]. Considering that complement has the capacity to functionally modulate immune cells within the TME, it may be expected that tumour-derived complement may differentially affect the immune milieu in rectal tumours, depending on which CMS they are characterised by. Furthermore, based on this heterogeneity, it is likely that immune subtypes in rectal cancer may differentially impact response to RT.

In conclusion, in this study, complement activation was demonstrated to be associated with inherent radioresistance in CRC cells. We also demonstrate, for the first time, a functional role for C3 in modulating the response to IR in CRC cells *in vitro*. CRC cell-derived C3 was demonstrated to alter the T cell phenotype, providing evidence that complement may modulate immune cells within the TME of rectal cancer. For the first time, a panel of complement components were profiled in pre-treatment rectal cancer patient sera, highlighting C3a and C5b-9 as potential predictive biomarkers of response to neo-CRT, and C5b-9 as a prognostic marker of worse RFS and OS in rectal cancer. Together, the data presented in this thesis provides evidence that complement contributes to radioresistance in rectal cancer, and may have clinical utility as a predictive and prognostic biomarker and novel therapeutic target, following large scale validation of these findings (**Figure 6-1**).

6.1. Future directions

This project has presented several future avenues to explore to further elucidate the role of complement in the response to IR in CRC.

1. Further *in vitro* study of CRC cells is necessary to elucidate the mechanism by which C3 and C5 are cleaved intracellularly. This would determine whether activation is occurring via the alternative complement activation pathway or other intracellular proteases.
2. Additional investigation of CRC cells using IF to assess if cytoplasmic C3aR is associated with a specific organelle is necessary to determine how intracellular C3 modulates the response to radiation.
3. Validation of C3 binding partners is required to further investigate the C3 interactome in rectal cancer.
4. As whole rectal tumour biopsies were used for this study, further investigation as to the source of tumour-derived complement (i.e. tumour epithelium versus stromal compartments) using FFPE tissue is required.
5. Further investigation of the relationship between complement expression and T cell dysfunction using IHC staining of tumour biopsies for T cell activation and exhaustion markers is required. This would provide further details on whether complement positively regulates the T cell immune response, importantly, in a TME in which other immune and stromal cells are present.
6. Profiling of complement components specific to activation pathways in pre-treatment rectal cancer sera is required to further characterise systemic complement activation in rectal cancer.
7. Further characterisation of circulating and tumour-derived complement in matched patients is required to elucidative the relationship between these two complement pools.
8. Validation of pre-treatment circulating C3a and C5b-9 as predictive biomarkers of response to neo-CRT, and C5b-9 as a prognostic marker in rectal cancer in larger, multi-centre, independent patient cohorts is required.

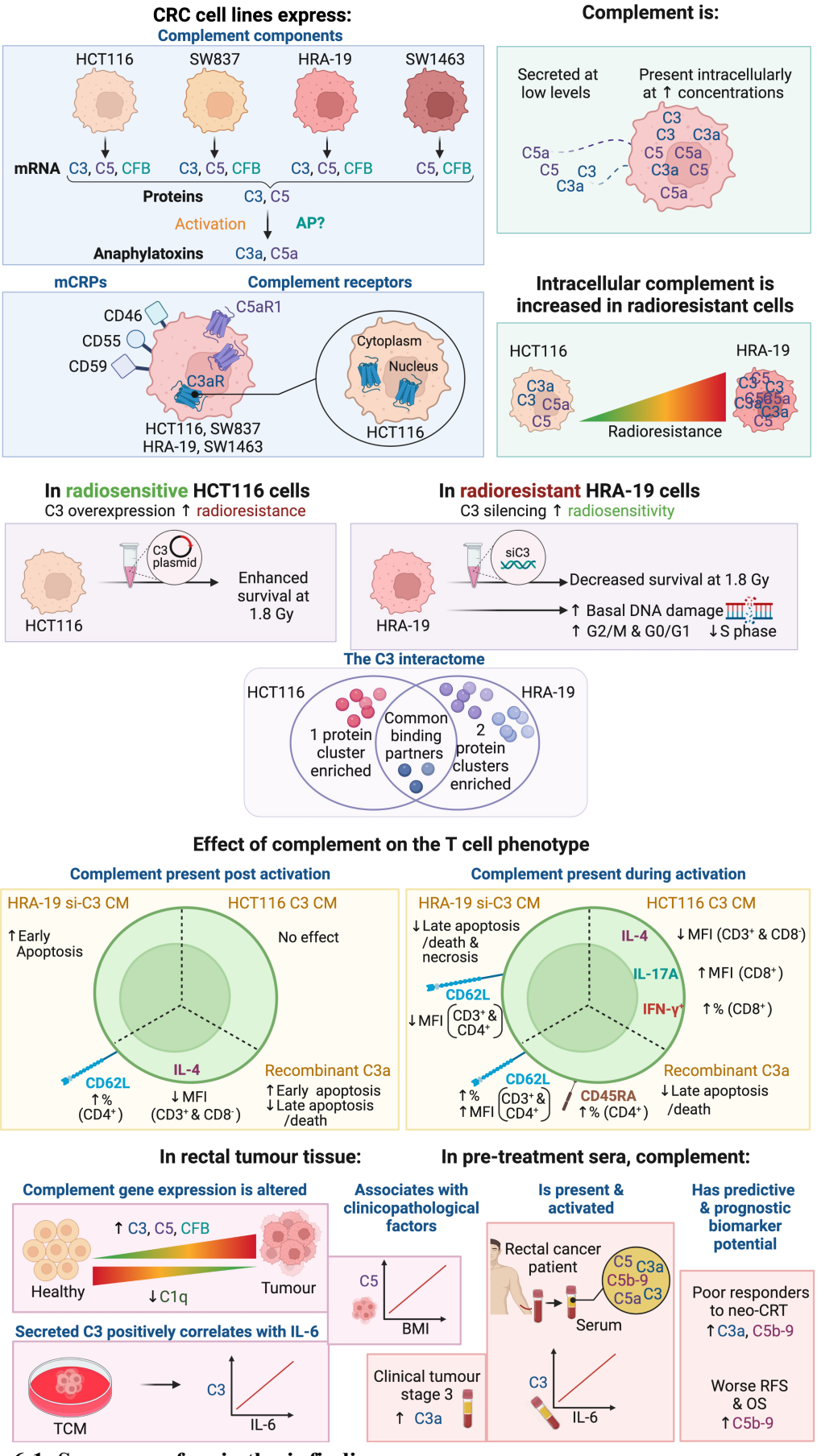

Figure 6-1: Summary of main thesis findings.

Appendices

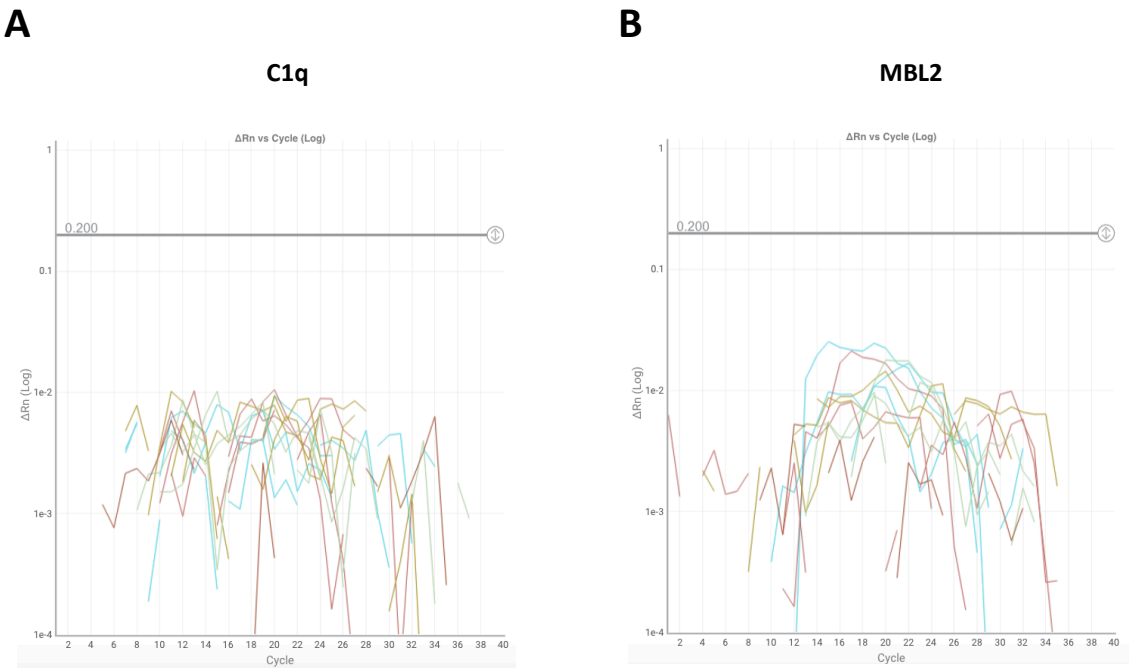

Appendix 1: Amplification plots for C1q and MBL2 which are not expressed by human colon carcinoma HCT116 and human rectal adenocarcinoma SW837, HRA-19 and SW1463 cell lines. C1q and MBL2 expression was assessed by qPCR. Data are representative of 3 independent experiments.

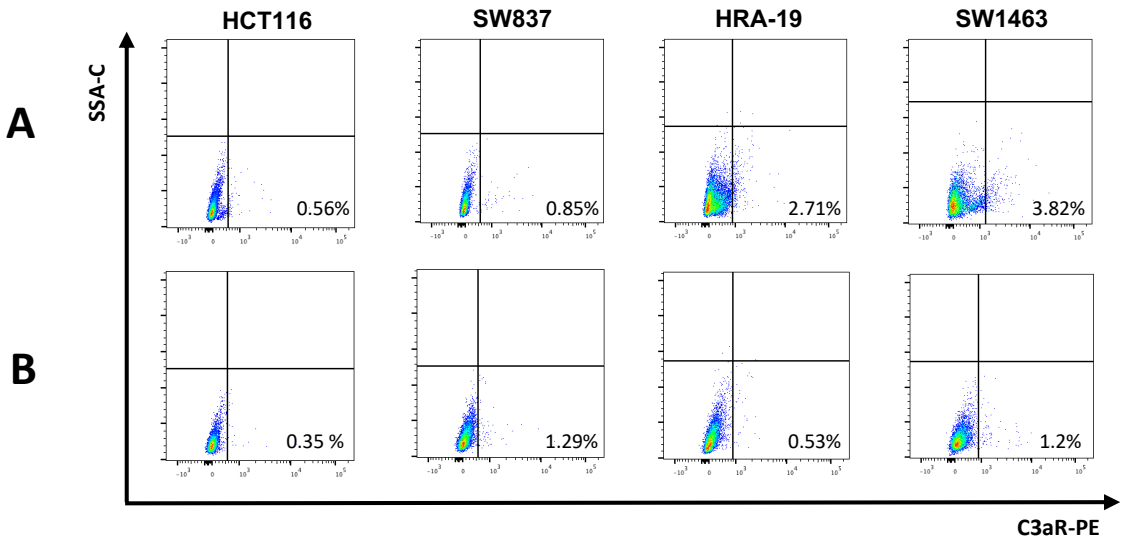

Appendix 2: C3aR is not expressed extracellularly by human colon carcinoma HCT116 or human rectal adenocarcinoma SW837, HRA-19 or SW1463 cells. Expression of C3aR was assessed by flow cytometry. C3aR expression detected in **(A)** unstained and **(B)** C3aR stained HCT116, SW837, HRA-19 and SW1463 cells. Dot plots are representative of data from 3 independent experiments.

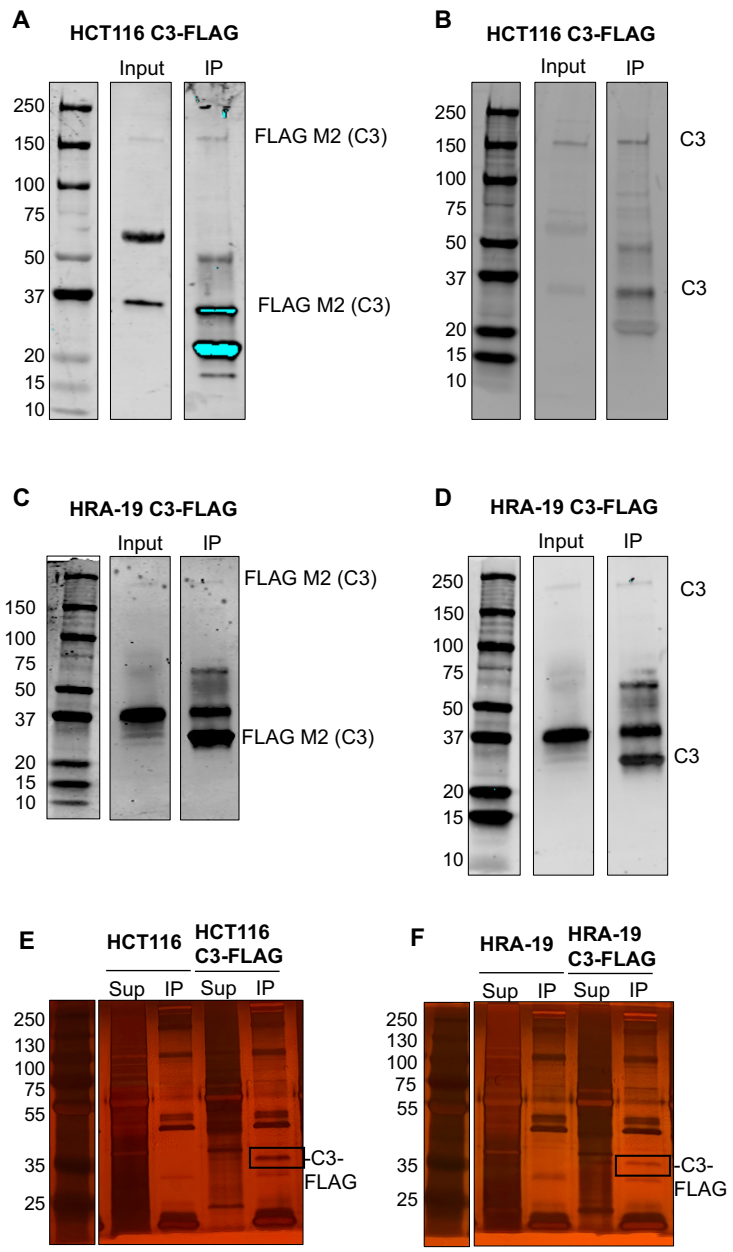

Appendix 3: Confirmation of expression of C3-FLAG in HCT116 and HRA-19 cells. Input (10%) and IP fractions of HCT116 and HRA-19 cells overexpressing C3-FLAG were separated by SDS-PAGE and western blotting of gels was performed. Detection of FLAG M2 (C3) (**A**) and C3 (**B**) in HCT116 cells overexpressing C3-FLAG. Detection of FLAG M2 (C3) (**C**) and C3 (**D**) in HRA-19 cells overexpressing C3-FLAG. Both HCT116 and HRA-19 cells alone and overexpressing C3-FLAG were incubated with FLAG-M2 magnetic beads. Silver stained gels from (**E**) HCT116 and HCT116 C3-FLAG supernatant (sup) and IP fractions and (**F**) HRA-19 and HRA-19 C3-FLAG sup and IP fractions. The IP fractions are representative of 5% of the total FLAG magnetic beads which were boiled in sample buffer for 5 min at 100°C. The supernatant fractions represent the protein lysate solution remaining when C3-FLAG was bound to the magnetic beads.

Appendix 4: Protein clusters identified when clustering analysis was performed using significantly altered proteins (as determined by *p*-adj) between the C3 interactome of HRA-19 and HCT116 cells. Mass Spectrometry was performed by the Discovery Proteomics Facility at the Target Discovery Institute, University of Oxford.

Cluster 1 (Upregulated in HRA-19)	Cluster 2 (Upregulated in HRA-19)	Cluster 3 (Upregulated in HCT116)
ELOA1	HMGB3	EI24
RCN1	CYH1;CYH2;CYH3	MAGB2
DHX37	CXL10	PLIN3
RRP36	P53	DNJA2
NUSAP	ISG15	NDUS7
DHX35	K1C19	AGM1
	H2AV;H2AZ	HS90B
	CCL5	LEG1
	UD16	HS71A;HS71B
	MANF	BIP
	LEG4	HSP7C
	SMD3	EF2
	CCL20	T2FB
	TFAM	CD44
	DHRS2	ERCC3
	TRI29	DNMT1
	SAFB2	ABCD3
	IPYR	TCPD
	SP6	HNRPM
	XAF1	NU107
	TRPT1	RS27A
	DDX60	RT10
	ESIP1	C1QBP
	DDX23	SF3B2
	CHID1	RRP1B
	DDX43	PHLA2
	FKB11	MPP7
	THYN1	UBR4
	KLK14	ECM29_
	LORF1	RL22L
	ZC3H4	FRMD5
	PUS1	RASEF
		CCAR2
		RM30
		NEUG
		RM24
		CC124
		ZC21A
		VAT1
		TCPH

	XRN2
	ESF1
	EXOS4
	XPP3
	SRPRB

Appendix 5: Common predicted interactors of C3 in both HRA-19 and HCT116 cells, which are not differentially expressed at significant levels. Mass Spectrometry was performed by the Discovery Proteomics Facility at the Target Discovery Institute, University of Oxford.

Protein	-log (*p*-value)	Fold change in HRA-19 cells relative to HCT116 cells
TSR3	0.798	-0.3434747
VCP	0.624	0.25092284
LTF	0.844	1.97265848
APOB	0.814	0.38459682
TXN	0.376	0.16089344
GAPDH	0.498	-0.5791136
ALB	0.550	0.6269811
APOE	0.297	-0.3927568
APOA1	0.206	-0.4446872
GSN	0.203	0.31421693
HP	0.25	0.31421693
APOC3	0.546	-0.4128882
F2	0.214	-0.4205588
HPX	0.419	1.07928967
C4A	0.537	0.32019838
ITIH1	0.261	0.46080621
SLC25A18	0.139	-0.208106
ADI1	0.085	0.20000124
HBA2	0.097	-0.182435
AFP	0.163	0.23258432
KNG1	0.125	0.20268504
ITIH4	0.096	0.06561597
NELFE	0.109	-0.1078533

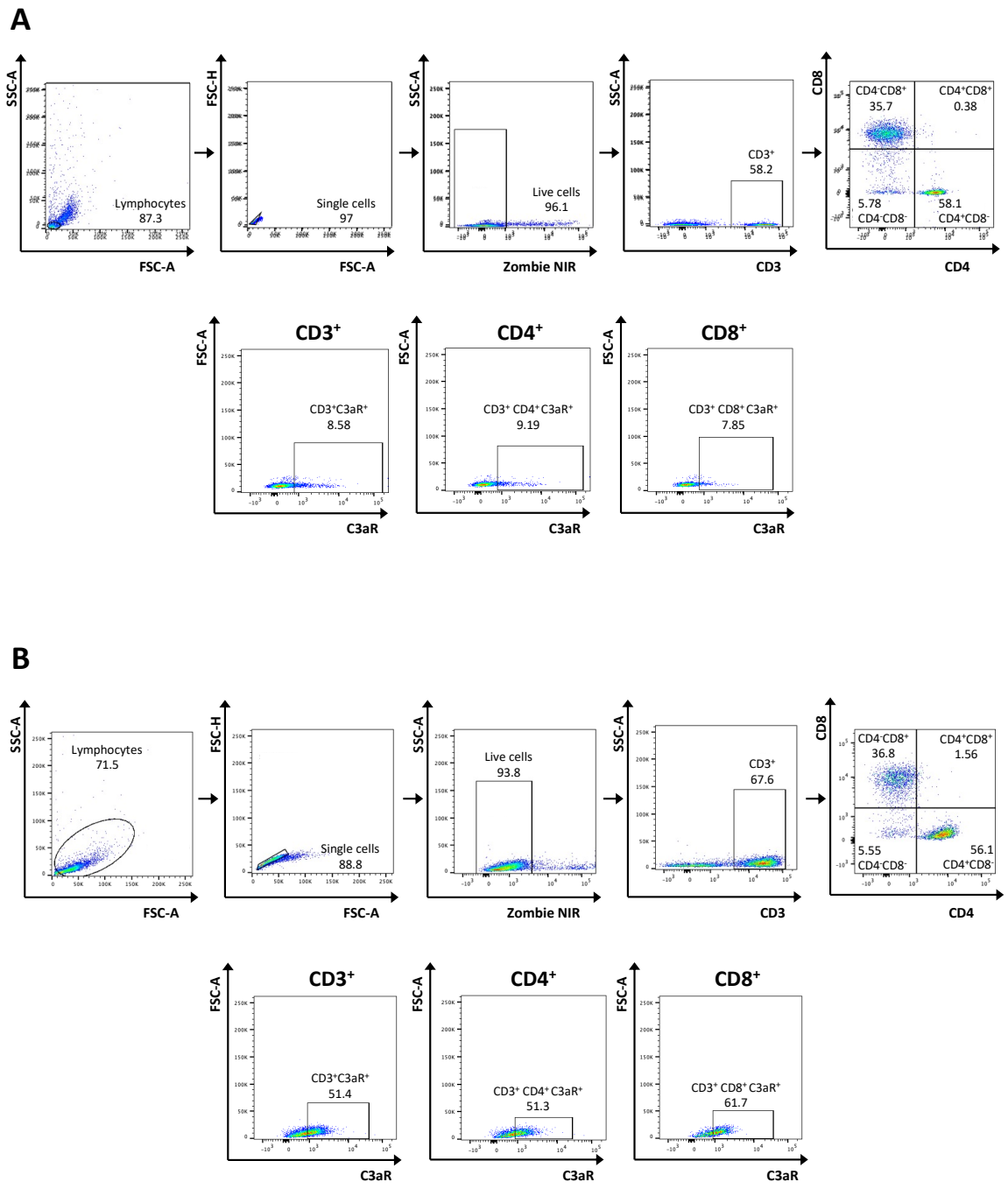

Appendix 6: Gating strategy and representative dot plots for assessing surface expression of C3aR on T cells using flow cytometry. (A) Unactivated and **(B)** activated T cells. FSC-A vs. SSC-A was used to gate on lymphocytes, and doublets were excluded using FSC-H vs. FSC-A. Zombie NIR viability dye was used to exclude dead cells. Expression of C3aR was assessed on $CD3^+$, $CD3^+$ $CD4^+$ and $CD3^+$ $CD8^+$ cells.

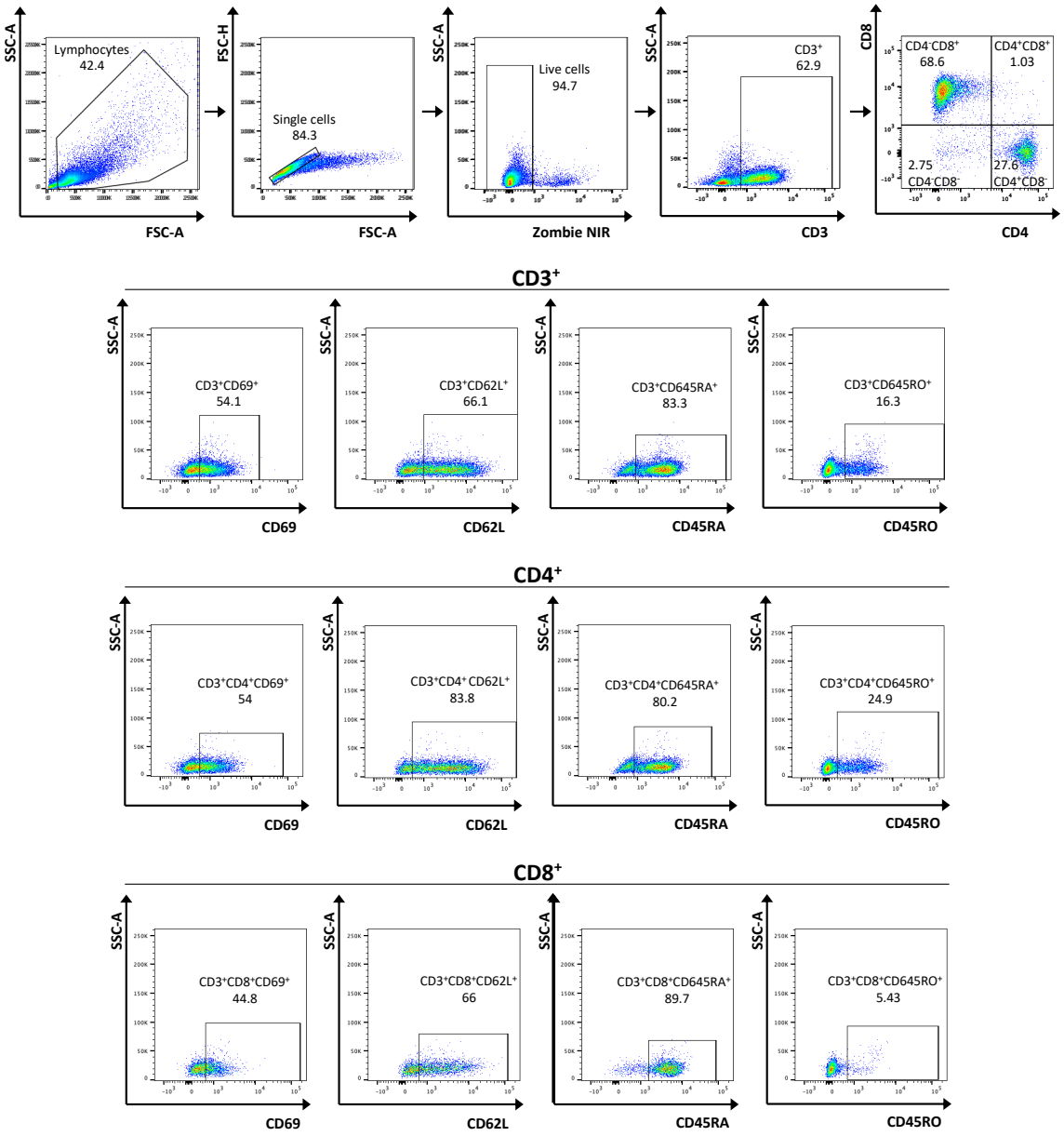

Appendix 7: Gating strategy and representative dot plots for assessing surface expression of activation markers on T cells using flow cytometry. FSC-A vs. SSC-A was used to gate on lymphocytes, and doublets were excluded using FSC-H vs. FSC-A. Zombie NIR viability dye was used to exclude dead cells. Expression of CD69, CD62L, CD45RA and CD45RO was assessed on $CD3^+$, $CD3^+$ $CD4^+$ and $CD3^+$ $CD8^+$ cells.

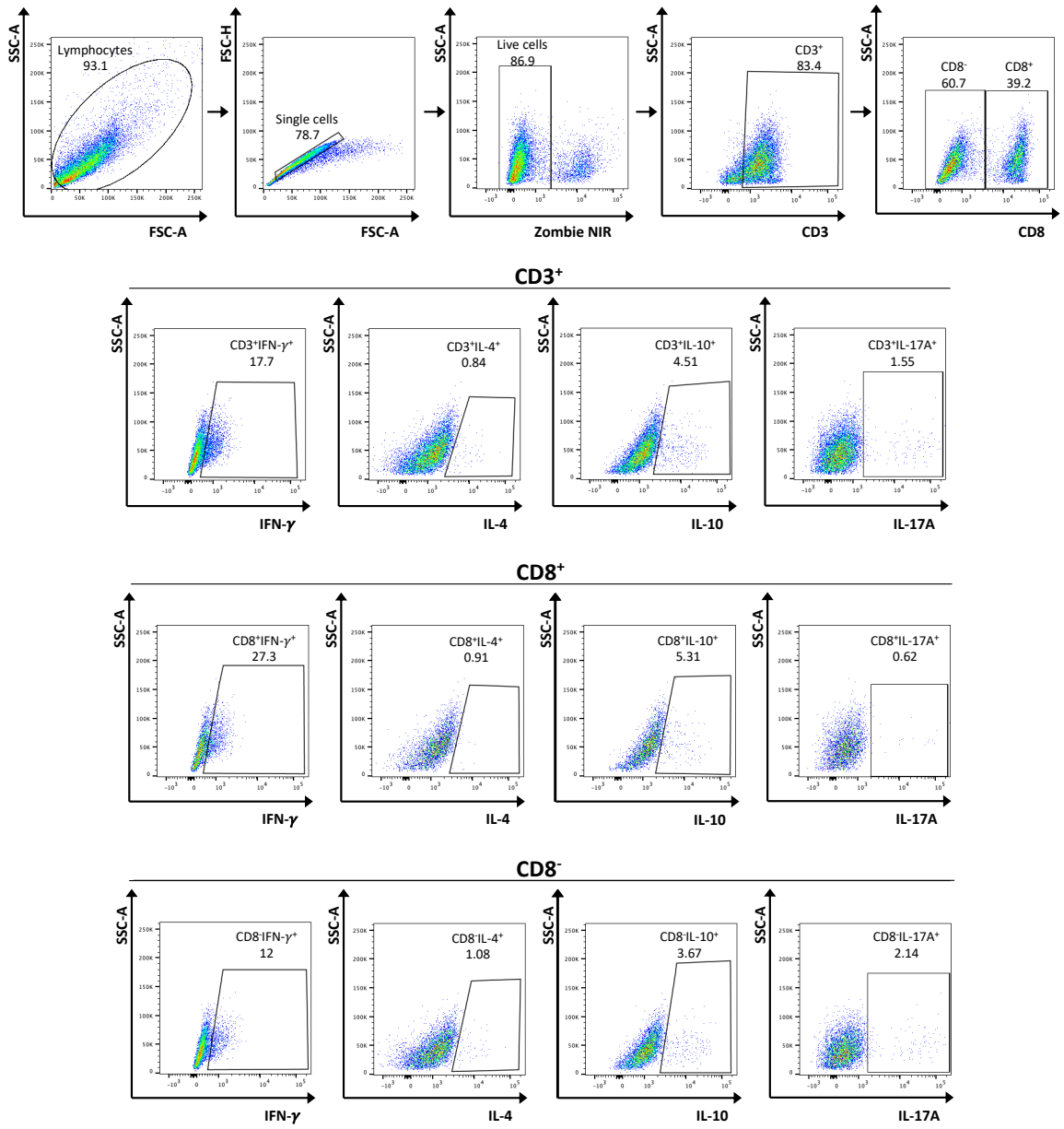

Appendix 8: Gating strategy and representative dot plots for assessing expression of intracellular cytokines by T cells using flow cytometry. FSC-A vs. SSC-A was used to gate on lymphocytes, and doublets were excluded using FSC-H vs. FSC-A. Zombie NIR viability dye was used to exclude dead cells. Expression of IFN-γ, IL-4, IL-10 and IL-17A was assessed on $CD3^+$, $CD3^+$ $CD8^+$ and $CD3^+$ $CD8^-$ cells.

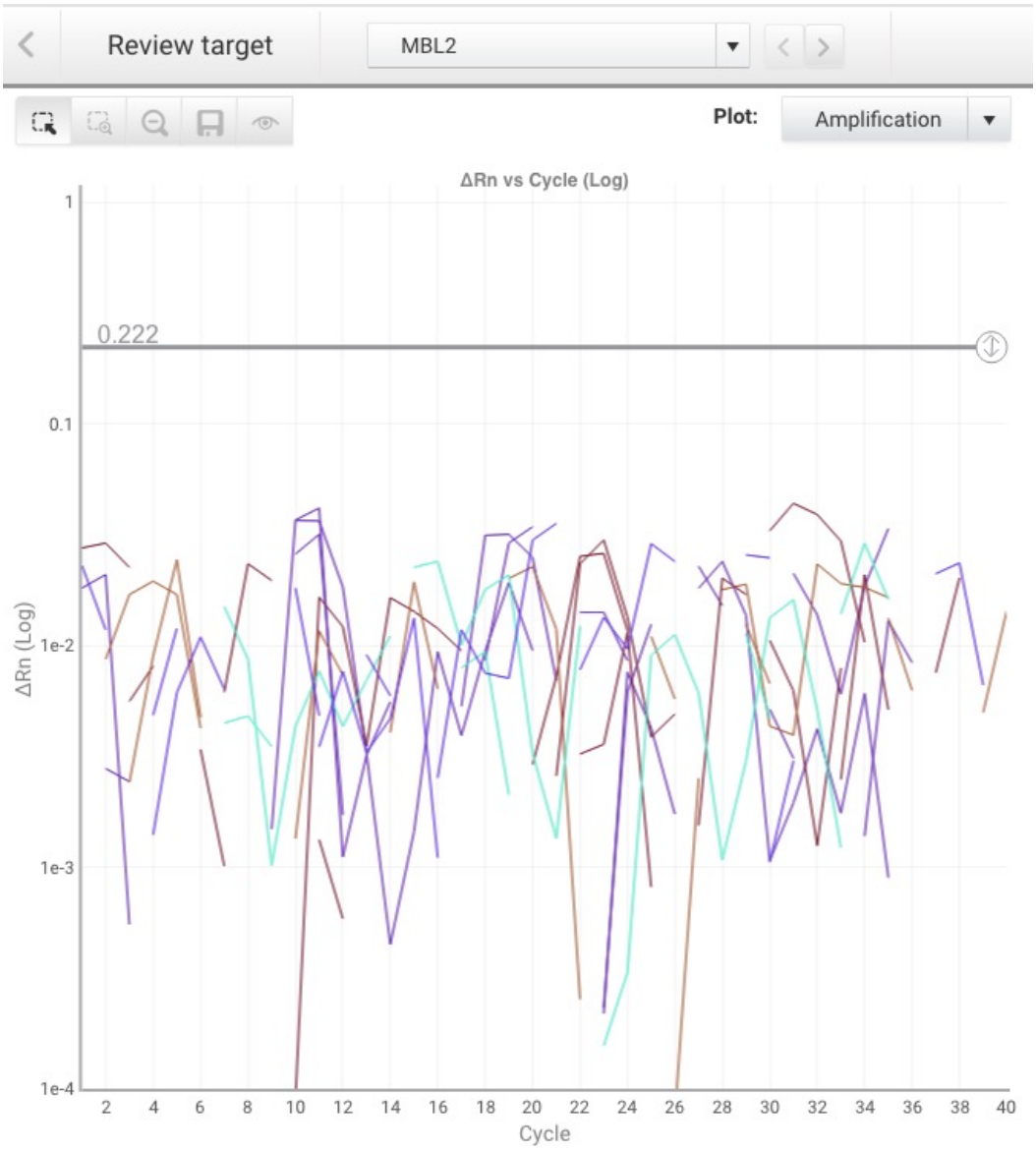

Appendix 9: Amplification plot for MBL2 which was not detected in cancer or non-cancer rectal tissue. MBL2 expression was assessed by qPCR. Data are representative of 3 biological replicates for both cancer and non-cancer tissue samples.

Bibliography

1. Sung H, Ferlay J, Siegel RL, et al. Global Cancer Statistics 2020: GLOBOCAN Estimates of Incidence and Mortality Worldwide for 36 Cancers in 185 Countries. *CA A Cancer J Clin*. 2021;71(3):209-249. doi:10.3322/caac.21660

2. *National Cancer Registry Ireland (2020) Cancer in Ireland 1994-2018 with Estimates for 2018-2020: Annual Report of the National Cancer Registry*. NCRI

3. Araghi M, Arnold M, Rutherford MJ, et al. Colon and rectal cancer survival in seven high-income countries 2010–2014: variation by age and stage at diagnosis (the ICBP SURVMARK-2 project). *Gut*. 2021;70(1):114-126. doi:10.1136/gutjnl-2020-320625

4. White A, Ironmonger L, Steele RJC, Ormiston-Smith N, Crawford C, Seims A. A review of sex-related differences in colorectal cancer incidence, screening uptake, routes to diagnosis, cancer stage and survival in the UK. *BMC Cancer*. 2018;18(1):906. doi:10.1186/s12885-018-4786-7

5. Morgan E, Arnold M, Gini A, et al. Global burden of colorectal cancer in 2020 and 2040: incidence and mortality estimates from GLOBOCAN. *Gut*. 2023;72(2):338-344. doi:10.1136/gutjnl-2022-327736

6. Fidler MM, Soerjomataram I, Bray F. A global view on cancer incidence and national levels of the human development index. *International Journal of Cancer*. 2016;139(11):2436-2446. doi:10.1002/ijc.30382

7. Araghi M, Soerjomataram I, Bardot A, et al. Changes in colorectal cancer incidence in seven high-income countries: a population-based study. *The Lancet Gastroenterology & Hepatology*. 2019;4(7):511-518. doi:10.1016/S2468-1253(19)30147-5

8. Stoffel EM, Murphy CC. Epidemiology and Mechanisms of the Increasing Incidence of Colon and Rectal Cancers in Young Adults. *Gastroenterology*. 2020;158(2):341-353. doi:10.1053/j.gastro.2019.07.055

9. Scott RB, Rangel LE, Osler TM, Hyman NH. Rectal cancer in patients under the age of 50 years: the delayed diagnosis. *The American Journal of Surgery*. 2016;211(6):1014-1018. doi:10.1016/j.amjsurg.2015.08.031

10. Palmer ML, Herrera L, Petrelli NJ. Colorectal adenocarcinoma in patients less than 40 years of age. *Dis Colon Rectum*. 1991;34(4):343-346. doi:10.1007/BF02050596

11. Taylor MC, Pounder D, Ali-Ridha NH, Bodurtha A, MacMullin EC. Prognostic factors in colorectal carcinoma of young adults. *Can J Surg*. 1988;31(3):150-153.

12. O'Connell JB, Maggard MA, Liu JH, Etzioni DA, Ko CY. Are survival rates different for young and older patients with rectal cancer? *Dis Colon Rectum*. 2004;47(12):2064-2069. doi:10.1007/s10350-004-0738-1

13. Araghi M, Soerjomataram I, Jenkins M, et al. Global trends in colorectal cancer mortality: projections to the year 2035. *International Journal of Cancer*. 2018;144(12):2992-3000. doi:10.1002/ijc.32055

14. *Breast, Cervical and Colorectal Cancer 1994-2019: National Trends for Cancers with Population-Based Screening Programmes in Ireland*. NCRI; 2022. Accessed January 25, 2023. https://www.ncri.ie/sites/ncri/files/pubs/Trendsreport_breast_cervical_colorectal_22092022.pdf

15. Bray F, Ferlay J, Soerjomataram I, Siegel RL, Torre LA, Jemal A. Global cancer statistics 2018: GLOBOCAN estimates of incidence and mortality worldwide for 36 cancers in 185 countries. *CA: a cancer journal for clinicians*. 2018;68(6):394-424. doi:10.3322/caac.21492

16. Kapiteijn E, Liefers GJ, Los LC, et al. Mechanisms of oncogenesis in colon versus rectal cancer. *J Pathol*. 2001;195(2):171-178. doi:10.1002/path.918

17. Salem ME, Weinberg BA, Xiu J, et al. Comparative molecular analyses of left-sided colon, right-sided colon, and rectal cancers. *Oncotarget*. 2017;8(49):86356-86368. doi:10.18632/oncotarget.21169

18. Li F ying, Lai M de. Colorectal cancer, one entity or three. *J Zhejiang Univ Sci B*. 2009;10(3):219-229. doi:10.1631/jzus.B0820273

19. van der Sijp MPL, Bastiaannet E, Mesker WE, et al. Differences between colon and rectal cancer in complications, short-term survival and recurrences. *Int J Colorectal Dis*. 2016;31(10):1683-1691. doi:10.1007/s00384-016-2633-3

20. Paschke S, Jafarov S, Staib L, et al. Are Colon and Rectal Cancer Two Different Tumor Entities? A Proposal to Abandon the Term Colorectal Cancer. *IJMS*. 2018;19(9):2577. doi:10.3390/ijms19092577

21. Glynne-Jones R, Wyrwicz L, Tiret E, et al. Rectal cancer: ESMO Clinical Practice Guidelines for diagnosis, treatment and follow-up. *Annals of Oncology*. 2017;28(Suppl 4):iv22-iv40. doi:10.1093/annonc/mdx224

22. Chan GHJ, Chee CE. Making sense of adjuvant chemotherapy in colorectal cancer. *J Gastrointest Oncol*. 2019;10(6):1183-1192. doi:10.21037/jgo.2019.06.03

23. Riihimäki M, Hemminki A, Sundquist J, Hemminki K. Patterns of metastasis in colon and rectal cancer. *Sci Rep*. 2016;6(1):29765. doi:10.1038/srep29765

24. Li M, Li JY, Zhao AL, Gu J. Colorectal Cancer or Colon and Rectal Cancer? *Oncology*. 2007;73(1-2):52-57. doi:10.1159/000120628

25. Guinney J, Dienstmann R, Wang X, et al. The consensus molecular subtypes of colorectal cancer. *Nature Medicine*. 2015;21(11):1350-1356. doi:10.1038/nm.3967

26. Wei EK, Giovannucci E, Wu K, et al. Comparison of risk factors for colon and rectal cancer. *Int J Cancer*. 2004;108(3):433-442. doi:10.1002/ijc.11540

27. Lengauer C, Kinzler KW, Vogelstein B. Genetic instability in colorectal cancers. *Nature*. Published online 1997:623-626.

28. Fleming M, Ravula S, Tatishchev SF, Wang HL. Colorectal carcinoma: Pathologic aspects. *Journal of Gastrointestinal Oncology*. 2012;3(3):153-173. doi:10.3978/j.issn.2078-6891.2012.030

29. Ruszkiewicz AR, Jass JR. Microsatellite Instability in Colorectal Cancer What, How, When and Why? *Pathology Case Reviews*. 2004;9(4):163-172. doi:10.1053/j.gastro.2009.12.064.Boland

30. Fernebro E, Halvarsson B, Baldetorp B, Nilbert M. Predominance of CIN versus MSI in the development of rectal cancer at young age. *BMC Cancer*. 2002;2(1):25. doi:10.1186/1471-2407-2-25

31. Pino MS, Chung DC. The Chromosomal Instability Pathway in Colon Cancer. *Gastroenterology*. 2010;138(6):2059-2072. doi:10.1053/j.gastro.2009.12.065

32. Toyota M, Ahuja N, Ohe-Toyota M, Herman JG, Baylin SB, Issa JPJ. CpG island methylator phenotype in colorectal cancer. *Proc Natl Acad Sci USA*. 1999;96:8681-8686.

33. Murphy N, Norat T, Ferrari P, et al. Dietary Fibre Intake and Risks of Cancers of the Colon and Rectum in the European Prospective Investigation into Cancer and Nutrition (EPIC). Lee JE, ed. *PLoS ONE*. 2012;7(6):e39361. doi:10.1371/journal.pone.0039361

34. Siegel RL, Miller KD, Jemal A. Colorectal Cancer Mortality Rates in Adults Aged 20 to 54 Years in the United States, 1970-2014. *JAMA*. 2017;318(6):572. doi:10.1001/jama.2017.7630

35. Troeung L, Sodhi-Berry N, Martini A, et al. Increasing Incidence of Colorectal Cancer in Adolescents and Young Adults Aged 15–39 Years in Western Australia 1982–2007: Examination of Colonoscopy History. *Front Public Health*. 2017;5:179. doi:10.3389/fpubh.2017.00179

36. Gram IT, Park SY, Wilkens LR, Haiman CA, Le Marchand L. Smoking-Related Risks of Colorectal Cancer by Anatomical Subsite and Sex. *American Journal of Epidemiology*. 2020;189(6):543-553. doi:10.1093/aje/kwaa005

37. Loud J, Murphy J. Cancer screening and early detection in the 21st century. *Semin Oncol Nurs*. 2017;33(2):121-128. doi:10.1016/j.soncn.2017.02.002

38. The US Preventive Services Task Force, Davidson KW, Barry MJ, et al. Screening for Colorectal Cancer: U.S. Preventive Services Task Force Recommendation Statement. *Ann Intern Med*. 2008;149(9):627. doi:10.7326/0003-4819-149-9-200811040-00243

39. National Screening Service. *BowelScreen Programme Report Round Three 2018-2019*.; 2021.

40. Department of Health. *Diagnosis, Staging and Treatment of Patients with Rectal Cancer (NCEC National Clinical Guideline No. 25)*.; 2020.

41. Hamilton W, Sharp D. Diagnosis of colorectal cancer in primary care: The evidence base for guidelines. *Family Practice*. 2004;21(1):99-106. doi:10.1093/fampra/cmh121

42. Burdan F, Sudol-Szopinska I, Staroslawska E, et al. Magnetic resonance imaging and endorectal ultrasound for diagnosis of rectal lesions. *Eur J Med Res*. 2015;20(1):4. doi:10.1186/s40001-014-0078-0

43. Penna C, Nordlinger B. Colorectal metastasis (liver and lung). *Surg Clin North Am*. 2002;82(5):1075-1090, x-xi. doi:10.1016/s0039-6109(02)00051-8

44. Van Cutsem E, Cervantes A, Adam R, et al. ESMO consensus guidelines for the management of patients with metastatic colorectal cancer. *Ann Oncol*. 2016;27(8):1386-1422. doi:10.1093/annonc/mdw235

45. Bach SP, Hill J, Monson JRT, et al. A predictive model for local recurrence after transanal endoscopic microsurgery for rectal cancer. *British Journal of Surgery*. 2009;96(3):280-290. doi:10.1002/bjs.6456

46. Stornes T, Wibe A, Nesbakken A, Myklebust TÅ, Endreseth BH. National Early Rectal Cancer Treatment Revisited. *Dis Colon Rectum*. 2016;59(7):623-629. doi:10.1097/DCR.0000000000000591

47. Delibegovic S. Introduction to Total Mesorectal Excision. *Med Arch*. 2017;71(6):434. doi:10.5455/medarh.2017.71.434-438

48. Quirke P, Steele R, Monson J, et al. Effect of the plane of surgery achieved on local recurrence in patients with operable rectal cancer: a prospective study using data from the MRC CR07 and NCIC-CTG CO16 randomised clinical trial. *Lancet*. 2009;373(9666):821-828. doi:10.1016/S0140-6736(09)60485-2

49. Taylor FGM, Quirke P, Heald RJ, et al. Preoperative High-resolution Magnetic Resonance Imaging Can Identify Good Prognosis Stage I, II, and III Rectal Cancer Best Managed by Surgery Alone: A Prospective, Multicenter, European Study. *Annals of Surgery*. 2011;253(4):711-719. doi:10.1097/SLA.0b013e31820b8d52

50. Erlandsson J, Holm T, Pettersson D, et al. Optimal fractionation of preoperative radiotherapy and timing to surgery for rectal cancer (Stockholm III): a multicentre, randomised, non-blinded, phase 3, non-inferiority trial. *The Lancet Oncology*. 2017;18(3):336-346. doi:10.1016/S1470-2045(17)30086-4

51. O'Connell MJ, Colangelo LH, Beart RW, et al. Capecitabine and Oxaliplatin in the Preoperative Multimodality Treatment of Rectal Cancer: Surgical End Points From National Surgical Adjuvant Breast and Bowel Project Trial R-04. *J Clin Oncol*. 2014;32(18):1927-1934. doi:10.1200/JCO.2013.53.7753

52. Amin MB, Edge SB, Greene FL, et al. *AJCC Cancer Staging Manual*. Vol 67.; 2017. Accessed February 5, 2023. https://onlinelibrary.wiley.com/doi/abs/10.3322/caac.21388

53. Maas M, Beets-Tan RGH, Lambregts DMJ, et al. Wait-and-see policy for clinical complete responders after chemoradiation for rectal cancer. *Journal of Clinical Oncology*. 2011;29(35):4633-4640. doi:10.1200/JCO.2011.37.7176

54. Maas M, Nelemans PJ, Valentini V, et al. Long-term outcome in patients with a pathological complete response after chemoradiation for rectal cancer: A pooled analysis of individual patient data. *The Lancet Oncology*. 2010;11(9):835-844. doi:10.1016/S1470-2045(10)70172-8

55. Janjan N a, Khoo VS, Abbruzzese J, et al. Tumor downstaging and sphincter preservation with preoperative chemoradiation in locally advanced rectal cancer: the M. D. Anderson Cancer Center experience. *International journal of radiation oncology, biology, physics*. 1999;44(5):1027-1038. doi:10.1016/S0360-3016(99)00099-1

56. Pucciarelli S, Toppan P, Friso ML, et al. Complete pathologic response following preoperative chemoradiation therapy for middle to lower rectal cancer is not a prognostic factor for a better outcome. *Diseases of the Colon and Rectum*. 2004;47(11):1798-1807. doi:10.1007/s10350-004-0681-1

57. Kidron D, Lahav L, Berkovich L, Mishaeli M, Yahya NH, Avital S. Lack of Pathological Response of Rectal Cancer to Neoadjuvant Chemoradiotherapy is

Associated with Poorer Long-Term Oncological Outcomes. *Clinical Oncology and Research*. 2019;2019(5):1-6. doi:10.31487/j.COR.2019.5.18

58. Jonathan Yang T, Goodman KA. Predicting complete response: Is there a role for non-operative management of rectal cancer? *Journal of Gastrointestinal Oncology*. 2015;6(2):241-246. doi:10.3978/j.issn.2078-6891.2014.110

59. Lange MM, den Dulk M, Bossema ER, et al. Risk factors for faecal incontinence after rectal cancer treatment. *British Journal of Surgery*. 2007;94(10):1278-1284. doi:10.1002/bjs.5819

60. Nesbakken A, Nygaard K, Bull-Njaa T, Carlsen E, Eri LM. Bladder and sexual dysfunction after mesorectal excision for rectal cancer. *Br J Surg*. 2000;87(2):206-210. doi:10.1046/j.1365-2168.2000.01357.x

61. Habr-Gama A, Perez RO, Nadalin W, et al. Operative versus nonoperative treatment for stage 0 distal rectal cancer following chemoradiation therapy: Long-term results. *Annals of Surgery*. 2004;240(4):711-718. doi:10.1097/01.sla.0000141194.27992.32

62. Dossa F, Chesney TR, Acuna SA, Baxter NN. A watch-and-wait approach for locally advanced rectal cancer after a clinical complete response following neoadjuvant chemoradiation: a systematic review and meta-analysis. *Lancet Gastroenterol Hepatol*. 2017;2(7):501-513. doi:10.1016/S2468-1253(17)30074-2

63. Dattani M, Heald RJ, Goussous G, et al. Oncological and Survival Outcomes in Watch and Wait Patients With a Clinical Complete Response After Neoadjuvant Chemoradiotherapy for Rectal Cancer: A Systematic Review and Pooled Analysis. *Ann Surg*. 2018;268(6):955-967. doi:10.1097/SLA.0000000000002761

64. Bitterman DS, Resende Salgado L, Moore HG, et al. Predictors of Complete Response and Disease Recurrence Following Chemoradiation for Rectal Cancer. *Front Oncol*. 2015;5. doi:10.3389/fonc.2015.00286

65. Zeng WG, Liang JW, Wang Z, et al. Clinical parameters predicting pathologic complete response following neoadjuvant chemoradiotherapy for rectal cancer. *Chin J Cancer*. 2015;34(10):468-474. doi:10.1186/s40880-015-0033-7

66. Dayde D, Tanaka I, Jain R, Tai MC, Taguchi A. Predictive and Prognostic Molecular Biomarkers for Response to Neoadjuvant Chemoradiation in Rectal Cancer. *International Journal of Molecular Sciences*. 2017;18(573). doi:10.3390/ijms18030573

67. Watanabe T, Komuro Y, Kiyomatsu T, et al. Prediction of sensitivity of rectal cancer cells in response to preoperative radiotherapy by DNA microarray analysis of gene expression profiles. *Cancer Res*. 2006;66(7):3370-3374. doi:10.1158/0008-5472.CAN-05-3834

68. Guo Y, Cheng J, Ao L, et al. Discriminating cancer-related and cancer-unrelated chemoradiation-response genes for locally advanced rectal cancers. *Sci Rep*. 2016;6:36935. doi:10.1038/srep36935

69. Gim J, Cho YB, Hong HK, et al. Predicting multi-class responses to preoperative chemoradiotherapy in rectal cancer patients. *Radiat Oncol*. 2016;11(1):50. doi:10.1186/s13014-016-0623-9

70. Gantt GA, Chen Y, DeJulius K, Mace AG, Barnholtz-Sloan J, Kalady MF. Gene expression profile is associated with chemoradiation resistance in rectal cancer. *Colorectal Disease*. 2014;16(1):57-66. doi:10.1111/codi.12395

71. Longley DB, Harkin DP, Johnston PG. 5-Fluorouracil: mechanisms of action and clinical strategies. *Nat Rev Cancer*. 2003;3(5):330-338. doi:10.1038/nrc1074

72. Wohlhueter RM, McIvor RS, Plagemann PG. Facilitated transport of uracil and 5-fluorouracil, and permeation of orotic acid into cultured mammalian cells. *J Cell Physiol*. 1980;104(3):309-319. doi:10.1002/jcp.1041040305

73. Sommer H, Santi DV. Purification and amino acid analysis of an active site peptide from thymidylate synthetase containing covalently bound 5-fluoro-2'-deoxyuridylate and methylenetetrahydrofolate. *Biochem Biophys Res Commun*. 1974;57(3):689-695. doi:10.1016/0006-291x(74)90601-9

74. Santi DV, McHenry CS, Sommer H. Mechanism of interaction of thymidylate synthetase with 5-fluorodeoxyuridylate. *Biochemistry*. 1974;13(3):471-481. doi:10.1021/bi00700a012

75. Houghton JA, Tillman DM, Harwood FG. Ratio of 2'-deoxyadenosine-5'-triphosphate/thymidine-5'-triphosphate influences the commitment of human colon carcinoma cells to thymineless death. *Clin Cancer Res*. 1995;1(7):723-730.

76. Yoshioka A, Tanaka S, Hiraoka O, et al. Deoxyribonucleoside triphosphate imbalance. 5-Fluorodeoxyuridine-induced DNA double strand breaks in mouse FM3A cells and the mechanism of cell death. *J Biol Chem*. 1987;262(17):8235-8241.

77. Miwa M, Ura M, Nishida M, et al. Design of a novel oral fluoropyrimidine carbamate, capecitabine, which generates 5-fluorouracil selectively in tumours by enzymes concentrated in human liver and cancer tissue. *European Journal of Cancer*. 1998;34(8):1274-1281. doi:10.1016/S0959-8049(98)00058-6

78. Cao D, Pizzorno G. Uridine phosophorylase: an important enzyme in pyrimidine metabolism and fluoropyrimidine activation. *Drugs Today (Barc)*. 2004;40(5):431-443. doi:10.1358/dot.2004.40.5.850491

79. Baskar R, Lee KA, Yeo R, Yeoh KW. Cancer and radiation therapy: Current advances and future directions. *International Journal of Medical Sciences*. 2012;9(3):193-199. doi:10.7150/ijms.3635

80. Harrington KJ, Billingham LJ, Brunner TB, et al. Guidelines for preclinical and early phase clinical assessment of novel radiosensitisers. *Br J Cancer*. 2011;105(5):628-639. doi:10.1038/bjc.2011.240

81. Borras JM, Lievens Y, Barton M, et al. How many new cancer patients in Europe will require radiotherapy by 2025? An ESTRO-HERO analysis. *Radiotherapy and Oncology*. 2016;119(1):5-11. doi:10.1016/j.radonc.2016.02.016

82. Chaput G, Regnier L. Radiotherapy: Clinical pearls for primary care. *Can Fam Physician*. 2021;67(10):753-757. doi:10.46747/cfp.6710753

83. Ellis F. Dose, time and fractionation: A clinical hypothesis. *Clinical Radiology*. 1969;20(1):1-7. doi:10.1016/S0009-9260(69)80043-7

84. Kye BH, Cho HM. Overview of radiation therapy for treating rectal cancer. *Annals of Coloproctology*. 2014;30(4):165-174. doi:10.3393/ac.2014.30.4.165

85. Marijnen CAM, Kapiteijn E, van de Velde CJH, et al. Acute Side Effects and Complications After Short-Term Preoperative Radiotherapy Combined With Total Mesorectal Excision in Primary Rectal Cancer: Report of a Multicenter Randomized Trial. *JCO*. 2002;20(3):817-825. doi:10.1200/JCO.2002.20.3.817

86. Bruheim K, Guren MG, Skovlund E, et al. Late Side Effects and Quality of Life After Radiotherapy for Rectal Cancer. *International Journal of Radiation Oncology*Biology*Physics*. 2010;76(4):1005-1011. doi:10.1016/j.ijrobp.2009.03.010

87. Peeters KCMJ, Velde CJH van de, Leer JWH, et al. Late Side Effects of Short-Course Preoperative Radiotherapy Combined With Total Mesorectal Excision for Rectal Cancer: Increased Bowel Dysfunction in Irradiated Patients—A Dutch Colorectal Cancer Group Study. *Journal of Clinical Oncology*. Published online September 21, 2016. doi:10.1200/JCO.2005.14.779

88. Guckenberger M, Saur G, Wehner D, et al. Long-term quality-of-life after neoadjuvant short-course radiotherapy and long-course radiochemotherapy for locally advanced rectal cancer. *Radiotherapy and Oncology*. 2013;108(2):326-330. doi:10.1016/j.radonc.2013.08.022

89. Withers HR. Four R's of radiotherapy. *Advances in Radiation Biology*. 1975;5:241-247.

90. Pajonk F, Vlashi E, McBride WH. Radiation Resistance of Cancer Stem Cells: The 4 R's of Radiobiology Revisited. *Stem Cells*. 2010;28(4):639-648. doi:10.1002/stem.318

91. Kim JJ, Tannock IF. Repopulation of cancer cells during therapy: an important cause of treatment failure. *Nat Rev Cancer*. 2005;5(7):516-525. doi:10.1038/nrc1650

92. Nordsmark M, Bentzen SM, Rudat V, et al. Prognostic value of tumor oxygenation in 397 head and neck tumors after primary radiation therapy. An international multi-center study. *Radiotherapy and Oncology*. 2005;77(1):18-24. doi:10.1016/j.radonc.2005.06.038

93. Brizel DM, Dodge RK, Clough RW, Dewhirst MW. Oxygenation of head and neck cancer: Changes during radiotherapy and impact on treatment outcome. *Radiotherapy and Oncology*. 1999;53(2):113-117. doi:10.1016/S0167-8140(99)00102-4

94. Höckel M, Schlenger K, Aral B, Mitze M, Schäffer U, Vaupel P. Association between tumor hypoxia and malignant progression in advanced cancer of the uterine cervix. *Cancer Research*. 1996;56(19):4509-4515. doi:10.1056/NEJM199604183341606

95. Sinclair WK, Morton RA. X-ray sensitivity during the cell generation cycle of cultured Chinese hamster cells. *Radiation research*. 1966;29(3):450-474. doi:10.2307/3572025

96. Sinclair WK, Morton RA. X-Ray and Ultraviolet Sensitivity of Synchronized Chinese Hamster Cells at Various Stages of the Cell Cycle. *Biophysical Journal*. 1965;5(1):1-25. doi:10.1016/S0006-3495(65)86700-5

97. Sinclair WK. Cyclic X-ray responses in mammalian cells in vitro. *Radiation Research*. 1968;33(3):620-643. doi:10.1667/RRAV09.1

98. Steel GG, McMillan TJ, Peacock JH. The 5Rs of radiobiology. *Int J Radiat Biol*. 1989;56(6):1045-1048. doi:10.1080/09553008914552491

99. Demaria S, Formenti SC. Role of T lymphocytes in tumor response to radiotherapy. *Frontiers in Oncology*. 2012;2(August):1-7. doi:10.3389/fonc.2012.00095

100. Apetoh L, Ghiringhelli F, Tesniere A, et al. Toll-like receptor 4-dependent contribution of the immune system to anticancer chemotherapy and radiotherapy. *Nature Medicine*. 2007;13(9):1050-1059. doi:10.1038/nm1622

101. Matsumura S, Wang B, Kawashima N, et al. Radiation-induced CXCL16 release by breast cancer cells attracts effector T cells. *Journal of Immunology*. 2008;181(5):3099-3107.

102. Dewan MZ, Galloway AE, Kawashima N, et al. Fractionated but not single-dose radiotherapy induces an immune-mediated abscopal effect when combined with anti-CTLA-4 antibody. *Clinical Cancer Research*. 2009;15(17):5379-5388. doi:10.1158/1078-0432.CCR-09-0265

103. Ngwa W, Irabor OC, Schoenfeld JD, Hesser J, Demaria S, Formenti SC. Using immunotherapy to boost the abscopal effect. *Nat Rev Cancer*. 2018;18(5):313-322. doi:10.1038/nrc.2018.6

104. Boustani, Grapin, Laurent, Apetoh, Mirjolet. The 6th R of Radiobiology: Reactivation of Anti-Tumor Immune Response. *Cancers*. 2019;11(6):860. doi:10.3390/cancers11060860

105. Dainiak N. Hematologic consequences of exposure to ionizing radiation. *Experimental Hematology*. 2002;30:513-528. doi:10.1016/S0301-472X(02)00802-0

106. Radford IR. The level of induced DNA double-Strand breakage correlates with cell killing after x-irradiation. *International Journal of Radiation Biology*. 1985;48(1):45-54. doi:10.1080/09553008514551051

107. Houtgraaf JH, Versmissen J, van der Giessen WJ. A concise review of DNA damage checkpoints and repair in mammalian cells. *Cardiovascular Revascularization Medicine*. 2006;7(3):165-172. doi:10.1016/j.carrev.2006.02.002

108. Ward JF. DNA Damage Produced by Ionizing Radiation in Mammalian Cells: Identities, Mechanisms of Formation, and Reparability. In: *Progress in Nucleic Acid Research and Molecular Biology*. Vol 35. Elsevier; 1988:95-125. doi:10.1016/S0079-6603(08)60611-X

109. Riley PA. Free radicals in biology: Oxidative stress and the effects of ionizing radiation. *International Journal of Radiation Biology*. 1994;65(1):27-33. doi:10.1080/09553009414550041

110. Desouky O, Ding N, Zhou G. Targeted and non-targeted effects of ionizing radiation | Elsevier Enhanced Reader. *Journal of Radiation Research and Applied Sciences*. 2015;8:247-254. doi:10.1016/j.jrras.2015.03.003

111. Roots R, Okada S. Protection of DNA Molecules of Cultured Mammalian Cells from Radiation-induced Single-strand Scissions by Various Alcohols and SH Compounds. *International Journal of Radiation Biology and Related Studies in Physics, Chemistry and Medicine*. 1972;21(4):329-342. doi:10.1080/09553007214550401

112. Corre I, Niaudet C, Paris F. Plasma membrane signaling induced by ionizing radiation. *Mutation Research/Reviews in Mutation Research*. 2010;704(1-3):61-67. doi:10.1016/j.mrrev.2010.01.014

113. Haimovitz-Friedman A, Kan CC, Ehleiter D, et al. Ionizing radiation acts on cellular membranes to generate ceramide and initiate apoptosis. *J Exp Med*. 1994;180(2):525-535.

114. Eriksson D, Stigbrand T. Radiation-induced cell death mechanisms. *Tumor Biology*. 2010;31(4):363-372. doi:10.1007/s13277-010-0042-8

115. Jackson SP, Bartek J. The DNA-damage response in human biology and disease. *Nature*. 2009;461(7267):1071-1078. doi:10.1038/nature08467

116. Pearl LH, Schierz AC, Ward SE, Al-Lazikani B, Pearl FMG. Therapeutic opportunities within the DNA damage response. *Nat Rev Cancer*. 2015;15(3):166-180. doi:10.1038/nrc3891

117. Khanna KK, Jackson SP. DNA double-strand breaks: Signaling, repair and the cancer connection. *Nature Genetics*. 2001;27(3):247-254. doi:10.1038/85798

118. Marechal A, Zou L. DNA Damage Sensing by the ATM and ATR Kinases. *Cold Spring Harbor Perspectives in Biology*. 2013;5(9):a012716-a012716. doi:10.1101/cshperspect.a012716

119. Jette N, Lees-Miller SP. The DNA-dependent protein kinase: A multifunctional protein kinase with roles in DNA double strand break repair and mitosis. *Progress in Biophysics and Molecular Biology*. 117(0). doi:10.1016/j.pbiomolbio.2014.12.003

120. Blackford AN, Jackson SP. ATM, ATR, and DNA-PK: The Trinity at the Heart of the DNA Damage Response. *Molecular Cell*. 66:801-817. doi:10.1016/j.molcel.2017.05.015

121. Stratton MR, Campbell PJ, Futreal PA. The cancer genome. *Nature*. 2009;458(7239):719-724. doi:10.1038/nature07943.The

122. Lynam-Lennon N, Reynolds JV, Pidgeon GP, Lysaght J, Marignol L, Maher SG. Alterations in DNA Repair Efficiency are Involved in the Radioresistance of Esophageal Adenocarcinoma. *Radiation Research*. 2010;174(6a):703-711. doi:10.1667/RR2295.1

123. Bao S, Wu Q, McLendon RE, et al. Glioma stem cells promote radioresistance by preferential activation of the DNA damage response. *Nature*. 2006;444(7120):756-760. doi:10.1038/nature05236

124. Rocha CRR, Silva MM, Quinet A, Cabral-Neto JB, Menck CFM. DNA repair pathways and cisplatin resistance: An intimate relationship. *Clinics*. 2018;73(8):1-10. doi:10.6061/clinics/2018/e478s

125. O'Connor MJ. Targeting the DNA Damage Response in Cancer. *Molecular Cell*. 2015;60(4):547-560. doi:10.1016/j.molcel.2015.10.040

126. Branzei D, Foiani M. Regulation of DNA repair throughout the cell cycle. *Nature Reviews Molecular Cell Biology*. 2008;9(4):297-308. doi:10.1038/nrm2351

127. Takata M, Sasaki MS, Sonoda E, et al. Homologous recombination and non-homologous end-joining pathways of DNA double-strand break repair have overlapping roles in the maintenance of chromosomal integrity in vertebrate cells. *EMBO J*. 1998;17(18):5497-5508. doi:10.1093/emboj/17.18.5497

128. Li X, Heyer WD. Homologous recombination in DNA repair and DNA damage tolerance. *Cell Res*. 2008;18(1):99-113. doi:10.1038/cr.2008.1

129. Chen C, Wang Y, Mei JF, et al. Targeting RAD50 increases sensitivity to radiotherapy in colorectal cancer cells. *neo*. 2018;65(01):75-80. doi:10.4149/neo_2018_170219N128

130. Ho V, Chung L, Singh A, et al. Overexpression of the MRE11-RAD50-NBS1 (MRN) complex in rectal cancer correlates with poor response to neoadjuvant radiotherapy and prognosis. *BMC Cancer*. 2018;18(1):869. doi:10.1186/s12885-018-4776-9

131. Yu Y, Liu T, Yu G, et al. PRDM15 interacts with DNA-PK-Ku complex to promote radioresistance in rectal cancer by facilitating DNA damage repair. *Cell Death Dis*. 2022;13(11):1-13. doi:10.1038/s41419-022-05402-7

132. Pucci S, Polidoro C, Joubert A, et al. Ku70, Ku80, and sClusterin: A Cluster of Predicting Factors for Response to Neoadjuvant Chemoradiation Therapy in Patients

With Locally Advanced Rectal Cancer. *International Journal of Radiation Oncology*Biology*Physics*. 2017;97(2):381-388. doi:10.1016/j.ijrobp.2016.10.018

133. Pawlik TM, Keyomarsi K. Role of cell cycle in mediating sensitivity to radiotherapy. *International Journal of Radiation Oncology Biology Physics*. 2004;59(4):928-942. doi:10.1016/j.ijrobp.2004.03.005

134. Huerta S, Gao X, Saha D. Mechanisms of resistance to ionizing radiation in rectal cancer. *Expert Review of Molecular Diagnostics*. 2009;9(5):469-480.

135. Esposito G, Pucciarelli S, Alaggio R, et al. p27kip1Expression Is Associated With Tumor Response to Preoperative Chemoradiotherapyin RectalCancer. *Ann Surg Oncol*. 2001;8(4):311-318. doi:10.1007/s10434-001-0311-2

136. Adell G, Sun XF, Stål O, Klintenberg C, Sjödahl R, Nordenskjöld B. p53 status: an indicator for the effect of preoperative radiotherapy of rectal cancer. *Radiother Oncol*. 1999;51(2):169-174. doi:10.1016/s0167-8140(99)00041-9

137. Fu CG, Tominaga O, Nagawa H, et al. Role of p53 and p21/WAF1 detection in patient selection for preoperative radiotherapy in rectal cancer patients. *Dis Colon Rectum*. 1998;41(1):68-74. doi:10.1007/BF02236898

138. Lin LC, Lee HH, Hwang WS, et al. p53 and p27 as predictors of clinical outcome for rectal-cancer patients receiving neoadjuvant therapy. *Surg Oncol*. 2006;15(4):211-216. doi:10.1016/j.suronc.2007.01.001

139. Qiu H, Sirivongs P, Rothenberger M, Rothenberger DA, Garciá-Aguilar J. Molecular prognostic factors in rectal cancer treated by radiation and surgery. *Dis Colon Rectum*. 2000;43(4):451-459. doi:10.1007/BF02237186

140. Visconti R, Della Monica R, Grieco D. Cell cycle checkpoint in cancer: A therapeutically targetable double-edged sword. *Journal of Experimental and Clinical Cancer Research*. 2016;35(1):1-8. doi:10.1186/s13046-016-0433-9

141. Galluzzi L, Maiuri MC, Vitale I, et al. Cell death modalities: classification and pathophysiological implications. *Cell Death & Differentiation*. 2007;14(7):1237-1243. doi:10.1038/sj.cdd.4402148

142. Roninson IB, Broude EV, Chang BD. If not apoptosis, then what? Treatment-induced senescence and mitotic catastrophe in tumor cells. *Drug Resistance Updates*. 2001;4(5):303-313. doi:10.1054/drup.2001.0213

143. Russell J, Wheldon TE, Wheldon TE, Stanton P. A Radioresistant Variant Derived from a Human Neuroblastoma Cell Line Is Less Prone to Radiation-induced Apoptosis. *Cancer Research*. 1995;55(21):4915-4921.

144. Pearce AG, Segura TM, Rintala AC, Rintala-Maki ND, Lee H. The generation and characterization of a radiation-resistant model system to study radioresistance in human breast cancer cells. *Radiation Research*. 2001;156(6):739-750. doi:10.1667/0033-7587(2001)156[0739:TGACOA]2.0.CO;2

145. Ji K, Sun X, Liu Y, et al. Regulation of Apoptosis and Radiation Sensitization in Lung Cancer Cells via the Sirt1/NF-κB/Smac Pathway. *Cellular Physiology and Biochemistry*. 2018;48(1):304-316. doi:10.1159/000491730

146. Rödel C, Grabenbauer GG, Papadopoulos T, et al. Apoptosis as a cellular predictor for histopathologic response to neoadjuvant radiochemotherapy in patients with rectal cancer. *International Journal of Radiation Oncology Biology Physics*. 2002;52(2):294-303. doi:10.1016/S0360-3016(01)02643-8

147. Scott N, Hale A, Deakin M, et al. A histopathological assessment of the response of rectal adenocarcinoma to combination chemo-radiotherapy: Relationship to apoptotic activity, p53 and bcl-2 expression. *European Journal of Surgical Oncology*. 1998;24(3):169-173. doi:10.1016/S0748-7983(98)92861-X

148. Adell GCE, Zhang H, Evertsson S, Sun XF, Stl OHG, Nordenskjld BA. Apoptosis in rectal carcinoma: prognosis and recurrence after preoperative radiotherapy. *Cancer*. 2001;91(10):1870-1875. doi:10.1002/1097-0142(20010515)91:10<1870::AID-CNCR1208>3.0.CO;2-1

149. Barker HE, Paget JTE, Khan AA, Harrington KJ. The tumour microenvironment after radiotherapy: Mechanisms of resistance and recurrence. *Nature Reviews Cancer*. 2015;15(7):409-425. doi:10.1038/nrc3958

150. Whiteside TL. The tumor microenvironment and its role in promoting tumor growth. *Oncogene*. 2008;27(45):5904-5912. doi:10.1038/onc.2008.271

151. Rankin EB, Giaccia AJ. Hypoxic control of metastasis. *Science*. 2016;352(6282):175-180. doi:10.1126/science.aaf4405

152. Hammond EM, Asselin MC, Forster D, O'Connor JPB, Senra JM, Williams KJ. The Meaning, Measurement and Modification of Hypoxia in the Laboratory and the Clinic. *Clinical Oncology*. 2014;26(5):277-288. doi:10.1016/j.clon.2014.02.002

153. Gray LH, Conger AD, Ebert M, Hornsey S, Scott OC. The concentration of oxygen dissolved in tissues at the time of irradiation as a factor in radiotherapy. *The British journal of radiology*. 1953;26(312):638-648. doi:10.1259/0007-1285-26-312-638

154. Graham K, Unger E. Overcoming tumor hypoxia as a barrier to radiotherapy, chemotherapy and immunotherapy in cancer treatment. *International Journal of Nanomedicine*. 2018;13:6049-6058. doi:10.2147/IJN.S140462

155. Goethals L, Debucquoy A, Perneel C, et al. Hypoxia in human colorectal adenocarcinoma: Comparison between extrinsic and potential intrinsic hypoxia markers. *International Journal of Radiation Oncology*Biology*Physics*. 2006;65(1):246-254. doi:10.1016/j.ijrobp.2006.01.007

156. Wendling P, Manz R, Thews G, Vaupel P. Heterogeneous oxygenation of rectal carcinomas in humans: a critical parameter for preoperative irradiation? *Adv Exp Med Biol*. 1984;180:293-300. doi:10.1007/978-1-4684-4895-5_28

157. Rasheed S, Harris AL, Tekkis PP, et al. Hypoxia-inducible factor-1α and -2α are expressed in most rectal cancers but only hypoxia-inducible factor-1α is associated with prognosis. *Br J Cancer*. 2009;100(10):1666-1673. doi:10.1038/sj.bjc.6605026

158. Theodoropoulos GE, Lazaris AC, Theodoropoulos VE, et al. Hypoxia, angiogenesis and apoptosis markers in locally advanced rectal cancer. *Int J Colorectal Dis*. 2006;21(3):248-257. doi:10.1007/s00384-005-0788-4

159. Toiyama Y, Inoue Y, Saigusa S, et al. Gene Expression Profiles of Epidermal Growth Factor Receptor, Vascular Endothelial Growth Factor and Hypoxia-inducible

Factor-1 with Special Reference to Local Responsiveness to Neoadjuvant Chemoradiotherapy and Disease Recurrence After Rectal Cancer Surgery. *Clinical Oncology*. 2010;22(4):272-280. doi:10.1016/j.clon.2010.01.001

160. Hanahan D, Coussens LM. Accessories to the Crime: Functions of Cells Recruited to the Tumor Microenvironment. *Cancer Cell*. 2012;21(3):309-322. doi:10.1016/j.ccr.2012.02.022

161. Chatila WK, Kim JK, Walch H, et al. Genomic and transcriptomic determinants of response to neoadjuvant therapy in rectal cancer. *Nature Medicine*. 2022;28(8):1646-1655. doi:10.1038/s41591-022-01930-z

162. O'Brien RM, Cannon A, Reynolds JV, Lysaght J, Lynam-lennon N. Complement in tumourigenesis and the response to cancer therapy. *Cancers*. 2021;13(1209):1-31. doi:10.3390/cancers13061209

163. Ricklin D, Hajishengallis G, Yang K, Lambris JD. Complement: A key system for immune surveillance and homeostasis. *Nature Immunology*. 2010;11(9):785-797. doi:10.1038/ni.1923

164. Cooper NR. *The Classical Complement Pathway: Activation and Regulation of the First Complement Component*. Vol 37.; 1985. doi:10.1016/S0065-2776(08)60340-5

165. Bordet J, Gengou O. Sur l'existence de substances sensibilisatrices dans la plu- part des serum antimicrobiens. *Annales de l'Institut Pasteur*. 1901;15:289−302.

166. Nesargikar PN, Spiller B, Chavez R. The complement system: History, pathways, cascade and inhibitors. *European Journal of Microbiology and Immunology*. 2012;2(2):103-111. doi:10.1556/EuJMI.2.2012.2.2

167. Brand E. Berlin Klin Woch 46. 1907;1075.

168. Ferrata A. Berlin Klin Woch 44. 1907;366.

169. Kolev M, Le Friec G, Kemper C. Complement-tapping into new sites and effector systems. *Nature Reviews Immunology*. 2014;14(12):811-820. doi:10.1038/nri3761

170. Morgan BP, Gasque P. Extrahepatic complement biosynthesis: where, when and why? *Clinical and Experimental Immunology*. 2003;107(1):1-7. doi:10.1046/j.1365-2249.1997.d01-890.x

171. Strainic MG, Liu J, Huang D, et al. Locally Produced Complement Fragments C5a and C3a Provide Both Costimulatory and Survival Signals to naive CD4+ T Cells. *Immunity*. 2008;28(3):425-435. doi:10.1016/j.immuni.2008.02.001.Locally

172. Lalli PN, Strainic MG, Yang M, Lin F, Medof ME, Heeger PS. Locally produced C5a binds to T cell expressed C5aR to enhance effector T-cell expansion by limiting antigen-induced apoptosis. *Blood*. 2008;112(5):1759-1766. doi:10.1182/blood-2008-04-151068

173. Roumenina LT, Daugan MV, Noé R, et al. Tumor Cells Hijack Macrophage-Produced Complement C1q to Promote Tumor Growth. *Cancer Immunology Research*. 2019;7(7):1091-1106. doi:10.1158/2326-6066.CIR-18-0891

174. Turner NA, Moake J. Assembly and Activation of Alternative Complement Components on Endothelial Cell-Anchored Ultra-Large Von Willebrand Factor Links Complement and Hemostasis-Thrombosis. Miyata T, ed. *PLoS ONE*. 2013;8(3):e59372. doi:10.1371/journal.pone.0059372

175. Monteran L, Ershaid N, Doron H, et al. Chemotherapy-induced complement signaling modulates immunosuppression and metastatic relapse in breast cancer. *Nat Commun*. 2022;13(1):5797. doi:10.1038/s41467-022-33598-x

176. Revel M, Daugan MV, Sautés-Fridman C, Fridman WH, Roumenina LT. Complement System: Promoter or Suppressor of Cancer Progression? *Antibodies*. 2020;9(4):57. doi:10.3390/antib9040057

177. Roumenina LT, Daugan MV, Petitprez F, Sautès-Fridman C, Fridman WH. Context-dependent roles of complement in cancer. *Nature Reviews Cancer*. Published online 2019. doi:10.1038/s41568-019-0210-0

178. Sarma JV, Ward PA. The Complement System. *Cell and Tissue Research*. 2011;343(1):227-235. doi:10.1007/s00441-010-1034-0.The

179. Qu H, Ricklin D, Lambris JD. Recent Developments in Low Molecular Weight Complement Inhibitors. *Molecular Immunology*. 2009;47(2-3):185-195. doi:10.1016/j.dcn.2011.01.002.The

180. Klos A, Tenner AJ, Johswich KO, Ager RR, Reis ES, Köhl J. The role of the anaphylatoxins in health and disease. *Molecular Immunology*. 2009;46(14):2753-2766. doi:10.1016/j.molimm.2009.04.027

181. Bokisch VA, Müller-Eberhard HJ. Anaphylatoxin inactivator of human plasma: its isolation and characterization as a carboxypeptidase. *J Clin Invest*. 1970;49(12):2427-2436. doi:10.1172/JCI106462

182. Matthews KW, Mueller-Ortiz SL, Wetsel RA. Carboxypeptidase N: a pleiotropic regulator of inflammation. *Molecular Immunology*. 2004;40(11):785-793. doi:10.1016/j.molimm.2003.10.002

183. Wilken HC, Götze O, Werfel T, Zwirner J. C3a(desArg) does not bind to and signal through the human C3a receptor. *Immunology Letters*. 1999;67(2):141-145. doi:10.1016/S0165-2478(99)00002-4

184. Webster RO, Hong SR, Johnston RB, Henson PM. Biological effects of the human complement fragments C5a and C5ades Arg on neutrophil function. *Immunopharmacology*. 1980;2(3):201-219. doi:10.1016/0162-3109(80)90050-8

185. Senior RM, Griffin GL, Perez HD, Webster RO. Human C5a and C5a des Arg exhibit chemotactic activity for fibroblasts. *The Journal of Immunology*. 1988;141(10):3570-3574. doi:10.4049/jimmunol.141.10.3570

186. Merle NS, Church SE, Fremeaux-Bacchi V, Roumenina LT. Complement system part I - molecular mechanisms of activation and regulation. *Frontiers in Immunology*. 2015;6:1-30. doi:10.3389/fimmu.2015.00262

187. Okinaga S, Slattery D, Humbles A, et al. C5L2, a nonsignaling C5A binding protein. *Biochemistry*. 2003;42(31):9406-9415. doi:10.1021/bi034489v

188. Van Lith LH c., Oosterom J, Van Elsas A, Zaman GJR. C5a-Stimulated Recruitment of ß-Arrestin2 to the Nonsignaling 7-Transmembrane Decoy Receptor

C5L2. *Journal of Biomolecular Screening*. 2009;14(9):1067-1075. doi:10.1177/1087057109341407

189. Croker DE, Halai R, Kaeslin G, et al. C5a2 can modulate ERK1/2 signaling in macrophages via heteromer formation with C5a1 and β-arrestin recruitment. *Immunology and Cell Biology*. 2014;92. doi:10.1038/icb.2014.32

190. Bamberg CE, Mackay CR, Lee H, et al. The C5a Receptor (C5aR) C5L2 Is a Modulator of C5aR-mediated Signal Transduction *. *Journal of Biological Chemistry*. 2010;285(10):7633-7644. doi:10.1074/jbc.M109.092106

191. Scola AM, Johswich KO, Morgan BP, Klos A, Monk PN. The human complement fragment receptor, C5L2, is a recycling decoy receptor. *Mol Immunol*. 2009;46(6):1149-1162. doi:10.1016/j.molimm.2008.11.001

192. Gaboriaud C, Thielens NM, Gregory LA, Rossi V, Fontecilla-Camps JC, Arlaud GJ. Structure and activation of the C1 complex of complement: Unraveling the puzzle. *Trends in Immunology*. 2004;25(7):368-373. doi:10.1016/j.it.2004.04.008

193. Kishore U, Ghai R, Greenhough TJ, et al. Structural and functional anatomy of the globular domain of complement protein C1q. *Immunology Letters*. 2004;95(2):113-128. doi:10.1016/j.imlet.2004.06.015

194. Szalai AJ, Agrawal A, Greenhough TJ, Volanakis JE. C-Reactive Protein: Structural Biology and Host Defense Function. *Clinical Chemistry and Laboratory Medicine*. 1999;37(3):265-270. doi:10.1515/CCLM.1999.046

195. Volanakis JE, Kaplan MH. Interaction of C-Reactive Protein Complexes with the Complement system. II. Consumption of Guinea Pig Complement by CRP Complexes: Requirement for Human C1q. *Journal of Immunology*. 1974;113(1):9-17.

196. Kang YS, Do Y, Lee HK, et al. A Dominant Complement Fixation Pathway for Pneumococcal Polysaccharides Initiated by SIGN-R1 Interacting with C1q. *Cell*. 2006;125(1):47-58. doi:10.1016/j.cell.2006.01.046

197. Ebenbichler CF. Human immunodeficiency virus type 1 activates the classical pathway of complement by direct C1 binding through specific sites in the

transmembrane glycoprotein gp41. *Journal of Experimental Medicine*. 1991;174:1417-1424. doi:10.1084/jem.174.6.1417

198. Spear GT, Jiang HX, Sullivan BL, Gewurz H, Landay AL, Lint TF. Direct Binding of Complement Component C1q to Human Immunodeficiency Virus (HIV) and Human T Lymphotrophic Virus-I (HTLV-I) Coinfected Cells. *AIDS Research and Human Retroviruses*. 1991;7(7):579-585. doi:10.1089/aid.1991.7.579

199. Thielens NM, Tacnet-Delorme P, Arlaud GJ. Interaction of C1q and Mannan-binding lectin with viruses. *Immunobiology*. 2002;205(4-5):563-574. doi:10.1078/0171-2985-00155

200. Holmskov U, Thiel S, Jensenius JC. COLLECTINS AND FICOLINS: Humoral Lectins of the Innate Immune Defense. *Annual Review of Immunology*. 2003;21:547-578. doi:10.1146/annurev.immunol.21.120601.140954

201. Thiel S, Vorup-Jensen T, Stover CM, et al. A second serine protease associated with mannan-binding lectin that activates complement. *Nature*. 1997;(386):506-510.

202. Megyeri M, Harmat V, Major B, et al. Quantitative characterization of the activation steps of mannan-binding lectin (MBL)-associated serine proteases (MASPs) points to the central role of MASP-1 in the initiation of the complement lectin pathway. *Journal of Biological Chemistry*. 2013;288(13):8922-8934. doi:10.1074/jbc.M112.446500

203. Pangburn MK, Schreiber RD, Müller-Eberhard HJ. Formation of the initial C3 convertase of the alternative complement pathway. Acquisition of C3b-like activities by spontaneous hydrolysis of the putative thioester in native C3. *The Journal of Experimental Medicine*. 1981;154(3):856-867. doi:10.1084/jem.154.3.856

204. Bexborn F, Andersson PO, Chen H, Nilsson B, Ekdahl KN. The Tick-Over Theory Revisited: Formation and Regulation of the soluble Alternative Complement C3 Convertase (C3(H2O)Bb). *Molecular immunology*. 2008;45(8):2370-2379. doi:10.1021/nl061786n.Core-Shell

205. Harboe M, Mollnes TE. The alternative complement pathway revisited. *Journal of Cellular and Molecular Medicine*. 2008;12(4):1074-1084. doi:10.1111/j.1582-4934.2008.00350.x

206. Reid KBM, Porter RR. The Proteolytic Activation Systems of Complement. *Annual Review of Biochemistry*. 1981;50:434-464.

207. Ganter MT, Brohi K, Cohen MJ, et al. Role of the alternative pathway in the early complement activation following major trauma. *Shock*. 2007;28(1):29-34. doi:10.1097/shk.0b013e3180342439

208. Walport MJ. Complement. First of Two Parts. *The New England Journal of Medicine*. 2001;344(14):1058-1066.

209. Ehrnthaller C, Ignatius A, Gebhard F, Huber-lang M. New Insights of an Old Defense System: Structure, Function and Clinical Relevance of the Complement System. *Molecular Medicine*. 2011;17(3-4):317-329. doi:10.2119/molmed.2010.00149

210. Koski CL, Ramm LE, Hammer CH, Mayer MM, Shin ML. Cytolysis of nucleated cells by complement: Cell death displays multi-hit characteristics. *Proceedings of the National Academy of Sciences of the United States of America*. 1983;80(12 I):3816-3820. doi:10.1073/pnas.80.12.3816

211. Morgan BP. Complement membrane attack on nucleated cells: Resistance, recovery and non-lethal effects. *Biochemical Journal*. 1989;264(1):1-14. doi:10.1042/bj2640001

212. Tegla CA, Cudrici C, Patel S, et al. Membrane attack by complement: The assembly and biology of terminal complement complexes. *Immunologic Research*. 2011;51(1):45-60. doi:10.1007/s12026-011-8239-5

213. Kim DD, Song W chao. Membrane complement regulatory proteins. *Clinical Immunology*. 2006;118:127-136. doi:10.1016/j.clim.2005.10.014

214. Schmidt CQ, Lambris JD, Ricklin D. Protection of host cells by complement regulators. *Immunological Reviews*. 2016;274(1):152-171. doi:10.1111/imr.12475

215. Fearon DT, Austen KF. Properdin: binding to C3b and stabilization of the C3b dependent C3 convertase. *Journal of Experimental Medicine*. 1975;142(4):856-863. doi:10.1084/jem.142.4.856

216. Spitzer D, Mitchell LM, Atkinson JP, Hourcade DE. Properdin Can Initiate Complement Activation by Binding Specific Target Surfaces and Providing a Platform for De Novo Convertase Assembly. *The Journal of Immunology*. 2007;179(4):2600-2608. doi:10.4049/jimmunol.179.4.2600

217. Fearon DT. Regulation of the amplification C3 convertase of human complement by an inhibitory protein isolated from human erythrocyte membrane. *Proceedings of the National Academy of Sciences of the United States of America*. 1979;76(11):5867-5871. doi:10.1073/pnas.76.11.5867

218. Fearon DT. Identification of the membrane glycoprotein that is the C3b receptor of the human erythrocyte, polymorphonuclear leukocyte, B lymphocyte, and monocyte. *Journal of Experimental Medicine*. 1980;152(1):20-30. doi:10.1084/jem.152.1.20

219. Iida K, Nussenzweig V. Complement receptor is an inhibitor of the complement cascade. *Journal of Experimental Medicine*. 1981;153(5):1138-1150. doi:10.1084/jem.153.5.1138

220. Medicus RG, Melamed J, Arnaout MA. Role of human factor I and C3b receptor in the cleavage of surface-bound C3bi molecules. *European Journal of Immunology*. 1983;13(6):465-470. doi:10.1002/eji.1830130607

221. Edward Medof M, Iida K, Mold C, Nussenzweig V. Unique role of the complement receptor CR1 in the degradation of C3b associated with immune complexes. *Journal of Experimental Medicine*. 1982;156(6):1739-1754. doi:10.1084/jem.156.6.1739

222. Seya T, Turner JR, Atkinson JP. Purification and characterization of a membrane protein (gp45-70) that is a cofactor for cleavage of C3B and C4B. *Journal of Experimental Medicine*. 1986;163(4):837-855. doi:10.1084/jem.163.4.837

223. Seya T, Ballard LL, Bora NS, Kumar V, Cui W, Atkinson JP. Distribution of membrane cofactor protein of complement on human peripheral blood cells. An altered

form is found on granulocytes. *European Journal of Immunology*. 1988;18(8):1289-1294. doi:10.1002/eji.1830180821

224. Liszewski MK, Post TW, Atkinson JP. Membrane cofactor protein (MCP or CD46): Newest member of the regulators of complement activation gene cluster. *Annual Review of Immunology*. 1991;9:431-455. doi:10.1146/annurev.iy.09.040191.002243

225. Nicholson-Weller A, Burge J, Fearon DT, Weller PF, Austen KF. Isolation of a human erythrocyte membrane glycoprotein with decay-accelerating activity for C3 convertases of the complement system . *The Journal of Immunology*. 1982;129:184-189.

226. Medof BYME, Kinoshita T, Nussenzweig V. Inhibition of Complement Activation on the Surface of Cells After of Incorporation of Decay-Accelerating Factor (DAF) Into Their Membranes. *Journal of Experimental Medicine*. 1984;160(November):1558-1578.

227. Kinoshita T, Medof ME, Nussenzweig V. Endogenous association of decay-accelerating factor (DAF) with C4b and C3b on cell membranes. *The Journal of Immunology*. 1986;136(9):3390-3395.

228. Meri S, Morgan BP, Davies A, et al. Human protectin (CD59), an 18,000-20,000 MW complement lysis restricting factor, inhibits C5b-8 catalysed insertion of C9 into lipid bilayers. *Immunology*. 1990;71(1):1-9.

229. Ninomiya H, Sims PJ. The human complement regulatory protein CD59 binds to the α-chain of C8 and to the "b" domain of C9. *Journal of Biological Chemistry*. 1992;267(19):13675-13680.

230. Davis AE, Mejia P, Lu F. BIOLOGICAL ACTIVITIES OF C1 INHIBITOR. *Mol Immunol*. 2008;45(16):4057-4063. doi:10.1016/j.molimm.2008.06.028

231. Nilsson SC, Sim RB, Lea SM, Fremeaux-Bacchi V, Blom AM. Complement factor I in health and disease. *Molecular Immunology*. 2011;48(14):1611-1620. doi:10.1016/j.molimm.2011.04.004

232. Ferreira VP, Pangburn MK, Cortés C. Complement control protein factor H: the good, the bad, and the inadequate. *Mol Immunol*. 2010;47(13):2187-2197. doi:10.1016/j.molimm.2010.05.007

233. Kühn S, Zipfel PF. Mapping of the domains required for decay acceleration activity of the human factor H-like protein 1 and factor H. *European Journal of Immunology*. 1996;26(10):2383-2387. doi:10.1002/eji.1830261017

234. Kühn S, Skerka C, Zipfel PF. Mapping of the complement regulatory domains in the human factor H-like protein 1 and in factor H1. *The Journal of Immunology*. 1995;155(12):5663-5670. doi:10.4049/jimmunol.155.12.5663

235. Fujita T, Gigli I, Nussenzweig V. Human C4-binding protein. II. Role in proteolysis of C4b by C3b-inactivator. *Journal of Experimental Medicine*. 1978;148(4):1044-1051. doi:10.1084/jem.148.4.1044

236. Gigli I, Fujita T, Nussenzweig V. Modulation of the classical pathway C3 convertase by plasma proteins C4 binding protein and C3b inactivator. *Proceedings of the National Academy of Sciences*. 1979;76(12):6596-6600. doi:10.1073/pnas.76.12.6596

237. Blom AM, Kask L, Dahlbäck B. CCP1–4 of the C4b-binding protein α-chain are required for factor I mediated cleavage of complement factor C3b. *Molecular Immunology*. 2003;39(10):547-556. doi:10.1016/S0161-5890(02)00213-4

238. Podak ER, Preissner KT, Müller-Eberhard HJ. Inhibition of C9 polymerization within the SC5b-9 complex of complement by S-protein. - Abstract - Europe PMC. *Acta Pathol Microbiol Scand Suppl*. 1984;284:89-96.

239. Tschopp J, Chonn A, Hertig S, French LE. Clusterin, the human apolipoprotein and complement inhibitor, binds to complement C7, C8 beta, and the b domain of C9. *J Immunol*. 1993;151(4):2159-2165.

240. Dunkelberger JR, Song WC. Complement and its role in innate and adaptive immune responses. *Cell Res*. 2010;20(1):34-50. doi:10.1038/cr.2009.139

241. Reis ES, Mastellos DC, Hajishengallis G, Lambris JD. New insights into the immune functions of complement. *Nature Reviews Immunology*. 2019;15. doi:10.1038/s41577-019-0168-x

242. Hartmann K, Henz BM, Krüger-Krasagakes S, et al. C3a and C5a stimulate chemotaxis of human mast cells. *Blood*. 1997;89(8):2863-2870. doi:10.1182/blood.v89.8.2863

243. Nilsson C, Johnell M, Hammer CH, et al. C3a and C5a Are Chemotaxins for Human Mast Cells and Act Through Distinct Receptors via a Pertussis Toxin-Sensitive Signal Transduction Pathway. *The Journal of Immunology*. 1996;157:1693-1998.

244. Daffern BPJ, Pfeifer PH, Ember JA, Hugli TE. C3a is a Chemotaxin for Human Eosinophils but Not for Neutrophils. I. C3a Stimulation of Neutrophils Is Secondary to Eosinophil Activation. *Journal of Experimental Medicine*. 1995;181:2119-2127.

245. Aksamit RR, Falk W, Leonard EJ. Chemotaxis by mouse macrophage cell lines. *The Journal of Immunology*. 1981;126:2194-2199.

246. Yancey KB, Lawley TJ, Dersookian M, S. B, Harvath L. Analysis of the Interaction of Human C5a and C5a des Arg with Human Monocytes and Neutrophils: Flow Cytometric and Chemotaxis Studies. *The Journal of Investigative Dermatology*. 1989;92:184-189.

247. Ehrengruber MU, Geiser T, Deranleau DA. Activation of human neutrophils by C3a and C5a. *FEBS Letters*. 1994;346:181-184.

248. Lett-Brown MA, Leonard EJ. Histamine-Induced Inhibition of Normal Human Basophil Chemotaxis to C5a. *The Journal of Immunology*. 1977;118:815-818.

249. Nataf S, Davoust N, Ames RS, Barnum SR. Human T Cells Express the C5a Receptor and Are Chemoattracted to C5a. *The Journal of Immunology*. 1999;162:4018-4023.

250. Ottonello L, Corcione A, Tortolina G, et al. rC5a Directs the In Vitro Migration of Human Memory and Naive Tonsillar B Lymphocytes: Implications for B Cell

Trafficking in Secondary Lymphoid Tissues. *The Journal of Immunology*. 1999;162:6510-6517.

251. van Lookeren Campagne M, Wiesmann C, Brown EJ. Macrophage complement receptors and pathogen clearance. *Cellular Microbiology*. 2007;9(9):2095-2102. doi:10.1111/j.1462-5822.2007.00981.x

252. Karsten CM, Köhl J. The immunoglobulin, IgG Fc receptor and complement triangle in autoimmune diseases. *Immunobiology*. 2012;217(11):1067-1079. doi:10.1016/j.imbio.2012.07.015

253. Zhang X, Kimura Y, Fang C, et al. Regulation of Toll-like receptor–mediated inflammatory response by complement in vivo. *Blood*. 2007;110(1):228-236. doi:10.1182/blood-2006-12-063636

254. Fang Y, Xu C, Fu YX, Holers VM, Molina H. Expression of Complement Receptors 1 and 2 on Follicular Dendritic Cells Is Necessary for the Generation of a Strong Antigen-Specific IgG Response. *Journal of immunology (Baltimore, Md : 1950)*. 1998;160(11):5273-5279.

255. Carroll MC. The complement system in regulation of adaptive immunity. *Nature Immunology*. 2004;5(10):981-986. doi:10.1038/ni1113

256. Matsumoto AK, Kopicky-Burd J, Carter RH, Tuveson DA, Tedder TF, Fearon DT. Intersection of the Complement and Immune Systems: A Signal Transduction Complex of the B Lymphocyte-containing Complement Receptor Type 2 and CD19. *Journal of Experimental Medicine*. 1991;173(1):55-64. doi:10.1084/jem.173.1.55

257. Carter RH, Fearon DT. CD19: lowering the threshold for antigen receptor stimulation of B lymphocytes. *Science (New York, NY)*. 1992;256(5053):105-107.

258. Cherukuri A, Cheng PC, Pierce SK. The Role of the CD19/CD21 Complex in B Cell Processing and Presentation of Complement-Tagged Antigens. *The Journal of Immunology*. 2001;167(1):163-172. doi:10.4049/jimmunol.167.1.163

259. Heeger PS, Lalli PN, Lin F, et al. Decay-accelerating factor modulates induction of T cell immunity. *Journal of Experimental Medicine*. 2005;201(10):1523-1530. doi:10.1084/jem.20041967

260. Lalli PN, Strainic MG, Lin F, Medof ME, Heeger PS. Decay Accelerating Factor Can Control T Cell Differentiation into IFN-γ-Producing Effector Cells via Regulating Local C5a-Induced IL-12 Production. *The Journal of Immunology*. 2007;179(9):5793-5802. doi:10.4049/jimmunol.179.9.5793

261. Cardone J, Friec GL, Vantourout P, et al. Complement regulator CD46 temporally regulates cytokine production by conventional and unconventional T cells. *Nature Immunology*. 2010;11(9):862-871. doi:10.1038/ni.1917

262. Arbore G, Kemper C, Kolev M. Intracellular complement − the complosome − in immune cell regulation. *Molecular Immunology*. 2017;89(May):2-9. doi:10.1016/j.molimm.2017.05.012

263. Liszewski MK, Kolev M, Le Friec G, et al. Intracellular Complement Activation Sustains T Cell Homeostasis and Mediates Effector Differentiation. *Immunity*. 2013;39(6):1143-1157. doi:10.1016/j.immuni.2013.10.018

264. Kolev M, Dimeloe S, Le Friec G, et al. Complement Regulates Nutrient Influx and Metabolic Reprogramming during Th1 Cell Responses. *Immunity*. 2015;42(6):1033-1047. doi:10.1016/j.immuni.2015.05.024

265. Arbore G, West EE, Spolski R, et al. T helper 1 immunity requires complement-driven NLRP3 inflammasome actvity in CD4+ T cells. *Science*. 2016;352(6292):1247-1262. doi:10.1002/jmri.25711.PET/MRI

266. Niyonzima N, Rahman J, Kunz N, et al. Mitochondrial C5aR1 activity in macrophages controls IL-1β production underlying sterile inflammation. *Science Immunology*. 2022;6(66). doi:10.1126/sciimmunol.abf2489.Mitochondrial

267. Nozaki M, Raisler BJ, Sakurai E, et al. Drusen complement components C3a and C5a promote choroidal neovascularization. *Proceedings of the National Academy of Sciences*. 2006;103(7):2328-2333. doi:10.1073/pnas.0408835103

268. Markiewski MM, DeAngelis RA, Strey CW, et al. The Regulation of Liver Cell Survival by Complement. *J Immunol*. 2009;182(9):5412-5418. doi:10.4049/jimmunol.0804179

269. Stevens B, Allen NJ, Vazquez LE, et al. The Classical Complement Cascade Mediates CNS Synapse Elimination. *Cell*. 2007;131(6):1164-1178. doi:10.1016/j.cell.2007.10.036

270. Hanahan D, Weinberg RA. Hallmarks of Cancer: The Next Generation. *Cell*. 2011;144:646-647. doi:10.1016/j.cell.2011.02.013

271. Coussens LM, Werb Z. Inflammation and cancer. *Nature*. 2012;420(6917):860-867. doi:10.1038/nature01322.Inflammation

272. De Visser KE, Eichten A, Coussens LM. Paradoxical roles of the immune system during cancer development. *Nature Reviews Cancer*. 2006;6(1):24-37. doi:10.1038/nrc1782

273. Ytting H, Jensenius JC, Christensen IJ, Thiel S, Nielsen HJ. Increased activity of the mannan-binding lectin complement activation pathway in patients with colorectal cancer. *Scandinavian Journal of Gastroenterology*. 2004;39(7):674-679. doi:10.1080/00365520410005603

274. Corrales L, Ajona D, Rafail S, et al. Anaphylatoxin C5a creates a favorable microenvironment for lung cancer progression. *Journal of Immunology*. 2012;189(9):4674-4683. doi:10.1038/jid.2014.371

275. Ajona D, Pajares MJ, Chiara M, et al. Complement activation product C4d in oral and oropharyngeal squamous cell carcinoma. *Oral Diseases*. 2015;21:899-904. doi:10.1111/odi.12363

276. Bu X, Zheng Z, Wang C, Yu Y. Significance of C4d deposition in the follicular lymphoma and MALT lymphoma and their relationship with follicular dendritic cells. *Pathology Research and Practice*. 2007;203(3):163-167. doi:10.1016/j.prp.2006.11.004

277. Bouwens TAM, Trouw LA, Veerhuis R, Dirven CMF, Lamfers MLM, Al-khawaja H. Complement activation in Glioblastoma Multiforme pathophysiology : Evidence from serum levels and presence of complement activation products in tumor tissue. *Journal of Neuroimmunology*. 2015;278:271-276. doi:10.1016/j.jneuroim.2014.11.016

278. Niculescu F, Rus HG, Retegan M, Vlaicu R. Persistent Complement Activation on Tumor Cells in Breast Cancer. *American Journal of Pathology*. 1992;140(5):1039-1043.

279. Chen J, Yang W jun, Sun H jian, Yang X, Wu Y zhang. C5b-9 Staining Correlates With Clinical and Tumor Stage in Gastric Adenocarcinoma. *Applied Immunohistochemistry and Molecular Morphology*. 2016;24(7):470-475.

280. Yamakawa M, Yamada K, Tsuge T, et al. Protection of Thyroid Cancer Cells by Complement-Regulatory Factors. *Cancer*. 1994;73(11):2808-2817.

281. Bjørge L, Hakulinen J, Vintermyr OK, et al. Ascitic complement system in ovarian cancer. 2005;92(February):895-905. doi:10.1038/sj.bjc.6602334

282. Fishelson Z, Kirschfink M. Complement C5b-9 and cancer: Mechanisms of cell damage, cancer counteractions, and approaches for intervention. *Frontiers in Immunology*. 2019;10:1-16. doi:10.3389/fimmu.2019.00752

283. Maestri CA, Nisihara R, Mendes HW, et al. MASP-1 and MASP-2 serum levels are associated with worse prognostic in cervical cancer progression. *Frontiers in Immunology*. 2018;9:1-5. doi:10.3389/fimmu.2018.02742

284. Ytting H, Christensen IJ, Thiel S, Jensenius JC, Nielsen HJ. Serum mannan-binding lectin-associated serine protease 2 levels in colorectal cancer: Relation to recurrence and mortality. *Clinical Cancer Research*. 2005;11(4):1441-1446. doi:10.1158/1078-0432.CCR-04-1272

285. Swierzko AS, Szala A, Sawicki S, et al. Mannose-Binding Lectin (MBL) and MBL-associated serine protease-2 (MASP-2) in women with malignant and benign ovarian tumours. *Cancer Immunology, Immunotherapy*. 2014;63(11):1129-1140. doi:10.1007/s00262-014-1579-y

286. Fishelson Z, Donin N, Zell S, Schultz S, Kirschfink M. Obstacles to cancer immunotherapy: Expression of membrane complement regulatory proteins (mCRPs) in tumors. *Molecular Immunology*. 2003;40(2-4):109-123. doi:10.1016/S0161-5890(03)00112-3

287. Olcina MM, Balanis NG, Kim RK, et al. Mutations in an Innate Immunity Pathway Are Associated with Poor Overall Survival Outcomes and Hypoxic Signaling in Cancer. *Cell Reports*. 2018;25(13):3721-3732.e6. doi:10.1016/j.celrep.2018.11.093

288. Ong HT, Timm MM, Greipp PR, et al. Oncolytic measles virus targets high CD46 expression on multiple myeloma cells. *Experimental Hematology*. 2006;34(6):713-720. doi:10.1016/j.exphem.2006.03.002

289. Lok A, Descamps G, Tessoulin B, et al. P53 regulates CD46 expression and measles virus infection in myeloma cells. *Blood Advances*. 2018;2(23):3492-3505. doi:10.1182/bloodadvances.2018025106

290. Kesselring R, Thiel A, Pries R, et al. The complement receptors CD46, CD55 and CD59 are regulated by the tumour microenvironment of head and neck cancer to facilitate escape of complement attack. *European Journal of Cancer*. 2014;50(12):2152-2161. doi:10.1016/j.ejca.2014.05.005

291. Watson NFS, Durrant LG, Madjd Z, Ellis IO, Scholefield JH, Spendlove I. Expression of the membrane complement regulatory protein CD59 (protectin) is associated with reduced survival in colorectal cancer patients. *Cancer Immunology, Immunotherapy*. 2006;55(8):973-980. doi:10.1007/s00262-005-0055-0

292. Geller A, Yan J. The Role of Membrane Bound Complement Regulatory Proteins in Tumor Development and Cancer Immunotherapy. *Frontiers in Immunology*. 2019;10(May):1-13. doi:10.3389/fimmu.2019.01074

293. Ajona D, Castaño Z, Garayoa M, et al. Expression of complement factor H by lung cancer cells: Effects on the activation of the alternative pathway of complement. *Cancer Research*. 2004;64(17):6310-6318. doi:10.1158/0008-5472.CAN-03-2328

294. Ajona D, Hsu YF, Corrales L, Montuenga LM, Pio R. Down-Regulation of Human Complement Factor H Sensitizes Non-Small Cell Lung Cancer Cells to Complement

Attack and Reduces In Vivo Tumor Growth. *The Journal of Immunology*. 2007;178(9):5991-5998. doi:10.4049/jimmunol.178.9.5991

295. Okroj M, Hsu YF, Ajona D, Pio R, Blom AM. Non-small cell lung cancer cells produce a functional set of complement factor I and its soluble cofactors. *Molecular Immunology*. 2008;45(1):169-179. doi:10.1016/j.molimm.2007.04.025

296. Ajona D, Ortiz-Espinosa S, Pio R, Lecanda F. Complement in Metastasis: A Comp in the Camp. *Frontiers in Immunology*. 2019;10(April):1-9. doi:10.3389/fimmu.2019.00669

297. Reis ES, Mastellos DC, Ricklin D, Mantovani A, Lambris JD. Complement in cancer: Untangling an intricate relationship. *Nature Reviews Immunology*. 2018;18(1):5-18. doi:10.1038/nri.2017.97

298. Markiewski MM, Deangelis RA, Benencia F, et al. Modulation of the anti-tumor immune response by complement. *Nature Immunology*. 2008;9(11):1225-1235. doi:10.1038/ni.1655.Modulation

299. Bulla R, Tripodo C, Rami D, et al. C1q acts in the tumour microenvironment as a cancer-promoting factor independently of complement activation. *Nature Communications*. 2016;7:1-11. doi:10.1038/ncomms10346

300. Cho MS, Vasquez HG, Rupaimoole R, et al. Autocrine Effects of Tumor-Derived Complement. *Cell Reports*. 2014;6(6):1085-1095. doi:10.1016/j.celrep.2014.02.014

301. Riihilä P, Nissinen L, Farshchian M, et al. Complement Component C3 and Complement Factor B Promote Growth of Cutaneous Squamous Cell Carcinoma. *American Journal of Pathology*. 2017;187(5):1186-1197. doi:10.1016/j.ajpath.2017.01.006

302. Riihilä P, Nissinen L, Farshchian M, et al. Complement factor I promotes progression of cutaneous squamous cell carcinoma. *Journal of Investigative Dermatology*. 2015;135(2):579-588. doi:10.1038/jid.2014.376

303. Nunez-Cruz S, Gimotty PA, Guerra MW, et al. Genetic and pharmacologic inhibition of complement impairs endothelial cell function and ablates ovarian cancer neovascularization. *Neoplasia*. 2012;14(11):994-1004. doi:10.1593/neo.121262

304. Fan Z, Qin J, Wang D, Geng S. Complement C3a promotes proliferation, migration and stemness in cutaneous squamous cell carcinoma. *Journal of Cellular and Molecular Medicine*. 2019;23(5):3097-3107. doi:10.1111/jcmm.13959

305. Yoneda M, Imamura R, Nitta H, et al. Enhancement of cancer invasion and growth via the C5a-C5a receptor system: Implications for cancer promotion by autoimmune diseases and association with cervical cancer invasion. *Oncology Letters*. 2019;17(1):913-920. doi:10.3892/ol.2018.9715

306. Maeda Y, Kawano Y, Wada Y, et al. C5aR is frequently expressed in metastatic renal cell carcinoma and plays a crucial role in cell invasion via the ERK and PI3 kinase pathways. *Oncology Reports*. 2015;33(4):1844-1850. doi:10.3892/or.2015.3800

307. Hu WH, Hu Z, Shen X, Dong LY, Zhou WZ, Yu XX. C5a receptor enhances hepatocellular carcinoma cell invasiveness via activating ERK1/2-mediated epithelial-mesenchymal transition. *Experimental and Molecular Pathology*. 2016;100(1):101-108. doi:10.1016/j.yexmp.2015.10.001

308. Ajona D, Zandueta C, Corrales L, et al. Blockade of the complement C5a/C5aR1 axis impairs lung cancer bone metastasis by CXCL16-mediated effects. *American Journal of Respiratory and Critical Care Medicine*. 2018;197(9):1164-1176. doi:10.1164/rccm.201703-0660OC

309. Abdelbaset-Ismail A, Borkowska-Rzeszotek S, Kubis E, et al. Activation of the complement cascade enhances motility of leukemic cells by downregulating expression of HO-1. *Leukemia*. 2017;31(2):446-458. doi:10.1038/leu.2016.198

310. Nitta H, Wada Y, Kawano Y, et al. Enhancement of Human Cancer Cell Motility and Invasiveness by Anaphylatoxin C5a via Aberrantly Expressed C5a Receptor (CD88). *Clinical Cancer Research*. 2004;19(8):2004-2014. doi:10.1158/1078-0432.CCR-12-1204

311. Cho MS, Rupaimoole R, Choi HJ, et al. Complement Component 3 Is Regulated by TWIST1 and Mediates Epithelial − Mesenchymal Transition. *The Journal of Immunology*. 2016;196(3):1412-1418. doi:10.4049/jimmunol.1501886

312. Kochanek DM, Ghouse SM, Karbowniczek MM, Markiewski MM. Complementing cancer metastasis. *Frontiers in Immunology*. 2018;9(JUL):1-11. doi:10.3389/fimmu.2018.01629

313. Block I, Müller C, Sdogati D, et al. CFP suppresses breast cancer cell growth by TES-mediated upregulation of the transcription factor DDIT3. *Oncogene*. 2019;38(23):4560-4573. doi:10.1038/s41388-019-0739-0

314. Bandini S, Curcio C, Macagno M, et al. Early onset and enhanced growth of autochthonous mammary carcinomas in C3-deficient Her2/neu transgenic mice. *OncoImmunology*. 2013;2(9):1-14. doi:10.4161/onci.26137

315. Bandini S, Macagno M, Hysi A, et al. The non-inflammatory role of C1q during Her2/neu-driven mammary carcinogenesis. *OncoImmunology*. 2016;5(12):1-13. doi:10.1080/2162402X.2016.1253653

316. Kim DY, Martin CB, Soon NL, Martin BK. Expression of complement protein C5a in a murine mammary cancer model: Tumor regression by interference with the cell cycle. *Cancer Immunology, Immunotherapy*. 2005;54(10):1026-1037. doi:10.1007/s00262-005-0672-7

317. Yuan K, Ye J, Liu Z, et al. Complement C3 overexpression activates JAK2/STAT3 pathway and correlates with gastric cancer progression. *Journal of Experimental and Clinical Cancer Research*. 2020;39(1):1-15. doi:10.1186/s13046-019-1514-3

318. Chen J, Li G qing, Zhang L, et al. Complement C5a/C5aR pathway potentiates the pathogenesis of gastric cancer by down-regulating p21 expression. *Cancer Letters*. 2018;412(October):30-36. doi:10.1016/j.canlet.2017.10.003

319. Imamura T, Yamamoto-Ibusuki M, Sueta A, et al. Influence of the C5a–C5a receptor system on breast cancer progression and patient prognosis. *Breast Cancer*. 2016;23(6):876-885. doi:10.1007/s12282-015-0654-3

320. Wang Y, Sun SN, Liu Q, et al. Autocrine complement inhibits IL10-dependent T-cell-mediated antitumor immunity to promote tumor progression. *Cancer Discovery*. 2016;6(9):1022-1035. doi:10.1158/2159-8290.CD-15-1412

321. Vadrevu SK, Chintala NK, Sharma SK, et al. Complement C5a receptor facilitates cancer metastasis by altering t-cell responses in the metastatic niche. *Cancer Research*. 2014;74(13):3454-3465. doi:10.1158/0008-5472.CAN-14-0157

322. Ajona D, Ortiz-Espinosa S, Moreno H, et al. A combined PD-1/C5a blockade synergistically protects against lung cancer growth and metastasis. *Cancer Discovery*. 2017;7(7):694-703. doi:10.1158/2159-8290.CD-16-1184

323. Downs-Canner S, Magge D, Ravindranathan R, et al. Complement Inhibition: A Novel Form of Immunotherapy for Colon Cancer. *Annals of Surgical Oncology*. 2016;23(2):655-662. doi:10.1245/s10434-015-4778-7

324. Ding P, Li L, Li L, et al. C5aR1 is a master regulator in colorectal tumorigenesis via immune modulation. *Theranostics*. 2020;10(19):8619-8632. doi:10.7150/thno.45058

325. Gunn L, Ding C, Liu M, et al. Opposing Roles for Complement Component C5a in Tumor Progression and the Tumor Microenvironment. *The Journal of Immunology*. 2012;189(6):2985-2994. doi:10.4049/jimmunol.1200846

326. Kwak JW, Laskowski J, Li HY, et al. Complement activation via a C3a receptor pathway alters CD4+ T lymphocytes and mediates lung cancer progression. *Cancer Research*. 2018;78(1):143-156. doi:10.1158/0008-5472.CAN-17-0240

327. Xu Y, Huang Y, Xu W, et al. Activated hepatic stellate cells (HSCs) exert immunosuppressive effects in hepatocellular carcinoma by producing complement C3. *OncoTargets and Therapy*. 2020;13:1497-1505. doi:10.2147/OTT.S234920

328. Guglietta S, Chiavelli A, Zagato E, et al. Coagulation induced by C3aR-dependent NETosis drives protumorigenic neutrophils during small intestinal tumorigenesis. *Nature Communications*. 2016;7:1-14. doi:10.1038/ncomms11037

329. Ning C, Li YY, Wang Y, et al. Complement activation promotes colitis-associated carcinogenesis through activating intestinal IL-1β/IL-17A axis. *Mucosal Immunology*. 2015;8(6):1275-1284. doi:10.1038/mi.2015.18

330. Nabizadeh JA, Manthey HD, Steyn FJ, et al. The Complement C3a Receptor Contributes to Melanoma Tumorigenesis by Inhibiting Neutrophil and CD4 + T Cell Responses. *The Journal of Immunology*. 2016;196(11):4783-4792. doi:10.4049/jimmunol.1600210

331. Davidson S, Efremova M, Riedel A, et al. Single-Cell RNA Sequencing Reveals a Dynamic Stromal Niche That Supports Tumor Growth. *Cell Reports*. 2020;31(7):107628. doi:10.1016/j.celrep.2020.107628

332. Bonavita E, Gentile S, Rubino M, et al. PTX3 is an extrinsic oncosuppressor regulating complement-dependent inflammation in cancer. *Cell*. 2015;160:700-714. doi:10.1016/j.cell.2015.01.004

333. Piao C, Cai L, Qiu S, Jia L, Song W, Du J. Complement 5a enhances hepatic metastases of colon cancer via monocyte chemoattractant protein-1-mediated inflammatory cell infiltration. *The Journal of Biological Chemistry*. 2015;290(17):10667-10676. doi:10.1074/jbc.M114.612622

334. Contractor T, Kobayashi S, da Silva E, et al. Sexual dimorphism of liver metastasis by murine pancreatic neuroendocrine tumors is affected by expression of complement C5. *Oncotarget*. 2016;7(21):30585-30596. doi:10.18632/oncotarget.8874

335. Piao C, Zhang WM, Li TT, et al. Complement 5a stimulates macrophage polarization and contributes to tumor metastases of colon cancer. *Experimental Cell Research*. 2018;366(2):127-138. doi:10.1016/j.yexcr.2018.03.009

336. Medler TR, Murugan D, Horton W, et al. Complement C5a Fosters Squamous Carcinogenesis and Limits T Cell Response to Chemotherapy. *Cancer Cell*. 2018;34:561-578. doi:10.1016/j.ccell.2018.09.003

337. Nandagopal S, Li CG, Xu Y, Sodji QH, Graves EE, Giaccia AJ. C3aR Signaling Inhibits NK-cell Infiltration into the Tumor Microenvironment in Mouse Models.

Cancer Immunology Research. Published online 2021:1-15. doi:10.1158/2326-6066.cir-21-0435

338. Sodji QH, Nambiar DK, Viswanathan V, et al. The Combination of Radiotherapy and Complement C3a Inhibition Potentiates Natural Killer cell Functions Against Pancreatic Cancer. *Cancer Research Communications*. 2022;2(7):725-738. doi:10.1158/2767-9764.CRC-22-0069

339. Janelle V, Langlois MP, Tarrab E, Lapierre P, Poliquin L, Lamarre A. Transient complement inhibition promotes a tumor-specific immune response through the implication of natural killer cells. *Cancer immunology research*. 2014;2(3):200-206. doi:10.1158/2326-6066.CIR-13-0173

340. Liu CF, Min XY, Wang N, et al. Complement receptor 3 has negative impact on tumor surveillance through suppression of natural killer cell function. *Frontiers in Immunology*. 2017;8(NOV):1-16. doi:10.3389/fimmu.2017.01602

341. Ding P, Xu Y, Li L, et al. Intracellular complement C5a/C5aR1 stabilizes b-catenin to promote colorectal tumorigenesis. *Cell Reports*. 2022;39(9):110851. doi:10.1016/j.celrep.2022.110851

342. Daugan MV, Revel M, Thouenon R, et al. Intracellular Factor H Drives Tumor Progression Independently of the Complement Cascade. *Cancer Immunology Research*. 2021;9(8):909-925. doi:10.1158/2326-6066.cir-20-0787

343. Olcina MM, Kim RK, Balanis NG, et al. Intracellular C4BPA levels regulate NF-κB dependent apoptosis. *iScience*. 2020;23(10):101594. doi:10.1016/j.isci.2020.101594

344. O'Brien RM, Lynam-Lennon N, Olcina MM. Thinking inside the box: intracellular roles for complement system proteins come into focus.

345. Lu Y, Zhao Q, Liao JY, et al. Complement Signals Determine Opposite Effects of B Cells in Chemotherapy-Induced Immunity. *Cell*. 2020;180(6):1081-1097.e24. doi:10.1016/j.cell.2020.02.015

346. Sautès-Fridman C, Roumenina LT. B cells and complement at the forefront of chemotherapy. *Nature Reviews Clinical Oncology*. Published online 2020. doi:10.1038/s41571-020-0376-0

347. Li Z, Meng X, Wu P, et al. Glioblastoma Cell–Derived lncRNA-Containing Exosomes Induce Microglia to Produce Complement C5, Promoting Chemotherapy Resistance. *Cancer Immunology Research*. 2021;9(12):1383-1399. doi:10.1158/2326-6066.CIR-21-0258

348. Murray KP, Mathure S, Kaul R, et al. Expression of complement regulatory proteins - CD 35, CD 46, CD 55, and CD 59 - In benign and malignant endometrial tissue. *Gynecologic Oncology*. 2000;76(2):176-182. doi:10.1006/gyno.1999.5614

349. Saygin C, Wiechert A, Rao VS, et al. CD55 regulates self-renewal and cisplatin resistance in endometrioid tumors. *The Journal of Experimental Medicine*. 2017;214(9):2715-2732. doi:10.1084/jem.20170438

350. Elvington M, Melissa Scheiber, Yang X, et al. Complement dependent modulation of anti-tumor immunity following radiation therapy. *Cell Reports*. 2014;8(3):818-830. doi:10.1016/j.celrep.2014.06.051.Complement

351. Surace L, Lysenko V, Fontana AO, et al. Complement Is a Central Mediator of Radiotherapy-Induced Tumor-Specific Immunity and Clinical Response. *Immunity*. 2015;42:767-777. doi:10.1016/j.immuni.2015.03.009

352. Liljedahl E, Konradsson E, Gustafsson E, et al. Combined anti-C1-INH and radiotherapy against glioblastoma. *BMC Cancer*. 2023;23(1):106. doi:10.1186/s12885-023-10583-1

353. Reits EA, Hodge JW, Herberts CA, et al. Radiation modulates the peptide repertoire, enhances MHC class I expression, and induces successful antitumor immunotherapy. *Journal of Experimental Medicine*. 2006;203(5):1259-1271. doi:10.1084/jem.20052494

354. Agata Y, Kawasaki A, Nishimura H, et al. Expression of the PD-1 antigen on the surface of stimulated mouse T and B lymphocytes. *International Immunology*. 1996;8(5):765-772. doi:10.1093/intimm/8.5.765

355. Ishida Y, Agata Y, Shibahara K, Honjo T. Induced expression of PD-1, a novel member of the immunoglobulin gene superfamily, upon programmed cell death. *The EMBO Journal*. 1992;11(11):3887-3895. doi:10.1002/j.1460-2075.1992.tb05481.x

356. Nowicki TS, Hu-Lieskovan S, Ribas A. Mechanisms of Resistance to PD-1 and PD-L1 blockade. *The Cancer Journal*. 2018;24(1):47-53. doi:10.1016/j.physbeh.2017.03.040

357. Sharma P, Hu-Lieskovan S, Wargo JA, Ribas A. Primary, Adaptive, and Acquired Resistance to Cancer Immunotherapy. *Cell*. 2017;168(4):707-723. doi:10.1016/j.cell.2017.01.017

358. Melero I, Berman DM, Aznar MA, Korman AJ, Gracia JLP, Haanen J. Evolving synergistic combinations of targeted immunotherapies to combat cancer. *Nature Reviews Cancer*. 2015;15(8):457-472. doi:10.1038/nrc3973

359. Weber JS, Sznol M, Sullivan RJ, et al. A Serum Protein Signature Associated with Outcome after Anti–PD-1 Therapy in Metastatic Melanoma. *Cancer Immunology Research*. 2018;6(1):79-86. doi:10.1158/2326-6066.cir-17-0412

360. Krieg C, Weber LM, Fosso B, et al. Complement downregulation promotes an inflammatory signature that renders colorectal cancer susceptible to immunotherapy. *J Immunother Cancer*. 2022;10(9):e004717. doi:10.1136/jitc-2022-004717

361. Zha H, Han X, Zhu Y, et al. Blocking C5aR signaling promotes the anti-tumor efficacy of PD-1/PD-L1 blockade. *OncoImmunology*. 2017;6(10):1-8. doi:10.1080/2162402X.2017.1349587

362. Zha H, Wang X, Zhu Y, et al. Intracellular activation of complement C3 leads to PD-L1 antibody treatment resistance by modulating tumor-associated macrophages. *Cancer Immunology Research*. 2019;7(2):193-207. doi:10.1158/2326-6066.CIR-18-0272

363. Gu J, Ding J yong, Lu C lai, et al. Overexpression of CD88 predicts poor prognosis in non-small-cell lung cancer. *Lung Cancer*. 2013;81(2):259-265. doi:10.1016/j.lungcan.2013.04.020

364. Lin K, He S, He L, et al. Complement component 3 is a prognostic factor of non-small cell lung cancer. *Molecular Medicine Reports*. 2014;10:811-817. doi:10.3892/mmr.2014.2230

365. Zhang J, Chen M, Zhao Y, et al. Complement and coagulation cascades pathway correlates with chemosensitivity and overall survival in patients with soft tissue sarcoma. *European Journal of Pharmacology*. 2020;879(January):173121. doi:10.1016/j.ejphar.2020.173121

366. Michlmayr A, Bachleitner-Hofmann T, Baumann S, et al. Modulation of plasma complement by the initial dose of epirubicin/docetaxel therapy in breast cancer and its predictive value. *British Journal of Cancer*. 2010;103(8):1201-1208. doi:10.1038/sj.bjc.6605909

367. Maher SG, McDowell DT, Collins BC, Muldoon C, Gallagher WM, Reynolds JV. Serum Proteomic Profiling Reveals That Pretreatment Complement Protein Levels are Predictive of Esophageal Cancer Patient Response to Neoadjuvant Chemoradiation. *Annals of Surgery*. 2011;254(5):809-817. doi:10.1097/SLA.0b013e31823699f2

368. Lynam-Lennon N, Bibby BAS, Mongan AM, et al. Low MiR-187 Expression Promotes Resistance to Chemoradiation Therapy In Vitro and Correlates with Treatment Failure in Patients with Esophageal Adenocarcinoma. *Molecular Medicine*. 2016;22(7):388-397. doi:10.2119/molmed.2016.00020

369. Bai Y, Wang W, Li S, et al. C1QBP Promotes Homologous Recombination by Stabilizing MRE11 and Controlling the Assembly and Activation of MRE11/RAD50/NBS1 Complex. *Molecular Cell*. 2019;75(6):1299-1314.e6. doi:10.1016/j.molcel.2019.06.023

370. Kurumizaka H, Ikawa S, Nakada M, et al. Homologous-pairing activity of the human DNA-repair proteins Xrcc3.Rad51C. *Proceedings of the National Academy of Sciences of the United States of America*. 2001;98(10):5538-5543.

371. Pei JS, Chang WS, Hsu PC, et al. The contribution of XRCC3 genotypes to childhood acute lymphoblastic leukemia. *Cancer Management and Research*. 2018;10:5677-5684. doi:10.2147/CMAR.S178411

372. Kuricova M, Naccarati A, Kumar R, et al. DNA repair and cyclin D1 polymorphisms and styrene-induced genotoxicity and immunotoxicity. *Toxicology and Applied Pharmacology*. 2005;207(2 SUPPL.):302-309. doi:10.1016/j.taap.2004.12.023

373. Rus HG, Niculescu FI, Shin ML. Role of the C5b-9 complement complex in cell cycle and apoptosis. *Immunological Reviews*. 2001;180:49-55. doi:10.1034/j.1600-065X.2001.1800104.x

374. National Cancer Research Institute. Cancer in Ireland 2013: Annual report of the National Cancer Registry. Published 2013. Accessed February 11, 2018. www.ncri.ie/publications/statistical-reports/cancer-ireland-2013-annual-report-national-cancer-registry%5Cn

375. Gaertner WB, Kwaan MR, Madoff RD, Melton GB. Rectal cancer: An evidence-based update for primary care providers. *World Journal of Gastroenterology*. 2015;21(25):7659-7671. doi:10.3748/wjg.v21.i25.7659

376. Glimelius B. Neo-adjuvant radiotherapy in rectal cancer. *World Journal of Gastroenterology*. 2013;19(46):8489-8501. doi:10.3748/wjg.v19.i46.8489

377. Petrelli F, Sgroi G, Sarti E, Barni S. Increasing the interval between neoadjuvant chemoradiotherapy and surgery in rectal cancer : A meta-analysis of published studies. *Annals of Surgery*. 2016;263(3):458-464. doi:10.1097/SLA.0000000000000368

378. Fernando NH, Hurwitz HI. Targeted Therapy of Colorectal Cancer: Clinical Experience with Bevacizumab. *The Oncologist*. 2004;9 Suppl 1(suppl 1):11-18. doi:10.1634/theoncologist.9-suppl_1-11

379. Walport MJ. Complement. Second of Two Parts. *The New England Journal of Medicine*. 2001;344(15):1140-1144. doi:10.1056/NEJM200104123441506

380. Pio R, Corrales L, Lambris JD. The Role of Complement in Tumour Growth. *Advances in Experimental Medicine and Biology*. 2014;772:229-262. doi:10.1007/978-1-4614-5915-6

381. Rutkowski MJ, Sughrue ME, Kane AJ, Mills SA, Parsa AT. Cancer and the Complement Cascade. *Molecular Cancer Research*. 2010;8:1453-1466. doi:10.1158/1541-7786.MCR-10-0225

382. Jackson WD, Gulino A, Fossati-Jimack L, et al. C3 Drives Inflammatory Skin Carcinogenesis Independently of C5. *Journal of Investigative Dermatology*. 2021;141(2):404-414.e6. doi:10.1016/j.jid.2020.06.025

383. Kaida T, Nitta H, Kitano Y, et al. C5α receptor (CD88) promotes motility and invasiveness of gastric cancer by activating RhoA. *Oncotarget*. 2016;7(51):84798-84809. doi:10.18632/oncotarget.12656

384. Franken NAP, Rodermond HM, Stap J, Haveman J, van Bree C. Clonogenic assay of cells in vitro. *Nature Protocols*. 2006;1(5):2315-2319. doi:10.1038/nprot.2006.339

385. Livak KJ, Schmittgen TD. Analysis of relative gene expression data using real-time quantitative PCR and the 2-ΔΔCT method. *Methods*. 2001;25(4):402-408. doi:10.1006/meth.2001.1262

386. Stirling DR, Swain-Bowden MJ, Lucas AM, Carpenter AE, Cimini BA, Goodman A. CellProfiler 4: improvements in speed, utility and usability. *BMC Bioinformatics*. 2021;22(1):433. doi:10.1186/s12859-021-04344-9

387. Spitzner M, Emons G, Kramer F, et al. A gene expression signature for chemoradiosensitivity of colorectal cancer cells. *International Journal of Radiation Oncology Biology Physics*. 2010;78(4):1184-1192. doi:10.1016/j.ijrobp.2010.06.023

388. Yokoi K, Yamashita K, Ishii S, et al. Comprehensive molecular exploration identified promoter DNA methylation of the CRBP1 gene as a determinant of radiation sensitivity in rectal cancer. *British Journal of Cancer*. 2017;116(8):1046-1056. doi:10.1038/bjc.2017.65

389. Huang MY, Wang JY, Chang HJ, Kuo CW, Tok TS, Lin SR. CDC25A, VAV1, TP73, BRCA1 and ZAP70 gene overexpression correlates with radiation response in colorectal cancer. *Oncology Reports*. 2011;25(5):1297-1306. doi:10.3892/or.2011.1193

390. Park JH, Kim Y heon, Park EH, et al. Effects of metformin and phenformin on apoptosis and epithelial-mesenchymal transition in chemoresistant rectal cancer. *Cancer Science*. 2019;110(9):2834-2845. doi:10.1111/cas.14124

391. Ma W, Yu J, Qi X, et al. Radiation-induced microRNA-622 causes radioresistance in colorectal cancer cells by down-regulating Rb. *Oncotarget*. 2015;6(18):15984-15994. doi:10.18632/oncotarget.3762

392. Emons G, Spitzner M, Reineke S, et al. Chemoradiotherapy resistance in colorectal cancer cells is mediated by Wnt/β-catenin signaling. *Molecular Cancer Research*. 2017;15(11):1481-1490. doi:10.1158/1541-7786.MCR-17-0205

393. Kendziorra E, Ahlborn K, Spitzner M, et al. Silencing of the Wnt transcription factor TCF4 sensitizes colorectal cancer cells to (chemo-) radiotherapy. *Carcinogenesis*. 2011;32(12):1824-1831. doi:10.1093/carcin/bgr222

394. Daugan MV, Revel M, Russick J, et al. Complement C1s and C4d as Prognostic Biomarkers in Renal Cancer: Emergence of Noncanonical Functions of C1s. *Cancer Immunology Research*. 2021;9(8):891-908. doi:10.1158/2326-6066.cir-20-0532

395. Bohlson SS, Garred P, Kemper C, Tenner AJ. Complement Nomenclature—Deconvoluted. *Frontiers in Immunology*. 2019;10(June):1-6. doi:10.3389/fimmu.2019.01308

396. Ytting H, Christensen IJ, Steffensen R, et al. Mannan-Binding Lectin (MBL) and MBL-Associated Serine Protease 2 (MASP-2) Genotypes in Colorectal Cancer. *Scandinavian Journal of Immunology*. 2011;73(2):122-127. doi:10.1111/j.1365-3083.2010.02480.x

397. Storm L, Christensen IJ, Jensenius JC, Nielsen HJ, Thiel S. Evaluation of complement proteins as screening markers for colorectal cancer. *Cancer Immunology, Immunotherapy*. 2015;64(1):41-50. doi:10.1007/s00262-014-1615-y

398. Kvarnström A, Sokolov A, Swartling T, Kurlberg G, Mollnes TE, Bengtsson A. Alternative Pathway Activation of Complement in Laparoscopic and Open Rectal Surgery. *Scandinavian Journal of Immunology*. 2012;76(1):49-53. doi:10.1111/j.1365-3083.2012.02702.x

399. Ikeda J ichiro, Morii E, Liu Y, et al. Prognostic significance of CD55 expression in breast cancer. *Clinical Cancer Research*. 2008;14(15):4780-4786. doi:10.1158/1078-0432.CCR-07-1844

400. King BC, Blom AM. Intracellular complement: Evidence, definitions, controversies, and solutions. *Immunological Reviews*. Published online September 13, 2022:imr.13135. doi:10.1111/imr.13135

401. Massagué J. G1 cell-cycle control and cancer. *Nature*. 2004;432(7015):298-306. doi:10.1038/nature03094

402. Curtin NJ. DNA repair dysregulation from cancer driver to therapeutic target. *Nature Reviews Cancer*. 2012;12(12):801-817. doi:10.1038/nrc3399

403. Demichev V, Messner CB, Vernardis SI, Lilley KS, Ralser M. DIA-NN: neural networks and interference correction enable deep proteome coverage in high throughput. *Nat Methods*. 2020;17(1):41-44. doi:10.1038/s41592-019-0638-x

404. Tyanova S, Temu T, Sinitcyn P, et al. The Perseus computational platform for comprehensive analysis of (prote)omics data. *Nat Methods*. 2016;13(9):731-740. doi:10.1038/nmeth.3901

405. Mah LJ, El-Osta A, Karagiannis TC. γh2AX: A sensitive molecular marker of DNA damage and repair. *Leukemia*. 2010;24(4):679-686. doi:10.1038/leu.2010.6

406. Satelli A, Rao PS, Thirumala S, Rao US. Galectin-4 functions as a tumor suppressor of human colorectal cancer. *Int J Cancer*. 2011;129(4):799-809. doi:10.1002/ijc.25750

407. Arbore G, Kemper C, Kolev M. Intracellular complement − the complosome − in immune cell regulation. *Molecular Immunology*. 2017;89(May):2-9. doi:10.1016/j.molimm.2017.05.012

408. Tang L, Wei F, Wu Y, et al. Role of metabolism in cancer cell radioresistance and radiosensitization methods. *J Exp Clin Cancer Res*. 2018;37(1):87. doi:10.1186/s13046-018-0758-7

409. Kremlitzka M, Colineau L, Nowacka AA, et al. Alternative translation and retrotranslocation of cytosolic C3 that detects cytoinvasive bacteria. *Cellular and Molecular Life Sciences*. 2022;79(291):1-17. doi:10.1007/s00018-022-04308-z

410. Rödel C, Haas J, Groth A, Grabenbauer GG, Sauer R, Rödel F. Spontaneous and radiation-induced apoptosis in colorectal carcinoma cells with different intrinsic radiosensitivities: Survivin as a radioresistance factor. *International Journal of Radiation Oncology Biology Physics*. 2003;55(5):1341-1347. doi:10.1016/S0360-3016(02)04618-7

411. Brown MJ, Wilson G. Apoptosis Genes and Resistance to Cancer Therapy: What Does the Experimental and Clinical Data Tell Us? *Cancer Biology & Therapy*. 2003;2(5):477-490.

412. Meyn RE, Milas L, Ang KK. The role of apoptosis in radiation oncology. *International Journal of Radiation Biologyc*. 2009;85(2):107-115.

413. Rödel F, Hoffmann J, Distel L, et al. Survivin as a radioresistance factor, and prognostic and therapeutic target for radiotherapy in rectal cancer. *Cancer Research*. 2005;65(11):4881-4887. doi:10.1158/0008-5472.CAN-04-3028

414. Yasukawa T, Kamura T, Kitajima S, Conaway RC, Conaway JW, Aso T. Mammalian Elongin A complex mediates DNA-damage-induced ubiquitylation and degradation of Rpb1. *EMBO J*. 2008;27(24):3256-3266. doi:10.1038/emboj.2008.249

415. Liu Z, Guan C, Lu C, et al. High NUSAP1 expression predicts poor prognosis in colon cancer. *Pathology - Research and Practice*. 2018;214(7):968-973. doi:10.1016/j.prp.2018.05.017

416. Li Z, Zhang Y, Sui S, et al. Targeting HMGB3/hTERT axis for radioresistance in cervical cancer. *Journal of Experimental & Clinical Cancer Research*. 2020;39(1):243. doi:10.1186/s13046-020-01737-1

417. Masuda Y, Takahashi H, Sato S, et al. TRIM29 regulates the assembly of DNA repair proteins into damaged chromatin. *Nat Commun*. 2015;6(1):7299. doi:10.1038/ncomms8299

418. Rentoft M, Coates PJ, Loljung L, Wilms T, Laurell G, Nylander K. Expression of CXCL10 is associated with response to radiotherapy and overall survival in squamous cell carcinoma of the tongue. *Tumor Biol*. 2014;35(5):4191-4198. doi:10.1007/s13277-013-1549-6

419. Elvington M, Liszewski MK, Bertram P, Kulkarni HS, Atkinson JP. A C3(H20) recycling pathway is a component of the intracellular complement system. *Journal of Clinical Investigation*. 2017;127(3):970-981. doi:10.1172/JCI89412

420. Hsieh C song, Macatonia SE, Tripp CS, et al. Development of TH1 CD4+ T Cells Through IL-12 Produced by Listeria-Induced Macrophages Anne O ' Garra and Kenneth M . Murphy Published by : American Association for the Advancement of Science Stable URL : http://www.jstor.org/stable/2880972 Development of. *Science*. 1993;260(5107):547-549.

421. Swain SL, Weinberg AD, English M, Huston G. IL-4 directs the development of Th2-like helper effectors. *Journal of immunology (Baltimore, Md : 1950)*. 1990;145(11):3796-3806.

422. McKenzie GJ, Emson CL, Bell SE, et al. Impaired development of Th2 cells in IL-13-deficient mice. *Immunity*. 1998;9(3):423-432. doi:10.1016/S1074-7613(00)80625-1

423. Groux H, O'Garra A, Bigler M, et al. A CD4+ T-cell subset inhibits antigen-specific T-cell responses and prevents colitis. *Nature*. 1997;389:737-742. doi:10.1038/39614

424. Trinchieri G. Interleukin-12 and the regulation of innate resistance and adaptive immunity. *Nature Reviews Immunology*. 2003;3(2):133-146. doi:10.1038/nri1001

425. Liu J, Lin F, Strainic MG, et al. IFN-γ and IL-17 Production in Experimental Autoimmune Encephalomyelitis Depends on Local APC–T Cell Complement Production. *The Journal of Immunology*. 2008;180(9):5882-5889. doi:10.4049/jimmunol.180.9.5882

426. Strainic MG, Shevach EM, An F, Lin F, Medof ME. Absent C3a and C5a receptor signaling into CD4+T cells enables auto-inductive TGF-β1 signaling and induction of

Foxp3+T regulatory cells. *Nature Immunology*. 2013;14(2):162-171. doi:10.1038/ni.2499.Absent

427. King BC, Esguerra JLS, Golec E, Eliasson L, Kemper C, Blom AM. CD46 Activation Regulates miR-150–Mediated Control of GLUT1 Expression and Cytokine Secretion in Human CD4 + T Cells. *The Journal of Immunology*. 2016;196(4):1636-1645. doi:10.4049/jimmunol.1500516

428. Yasuda K, Nirei T, Sunami E, Nagawa H, Kitayama J. Density of CD4(+) and CD8(+) T lymphocytes in biopsy samples can be a predictor of pathological response to chemoradiotherapy (CRT) for rectal cancer. *Radiation Oncology*. 2011;6(49). doi:10.1186/1748-717X-6-49

429. Anitei MG, Zeitoun G, Mlecnik B, et al. Prognostic and predictive values of the immunoscore in patients with rectal cancer. *Clinical Cancer Research*. 2014;20(7):1891-1899. doi:10.1158/1078-0432.CCR-13-2830

430. Wang Y, Zhang H, He YW. The Complement Receptors C3aR and C5aR Are a New Class of Immune Checkpoint Receptor in Cancer Immunotherapy. *Frontiers in immunology*. 2019;10(July):1574. doi:10.3389/fimmu.2019.01574

431. Ivetic A, Green HLH, Hart SJ. L-selectin: A major regulator of leukocyte adhesion, migration and signaling. *Frontiers in Immunology*. 2019;10(MAY):1-22. doi:10.3389/fimmu.2019.01068

432. Jones D, Pereira ER, Padera TP. Growth and immune evasion of lymph node metastasis. *Frontiers in Oncology*. 2018;8(FEB). doi:10.3389/fonc.2018.00036

433. van Pul KM, Fransen MF, van de Ven R, de Gruijl TD. Immunotherapy Goes Local: The Central Role of Lymph Nodes in Driving Tumor Infiltration and Efficacy. *Frontiers in Immunology*. 2021;12(March):1-8. doi:10.3389/fimmu.2021.643291

434. Guo L, Wang C, Qiu X, Pu X, Chang P. Colorectal Cancer Immune Infiltrates: Significance in Patient Prognosis and Immunotherapeutic Efficacy. *Frontiers in Immunology*. 2020;11(May):1-13. doi:10.3389/fimmu.2020.01052

435. Xiong Y, Wang K, Zhou H, Peng L, You W, Fu Z. Profiles of immune infiltration in colorectal cancer and their clinical significant: A gene expression-based study. *Cancer Medicine*. 2018;7(9):4496-4508. doi:10.1002/cam4.1745

436. Soldevilla B, Carretero-Puche C, Gomez-Lopez G, et al. The correlation between immune subtypes and consensus molecular subtypes in colorectal cancer identifies novel tumour microenvironment profiles, with prognostic and therapeutic implications. *European Journal of Cancer*. 2019;123:118-129. doi:10.1016/j.ejca.2019.09.008

437. Woo SR, Fuertes MB, Corrales L, et al. STING-dependent cytosolic DNA sensing mediates innate immune recognition of immunogenic tumors. *Immunity*. 2014;41(5):830-842. doi:10.1016/j.immuni.2014.10.017

438. Deng L, Liang H, Xu M, et al. STING-dependent Cytosolic DNA Sensing Promotes Radiation- induced Type I interferon-dependent Antitumor Immunity in Immunogenic Tumors. *Immunity*. 2014;41(5):843-852. doi:10.1016/j.immuni.2014.10.019

439. Chen J, Wu W, Zhen C, et al. Expression and clinical significance of complement C3, complement C4b1 and apolipoprotein E in pancreatic cancer. *Oncology Letters*. 2013;6:43-48.

440. Kwan W hong, van der Touw W, Paz-Artal E, Li MO, Heeger PS. Signaling through C5a receptor and C3a receptor diminishes function of murine natural regulatory T cells. *Journal of Experimental Medicine*. 2013;210(2):257-268. doi:10.1084/jem.20121525

441. Chen DS, Mellman I. Oncology meets immunology: The cancer-immunity cycle. *Immunity*. 2013;39(1):1-10. doi:10.1016/j.immuni.2013.07.012

442. Arbonés ML, Ord DC, Ley K, et al. Lymphocyte Homing and Leukocyte Rolling and Migration Are Impaired in L-Selectin-Deficient Mice. *Immunity*. 1994;1:247-260.

443. Ziegler SF, Ramsdell F, Alderson MR. The activation antigen CD69. *STEM CELLS*. 1994;12(5):456-465. doi:10.1002/stem.5530120502

444. Romagnani S. The Thl/Th2 paradigm. *Immunology Today*. 1997;18(6):263-266.

445. Mosmann TR, Coffman RL. TH1 and TH2 Cells: Different Patterns of Lymphokine Secretion Lead to Different Functional Properties.

446. Denardo DD, Barreto JB, Andreu P, et al. CD4+ T Cells Regulate Pulmonary Metastasis of Mammary Carcinomas by Enhancing Protumor Properties of Macrophages. *Cancer Cell*. 16:91-102. doi:10.1056/NEJMoa1215637

447. Zheng Z, Li Y nan, Jia S, et al. Lung mesenchymal stromal cells influenced by Th2 cytokines mobilize neutrophils and facilitate metastasis by producing complement C3. *Nat Commun*. 2021;12(1):6202. doi:10.1038/s41467-021-26460-z

448. Castro F, Cardoso AP, Gonçalves RM, Serre K, Oliveira MJ. Interferon-gamma at the crossroads of tumor immune surveillance or evasion. *Frontiers in Immunology*. 2018;9(MAY):1-19. doi:10.3389/fimmu.2018.00847

449. Kuen DS, Kim BS, Chung Y. Il-17-producing cells in tumor immunity: Friends or foes? *Immune Network*. 2020;20(1):1-20. doi:10.4110/in.2020.20.e6

450. Popeda M, Markiewicz A, Stokowy T, et al. Reduced expression of innate immunity-related genes in lymph node metastases of luminal breast cancer patients. *Scientific Reports*. 2021;11(1):1-9. doi:10.1038/s41598-021-84568-0

451. Feeney G, Sehgal R, Sheehan M, et al. Neoadjuvant radiotherapy for rectal cancer management. *WJG*. 2019;25(33):4850-4869. doi:10.3748/wjg.v25.i33.4850

452. Department of Health Ireland (An Roinn Slainte). Diagnosis, staging and treatment of patients with gestational trophoblastic disease: National Clinical Guideline No. 25. 2020;December.

453. Li M, Xiao Q, Venkatachalam N, et al. Predicting response to neoadjuvant chemoradiotherapy in rectal cancer: from biomarkers to tumor models. *Ther Adv Med Oncol*. 2022;14:175883592210779. doi:10.1177/17588359221077972

454. Beets GL, Figueiredo NF, Beets-Tan RGH. Management of Rectal Cancer Without Radical Resection. *Annu Rev Med*. 2017;68(1):169-182. doi:10.1146/annurev-med-062915-021419

455. Garcia-Aguilar J, Patil S, Gollub MJ, et al. Organ Preservation in Patients With Rectal Adenocarcinoma Treated With Total Neoadjuvant Therapy. *J Clin Oncol*. 2022;40(23):2546-2556. doi:10.1200/JCO.22.00032

456. Kolev M, Das M, Gerber M, Baver S, Deschatelets P, Markiewski MM. Inside-Out of Complement in Cancer. *Front Immunol*. 2022;13:931273. doi:10.3389/fimmu.2022.931273

457. Gebski V, Burmeister B, Smithers BM, Foo K, Zalcberg J, Simes J. Survival benefits from neoadjuvant chemoradiotherapy or chemotherapy in oesophageal carcinoma: a meta-analysis. *The Lancet Oncology*. 2007;8(3):226-234. doi:10.1016/S1470-2045(07)70039-6

458. Janse van Rensburg HJ, Spiliopoulou P, Siu LL. Circulating Biomarkers for Therapeutic Monitoring of Anti-cancer Agents. *The Oncologist*. 2022;27(5):352-362. doi:10.1093/oncolo/oyac047

459. Zhang Z, Qin K, Zhang W, et al. Postoperative recurrence of epithelial ovarian cancer patients and chemoresistance related protein analyses. *J Ovarian Res*. 2019;12(1):29. doi:10.1186/s13048-019-0499-z

460. Reese B, Silwal A, Daugherity E, et al. Complement as Prognostic Biomarker and Potential Therapeutic Target in Renal Cell Carcinoma. *The Journal of Immunology*. 2020;205(11):3218-3229. doi:10.4049/jimmunol.2000511

461. McShane LM, Altman DG, Sauerbrei W, et al. Reporting recommendations for tumor marker prognostic studies (REMARK). *J Natl Cancer Inst*. 2005;97(16):1180-1184. doi:10.1093/jnci/dji237

462. De Pergola G, Silvestris F. Obesity as a Major Risk Factor for Cancer. *Journal of Obesity*. 2013;2013:1-11. doi:10.1155/2013/291546

463. Gallo M, Adinolfi V, Barucca V, et al. Expected and paradoxical effects of obesity on cancer treatment response. *Rev Endocr Metab Disord*. 2021;22(4):681-702. doi:10.1007/s11154-020-09597-y

464. Lee SY, Kim CH, Kim YJ, Kwak HD, Ju JK, Kim HR. Obesity as an independent predictive factor for pathologic complete response after neoadjuvant chemoradiation in rectal cancer. *Ann Surg Treat Res*. 2019;96(3):116. doi:10.4174/astr.2019.96.3.116

465. Aronne LJ. Classification of Obesity and Assessment of Obesity-Related Health Risks. *Obesity Research*. 2002;10(S12):105S-115S. doi:10.1038/oby.2002.203

466. Weber R, Groth C, Lasser S, et al. IL-6 as a major regulator of MDSC activity and possible target for cancer immunotherapy. *Cellular Immunology*. 2021;359:104254.

467. Waldner MJ, Foersch S, Neurath MF. Interleukin-6 - A Key Regulator of Colorectal Cancer Development. *Int J Biol Sci*. 2012;8(9):1248-1253. doi:10.7150/ijbs.4614

468. Bao D, Zhang C, Li L, et al. Integrative Analysis of Complement System to Prognosis and Immune Infiltrating in Colon Cancer and Gastric Cancer. *Frontiers in Oncology*. 2021;10. Accessed February 22, 2023. https://www.frontiersin.org/articles/10.3389/fonc.2020.553297

469. Bardou M, Barkun AN, Martel M. Obesity and colorectal cancer. *Gut*. 2013;62(6):933-947. doi:10.1136/gutjnl-2013-304701

470. Gabrielsson BG, Johansson JM, Lönn M, et al. High Expression of Complement Components in Omental Adipose Tissue in Obese Men. *Obesity Research*. 2003;11(6):699-708. doi:10.1038/oby.2003.100

471. Hayder A Al-Domi, Reem M Al Haj Ahmad. Association between complement component C3 and body composition: a possible obesity inflammatory biomarker for insulin resistance. *Asia Pacific Journal of Clinical Nutrition*. 2017;26(6). doi:10.6133/apjcn.012017.02

472. Moreno-Navarrete JM, Fernández-Real JM. The complement system is dysfunctional in metabolic disease: Evidences in plasma and adipose tissue from obese and insulin resistant subjects. *Semin Cell Dev Biol*. 2019;85:164-172. doi:10.1016/j.semcdb.2017.10.025

473. Gadekar T, Dudeja P, Basu I, Vashisht S, Mukherji S. Correlation of visceral body fat with waist–hip ratio, waist circumference and body mass index in healthy adults: A

cross sectional study. *Medical Journal Armed Forces India*. 2020;76(1):41-46. doi:10.1016/j.mjafi.2017.12.001

474. Bromberg J, Wang TC. Inflammation and Cancer: IL-6 and STAT3 Complete the Link. *Cancer Cell*. 15:79-80. doi:10.1016/j.ccr.2009.01.009

475. Mahdi NK, Al-Jowher MH, Ali HQ. Can IgA, C3, IL-6 and TNF-α act as predictors for reoccurrence of breast cancer among Iraqi women? *Qatar Medical Journal*. 2013;2013(1). doi:10.5339/qmj.2013.6

476. Tada N, Tsuno NH, Kawai K, et al. Changes in the plasma levels of cytokines/chemokines for predicting the response to chemoradiation therapy in rectal cancer patients. *Oncology Reports*. 2014;31(1):463-471. doi:10.3892/or.2013.2857

477. Debucquoy A, Goethals L, Geboes K, Roels S, Mc Bride WH, Haustermans K. Molecular responses of rectal cancer to preoperative chemoradiation. *Radiotherapy and Oncology*. 2006;80(2):172-177. doi:10.1016/j.radonc.2006.07.016

478. Katz Y, Revel M, Strunk RC. Interleukin 6 stimulates synthesis of complement proteins factor B and C3 in human skin fibroblasts. *Eur J Immunol*. 1989;19(6):983-988. doi:10.1002/eji.1830190605

479. Kopf M, Herren S, Wiles MV, Pepys MB, Kosco-Vilbois MH. Interleukin 6 Influences Germinal Center Development and Antibody Production via a Contribution of C3 Complement Component. *Journal of Experimental Medicine*. 1998;188(10):1895-1906. doi:10.1084/jem.188.10.1895

480. Heinrich PC, Castell JV, Andus T. Interleukin-6 and the acute phase response. 1990;265.

481. Wilkins A, Fontana E, Nyamundanda G, et al. Differential and longitudinal immune gene patterns associated with reprogrammed microenvironment and viral mimicry in response to neoadjuvant radiotherapy in rectal cancer. *Journal for ImmunoTherapy of Cancer*. 2021;9(3). doi:10.1136/jitc-2020-001717

482. Koncina, Haan, Rauh, Letellier. Prognostic and Predictive Molecular Biomarkers for Colorectal Cancer: Updates and Challenges. *Cancers*. 2020;12(2):319. doi:10.3390/cancers12020319

483. Liang JZ, Liang XL, Zhong LY, Wu CT, Zhang J, Wang Y. Comparative Proteome Identifies Complement Component 3-Mediated Immune Response as Key Difference of Colon Adenocarcinoma and Rectal Adenocarcinoma. *Front Oncol*. 2021;10:617890. doi:10.3389/fonc.2020.617890

484. Gordon Steel G, Peckham MJ. Exploitable mechanisms in combined radiotherapy-chemotherapy: The concept of additivity. *International Journal of Radiation Oncology*Biology*Physics*. 1979;5(1):85-91. doi:10.1016/0360-3016(79)90044-0

485. Aykut B, Pushalkar S, Chen R, et al. The fungal mycobiome promotes pancreatic oncogenesis via activation of MBL. *Nature*. 2019;574(7777):264-267. doi:10.1038/s41586-019-1608-2

486. Dho SH, Cho EH, Lee JY, et al. A novel therapeutic anti-CD55 monoclonal antibody inhibits the proliferation and metastasis of colorectal cancer cells. *Oncology Reports*. 2019;42(6):2686-2693. doi:10.3892/or.2019.7337

487. Durrant LG, Chapman MA, Buckley DJ, Spendlove I, Robins RA, Armitage NC. Enhanced expression of the complement regulatory protein CD55 predicts a poor prognosis in colorectal cancer patients. *Cancer Immunol Immunother*. 2003;52(10):638-642. doi:10.1007/s00262-003-0402-y

488. Bauer KM, Hummon AB, Buechler S. Right-side and left-side colon cancer follow different pathways to relapse: RELAPSE IN RIGHT-SIDE AND LEFT-SIDE COLON CANCER. *Mol Carcinog*. 2012;51(5):411-421. doi:10.1002/mc.20804

489. Ajona D, Ortiz-Espinosa S, Pio R. Complement anaphylatoxins C3a and C5a: Emerging roles in cancer progression and treatment. *Seminars in Cell and Developmental Biology*. 2019;85:153-163. doi:10.1016/j.semcdb.2017.11.023

490. Kanehisa M, Goto S. KEGG: kyoto encyclopedia of genes and genomes. *Nucleic acids research*. 2000;28(1). doi:10.1093/nar/28.1.27

491. Kanehisa M, Furumichi M, Sato Y, Kawashima M, Ishiguro-Watanabe M. KEGG for taxonomy-based analysis of pathways and genomes. *Nucleic Acids Research*. 2023;51(D1):D587. doi:10.1093/nar/gkac963

492. Kanehisa M. Toward understanding the origin and evolution of cellular organisms. *Protein science : a publication of the Protein Society*. 2019;28(11). doi:10.1002/pro.3715

493. Lynam-Lennon N, Maher SG, Maguire A, et al. Altered mitochondrial function and energy metabolism is associated with a radioresistant phenotype in oesophageal adenocarcinoma. *PLoS One*. 2014;9(6):e100738. doi:10.1371/journal.pone.0100738

494. Mastellos DC, Reis ES, Lambris JD. Complement C5a-Mediated TAM-ing of Antitumor Immunity Drives Squamous Carcinogenesis. *Cancer Cell*. 2018;34:531-533. doi:10.1016/j.ccell.2018.09.005

495. He L, Jin M, Jian D, et al. Identification of four immune subtypes in locally advanced rectal cancer treated with neoadjuvant chemotherapy for predicting the efficacy of subsequent immune checkpoint blockade. *Front Immunol*. 2022;13:955187. doi:10.3389/fimmu.2022.955187